

**Biomechanical Study of Rigid Ankle-Foot Orthoses in
the Treatment of Stroke Patients.**

By

Amneh Alshawabka (MPhil, BSc)

University of Strathclyde
Department of Biomedical Engineering

Thesis Submitted in Total Fulfilment of the Requirements for the
Degree of Doctor of Philosophy

2020

Declaration

This thesis is the result of the author's original research. It has been composed by the author and has not been previously submitted for examination which has led to the award of a degree.

The copyright of this thesis belongs to the author under the terms of the United Kingdom Copyright Act as qualified by University of Strathclyde Regulation 3.50. Due acknowledgement must always be made of the use of any material contained in, or derived from, this thesis.

Signed: *Amneh Alshawabka*

Date: 1st Sep 2020

Abstract

Rigid Ankle-Foot Orthoses (AFOs) are commonly prescribed for stroke patients who exhibit equinovarus deformity as an orthotic intervention. The main purpose of prescribing a rigid AFO is to provide appropriate control of unwanted ankle and foot motions in any plane. To achieve the optimal effects of the AFO, appropriate stiffness and alignment optimisation (tuning) should be considered. The AFO provides moments (referred to as the orthotic moments) to control ankle motion. Orthotic moments are different from the moments generated by ground reaction forces, the later are known as total ankle moments. Reviewing the literature showed limited research in this area. The aims of this study are to investigate the biomechanical effects of using rigid AFO (before and after tuning) and to investigate the orthotic moment during walking in stroke patients.

Gait data were collected from six stroke participants (2 females, 4 males) and six healthy participants (3 females, 3 males) using a Motekforce Link dual belt instrumented treadmill and a Vicon 3-dimensional motion analysis system. Each participant was fitted with a custom made rigid AFO instrumented using four strain gauges. Walking at a self-selected speed was investigated while wearing: **(1)** Standard shoes only **(2)** Rigid AFO with standard shoes **(3)** Rigid Tuned-AFO with standard shoes. Lower limb temporal-spatial, kinetic and kinematic parameters, and electromyographic activity (Delsys TrignoTM) of the knee muscles were compared among the test conditions. The orthotic moments were also quantified using the strain gauges data combined with gait analysis. Repeated measures ANOVA and Friedman's ANOVA were used for statistical analysis.

The rigid AFO showed immediate improvement in the temporal-spatial parameters and the kinematics and the kinetics of post stroke gait. Greater improvement in knee kinematics and kinetics was achieved when tuning the rigid AFO. The rigid AFO (before and after tuning) increased quadriceps muscle activity and reduced hamstring muscle activity compared to walking with standard shoes only. Tuning a rigid AFO further increased quadriceps muscle activity and reduced hamstring muscle activity compared to AFO before tuning. Strain gauges data combined with gait analysis can be used in evaluating the orthotic moment around the ankle in sagittal and frontal planes. Tuning a rigid AFO had no clear changes in the orthotic moment, and it did not alter the anatomical moments at the ankle joint in sagittal and at the subtalar joint in frontal plane.

Abbreviations

| | |
|--------|-----------------------------------------------------------|
| 2D | 2-Dimensional |
| 3D | 3-Dimensional |
| AA-AFO | Ankle Angle of the Ankle-Foot Orthosis |
| AFO | Ankle-Foot Orthosis |
| AFO-FC | Ankle-Foot Orthosis Footwear Combination |
| BA | Brodman Areas |
| BRUCE | Bi-articular Reciprocating Universal Compliance Estimator |
| CAST | Calibrated Anatomical System Technique |
| COM | Centre of Mass |
| COP | Centre of Pressure |
| CVA | Cerebrovascular Accident |
| CWS | Comfortable Walking Speed |
| EMG | Electromyography |
| GC | Gait Cycle |
| GRAFO | Ground Reaction Ankle-Foot Orthosis |
| GRF | Ground Reaction Force |
| HAFO | Hinged Ankle-Foot Orthosis |
| HPP | Homopolymer Polypropylene |
| ISPO | International Society of Prosthetics and Orthotics |
| JCS | Joint Coordinate System |
| MMT | Manual Muscle Test |
| MCID | Minimal Clinically Important Difference |
| MTP | Metatarsal Phalangeal |
| MAS | Modified Ashworth Scale |

| | |
|-----------|---------------------------------|
| NHS | National Health Service |
| PLS | Posterior Leaf Spring |
| SAF | Shank Angle to Floor |
| SVA | Shank to Vertical Angle |
| SP | Stroke Participant |
| SSO | Standard Shoes Only |
| SG | Strain Gauge |
| TIA | Transient Ischemic Attack |
| Tuned-AFO | Tuned Rigid Ankle-Foot Orthosis |
| UMN | Upper Motor Neuron |
| UV | Ultraviolet |
| GRFv | Vertical Ground Reaction Force |
| BW | Body Weight |
| WHO | World Health Organization |

Acknowledgments

Chasing a dream requires effort, passion, and hard work. I have been truly blessed to have the unique opportunity to study at the University of Strathclyde. Completing this thesis would not have certainly been possible without the contributions of many supportive and knowledgeable people.

First and foremost, I would like to thank my supervisor, Stephanos Solomonidis for his invaluable guidance, encouragement, academic stimulus, and generous help. You always gave me a lot of freedom, encouraged me to treat myself as a lab manager, and be confident to discover and verify new thoughts. I would like to extend my sincere gratitude to my co-supervisor, Roy Bowers, for his continuous support and endless help, for taking hours of the time reviewing my thesis. Thank you for your valuable feedback and advice, and for providing your expertise and for fabrication the AFOs. Your personality of optimism and self-confident always inspired me when I met problems during my PhD journey.

I am thankful to Vojtech Nedved for assisting me in the Instron tensile testing and being always very helpful. I am grateful also for Moutaz Hamdan and John Maclean, for their technical help and assistance. Thank you and I have learned so much from all of you.

I would like to extend my appreciation to the staff of the National Centre for Prosthetics and Orthotics at the University of Strathclyde, for their support and assistance during data collection. I would also like to thank Stephen Murray, for his support and technical assistance. I am also indebted to Craig Childs, thank you for your assistance with my data collection, great discussions, and feedback.

I thank Heba Lakany, for sharing her vast experience in the field of EMG analysis which has made an invaluable contribution to this work. Thank you for being available, for your encouragement, and for your guidance.

Most importantly, I would like to acknowledge and thank all the participants in this study. Without their willingness to give their time so generously this work would not be possible. I would also like to acknowledge the University of Strathclyde which offered me all the

facilities needed to complete my research project. I am always indebted to the University of Jordan for the financial support offered throughout my study.

I would also like to extend my deepest gratitude to my friends and the entire staff in the Biomedical Engineering department. Especial thanks go to Sara, Shima, Esraa, Eunice, Ansu and Mahmoud. It is impossible to say enough for Noor Almansor and Maareb Araim. I am humbled by your support and friendship. Each of you always found a way to keep things light when tensions were high.

My gratitude is beyond words to my great family; Mum, Nuha, Rasha, Ayaat and Mohammad. Your permanent love and confidence in me have encouraged me to go ahead in my study and career. Specifically, I want to appreciate you all for taking care of my daughter when I was studying in Glasgow. This thesis is dedicated to my superhero, Mum, I hope you will always be proud of me.

To my sweet little girl, Sarah, for your amazing smile that brings joy to my life. For your words that motivate me to work. My love and longing for you are beyond words. For your patience and for hiding your feelings so not upset me. I am sorry for not being able to accompany or witness every step of your growing up. Last, but definitely not the least, I express my gratitude to my beloved husband, Wa'el. I am so appreciative for your constant love, understanding and encouraging, for taking up the whole responsibilities to our family and bearing the pressure both from working and living during my studying abroad.

Thank Allah for every blessing you have given us.

Table of Contents

| | |
|--------------------------------------------------------------------------------------|-----------|
| Declaration | 1 |
| Abstract..... | 2 |
| Abbreviations | 3 |
| Acknowledgments | 5 |
| Table of Contents | 7 |
| List of Figures..... | 11 |
| List of Tables | 18 |
| Chapter 1: Introduction | 20 |
| Chapter 2 Background and Literature review..... | 24 |
| 2.1 Chapter overview | 24 |
| 2.2 Stroke | 24 |
| 2.2.1 “Stroke” an overview | 24 |
| 2.2.2 Impact of stroke on key motor functions | 27 |
| 2.2.3 Stroke incidence and recovery | 29 |
| 2.3 Normal and post stroke gait..... | 31 |
| 2.3.1 Introduction..... | 31 |
| 2.3.2 Normal gait | 32 |
| 2.3.3 Post stroke gait..... | 46 |
| 2.4 Post stroke gait rehabilitation..... | 51 |
| 2.5 Orthotic management of stroke patients with plantarflexion deformity..... | 54 |
| 2.5.1 Introduction..... | 54 |
| 2.5.2 Prescription of AFOs | 55 |
| 2.5.3 Biomechanical effects of AFOs | 64 |
| 2.5.4 The AFO alignment | 69 |
| 2.6 Tuning rigid AFOs..... | 75 |

| | | |
|------------------|------------------------------------------------------------------------|------------|
| 2.7 | The efficacy of rigid AFOs on post stroke gait parameters | 79 |
| 2.8 | AFO stiffness | 92 |
| 2.8.1 | AFO stiffness definition and measurement techniques | 92 |
| 2.8.2 | Impact of AFOs stiffness on post stroke gait parameters | 93 |
| 2.9 | Orthotic moment measurement techniques | 94 |
| 2.10 | Literature considerations | 104 |
| 2.11 | Aims and objectives | 105 |
| Chapter 3 | Methods | 107 |
| 3.1. | Design of the methods..... | 107 |
| 3.2. | Participants..... | 107 |
| 3.2.1 | Control participants..... | 107 |
| 3.2.2 | Stroke participants | 108 |
| 3.3. | Experimental procedure..... | 109 |
| 3.3.1 | Experimental AFO | 109 |
| 3.3.2 | Motion capture system set up | 122 |
| 3.3.3 | Electromyography (EMG) setup..... | 131 |
| 3.4. | Data collection | 136 |
| 3.4.1 | Gait laboratory preparation..... | 136 |
| 3.4.2 | Manual muscle test (MMT) | 139 |
| 3.4.3 | Gait laboratory testing procedure | 141 |
| 3.5 | Motion data processing | 148 |
| 3.5.1 | Lower limb modelling | 150 |
| 3.5.2 | Kinematics calculation..... | 155 |
| 3.5.3 | Kinetics calculation..... | 157 |
| 3.6 | Data analysis..... | 158 |
| 3.6.1 | Kinetic and kinematic analysis | 158 |
| 3.6.2 | EMG data analysis | 160 |
| 3.6.3 | SG data analysis..... | 165 |
| Chapter 4 | Case Studies: Results and Discussion. | 170 |

| | |
|---------------------------------------------------------------------------------------------------------------------------------------|------------|
| 4.1 Control participants | 171 |
| 4.1.1 Comparing AFO condition with SSO condition:..... | 171 |
| 4.1.2 Comparing Tuned-AFO condition with AFO condition: | 173 |
| 4.2 Case study one (SP1)..... | 181 |
| 4.2.1 Comparing AFO condition with SSO condition:..... | 181 |
| 4.2.2 Comparing Tuned-AFO condition with AFO condition: | 184 |
| 4.3 Case study two (SP2) | 192 |
| 4.3.1 Comparing AFO condition with SSO condition:..... | 193 |
| 4.3.2 Comparing Tuned-AFO condition with AFO condition: | 195 |
| 4.4 Case study three (SP3)..... | 203 |
| 4.4.1 Comparing AFO condition with SSO condition:..... | 203 |
| 4.4.2 Comparing Tuned-AFO condition with AFO condition: | 205 |
| 4.5 Case study four (SP4) | 214 |
| 4.5.1 Comparing AFO condition with SSO condition:..... | 215 |
| 4.5.2 Comparing Tuned-AFO condition with AFO condition: | 216 |
| 4.6 Case study four (SP5) | 225 |
| 4.5.1 Comparing AFO condition with SSO condition:..... | 226 |
| 4.6.2 Comparing Tuned-AFO condition with AFO condition: | 228 |
| 4.7 Case study four (SP6) | 236 |
| 4.7.1 Comparing Tuned-AFO condition with AFO condition: | 237 |
| Chapter 5 Discussion | 246 |
| 5.1 The immediate effects of rigid Tuned-AFO, rigid AFO (before tuning), and SSO on control and stroke participants gait. | 249 |
| 5.1.1 Shank to vertical angle (SVA) | 249 |
| 5.1.2 Temporal-spatial parameters..... | 251 |
| 5.1.3 Kinematic parameters | 252 |
| 5.1.4 Kinetic parameters | 259 |
| 5.1.5 EMG outputs..... | 264 |
| 5.2 The immediate effects of Tuned-AFO and rigid AFO (before tuning) on the orthotic and the anatomical moments..... | 271 |

| | | |
|-------------------------|-----------------------------------------------------------------------------------------|------------|
| 5.2.1 | Anatomical and Orthotic moments at the ankle in the sagittal plane | 273 |
| 5.2.2 | Anatomical and Orthotic moments at assumed subtalar joint in the frontal plane | 275 |
| 5.3 | The limitations of the study..... | 276 |
| Chapter 6 | Conclusions and suggested future studies | 278 |
| 6.1 | Clinical implications | 278 |
| 6.2 | Conclusions..... | 279 |
| 6.3 | Suggested future studies | 280 |
| Chapter 7 | Appendices | 282 |
| Appendix (A): | Clinical recommendations for AFOs..... | 282 |
| Appendix (B): | Randomization plan from | 285 |
| Appendix (C): | West of Scotland Research Ethics Service letter..... | 286 |
| Appendix (D): | The Study poster..... | 290 |
| Appendix (E): | The Study Advert..... | 291 |
| Appendix (F): | Participant information sheet and consent form | 292 |
| Appendix (G): | Demographic data collection | 304 |
| Appendix (H): | Strain Gauge Reliability Test | 305 |
| Appendix (I): | Matlab codes | 322 |
| Appendix (J): | Supplementary Results | 327 |
| References | | 356 |

List of Figures

Chapter 2: Background and Literature review

| | |
|----------------------------------------------------------------------------------------------------------------------------------------------------|----|
| Figure 2.1: Blood supply to the brain. | 25 |
| Figure 2.2: Stroke types; ischaemic and haemorrhagic stroke. | 27 |
| Figure 2.3: Gait cycle phases and sub-phases..... | 34 |
| Figure 2.4: Spatial parameters of normal gait..... | 35 |
| Figure 2.5: The stance time percentage of COP progression | 36 |
| Figure 2.6: Vertical ground reaction force (GRFv) during stance phase..... | 37 |
| Figure 2.7: Functional rockers of the foot and ankle | 39 |
| Figure 2.8: Normal range of motion pattern of the ankle joint during a gait cycle | 40 |
| Figure 2.9: Normal range of motion pattern of the knee joint during a gait cycle.. | 41 |
| Figure 2.10: Normal range of motion pattern of the hip joint during a gait cycle..... | 43 |
| Figure 2.11: Shank to Vertical Angle (SVA) measurement. | 44 |
| Figure 2.12: Shank to Vertical Angle (SVA) measurement | 45 |
| Figure 2.13: Affected and non-affected step length of stroke patient. | 47 |
| Figure 2.14: An example of a typical stance phase in a stroke patient with hemiplegic gait. | 48 |
| Figure 2.15: The GRFv patterns of stroke patients during walking. | 50 |
| Figure 2.16: Thermoplastic AFO type examples | 56 |
| Figure 2.17: AFO stiffness can be affected by the location of its trimlines. | 58 |
| Figure 2.18: The terms used to describe the rigid AFO parts and trimlines..... | 58 |
| Figure 2.19: The AFO force system | 66 |
| Figure 2.20: Single ankle strap (A) and “figure-8” crossover ankle strap (B)..... | 67 |
| Figure 2.21: The GRF and tibia alignments in a stroke patient..... | 68 |
| Figure 2.22: A diagram showing the ankle angle of the AFO (AA-AFO), the shank to vertical angle (SVA), and the shank to the floor angle (SAF)..... | 71 |
| Figure 2.23: Measuring the SVA using the anterior (A) and lateral (B) markers placement methods..... | 73 |
| Figure 2.24: Measuring the effective heel height | 74 |
| Figure 2.25: The effects of tuning a rigid AFO on the GRF alignment during mid stance.. | 77 |
| Figure 2.26: The effects of tuning on the SVA, knee, and hip joints. | 77 |
| Figure 2.27: Factors preventing orthotists from using AFO tuning | 78 |
| Figure 2.28: Walking speed variation during walking with and without rigid AFO..... | 82 |

| | |
|---------------------------------------------------------------------------------------------------------------------------------------------------------------------------------------------------------------------|-----|
| Figure 2.29: The peak knee flexion angle during walking with rigid AFO and without AFO. | 84 |
| Figure 2.30: The sagittal knee angle (A) and the sagittal knee external moment (B) for stroke patients with moderate plantarflexion contracture during walking with different types of AFO and with shoes only..... | 84 |
| Figure 2.31: The rigid AFO (A) and the rigid AFO with rocker bar..... | 86 |
| Figure 2.32: Muscle operation length of the long head of biceps femoris (A), medial gastrocnemius (B) and tibialis anterior (C) during walking with different conditions... .. | 88 |
| Figure 2.33: A schematic drawing of the BRUCE | 96 |
| Figure 2.34: The articulated AFO (A) and the bench testing (B) of the articulated AFO used in Kobayashi et al. (2017) study..... | 97 |
| Figure 2.35: The ankle angle-plantarflexion resistive moment relationship | 98 |
| Figure 2.36: A schematic drawing of the strain gauge (SG) | 99 |
| Figure 2.37: The strain gauged AFOs used in Chu and Feng (1998) study | 100 |
| Figure 2.38: The strain gauged AFO used in the study by Papi et al (2015)..... | 102 |
| Figure 2.39: SGs outputs against load for static AFO calibration of the 45° three-element rosette..... | 103 |
| Figure 2.40: The orthotic moment measured in a rigid AFO during walking in the study by Papi et al. (2015)..... | 103 |

Chapter 3: Methods

| | |
|----------------------------------------------------------------------------------------------------------------------------------------------------------------------------------------------------|-----|
| Figure 3.1: AFO casting process..... | 110 |
| Figure 3.2: Carbon fibre reinforcement used in rigid AFO. | 112 |
| Figure 3.3: A schematic drawing of the single SG used in this study | 113 |
| Figure 3.4: The location of the strain gauges used in this study and a schematic drawing of the Wheatstone bridge configuration..... | 116 |
| Figure 3.5: Lever arm measurement. | 118 |
| Figure 3.6: The Instron tensile testing machine..... | 119 |
| Figure 3.7: AFO calibration protocol (A). An example of load data from Wavematrix software (B), SGs data from LabVIEW software (C), synchronised load and SGs data using Matlab software (D) | 120 |
| Figure 3.8: AFO calibration orientations to produce dorsiflexion (A), plantarflexion (B), inversion (C) and eversion (D) moments at the ankle joint..... | 121 |
| Figure 3.9: A schematic drawing of the CAREN system laboratory..... | 122 |
| Figure 3.10: A schematic drawing of the instrumented treadmill with the two force plates. | 123 |

| | |
|------------------------------------------------------------------------------------------------------------------------------------------------------------------------------|-----|
| Figure 3.11: The three components of the ground reaction force (GRF) with the coordinate system used in this study (A and B) and the coordinate system adapted by (ISB)..... | 124 |
| Figure 3.12: The setup position of the static calibration with global reference frame axes as defined by the calibration wand | 126 |
| Figure 3.13: Representation of Vicon cameras beams of infrared light | 127 |
| Figure 3.14: An example of using a “least squares” method to calculate the marker centre residual with three cameras beams | 128 |
| Figure 3.15: Rigid cluster consisting of four reflective markers. | 129 |
| Figure 3.16: Anatomical and technical reflective markers positions..... | 131 |
| Figure 3.17: The wireless base station of Delsys Trigno™ system..... | 132 |
| Figure 3.18: Bipolar electrode configuration..... | 133 |
| Figure 3.19: Delsys EMG sensor locations | 134 |
| Figure 3.20: The Trigger module (A) and Delsys Trigno software interface (B). | 136 |
| Figure 3.21: The experimental set up for gait analysis..... | 137 |
| Figure 3.22: Standard Shoes (Potenza Renace). | 138 |
| Figure 3.23: Anatomical and technical markers. | 141 |
| Figure 3.24: The supportive harness used during treadmill walking..... | 143 |
| Figure 3.25: Tuning heel wedges..... | 144 |
| Figure 3.26: Example of an AFO before tuning (A) and after tuning (B). | 145 |
| Figure 3.27: The GRF location relative to hip and knee joints during midstance | 147 |
| Figure 3.28: Demonstration of SVA with SSO (A), AFO (B), and Tuned-AFO (C)... | 148 |
| Figure 3.29: Static participant’s markers before (A) and after (B) labelling..... | 149 |
| Figure 3.30: Examples of some walking scenarios..... | 150 |
| Figure 3.31: Six- degrees of freedom movements | 151 |
| Figure 3.32: Pelvic depth, height and width | 152 |
| Figure 3.33: The modelled markers that represent the hip, knee, and ankle joints centres. | 153 |
| Figure 3.34: The hip, knee, and Ankle coordinate systems | 156 |
| Figure 3.35: Determination of gait events using vertical GRF..... | 159 |
| Figure 3.36: The maximum/minimum peak values calculation of the knee angle joint | 160 |
| Figure 3.37: An example of EMG data processing steps | 162 |
| Figure 3.38: An example of EMG normalization processes..... | 163 |
| Figure 3.39: An example of determining the activation period..... | 164 |
| Figure 3.40: An example of processed EMG data..... | 165 |

| | |
|------------------------------------------------------------------------------------------------------------------------------------------------------|-----|
| Figure 3.41: SGs raw data examples for SG2 (A) and SG4 (B)..... | 166 |
| Figure 3.42: SGs AFO calibration outputs against load | 167 |
| Figure 3.43: Linear regression of SG2 outputs versus dorsiflexion/plantarflexion moments (A), SG4 outputs versus inversion/eversion moments (B)..... | 168 |
| Figure 3.44: Orthotic moments in sagittal plane based on SG2 voltage output (A), and in frontal plane based on SG4 voltage outputs (B). | 168 |
| Figure 3.45: Ankle moments in sagittal plane (A) and in frontal plane (B). | 169 |

Chapter 4: Case studies: Results and Discussion

| | |
|---------------------------------------------------------------------------------------------------------------------------------------------------------------------------------------------------------------|-----|
| Figure 4.1: Sagittal kinematic graphs for control participants..... | 176 |
| Figure 4.2: Sagittal kinetic graphs and the vertical GRF graph for control participant. | 177 |
| Figure 4.3: Quadriceps and hamstring EMG RMS amplitude and timing during walking on treadmill for control participant | 178 |
| Figure 4.4: Total ankle moment, orthotic moment, and anatomical moment in sagittal plane (A) and frontal plane (B) for control participants derived from SG2 and SG4 data outputs, respectively. | 181 |
| Figure 4.5: Sagittal kinematic graphs for case study 1 (<i>SP1</i>)..... | 187 |
| Figure 4.6: Sagittal kinetic graphs and the vertical GRF graph for case study 1 (<i>SP1</i>) | 188 |
| Figure 4.7: Quadriceps and hamstring EMG RMS amplitude and timing during walking on treadmill for case study 1 (<i>SP1</i>) | 189 |
| Figure 4.8: Total ankle moment, orthotic moment, and anatomical moment in sagittal plane (A) and frontal plane (B) for case study 1 (<i>SP1</i>) derived from SG2 and SG4 data outputs, respectively. | 192 |
| Figure 4.9: Sagittal kinematic graphs for case study 2 (<i>SP2</i>)..... | 198 |
| Figure 4.10: Sagittal kinetic graphs and the vertical GRF graph for case study 2 (<i>SP2</i>) | 199 |
| Figure 4.11: Quadriceps and hamstring EMG RMS amplitude and timing during walking on treadmill for case study 2 (<i>SP2</i>). | 200 |
| Figure 4.12: Total ankle moment, orthotic moment, and anatomical moment in sagittal plane (A) and frontal plane (B) for case study 2 (<i>SP2</i>) derived from SG2 and SG4 data outputs, respectively. | 203 |
| Figure 4.13: Sagittal kinematic graphs for case study 3 (<i>SP3</i>)..... | 209 |
| Figure 4.14: Sagittal kinetic graphs and the vertical GRF graph for case study 3 (<i>SP3</i>) | 210 |
| Figure 4.15: Quadriceps and hamstring EMG RMS amplitude and timing during walking on treadmill for case study 3 (<i>SP3</i>) | 211 |
| Figure 4.16: Total ankle moment, orthotic moment, and anatomical moment in sagittal plane (A) and frontal plane (B) for case study 3 (<i>SP3</i>) derived from SG2 and SG4 data outputs, respectively. | 214 |

| | |
|---------------------------------------------------------------------------------------------------------------------------------------------------------------------------------------------------------------------|-----|
| Figure 4.17: Sagittal kinematic graphs for case study 4 (<i>SP4</i>)..... | 220 |
| Figure 4.18: Sagittal kinetic graphs and the vertical GRF graph for case study 4 (<i>SP4</i>) | 221 |
| Figure 4.19: Quadriceps and hamstring EMG RMS amplitude and timing during walking on treadmill for case study 4 (<i>SP4</i>) | 222 |
| Figure 4.20: Total ankle moment, orthotic moment, and anatomical moment in sagittal plane (A) and frontal plane (B) for case study 4 (<i>SP4</i>) derived from SG2 and SG4 data outputs, respectively. | 225 |
| Figure 4.21: Sagittal kinematic graphs for case study 5 (<i>SP5</i>)..... | 231 |
| Figure 4.22: Sagittal kinetic graphs and the vertical GRF graph for case study 5 (<i>SP5</i>) | 232 |
| Figure 4.23: Quadriceps and hamstring EMG RMS amplitude and timing during walking on treadmill for case study 5 (<i>SP5</i>). | 233 |
| Figure 4.24: Total ankle moment, orthotic moment, and anatomical moment in sagittal plane (A) and frontal plane (B) for case study 5 (<i>SP5</i>) derived from SG2 and SG4 data outputs, respectively. | 236 |
| Figure 4.25: Sagittal kinematic graphs for case study 6 (<i>SP6</i>)..... | 240 |
| Figure 4.26: Sagittal kinetic graphs and the vertical GRF graph for case study 6 (<i>SP6</i>) | 241 |
| Figure 4.27: Quadriceps and hamstring EMG RMS amplitude and timing during walking on treadmill for case study 6 (<i>SP6</i>) | 242 |
| Figure 4.28: Total ankle moment, orthotic moment, and anatomical moment in sagittal plane (A) and frontal plane (B) for case study 6 (<i>SP6</i>) derived from SG2 and SG4 data outputs, respectively. | 245 |
| Chapter 5: Discussion | |
| Figure 5.1: The SVA values for stroke participants and the mean SVA value for control participants during mid stance. | 250 |
| Figure 5.2: Vastus lateralis and Vastus medialis muscles activation time duration for all participants..... | 265 |
| Figure 5.3: Rectus femoris muscle activation time duration for all participants..... | 268 |
| Figure 5.4: Biceps femoris and Semitendinosus muscles activation time duration for all participants..... | 270 |
| Chapter 7: Appendices | |
| Figure 7.1: Test sample dimensions | 305 |
| Figure 7.2: Two-element 90° degrees rosette SG used for strain measurement..... | 306 |
| Figure 7.3: Single SG used for strain measurement | 307 |
| Figure 7.4: Strain-gauged samples with the two two-element 90° degrees rosette SGs | 309 |

| | |
|------------------------------------------------------------------------------------------------------------------------------------------------------------------------------------------------------|-----|
| Figure 7.5: The Instron tensile testing machine..... | 310 |
| Figure 7.6: The tensile test protocol applied to strain-gauged samples with an Instron tensile testing machine..... | 311 |
| Figure 7.7: Stress-strain graph of selected strain-gauged samples with full Wheatstone bridge..... | 314 |
| Figure 7.8: Strain against time measured by the extensometer and full Wheatstone bridge SGs (two two-element SGs) during 100 cycles..... | 315 |
| Figure 7.9: Strain against time measured by the extensometer and quarter Wheatstone bridge SG (single SG) during 100 cycles..... | 316 |
| Figure 7.10: The first 10 cycles of strain against time measured by the extensometer, quarter Wheatstone bridge SG (strain-gauged sample 5) and full Wheatstone bridge..... | 318 |
| Figure 7.11: The first 10 cycles of strain against time measured by the extensometer, quarter Wheatstone bridge SG (strain-gauged sample 6) and full Wheatstone bridge (strain-gauged sample 3)..... | 319 |
| Figure 7.12: The SVAs mean of the non-orthotic side for control participants while walking on treadmill..... | 327 |
| Figure 7.13: Sagittal ankle motion of non-orthotic side for control participants..... | 328 |
| Figure 7.14: Sagittal knee motion of non-orthotic side for control participants..... | 328 |
| Figure 7.15: Sagittal hip motion of non-orthotic side for control participants..... | 329 |
| Figure 7.16: Sagittal ankle moment of non-orthotic side for control participants..... | 329 |
| Figure 7.17: Sagittal knee moment of non-orthotic side for control participants..... | 330 |
| Figure 7.18: Sagittal hip moment for control participants..... | 330 |
| Figure 7.19: Vertical GRF for control participants..... | 331 |
| Figure 7.20: Stance and swing as a percentage of %100 gait cycle for the affected and unaffected sides..... | 332 |
| Figure 7.21: The SVA of the unaffected side for stroke participants..... | 334 |
| Figure 7.22: Sagittal knee motion of the unaffected side for stroke participants..... | 336 |
| Figure 7.23: Sagittal hip motion of the unaffected side for stroke participants..... | 338 |
| Figure 7.24: Sagittal ankle motion of the unaffected side for stroke participants..... | 340 |
| Figure 7.25: Sagittal knee moment for stroke participants..... | 342 |
| Figure 7.26: Sagittal hip moment for stroke participants..... | 344 |
| Figure 7.27: Sagittal ankle moment for stroke participants..... | 346 |
| Figure 7.28: Vertical GRF for stroke participants..... | 348 |
| Figure 7.29: Vastus lateralis muscle peaks and their time of occurrence for all participants. The VL peaks for each participant..... | 349 |
| Figure 7.30: Vastus medialis muscle peaks and their time of occurrence for all participants..... | 349 |

| | |
|-------------------------------------------------------------------------------------------------------------------------------------|-----|
| Figure 7.31: Rectus femoris muscle peaks and their time of occurrence for all participants. | 350 |
| Figure 7.32: Biceps femoris muscle peaks and their time of occurrence for all participants. | 350 |
| Figure 7.33: Semitendinosus muscle peaks and their time of occurrence for all participants..... | 351 |
| Figure 7.34: The relationship between the total ankle moment and the ankle angle for control participants. | 352 |
| Figure 7.35: The relationship between the total ankle moment and the ankle angle for SP1 , SP2 , and SP3 | 354 |
| Figure 7.36: The relationship between the total ankle moment and the ankle angle for SP4 , SP5 , and SP6 | 355 |

List of Tables

Chapter 2: Background and Literature review

| | |
|--------------------------------------------------------------------------------------------------------------------------------------------------------------------------|----|
| Table 2.1: The Modified Ashworth Scale (MAS) | 28 |
| Table 2.2: Summary of some research studies that investigated the effects of AFOs on gait parameters of stroke patients. | 61 |
| Table 2.3: Summary of research studies that investigated the effects of rigid AFOs on temporal-spatial, kinematics, kinetics, and EMG parameters of stroke patients..... | 89 |

Chapter 3: Methods

| | |
|---------------------------------------------------------------------------------------------------------|-----|
| Table 3.1: Delsys EMG sensor placement location over tested muscles according to SENIAM guidelines..... | 135 |
| Table 3.2: Manual muscle test for quadriceps and hamstring muscles | 140 |
| Table 3.3: The model segments and their anatomical reference frames definitions..... | 154 |

Chapter 4: Case studies: Results and Discussion

| | |
|-----------------------------------------------------------------------------------------------------------------------------|-----|
| Table 4.1: Temporal-spatial, kinematic and kinetic data for control participant..... | 179 |
| Table 4.2: Quadriceps and hamstring EMG RMS amplitude for control participant... | 180 |
| Table 4.3: The anatomical and the orthotic ankle moment for control participant derived from SG2 and SG4 data outputs | 180 |
| Table 4.4: Temporal-spatial, kinematic and kinetic data for <i>SP1</i> | 190 |
| Table 4.5: Quadriceps and hamstring EMG RMS amplitude for <i>SP1</i> | 191 |
| Table 4.6: The anatomical and the orthotic ankle moment for <i>SP1</i> derived from SG2 and SG4 data outputs..... | 191 |
| Table 4.7: Temporal-spatial, kinematic and kinetic data for <i>SP2</i> | 201 |
| Table 4.8: Quadriceps and hamstring EMG RMS amplitude for <i>cSP2</i> | 202 |
| Table 4.9: The anatomical and the orthotic ankle moment for <i>SP2</i> derived from SG2 and SG4 data outputs..... | 202 |
| Table 4.10: Temporal-spatial, kinematic and kinetic data for <i>SP3</i> | 212 |
| Table 4.11: Quadriceps and hamstring EMG RMS amplitude for <i>SP3</i> | 213 |
| Table 4.12: The anatomical and the orthotic ankle moment for <i>SP3</i> derived from SG2 and SG4 data outputs..... | 213 |
| Table 4.13: Temporal-spatial, kinematic and kinetic data for <i>SP4</i> | 223 |
| Table 4.14: Quadriceps and hamstring EMG RMS amplitude for <i>SP4</i> | 224 |
| Table 4.15: The anatomical and the orthotic ankle moment for <i>SP4</i> derived from SG2 and SG4 data outputs..... | 224 |
| Table 4.16: Temporal-spatial, kinematic and kinetic data for <i>SP5</i> | 234 |

| | |
|---------------------------------------------------------------------------------------------------------------------|-----|
| Table 4.17: Quadriceps and hamstring EMG RMS amplitude for <i>SP5</i> | 235 |
| Table 4.18: The anatomical and the orthotic ankle moment for <i>SP5</i> derived from SG2 and SG4 data outputs | 235 |
| Table 4.19: Temporal-spatial, kinematic and kinetic data for <i>SP6</i> | 243 |
| Table 4.20: Quadriceps and hamstring EMG RMS amplitude for <i>SP6</i> | 244 |
| Table 4.21: The anatomical and the orthotic ankle moment for <i>SP6</i> derived from SG2 and SG4 data outputs | 244 |

Chapter 7: Appendices

| | |
|-------------------------------------------------------------------------------------------------------------------------------------------------------|-----|
| Table 7.1: Young’s Modulus mean (100 cycles)..... | 313 |
| Table 7.2: Means percentage of difference between strain gauges and extensometer values of strain for the 100 cycles..... | 317 |
| Table 7.3: The SVA values in mid stance of the non-orthotic side and unaffected side for control and stroke participants, respectively..... | 333 |
| Table 7.4: Sagittal knee angle of the non-orthotic side and unaffected side for control and stroke participants, respectively..... | 335 |
| Table 7.5: Hip extension and flexion angle peaks of the non-orthotic side and unaffected side for control and stroke participants, respectively. | 337 |
| Table 7.6: Sagittal ankle motion peaks of the non-orthotic side and unaffected side for control and stroke participants, respectively..... | 339 |
| Table 7.7: Sagittal knee moment of the non-orthotic side and unaffected side for control and stroke participants, respectively. | 341 |
| Table 7.8: Sagittal hip moment of the non-orthotic side and unaffected side for control and stroke participants, respectively..... | 343 |
| Table 7.9: Sagittal ankle moment of the non-orthotic side and unaffected side for control and stroke participants, respectively..... | 345 |
| Table 7.10: Vertical GRF of the non-orthotic side and unaffected side for control and stroke participants, respectively..... | 347 |

Chapter 1: Introduction

Stroke is among the common disorders and affects more than 100,000 people in the UK each year (Bray et al., 2017). Stroke is the fourth leading cause of death in the UK and the third cause of death in Scotland (NHS Scotland, 2019). Stroke causes a disturbance in brain functions as the blood supply to a part of the brain is interrupted due to either blockage caused by a clot in a blood vessel in the brain (Ischemic stroke) or a bleeding in the brain (Haemorrhagic stroke), resulting in damage or death to the brain tissue that depends on that blood supply (Hans, 2011). The severity and clinical features of the stroke are determined by the site affected within the brain and how quickly treatment was given after onset (Belagaje and Kissela, 2010, Harvey et al., 2008). Stroke can disrupt a wide range of neural processes and can cause a range of possible impairments such as; difficulties in generation or control of muscle activity (motor impairments), problems with balance and coordination, sensory disturbances, and cognitive problems (Emos and Agarwal, 2018, Rathore et al., 2002). Motor impairment is expected to be a main clinical feature of stroke indicating problems with movement, coordination, and balance. Symptoms such as muscle spasticity and weakness or paralysis are very common among stroke patients (Evers et al., 2004). Improper dorsiflexion/plantarflexion strength ratio due to spasticity in the plantarflexor muscles and/or weakness in the dorsiflexor muscles generate a plantarflexion deformity which is characterised by ankle resting in a plantarflexed position (Barrett and Taylor, 2010, Stewart, 2008). Frequently, the plantarflexed position of the ankle (equinus) in stroke patients is accompanied with a supination foot deformity (inversion at the subtalar joint and forefoot adduction at the midtarsal joints), which is termed as equinovarus deformity (Condie and Bowers, 2008, Kinsella and Moran, 2008, Reynard et al., 2009).

Improving walking in patients with plantarflexion deformity is a priority in stroke rehabilitation, and is generally attempted through physiotherapy (Begg et al., 2019, Lindquist et al., 2007, Teasell et al., 2003). However, the International Society of Prosthetics and Orthotics (ISPO) and the NHS Quality Improvement Scotland have recommended prescribing Ankle-foot orthosis (AFOs) as an adjunct to physiotherapy in stroke management (Condie et al., 2004, NHS Quality Improvement Scotland, 2009). Rigid AFO is commonly prescribed for stroke patients to promote initial contact with the

heel strike (by controlling excessive plantarflexion position of the ankle), to facilitate foot ground clearance in swing phase, to support and improve the alignment of the foot (control the equinovarus deformity), and to reduce knee extension and promote hip extension during stance (Condie et al., 2004, Lehmann, 1986, NHS Quality Improvement Scotland, 2009). A rigid AFO is designed to restrict/prevent the motion of the shank relative to the foot and vice versa. Lack of the required forward inclination of the rigid AFO will lead to a lack of the required forward inclination of the tibia during mid stance, which in turn can badly affect the stance stability. Both alignment and the mechanical characteristics of AFO are important factors to achieve the optimal functional performance of the AFO (Bowker et al., 1993, NHS Quality Improvement Scotland, 2009, Totah et al., 2019, Tyson et al., 2013).

Healthcare Improvement Scotland has recommended “tuning” rigid AFOs in order to achieve optimal effects (NHS Quality Improvement Scotland, 2009). Tuning a rigid AFO involves adjusting the alignment of the AFO in relation to the shoes by modifying the height, type, or/and design of the heel, or/and the rocker type (Meadows et al., 2008, Meadows, 1984, Owen, 2004b). However, only few published studies have attempted to examine the impact of tuning AFOs on gait parameters among stroke patients (Carse et al., 2015, Choi et al., 2016, Cruz and Dhaher, 2009, Gatti et al., 2012, Jagadamma et al., 2010). Most of the published studies focus on the impact of AFOs on temporal-spatial and knee joint kinematics and kinetics. Only a limited number of studies investigated hip joint kinematics and kinetics. Additionally, none of the studies has focused on comparing the effects of tuning on knee muscle activation patterns during walking.

In order to achieve the optimal effects of the AFO, the stiffness of the AFO should also be considered (NHS Quality Improvement Scotland, 2009, Totah et al., 2019). AFOs should be sufficiently stiff in order to provide adequate structural support. However, they should not be too stiff, as this would unnecessarily limit existing functional motion which may lead to an inability to adapt to disruptions in balance. Providing excessively stiff AFO might put added stress on the extensor muscles of the knee joint, potentially creating fatigue and future pathologies (Allen et al., 2008, Halim et al., 2012, Singer et al., 2014). The AFO stiffness is usually measured via determining the AFO resistance to sagittal plane rotation, demonstrated by moment -ankle angle or moment -deflection relationships (Kobayashi et al., 2011, Totah et al., 2019). Most of the published studies put an

inaccurate assumption that external forces and ankle joint moment are resisted solely by the orthosis. This is not true as soft tissues of the ankle, and the activity and/or the stiffness of the calf muscles may contribute in assisting/resisting these external forces and moments actively or passively (Miyazaki et al., 1993). Measuring the orthotic moments during walking is considered as a key criterion for the current study. The orthotic moment has an important role in assisting post stroke gait (Kobayashi et al., 2019, Kobayashi et al., 2016, Yamamoto et al., 1993b). In a rigid AFO, the orthotic moment can be in the form of plantarflexion resistive moment (which resists movement of the ankle in a plantarflexion direction) and dorsiflexion resistive moment (which resists movement of the ankle in a dorsiflexion direction) (Kobayashi et al., 2015). Thus, the magnitude of the orthotic moment may have a significant effect on ankle motion, and therefore potentially knee and hip motion, in stroke patients. Measuring the orthotic moment would also reflect the individual differences in the influence of anatomical structures, such as muscle spasticity/weakness/contracture at the ankle joint during walking. Few studies have investigated the orthotic moment during walking (Bregman et al., 2010, Kobayashi et al., 2017, Papi et al., 2015). However, the contribution of a rigid AFO in improving gait parameters in stroke patients is still not clear. A study by Papi et al. (2015) successfully measured the orthotic moment exerted by a rigid AFO around the ankle joint in a healthy participant using strain gauges data combined with gait analysis. This method was considered a reliable method to directly measure the orthotic moment during walking without the need for destroying the AFO or changing the mechanical properties of the AFO by inserting metal bars on which the strain gauges would be attached. Furthermore, measuring the orthotic moment using an experimental AFO would provide more precise results than using indirect methods which are totally based on the stiffness values determined during bench testing. The aim of the Papi et al. (2015) study was to introduce a new method for measuring the orthotic moment rather than studying the orthotic moment itself, and thus further research regarding orthotic moment is recommended.

In summary, there are still many challenges and questions that need to be addressed to improve the design of AFOs, as there is a large variation of AFOs used in clinical practice. These AFOs are characterized by their designs, materials, trim lines, and AFO footwear combinations. These variables should be considered in clinical decision making to achieve the optimal therapeutic benefits of the AFOs. There is limited information in the

literature regarding the most appropriate and effective orthosis that best fits the functional needs of the patients. Understanding the mechanical and biomechanical properties of AFOs has a great value in improving AFO function and in accomplishing a successful treatment (Bowker et al., 1993).

The first aim of the current study was to gain a more thorough understanding of the biomechanical effectiveness of using rigid AFO (before and after tuning) during walking in stroke patients. A better understanding of how AFOs alter the gait performance of individuals with stroke will improve the prescription procedure so that it is based on biomechanical principles rather than reliant on subjective judgements and orthotist experience.

The second aim of the current study was to quantify the magnitude of moment generated from the rigid AFO (before and after tuning) to control the ankle joint motion. As mentioned earlier, stroke patients usually show equinovarus deformity which is considered as a multiplanar deformity (Kinsella and Moran, 2008, Reynard et al., 2009). The rigid AFO is prescribed to control equinovarus deformity. This highlights the importance of evaluating the AFO contribution in planes other than the sagittal plane (dorsi/plantarflexion) in order to demonstrate how effectively the rigid AFO can control inversion/eversion and supination/pronation along with evaluating the plantarflexion/dorsiflexion.

The outline of the conducted work in this study is as follows: **Chapter2** follows this introduction chapter, introducing the essential background to the study and discusses the limited available literature; **Chapter3** describes the methods and materials used in this study; **Chapter 4** presents the experimental results obtained by the methods outlined in Chapter 3; **Chapter 5** critically discusses the obtained results and highlights the study limitations; **Chapter 6** concludes the findings of the thesis and suggests future work; and **Chapter 7** includes the appendices containing additional information/evidence and supplementary results. The study **References** were then provided.

Chapter 2 Background and Literature review

2.1 Chapter overview

In this chapter, stroke definition and its most common effects on human body are briefly described. A more detailed description of the effects on motor functions is also included. In order to understand the functional consequences of abnormal foot and ankle motion, resulting from stroke, it is necessary to understand normal biomechanics of gait. Therefore, normal gait biomechanics is reviewed, outlining the gait cycle, the main events of the gait cycle, the spatial and temporal parameters, ground reaction force, and the kinematic and the kinetic parameters. Additionally, the main actions of muscles and joints are described. The effects of stroke on gait are then covered, describing the typical deviations from normal gait and, in particular, highlighting plantarflexion deformity on stroke patients. Ankle-foot orthosis (AFOs) are then introduced as a method to assist in limiting the impacts of post stroke gait. Different designs of AFOs and their biomechanical effects, concentrating on rigid AFO, will then be discussed. Additionally, the importance of clinical assessment and several elements of prescription criteria will be reviewed. Afterwards, AFOs tuning and describing the tuning process and its effects on the AFOs biomechanics are introduced. This is followed by a review of the effects of tuned AFO on several outcomes of gait including speed, energy cost and balance, followed by the effects of the AFOs on the kinematics and kinetics of gait and lower limb muscle activities. The AFO stiffness is then introduced followed by a description of the impact of AFOs stiffness on post stroke gait parameters, with a detailed focus on the orthotic moment measurement techniques. A summary of the literature is then provided. The chapter concludes with a discussion of the study aims and objectives.

2.2 Stroke

2.2.1 “Stroke” an overview

Stroke, also known as cerebrovascular accident (CVA), is defined by the World Health Organization (WHO) as “a focal or global neurological impairment of sudden onset of cerebral function, lasting more than 24 hours or leading to death, with no apparent cause other than of vascular origin.” (World Health Organisation, 2002). When the disturbance

of cerebral functions is lasting less than 24 hours, from minutes to hours, it is termed as “mini-stroke” or Transient Ischemic Attack (TIA) (Swaffield, 1996).

Like all organs in the human body, the brain needs oxygen and nutrients to function properly. These life-sustaining products are delivered to the brain via blood that travels through the circulatory system. Blood reaches the brain through two main arterial systems: internal carotid arteries and vertebral arteries (Hans, 2011) (Figure 2.1). After passing through the base of the skull, the right and left vertebral arteries fuse together to form the basilar artery. The internal carotid arteries and the basilar artery merge with each other in a ring shaped arterial network at the base of the brain called the arterial cerebral circle, or the circle of Willis (Hans, 2011, Heimer, 2012). The Circle of Willis distributes blood throughout the brain and provides interconnections between the arteries. Thus, in case one of the supplying arteries is occluded or narrowed, the circle of Willis provides a constant cerebral perfusion to the brain tissues (Hans, 2011). However, interruption of a vessel beyond the circle can result in serious damage (Heimer, 2012, Parmar, 2019). Stroke occurs when there is a reduction or disruption of cerebral blood circulation, resulting in tissue death and loss of brain functions (Hans, 2011, Parmar, 2019).

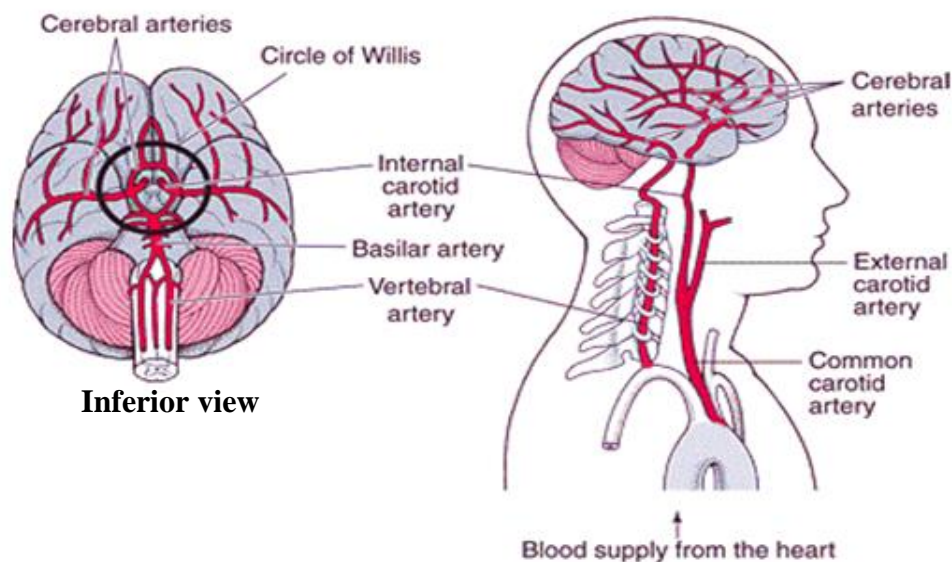


Figure 2.1: Blood supply to the brain. The figure shows the main arteries of the brain and the inferior view shows the circle of Willis. Adapted from (Giraldo, 2018).

Stroke can be typically classified into two main types: ischaemic (blockage caused by a clot in a blood vessel in the brain), or haemorrhagic (i.e. caused by a bleeding in the brain) (Hans, 2011) (Figure 2.2). The majority of strokes are reported to be ischaemic, with this type accounting for approximately 85% of all cases (Adeoye and Broderick, 2010), and is caused by a blood clot forming in the main artery or one or more of the small vessels of the brain, or a blockage transported from another blood vessel in the body by the blood stream to the brain (embolus) (Hans, 2011, Parmar, 2019). The haemorrhagic stroke, affecting about 15% of cases, occurs when a blood vessel either within or on the surface of the brain bursts (Adeoye and Broderick, 2010). The expanding blood leakage causes cerebral tissue injuries near the site of the bleeding (Hans, 2011). This type of stroke tends to be more severe and is associated with higher early mortality (Adeoye and Broderick, 2010). The most common symptoms of stroke are sudden weakness or numbness of the face, arm or leg, especially on one side of the body, loss of walking function, difficulty in speaking and understanding, loss of vision, and poor balance and coordination. The more typical symptoms of haemorrhagic strokes are sudden headache, loss of consciousness, and high blood pressure (World Health Organisation, 2002).

The severity and clinical features of stroke are determined by the site affected within the brain and how quickly treatment was given after onset (Belagaje and Kissela, 2010, Harvey et al., 2008). Stroke can disrupt a wide range of neural processes and can cause a range of possible impairments. These including difficulties in generation or control of muscle activity (motor impairments) (Rathore et al., 2002), problems with balance and coordination (ataxia) (Bonni et al., 2014), sensory disturbances (altered ability to feel touch, pain, proprioception, and temperature) (Cahill et al., 2018), dysphagia (problem with swallowing) (Helldén et al., 2018), continence problems (poor bowel and bladder control) (Getliffe and Thomas, 2019), vision disturbance (Banerjee et al., 2018), emotional disturbance, depression, fear, loss of motivation, and sleep disturbance (Lennon and Bassile, 2018). Additionally, stroke can cause cognitive problems (loss of memory, poor concentration) (Loetscher et al., 2019), and communication problems (either misunderstanding and misinterpretation abilities such as aphasia (an impairment of the ability to form and understand words) and dysarthria (characterised by slow, weak, imprecise and/or uncoordinated movements of the speech musculature)) (Ali et al., 2015).

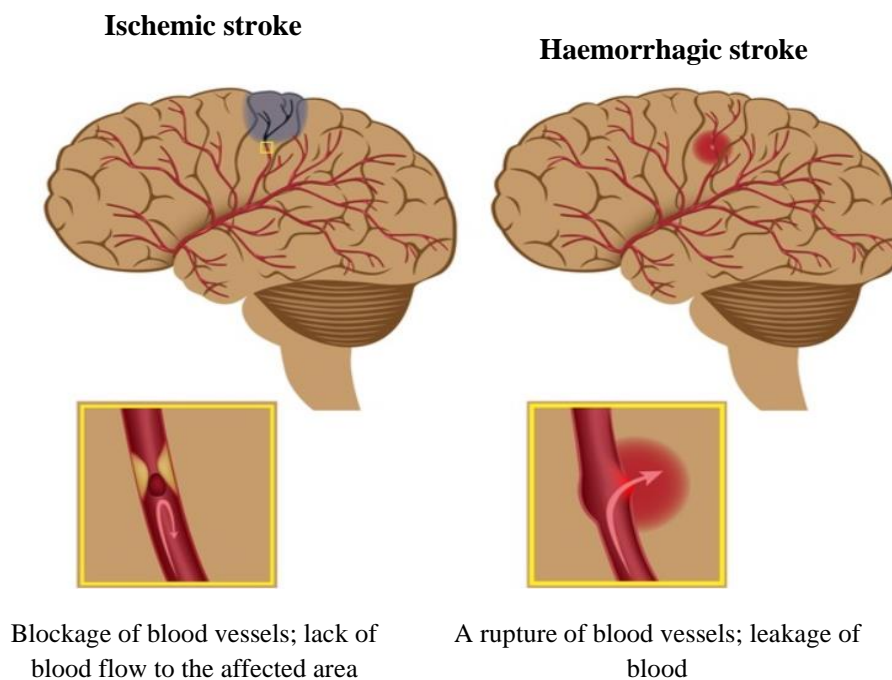


Figure 2.2: Stroke types; ischaemic and haemorrhagic stroke. Adapted from (Mueller, 2014).

2.2.2 Impact of stroke on key motor functions

Motor impairment is expected to be a main clinical feature of stroke. It may be the most frequently diagnosed neurologic problem after stroke (Emos and Agarwal, 2018, Rathore et al., 2002). The motor areas of the cerebral cortex can be damaged if the stroke occurs in the middle cerebral artery or anterior cerebral artery (Lee et al., 2017). A stroke that targets the internal capsule, vertebral artery branches, or basilar artery can also lead to motor impairment (Lee et al., 2017). The Upper Motor Neuron (UMN) syndrome (discussed shortly), also known as pyramidal insufficiency, is common after stroke and occurs due to any damage of the UMN pathways (Emos and Agarwal, 2018, Rathore et al., 2002).

As stroke occurs on the brain, before the pyramidal decussation, this will result in symptoms contralateral to the site of the lesion, that is, on the other side of the body. For Instance, a unilateral lesion on the right corticospinal tract would cause motor impairment on the left side of the body, and vice versa. The severity can range from slight

coordination problems to complete paralysis of the face, upper, and lower limbs on one side of the body (i.e. hemiplegia or hemiparesis). The initial effects of impaired innervation to the muscles include muscle weakness, lack of fine motor control, poor control of muscle activity, and poor timing of forces leading to slow movements (Carr, 2011, Emos and Agarwal, 2018). Spasticity is one of the common complications following stroke. It is widely defined as “a motor disorder characterised by velocity dependent hyperexcitability of muscles to stretch, characterized by exaggerated tendon reflexes, increased resistance to passive movement, and hypertonia resulting from loss of upper motor neuron inhibitory control” (Lance, 1980). The Modified Ashworth scale (MAS) is one of the common scales that are used to measure the severity of the muscle spasticity (Bohannon et al., 1987, Charalambous, 2014, Gregson et al., 1999). The MAS contains a 6-point scale with a grade score of 0, 1, 1+, 2, 3, or 4; as illustrated in Table 2.1. Furthermore, secondary complications such as joint stiffness and muscle contracture may occur due to disuse, limitation of functional activity, and the weakness of certain muscle groups (Carr, 2011).

Table 2.1: The Modified Ashworth Scale (MAS). Adapted from (Bohannon and Smith, 1987).

| <u>Grade</u> | <u>Description</u> |
|--------------|--------------------------------------------------------------------------------------------------------------------------------------------------------------------------------------------|
| 0 | Normal muscle tone |
| 1 | Slight increase in muscle tone, manifested by a catch and release or by minimal resistance at the end of the range of motion (ROM) when the affected part is moved in flexion or extension |
| 1+ | Slight increase in muscle tone, manifested by a catch, followed by minimal resistance throughout the remainder (less than half) of the ROM |
| 2 | More marked increase in muscle tone through most of the ROM, but affected parts easily moved |
| 3 | Considerable increase in muscle tone, passive movement difficult |
| 4 | Affected part rigid in flexion or extension |

2.2.3 Stroke incidence and recovery

Stroke affects more than 100,000 people in the UK each year (Bray et al., 2017). Stroke is the fourth leading cause of death in the UK and the third cause of death in Scotland (NHS Scotland, 2019). Incidences of stroke-related deaths and disability are expected to rise even higher as the population ages (Bray et al., 2017, Wang et al., 2013). Stroke causes a greater disability impact than any other condition (Bray et al., 2017, Wang et al., 2013). Up to a third of stroke patients show a natural ability of motor recovery (Kwakkel et al., 2002). The main pattern of recovery after stroke is determined by certain unknown biological processes, often prescribed as Spontaneous Neurological Recovery (SBR) that follows a proportional recovery rule (Prabhakaran et al., 2008). The proportional recovery rule states that, within three months, patients should get approximately 70% of their maximum potential recovery back (Winters et al., 2015, Zarahn et al., 2011). However, some patients with severe hemiparesis show no recovery within three months of onset (Krakauer and Marshall, 2015). There is no absolute end to recovery after stroke, however, most improvement in function occurs within three to six months of onset (Bray et al., 2017, NHS Scotland, 2019). More complex aspects of physical recovery, such as speech, may continue to improve over years (Stevens et al., 2018).

Recovery in function following stroke is believed to be due to neuroplasticity of the brain. Neuroplasticity is defined as “the ability of the nervous system to respond to intrinsic or extrinsic stimuli by reorganising its structure, function and connections” (Cramer et al., 2011). The ability of the brain to reorganise (or to change) the anatomical and functional mechanisms of the central nervous system (brain and spinal cord) may occur on both micro and macro scale connectivity levels, such as changes in neural pathways and synapses (Cramer and Riley, 2008, Dimyan and Cohen, 2011). The process of recovery is undoubtedly complex, occurring through a combination of spontaneous and learning-dependent processes (Sathian et al., 2011). The functional recovery theories after stroke involve both restitution and/or substitution of function (Hyllin et al., 2017, Kwakkel et al., 2004, Rothi and Horner, 1983). The restitution model suggests that the lesioned area recovers as a result of tissue repair, while its function is assumed by other cortical and subcortical structures, either adjacent to or remote from the damaged area (Finger et al., 2004, Nudo et al., 2001). Functional recovery is largely due to a reactivation of functionally suppressed areas remote from, but connected to, the area of primary injury.

This process is known as resolution of diaschisis (Feeney and Baron, 1986, Finger et al., 2004, Nudo et al., 2001).

On the other hand, the substitution model suggests that functional recovery after stroke occurs largely by behavioural compensation, in which patients learn to compensate for their acquired deficits (Nudo et al., 2001, Rothi and Horner, 1983). Learning and new experiences enhance the lifelong ability of the brain for neural plastic change (Bruehl-Jungerman et al., 2007, Kolb et al., 2010). The maintenance of the ability of learning and re-learning skills is considered as a motivating force for recovery in stroke patients (Kolb et al., 2010). There are two types of behavioural model that can stimulate the neuroplasticity of the brain; first is 'use/experience-dependent' plasticity, which indicates that repetitive training of a simple motor task can produce changes of motor cortex area (Classen et al., 1998, Nudo et al., 1996), and second is 'learning-dependent' plasticity, which involves practice, but with the addition of monitored improvements in a certain skill, requiring complex task-specific training (Plautz et al., 2000). There is a strong evidence from animal (Nudo, 2007, Nudo, 2011, Plautz et al., 2000) and human (Dayan and Cohen, 2011, Dimyan and Cohen, 2011, Hallett, 2001) studies that performing difficult skill task was associated with more functional improvement, showed further growth, and stimulated more changes in motor cortex area than performing basic repetition movement task. Furthermore, the motor cortex area that represents the hand function has diminished in monkeys' brains who did not receive any hand rehabilitation training at all, suggesting a complete lack of activity may result in a further deterioration of function (Nudo et al., 1996). Thus, this relationship between learning-dependent model and functional recovery forms the basis for the rehabilitation gait-training programme after stroke (Hodics et al., 2006, Richards et al., 2008), this will be discussed further in section 2.4 under the heading 'Post stroke gait rehabilitation'.

There are currently more than 124,000 people who have survived a stroke living in Scotland, with approximately half of them dependent on others for everyday activities, following a period of recovery (NHS Scotland, 2019). Thus, the main burden of stroke is the number of survivors left with some degree of functional impairment or disability and their effects on economy. These impairments have an important impact on a patient's life and considerable costs for health and social services (Evers et al., 2004). Although the majority of stroke patients will be able to walk independently, approximately 70% will

have a reduction in walking performance during their daily activities (Belda-Lois et al., 2011, Emos and Agarwal, 2018). Walking is a fundamental human activity. The loss of the ability to walk can sufficiently influence an individual's capacity to participate in a broad range of activities (Paul et al., 2005).

2.3 Normal and post stroke gait

2.3.1 Introduction

Bipedal ambulation, or gait, is a method of locomotion involving the use of two lower limbs in an alternating pattern, to provide both support and progression. This apparently simple task is achieved through a very complicated combination of neuro-musculo-skeletal system activity in order to move the lower limbs and Head, Arms and Trunk (HAT) safely (Perry and Burnfield, 2010, Richards, 2018, Shumway-Cook and Woollacott, 2007).

Gait impairments following stroke can vary due to the size and site affected within the brain (Emos and Agarwal, 2018, Handelzalts et al., 2019). Consequently, the gait impairments depends on the level of muscle weakness, severity of spasticity, compensatory mechanisms, and their interactions (Bohannon, 1987, Handelzalts et al., 2019). Before examining the gait impairments following stroke, it is necessary to review normal (able-bodied) gait. Being able to understand normal gait could significantly enhance the quality of life of a person with physical impairments through improving rehabilitation and treatment planning, as well as improving the design of public environments (Zukowski et al., 2019). For this reason, normal and stroke gait will be described in the following sections to give the reader a brief overview.

Gait analysis involves a variety of quantitative methods that have been used to examine normal and abnormal gait including; temporal-spatial parameters (timing and distance of movement), kinematic parameters (joint and segment positions and arc of motions), kinetic parameters (forces and moments) and dynamic electromyography (EMG) recording (Perry and Burnfield, 2010, Richards, 2018). These methods will be discussed further in section 3.3 and section 3.4. In general, the kinematic and kinetic parameters have usually been examined in terms of peak values, values at key points, or the total excursion during the gait cycle. The following section will focus only on the contribution

of the lower limbs to achieve this motion as the HAT unit, also known as the passenger unit, acts mainly to preserve the body stability by maintaining a neutral alignment (Perry and Burnfield, 2010, Richards, 2018). In addition, as the contribution of lower limb kinematics, kinetics, and muscles are complex, this section will focus only on those parameters that are considered to be most relevant to the topic of this thesis. Key parameters for the current study are considered to be the kinematics and kinetics of the lower limbs in the sagittal plane. This is in part because sagittal plane motions are larger in magnitude than motions in other planes and thus, they are the main contributors to body progression from one point to another. Also, this section will highlight the importance of the knee muscles on controlling the knee joint during walking and how they may cause a change in the gait pattern by interfering with the movement of the joint.

2.3.2 Normal gait

Human walking or gait is characterised by smooth and efficient progression of the body's centre of mass. It is also characterised by its repetitive sequence of limb motion (Perry and Burnfield, 2010, Whittle, 2014). The gait cycle (GC) represents the period of time between two identical events which recur on the same lower limb; typically initial contact (the moment when the foot contacts the ground) of one foot is chosen as the defining event (Perry and Burnfield, 2010, Richards, 2018). In studies of human locomotion, the GC is typically divided into two main phases; stance phase and swing phase (Perry and Burnfield, 2010, Richards, 2018, Whittle, 2014). The stance (support) phase is the period where the lower limb is in contact with the ground, and it comprises about (60±4%) of the GC at normal walking speeds. The swing phase of the GC, where the lower limb is not in contact with the ground, occupies the remaining period (40±4%) (Perry and Burnfield, 2010, Richards, 2018, Whittle, 2014). There are periods of single support when the alternate leg is in swing phase, and double support when both limbs are in contact with the ground. Each double support phase lasts for approximately 10-12% of the gait cycle time, at the start/end of each stance phase. The speed of walking will affect these proportions; as speed increases, swing phase increases and stance and double support phases decrease (Whittle, 2014). In this section, all values reported are for normal adults at a self-selected comfortable walking speed which ranges between 1.2 (±0.2) and 1.4 (±0.2) m/s (Bohannon and Andrews, 2011, Perry and Burnfield, 2010, Riley et al., 2001).

❖ *GC phases*

As aforementioned, the normal walking GC is divided into stance and swing phases. These phases are both further divided into eight sub-phases which are expressed in terms of a percentage of the entire gait cycle (Figure 2.3), as below (Perry and Burnfield, 2010):

- 1) **Initial contact (0-2%)**: The moment at which the foot comes in contact with the ground. Also known as heel strike as usually it happens with the heel contact. Initial contact is usually considered the beginning of the GC.
- 2) **Loading response (2-12%)**: The first double limb support period when the body weight is transferred from one side to the other.
- 3) **Mid stance (12-31%)**: The first half of the single limb support period when the body progresses forward over the stationary foot on the ground. It begins when the contralateral foot leaves the ground and ends with heel rise.
- 4) **Terminal stance (31-50%)**: The second half of the single limb support period when the body continues to progress forward over the foot. It begins with heel rise and ends with contralateral foot initial contact.
- 5) **Pre swing (50-62%)**: The second double limb support period when the body weight transfers rapidly to the contralateral foot to start progressing forward during the swing period. It begins with the contralateral foot initial contact and ends with ipsilateral toe off, or when the foot completely leaves the ground. The term “**Push off**” is also frequently used to describe this phase (Richards, 2018, Whittle, 2014).
- 6) **Initial swing (62-75%)**: The first third of the swinging period when the limb is progressing forward. It begins with the toe off and ends when the swinging foot is opposite to the contralateral limb which is in stance phase.
- 7) **Mid swing (75-87%)**: The second third of the swinging period when the limb is further progressing forward. It ends when the swinging limb moves forward, and the tibia reaches a vertical position.
- 8) **Terminal swing (87-100%)**: The last third of the swinging period when the limb is still progressing forward until its advancement finishes in preparation for the

subsequent initial contact. It begins with the vertical tibia and ends with initial contact.

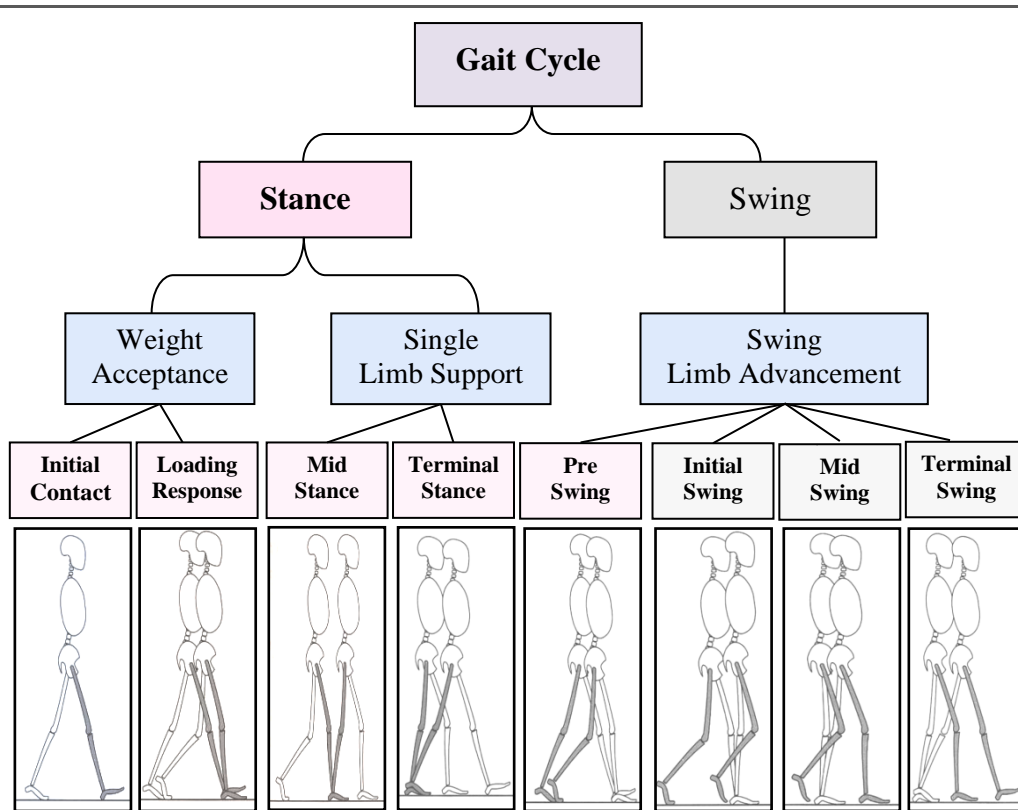


Figure 2.3: Gait cycle phases and sub-phases. Shaded limb side represents a complete GC that begins with initial contact and ends with terminal swing. Adapted from (Perry and Burnfield, 2010).

Three main basic tasks are accomplished through each GC; weight acceptance, single limb support, and swing limb advancement as shown in Figure 2.3 (Perry and Burnfield, 2010). Weight acceptance is the most demanding task in the GC, because the body is trying to accept the weight that is transferred from one limb to the other. It is also the same time for absorbing the shock and impact forces of the free-falling body. Additionally, initial stabilization of the stance limb and preservation of forward momentum occur at the same time (Perry and Burnfield, 2010, Richards, 2018). This task comprises the first two GC phases, namely; initial contact and loading response. Stance continues with single limb support, the second task, comprising mid stance and terminal stance phases. During this task, the stance limb has total responsibility for supporting body weight while the other limb is in swing (Perry and Burnfield, 2010). Swing limb

advancement begins in the final phase of stance, pre-swing, and continues through the three phases of swing: initial swing, mid swing and terminal swing (Perry and Burnfield, 2010). During swing, the limb must be shortened in vertical length in order to provide sufficient foot ground clearance (Marasović et al., 2009, Perry and Burnfield, 2010).

❖ *Temporal-spatial parameters*

The primary temporal parameters are cadence, stance and swing durations, as well as the duration of single limb and double limb support (Perry and Burnfield, 2010). Cadence is the number of steps taken per unit time (steps/minute). The most common temporal-spatial parameters examined during gait are step length, stride length, and walking speed (Richards, 2018). Step length refers to the distance between heel strike of one limb and heel strike of the contralateral limb, while stride length is the distance between subsequent heel strikes of the same limb (Richards, 2018) (Figure 2.4). Walking speed is defined as the distance travelled per period of time (meters/second) (Richards, 2018). In healthy adults, the normal walking speed is approximately 1.21–1.32 m/s (Bohannon and Andrews, 2011). Walking speed is an important parameter, and must be given great consideration when measuring other gait parameters that are correlated with the ground reaction force (Andriacchi et al., 1977). In comparison to normal speed, faster acceleration in the body's Centre of Mass (COM) will result in higher ground reaction force magnitude, and then the outcome will be higher moments acting on the lower limb joints (Richards, 2018).

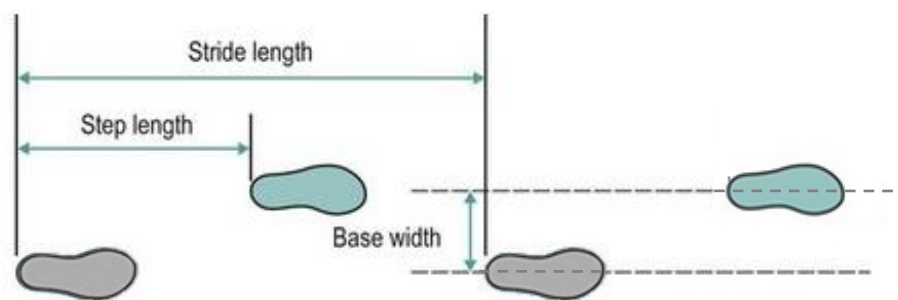


Figure 2.4: Spatial parameters of normal gait. Adapted from (Richards, 2018).

❖ *Vertical ground reaction force (GRFv)*

During gait, once the foot contacts the ground, forces are applied from the foot to the ground. Thus, based on Newton's third law, the ground applies the same magnitude of the force back to the body in the opposite, direction; this is called the Ground Reaction Force (GRF). The GRF is composed of three components: vertical, mediolateral, and anteroposterior. These forces are located at the centre of pressure (COP) which changes throughout stance (Figure 2.5). In this thesis, only the vertical GRF (GRFv) is investigated. The mediolateral and anteroposterior GRF are small compared to the GRFv and result from any non-vertical components of the GRF (Richards, 2018, Winter, 2009).

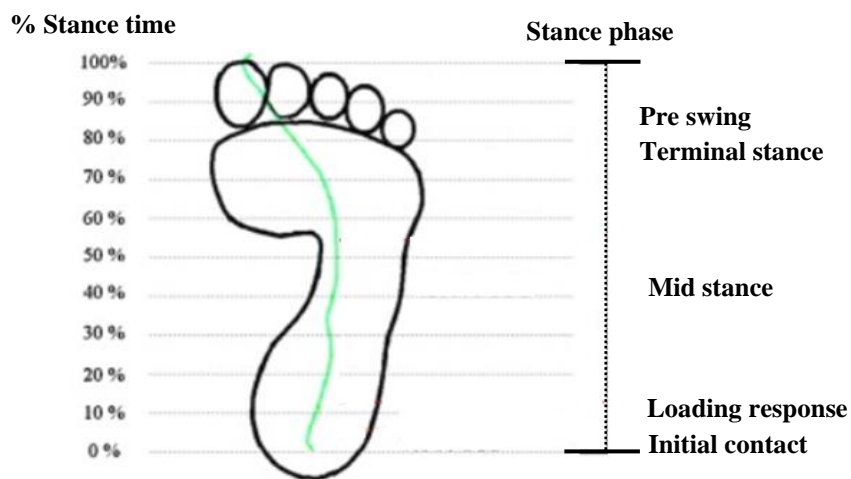


Figure 2.5: The stance time percentage of COP progression during 1.3 m/s walking speed projected onto the right foot from initial contact to toe off. The green line represents the path of COP that is formed by a series of COPs that start slightly laterally to the midline of the heel at initial contact, pass along the midline of the foot up to the metatarsal heads and then transfer medially between the first and second toe at toe off. Deviation in the normal COP can provide useful information in assessing or detecting gait pathologies. Adapted from (Chiu et al., 2013).

Inspecting the GRFv profile associated with each step provides essential information about the complete function of the lower limb and provides a means of identifying the timing of stance phase. The GRFv normally exhibits a bimodal M pattern; two peaks separated by a trough (or valley) as illustrated in Figure 2.6. The peaks of GRFv are greater than body weight and varies with gait velocity. The peaks are approximately 1.2

times body weight and the trough is about 0.7 times body weight (Richards, 2018, Winter, 2009). The GRFv increases above or decreases below the body weight in response to upward and downward movements of the Centre Of Mass (COM) (Marasović et al., 2009, Richards, 2018). The first peak occurs at the end of the loading response (Perry and Burnfield, 2010). During loading response, the COM is accelerating downwards in response to limb loading, in an attempt to decelerate the downward fall of the COM an upward force must be generated (including inertia) (Marasović et al., 2009, Richards, 2018). This upward force is added to the GRFv resulting in the first peak that is higher than body weight. The trough occurs during mid stance and as the body's COM is accelerated upward the body generates a counter acting force (including inertia) to decelerate the upward travel of COM (Perry and Burnfield, 2010). This results in a GRFv magnitude that is less than body weight (as GRFv is directed upward and the decelerating force is directed downwards) (Marasović et al., 2009, Richards, 2018). Towards the end of terminal stance, the second peak of the GRFv occurs (Perry and Burnfield, 2010). The second peak is the results of body's attempt to decelerate the downward fall of COM by an upward directed force (Marasović et al., 2009, Perry and Burnfield, 2010).

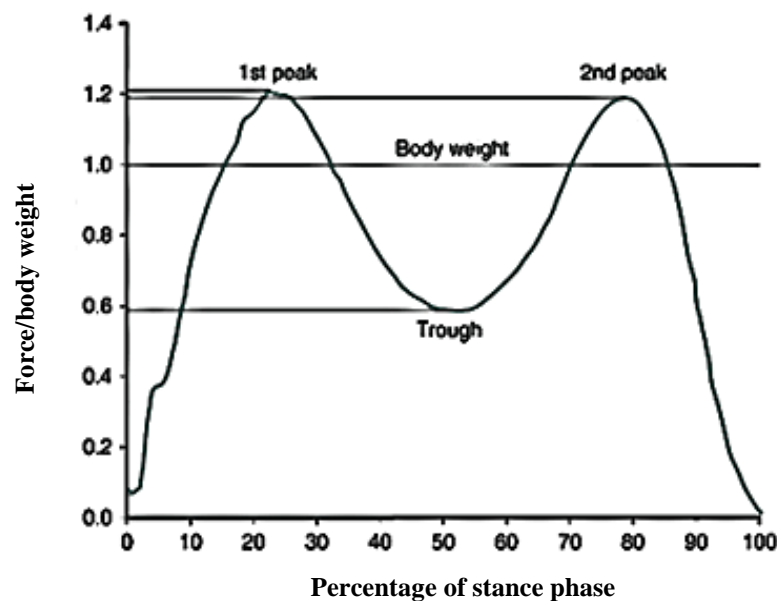


Figure 2.6: Vertical ground reaction force (GRFv) during stance phase. Adapted from (Richards, 2018).

The first peak of the GRFv is an indication of the magnitude of loading that the individual is putting on the foot commencing stance during initial double support time. Reduction in the magnitude of the first peak may be related to the presence of any discomfort, pain, poor functional movement of the lower limb joints, or slow walking speed. In orthotic/prosthetic users, it may also reflect the individual's confidence in the orthotic device or the prosthetic limb; as poor confidence to put/transfer load on the foot commencing stance may also reduce the first peak (Richards, 2018, Winter, 2009). The trough of the GRFv occurs as the body moves over the foot. Thus, the depth of the trough reflects the quality of forward body transition over the stance foot. A fast walking speed can produce a low trough value (Perry and Burnfield, 2010, Richards, 2018). While slow walking speed or poor movement of the lower body joints may produce a high trough value (Richards, 2018, Winter, 2009). The second peak of the GRFv occurs as the body falls forward over the forefoot (Perry and Burnfield, 2010). A low second peak may indicate a poor ability to accomplish toe off, whereas a high peak could relate to the person's acceleration (Richards, 2018).

❖ *Kinematics and kinetics of gait*

Kinematics observes and describes the spatial movement of the body, without considering the forces that cause the movement, including joint motion, displacement, velocity, and acceleration of body segments (Winter, 2009). Kinetics describes the factors causing the movements, specifically the forces which produce moments and powers (Kerr and Rowe, 2019, Winter, 2009). The following headings describe the kinematics and kinetics of GC for the ankle and the foot, knee, and hip joints. The segmental movement of the shank (the body segment located between knee and ankle joints) to vertical line is also described.

➤ **The ankle and the foot**

The arcs of motion of the ankle are not large, but they are critical for progression and shock absorption during stance. This is accomplished through four rockers in the heel, ankle, forefoot and toe that allow the body to advance forward while the foot remains stationary on the ground (Perry and Burnfield, 2010) (Figure 2.7).

Initial contact is the moment at which the foot comes in contact with the ground. Although this is a momentary posture, it is significant because of its influence on subsequent knee action. At initial contact, the ankle is at a neutral angle (the foot is at a right angle relative to the shank) pulled by the tibialis anterior muscle. To keep the body moving forward without interruption, a heel rocker is used (Perry and Burnfield, 2010). Rapid loading of the limb generates a plantarflexion moment that drives the foot toward the ground. The external plantarflexion moment is resisted by the internal dorsiflexion moment of the dorsiflexors muscles (tibialis anterior, extensor digitorum longus, extensor hallucis longus and peroneus tertius) as they provide a controlling, eccentric contraction (Perry and Burnfield, 2010, Richards, 2018). This extends the heel support period, draws the tibia forward, and rolls the body weight forward on the heel. This also provides shock absorption for the brief period when the body weight falls freely before heel strike.

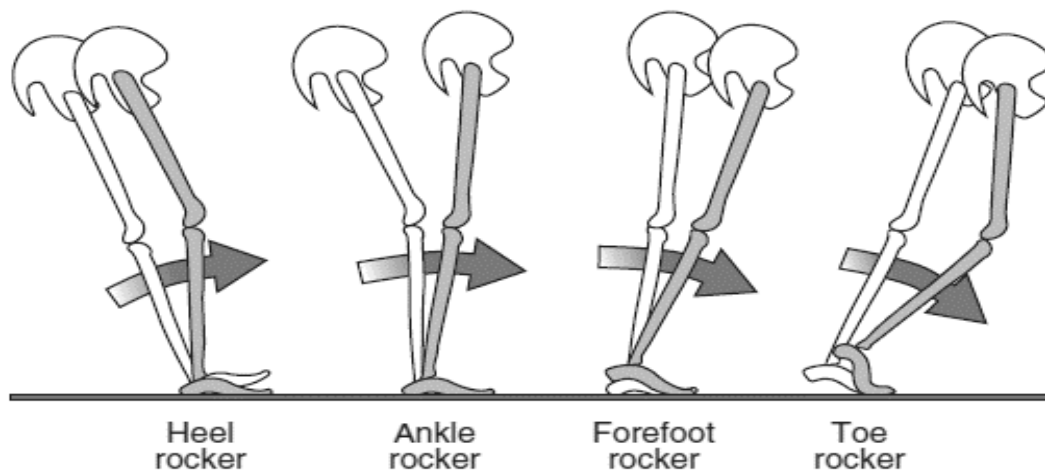


Figure 2.7: Functional rockers of the foot and ankle. Adapted from (Webster and Darter, 2019)

The displacement of the body over the foot creates an increasing dorsiflexion moment that rolls the tibia forward from an initial 10 degrees of plantarflexion position achieved by the end of loading response to 5 degrees of dorsiflexion by the end of mid stance, while the entire foot remains in contact with the ground (Perry and Burnfield, 2010) (Figure 2.8). This motion towards dorsiflexion enables the ankle rocker to take place leading to heel rise at the beginning of terminal stance; facilitating the forefoot rocker. Thus, ankle

rocker assists in limb progression. The gastrocnemius and soleus muscles slow the rate of tibial advancement until the end of mid stance to restrain the forward movement of the tibia on the foot (Whittle, 2014). Soleus activity is the dominant decelerating force because of its larger size and its direct attachment between the tibia and calcaneus.

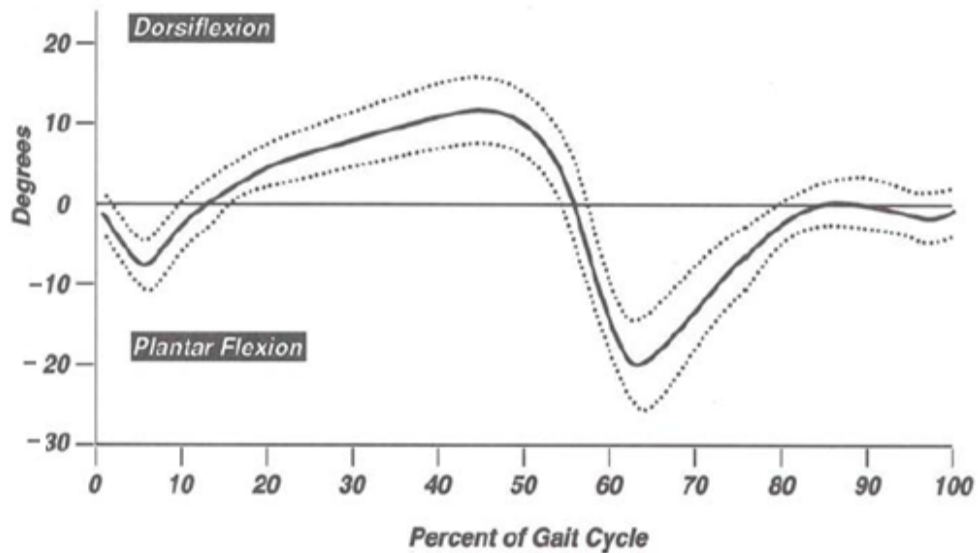


Figure 2.8: Normal range of motion pattern of the ankle joint during a gait cycle. Adapted from (Perry and Davids, 1992).

By the end of mid stance, the ankle is almost locked by the gastrocnemius and soleus, and the heel rises due to continued tibial advancement. The ankle continues to dorsiflex to reach maximum of 10 degrees by the end of terminal stance (Figure 2.8). The limitation of ankle dorsiflexion motion during terminal stance enables the limb to pivot at the forefoot and creates a forefoot rocker to allow for forward progression (Perry and Burnfield, 2010). During terminal stance, a combination of limited ankle dorsiflexion and heel rise places the GRF anterior to the source of foot support. As the GRF moves more anterior to the metatarsal heads axis, the foot rolls with the body, leading to a greater heel rise and an increasing dorsiflexion moment. This creates a free forward fall situation that passively generates the major progression force used in gait. Peak soleus and gastrocnemius activities only support a heel rise and accelerates advancement of the unloaded limb. By the end of terminal stance and the beginning of pre swing, there is no stabilizing force within the foot, so it is free to plantarflex in response to the

gastrocnemius and soleus muscles action, commonly called push off (Perry and Burnfield, 2010).

Following the onset of double limb support, the body weight is transferred to the other limb in preparation for pre swing. The tibia moves forward as the toe is stabilized by ground contact and the knee flexes in preparation for swing (Perry and Burnfield, 2010).

During toe off, the ankle is plantarflexed approximately (20-25) degrees (Figure 2.8). The dorsiflexor muscles increase their intensity in initial swing to dorsiflex the foot to neutral during mid swing. The neutral position of the ankle is required to help in foot ground clearance. During terminal swing, dorsiflexor muscles activity increases to assure the ankle is at neutral position for optimal heel contact and in preparation for the increased force requirement of initial contact (Perry and Burnfield, 2010).

➤ **The knee**

During stance, the knee is the basic determinant of limb stability. In swing, knee flexibility is the primary factor in the limb's freedom to advance (Perry and Burnfield, 2010). Figure 2.9 shows the typical motion pattern of the knee joint during a GC.

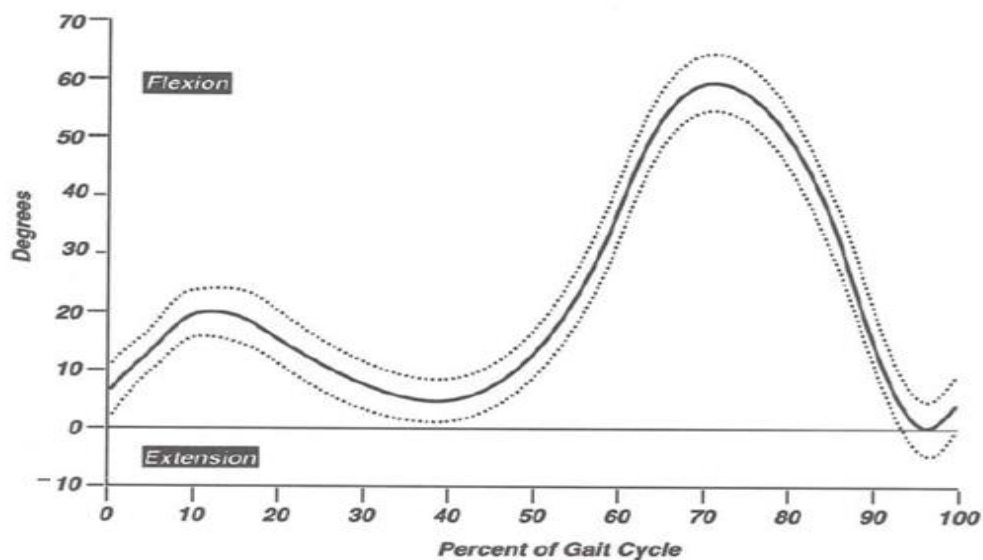


Figure 2.9: Normal range of motion pattern of the knee joint during a gait cycle. Adapted from (Perry and Davids, 1992).

At initial contact, the knee may range from slight hyperextension to slight flexion among individuals. The knee begins to flex immediately after initial contact to reach a peak of 15-20 degrees by the end of loading response or early in mid stance. This knee flexion serves to decrease energy requirements of locomotion and act as a shock absorber. The body weight is accepted with the knee flexed and the GRF falls behind the knee to produce an external flexion moment. This moment is counteracted by contraction of the quadriceps muscle, including the vastus lateralis, medialis, and intermedius, to prevent the knee from buckling and to place the knee under maximum weight-bearing load (Davis III et al., 1991).

During mid stance, total body weight is transferred onto the flexed knee, resulting in an additional five degrees of flexion that occur early in mid stance. The quadriceps muscle reacts to inhibit further flexion. Quadriceps muscle is then assisted by the tibial stability gained through the combined action of the soleus and the forward motion of the body weight. Three mechanisms extend and stabilise the knee during terminal stance. These are: firstly; the strong plantarflexor muscles control on dorsiflexion that provides a stable tibia over which the femur advances, secondly; swing limb momentum, and thirdly; the forefoot rocker that facilitates the forward fall of the body weight over the leg which also assists in stabilizing the knee. To avoid knee hyperextension, the popliteus and gastrocnemius provide a flexor action posteriorly. The knee begins to slightly flex at the end of terminal stance from the rolling of the leg. Tibial stability is then lost and the gastrocnemius, popliteus and short head of biceps femoris muscles can initiate knee flexion (Perry and Burnfield, 2010).

Body weight is transferred to the opposite limb and as the trailing limb reduces its ground contact, the lower leg is free to roll forward. This is accelerated by the release of the tension stored in the stretched soleus, gastrocnemius, and hip flexors. This force and the force from the adductor longus initiate early hip flexion and assist knee flexion. The critical issue during initial swing is to achieve sufficient knee flexion to aid in toe clearance as the thigh advances (Perry, 1997). Attainment of full knee flexion largely depends on the imbalance between the forward momentum of the femur generated by hip flexion and inertia of the tibia and the active knee flexion by the biceps femoris. Only gravitational forces and the momentum generated by hip flexion are required during mid swing. The quadriceps muscle is involved in knee extension during terminal swing to lift

the weight of the lower leg. These counteracted by the hamstrings muscle, which prevent knee hyperextension and decelerate the hip flexion (Perry and Burnfield, 2010).

➤ The hip

The hip provides the connection between the dynamic lower body and the almost stationary upper body. The hip moves through only two arcs of motion during a normal stride: extension during most of stance and flexion in swing (Figure 2.10). During stance, the primary hip role is stabilization of the trunk; while during swing, its role is control and advancement of the limb (Perry and Burnfield, 2010).

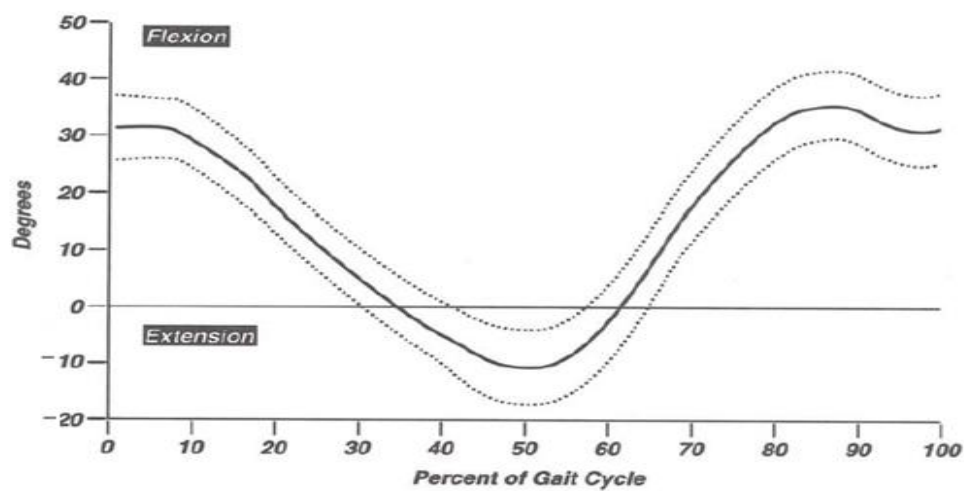


Figure 2.10: Normal range of motion pattern of the hip joint (thigh relative to pelvis) during a gait cycle. Adapted from (Perry and Davids, 1992).

The hip is flexed to a maximum of 25 degree at initial contact, whereby the acquired angle can range between (15-35) degrees (Baker, 2003, Perry and Burnfield, 2010, Richards, 2018). All the five hip extensors (biceps femoris, semimembranosus, semitendinosus, adductor magnus, gluteus maximus) contract to resist the flexor moment created by the vertical ground reaction force (GRFv) and to keep thigh position relatively stable (Richards, 2018). During mid and terminal stance, the hip progressively extends, reaching neutral position at 38% of the GC. In terminal stance, the erect pelvis and trunk roll forward over by the forefoot rocker causing the GRF to move posterior to the hip joint and the thigh to be pulled into hyperextension.

Hip flexion to neutral position during pre and initial swing results from two events. First, contraction of the Iliopsoas muscle aided by gravity, the rectus femoris and the adductors (Davis III et al., 1991). The second event is the ankle mechanics that advance the tibia, induce knee flexion and carry the thigh forward. When tibial inertia causes excessive knee flexion during initial swing, the rectus femoris preserves accelerated hip flexion while correcting knee motion. Minimal hip flexion and partial knee extension continue to advance the limb during mid swing. During terminal swing, strong action by the hamstring muscles prepares the limb for stance by stopping further hip flexion. The reduction of hamstring muscle activity and accompanying onset of the gluteus maximus and adductor magnus activity limit hip flexion. As a result of these actions, the limb is positioned for initial contact (Perry and Burnfield, 2010).

➤ **Shank to vertical angle (SVA)**

During the stance phase, in the sagittal plane, the shank moves from a reclined position (leaning backward from the vertical) to an inclined position (leaning forward from the vertical). The position of the shank can be determined at any point of gait by measuring the angle of the segment (tibia) relative to the vertical. The shank to vertical angle (SVA) is the angle of the shank relative to the vertical (Meadows et al., 2008) (Figure 2.11).

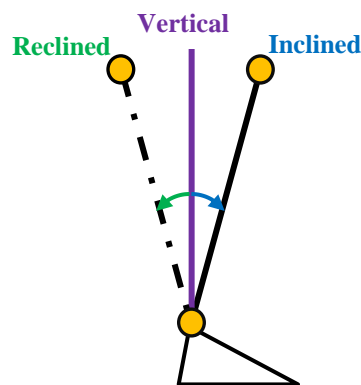


Figure 2.11: Shank to Vertical Angle (SVA) measurement.

The angular velocity (the rate of change of angular position) of the shank movement differs during stride period (Meadows et al., 2008) (Figure 2.12). At mid stance, the angular velocity of the shank slows down as it moves into forward inclination (Inman et

al., 1981, Winter, 2009). Mid stance and terminal stance are challenging phases as they are single support phases, and many kinematic and kinetic changes occur during these phases. The slowing angular velocity of the shank with the optimum inclination of it (10-12° inclination) in mid stance is important for several reasons (Owen, 2010) (Figure 2.12). It aids in achieving the required stability in stance, it enhances smooth movement of the thigh, pelvis and trunk, it determines thigh, pelvis, trunk and head kinematics, it facilitates appropriate GRF alignment to the knee and hip, and it contributes to conservation of energy (Meadows et al., 2008, Owen, 2010, Roelker et al., 2019).

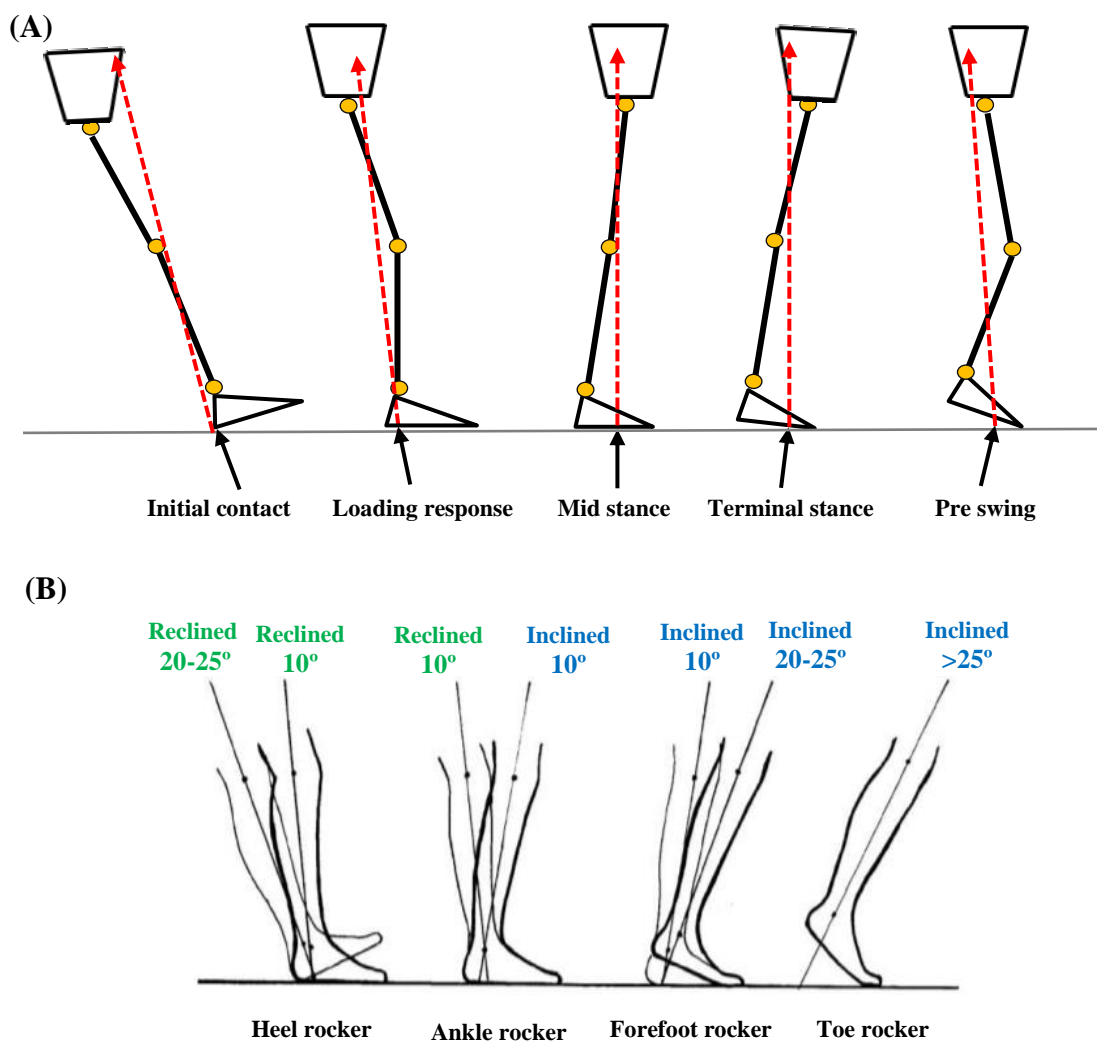


Figure 2.12: Normal shank inclination and the alignment of GRF in relation to the hip and knee joint in stance phase (A). Forward progression of shank produced by the rockers (B), adapted from (Owen, 2010).

2.3.3 Post stroke gait

As aforementioned, gait impairments following stroke can vary due to the size of the lesion and the site affected within the brain, as well as the time passed since the stroke (Jorgensen et al., 1995, Wall and Ashburn, 1979). However, stroke typically may cause hemiparesis that results in the weakness and loss of some function on one side of the body, or hemiplegia that results in total paralysis on one side of the body. Hemiparesis and hemiplegia can affect an individual's gait (Emos and Agarwal, 2018). Several studies have shown alteration in the kinematic and kinetic parameters of post stroke gait in both magnitude (range and peak values) and pattern (profile of curves) as compared to normal gait parameters (Handelzalts et al., 2019, Jorgensen et al., 1995, Olney and Richards, 1996, Patterson et al., 2008, Wall and Ashburn, 1979, Woolley, 2001).

The term hemiplegic (or hemiparetic) gait is usually used to describe post stroke gait. Hemiplegic gait is characterised by an asymmetric gait pattern and slow and stiff gait with poor coordination of the affected side (Olney and Richards, 1996). Patients with hemiplegic gait generally have slower walking speeds ranging from (0.23 ± 0.11) m/s to (0.73 ± 0.38) m/s (Olney and Richards, 1996). Hemiplegic gait is also characterised by abnormal temporal-spatial parameters. For instance, cadence and step and stride length of the affected limb are typically reduced (Figure 2.13) (Esquenazi et al., 2009, Goldie et al., 1996, Hausdorff and Alexander, 2005, Nickel, 1995). Additionally, the swing phase duration of the affected limb is typically longer than the unaffected limb (Chen et al., 2005). Stroke patients usually attempts to shift their weight as early as possible to the unaffected limb due to muscle weakness, spasticity, and joint contractures that restrict joint mobility (Chen et al., 2005, Esquenazi et al., 2009). Stroke patients also require more energy to ambulate the same distance when compared to age-matched healthy participants (Michael et al., 2005, Platts et al., 2006). The differences in step length, swing time, muscle strength, and range of motion between the affected and unaffected limbs result in an asymmetric gait pattern (Goldie et al., 1996, Olney and Richards, 1996) and increased energy expenditure (Patterson et al., 2008).

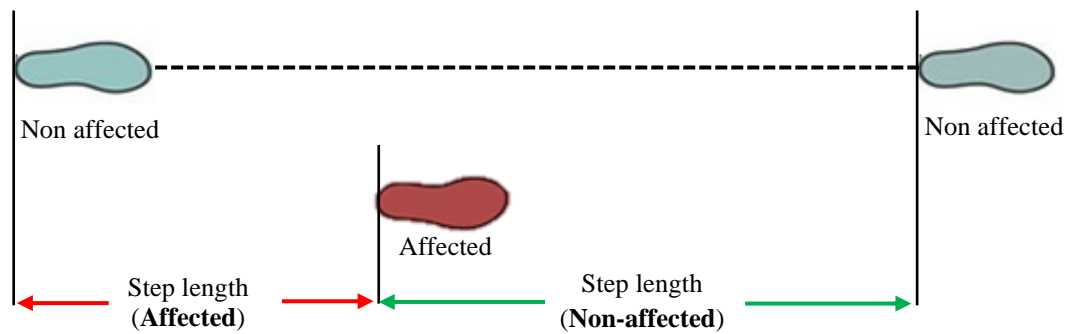


Figure 2.13: Affected and non-affected step length of stroke patient. Adapted from (Kim and Eng, 2003).

Furthermore, in hemiplegic gait about 20% of stroke patients worldwide have shown plantarflexion deformity (Barrett and Taylor, 2010, BurrIDGE et al., 1997). Plantarflexion deformity is characterised by ankle resting in a plantarflexed position. The reason behind this deformity is complex but is thought to be caused by an improper dorsiflexion/plantarflexion strength ratio due to spasticity in the plantarflexor muscles and/or weakness in the dorsiflexor muscles which counteract this position (Barrett and Taylor, 2010, Olney and Richards, 1996, Stewart, 2008, VerdIE et al., 2004). Thus, calf muscle stiffness and shortening develop, resulting in reduced range of motion at the ankle (Carr, 2011). Additionally, stroke patients usually show a supination deformity in the foot on the affected side (NHS Quality Improvement Scotland, 2009, Reynard et al., 2009), which is defined as an inversion at the subtalar joint and forefoot adduction at the midtarsal joints (McDonald and Tavener, 1999). Frequently, the plantarflexed position of the ankle (equinus) in stroke patients is accompanied with a supination foot deformity, which is termed as equinovarus deformity (Condie and Bowers, 2008, Kinsella and Moran, 2008, Reynard et al., 2009). Therefore, the initial contact with the ground occurs either with the foot flat or with the forefoot; instead of contact with the heel (heel strike) (Meadows et al., 2008, Perry and Burnfield, 2010, Webster and Darter, 2019). If equinovarus deformity is present, the contact occurs on the lateral border of the foot. The inversion position of the foot creates an unstable configuration of the ankle (Esquenazi, 2008).

The foot maintains a plantarflexed position throughout the stance and swing phases of gait with consequences at the knee and the hip joint (Gard and Fatone, 2003, Meadows et al., 2008). This impairment has significant effects on the magnitude and patterns of gait kinetics and kinematics. Excessive plantarflexion during stance phase leads to transferring the weight of the limb through the front part of the foot rather than smoothly transferring it from the heel throughout the length of the foot (Meadows et al., 2008, Perry and Burnfield, 2010), as illustrated in Figure 2.14. As the forefoot is the initial point of contact with ground, the heel rocker of the loading response is lost. Additionally, the tibia is driven backward as the heel drops to the ground. Thus, the knee is more posteriorly placed (hyperextended) than normal (NHS Quality Improvement Scotland, 2009, Perry and Burnfield, 2010).

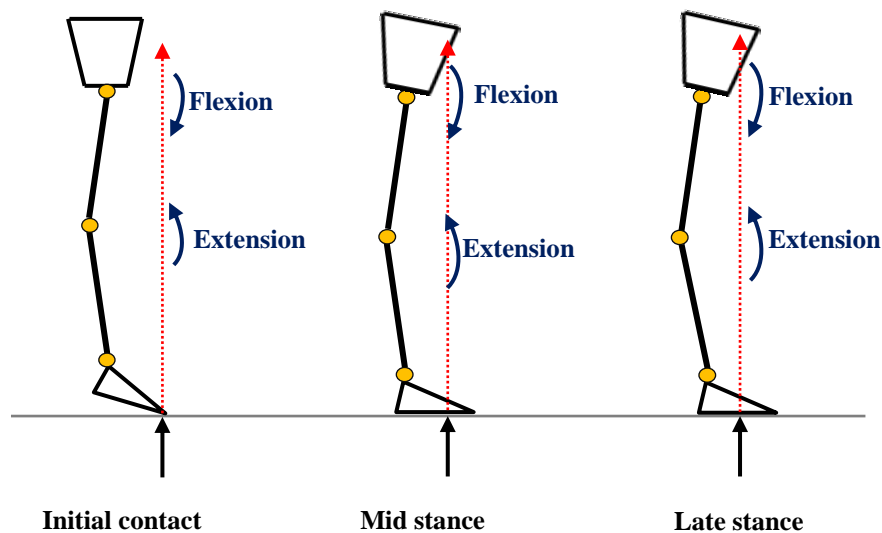


Figure 2.14: An example of a typical stance phase in a stroke patient with hemiplegic gait. The red dotted line represents the GRF.

The persistent plantarflexion during mid stance resists also the forward progression of the tibia and leads to loss of the ankle rocker (Esquenazi, 2008, Kinsella and Moran, 2008). The femur follows body momentum and rolls over the immobile tibia, thus the knee hyperextension is maintained also in mid stance (Perry and Burnfield, 2010) (Figure 2.14). Body weight advances as the patient rolls across the forefoot and the patient proceeds immediately into the late stance. However, if there is no heel rise, the advancement of the body is limited to the extent that knee hyperextension and trunk lean

improve the forward reach of the opposite limb (Meadows et al., 2008, Olney and Richards, 1996) (Figure 2.14). The location of the GRF (in front of the knee and hip) and the knee hyperextension position make hip extension difficult due to the presence of an external hip flexion moment (Kinsella and Moran, 2008) (Figure 2.14). Hence, the GRF alignment is inappropriately altered to pass further anteriorly to the knee centre and anteriorly to the hip joint centre, which will lead to an increase in the moment arms and thus an increase in the magnitude of the external moments at these two joints. Therefore, abnormal muscle activities are required to oppose the generated external moments.

As one of the key requirements of gait is foot ground clearance during the swing phase (Perry and Burnfield, 2010, Richards, 2018, Whittle, 2014), a lack of knee flexion at terminal stance phase accompanied with excessive ankle plantarflexion prevent the leg from being shortened and lead to difficulty with ground clearance (Esquenazi, 2008, Winters et al., 1987). Without any substitutive movements, this causes the foot to drag along the ground, or “toe drag”. There are many common substitutive movements to achieve better foot ground clearance, including; hip hiking (increasing hip abduction of the unaffected stance limb with simultaneous elevation of the affected swing limb), vaulting (increasing plantarflexion of the unaffected stance limb during mid and terminal stance), leg circumduction, and lateral trunk lean toward the stance limb (Chen et al., 2005, Gard and Fatone, 2003, Kerrigan et al., 2000). These substitutive movements may allow for the advance of the swing limb but increase energy demand (Chen et al., 2005, Olney and Richards, 1996). Also, these substitutive movements may improve the impaired forward progression in the affected side but decrease the walking speed (Awad et al., 2015, van de Port et al., 2008). Additionally, if these substitutive movements were insufficient for foot ground clearance, there may be an increased risk of falling, reduced physical activity and loss of independence (Esquenazi, 2008, Hausdorff and Alexander, 2005). Therefore, patients with plantarflexion deformity require some form of treatment to improve foot ground clearance and to decrease their risk of falling.

Furthermore, several studies have shown alteration in the GRFv of post stroke gait in both magnitude and pattern as compared to normal GRF, this may be considered as a consequence of losing heel strike, limited use of the foot rockers and insufficient push off (Campanini and Merlo, 2009, Chen et al., 2001, Chen et al., 2007, Wong et al., 2004). As mentioned earlier, in normal gait, the knee is extended (or hyperextended) at initial

contact and then immediately flexes to absorb the resultant shock (Perry and Burnfield, 2010). In post stroke gait, the first peak of GRFv occurs when the foot contacts the ground. Stroke patients usually lack the ability to flex their knee and hence subject the affected limb to a shock loading (Chen et al., 2007, Winters et al., 1987). Three common patterns of GRFv were reported in post stroke gait; bimodal M pattern, inverted U pattern and A pattern as illustrated in Figure 2.15 (Wong et al., 2004). These GRFv patterns were strongly correlated with motor recovery status and walking speed (Chen et al., 2007, Wong et al., 2004). Stroke patients with bimodal M pattern showed a good motor control and their walking patterns could be closer to normal. Although the bimodal M pattern in stroke patients is similar in shape to the normal GRFv, it might have smaller first and second peaks, with magnitude less than the patient's body weight. Additionally, the walking speed in bimodal M pattern was higher than the other patterns, but lower than normal walking speed (Chen et al., 2007, Wong et al., 2004). In the inverted U pattern, the GRFv has no obvious peaks as the GRFv is relatively remaining constant (Figure 2.15). The inverted U pattern was found in stroke patients with fair motor control with limited ability to use the foot rockers in the affected limb during walking (Chen et al., 2007, Wong et al., 2004). In the A pattern, The GRFv has only one vertical peak (Figure 2.15). This pattern was correlated with poor motor control, poor stability and slow walking speed (Chen et al., 2007, Wong et al., 2004). Additionally, an irregular pattern has also been reported in stroke patients with poor motor control and poor stability (Chen et al., 2007).

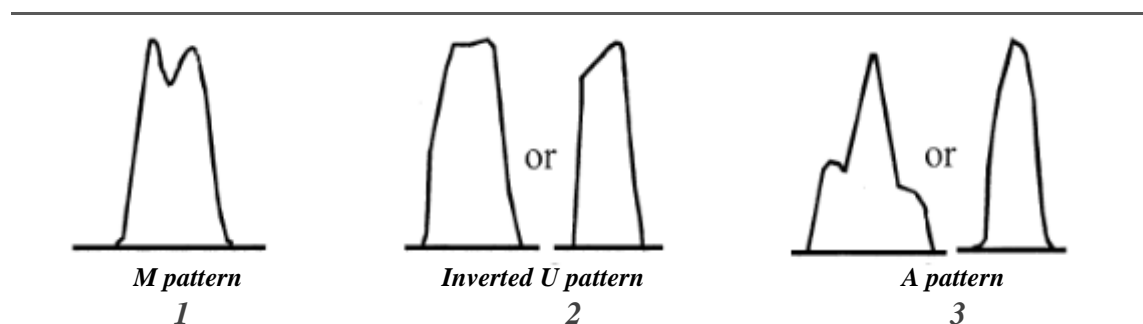


Figure 2.15: The GRFv patterns of stroke patients during walking. Adapted from (Wong et al., 2004).

2.4 Post stroke gait rehabilitation

Rehabilitation is defined as “an organised therapeutic programme directed towards recovering maximal function in patients with permanent or severely protracted physical disability” (Roper, 1982). Rehabilitation after stroke aims to aid physical recovery and prevent secondary complications (Langhorne et al., 2011). Gait recovery (restoring walking ability) is a main goal in the rehabilitation programme for stroke patients (Belda-Lois et al., 2011). A specific rehabilitation gait-training programme is needed to improve walking performance. The rehabilitation programme must focus on the individual patient needs and must be task-oriented (Dean et al., 2000, Langhorne et al., 2011, Salbach et al., 2004, Teixeira-Salmela et al., 1999). This rehabilitation programme consists of a multidisciplinary approach involving a range of health care professionals such as healthcare medical consultants, physiotherapists, occupational therapists, and orthotists. Several gait rehabilitation techniques/approaches are used for post stroke gait rehabilitation. The most widely adopted approaches include muscle strengthening and stretching exercises, conventional overground training, treadmill training, body weight support, functional electrical stimulation, and training with orthoses (Belda-Lois et al., 2011, Kerr et al., 2019, Kobayashi et al., 2019, Moseley et al., 2005, Nikamp et al., 2019, Park et al., 2015).

Compensatory strategies based on rehabilitation training programmes, such as using the non-affected side or using supportive equipment, can also be useful in restoring function after stroke (Cirstea and Levin, 2000). Although the compensatory strategies may increase the independence of a patient in the short term, they are suboptimal for physiological recovery and have the potential to be mal-adaptive on the long term (Carey 2012). The concept of learning-dependent neuroplasticity (see section 2.2.3 under the heading “Stroke incidence and recovery”) has been used as a treatment strategy in rehabilitation programmes to increase the motor/functional recovery after stroke. High intensity practice with repetitive, task-oriented and task-specific exercises are considered the most effective current interventions for restoring motor function after stroke (French et al., 2016, Langhorne et al., 2011, Veerbeek et al., 2014). Restoring motor function has been strongly associated with several training therapy modalities such as constraint-induced movement therapy with guided practice (Boake et al., 2007, Wolf et al., 2006),

training within enriched environments, e.g. action observation training (Celnik et al., 2008), and motor imagery training (Page et al., 2007).

Following the clinical practice guidelines around the world, stroke patients are recommended to receive between 45 to 60 minutes of daily physiotherapy and occupational therapy during their rehabilitation programme (National Stroke Foundation, 2010, NICE Stroke rehabilitation, 2013, Otterman et al., 2017, Party, 2010, Van Peppen et al., 2007). However, several studies reported that stroke patients usually receive less than the recommended period of training per day (Birkenmeier et al., 2010, French et al., 2010, Hayward and Brauer, 2015). This might be due to the limited resources of the rehabilitation services; specifically the low availability and the high costs of trained therapists (Bernhardt et al., 2007). Several types of technology-based solutions have been proposed in rehabilitation programmes, such as robot-assisted devices and passive sensor-based devices. The robot-assisted devices are self-operating systems, providing movement assistance in a similar manner as therapists (Fasoli et al., 2004, Hobbs and Artemiadis, 2020, Takahashi et al., 2008). However, the high cost of robot-assisted devices and their complex nature limits their use in hospitals or in patients' homes (Takahashi et al., 2008). Passive sensor-based devices provide assessment and feedback of function to both patients and therapists by tracking movement, however; they do not provide any movement assistance (Lee et al., 2018, Saposnik et al., 2011). Both robot-assisted and passive sensor-based devices have been used to produce a virtual reality gaming interfaces in order to improve the quality and quantity of therapy, by motivating patients through simulating environments (Gibbons et al., 2016, Saposnik et al., 2011, Zakharov et al., 2020).

Surveying the literature reveals that it is unclear which rehabilitative approach is more effective than the others (Combs-Miller et al., 2014, Langhorne et al., 2011, Pollock et al., 2007). The muscle strengthening approach was found to improve walking speed, endurance, balance, and post stroke gait pattern (Dorsch et al., 2012, Kim et al., 2011, Ng and Hui-Chan, 2012, Teixeira-Salmela et al., 1999). For instance, strengthening ankle dorsiflexors, hip flexors, ankle evertors, and knee flexor muscles was significantly correlated with walking speed (Dorsch et al., 2012). Using conventional overground and treadmill training in stroke patients who were able to walk independently showed low-to-moderate quality evidence of rehabilitation benefits (Mehrholz et al., 2017). Additionally,

performing treadmill training with body weight support showed more improvement in the ability to walk independently than conventional over ground training in stroke patients who were unable to walk (Ada et al., 2010b). However, some stroke patients preferred to use the conventional overground training rather than treadmill training as they felt anxious about using the treadmill although a safety harness was provided (Ada et al., 2010a, Mehrholz et al., 2017). Furthermore, no significant differences were found in improvement of walking speed, motor recovery, balance, and quality of life between using treadmill training with body weight support and home exercises managed by a physiotherapist (Duncan et al., 2011). Regardless of the rehabilitation gait-training programme used, most of the studies showed an improvement of walking speed from 0.71 m/s to by approximately 0.9 m/s (Dickstein, 2008, Kerr et al., 2019, Mehrholz et al., 2017) which, however, is still below the required walking speed to safely cross the road using pedestrian crossing in the United Kingdom (1.2 m/s) (Asher et al., 2012).

Using Ankle-foot orthosis (AFOs) has been shown to increase walking speed and to improve post stroke gait pattern (Condie et al., 2004, Lehmann, 1986, NHS Quality Improvement Scotland, 2009). This will be discussed further in the next section (2.5) under the heading “Orthotic management of stroke patients with plantarflexion deformity”. Two studies reported the effects of AFOs on functional recovery after stroke, comparing stroke patients who wore AFOs to stroke patients who did not (Momosaki et al., 2015, Teasell et al., 2001). Both studies found that using AFOs was associated with good functional recovery in stroke patients, by improving the quality of gait and reducing the risk of falls. However, both studies lack important information, including the type/design of the AFOs, time of AFOs prescription, and how often the prescribed AFOs were used during rehabilitation. Additionally, the improvement in functional recovery might also be associated with other confounding factors such as the rehabilitation gait-training programme used by individual patients.

Physical therapy in conjunction with AFO has been used to reduce mild to moderate spasticity in stroke patients (Cakar et al., 2010, Francisco and McGuire, 2012, Logan, 2011). Pharmacological intervention may also be necessary to reduce patient’s spasticity especially in moderate to severe cases (Francisco and McGuire, 2012, Goldstein, 2001). Treatment of severe spasticity may be achieved surgically by releasing the appropriate

tendons by selected neurectomies or by transferring tendons to produce the antagonist action (Francisco and McGuire, 2012, Goldstein, 2001).

2.5 Orthotic management of stroke patients with plantarflexion deformity

2.5.1 Introduction

Improving walking in patient with plantarflexion deformity is a priority in stroke rehabilitation, and is generally attempted through physiotherapy (Begg et al., 2019, Lindquist et al., 2007, Teasell et al., 2003). However, the International Society of Prosthetics and Orthotics (ISPO), the American Heart Association/American Stroke Association (AHA/ASA), and the NHS Quality Improvement Scotland have recommended prescribing Ankle-foot orthosis (AFOs) as an adjunct to physiotherapy in stroke management (Condie et al., 2004, NHS Quality Improvement Scotland, 2009, Winstein et al., 2016). An AFO is an externally applied device used to modify the structural and functional characteristics of the neuromuscular and skeletal system, which encompasses the ankle joint and the whole or part of the foot (Condie, 2008, Lehmann, 1986). AFOs are the most commonly prescribed category among lower limb orthoses in clinical practice (Condie and Bowers, 2008, Meadows et al., 2008, Teasell et al., 2001). They are commonly prescribed for stroke patients to promote initial contact with the heel strike (by preventing/reducing excessive plantarflexion position of the ankle), to facilitate foot ground clearance in swing phase, to support and improve the alignment of the foot (manage equinovarus deformity), and to reduce knee extension and promote hip extension during stance (Condie et al., 2004, Lehmann, 1986, NHS Quality Improvement Scotland, 2009). Thus, using AFOs in stroke rehabilitation is recommended to restore independent walking (Teasell et al., 2001) and to reduce the energy expenditure of walking (Bregman et al., 2010). Early prescriptions of AFOs emphasised their role in the management of post stroke gait primarily for patients with plantarflexion deformity (Lehmann, 1986). NHS Healthcare Improvement Scotland has issued a Best Practice Statement which aims to provide guidelines and to improve practice in using AFOs for stroke patients (NHS Quality Improvement Scotland, 2009). However, there are still many challenges and questions that need to be addressed to improve the design of AFOs, as there is a large

variation of AFOs used in clinical practice, characterized by their designs, materials, trim lines, and AFO footwear combination. These variables should be considered in clinical decision making to achieve the optimal therapeutic benefits of the AFOs. There is limited information in the literature regarding the most appropriate and effective orthosis that best fits the functional needs of the patients. Understanding the mechanical and biomechanical properties of AFOs has a great value in improving AFO function and in accomplishing a successful treatment (Bowker et al., 1993).

2.5.2 Prescription of AFOs

A variety of AFO types/designs can be useful for patients with plantarflexion deformity. Evaluating the patient's gait impairment should be conducted accurately. Identifying the functional loss, describing the gait deviations in a reference to the joint (ankle, knee and hip) and in reference to the body segment (shank and thigh), the timing of the gait event, and the musculoskeletal impairments are essential to clarify the functional objectives desired from an AFO (Condie et al., 2004). The main functional objectives of using an AFO are to prevent/accommodate deformity, promote a base of support, improve function and/or increase or maintain range of motion (NHS Quality Improvement Scotland, 2009).

Traditionally, AFOs were fabricated from metal and leather materials, which are called conventional AFOs. They consist of a leather covered calf band with a single or double metal upright attached distally to shoes and an adjustable ankle joint to control the ankle motion (Chu, 2001). Conventional AFOs are sometimes prescribed in cases of fluctuating peripheral oedema or based on patient's preference, as they may be accustomed to this type from several years (Chu, 2001, Good et al., 1989). However, nowadays conventional AFOs have almost been replaced by thermoplastic AFOs because they are lighter and possess a more cosmetic appearance compared to the conventional AFOs (Chu, 2001, Showers and Strunck, 1984, Yamane, 2019). Polypropylene is the most common type of thermoplastic material used in AFO fabrication (Chu, 2001). Various designs of thermoplastic AFOs are made available, offering many choices of mechanical features to fit an individual's requirements. This is achieved by varying material thicknesses, altering the ankle trim-line, and adjusting the angle at the ankle region of the AFO (Bowker et al., 1993, Lehmann, 1986). Thermoplastic AFOs may be either prefabricated (off-the-shelf) or custom made (Condie, 2008). In the presence of complex deformities (as in

equinovarus deformity), custom made AFOs provide better biomechanical control than prefabricated AFOs. This is because custom made AFOs are fabricated over a positive model of the patient's own limb, thus, an intimate fit and a more precise control can be achieved to meet the individual patient needs (Condie et al., 2004, Condie and Bowers, 2008). Several designs of custom made AFOs are available (Figure 2.16), which include posterior leaf spring (PLS), ground reaction AFO (GRAFO), rigid AFO, and hinged or articulated AFO (HAFO). Electrical stimulation, such as Functional Electrical Stimulation, (FES) has also been used to improve post stroke gait (Hong et al., 2018, Pereira et al., 2012).

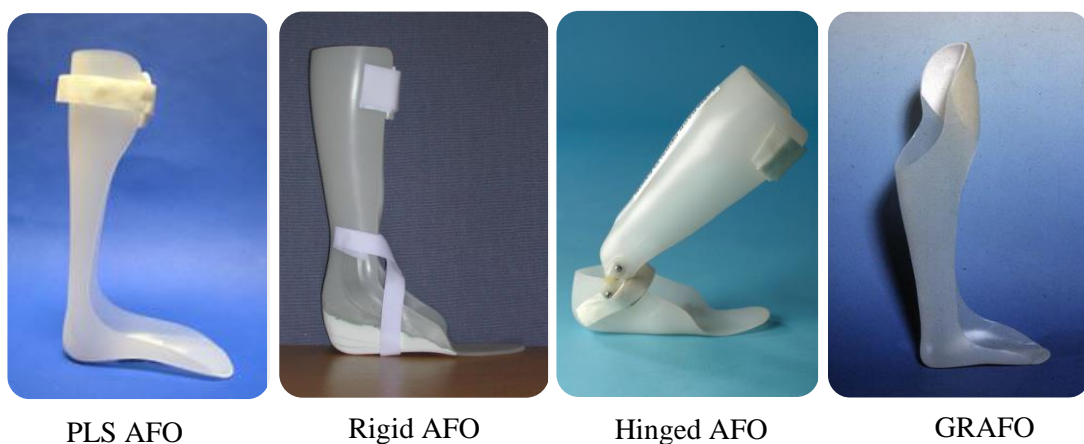


Figure 2.16: Thermoplastic AFO type examples: PLS AFO, Rigid AFO, Hinged AFO, and Ground Reaction AFO (GRAFO). Adapted from (NHS Quality Improvement Scotland, 2009).

❖ *Posterior leaf spring (PLS) AFO*

Posterior leaf spring (PLS) has a flexible design, and is usually a prefabricated AFO (Sumiya et al., 1996) (Figure 2.16). The primary indication for the PLS is isolated dorsiflexor weakness to improve foot ground clearance in swing phase (NHS Quality Improvement Scotland, 2009). The material properties of the PLS allow the AFO to restore stored energy during stance and to release it during swing phase to assist dorsiflexion (Condie and Bowers, 2008, Richards, 2018). This type of AFO is contraindicated in the presence of muscle spasticity (high tone), mediolateral instability

of the foot, and stance problems affecting the knee and hip joints (NHS Quality Improvement Scotland, 2009).

❖ ***Ground reaction AFO (GRAFO)***

Ground reaction AFO (GRAFO) is a type of rigid AFO with a plastic anterior shell (pretibial shell) close to the knee (Condie, 2008) (Figure 2.16). Considering the intimate fit and an adequate stiffness, the GRAFO intends to assist knee extension in patients with excessive tibial inclination. It works by ensuring that the GRF is passing anterior to the knee joint in mid stance to terminal stance (Meadows et al., 2008). It is contraindicated in the presence of fixed deformity and in the presence of knee and/or hip contracture (NHS Quality Improvement Scotland, 2009).

❖ ***Rigid AFO***

Rigid or solid AFO aims to prevent all motions at the foot and ankle (Condie, 2008). The primary indications for the rigid AFO are plantarflexor muscles spasticity (high tone), a gastrocnemius and/or soleus contracture, significant mediolateral instability of the foot, and/or stance problems affecting hip and knee joints (NHS Quality Improvement Scotland, 2009). Rigid AFO is usually a custom made design, and it is fabricated as one piece of a thermoplastic material (Lehmann, 1986) (Figure 2.16). To achieve the best control of the ankle joint, the stiffness of the AFO should be appropriate to prevent foot and ankle motion. Material type, material thickness, location of trimlines (edges), intimacy of fit, and use of ankle reinforcement (such as carbon fibre inserts) influence the stiffness of the AFO (Figure 2.17, B) (Convery et al., 2004, Lin, 2007, Major et al., 2004). At the ankle, the trimline of rigid AFO should be anterior to the malleoli (NHS Quality Improvement Scotland, 2009), but if stiffness needs to be reduced, the trimlines can be shifted posterior to the malleoli as illustrated in figure (Figure 2.17, A) which is then called a semi-rigid AFO (Lehmann, 1986, Major et al., 2004). The terms used to describe the rigid AFO parts and trimlines are illustrated in Figure 2.18.

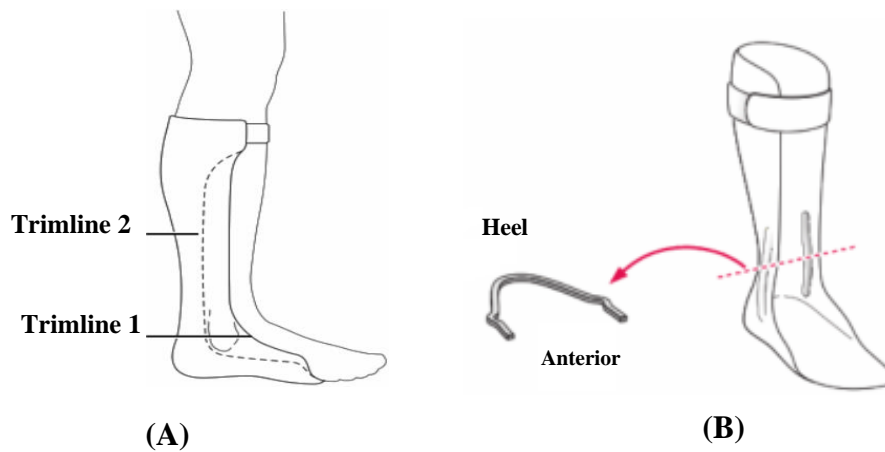


Figure 2.17: AFO stiffness can be affected by the location of its trimlines (A); the typical rigid AFO (Trimline 1) is stiffer and more effective in restricting ankle motion than the semi-rigid AFO (Trimline 2). A reinforced rigid AFO at the ankle area (B) increases the AFO stiffness at the high stress ankle area. The increased curved shape illustrated in the cross section of the AFO shell at the level of the reinforcement (B) contributes to improving AFO stiffness. Adapted from (May and Lockard, 2011).

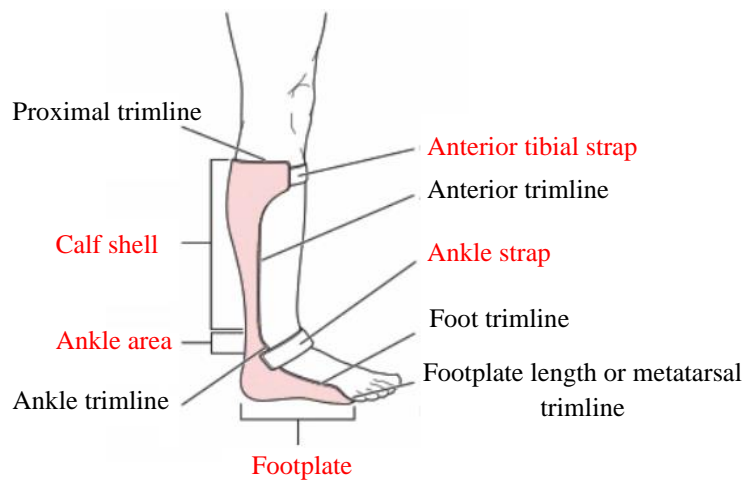


Figure 2.18: The terms used to describe the rigid AFO parts and trimlines. Adapted from (May and Lockard, 2011).

❖ *Hinged or articulated AFO (HAFO)*

Hinged or articulated AFO (HAFO) is fabricated from two pieces of thermoplastic (one for the shank segment and one for the foot) joined together by a mechanical ankle joint

that can be set to allow or assist motion in one direction, while preventing or limiting motion in the other direction (Condie, 2008, NHS Quality Improvement Scotland, 2009) (Figure 2.16). The most common prescribed HAFO design is the one that allows dorsiflexion and prevents plantarflexion beyond neutral ankle angle (90°) (NHS Quality Improvement Scotland, 2009). This design should only be considered when there is sufficient gastrocnemius length and when the patient is able to dorsiflex his ankle up to 10° with full knee extension (without any spastic catch and/or tone in the plantarflexor muscles) (Boyd and Graham, 1999, Condie and Bowers, 2008, Meadows et al., 2008). The presence of the mechanical joint reduces the intimate fit of the AFO at the ankle. Therefore, it is contradicted in the presence of moderate to severe mediolateral instability of the foot (NHS Quality Improvement Scotland, 2009).

Based on the aforementioned information, all AFOs are often prescribed for stroke patients to inhibit plantarflexion, but the amount of dorsiflexion allowed depends on the type/design of AFO used. PLS creates resistance when it is deformed into dorsiflexion (Nagaya, 1997). The PLS is design to restore stored energy during stance and to release it during swing to assist dorsiflexion (Lehmann, 1986), but the amount of resistive moment to dorsiflexion is minimal (Ounpuu et al., 1996). Rigid AFO is design to assist the activity of the plantarflexor muscles during gait by generating a dorsiflexion resistance (Lehmann, 1986). However, using rigid AFO for stroke patients with mild plantarflexion contracture showed restriction of dorsiflexion motion during mid stance (ankle rocker) (Mulroy et al., 2010) and thus, hinders limb progression. Several studies found improvement in post stroke gait during mid stance when tuning rigid AFO is considered (Butler and Nene, 1991, Meadows et al., 2008, Owen, 2004b, Owen, 2010), this will be discussed further in section 2.6 under the heading “Tuning of rigid AFO”. Previous studies reported that using articulated AFOs improves heel and ankle rocker during walking (Brunner et al., 1998, Desloovere et al., 2006, Romkes and Brunner, 2002, Yamamoto et al., 2011). However, walking with excessive plantarflexion resistance generated by the articulated AFOs with a plantarflexion stop may lead to knee instability as a result of increasing the external knee flexion moment during loading response (Gök et al., 2003, Lehmann et al., 1983, Mulroy et al., 2010). Using articulated AFO with an oil damper showed improvement in heel and ankle rocker function without changing the knee moment as the knee was prevented from moving forward excessively due to the

gradual plantarflexion supported by the oil damper (Yamamoto et al., 2005), however, the peak ankle plantarflexion power generated in pre swing was not improved and thus, resulted in insufficient forefoot rocker function (Yamamoto et al., 2011). A summary of some studies investigating the effects of wearing AFOs on stroke patients is in Table 2.2.

Recommendations for prescribing the most appropriate AFO type/design for stroke patients have been developed during a consensus conference of the International Society of Prosthetics and Orthotics (ISPO) (Appendix A), however; the final decision is left to the orthotist (Condie et al., 2004). Several systematic reviews and meta-analysis studies have investigated the effects of several types/designs of AFOs which provide evidence for the benefits of using AFOs in stroke patients (Daryabor et al., 2018, Daryabor et al., 2020, Ferreira et al., 2013, Leung and Moseley, 2003, Padilla et al., 2014, Shahabi et al., 2020, Totah et al., 2019, Tyson et al., 2013). Nonetheless, most of the included studies examined only the immediate effects of the AFOs. Additionally, there is some controversy regarding the AFO type/design which may be most appropriate to manage the post stroke gait. Some studies recommend the use of articulated AFOs, which allow some movement at the ankle (Daryabor et al., 2018, Ramstrand and Ramstrand, 2010), whereas others recommend a rigid AFO, which blocks ankle motion, and, as a result, encourages a more normal-like gait pattern of hip and knee extension in terminal stance (Bowers and Ross, 2010, Carse et al., 2015). There is insufficient evidence to allow any conclusive result on the most appropriate AFO types/designs for stroke (Shahabi et al., 2020, Tyson et al., 2013).

Table 2.2: Summary of some research studies that investigated the effects of AFOs on gait parameters of stroke patients.

| Author | Design and participants | Intervention | Outcome measures and key findings |
|--------------------------|----------------------------------------------------------------------------------------------------------------------------------------------------------|-----------------------------------------------------------------------------|-------------------------------------------------------------------------------------------------------------------------------------------------------------------------------------------------------------------------------------------------------------------------------------------------------------------------------------------------------------------------------------------------------------------------------------------------|
| (Park et al., 2009) | One session: within-subject comparison. 17 stroke patients able to walk independently with canes. Mean age: 58 years. Mean time from stroke: 36 days. | PLS compared to barefoot condition. | Ankle kinematics: PLS reduced the excessive ankle plantarflexion in stance (PLS 23.9 , barefoot 18.8) and increased swing dorsiflexion (PLS 2.9 , barefoot -2.9). Knee and hip kinematics: No significant differences were found between PLS and barefoot conditions. |
| (Lairamore et al., 2011) | One session: within-subject comparison. 15 subacute stroke patients able to walk without assistance. Mean age: 55 years. Mean time from stroke: 86 days. | PLS and dynamic ankle orthosis compared to shoes only condition. | Ankle kinematics: No significant differences were found between the tested conditions. Walking speed: No significant differences were found between the tested conditions. |
| (Gatti et al., 2012) | A cross-sectional study. 10 stroke patients able to walk without assistance. Mean age: 46 years. Mean time from stroke: 40 months. | Custom made rigid AFO compared to shoes only condition. | Walking speed: Significant walking speed when walking with rigid AFO (0.62±0.08m/s) compared to shoes condition (0.47±0.13m/s) (P < 0.05). Knee kinematics: No significant increase in difference in the knee flexion angle at the toe off between AFO and shoes only conditions (18.64° vs. 17.22°). Significant increase in the peak knee flexion angle during swing using AFO as compared to shoes only (30.71° vs. 26.3°). |
| (Lee et al., 2015) | Randomised controlled trial. 15 chronic stroke patients able to walk without assistance. Mean age: 46.5 years. Mean time from stroke: 26.5 months | Custom made articulated AFO (0°, 5°, 10°, 15°, and 20°plantarflexion stop). | Knee kinematics: Significant increase in knee flexion angle was found at orthotic limitation angles more than 10° at mid stance. |

Table 2.2/continued

| | | | |
|------------------------------------|--------------------------------------------------------------------------------------------------------------------------------------------------------------|--------------------------------------------------------------------------------------------------------------------------------|-----------------------------------------------------------------------------------------------------------------------------------------------------------------------------------------------------------------------------------------------------------------------------------------------------------------------------------------------------------------------------------------------------------------------|
| (Silver-Thorn et al., 2011) | Randomised controlled trial. 8 chronic stroke patients, able to actively ambulate within the community. Mean age:43 years. Mean time from stroke: 3.3 years. | Articulated AFO (5 dorsiflexion, 5 plantarflexion, and neutral alignment). | Knee kinematics: AFO with 5° plantarflexion reduced the flexion angle during loading response compared to AFO with 5° dorsiflexion and neutral alignment. Knee Kinetics: knee flexion moment increased during loading response when using an AFO with 5° plantarflexion. |
| (Yamamoto et al., 2011) | Crossover study. 8 chronic stroke patients, able to walk without assistance. Mean age: 55.25 years. Mean time from stroke: 3 years. | Articulated AFOs (oil damper) compared to shoes only condition. | Ankle kinematics: Ankle dorsiflexion at initial contact, loading response, and mid swing were improved with the articulated AFO. No significant differences were found in the ankle power, anterior-posterior GRF and knee and hip kinetics and kinematics ($P > 0.005$). |
| (Kobayashi et al., 2015) | Randomized controlled trials. 10 chronic stroke patients able to walk without assistance. Mean age: 56 year. Mean time from stroke: 6 years | Metal articulated AFO under four different plantarflexion resistive moments | Joint kinematics Increasing the plantarflexion resistive moment of the AFO caused significant decreases both in the peak ankle plantarflexion angle and the peak knee extension angle. Joint Kinetics: Increasing the plantarflexion resistive moment of the AFO caused significant increase in the internal ankle dorsiflexion moment and significant decrease in the internal knee flexion moment. |
| (Yamamoto et al., 2018) | Randomized controlled trials. 42 subacute stroke patients (<6 months duration). Mean age: 59±13 years. Mean time from stroke: 3.4±1.7 months. | Articulated AFO with plantarflexion resistance (oil damper) Articulated AFO with plantarflexion stop compared to shoes only | In Articulated AFO with plantarflexion stop the pelvis was inclined forward to a greater degree at initial contact compared with the shoes only condition. In the articulated AFO with plantarflexion resistance (oil damper), the thoracic tilt angle was reduced throughout the stance phase compared with the shoes only condition. |

❖ *Functional Electrical Stimulation (FES)*

Functional electrical stimulation (FES) has been used to overcome plantarflexion deformity by improving muscle strength and decreasing spasticity in stroke patients (Glanz et al., 1996, Pereira et al., 2012). The FES system consists of electrodes (either placed on the skin surface or implanted) in order to stimulate the common peroneal nerve to elicit ankle dorsiflexion during swing phase. The FES has a heel switch or tilt sensor to detect stance and swing phases of the GC. Using FES in stroke patients with plantarflexion deformity has demonstrated positive effects on many gait parameters, such as increased walking speed, improved gait symmetry, and reduced energy expenditure (Hausdorff and Ring, 2008, Stein et al., 2010). Furthermore, the use of FES showed an immediate improvement in ankle dorsiflexion during swing phase and reduced ankle plantarflexion at toe off (Kesar et al., 2010).

To date, a few studies have compared the effects of using different types of AFOs and FES on gait parameters of stroke patients. Chisholm (2012) compared the effects of wearing different types of AFOs (rigid, PLS, and HAFO) and FES among 4 stroke patients on gait kinematics. The improvement on hip and knee joint kinematics during walking were higher with the AFOs compared to the FES. The ankle dorsiflexion and the muscle activity of gastrocnemius were improved during swing phase with the AFOs, while the response to FES was less consistent among stroke patients. The stroke patients in this study regularly used an AFO for walking within the community, thus they may have the opportunity to become familiar with and feel confident when wearing the AFOs. The patients in the study by Chisholm (2012) may have needed more time to become familiar with FES, as FES requires a long training process (Popovic et al., 2001). The impact of training on gait parameters might be noticed/improved if the stroke patients had a long training process with FES (Embrey, 2010). Although FES and AFO showed similar effect in improving walking speed and activity level in chronic stroke patients (Sannyasi, 2019, van Swigchem et al., 2010), these improvements were considered clinically insufficient (less than the Minimal Clinically Important Differences (MCID)). “The MCID is the minimal amount of change in walking speed (0.16m/s) that is clinically meaningful and associated with an important difference in function for stroke patients” (Tilson et al., 2010).

The American Heart Association/American Stroke Association (AHA/ASA) recommends FES as a proper alternative to AFO for stroke patients (Winstein et al., 2016). A recent systematic review showed that AFOs and FES had similar effects on walking speed (Shahabi et al., 2020). Only one study showed more improvement in walking speed with FES compared to AFO (the type/design of the AFO was not mentioned) (Kottink et al., 2012). The improvement in the walking speed may be due to the using 2-channel peroneal nerve stimulator, which may lead to improved performance (Berenpas et al., 2018).

Based on patients' feedback, some patients preferred the use of FES, because it is easy and comfortable to fit with shoes (Chisholm, 2012) and because it does not restrict ankle motion (Bulley et al., 2011), whereas others preferred the use of AFO for providing more support when loading weight onto their affected side (Chisholm, 2012, de Wit et al., 2004). Additionally, several FES users also used AFO when FES equipment failed or during travelling (Bulley et al., 2011). Stroke patients have previously indicated greater self-confidence and improved ability to perform functional tasks when wearing an AFO compared to without wearing AFO (de Wit et al., 2004), although AFOs have negative aspects such as an unappealing appearance (Hesse et al., 1996).

2.5.3 Biomechanical effects of AFOs

AFO designs are based entirely on biomechanical principles, with emphasis on force systems that act upon body segments for corrective, assistive, preventive, and substitutive functions (Bowker et al., 1993, Condie and Bowers, 2008, Lehmann, 1986). Both comfort and effective force application are essential in AFOs design to achieve the therapeutic benefits of the orthoses (Lehmann, 1986, Silva et al., 2010). AFOs, in general, have both direct and indirect effects on the patients. The AFO applies forces to the patient's leg and foot to directly control movements of the foot and ankle. Indirectly, the AFO affects the alignment of the ground reaction force with respect to the proximal lower limb joints (Bowers and Ross, 2010, Bowker et al., 1993, McHugh, 1999).

(i). Direct biomechanical effects of AFOs

The AFO can provide a direct impact on the segments and joints that are encompassed by the AFO (Meadows et al., 2008). Regardless of the type of the AFO, each AFO is

designed to restore functions normally controlled by either passive tissues (ligaments, joint capsules) or active tissues (muscles) (Lin, 2007, Meadows et al., 2008). The direct aims of using AFO in stroke patients are to control the equinovarus deformity and to compensate the excessive plantarflexion position of the ankle. This can be achieved by the application of external balanced three-force system around the patient's joints through changing the shear force, the axial force, or/and the moment, directly at the joint (Bowker et al., 1993, Meadows et al., 2008, Richards, 2018). This force system is illustrated in (Figure 2.19). Thus, to control/prevent excessive plantarflexion, the AFO applies forces to the posterior calf section (F_1), to the plantar surface of the foot near the metatarsal heads (F_2), and to the dorsum of the foot near the ankle joint (F_3) (Meadows et al., 2008). F_3 can be provided by the upper of the shoes or/and by the ankle strap (Figure 2.19, A). The ankle strap can be either a single strap that is positioned to apply force at approximately 45° angle, or a "figure-8" crossover ankle strap as shown in (Figure 2.20) (NHS Quality Improvement Scotland, 2009). Using an ankle strap is recommended in the presence of muscle spasticity (high tone) and to ensure sustaining the heel within the AFO, especially when the shoes do not provide enough support (Major et al., 2004). However, the patient's upper limb function should be considered in placing and choosing the ankle strap design (NHS Quality Improvement Scotland, 2009). The anterior tibial strap (Figure 2.18) is another strap in the AFOs that is used to improve the intimate fit of the AFO and to ensure sustaining the tibia within the AFO. The anterior tibial strap applies a posteriorly directed force on tibia proximally to control/prevent forward movement of the tibia over the foot (Meadows et al., 2008, Richards, 2018).

The three-force system can also be used to control supination deformity of the foot (Chen et al., 2010, NHS Quality Improvement Scotland, 2009). Applying forces to the medial aspect of the heel (calcaneus), the area above the lateral malleolus, and at the medial aspect of the proximal calf can control the inversion at the subtalar joint (Meadows et al., 2008) (Figure 2.19, B). Adduction at the midtarsal joint is controlled by applying forces at the medial heel (calcaneus), the lateral mid foot (midtarsal joint) and along the first metatarsal shaft (Meadows et al., 2008) (Figure 2.19, C). During the casting process, the ankle angle and the foot position must be considered. If the foot deformity is flexible, correction of the supination deformity must be applied during casting. This can be achieved by initially fully plantarflexing the ankle to release the tension on the Achilles

tendon. Then, the subtalar joint is pronated, and the forefoot is abducted to the neutral position. Finally, the ankle can be set in the desired angle, this will be discussed below under the heading “The ankle angle of the AFO (AA-AFO)”. If the supination deformity has not been controlled, the foot position may increase adduction moment at the knee joint, which can lead to ligamentous laxity, at the lateral collateral ligament of the knee, and to increase the knee varus alignment (NHS Quality Improvement Scotland, 2009).

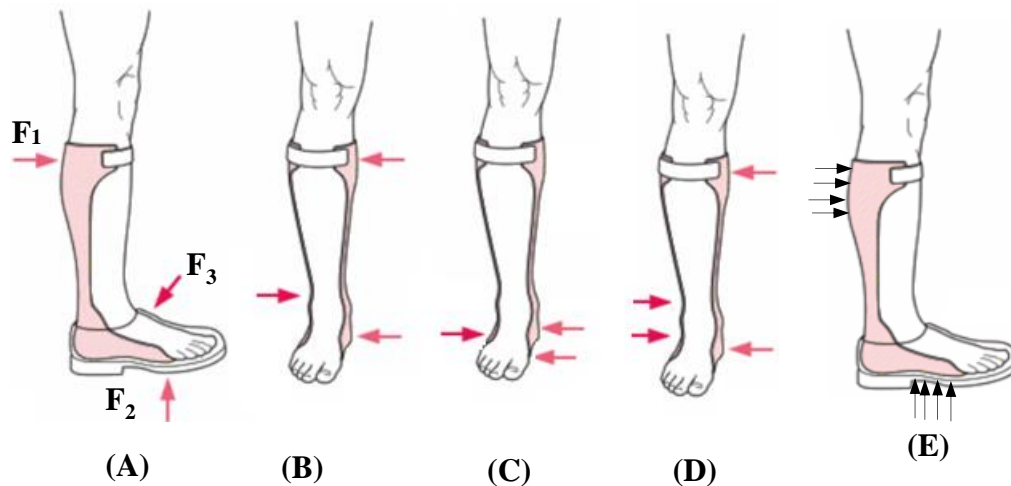


Figure 2.19: The AFO force system; three-force system to control plantarflexion (A), inversion (B) and forefoot adduction (C), four-force system to control inversion at subtalar joint (D), the distribution of force over a broad area (E). Adapted from (May and Lockard, 2011).

Although forces are represented as vectors acting about a single point, distribution of these forces over a broad area of the patient’s leg can be provided (Figure 2.19, E) when the AFO is fitted properly to match the contour of the skeletal structures in respect to the underlying anatomy (Bowker et al., 1993, McHugh, 1999, Meadows et al., 2008). Furthermore, a direct force over bony prominences or sensitive areas should be avoided to reduce the risk of high localised pressure and thus discomfort and skin damage (McHugh, 1999). This can be achieved by a special care of these areas during the casting process, adding pads over the sensitive areas, and maximizing the AFO lever arm and the areas of the force application (Meadows et al., 2008). Additionally, the application point of the force can be transferred slightly above and/or below the joint to reduce the high

pressure at the joint, producing a four-force system as illustrated in (Figure 2.19, D) (May and Lockard, 2011).

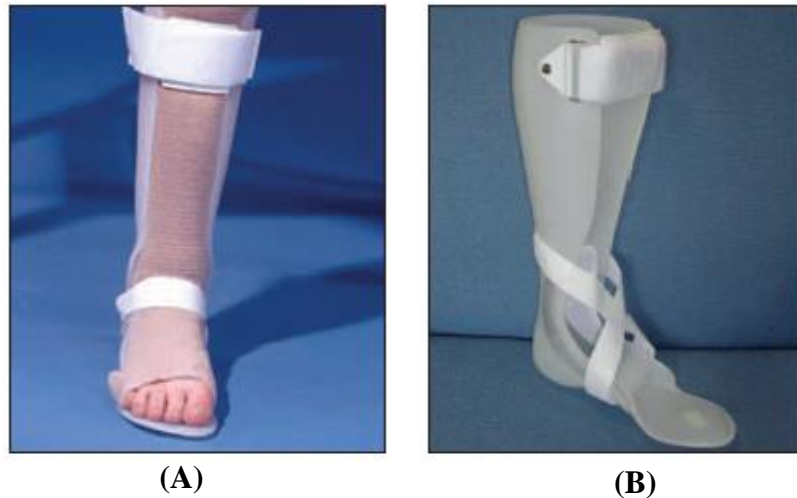


Figure 2.20: Single ankle strap (A) and “figure-8” crossover ankle strap (B). Adapted from (NHS Quality Improvement Scotland, 2009).

(ii). Indirect biomechanical effects of AFOs

The influence of AFOs can extend beyond the foot and the ankle to the knee and hip joints (Bowers and Ross, 2010, Eddison et al., 2017, Farmani et al., 2016a, Meadows et al., 2008, Owen, 2010). Controlling the alignment and motion of the ankle can affect the alignment of the tibia to become closer to normal. For instance, in the case of walking with a hyperextended knee (e.g. stroke), if the AFO realign the tibia to be approximately 10° forward inclined during static (quiet standing) or dynamic (at mid stance) alignments, the knee joint will be placed anteriorly during mid to terminal stance (Eddison et al., 2017). Subsequently, the GRF will be shifted posteriorly toward the knee joint centre during mid to terminal stance (Bowers and Ross, 2010). Both anterior placement of the tibia and posterior placement of the GRF realign the GRF to pass closer to the knee joint. Thus, rigid AFO can reduce the external knee extension moment during stance phase (Figure 2.21) and can facilitate knee flexion during swing phase (Meadows et al., 2008, NHS Quality Improvement Scotland, 2009). Furthermore, altering the alignment of the tibia so that it is 10° forward inclined can also realign the femur to be approximately 10° forward inclined; which leads to GRF moving posteriorly relative to the hip during mid

to terminal stance and the hip joint to be shifted anteriorly (Bowers and Ross, 2010, NHS Quality Improvement Scotland, 2009) (Figure 2.21). Thus, rigid AFO can reduce the undesirable external hip flexion moment or even to be replaced with a suitable external extension moment (Meadows et al., 2008, NHS Quality Improvement Scotland, 2009).

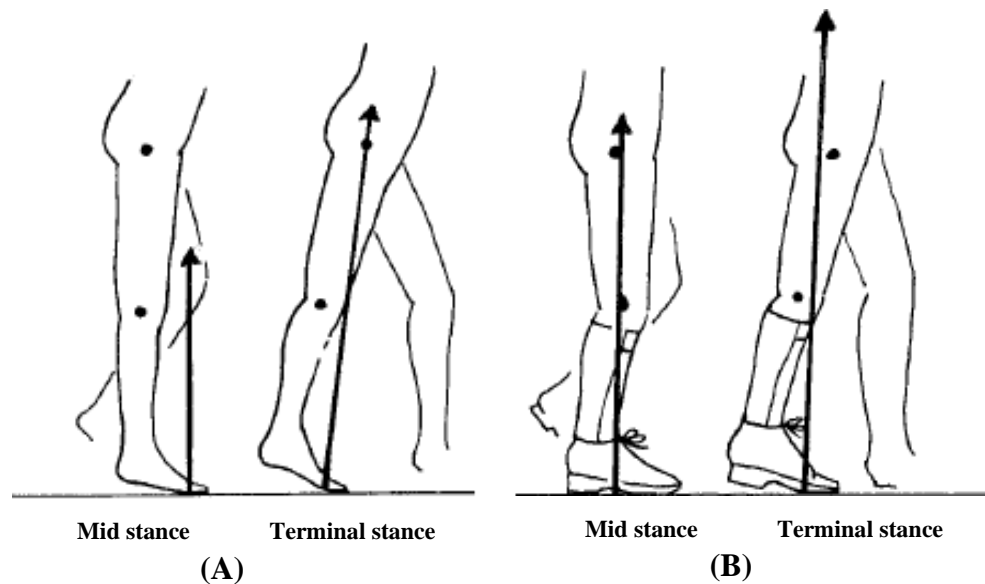


Figure 2.21: The GRF and tibia alignments with and without rigid AFO in a stroke patient. Without AFO (A); the tibia is insufficiently inclined at mid stance and terminal stance, and the GRF is excessively anteriorly aligned at knee and hip joints. The biomechanical effects of rigid AFO (B); the inclination of tibia is increased at mid stance and terminal stance, and the GRF is realigned to reduce the external knee extension moment and to create external hip extension moment. Adapted from (Owen, 2004b).

Additionally, it is clear that any deviation in foot position would lead to an alteration in the GRF, which consequently alters the plantar foot pressure pattern (the distribution of pressures at the plantar surface of the foot, the total sum of which represents the centre of pressure). If foot position is altered, there would be a corresponding alteration in the static and dynamic alignments of the lower limb (Guichet et al., 2003). Several previous studies have reported the association between the alteration of centre of pressure (COP) and post stroke gait (Chen et al., 2007, Chisholm et al., 2011, Nardone et al., 2009, Rodgers et al., 2004, Wong et al., 2004). As mentioned earlier, stroke patients usually show a supinated foot deformity. Increased foot supination will shift the centre of pressure (COP) laterally

(Lugade and Kaufman, 2014) followed by shifting the GRF farther laterally from the knee joint centre in the frontal plane and that could potentially increase the varus (or adduction) moment at the knee joint (Guichet et al., 2003). This in turn can contribute to increased risk of ligamentous laxity (lateral collateral ligament) and generate a varus knee deformity over time (NHS Quality Improvement Scotland, 2009). Thus, controlling the alignment of the supinated foot will lead to modifying the point of application of the GRF to be closer to the knee centre, which consequently reduces the varus moment at the knee joint (Schmalz et al., 2006).

2.5.4 The AFO alignment

As previously mentioned, AFO encompasses the ankle and the foot; consequently, the AFO directly controls the alignment and the movement of the ankle and foot, and indirectly controls the alignment and the movement of lower limb joints. Proper alignment of AFO is considered essential as it helps to control postural stability (Abe et al., 2009, Owen, 2010) and energy expenditure during gait (Bennett et al., 2012, Bregman et al., 2011, Condie and Meadows, 1993). The AFO alignment can be achieved during static alignment (“process whereby the bench alignment is refined while the prosthesis or orthosis is being worn by the stationary patient” (ISO, 1989)) and dynamic alignment (“process whereby the alignment of the prosthesis or orthosis is optimised by using observations of the movement pattern of the patient” (ISO, 1989)). It is generally accepted that proper alignment of a rigid AFO, and any other type of AFO, depends on the patient’s gait. This means that the proper alignment of the AFO is unique for each patient. Therefore, consideration must be given to align the AFO properly to produce a controlled and energy-efficient gait that meets the patient’s need. There are common guidelines that should be considered while aligning an AFO. Proper alignment of AFO requires a clear consideration of the ankle angle of the AFO, the AFO alignment in the shoes and the shank alignment in order to obtain the maximum effects from AFO (Eddison and Chockalingam, 2015, Fatone et al., 2009, Malas, 2011, Owen, 2004a, Owen, 2005a). These variables will be discussed further below.

➤ **The ankle angle of the AFO (AA-AFO)**

The ankle angle of the AFO (AA-AFO) is the angle between the shank section (calf shell) and the footplate of the AFO in the sagittal plane (Owen, 2005b), as illustrated in Figure 2.22. The AA-AFO is usually either described in degrees of dorsiflexion, plantarflexion, or plantargrade (at 90°) positions (Owen, 2005b). The AA-AFO was commonly set in plantargrade position regardless of the length of gastrocnemius. The dorsiflexion position was also acceptable, but not the plantarflexion position (Churchill et al., 2003, Gök et al., 2003, Hesse et al., 1996, Lehmann, 1979, Mulroy et al., 2010). It has been believed that setting the AA-AFO at 90° can always improve knee alignment during gait (Owen, 2010). However, the gastrocnemius muscle is a tri-articular muscle which crosses the knee, the ankle and the subtalar joints. It induces ankle plantarflexion and knee flexion (Jenkins et al., 2006). Hence, the available length of gastrocnemius will influence the range of motion (ROM) at the knee and ankle joints. The AA-AFO is determined by the available gastrocnemius length so that the AA-AFO should never prevent the knee from fully extending regardless of the ankle being in plantargrade or in a plantarflexion positions (Carse et al., 2011, Owen, 2005a). Spastic and/or short gastrocnemius can limit the dorsiflexion ROM at the ankle joint when the knee joint is fully extended or it can limit the knee extension ROM when the ankle is dorsiflexed (Owen). In the presence of gastrocnemius spasticity and if the AA-AFO was set at 90, the length of the gastrocnemius will be insufficient to allow full extension at the knee joint (Owen, 2005b). Thus, the required amount of knee extension during mid stance, terminal stance and terminal swing will be limited/prevented which in turn can badly affect knee and hip kinetics (Becher, 2002, Meadows et al., 2008, Owen, 2005b). The moment arms ratio of the muscle pull for the gastrocnemius at the knee and ankle joints was measured to be 1:2 during terminal stance (Stewart et al., 2004). For instance, in the presence of gastrocnemius muscle spasticity, 5 degrees increment of ankle dorsiflexion will lead to a reduction in knee extension by 10°. Thus, if the AA-AFO does not consider the gastrocnemius length, knee extension which is required to achieve stance stability can be limited (NHS Quality Improvement Scotland, 2009, Stewart et al., 2004). Therefore, it is essential to set the ankle angle of the AFO (AA-AFO) properly so that it meets the individual patient needs (Meadows et al., 2008, NHS Quality Improvement Scotland, 2009, Owen, Owen, 2005b). The AA-AFO must be considered during casting of the AFO to accommodate the

shortness and tone of gastrocnemius muscle (NHS Quality Improvement Scotland, 2009). Owen (2005b) has proposed an algorithm (Appendix A) for determining the optimum AA-AFO that has been recommended to be considered in AFO design for stroke patients (Bowers and Ross, 2010, NHS Quality Improvement Scotland, 2009).

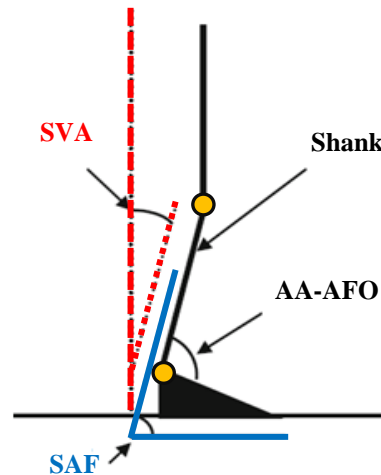


Figure 2.22: A diagram showing the ankle angle of the AFO (AA-AFO), the shank to vertical angle (SVA), and the shank to the floor angle (SAF). Adapted from (Malas, 2011).

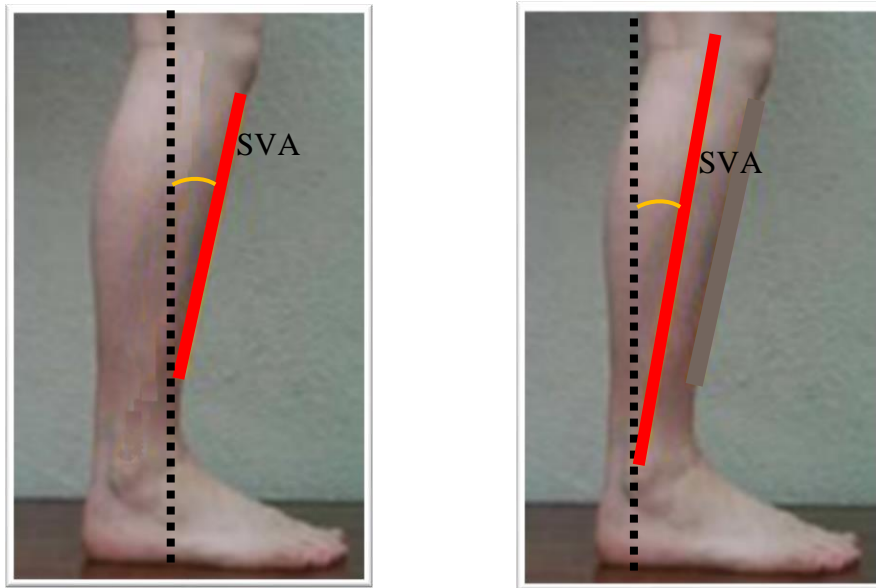
➤ Shank alignment

Several terms and measures have been used to describe the shank alignment. Firstly, the term “Foot-Shank Angle” was used to describe the angle between the shank and the foot (Hullin et al., 1992). Then the term “Shank Angle to Floor” (SAF) was used to express the angle between the shank and the floor (Owen, 2002), Figure 2.22. While the term “Shank to Vertical Angle” (SVA) is the most common term used to measure the shank alignment (Carse et al., 2015, Choi et al., 2016, Eddison et al., 2017, Kerkum et al., 2015b, Kessels et al., 2013, Meadows et al., 2008, Nguyen et al., 2020, Owen, 2010, Pratt et al., 2007). The SVA is the angle of the long axis of the shank relative to the imaginary line drawn perpendicular to the horizontal (see section 2.3.1 under the heading “Shank to vertical angle”), Figure 2.22. The SVA and SAF are described as inclined (leaning forward from the vertical), reclined (leaning backward from the vertical) or vertical (0° degree from the vertical) (Owen, 2002, Owen, 2010). Based on anthropometric measures,

10-12° of forward inclination of the SVA is considered as the optimal SVA required to align the knee joint centre directly above the middle of the foot (Choi et al., 2016, Tilley, 2001, Winter, 2009). This inclination facilitates the forward inclination of the thigh, pelvis, and trunk, and allows the COM to remain within the base of support and thus improves stance stability (Owen, 2010, Owen, 2016, Roelker et al., 2019).

Two methods were used to define the long axis of the shank, as illustrated in Figure 2.23. The first method is by using the anterior surface of tibia (the line extended between the tibial tuberosity and the anterior distal edge of tibia, or talus) (Kerkum et al., 2015b, Kessels et al., 2013). The second method by using the lateral surface of tibia (the line extended between the lateral epicondyle and lateral malleolus) (Choi et al., 2016, Owen, 2010, Owen et al., 2018). In a recent study (Nguyen et al., 2020), measuring the SVA using the anterior markers placement method showed $1.48 \pm 0.97^\circ$ greater inclination than the lateral markers placement method. This difference is expected due to the anatomical structure of the tibia; the anterior surface of tibia is more inclined than the lateral surface of tibia as illustrated in Figure 2.23. Measuring the SVA using the anterior markers placement method was more accurate and more repeatable than using lateral markers placement method (Nguyen et al., 2020). The presence of more soft tissue, tendons and muscles on the lateral surface of tibia compared to the anterior surface of tibia may affect the ability to accurately palpate the anatomical landmarks and place the markers precisely on these landmarks.

The SVA is considered to have a greater influence on gait than the ankle angle of the AFO (AA-AFO) (Jagadamma et al., 2010, Owen, 2005a). The effects of rigid AFO can be improved by small changes in the shank alignment (Hullin et al., 1992). A properly aligned shank can facilitate proper GRF alignment relative to knee and hip joint centres (Owen, 2005a). This leads to reducing the abnormal moments acting on knee and hip, decreasing knee hyperextension and decreasing hip flexion during stance phase (Choi et al., 2016, Kerkum et al., 2015b) thus, improving stability and spatiotemporal parameters of gait (Carse et al., 2015). Furthermore, the SVA was significantly associated with increased walking speed in stroke patients (Kerr et al., 2019). This will be discussed further in section 2.6 under the heading “Tuning of rigid AFO”.



(A) Anterior markers placement

(B) Lateral markers placement

Figure 2.23: Measuring the SVA using the anterior (A) and lateral (B) markers placement methods. The red and black lines represent the long axis of the shank and a vertical line, respectively. Adapted from (Kessels et al., 2013).

➤ **Role of shoes on the biomechanical effects of AFOs**

AFOs are used in conjunction with shoes. The characteristics of the shoes (stiffness, contour, the width of the heel and sole, and the height of the heel and sole) are important factors influencing the biomechanical alignment of AFOs (Condie and Meadows, 1993, NHS Quality Improvement Scotland, 2009, Owen, 2004a, Sungkarat et al., 2011). As aforementioned, the shoe has a vital part in the three-force system; it applies forces on the dorsum of the foot to prevent abnormal plantarflexion (Figure 2.19, A). The effective heel height of the shoes should be considered in aligning the AFO. The effective heel height, also known as heel sole differential, is defined as the difference in thickness between the heel and sole, as illustrated in Figure 2.24. The effective heel height of the shoes can influence the SVA and thus, alter the GRF alignment with respect to the ankle, knee, and hip joints (Condie and Meadows, 1993, Meadows et al., 2008, NHS Quality Improvement Scotland, 2009, Owen, 2005a). The stiffness of the heel also should be considered, as using too soft heel may be inadequate to contribute to the tibial progression, and the knee joint may be hyperextended (Kerkum et al., 2015b, NHS Quality Improvement Scotland,

2009, Owen et al., 2018). Moreover, additional shoe modifications can be helpful in some cases. For instance, adding a rocker sole can be used to increase the walking speed and to allow stance phase roll over given that ankle motion is restricted (Farmani et al., 2016b, Owen, 2004a). Using a flare heel (extending the heel width medially or/and laterally) on the other hand can improve the mediolateral stability of the heel (NHS Quality Improvement Scotland, 2009).

Consequently, to achieve the optimal effects of the AFO, the influence of both the AFO and the shoe designs/characteristics on manipulating the GRF point of application, magnitude, and line of action must be considered in orthotic prescription (Meadows et al., 2008, NHS Quality Improvement Scotland, 2009, Owen, 2005b, Owen, 2010). To emphasize the importance of the shoes on orthotics prescription and to consider the AFO and the shoe as a single unit, the term “AFO footwear combinations (AFO-FCs)” has been recommended to be used in the clinical notations (Condie and Meadows, 1993, Condie, 2008, NHS Quality Improvement Scotland, 2009, Owen, 2005a). Owen (2005b) has proposed an algorithm (Appendix A) for determining the optimum AFO-FCs that has been recommended to be considered in AFO design for stroke patients (Bowers and Ross, 2010, NHS Quality Improvement Scotland, 2009).

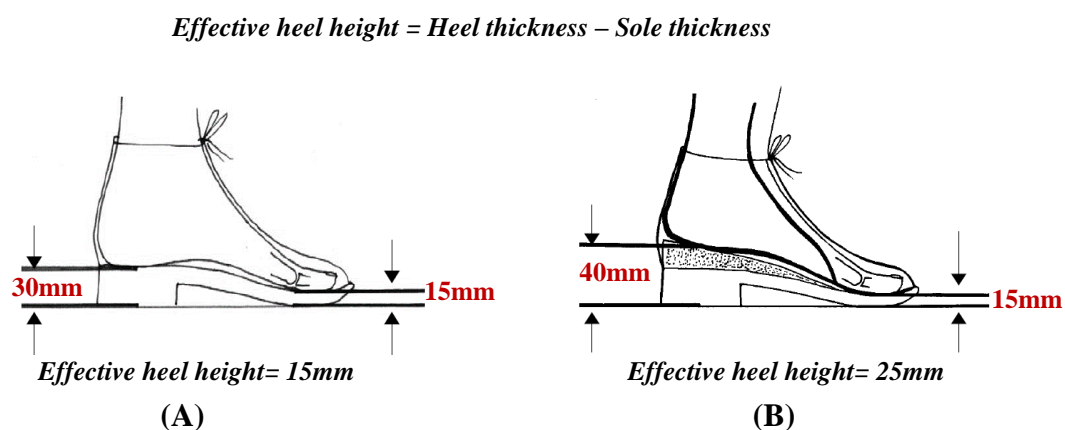


Figure 2.24: Measuring the effective heel height by measuring the difference between the heel thickness of the shoe and the sole thickness (A), and with additional heel (B). Adapted from (Owen, 2005a).

In summary, to achieve the optimal effect of rigid AFO-FCs; the AA-AFO should be set at an adequate ankle angle based on the gastrocnemius length (NHS Quality Improvement

Scotland, 2009, Owen, 2005b), the shank should be realigned to manipulate the GRF alignment to be as close as possible to the knee and hip joint centres during mid and terminal stance (Meadows et al., 2008, NHS Quality Improvement Scotland, 2009, Owen, 2005a) (Figure 2.21), and the shoes should be modified, if necessary, to fit the individual patient need (NHS Quality Improvement Scotland, 2009, Owen, 2004a).

2.6 Tuning rigid AFOs

Tuning a rigid AFO involves fine adjustment of the AFO-FCs to optimise the alignment of the GRF relative to the knee and hip joints during gait (Meadows et al., 2008, Owen, 2004b, Owen, 2010). This can be achieved by modifying the height, type or/and design of the heel, or/and the rocker type (Butler and Nene, 1991, Meadows et al., 2008, Owen, 2004b, Owen, 2010). GRF alignment has been recommended to be used as the key parameter for the tuning process (Bowers and Ross, 2010, Butler and Nene, 1991, Carse et al., 2015, Meadows et al., 2008, Owen, 2004b). As discussed earlier, changing the alignment of the GRF to be as close as possible to the joint centre so that it passes anterior to the knee and posterior to the hip during mid and terminal stance can increase stance stability (Meadows et al., 2008, NHS Quality Improvement Scotland, 2009). In normal gait, stance stability (in mid to terminal stance) is achieved by forward inclination of the thigh and the shank (SVA=10-12° in mid stance) in order to facilitate the GRF alignment to pass anterior to the knee joint centre and posterior to the hip joint centre, as illustrated in Figure 2.25 (A) (Owen, 2005a, Perry and Burnfield, 2010). This highlights the importance of considering the GRF alignment during mid to terminal stance while wearing a rigid AFO. A rigid AFO is designed to restrict/prevent the motion of the shank over the foot. Lack of the required forward inclination of the rigid AFO will lead to a lack of the required forward inclination of the tibia during mid stance which in turn can badly affect the stance stability. Consequently, rigid AFO tuning is essential (Condie and Meadows, 1993, Meadows et al., 2008, Owen, 2005a).

Investigating the SVA while wearing rigid AFO in mid stance is considered as the key starting point for optimising the alignment of the GRF relative to the knee and hip joints (Bowers and Ross, 2010, Jagadamma et al., 2010, Kessels et al., 2013, Owen, 2002, Owen, 2004b). With a vertical SVA (Figure 2.25, B), the GRF is aligned anterior to the hip and knee joint centres, unless the knee hyperextends (Figure 2.25, C), which is not

desirable (Bowers and Ross, 2010). Optimising the GRF alignment requires the SVA to be 10-12° inclined during mid stance (Owen, 2010). This can be achieved by altering the effective heel height through adding wedges under the heel (heel raise) as required (Meadows et al., 2008, Owen, 2004b, Owen et al., 2018), Figure 2.25 (D and E). The SVA in mid stance was significantly increased with increasing the effective heel height (Kerkum et al., 2015b, Owen et al., 2018). Additionally, knee and hip flexion angles and the internal knee extension moment in mid stance were also increased significantly with increasing the effective heel height (Kerkum et al., 2015b, Kessels et al., 2013). The SVA is very sensitive to small changes in the effective heel height. In adults, adding 5 mm heel wedge will increase the inclination of the SVA by 2°, and will move the knee and hip joint centres forward approximately 17 mm and 30 mm, respectively (Meadows et al., 2008) as shown in Figure 2.26. Consequently, a small alteration in the SVA may significantly change the kinematic and kinetic parameters of the knee and hip joints (Kerkum et al., 2015b, Owen et al., 2018). Tuning a rigid AFO may be performed gradually over a period of several weeks (Choi et al., 2016, Jagadamma et al., 2010) or non-gradually in one session (Carse et al., 2015, Kessels et al., 2013). The benefits and drawbacks of each way were not mentioned. Additionally, the reasons behind using either of these ways were not clarified. Nevertheless, it is expected that some patients may need time to adapt to the tuning.

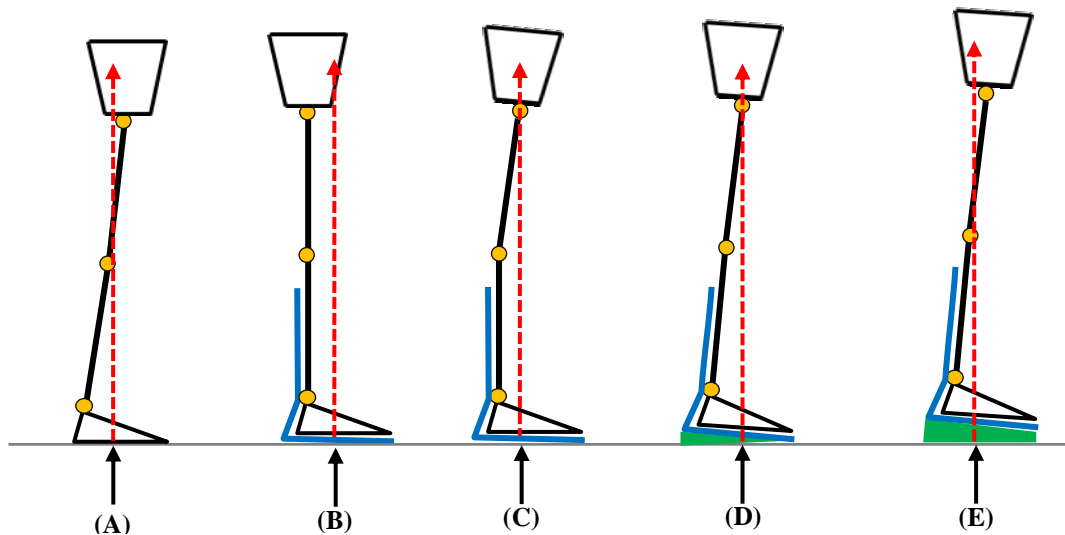


Figure 2.25: The effects of tuning a rigid AFO on the GRF alignment during mid stance. Normal GRF alignment without AFO (A). The GRF alignment with a vertical SVA without (B) and with knee hyperextension (C). The GRF alignment with forward inclined SVA by progressively adding wedges under the heel (D and E). The red dashed line represents the GRF. Adapted from (Meadows et al., 2008).

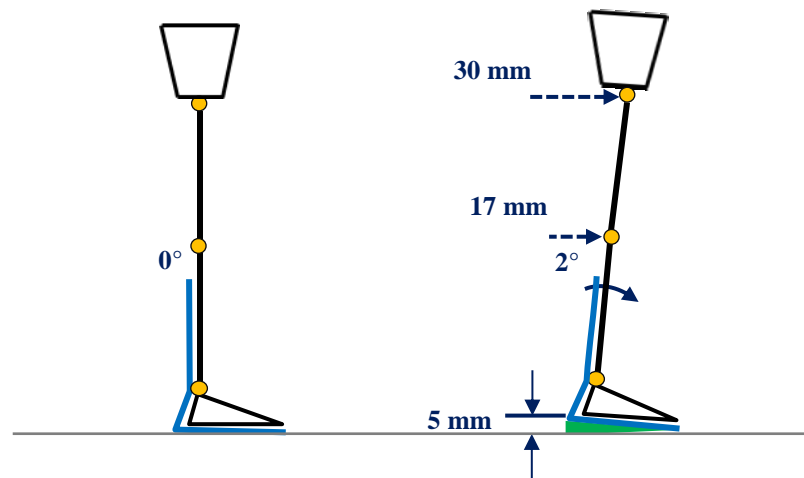


Figure 2.26: The effects of tuning on the SVA, knee, and hip joints. Adapted from (Meadows et al., 2008).

Although tuning rigid AFOs has been considered as an essential procedure of clinical practice (Eddison and Chockalingam, 2015, NHS Quality Improvement Scotland, 2009), the success of tuning process depends on the patient's physical characteristics (Owen et

al., 2004). Several factors may limit the success of tuning such as the inability to passively extend the hip and/or the knee fully (or almost fully) during walking due to insufficient musculotendinous length or excessive joint stiffness (Owen et al., 2004). Furthermore, the success of tuning also relies on the orthotist who should be fully understanding the process of tuning and its aims. In a cross-sectional survey study, only 50% of the registered orthotists in the UK who participated in the study (41 orthotists) performed tuning AFO as a standard clinical practice (Eddison et al., 2015). Although the vast majority of the orthotists (95%) indicated that they know about tuning, their responses in the study showed lack of thorough understanding of it. Based on the orthotists' response, several factors made tuning AFOs impossible, as illustrated in Figure 2.27. The most frequently mentioned factor was the lack of access to 3D gait analysis system (37%). This factor indicates that the orthotists lack thorough understanding of tuning process as it can be achieved by several other methods such as video recording and 2D gait analysis. The second frequently mentioned factor was the long time required to complete the tuning (27%). This may be the result of unclear literature regarding tuning process or inappropriate training of these orthotists (Eddison et al., 2015).

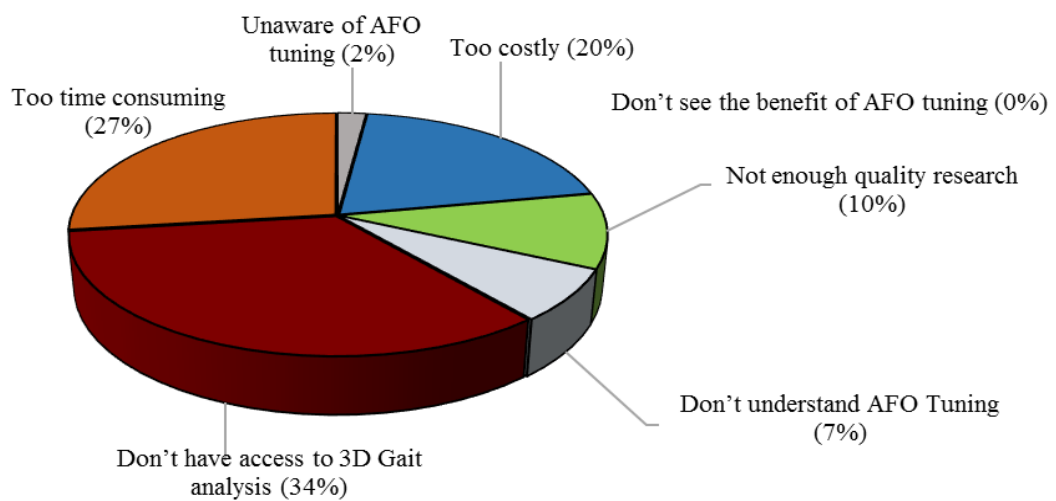


Figure 2.27: Factors preventing orthotists from using AFO tuning. Adapted from (Eddison et al., 2015)

2.7 The efficacy of rigid AFOs on post stroke gait parameters

Several publications including systematic reviews have been published to quantify the effects of using different types of AFOs on gait parameters of stroke patients (Daryabor et al., 2018, Ferreira et al., 2013, Leung and Moseley, 2003, Padilla et al., 2014, Shahabi et al., 2020, Tyson et al., 2013, Tyson and Kent, 2013). The temporal-spatial, joint kinematics and kinetics, energy expenditure, muscle length, and activity parameters were investigated. The findings of these parameters were varying and inconclusive. The varying results may be due to the different participants' characteristics that are often not fully described in the literature. As mentioned earlier, the gait impairments following stroke are different from one patient to another, making variability in the studies expected and demanding extreme care when interpreting the results. Using several types/designs of AFO (rigid, PLS, HAFO, and GRAFO) may also explain the varying results in the literature. The current study is investigating the effects of rigid AFOs on the gait parameters of stroke patients, and thus, other AFO types will not be considered in this section. A few variations were also found in the gait parameter outcomes when stroke patients were fitted with rigid AFOs. These variations may be considered to be the result of the variation in the rigid AFO characteristics in the literature such as the AA-AFO, material type and thickness, trimlines, and shoe types. Additionally, most studies have not considered tuning rigid AFOs (Farmani et al., 2016b, Gatti et al., 2012, Geboers et al., 2002, Zollo et al., 2015) or have not fully described the tuning process (Farmani et al., 2016a) which may have affected the studies' outcomes and making comparison among them difficult. Although the Healthcare Improvement Scotland has recommended tuning rigid AFOs in order to achieve optimal effects (NHS Quality Improvement Scotland, 2009), none of the previous mentioned systemic reviews considered tuning AFOs as an evaluation criterion. While acknowledging the variability amongst the studies, attempts are made to identify the influence rigid AFOs have on gait parameters and draw conclusions. Some studies have compared the effects of rigid AFOs to a baseline condition on post stroke gait. The baseline was either barefoot condition (Farmani et al., 2016a, Kesikburun et al., 2017) or wearing shoes condition (Carse et al., 2015, Gatti et al., 2012, Geboers et al., 2002, Zollo et al., 2015). Other studies have compared the effects of rigid AFOs with other types of AFOs (Choi et al., 2016, Mulroy et al., 2010, Zollo et al., 2015). A summary of the studies investigating the effects of wearing rigid AFO on

stroke patients (as some studies were not mentioned in the aforementioned systemic reviews) is described in Table 2.3.

The effects of using AFOs on balance and stability have been assessed using the Berg Balance scale (BBS) (Tyson and Kent, 2013). The BBS is a standardized measure of functional balance, used to assess balance during 14 static and dynamic tasks relevant to activities of daily living (e.g. walking, sit to stand, sitting and standing unsupported). The BBS score ranges from 0 to 4 for each task (total score ranging from 0 to 56), with the higher score indicating improved balance (Berg et al., 1989). The effect of rigid AFOs on balance is an issue of debate. Two studies reported the effect of rigid AFOs on balance when stroke patients wore a rigid AFO as compared to the no wearing AFO condition. One study did not find any improvement in the BBS score (with off-the-shelf AFO the BBS score was 51 ± 4.9 , without AFO the score was 51 ± 4.9) (Wang et al., 2005), while the other study reported significant improvement in the BBS (with custom made rigid AFO the BBS score was 48.0 ± 4.8 , without AFO the score was 46.2 ± 5.59) (Simons et al., 2009). The improvement in the BBS may be due to the external stability of the ankle joint provided through the AFO that, in turn, improves the ability of transferring weight to the affected side (Marigold and Eng, 2006). The contradictions in the results of these two studies may be due to using different designs of rigid AFOs and/or different reactions and responses among patients upon wearing the AFO. Both studies did not describe whether optimising (tuning) the AFOs alignment was considered in their methodology.

Several systematic review studies have investigated the effects of several types of AFOs, including rigid AFO, on temporal-spatial parameters (Daryabor et al., 2018, Ferreira et al., 2013, Leung and Moseley, 2003, Padilla et al., 2014, Shahabi et al., 2020, Tyson et al., 2013, Tyson and Kent, 2013). Walking speed has been reported to increase significantly while wearing an AFO compared to a baseline (shoes or barefoot without the use of an AFO) condition. Additionally, the time required to complete a 10 metre walk (Simons et al., 2009) or to perform several mobility tasks such as walking 5 metres on various surfaces, climbing up and down stairs, standing up from chair, walking 3 metres, and returning to seated position (Sheffler et al., 2006) was found to be less with wearing an AFO; which is again reflecting the improvement of walking speed. However, the improvement of walking speed remained limited and the walking speed remained slower than normal walking speed and it may be considered clinically insufficient (less than 0.8

m/s) to accomplish the basic community walking activities based on the classification by Perry et al. (1995), which used walking speed to predict the clinically meaningful community walking status of stroke patients as follows: household walking (<0.4 m/s), limited community walking (0.4–0.8 m/s), and full community walking (> 0.8 m/s). Furthermore, the differences in walking speed with and without rigid AFOs was greater in acute stroke patients than in chronic stroke patients (Rao et al., 2008, Wang et al., 2005, Wening et al., 2009), as exemplified in Figure 2.28. For instance, in Wening et al.'s (2009) study, walking speed was increased from 0.36 to 0.45 m/s in acute stroke group and from 0.54 to 0.61 m/s in chronic stroke group. In the chronic stroke group, the improvement in walking speed with the delay of using AFOs may indicate that gait recovery had already taken place so that the improvement of walking speed when finally using the AFO would be expected to be smaller. Although the improvement in walking speed was statistically significant for both acute and chronic stroke groups, these improvements were considered as clinically insufficient (less than 0.16m/s). In contrast, several studies reported that the improvement in walking speed in stroke patients was clinically significant ($\geq 0.16\text{m/s}$) with wearing different designs of AFO, including rigid AFOs compared to without AFO (Bethoux et al., 2014, Kluding et al., 2013, Rao et al., 2008). The walking speed was clinically significantly increased with tuned rigid AFO (SVA12°: 0.66m/s, SVA15°: 0.59m/s) compared to PLS (0.26m/s) or shoes only condition (0.20m/s) (Choi et al., 2016). Also, using rigid AFO (SVA 15°) reduced the stance time from 88% to 76% of the gait cycle as compared to shoes only condition (Choi et al., 2016).

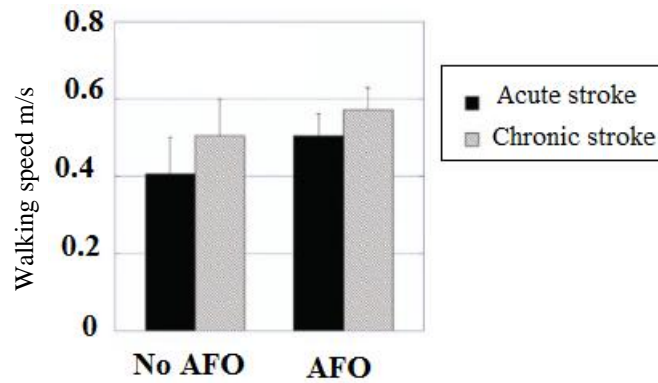


Figure 2.28: Walking speed variation during walking with and without rigid AFO in acute and chronic stroke groups. Adapted from (Rao et al., 2008).

Cadence and step/stride length were also investigated with and without wearing different designs of AFO, including rigid AFOs. The systematic review and meta-analysis by Tyson and Kent (2013) (9 trials and 144 stroke participants) showed significant increase of step/stride length and cadence of the affected limb, demonstrating that stroke patients had a longer step/stride length when using an AFO compared to not wearing an AFO. Furthermore, a positive correlation was found between walking speed and cadence (Esquenazi et al., 2009, Rao et al., 2008, Wening et al., 2009). Gok et al. (2003) compared the effect of wearing rigid AFO and metal AFO among 12 acute stroke patients on temporal-spatial parameters during walking. The walking speed and cadence were significantly greater with metal AFO (0.41 ± 0.16 , 67.3 ± 17.5 steps/min, respectively), due to its stiffness, compared to rigid AFO (0.37 ± 0.14 , 65.0 ± 19.2 steps/min, respectively). On the other hand, no significant difference was found in walking speed and cadence when comparing walking with rigid AFO and articulated AFOs (dorsiflexion assist and plantarflexion stop) (Mulroy et al., 2010).

A recent systematic review (Daryabor et al., 2020), using different designs of AFO, including rigid AFOs, showed that energy expenditure can immediately improve during walking in stroke patients (15 trials involving 195 participants). However, there were insufficient studies to assess the long-term effect of using AFO or comparing the effects of AFO designs on energy expenditure.

Although several studies investigated the effects of tuning AFO among cerebral palsy patients, only few published studies attempted to examine the impact of tuning AFOs on gait parameters among stroke patients. A single case study was performed on a chronic stroke patient during walking with a rigid AFO (Jagadamma et al., 2010). Four conditions were tested in this study, walking with non-tuned AFO (SVA 0°), partially tuned AFO (SVA 12°), tuned AFO (SVA 14°), and the tuned AFO (SVA 14°) after three months (visit 2). In this study, knee flexion angle increased at initial contact with partial tuned AFO (18.3°), immediate (17.9°) or after three months (19.4°) tuned AFO compared to non-tuned AFO (8.1°). In mid stance, the maximum reduction in knee hyperextension was achieved with the tuned AFO decreasing from 12.7° (non-tuned) to 0.1° immediately after tuning. Additionally, the external knee flexion moment peak at mid stance increased after tuning, while the external knee extension moment peak at terminal stance decreased after tuning. Knee flexion angle during swing on the other hand did not improve (Jagadamma et al., 2010). A previous study performed on 9 chronic stroke patients showed similar results regarding no improvement of the knee flexion angle at swing phase (Cruz and Dhaher, 2009). However, another study performed on 10 chronic stroke patients found significant improvement in the knee flexion peak at swing phase (Gatti et al., 2012) when walking with AFO compared to no AFO (Figure 2.29). The difference between these two studies may be due to variation in the design of the AFOs used and in participants' impairments. In the study by Gatti et al. (2012), all the 10 stroke patients were fitted with rigid AFOs, and were provided with standard shoes with zero effective heel height, the AA-AFO was set at 90°, while 3 rigid and 6 articulated AFOs were used in the study by Cruz and Dhaher (2009). Additionally, although two types of AFO (rigid and articulated) were used in the study by Cruz and Dhaher (2009), the result outcomes were based on sample mean omitting the individual analysis response for each AFO type. Furthermore, both studies did not describe whether optimising (tuning) the AFOs alignment was considered in their methodology. The rigid AFO showed the greatest improvement on the knee flexion angle (at initial contact and during loading response) and the external knee extension moment compared to articulated AFO with dorsiflexion assist, articulated AFO with plantarflexion stop, or with baseline (shoes only) (Mulroy et al., 2010), as shown in Figure 2.30.



Figure 2.29: The peak knee flexion angle during walking with rigid AFO and without AFO (barefoot) among 10 chronic stroke patients. Adapted from (Gatti et al., 2012).

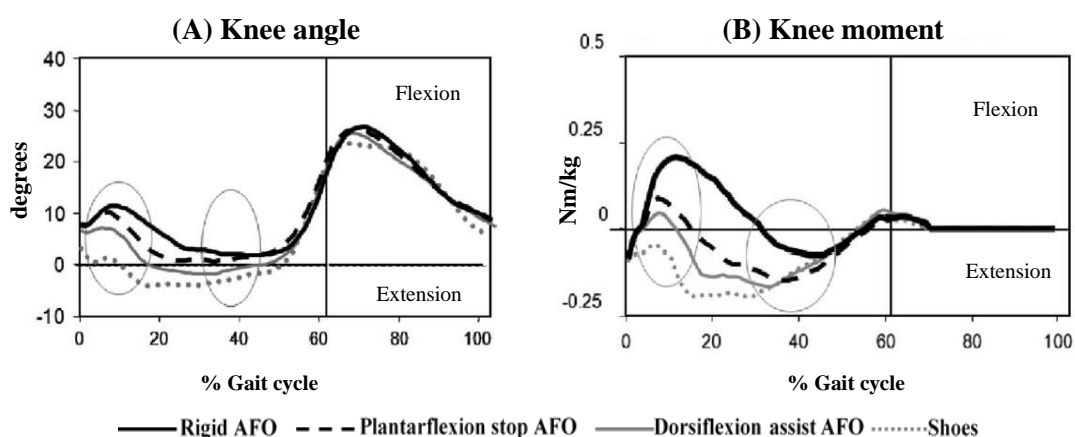


Figure 2.30: The sagittal knee angle (A) and the sagittal knee external moment (B) for stroke patients with moderate plantarflexion contracture during walking with different types of AFO and with shoes only. The vertical line represents the end of stance phase (toe off). The knee flexion at initial contact and loading response increased in the rigid AFO. While the knee extension angle decreased in rigid AFO as compared to shoes only condition. In rigid AFO, the knee flexion moment increased during loading response, and the knee extension moment decreased during terminal stance. Adapted from (Mulroy et al., 2010).

In a case study (Choi et al., 2016), four different conditions were investigated during three visits; off-the-shelf PLS AFO (in the first visit), custom made rigid AFO with 15° of SV

after tuning (second visit, after 5 months of wearing the rigid AFO), re-tuned the rigid AFO with 12° of SVA (third visit, 1 month later), and shoes only (third visit). The results of Choi et al. (2016) study demonstrated that the hip, knee, and ankle motions were improved with tuned rigid AFO (SVA 12° or SVA 15°) as compared to PLS or shoes only conditions. Altering the alignment of the SVA from 15° to 12° increased the peak knee flexion from 30.4° to 36.5° during swing and increased the hip flexion from 14.1° to 18.8° at initial contact. Additionally, this reduction in the SVA also increased the internal ankle plantarflexion moment and decreased the internal knee extension moment and internal hip flexion moment during terminal stance. This highlights that slight adjustments in the SVA alignment may have a great impact on gait parameters. As the tested conditions in the study by Choi et al. (2016) were investigated at different sessions, the results of gait parameters may have been influenced by carryover effects between test sessions. However, tuned rigid AFO (SVA 12°) showed an improvement of gait parameters as compared to shoes only condition and both were investigated at the same testing session (third visit).

A study by Carse et al. (2015) involving 8 stroke patients fitted with tuned rigid AFOs, found immediate improvement in walking speed, cadence and step length compared to walking with shoes only. However, no clear conclusions were found in hip and knee motions. The SVA after tuning ranged from 6.2° to 16.4°, indicating that the optimal tuning may have not been accomplished for all participants. The participants were early stroke patients, mean time from stroke was 3.5±3 weeks, so they were quickly exhausted during testing. Consequently, the number of inserted wedges to achieve the optimal SVA alignment (10°-12°) was restricted, as wedges were applied gradually.

Farmani et al (2016a) compared the effects of rigid AFO, rigid AFO with a rocker bar (forefoot rocker) and barefoot walking (Figure 2.31). The thickness of the rocker bar was 20 mm and located proximal to the metatarsal heads. The rocker bar was attached to the rigid AFO foot plate. The spasticity in the gastrocnemius and soleus was recorded with a maximum grade score of 2 in Modified Ashworth Scale among all participants. The AA-AFO was set for all 18 stroke participants at 90° without mentioning/linking this to the available length of gastrocnemius. Furthermore, the rigid AFOs were not tuned. Both walking with rigid AFO or rigid AFO with a rocker bar significantly increased the walking speed, cadence, and step length as compared to barefoot walking ($p < 0.05$).

Additionally, walking with rigid AFO with a rocker bar significantly increased hip extension and knee flexion by 10° and 9°, respectively at toe off compared to AFO without rocker bar or barefoot conditions ($p < 0.05$). The pre swing time and the plantarflexion peak angle in pre swing parameters were measured to evaluate the improvement in forefoot rocker. Both the pre swing time and the plantarflexion peak angle in pre swing were significantly decreased when walking with rigid AFO with a rocker bar compared to AFO without rocker bar or barefoot conditions ($p < 0.05$). This was considered as a positive result of using the forefoot rocker on improving push off, thus facilitating the forward fall of the body weight over the leg also assist in stance stability. Although the study highlights the effects of using rocker bar on temporal-spatial and kinematic parameters of stroke patients, no attempt was made to clarify the reasons behind using this specific thickness of rocker bar (and the effective heel height) for all participants.

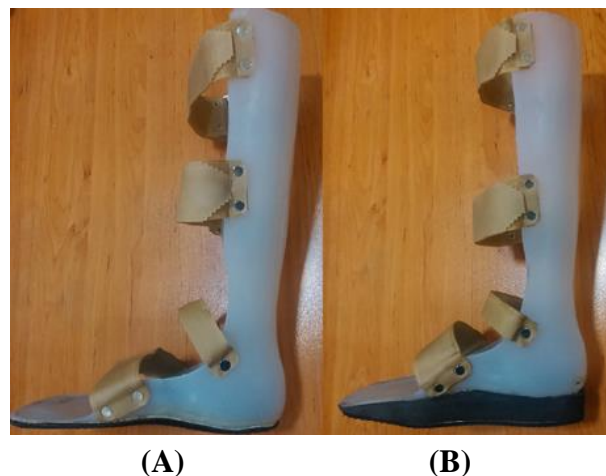


Figure 2.31: The rigid AFO (A) and the rigid AFO with rocker bar that were used in the Farmani et al (2016a) study. Adapted from (Farmani et al., 2016a).

Although several studies have investigated the impact of using AFOs on temporal-spatial parameters (Daryabor et al., 2018, Ferreira et al., 2013, Leung and Moseley, 2003, Padilla et al., 2014, Shahabi et al., 2020, Tyson et al., 2013, Tyson and Kent, 2013), few have considered the impact of using AFOs on muscle activity (Leung and Moseley, 2003). In a systemic review (Leung and Moseley, 2003), only four studies were found identifying the influence of using various AFO designs, all not including rigid AFOs, on different

muscle group during walking. The authors concluded that the overall evidence from these studies is not adequate to draw conclusions about the impact of using AFOs on muscle activity due to the vast variation of the participants' characteristics and AFO types/designs, making the studies' findings difficult to generalise (Leung and Moseley, 2003). A recent systemic review conducted by Daryabor et al. (2018) showed that since the time of the Leung and Moseley review (2003), only five additional studies have investigated the influence of using AFOs on muscle activity with only two of these attempting to evaluate the effects of rigid AFOs on muscle activity (Mulroy et al., 2010, Zollo et al., 2015). Mulroy et al. (2010) compared the muscle activity of the tibialis anterior, soleus and vastus intermedius muscles during walking with a custom made rigid AFO, dorsiflexion assist AFO (articulated AFO), plantarflexion stop AFO (articulated AFO) and shoes only, among 30 chronic stroke patients. The ankle angle of the three AFO types was adjusted to neutral (90°) or 5° of dorsiflexion to accommodate the varying heel heights of the participants' shoes regardless of the length of gastrocnemius. No significant differences in the muscles' activity of the three tested muscles were found between walking with rigid AFO or with shoes only. Walking with the plantarflexion stop AFO increased the activity of soleus (48% of maximum manual muscle test value (MMT)) compared to rigid AFO (30% MMT), dorsiflexion assist AFO (30% MMT) or shoes only (32% MMT). The activity of tibialis anterior was significantly decreased when walking with the plantarflexion stop AFO (8% MMT) compared to rigid AFO (16% MMT), dorsiflexion assist AFO (16% MMT) or shoes only (16% MMT). The activity of the vastus intermedius did not change among walking with different AFO types or with shoes only.

In the study by Zollo et al. (2015), the authors compared the effects of using off-the-shelf AFO with heel opening (the authors considered them as off-the-shelf rigid AFO), a dynamic AFO (made from carbon fibre with anterior shell) and with no AFO (shoes only) on the co-contraction of the tibialis anterior-lateral gastrocnemius and rectus femoris-biceps femoris muscles among 10 stroke patients during walking at self-selected walking speed. Although no significant differences were found among the three tested conditions, the dynamic AFO showed close to normal pattern and led to a decrease in the co-contraction of the two couples of muscles than rigid AFO. Both studies (Mulroy et al.,

2010, Zollo et al., 2015) have made no attempt to optimise (tuning) the AFOs alignment, which may limit the benefits from the AFOs.

Tuning an AFO may aid in reducing the effects of gastrocnemius contracture and spasticity on gait parameters by reducing the operating length of the gastrocnemius (Choi et al., 2016). The muscle's operating length is the length of the muscle from origin to insertion during movement (Arnold et al., 2001). In a case study (Choi et al., 2016), the operation length of the gastrocnemius (medial head), tibialis anterior and biceps femoris (long head) was estimated using an open-source musculoskeletal modelling and simulation software platform (Delp et al., 2007). The results of Choi et al. (2016) study demonstrated that the tuned rigid AFO (12° or 15° of SVA) increased peak biceps femoris operating length (close to the normal estimated pattern), increased the peak tibialis anterior operating length and reduced the peak gastrocnemius operating length compared to PLS AFO or shoes conditions (Figure 2.32).

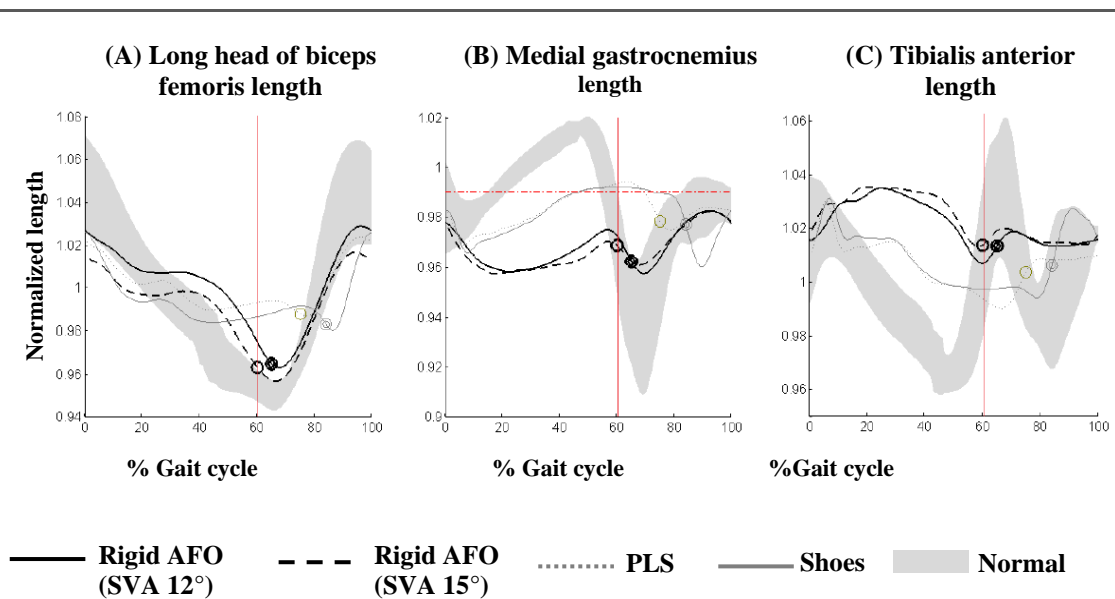


Figure 2.32: Muscle operation length of the long head of biceps femoris (A), medial gastrocnemius (B) and tibialis anterior (C) during walking with different conditions. The muscle operation length of each muscle was normalized to the muscle length in the anatomical position. The vertical line and circles represent the end of stance phase (toe off). The horizontal red dotted line in (B) represents the length of the gastrocnemius at maximum ankle dorsiflexion with the knee extended during clinical examination. Adapted from (Choi et al., 2016).

Table 2.3: Summary of research studies that investigated the effects of rigid AFOs on temporal-spatial, kinematics, kinetics, and EMG parameters of stroke patients.

| Author | Design and participants | Intervention | Tuning process | Outcome measures and key findings |
|---------------------------------|-----------------------------------------------------------------------------------------------------------------------------------------------------------------------|------------------------------------------------------------------------------------------------------------|--------------------------------------------------------------------|-------------------------------------------------------------------------------------------------------------------------------------------------------------------------------------------------------------------------------------------------------------------------------------------------------------------------------------------------------------------------------------------------------------------------------------------------------------------------------------------------------------------------------------------------------------------------------------------------------------------------------------------------------------------------------------------------------------------|
| Kesikburun et al. (2017) | One session: within-subject comparison. 28 chronic stroke patients able to walk without assistance. Mean age: 43.2±15.9 years. Mean time from stroke: 8.4±2.3 months. | Custom made thermoplastic rigid AFO. | Tuning: not reported | Walking speed: Significantly increased when walking with an AFO compared to barefoot condition ($P < 0.001$). Ankle kinematics: Ankle dorsiflexion angle at initial contact and mid swing significantly increased when walking with an AFO compared to barefoot condition ($P < 0.001$). |
| Farmani et al. (2016a) | Randomised block design. 18 chronic stroke patients able to walk without assistance. Mean age: 57.8±10.44 years. Mean time from stroke: 25.31±16 months. | Custom made thermoplastic (3mm thick) rigid AFO with and without rocker bar attached to the AFO footplate. | AA-AFO: 90°. Using a rocker bar (20 mm thick) | Temporal-spatial parameters: Significant increases in walking speed, cadence, and step length when walking with AFO and rocker bar AFO compared to barefoot condition ($P < 0.05$). Knee and hip kinematics: The AFO with rocker bar significantly increased hip extension and knee flexion at toe off compared to AFO without rocker bar or barefoot conditions ($P < 0.05$). |
| Choi et al. (2016) | Case study. One left side stroke patient with short gastrocnemius (10° of dorsiflexion at 90° knee flexion). Age 56 year. Time from stroke: 11 months. | Off-the-shelf PLS, tuned rigid AFO (SVA 12° and SVA 15°) and shoes only. | AA-AFO: 8° plantarflexion. The rigid AFO was tuned SVA 12° and 15° | Muscle operation length: Tuned rigid AFO reduced the operation length of the gastrocnemius, tibialis anterior and increased the operation length of biceps femoris compared to PLS or shoes conditions. Walking speed: Significant increase in walking speed when walking with tuned rigid AFO compared to PLS or shoes conditions. Joint kinematics: Hip, knee, and ankle motions were improved with tuned rigid AFO compared to PLS or shoes conditions. Joint kinetics: In comparison to the PLS or shoes conditions, tuned rigid AFO decreased internal plantarflexion moment at early stance and increased it at terminal stance. Increased the internal knee extension |

Table 2.3/continued

| | | | | |
|-----------------------------|--------------------------------------------------------------------------------------------------------------------------------------------------------------------------------------------------------------------------------------------------------|-----------------------------------------------------------------------------------------------------------------------------------------------|-----------------------------------------------------------|-----------------------------------------------------------------------------------------------------------------------------------------------------------------------------------------------------------------------------------------------------------------------------------------------------------------------------------------------------------------------------------------------------------------------------------------------------------------------------------------------------------------------------------------------------------------------------------------------------------------------------------------------------------------------------------|
| | | | | moment peak at terminal stance. Increased internal hip extension moment at initial contact and terminal stance. |
| Carse et al. (2015) | Randomised controlled trial. 8 early stroke patients able to walk with assistance but had difficulty flexing knee and extending hip during gait. Mean age: 57±16 years. Mean time from stroke: 0.83±0.7 month. | Custom made thermoplastic rigid AFO compared to shoes condition | Tuned by heel wedges | <p>Temporal-spatial parameters: Significant improvement in walking speed, cadence, and step length ($P < 0.05$) with AFO compared to shoes condition.</p> <p>Joint kinematics: No clear changes were found in hip and knee kinematic.</p> |
| Zollo et al.(2015) | Randomised crossover trial. 10 chronic stroke patients, able to walk without assistance. Mean age:64.3 years. Mean time from stroke: 11-205 months. | Off-the-shelf rigid AFO (with a heel opening) compared to dynamic AFO (made from carbon fibre and has an anterior shell) and shoes condition. | Tuning: not reported | <p>Temporal-spatial parameters: Significant increase in walking speed, cadence, and step length when walking with AFOs compared to shoes only condition. No significant differences among the two AFOs.</p> <p>Joint kinematics: Both AFOs reduced ankle dorsiflexion/plantarflexion during stance compared with shoes condition. No significant differences in the knee and hip joint motion when walking with AFOs compared to shoes condition.</p> <p>Muscles activity: The rigid AFO led to an insignificant increase of co-contraction of the 2 couples (tibialis anterior-lateral gastrocnemius and rectus femoris-biceps femoris) during walking.</p> |
| Mulroy et al. (2010) | Randomized controlled trials. 30 chronic stroke patients without (n:9) and with (n:21) moderate ankle plantarflexion contracture, able to walk without assistance. Mean age: 58.3year (36-78 year). Mean time from stroke: 25.3 months (5–127 months). | Rigid AFO, articulated AFOs (dorsiflexion assist, and plantarflexion stop), and shoes condition | AA-AFO: 90° or 5° of dorsiflexion Tuning: not reported | <p>Joint kinematics: Ankle dorsiflexion at initial contact, loading response and mid swing and knee flexion at initial contact and loading response were significantly increased in all three AFOs compared to shoes only. Knee extension was decreased at mid to terminal stance with rigid AFO. No significant differences were found in the peak knee flexion at swing phase among the tested conditions.</p> <p>Joint kinetics: Ankle plantarflexion moment in loading response was greatest in the rigid AFO, intermediate in the plantarflexion stop and dorsiflexion assist AFOs, and lowest in shoes only. The rigid AFO showed</p> |

Table 2.3/continued

| | | | | |
|-----------------------------|--------------------------------------------------------------------------------------------------------------------------------------------------------------------------------------------------------------------------------------------------------------------------------------------------------------------------------------------------|----------------------------------------------------------------------------------------------------------------------------------------------|-------------------------------------|-----------------------------------------------------------------------------------------------------------------------------------------------------------------------------------------------------------------------------------------------------------------------------------------------------------------------------------------------------------------|
| | | | | the greatest knee flexion moment at loading response and the lowest knee extension moment in terminal stance. Muscles activity: No significant differences were found in the muscle activity of the vastus intermedius, tibialis anterior, nor soleus when walking with rigid AFO or with shoes only. |
| Simons et al. (2009) | Randomized controlled trials. 20 chronic stroke patients able to walk without assistance. Mean age: 57year (36-78 year). Mean time from stroke: 39 months (5–127 months). | Patients wear their own AFOs (Rigid AFO, PLS AFO, and plastic AFO with a heel opening and articulated metal AFO) compared to shoes condition | Tuning: not reported | Balance (Berg Balance Scale): significantly improved when walking with AFOs compared to shoes condition (P < 0.05). Walking speed: significantly increased when walking with an AFO (P < 0.05). |
| Wang et al.(2005) | Randomized controlled trials. 42 acute stroke patients (<6 months duration). Mean age: 59±13 years. Mean time from stroke: 3.4±1.7 months. 61 chronic stroke patients (6-12 months duration). Mean age: 62±12 years. Mean time from stroke: 34.7±36.8 months. Able to stand without support for 1min and walk 10m with an assistive device | Off-the-shelf thermoplastic rigid AFOs compared to no AFO condition (Not stated whether barefoot or shoes) | AA-AFO: 90° Tuning: not reported | Balance (Berg Balance Scale): No significant differences were found when walking with an AFO compared to no AFO condition (P > 0.005) for both stroke groups (<6 and (6-12) months durations). Walking speed and cadence: significantly increased when walking with an AFO (P < 0.05) for both stroke groups (<6 and (6-12) months durations). |

2.8 AFO stiffness

2.8.1 AFO stiffness definition and measurement techniques

“Stiffness is a term used to describe the force needed to achieve a certain deformation of a structure” (Baumgart, 2000). In biomechanical studies, stiffness of the AFO is defined as the load divided by the AFO deformation (Baumgart, 2000). The load can be force, moment, or stress and the deformation can be strain, displacement or angle (Baumgart, 2000, Kobayashi et al., 2011, Totah et al., 2019).

Several techniques were used to measure AFO stiffness, however, no attempts have been made to compare between these techniques (Kobayashi et al., 2011, Totah et al., 2019). The stiffness of an AFO has been measured either by computational (typically finite element analysis) or mechanical techniques. The mechanical techniques vary between bench and functional methods. In the bench methods, the AFOs were attached/fixed to a specific custom-made device designed to measure stiffness. Several methods have been used to assess stiffness during bench testing including tensiometer (DeToro, 2001, Golay et al., 1989, Sumiya et al., 1996), a dial micrometre (Polliack et al., 2001, Ross et al., 1999), a strain gauge or a load cell (Bregman et al., 2009, Bregman et al., 2010, Cappa et al., 2005, Nagaya, 1997), a force plate (Novacheck et al., 2007), a BIODEX muscle training machine (Yamamoto et al., 1993a, Yamamoto et al., 2005), and a tensile testing machine (Braund et al., 2005, Major et al., 2004). In the functional methods, the AFOs stiffness was measured, during walking, using a strain gauged AFO (Chu and Feng, 1998, Papi et al., 2015) or an experimental AFO (Kobayashi et al., 2017, Miyazaki et al., 1997, Yamamoto et al., 1993b) in conjunction with gait analysis.

Various factors can determine the AFO stiffness such as material type, material thickness, AFO trimlines, AFO geometry and the ankle joint types in articulated AFOs (Convery et al., 2004, Kobayashi et al., 2011, Major et al., 2004). The non-articulated AFO stiffness level can generally be adjusted by altering its trimlines, materials, or exchanging its components (Kobayashi et al., 2011, Miyazaki et al., 1997, Sumiya et al., 1996). For instance, adding a carbon fibre reinforcement at the ankle region of the AFO or more forward AFO trimlines lead to an increase in the AFO stiffness, as illustrated in Figure 2.17 (Bielby et al., 2010, Major et al., 2004).

2.8.2 Impact of AFOs stiffness on post stroke gait parameters

The impact of AFO stiffness on gait parameters was also investigated in the literature. The effectiveness of the AFOs to reduce energy cost and to improve gait parameter is stiffness dependent (Bregman et al., 2011, Totah et al., 2019). In order to achieve the optimal effects of the AFO, the stiffness of the AFO should also be considered (NHS Quality Improvement Scotland, 2009, Totah et al., 2019). As aforementioned, both alignment and mechanical characteristics of AFO are important factors in order to achieve the optimal functional performance of the AFO (Bowker et al., 1993, NHS Quality Improvement Scotland, 2009, Totah et al., 2019, Tyson et al., 2013). Furthermore, changing the joint alignments of an articulated AFO showed significant effects on the stiffness of the AFO (Gao et al., 2011). Setting the ankle joint in the articulated AFO to be aligned at the same level of the anatomical ankle joint showed the lowest stiffness level compared to other joint alignments (10mm superior, inferior, anterior, and posterior with respect to the anatomical ankle joint) (Gao et al., 2011).

Bregman et al. (2010) demonstrated that low stiffness AFO (0.19Nm/degree) was adequate to control the ankle joint at neutral position during swing phase in patients with plantarflexion deformity, however, no effects on ankle motion was found during stance phase. Additionally, another study (Kobayashi et al., 2016) performed by increasing articulated AFO stiffness individually on 6 stroke patients (ranging from 1.98Nm at 0° to 20.35 Nm at 20° of plantarflexion) investigated the effects on ankle and knee parameters and revealed a unique response for each participant. This finding indicates that AFO stiffness should be adjusted to meet the patients' individual impairment in order to obtain the optimal effect from the AFO.

A recent systematic review (Totah et al., 2019) reviewed the influence of AFO stiffness in 25 studies including different sample groups (e.g. healthy, stroke, cerebral palsy), in a variety of AFO types/designs on several gait parameters. The review concluded that ankle and knee kinematics changed significantly with alteration of the AFO stiffness level. Increasing the AFO stiffness decreases ankle range of motion (dorsiflexion and plantarflexion) and increases knee flexion angle during stance, suggesting that patients with hyperextended knee should be fitted with a stiffer AFO. Five studies reported that AFO stiffness did not affect peak plantarflexion moment nor the dorsiflexion moment

(Collins et al., 2015, Esposito et al., 2014, Harper et al., 2014, Kerkum et al., 2015a, Telfer et al., 2012). In contrast, three studies reported that internal dorsiflexion moment in stroke patients was significantly increased with increasing the AFO stiffness (Kobayashi et al., 2019, Kobayashi et al., 2016, Yamamoto et al., 1993b). The contradicting results can be explained by the different participants' aetiology, and the different AFO type and design. There is a low evidence of the impact of stiffness on other gait parameters such as, temporal-spatial, knee kinetics, hip kinetics and kinematics, GRF, and energy expenditure. The varying techniques used to measure AFO stiffness, the variation among the measured outcomes, and the different participants' characteristics made drawing a conclusion about the influence of AFO stiffness on walking performance difficult.

2.9 Orthotic moment measurement techniques

Orthotic moment, or AFO moment, or resistive moment, can be defined as the moment exerted by the AFO around the ankle joint (Kobayashi et al., 2017, Kobayashi et al., 2015, Papi et al., 2015, Yamamoto et al., 1993b). Consequently, orthotic moment is the moment generated by the mechanical properties of the orthosis to resist/assist motions around the ankle. These motions can be elicited by external (GRF) or internal (soft tissue) forces. Based on mechanical properties of the AFO, the orthotic moment during walking can be derived from the stiffness and the angle of the AFO (Bregman et al., 2010). Due to the vast variation of aims and methods among the AFO stiffness studies, this section will focus only on those studies that are considered to be most relevant to the topic of this thesis. The AFO stiffness is usually measured via determining the AFO resistance to sagittal plane rotation, demonstrated by moment -ankle angle or moment -deflection relationships (Kobayashi et al., 2011, Totah et al., 2019). Most of these methods put an inaccurate assumption that external forces and ankle joint moment are resisted solely by the orthosis. This is not true as soft tissues of the ankle, and the activity and/or the stiffness of the calf muscles may contribute in assisting/resisting these external forces and moments actively or passively (Miyazaki et al., 1993). Measuring the orthotic moments during walking is considered as a key criterion for the current study. The orthotic moment has an important role in assisting post stroke gait (Kobayashi et al., 2019, Kobayashi et al., 2016, Yamamoto et al., 1993b). In a non-articulated AFO, the orthotic moment can

be in the form of plantarflexion resistive moment (which resists moving the ankle in a plantarflexion direction) and dorsiflexion resistive moment (which resists moving the ankle in a dorsiflexion direction) (Kobayashi et al., 2015). Thus, the magnitude of the orthotic moment may have a significant contribution on ankle motion, and therefore potentially on knee and hip motion, in stroke patients. A few studies have investigated the orthotic moment during walking (Bregman et al., 2010, Kobayashi et al., 2017, Papi et al., 2015). However, the contribution of the AFO in improving gait parameters in stroke patients is still not clear.

Bregman et al. (2009) developed an AFO testing apparatus called BRUCE (Bi-articular Reciprocating Universal Compliance Estimator, Figure 2.33) in order to measure the AFO stiffness using force sensors. The BRUCE consists of a dummy of the human leg and foot with mechanical joints (hip, knee, ankle and metatarsal phalangeal (MTP)) in order to imitate human gait. The location of the axis of the joint centres was assembled based on the anatomical anthropomorphic data. Ankle dorsiflexion/plantarflexion (-10° - 20°) and MTP flexion/extension (0° - 30°) can be manually applied to deform the AFO. Six dummy feet with different foot lengths ranging from 175 to 300mm were manufactured in order to accommodate the variety of AFO sizes that could be measured. The AFO is non-destructively secured into the device with two clamps (Figure 2.33), but without providing total contact between the AFO and the device. The BRUCE was considered as a reliable method to measure the AFO stiffness around the ankle and MTP joints. The orthotic moments for 7 participants (multiple sclerosis and stroke) during walking were then calculated based on the mechanical characteristics driven from the BRUCE bench testing (Bregman et al., 2010). The study involved two types of AFOs; 4 PLS AFOs and 3 AFOs trimmed posterior to the malleoli with dorsal notches for flexibility. Regardless the AFO types, all AFOs were made from polypropylene material. It was found that the orthotic moment contributes only about 13.7% of the total ankle moment (total moment about the ankle joint measured by a force plate and gait analysis system). This small contribution of orthotic moment may be related to the flexible AFO types involved in the study, as the mean measured stiffness was 0.19 Nm/deg. The method is considered as simple, easy to be applied, and can be performed without destroying the AFO. However, the AFO is not totally contacting the device which may be considered as a limitation of the BRUCE as this is not presenting the actual interface between the AFO

and participant's leg. Additionally, the reliability of the results was found to be dependent on the testers. Furthermore, measuring the orthotic moment using an experimental AFO would provide more precise results than using indirect method totally based on the stiffness values determined during bench testing.

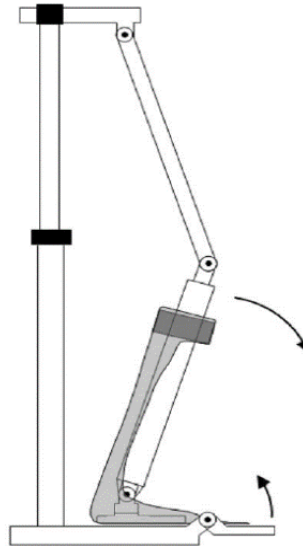


Figure 2.33: A schematic drawing of the BRUCE developed by Bregman et al. (2009). Plantar/dorsiflexion motion at the ankle and flexion/extension at MTP joint are shown by the two arrows. Note: The two clamps are not shown in the figure. Adapted from (Bregman et al., 2009).

Kobayashi et al. (2017, 2015) studied the contribution of the orthotic moment during walking on a treadmill for 10 stroke patients. The authors used an articulated AFO (the authors considered them as off-the-shelf AFO) with adjustable plantarflexion resistive moment (Figure 2.34, A). Initially, a bench test was performed in order to measure orthotic moment using a custom automated device (Figure 2.34, B) that was developed in a previous study (Gao et al., 2011). The plantarflexion resistive moment was adjusted under 4 different spring (S1, S2, S3 and S4) conditions. The S1 condition represented the baseline condition where no steel spring was installed on the AFO with the minimum level of plantarflexion resistive moment. While the level of the plantarflexion resistive moments in S2, S3 and S4 conditions were adjusted to be gradually increased so that the maximum level was in S4 condition (Figure 2.35). Increasing the plantarflexion resistive moment showed significant decreases in the peak ankle plantarflexion angle during

loading response (Figure 2.35, B), in the peak knee extension angle (Figure 2.35, C), and in the internal knee flexion moment (Figure 2.35, D) during terminal stance ($p < 0.01$). Additionally, the internal dorsiflexion moment of the ankle joint was significantly increased with increased plantarflexion resistive moment ($p < 0.01$). Consequently, increasing the plantarflexion resistive moment induced the ankle angle in more dorsiflexion and the knee angle in more flexion throughout the gait cycle (Figure 2.35, C). However, the AFO used in this study was an off-the-shelf AFO, not custom made AFO, thus, the AFO may not provide appropriate intimate fit and an accurate control for the patient's pathology. Furthermore, although the sample size was small (10 stroke patients), the result outcomes were based on sample mean omitting the individual analysis response for each patient.

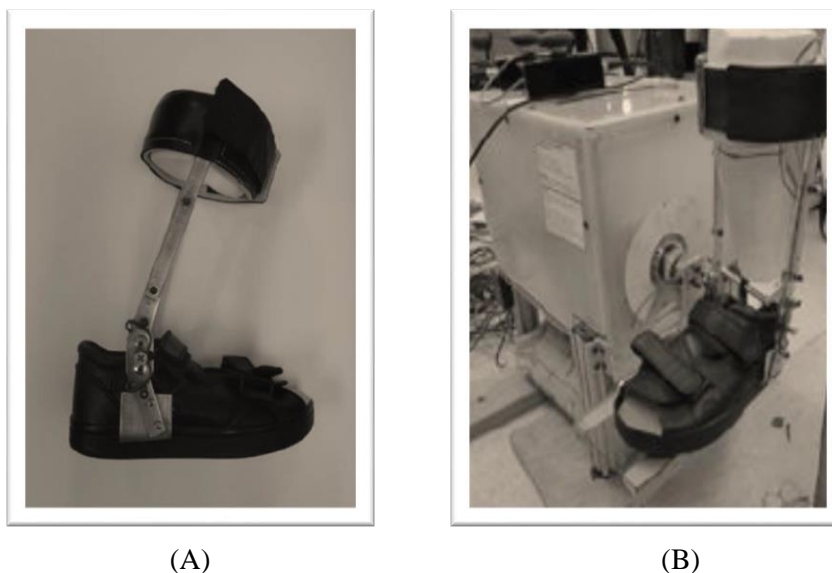


Figure 2.34: The articulated AFO (A) and the bench testing (B) of the articulated AFO used in Kobayashi et al. (2017) study. Adapted from (Kobayashi et al., 2017).

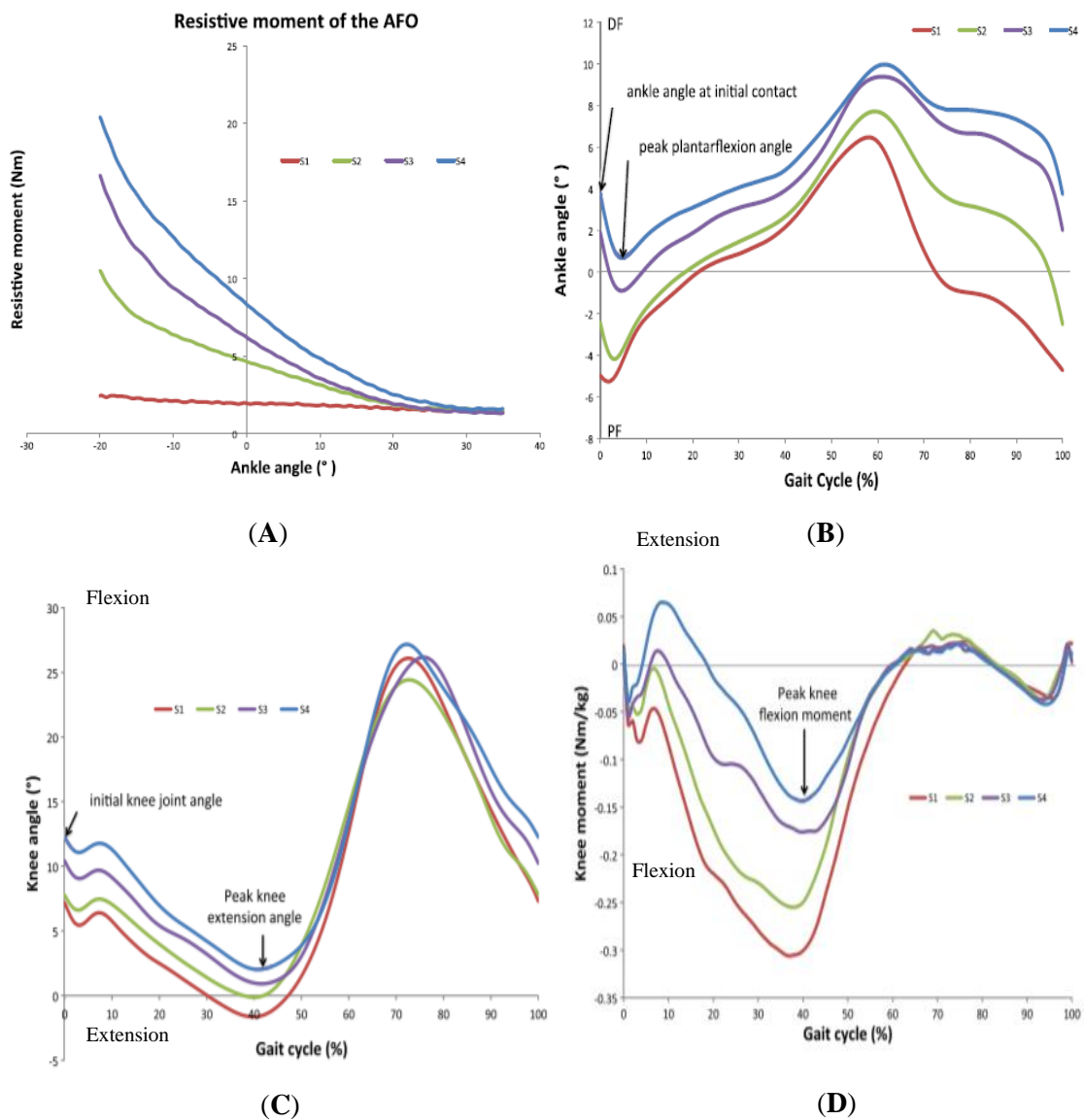


Figure 2.35: The ankle angle-plantarflexion resistive moment relationship of the articulated AFO during bench testing (A) used in Kobayashi et al. (2017) study. The effects of changes in plantarflexion resistive moments on the mean ankle joint angles (B), on the mean knee joint angle (C), and on the internal knee moment (D). Adapted from (Kobayashi et al., 2017).

As mentioned previously, strain gauges have also been used to measure the orthotic moment during walking. The strain gauge (SG) is an electrical sensor that is used to measure strain, as illustrated in Figure 2.36 (Hoffmann, 2012). The SG has a fine metal foil used to measure changes in electrical resistance that occurs due to a change in the applied force, pressure, tension, strain, etc. Using SG offers a high accuracy and

repeatability results (Hoffmann, 2012). Chu and Feng (1998) introduced using SGs on polypropylene (plastic) AFO. However, polypropylene is an inert material that cannot be bonded/adhered easily to any other materials. The authors suggested using ultraviolet (UV) light in the preparation of polypropylene surface prior to attachment of SGs. The UV light can break the surface molecular bonding so that the other material can be bonded without causing any change of its proprieties (Papi, 2008).

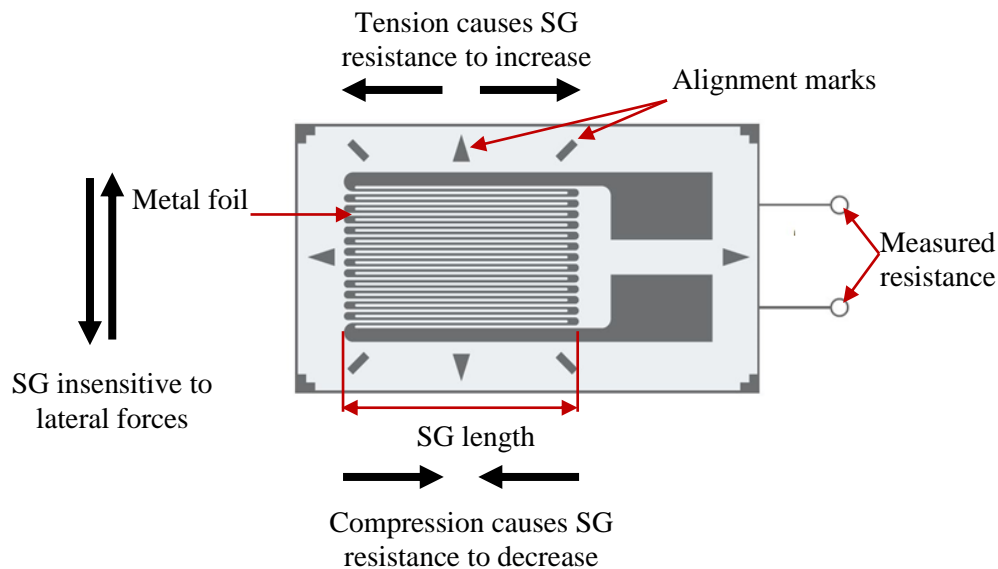


Figure 2.36: A schematic drawing of the strain gauge (SG). The resistance increases with tension forces and decreases with compression forces. While the SG resistance remains unchanged with lateral (shear) forces. The alignment marks are used as a guide to properly attach the SG on the tested material. Adapted from (Hoffmann, 2012).

Chu and Feng (1998) used SGs to measure the stress distribution on the AFOs during walking. Eight SGs were attached at different locations on five different non articulated polypropylene AFO designs (Figure 2.37). The peak stress concentration in the AFOs was significantly different among the AFO designs. Each AFO showed a specific stress concentration during walking. For example, the peak stress in the rigid AFO was concentrated at 20-30mm above the narrowest place in the ankle area of the AFO. While the peak stress in PLS AFO was concentrated at the narrowest place in the ankle area of the AFO and at 20-30mm below. The aim Chu and Feng's (1998) study was to measure

the stress concentration during walking and no attempts were made to measure the gait parameters.

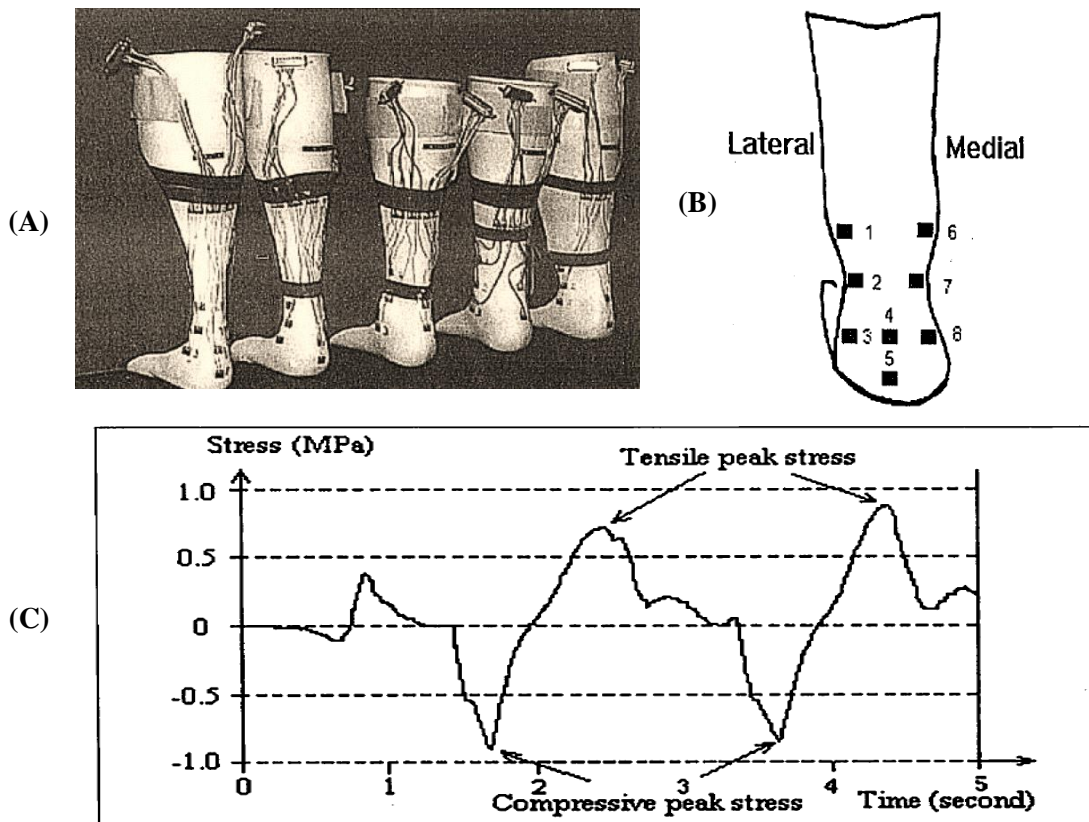


Figure 2.37: The strain gauged AFOs used in Chu and Feng (1998) study (A). The five AFOs are (from left) PLS, Standard, Moderate, Rigid, and Varus AFOs. A schematic view of the SGs location on the AFO (B). An example of the SG output (SG number 2) during walking. Adapted from Chu and Feng (1998).

A study by Papi et al. (2015) successfully measured the orthotic moment exerted by a rigid homopolymer polypropylene AFO around the ankle joint during walking in a healthy participant. The authors attached two types of SGs (two two-element parallel and 45° three-element rosette SGs) on the AFO at the ankle area as illustrated in Figure 2.38. Papi et al. (2015) also used UV light in order to facilitate attachment of the SGs on the polypropylene plastic material. However, the SGs manufacturer company of their study has not mentioned/recommended using UV light in the preparation of plastic surface prior to attachment of SG (VISHAY, 2008). The two two-element parallel SGs were attached at the inside and outside surface of the AFO calf shell just 35mm above the malleoli level

(Figure 2.38, level A). The two two-element parallel SGs were connected to create a full Wheatstone bridge circuit. Wheatstone bridge is an electrical circuit used to measure an unknown electrical resistance by connecting it with three known resistances. The 45° three-element rosette SG was attached on the posterior aspect of the AFO at the malleoli level (Figure 2.38, level B). Each element of the 45° three-element rosette SG was arranged in a quarter Wheatstone bridge configuration and connected to three resistors to complete a full Wheatstone bridge circuit. A static calibration (bench) test was then conducted on the strain gauged AFO to investigate the linearity of the SGs response. The strain gauged AFO was clamped from the foot section in a position to produce dorsiflexion and plantarflexion moments at the ankle (Figure 2.38). A hanger was attached perpendicular to the proximal calf section of the AFO creating a lever arm of 260mm from the ankle joint (Figure 2.38). The calibration was started without any mass added. Masses of 1 Kg were then added onto the hanger to a maximum of 4 Kg (39.2N) on intervals of 30 seconds each. Afterwards, the hanger was unloaded by 1 kg every 30 seconds. The two two-element parallel SGs showed a non-linear stress/strain relationship on the strain gauged AFOs (B and C, Figure 2.39). Thus, the results from the two-element parallel SGs were not further used in the study. The curvature of the AFO, where the SGs were attached, caused the Wheatstone bridge to be unbalanced, which led to the observed non-linear behaviour of the SGs' outputs. This could be overcome by using a different set up of SGs' positions on the AFO where the shape is identical for each SG. This, however, is not promising due to the geometry of the AFO. The three-element 45° rosette SG on the other hand showed a linear stress/strain relationship on strain gauged AFO (Figure 2.39, A), within the linear region of homopolymer polypropylene (0-7 MPa) (Papi et al., 2015). Using a quarter Wheatstone bridge configuration for each element of the three-element 45° rosette SG could eliminate the AFO's geometry problem, and the need to find two identical positions on the AFO. The moments generated by the load were then calculated by multiplying the loads applied by the distance (260 mm) between the point of load application (the hanger) and the axis of the ankle joint. The resulting moments were plotted against the SG outputs for dorsiflexion and plantarflexion to generate the regression equation which was then used to calculate the orthotic moment. The results obtained from the 45° three-element rosette SG during walking displayed a consistent and good repeatability across the analysed steps as shown in Figure 2.40. Thus, using a strain

gauged AFO data combined with gait analysis can be used to measure the orthotic moment during walking. However, performing the static calibration manually may increase the risk of errors and mistakes, and it is a time-consuming procedure. Furthermore, the rate of adding/removing masses may not be accurate through the calibration test as it is difficult for a human tester to apply the masses at regular intervals of time. The viscoelastic nature of the homopolymer polypropylene (the material of which the AFO was made in this study) that involves molecular movement and rearrangement when a stress is applied (creep), is a time-dependant (Crawford and Martin, 2019), thus this needs to be considered during the static calibration. The aim of the Papi et al. (2015) study was to introduce a new method for measuring the orthotic moment rather than studying the orthotic moment itself, and thus further research regarding orthotic moment is recommended.

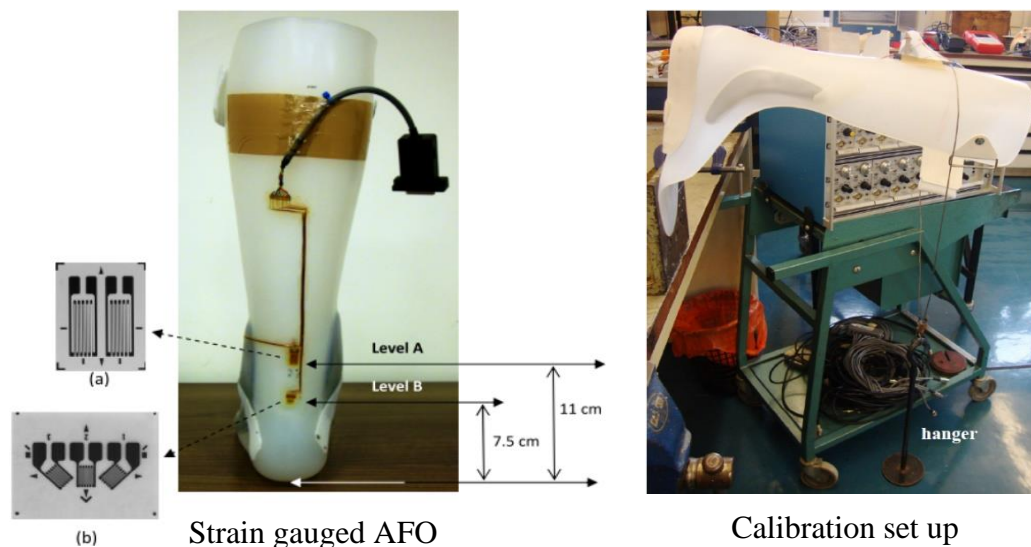


Figure 2.38: The strain gauged AFO used in the study by Papi et al (2015). Two types of SGs were used; two-element parallel SGs (a), the picture shows only the SG attached on the outer surface of the AFO, and 45° three-element rosette (b). The SGs were attached on the posterior aspect of the AFO at the malleoli level (level B) and at level A (35mm above level B). The right picture shows the plantarflexion static calibration test, and for the dorsiflexion static calibration test, the AFO is reversed by 180°.

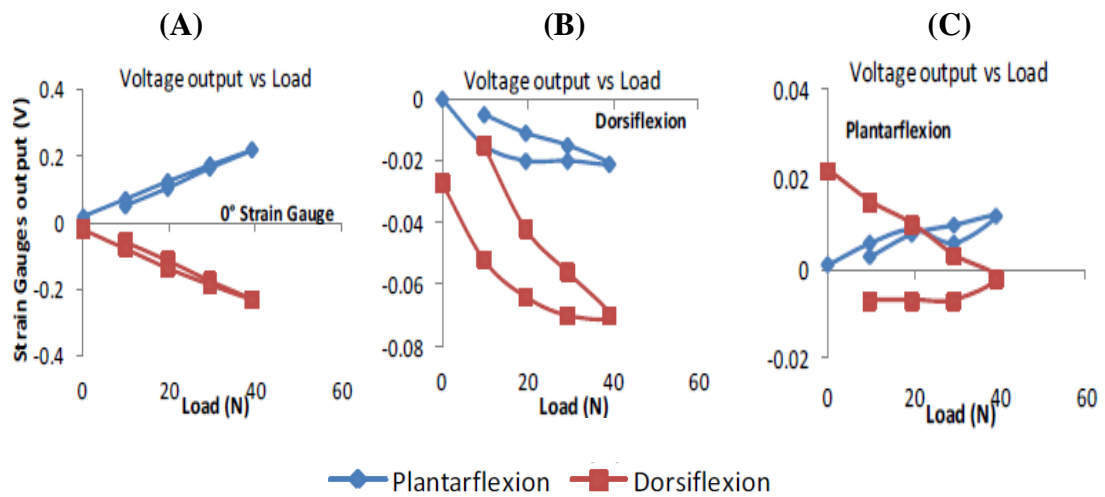


Figure 2.39: SGs outputs against load for static AFO calibration of the 45° three-element rosette (the vertical SG element (0°) only) SG in dorsiflexion and plantarflexion (A), and the two two-element parallel SGs in dorsiflexion (B) and plantarflexion (C). Adapted from (Papi, 2012).

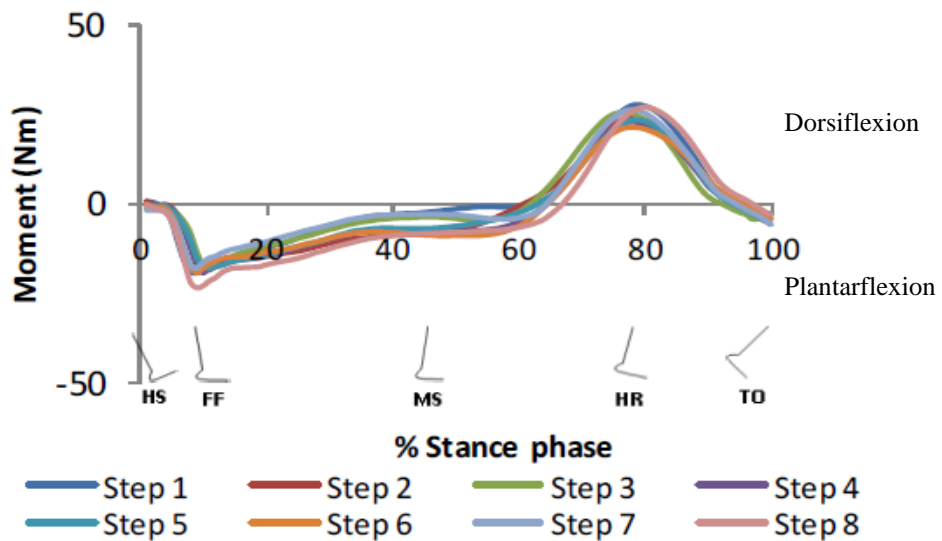


Figure 2.40: The orthotic moment measured in a rigid AFO during walking in the study by Papi et al. (2015). Adapted from (Papi, 2012).

2.10 Literature considerations

Overall, there is a strong evidence that the ankle-foot impairments greatly contribute to post stroke gait dysfunction. As reviewed in sections 2.7, 2.8 and 2.9, the quality of evidence supporting application of AFOs to improve gait function is affected by significant limitations. Most studies involved a small sample size and provided insufficient information about the participants characteristics. Additionally, the studied parameters were frequently reported based on sample mean of the parameter (which is based on a limited number of trials), however, for heterogenous populations, such as stroke patients, the mean results may be misleading because of the uncertainty about whether all patients had the same response to the AFO. Thus, individual analysis response for each patient may be more meaningful in order to understand individual responses to the AFO.

Furthermore, several studies provided insufficient details on the AFO characteristics such as; AA-AFO, material properties, AFO trimlines, AFO stiffness, and shoe characteristics. Noticeably, most of the literature on AFO did not consider tuning of the AFOs in order to optimise the biomechanical effects of the AFOs. There is a lack of published evidence on the consequence of AFO tuning in stroke patients. Most of the published studies focus on the impact of AFOs on temporal-spatial and knee joint kinematics and kinetics with a limited number of studies investigating the hip joint kinematics and kinetics. Also, none of the studies has focused on comparing the effects of tuning on knee muscle activation patterns during walking. A better understanding of how AFOs alter the gait performance of individuals with stroke will improve the prescription procedure so that it is based on biomechanical principles rather than reliant on subjective judgements and orthotist experience.

Furthermore, none of the studies has considered investigating the effects of tuning on the orthotic moment. Altering the orthotic moment in non-articulated AFOs during real walking may not be applicable without changing the AFO trimlines and material characteristics. Therefore, it may be ideal to investigate the contribution of the non-articulated AFO before and after tuning during walking. To the author's knowledge, the effects of tuning a rigid AFO (or any other non-articulated AFOs) on the orthotic moment have not been evaluated.

The main purpose of prescribing an AFO is to provide appropriate control of unwanted motion in any plane. As mentioned earlier, stroke patients usually show equinovarus deformity which is considered as a multiplanar deformity (Kinsella and Moran, 2008, Reynard et al., 2009). The rigid AFO is prescribed to manage equinovarus deformity. This highlights the importance of evaluating the AFO contribution in other than the sagittal plane (dorsi/plantarflexion) in order to demonstrate how effectively the rigid AFO can manage inversion/eversion and supination/pronation along with evaluating the plantarflexion/dorsiflexion. To the author's knowledge, no attempt has been made to measure the orthotic moment of a rigid AFO in frontal plane during walking.

2.11 Aims and objectives

The study aims to investigate the differences in gait characteristics between three conditions; standard shoes only (SSO), rigid AFO before tuning (AFO), and rigid AFO after tuning (Tuned-AFO). This comparison was carried out during walking on a treadmill and in two separate groups (control participants and stroke patients). Additionally, the study aims to measure the orthotic moment in the sagittal and frontal planes and to compare the effects of tuning a rigid AFO on the orthotic moment. The study focused on the following parameters:

- 1) Kinematic data in the sagittal plane: ankle motion, knee motion, hip motion, and SVA.
- 2) Kinetic data: vertical GRF (GRFv), ankle sagittal plane moment, knee sagittal plane moment, and hip sagittal plane moment.
- 3) Temporal-spatial parameters: speed, stride length, stance and swing time.
- 4) EMG data: EMG amplitude and activation period of quadriceps and hamstring muscles.
- 5) Orthotic moment in the sagittal and frontal planes.

❖ Hypotheses:

Hypothesis 1: Rigid AFO immediately improves gait parameters (temporal-spatial, kinematics, kinetics, and knee muscles' EMG) of stroke participants during walking on a treadmill.

Hypothesis 2: Tuning a rigid AFO immediately optimises gait parameters (temporal-spatial, kinematics, kinetics, and knee muscles' EMG) of stroke participants during walking on a treadmill.

Chapter 3 Methods

3.1. Design of the methods

The study was of within-subject comparison design, where all participants were exposed to every study condition or test. It was not possible to make this study blind, since the treatment conditions were easily recognisable by the participants and investigator. Each participant was randomised to a sequence of three conditions (Standard Shoes Only (SSO), AFO with standard shoes, and Tuned-AFO with standard shoes) during walking on treadmill (this will be discussed further in section “3.4.3 Gait laboratory testing procedure”) following the randomisation plan (www.randomization.com) (Appendix B).

3.2. Participants

3.2.1 Control participants

The Biomedical Engineering Departmental Ethics Committee, University of Strathclyde approved this part of the study (DEC/BioMed/2018/240) to recruit a baseline group for comparison. The participants were recruited within the Department of Biomedical Engineering at the University of Strathclyde, where the department administrative staff distributed an e-mail invitation on behalf of the researchers to the students and staff in the Department of Biomedical Engineering.

The inclusion criteria for control participants were:

- ✓ Over 18 years of age
- ✓ Good general health condition (have no musculoskeletal, cardiovascular, neurological, skin conditions or conditions affecting balance).
- ✓ No pre-existing condition or injury that may likely influence the performance of test activities (e.g. hip or knee flexion contracture, ankle plantar/dorsiflexion contractures)
- ✓ Not pregnant.
- ✓ Able to give informed consent

3.2.2 Stroke participants

In order to recruit the highest possible number of stroke participants, approvals were obtained through a range of channels including; West of Scotland Research Ethics Service (WoSRES), Clinical Research & Development Office of Greater Glasgow & Clyde and Lanarkshire Health Boards and hospital managements (18/WS/0178) (Appendix C) and from the University of Strathclyde Ethics Committee (UEC18/28). The recruitment process was firstly; through a poster (Appendix D), which was pinned onto notice boards in the waiting area of the orthotics and physiotherapy departments at Greater Glasgow and Clyde and Lanarkshire Health Boards; and secondly, by an advert (Appendix E), which was displayed in the Stroke association, Chest Heart & Stroke Scotland and in Port-ER, Mobility Matters websites.

A participant information sheet and a consent form (Appendix F) were sent out by email to potential participants (control and stroke participants) who contacted the research team showing their interest to take part in the study. Participants were given a minimum of 48 hours after receiving the participant information sheet and consent form to decide whether or not to take part. This time allowed participants to familiarise themselves with all the given information and ask about any aspect of the study by contacting the research team to fully understand the steps included.

❖ *The inclusion and exclusion criteria*

- The inclusion criteria for stroke participants were:
 - ✓ Patients who have suffered from a stroke (at least six months ago).
 - ✓ Over 18 years of age.
 - ✓ Able to walk 10- 15 steps on a treadmill (this corresponds to 10 metres per tested condition) without walking aids.
 - ✓ No spasticity or mild to moderate spasticity (Modified Ashworth scale less than 3).
 - ✓ No hip flexion contracture.
 - ✓ No knee flexion contracture.
 - ✓ Able to give informed consent.
 - ✓ Using Ankle-foot orthosis (lower leg splint).

- The exclusion criteria for stroke participants were:
 - ✓ Pregnant.
 - ✓ Suffering from motion sickness.
 - ✓ Having conditions other than stroke affecting balance.
 - ✓ Having any existing condition or previous surgical procedure that limits the required range of motion needed for normal walking (e.g. arthritis, arthrodesis).
 - ✓ Known to be epileptic.
 - ✓ Living outside Glasgow and Clyde and Lanarkshire health board areas.

3.3. Experimental procedure

Each participant was invited to attend three study sessions for no longer than 2 hours each. The research took place at the National Centre for Prosthetics and Orthotics (NCPO) at the University of Strathclyde. The first session was a screening session to determine whether the participant could be included in the study; if so, a plaster of Paris cast of the participant's lower leg was taken. The second session (one week later) was to check the orthosis fitting, comfort and function. The third session (one week after the second session) was to record the participant's gait.

3.3.1 Experimental AFO

(i). AFO casting and fabrication

In the first visit, the study was fully explained to the participants and any questions that the participants may have were answered. All participants were asked to sign the informed consent form (Appendix F) and to complete their demographic information such as the date of birth, height, mass and shoe size (Appendix G).

Participants, who matched all the selection criteria, were seated on a casting chair and cotton stockinet was attached over the desired limb (the affected limb for stroke participants and a limb was selected randomly for the control participants). An indelible pencil was used to mark the positions of the following anatomical landmarks: the medial and lateral malleoli, the head of fibula, first and fifth metatarsal heads, 5th metatarsal base, navicular and any other pressure-sensitive areas. A plastic tube was placed over the anterior aspect of the leg to facilitate cast removal (Figure 3.1, A). Plaster of Paris

bandages were then attached from just below the head of fibula to the toes. The plaster was strengthened over the ankle joint area to avoid cast breakage during cast removal. During the casting process, the ankle angle and the foot position were considered. If the foot deformity was flexible, then correction of the tri-planar deformity was applied during casting. This manual correction was applied up to a maximal position (that does not exceed the neutral position) where the participant felt he/she could tolerate. The ankle was set in a position to accommodate the available gastrocnemius length (i.e. the ankle angle of the AFO should never prevent the knee from fully extending). The ankle and the foot were held in this position until the plaster had set. Following that, the negative cast was removed using a cast cutter along the plastic tube, and the stockinet was cut off and removed (Figure 3.1, B and C).

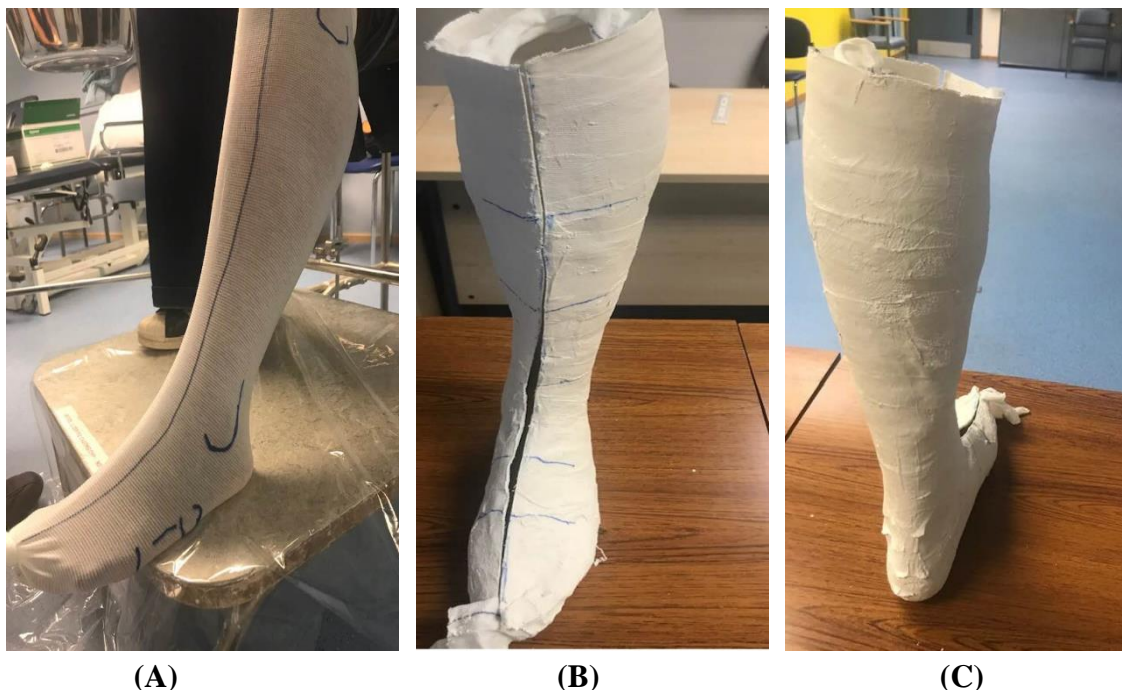


Figure 3.1: AFO casting process: Casting preparation (A). Anterior view of the negative cast (B). Posterior view of the negative cast (C).

In order to make a positive cast for the participants' lower leg, liquid plaster of Paris was poured inside the negative cast. A steel tube was inserted inside the cast but kept away from the bottom of the cast until the plaster was set and had become solid. After that, the outer plaster shell was removed to obtain the positive cast. This was followed by cast

modification where appropriate corrective forces were to be applied. Cast shaping was done in a way that matches the contours of the underlying skeletal structure. Furthermore, the forces were applied as far apart as possible and over large areas to maximise the force lever arms and to reduce pressure. These steps aid in increasing the comfort of the AFO.

A 5mm homopolymer polypropylene plastic sheet (North Sea Plastics Ltd., Glasgow, UK) was vacuum moulded over the positive cast with carbon fibre reinforcement (PolyCar-C Ankle Inserts, Fillauer Inc., Tennessee, USA) where their leading edge placed at the midline of each malleolus (Figure 3.2). The AFO trimlines were cut as follows:

- Proximally, 20 mm horizontally below the head of fibula.
- At the ankle, approximately 10mm anterior to the midline of the malleoli.
- At the forefoot, close to the metatarsal heads at the medial and lateral borders to control the forefoot abduction /adduction and supination/pronation.
- At the sole plate, 5mm extended beyond the toes.

Two Velcro straps were placed on the AFO; proximal strap 15 mm below the proximal trimline and distal strap at an angle of 45° passing through the posterior distal tip of the calcaneus in order to hold the calcaneus firmly inside the orthosis and to maintain proper foot alignment (Figure 3.2, C).

In the second session, once the AFO had been made, approximately after one week, the participant was invited to visit the NCPO for checking the fitting, comfort, and function of the AFO. At the time of fitting, preliminary tuning of the AFO with heel wedges was performed to achieve the optimal posture/alignment/inclination for the lower leg (as discussed in section 2.6) and to achieve comfort to the stroke participant during walking. Additionally, another heel wedge was placed under the other foot in order to equalise the leg length. The AFO casting, modification, fabrication and fitting were performed by the same registered orthotist.

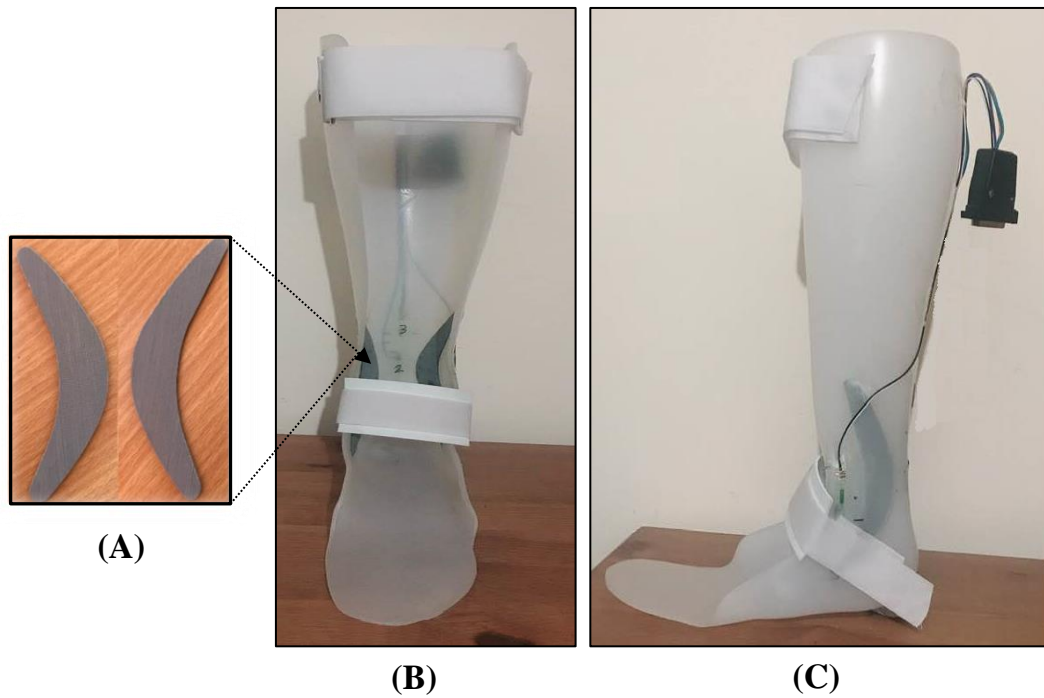
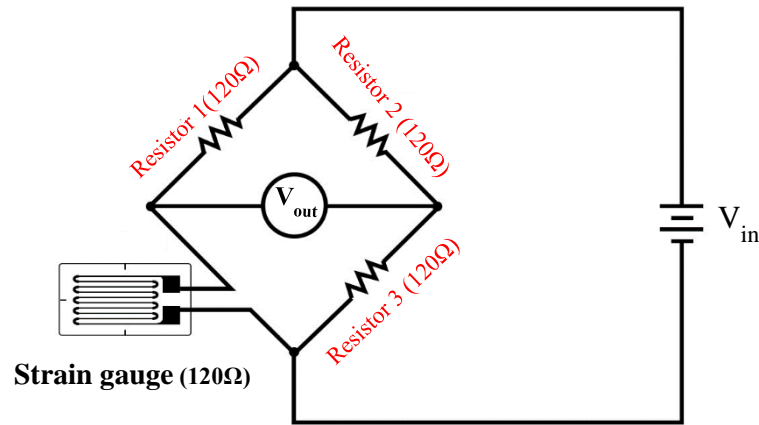


Figure 3.2: Carbon fibre reinforcement (A) used in rigid AFO. Anterior view of the AFO with the moulded carbon fibre reinforcement (B). Lateral view of the AFO (C).

(ii). Strain gauges attachments

Four single Strain Gauges (SGs) (each arranged in a quarter Wheatstone bridge configuration, 5mm length, 120 Ω ; Techni Measure Lab (TML), Tokyo, Japan) were used to measure the orthotic moment at the ankle joint, following the same methods introduced by Papi et al (2015). This method was considered a reliable method to directly measure the orthotic moment during walking without the need to destroying the AFO or to change the mechanical properties of the AFO by inserting metal bars on which SGs would be attached. Measuring the orthotic moment using an experimental AFO would provide more precise results than using indirect methods which are totally based on the stiffness values determined during bench testing. As aforementioned in section “2.9 Orthotic moment measurement techniques”, using SG arranged in a quarter Wheatstone bridge configuration could eliminate the AFO’s geometry problem and showed a linear stress/strain relationship on polypropylene plastic AFO (Papi et al., 2015). Therefore, a single SG (arranged in a quarter Wheatstone bridge configuration) was chosen to be used in this study (Figure 3.3).



A full Wheatstone bridge circuit

Figure 3.3: A schematic drawing of the single SG used in this study (Techni Measure Lab (TML), Tokyo, Japan) and the full Wheatstone bridge circuit.

Prior to attaching the SGs to the AFOs, a reliability test was conducted on six homopolymer polypropylene plastic tensile specimen samples with a 5mm thickness (of the same thickness and material used in AFOs fabrication) (Appendix H). Two types of SGs were used in the reliability test; two-element 90° rosette strain gauges (2 mm long, 120 Ω; Techni Measure Lab (TML), Tokyo, Japan) and single SG (5 mm length, 120 Ω; Techni Measure Lab (TML), Tokyo, Japan), this will be discussed further in appendix H. The aim of this test was to assess the SGs repeatability and performance. Therefore, SGs were attached to the homopolymer polypropylene plastic samples using the standard surface preparation technique (Window and Holister, 1992) and in agreement with SG manufacture’s recommendations (Techni Measure Lab (TML), Tokyo, Japan). This technique was performed as follows: **(1)** degreasing and cleaning a larger area than the area required for SG attachment from all dust, paint, oil, and grease with a solvent (Chlorothene, Micro-Measurements). **(2)** abrading the surface to make it slightly rough using fine sandpaper (400 grit size) to allow good bonding surface of the SGs. **(3)** scrubbing the area with a conditioner (M-Prep Conditioner A, Micro-Measurements) to remove any contamination caused by the abrading procedure. **(4)** neutralising the area by scrubbing the surface using absorbent cotton with a neutralizer (M-Prep Neutralizer 5A, Micro-Measurements) to bring the surface alkalinity to the optimum condition of PH value of around seven in order to facilitate bonding the SGs; as some adhesives will not

bond to an acidic surface. (5) transferring the SGs to the samples using a specific SG installation tape (MJG-2 MYLAR tape, Micro-Measurements, UK). (6) aligning the transferred SGs in the principal stress direction (i.e. the SG foil was aligned to the main axes of the tensile sample, to be parallel to the long axis direction of the sample). (7) adhering the SG to the prepared surface using cyanoacrylate adhesive (200 Catalyst-C and M-Bond 200, Micro-Measurements, UK). Constant thumb pressure was immediately applied to the SG for at least two minutes. Once the adhesive was cured, the SG installation tape was then carefully removed. (8) soldering the SG lead wires to the soldering path (connecting the two, two-element 90° degrees rosette SGs together to create the full Wheatstone bridge or connecting the single SG to the three compensating resistors to create the quarter Wheatstone bridge). (9) applying a coating agent (M-Coat-A Polyurethane, Micro-Measurements) over the SGs and the lead wires, and this was allowed to dry for at least two hours. The aim of using the coating agent was to prevent the SGs from absorbing moisture in outdoor or long-term measurement and to protect them from any excessive movements of the wire that may damage them.

A tensile test was then performed for the homopolymer polypropylene plastic samples using an Instron tensile testing machine (Electroplus™ E10000 Instron, USA). The strain was measured using both the attached strain gauges on the homopolymer polypropylene plastic samples and an Instron extensometer (Instron reference 2620-60, USA). The full details on the test protocol, methods and results can be found in appendix H. No significant differences were found between the strain readings obtained from the SGs and the Instron extensometer. Moreover, the SGs showed repeatable readings over 100 cycles (Appendix H). Thus, the use of SGs was considered as an adequate technique to proceed toward strain gauging the AFOs.

The surfaces of the AFO where the strain gauges (SGs) were to be attached were prepared using the aforementioned technique. The four SGs were attached to the AFO at specific locations as follows (Figure 3.4):

- The first strain gauge (SG1) attached on the medial aspect of the AFO at the medial malleolus.
- The second strain gauge (SG2) attached on the ankle region of the AFO at the intersection of a line drawn between the medial and lateral malleoli and the

perpendicular line passing midway of the widest medial-lateral diameter of the ankle, at the same level of the ankle joint centre (which is located at the midpoint of the distance between medial and lateral malleoli).

- The third strain gauge (SG3) attached on the posterior aspect of the AFO 30mm above and in line with SG2.
- The fourth strain gauge (SG4) attached on the lateral aspect of the AFO at the lateral malleolus.

These locations were selected specifically based on the results of previous research, as the ankle moment in the sagittal plane was successfully measured at the location of SG2, for the determination of the anterior- posterior ankle moment (Papi et al., 2015). Additionally, the maximum compression and tensile stresses were previously found to be produced at the location of SG2 and SG3 during initial contact and toe off respectively (Chu and Feng, 1998). The location of SG1 and SG4 were chosen in order to measure the ankle moment in the frontal plane. The aim of using two SGs to measure the ankle moment for both sagittal and frontal planes (i.e. SG2 and SG3 in sagittal plane and SG1 and SG4 in frontal plane) was to provide a backup of the data in case of any failure that might occur in the SGs during the data collection.

The strain gauge has a fine metal foil used to measure changes in electrical resistance that are caused by the strain occurring on the AFO. Each strain gauge was connected to three compensating resistors (Surface Mount Device (SMD) resistor, 120 Ω , Panasonic, New Jersey, USA) to compensate/complete a full Wheatstone bridge circuit, which is used to detect these changes as electrical signals (Figure 3.4). The SMD resistor offers superior stability, temperature performance, lower power consumption, and flexibility of design (Macleod, 2002). The changes in resistance are very small (i.e. in the order of 10^{-5} Ω), subsequently they are very difficult to detect. Therefore, a high gain instrumentation amplifier was used to detect changes in voltage levels, rather than changes in resistance. Amplifier gain and bridge voltage were set at 200 and 3 V, respectively. For each AFO, all the compensating resistors for the four SGs used were incorporated in a connector plug (25 Pin D-sub Connector Plug, Micro-Measurements, UK) as illustrated in Figure 3.4, which in turn was connected to the amplifier (Figure 3.6).

Four Wheatstone bridges: each Wheatstone bridge consists of three SMDs compensators connected to a single SG.

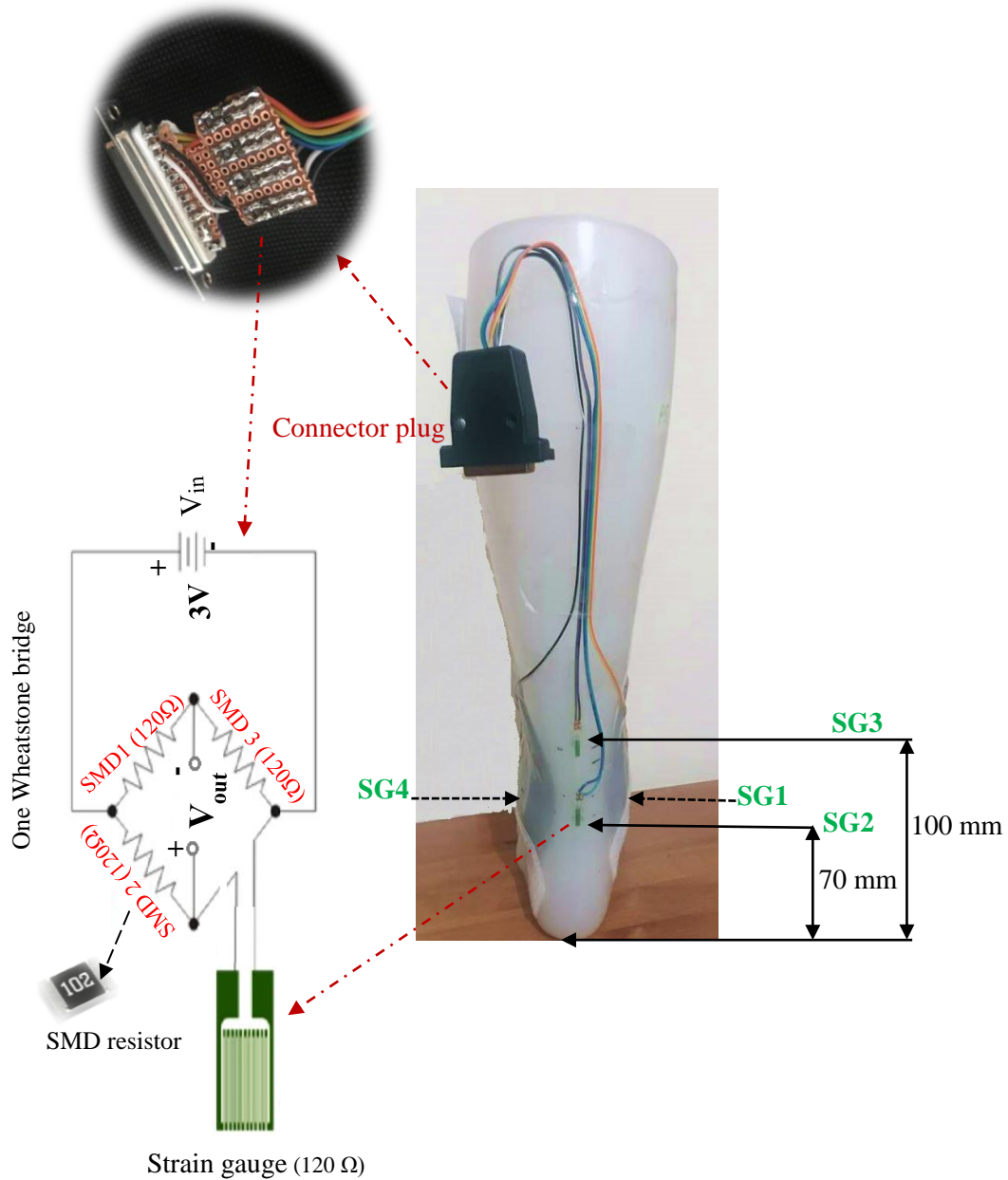


Figure 3.4: The location of the strain gauges used in this study and a schematic drawing of the Wheatstone bridge configuration.

(iii). AFO calibration

Prior to data collection, a static calibration test was conducted on the strain gauged AFOs to investigate the linearity and the repeatability of the SGs response using the Instron

tensile testing machine (Electroplus™ E10000 Instron, USA). A wooden foot block was inserted in the foot section of the AFO to facilitate attachment of the AFO to the Instron (Figure 3.5). Thus, the AFO was clamped from the foot section to a calibration frame that was firmly attached with four 10mm bolts to the Instron base plate (Figure 3.5, Figure 3.6). A stainless-steel loading bar was secured to the upper jaw of the Instron machine (Figure 3.6). The position of the upper crosshead was adjusted at a desired position allowing the stainless steel loading bar to be perpendicular in contacting the proximal calf section of the AFO (without applying any pressure on the AFO) in order to transfer the produced load from the Instron to the AFO while performing the calibration test (Figure 3.6). Thus, the contact point was considered as the load application point and the created lever arm was measured (the distance from this point to a point on the AFO against the ankle joint centre) (Figure 3.5). Then, the four Wheatstone bridges of the AFO were connected to a bank of four amplifiers. For each SG, the amplifier gain and the bridge voltage were set at 200 and 3V, respectively. Then, the output for each SG was zeroed before starting the calibration test.

The calibration test protocol was created and applied to each AFO using the Instron WaveMatrix software at a sample rate of 50Hz. The protocol consisted of 20 loading cycles up to 100N. For each cycle, one second was allowed for the load to reach the maximum value and one second to return to 0N (Figure 3.7, A). The load was chosen to be approximating the load expected to be exerted on an AFO (Papi et al., 2015) (derived from the 2 MPa stress based on experimental and finite element analysis studies conducted on a plastic AFO (Chu and Feng, 1998, Chu, 2000)). Output data from the SGs were transferred to a laptop via data acquisition system (Analog-to-digital convertor, National Instruments (USB-8009), USA). Data from the four SGs were collected at sample rate of 50Hz using a custom –built LabVIEW program (LabVIEW software 18, National Instruments, USA) installed on the laptop. The data from both WaveMatrix and the LabVIEW were exported to Excel (Microsoft Office Professional Edition 2016, Microsoft Corporation, USA) for further analysis. The synchronization of both sets of data was not feasible at the time of data collection. Therefore, synchronization was performed manually by using the first load cycle as the starting point (Figure 3.7). Thus, 19 load cycles were analysed using Matlab software (Math Works 2017, Massachusetts, USA).

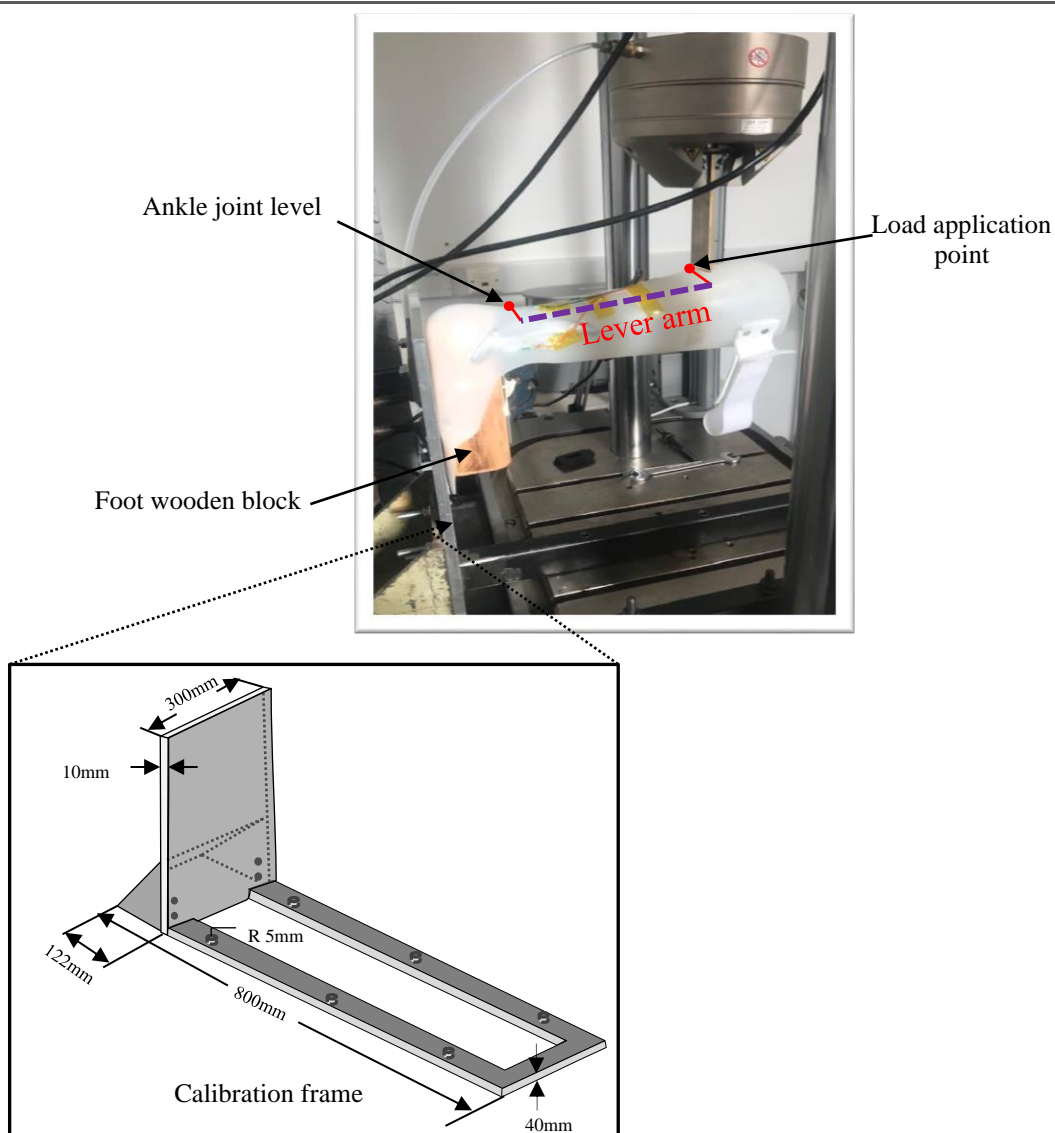


Figure 3.5: Lever arm measurement (the AFO is placed in a position to produce dorsiflexion moment). The focused picture shows a sketch of the calibration frame.

The aforementioned calibration protocol was performed four times in a random sequence for each AFO. For each time, the AFO orientation was changed in order to produce dorsiflexion, plantarflexion, inversion and eversion moments at the ankle joint, thus, the load was applied on the posterior, anterior (inner surface), lateral and medial side of the proximal calf section of the AFO, respectively, as shown in Figure 3.8.

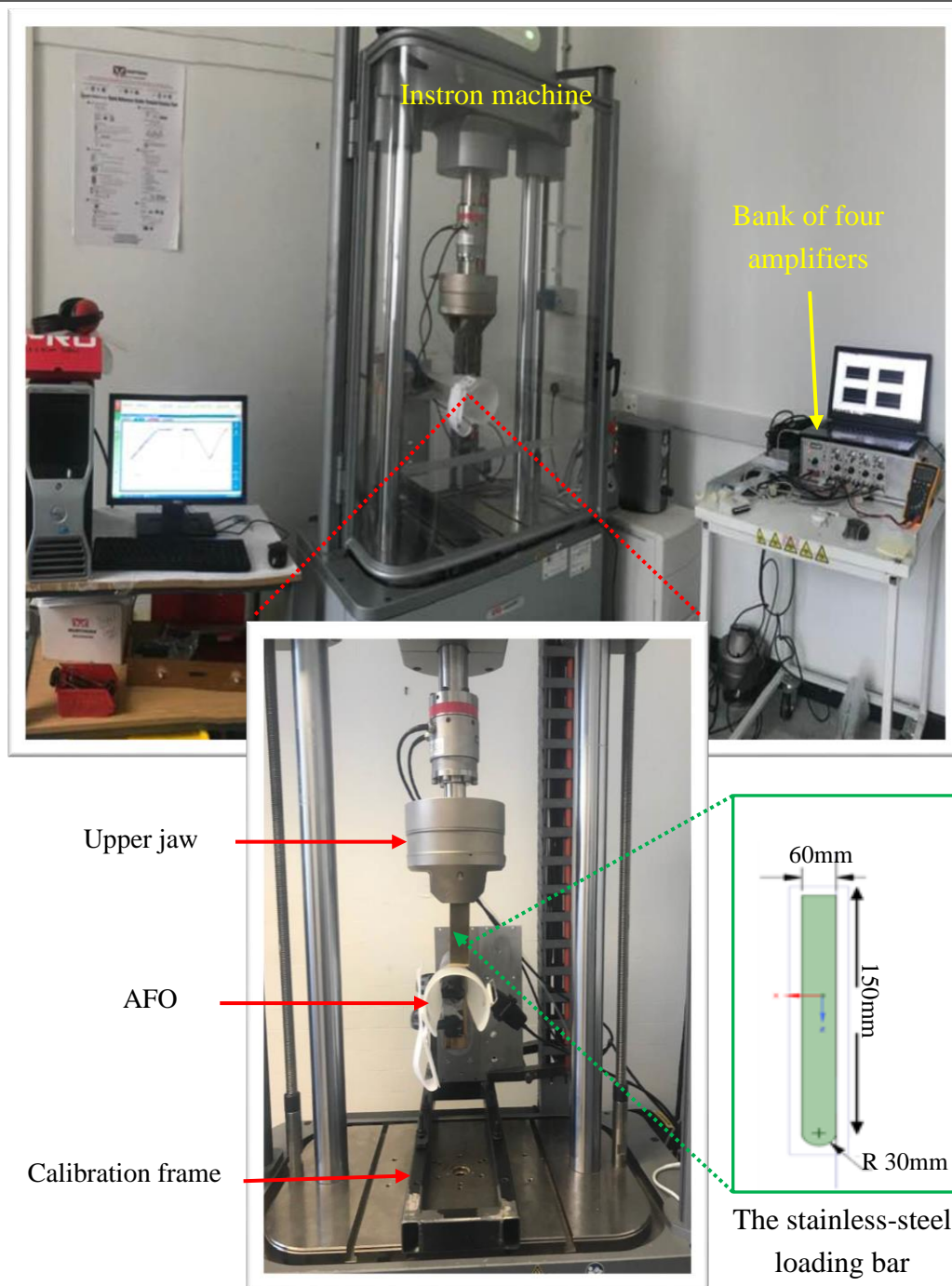


Figure 3.6: The Instron tensile testing machine (Electroplus™ E10000 Instron, USA). The focused pictures show the attachment of the AFO to the Instron and the stainless-steel loading bar dimensions.

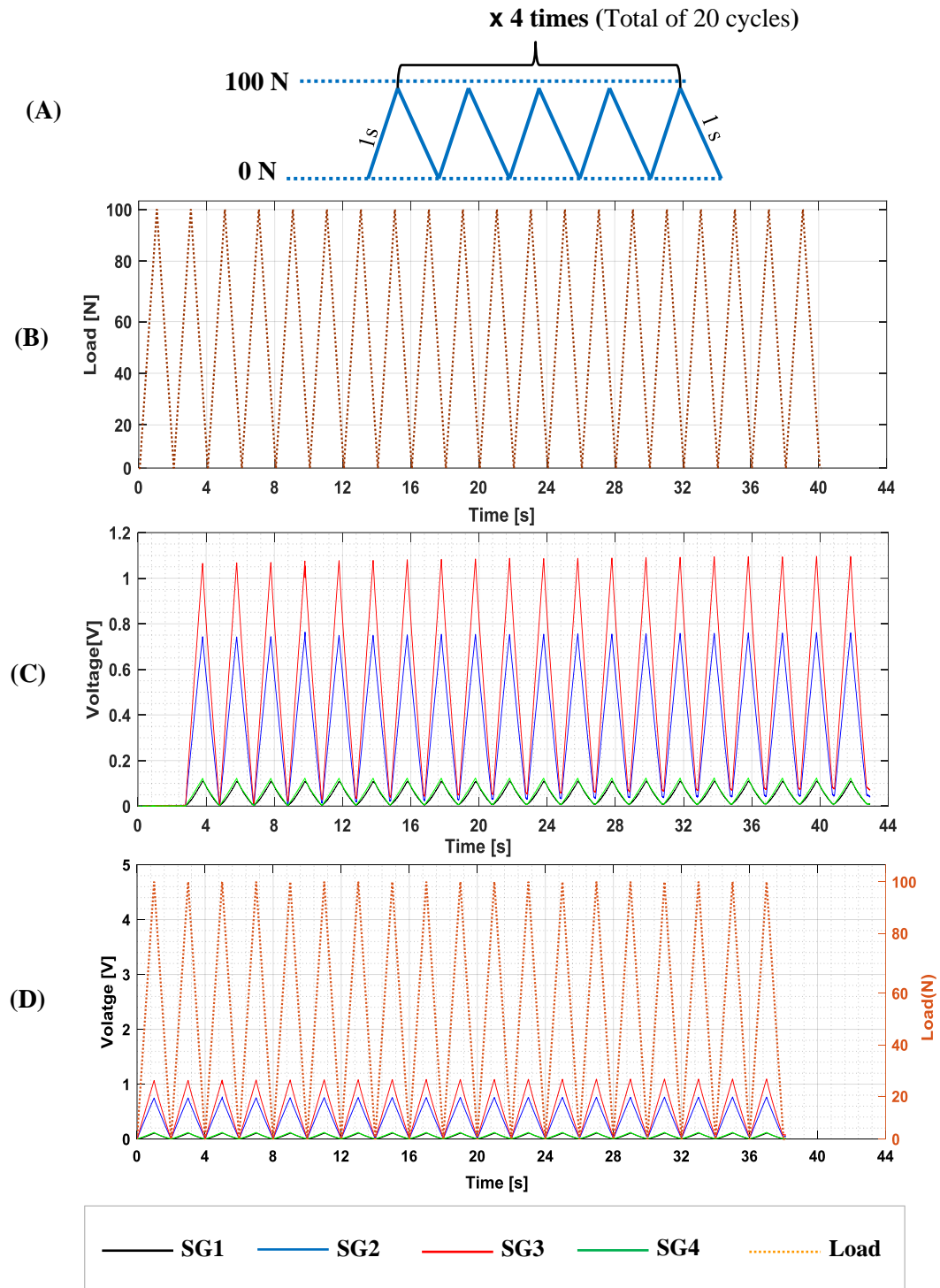


Figure 3.7: AFO calibration protocol (A). An example of load data from Wavematrix software (B), SGs data from LabVIEW software (C), synchronised load and SGs data using Matlab software (D). The AFO in this example was placed in a position to provide dorsiflexion moment.

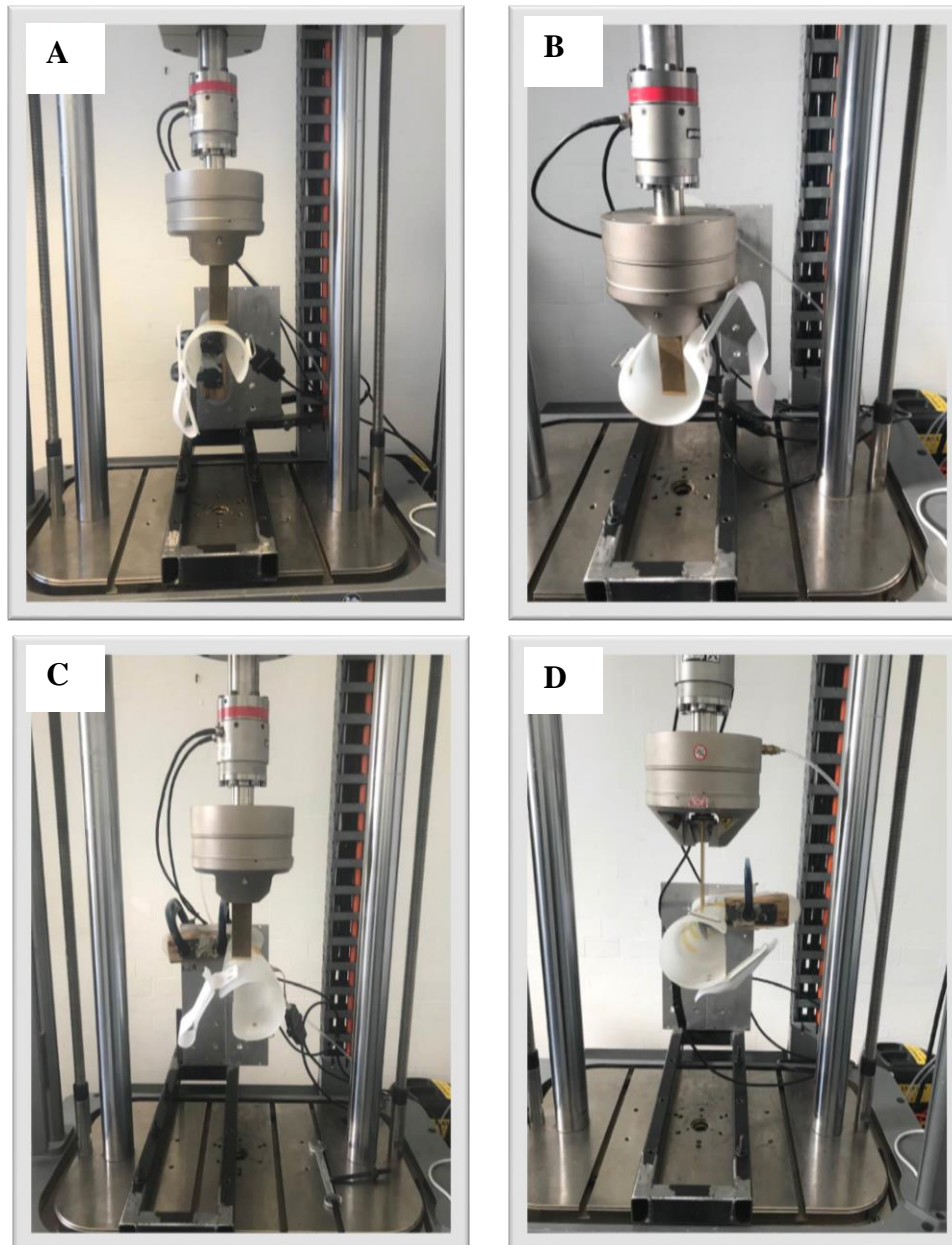


Figure 3.8: AFO calibration orientations to produce dorsiflexion (A), plantarflexion (B), inversion (C) and eversion (D) moments at the ankle joint.

The SGs data showed repeatable readings for all tested AFOs. These data will be used later to find the conversion factor to calculate ankle moment from the strain gauge voltage output. This will be discussed further in section “3.6.3 SG data analysis”.

3.3.2 Motion capture system set up

The third session was conducted in the motion analysis gait laboratory at the NCPO in the University of Strathclyde. Motek Medical's Computer Assisted Rehabilitation Environment (CAREN) system (Motekforce Link, the Netherlands) was used in this study (Figure 3.9). The system consists of:

- A dual belt treadmill instrumented with two force plates (Motekforce Link, the Netherlands) to collect the kinetic data at a sample rate of 2000Hz.
- A three-dimensional motion capture system equipped with twelve infrared cameras (Vicon Bonita, Oxford Metrics, Oxford UK) along with the Nexus software suite (Vicon Motion Systems, Oxford, UK) that captures the location in space of reflective markers placed on the participants' body during the test. The kinematic data were acquired at a sampling frequency of 100Hz.

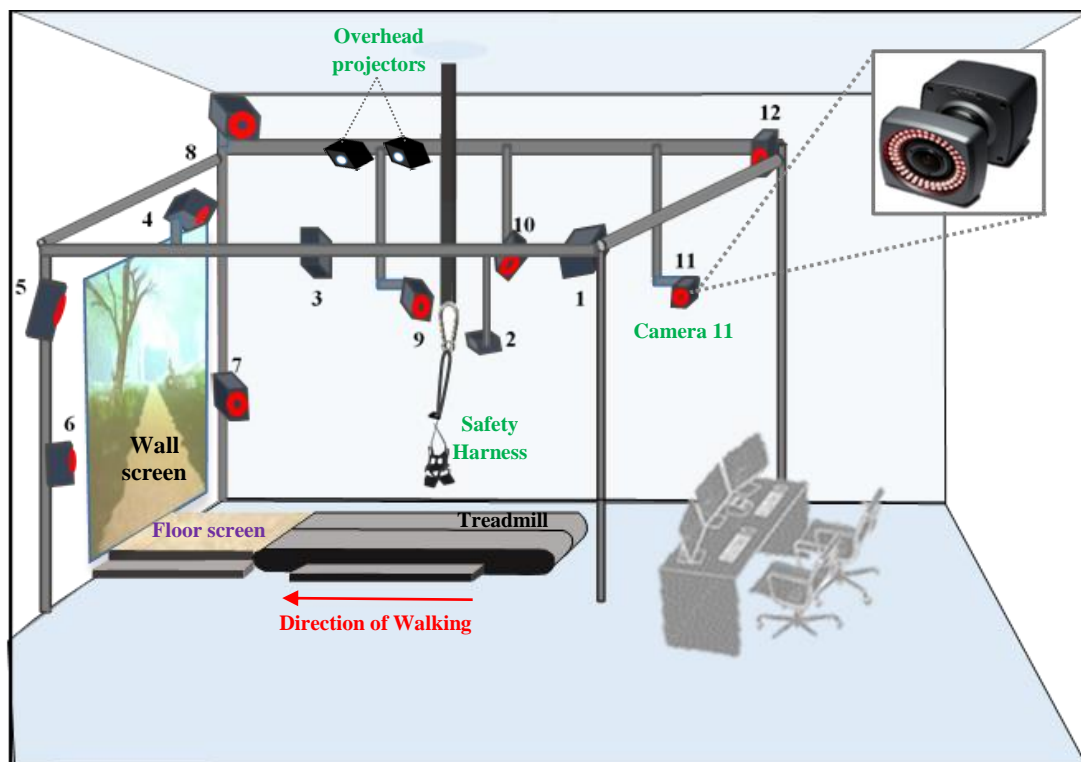


Figure 3.9: A schematic drawing of the CAREN system laboratory showing the location of the twelve Vicon Bonita infrared cameras and the treadmill. The focused picture shows a Vicon Bonita infrared camera.

(i). *The instrumented treadmill*

A dual 1 × 2 m split-belt treadmill with two force plates underneath of all the surface of the treadmill belts (Motekforce Link, Amsterdam, Netherlands) was used in this study (Figure 3.10). These two force plates allowed collection of the ground reaction force, centre of pressures and temporal-spatial parameters data. The force plates have a resolution of +/- 0.5 N and a centre of pressure sensitivity less than 2mm with loads under 1000 N. The treadmill has left and right belts with a force plate underneath each belt, which allows independent measurement of the forces over each belt/limb during walking.

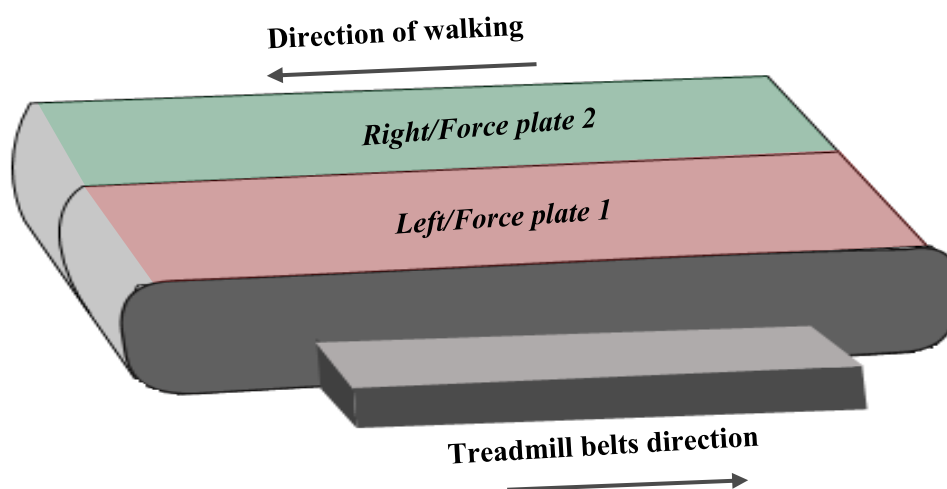


Figure 3.10: A schematic drawing of the instrumented treadmill with the two force plates.

During quiet standing on the force plate, a ground reaction component acts in opposition to body weight. During dynamic walking, the ground reaction vector magnitude and direction is further composed by three vector forces as shown in (Figure 3.11) (Richards, 2018). The ground reaction force (GRF) is the resultant of F_x , F_y and F_z , which can be calculated by the following equation:

$$\mathbf{GRF} = \sqrt{\mathbf{F}_x^2 + \mathbf{F}_y^2 + \mathbf{F}_z^2} \quad \text{Equation 1}$$

Where; \mathbf{F}_x : the mediolateral component of the GRF, \mathbf{F}_y : the anteroposterior component of the GRF and \mathbf{F}_z is the vertical component of the GRF.

Following recommendations for setting up and using a Motekforce Link treadmill with Nexus, the gait laboratory coordinate system used in this study was different from that used by the International Society of Biomechanics (ISB) system (Figure 3.11). In this study, the gait laboratory was set up so that the positive X-axis points to the left, the positive Y-axis points backward and the positive Z-axis points upward as shown in figures (Figure 3.11, Figure 3.12). Prior to data collection, the force plates were manually offset to zero load by pressing the zero button when there was no load acting on them. This is done to ensure that the reading was equal to zero.

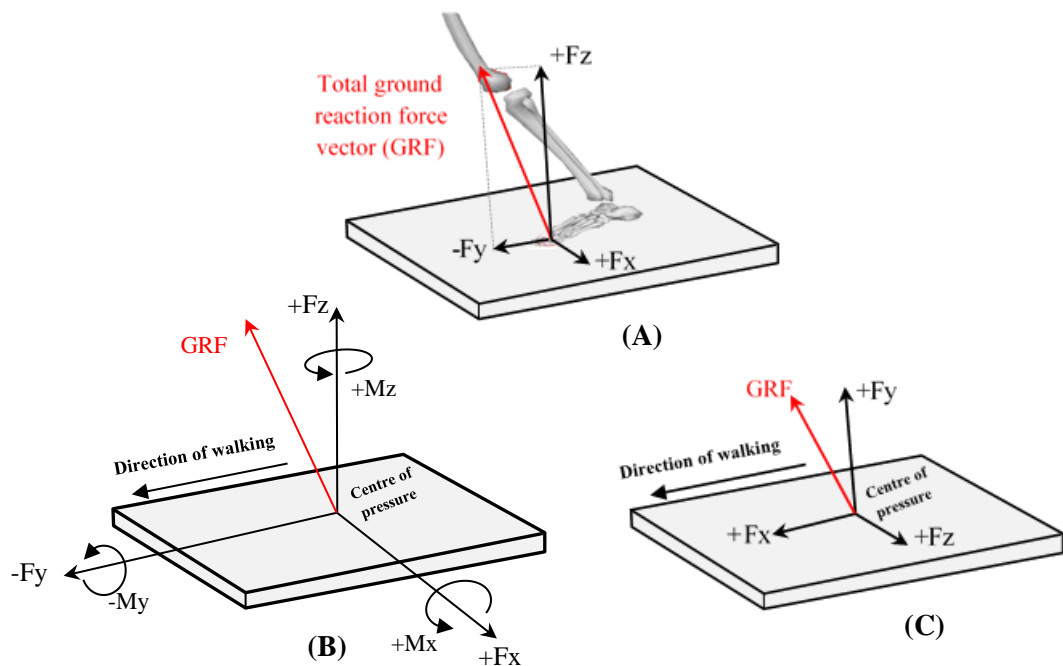


Figure 3.11: The three components of the ground reaction force (GRF) with the coordinate system used in this study (A and B) and the coordinate system adapted by (ISB) (C). B also shows the moment directions (M_x , M_y , and M_z).

In clinical gait analysis, walking on an instrumented treadmill or overground at comparable speeds showed similar results in the kinematic and kinetic gait parameters (Parvataneni et al., 2009, Riley et al., 2007, Watt et al., 2010). Clinical gait analysis based on using an instrumented treadmill has several advantages as compared to overground testing. One of these advantages is that walking speed can be controlled and kept constant between sessions. Using an instrumented treadmill also allows to record several successful consecutive gait cycles in a short period of time (Papegaij and Steenbrink,

2017), thus increasing the test reliability (Kesar et al., 2011, Mills et al., 2007, Tesio and Rota, 2008) and increasing data collection efficiency (Papegaaij and Steenbrink, 2017).

(ii). Cameras configuration and setup

Twelve infrared cameras (Vicon Bonita, Oxford Metrics, Oxford UK) are mounted using mounting brackets onto a metal frame around the wall of the room (Figure 3.9). They are adjusted and aligned in proper positions to obtain complete data collection from the measurement volume during walking on treadmill (Figure 3.9). Prior to data collection, static and dynamic calibrations were performed using the active calibration wand manufactured by Vicon (Figure 3.12). The active wand has five illuminating light emitting diode (LED) markers mounted on it in known locations and with a known fixed distance between them (rather than reflecting the infrared light projected from the camera as in the passive wand). The active wand has the advantage of recognizing and capturing the LED markers only, excluding any interference from other illuminating or illuminated structures. This results in a more precise calibration (Summan et al., 2015). Dynamic calibration was performed by waving the active wand throughout the capture volume, ensuring that the wand markers are visible to all the cameras. The purpose of the calibration is to define the precise position of the wand markers in the field of view of each camera; thus, the Vicon software can accurately estimate the orientation and position of each camera in relation to the wand and each other to ensure that any motion in the measurement volume will be recorded.

The static calibration was then performed by placing the calibration wand on a specific location over the treadmill to define the lab origin and the global reference frame as shown in Figure 3.12.

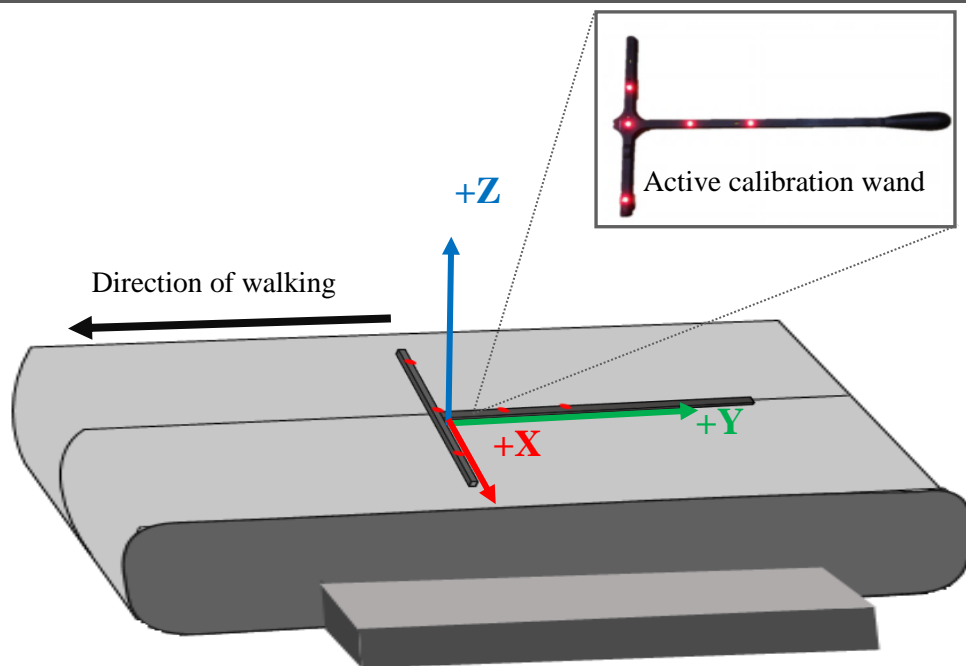


Figure 3.12: The setup position of the static calibration with global reference frame axes as defined by the calibration wand. The focused picture shows the active calibration wand.

Each camera provides a two-dimensional (2D) coordinate image of the wand markers. The Vicon software uses several types of internal and external camera parameters (e.g. the focal length of the infrared camera lens, the orientation of the infrared camera sensor relative to the global coordinate system, etc..) to convert the 2-D position of the marker into a beam of infrared light. This beam originates in the location of the marker from the active wand and terminates in the infrared camera. At least two such beams, and thus two infrared cameras, are needed to find the 3-D location of a marker in the global coordinate system (Payton and Burden, 2008). Ideally, it can be assumed that this marker should lie on a point where these two beams intersect. The system then calculates the location of the point where the beams intersect to find the marker position. The 3-D location of the markers is relatively accurate; as the greater the number of beams (captured by infrared cameras) the more accurate is the 3-D localisation of a marker in space (Figure 3.13). However, as the beams of multiple cameras do not necessarily intersect; this method cannot be relied upon to calculate the position of the marker.

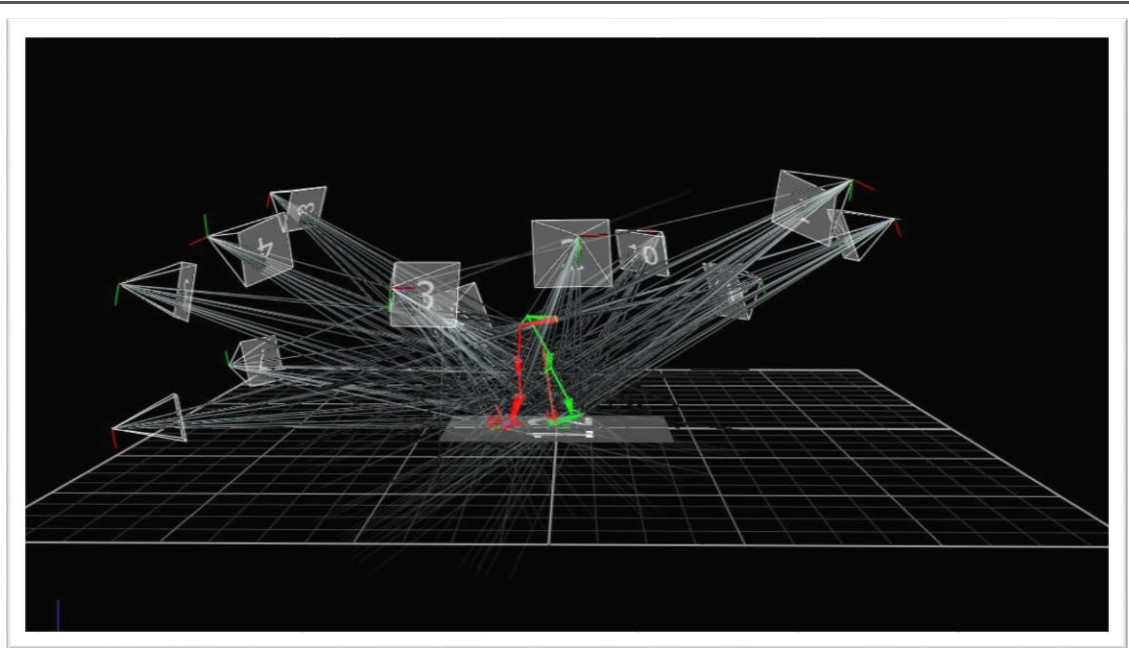


Figure 3.13: Representation of Vicon cameras beams of infrared light.

The Vicon software instead uses a “least-squares” method that identifies the best estimate of the marker centre location by minimizing the sum of the squares of the shortest distances from assumed point location to each beam (Figure 3.13, Figure 3.14). These distances are the residuals for each camera and they are measured in millimetres. The higher the residual number, the less accurately the calibration was performed. According to the manufacturer, the accuracy of residual values is considered successful if each camera mean residual values are ≤ 0.2 mm as this indicates that a marker’s position in space is located within 0.2 mm of its true position (Motion Lab Systems, 2016).

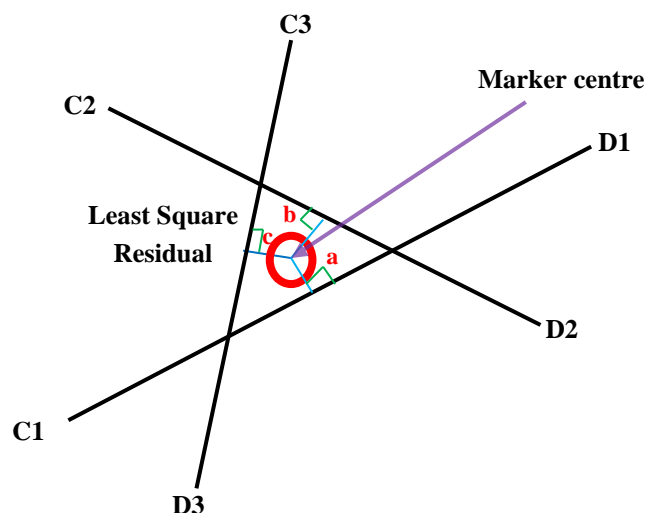


Figure 3.14: An example of using a “least squares” method to calculate the marker centre residual with three cameras beams; C1-D1, C2-D2 and C3-D3 (Motion Lab Systems, 2016).

(iii). *Skin reflective markers setup*

The orientation and position of the body segments and the underlying bones are required to calculate 3D kinetic and kinematic data. A minimum of three non-collinear markers is required per rigid segment to provide full information about its movement in 3D (Cappozzo et al., 1995), (Figure 3.15). To accomplish this, skin based reflective markers were attached to the skin of the participants at specifically chosen anatomical landmarks. These markers are lightweight and are composed of a reflective sphere and a plastic base (Figure 3.15). They reflect the infrared light that is emitted from LED placed around the camera lenses. Consequently, each camera provides a two-dimensional (2D) coordinate image of the reflective markers. Thus, the markers can be used for tracking segments and subsequently, calculating kinetic and kinematic data.

A number of studies have demonstrated that if markers are placed directly onto the skin, soft tissue motion artefacts can be produced during dynamic motion data collection (Andersen et al., 2010, Leardini et al., 2005, Peters et al., 2010). Soft tissue artefacts arise from the relative movement between markers and the underlying bone or the subcutaneous tissues that results from inertial effects, muscular contraction and skin movement (Cappozzo et al., 1996). For instance, 22-30 mm and 12-15 mm of soft tissue

artefact were detected on the thigh and tibia segments, respectively (Sangeux et al., 2006, Stagni et al., 2005). Moreover, markers placed over bony prominences produced greater skin movement artefact than over fleshy areas (Cappozzo et al., 1996, Peters et al., 2010, Sangeux et al., 2006). It is an important issue while setting up this study to choose the methodology that presents the least inaccuracy. Therefore, the Calibrated Anatomical System Technique (CAST) was used to minimise skin movement artefacts (Cappozzo et al., 1996, Papi et al., 2014, Richards, 2018). This technique is based on identifying body segments through technical markers (which are the markers positioned over fleshy areas) and anatomical markers (the markers positioned over bony prominences). In a static trial, the global coordinates of the anatomical landmarks are used to define the segments anatomical reference frames to determinate the joints' positions and axes, while the technical markers are grouped in rigid clusters (so that orientation and distances between markers are fixed) to represent the bones' motion trajectories during dynamic trials (Figure 3.15). Therefore, the anatomical markers are only necessary during the static trial and thus reduce marker displacement error.

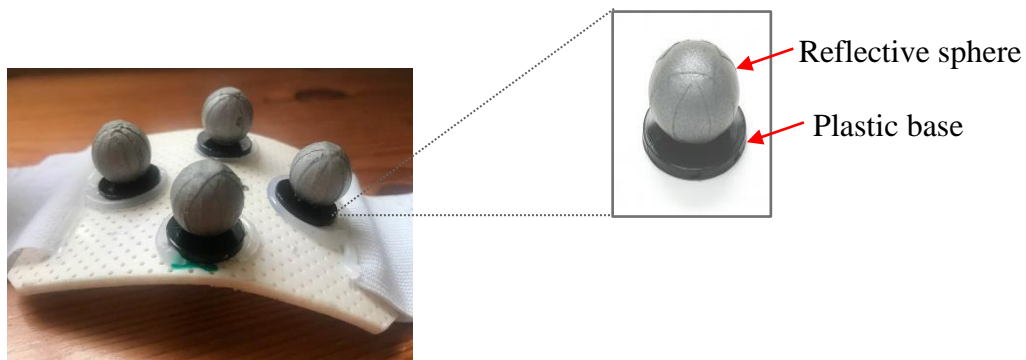


Figure 3.15: Rigid cluster consisting of four reflective markers. The focused picture shows the reflective marker components.

(iv). *Reflective marker positions*

Forty-four anatomical and technical reflective markers (14 mm diameter) were used in this study. The markers were directly placed on the skin of both lower limbs using clusters or hypoallergenic double-sided adhesive tape on the marker's base.

❖ *Anatomical markers*

Reflective markers were attached to bony landmarks on both lower limbs; ankle (medial malleolus (MM) and lateral malleolus (LM)), knee (lateral femoral condyle (LC) and medial femoral condyle (MC)), and pelvis (right and left anterior superior iliac spine (ASIS), and right and left posterior superior iliac spine (PSIS), (Figure 3.16)). Extra markers were also placed on the tibial tuberosity (TT) and the anterior distal edge of tibia (DT), as illustrated in Figure 3.16, in order to measure the Shank Vertical Angle (SVA) (this will be discussed further in section 3.4.3 under the heading ‘‘Gait laboratory testing procedure: Condition 3: Tuned-AFO’’).

❖ *Technical markers*

Fixed cluster pads made of rigid plastic material (four markers on each, (Figure 3.15) were attached to the pelvis and on both shanks and thighs. Elastic Velcro fastening straps and elastic super-wrap bandages (Fabriofam, USA) were used to securely fasten clusters on the segments to reduce rotation and downward migration of these cluster pads. The thigh and shank clusters were placed on the lateral aspect of each segment at the mid-segment level (Figure 3.16). The pelvis cluster pad was placed securely at the mid-point between the posterior superior iliac spines, on the sacrum. Additionally, the shoes were assumed as a rigid body, and the markers were firmly attached onto them (over the first and fifth metatarsal heads (MTS), big toe and calcaneus) to minimise marker displacement error among trials (Figure 3.16). The markers were attached exactly over the areas that represent the aforementioned landmarks of the foot.

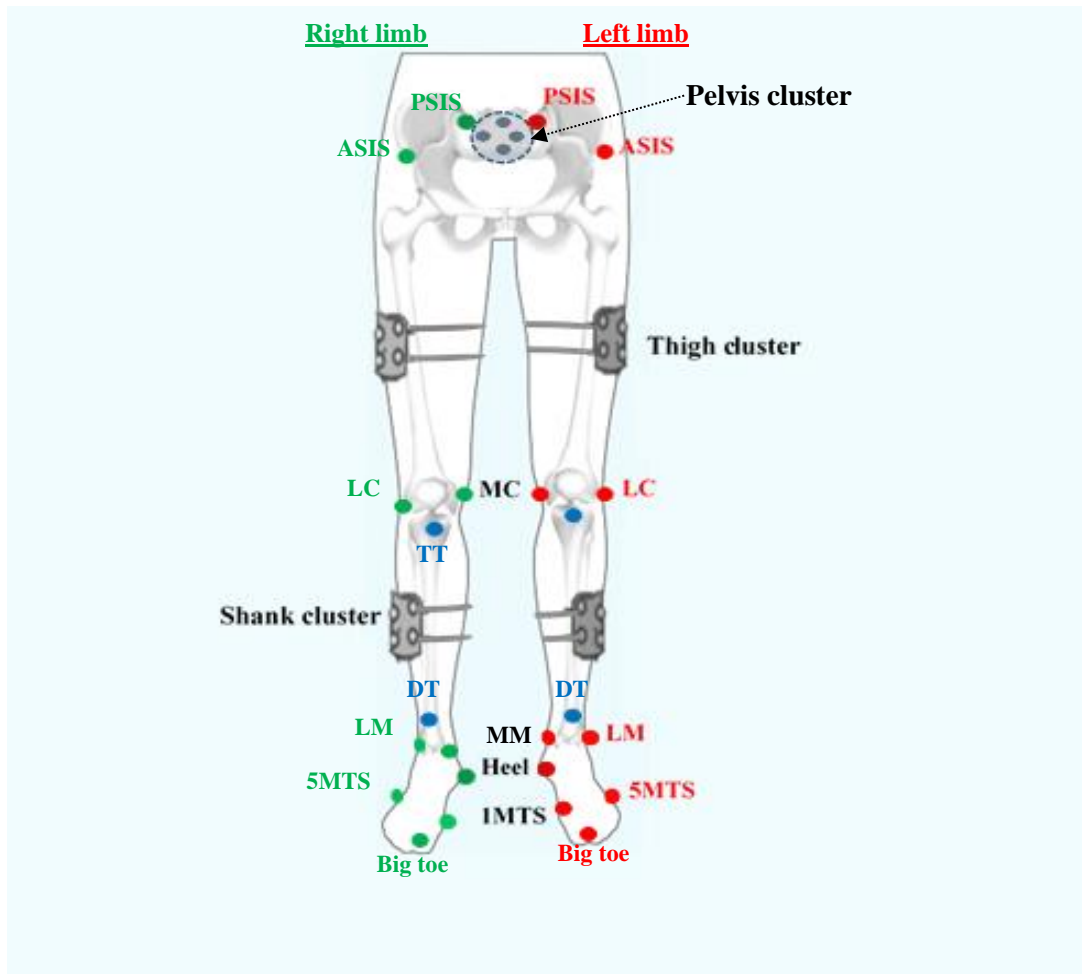


Figure 3.16: Anatomical and technical reflective markers positions.

3.3.3 Electromyography (EMG) setup

(i). *Electromyography equipment*

A wireless surface electromyography (EMG) recording system (Delsys Trigno™, Boston, USA) was used to measure the myoelectrical activity of the knee muscles at a sampling frequency of 2000Hz. Ten wireless active sensors were used in this study (Figure 3.17), with each sensor attached to an amplifier. The Delsys system is a real-time EMG system that sends the pre-amplified and synchronized data signals from each sensor across a distance of up to 20 metres by wireless transmission to a PC-connected base station (DELSYS Trigno, 2019), (Figure 3.17).

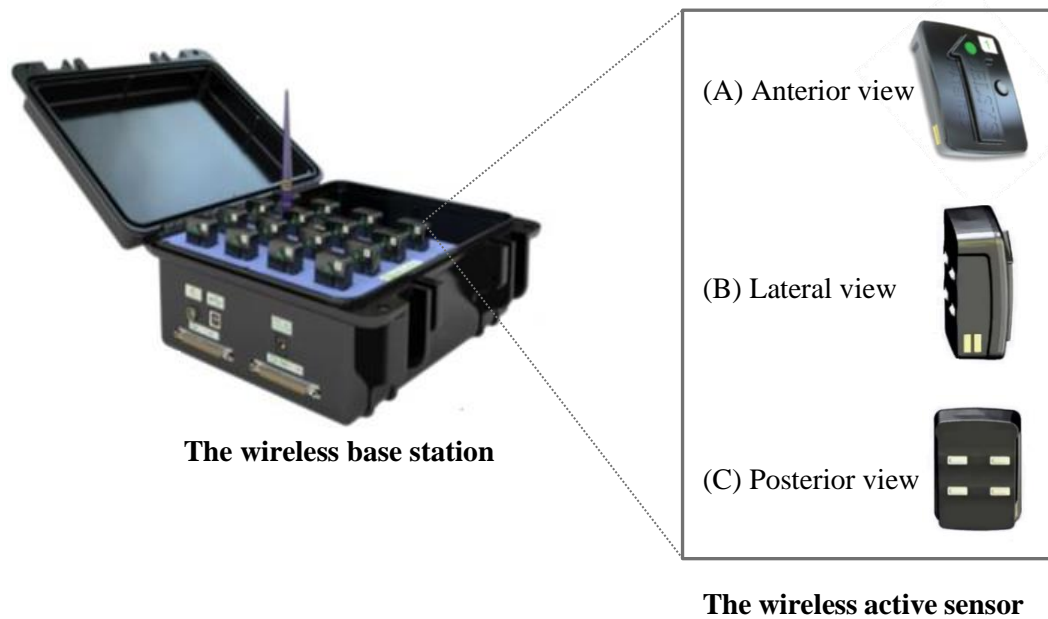


Figure 3.17: The wireless base station of Delsys Trigno™ system. The focused picture shows the wireless active sensor in anterior view (A), lateral view (B) and posterior view (C).

It is well known that EMG signals are highly affected by noise (Amrutha and Arul, 2017). EMG noise can be generated from various sources such as electromagnetic radiation sources, motion artefacts, EMG equipment and circuitry, cross talk interference from adjacent muscles, existence of dead cells or hairs on the skin, and other issues. (De Luca et al., 2010, Roy et al., 2007). Delsys surface EMG sensors have in-built significant features in order to eliminate the noise interference and improve the quality of the detected signals, such as; the bipolar configuration as each sensor has two stabilizer references and two electrodes EMG detecting surfaces (Figure 3.18). The two electrode surfaces detect signals from both surfaces. Immediately, the differential amplifier allows the sensor to react by removing the signal that is common to both electrodes, and then amplifies the difference. Thus, reducing the noise detected on the surface of the skin (Jamal, 2012, Richards, 2018). Additionally, the distance between the two EMG electrodes surfaces is 10 mm (Figure 3.18), which has been considered to provide the optimal EMG signal amplitude with the minimum cross talk interference from undesired muscles (De Luca et al., 2010). The curved surface of the electrode sensor improves the

contact of the sensor surfaces with the skin, which also may eliminate the motion artefact (Figure 3.17).

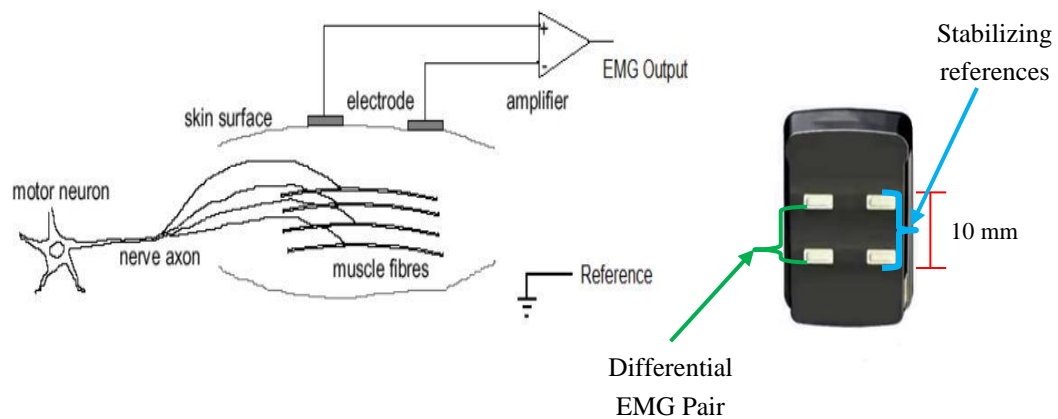


Figure 3.18: Bipolar electrode configuration. Adapted from (Jamal, 2012).

(ii). EMG signal placements

Surface EMG data were obtained from the following muscles on both sides of the body:

- Rectus Femoris.
- Vastus Lateralis.
- Vastus Medialis.
- Biceps Femoris (long head).
- Semitendinosus.

Before application of the electrodes, the hair underlying the electrodes was removed using a standard disposable safety razor and the skin was cleansed with an alcohol wipe. Although Delsys sensors are designed to be used as “dry electrodes”, abrasive skin preparation gel (Nuprep™) was used in persons with dry skin to remove the outer layer of dead skin and thus facilitate ionic currents between the sensor and the skin (Roy et al., 2007). On the top of each Delsys EMG sensor, there is an arrow used to illustrate the direction of how the sensor was aligned with respect to the muscle fibres. Following the guidelines issued by SENIAM (Surface EMG for a Non-Invasive Assessment of Muscles), the sensors were placed on the centre of the muscles belly with the arrows laid parallel to the direction of the tested muscle fibres (Hermens et al., 2000). These locations are illustrated in Figure 3.19 and Table 3.1. In addition, each Delsys EMG sensor has its

own number from (1-10) to identify to which muscle it belonged for further data processing. The sensors were then firmly attached to the skin using hypo-allergenic adhesive tape.

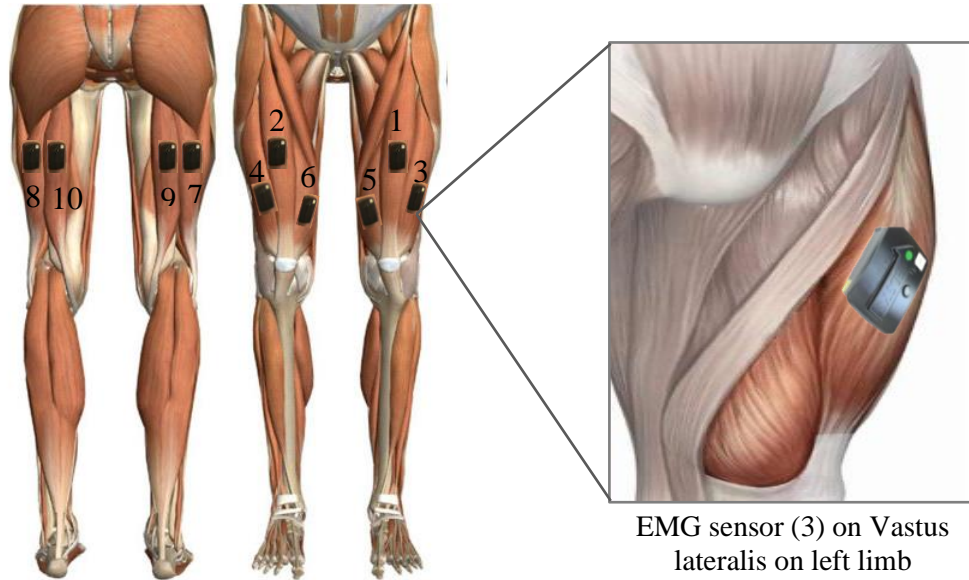
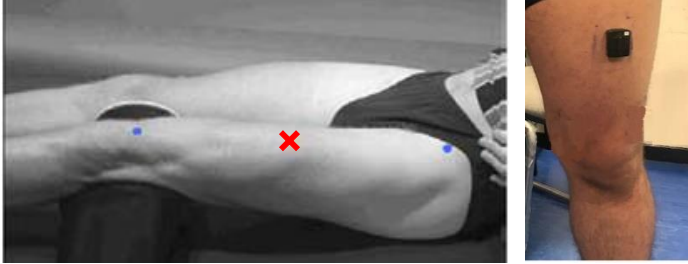

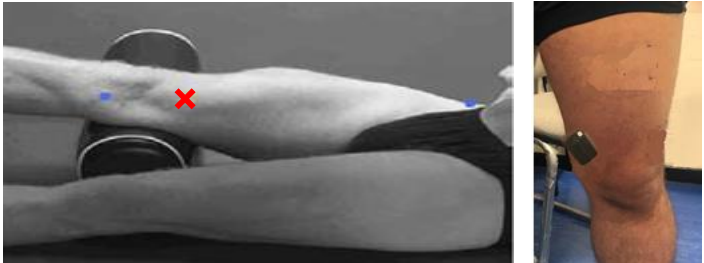
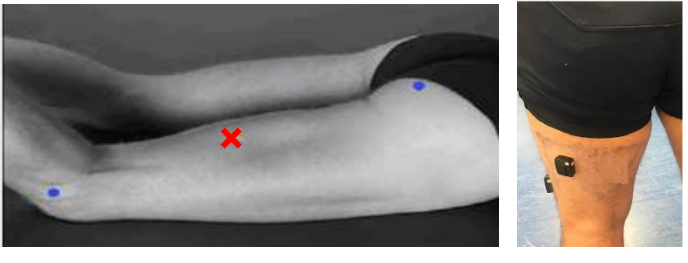
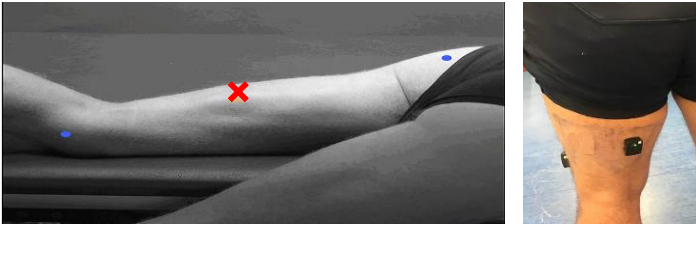


Figure 3.19: Delsys EMG sensor locations on: Rectus femoris (1, 2), Vastus lateralis (3, 4), Vastus medialis (5, 6), Biceps femoris (7, 8) and Semitendinosus (9, 10). The focused picture shows an example of the electrode orientation with respect to the muscle (Vastus lateralis) fibres.

Table 3.1: Delsys EMG sensor placement location over tested muscles according to SENIAM guidelines. Adapted from (SENIAM Organisation, 1999). The red and blue marks represent the sensor location and the anatomical landmarks, respectively.

| Delsys EMG sensor location and placement position for the following muscles: | |
|--------------------------------------------------------------------------------------------------------------------------------------------------------------------------------------------|--------------------------------------------------------------------------------------|
| <p>Rectus femoris: The sensor was placed on the anterior thigh surface at halfway of the line between the anterior superior iliac spine and the patella.</p> |  |
| <p>Vastus lateralis: The sensor was placed on the anterolateral side of the thigh at the lower third of the line between the anterior superior iliac spine and the patella.</p> |  |
| <p>Vastus medialis: The sensor was placed on the anteromedial thigh surface (5-7.5cm above the patella).</p> |  |
| <p>Biceps femoris: The sensor was placed on the posterolateral thigh surface at halfway of the line between the ischial tuberosity and the lateral epicondyle of the tibia.</p> |  |
| <p>Semitendinosus: The sensor was placed on the posteromedial thigh surface at halfway of the line between the ischial tuberosity and the medial epicondyle of the tibia.</p> |  |

The EMG data outputs were recorded as a voltage using Delsys Trigno software (Delsys Trigno™, Boston, USA) along with Nexus software (Oxford Metrics Ltd., UK) that is installed on the laboratory computer. Trigger module (Delsys Trigno™, Boston, USA) was connected to motion capture system to provide complete information about each EMG sensor condition and to make sure that input signals, Delsys hardware, output signals and motion capture system were all properly synchronised with each other (Figure 3.20). Motion capture and EMG data were synchronised during the data collection session.

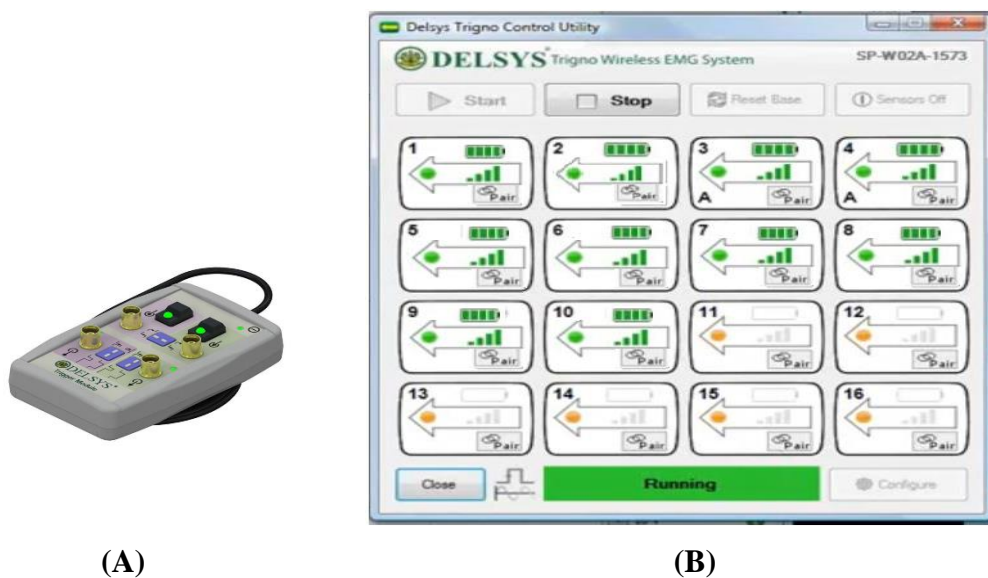


Figure 3.20: The Trigger module (A) and Delsys Trigno software interface (B) (Delsys Trigno™, Boston, USA).

3.4. Data collection

3.4.1 Gait laboratory preparation

The gait laboratory was prepared, and all the equipment was calibrated and checked before each of the participants arrive. The following is a summary of how the gait laboratory was prepared for testing (Figure 3.21):

- An acceptable calibration of the Vicon was performed (as mentioned in section 3.3.2 under the heading “Cameras configuration and setup”).

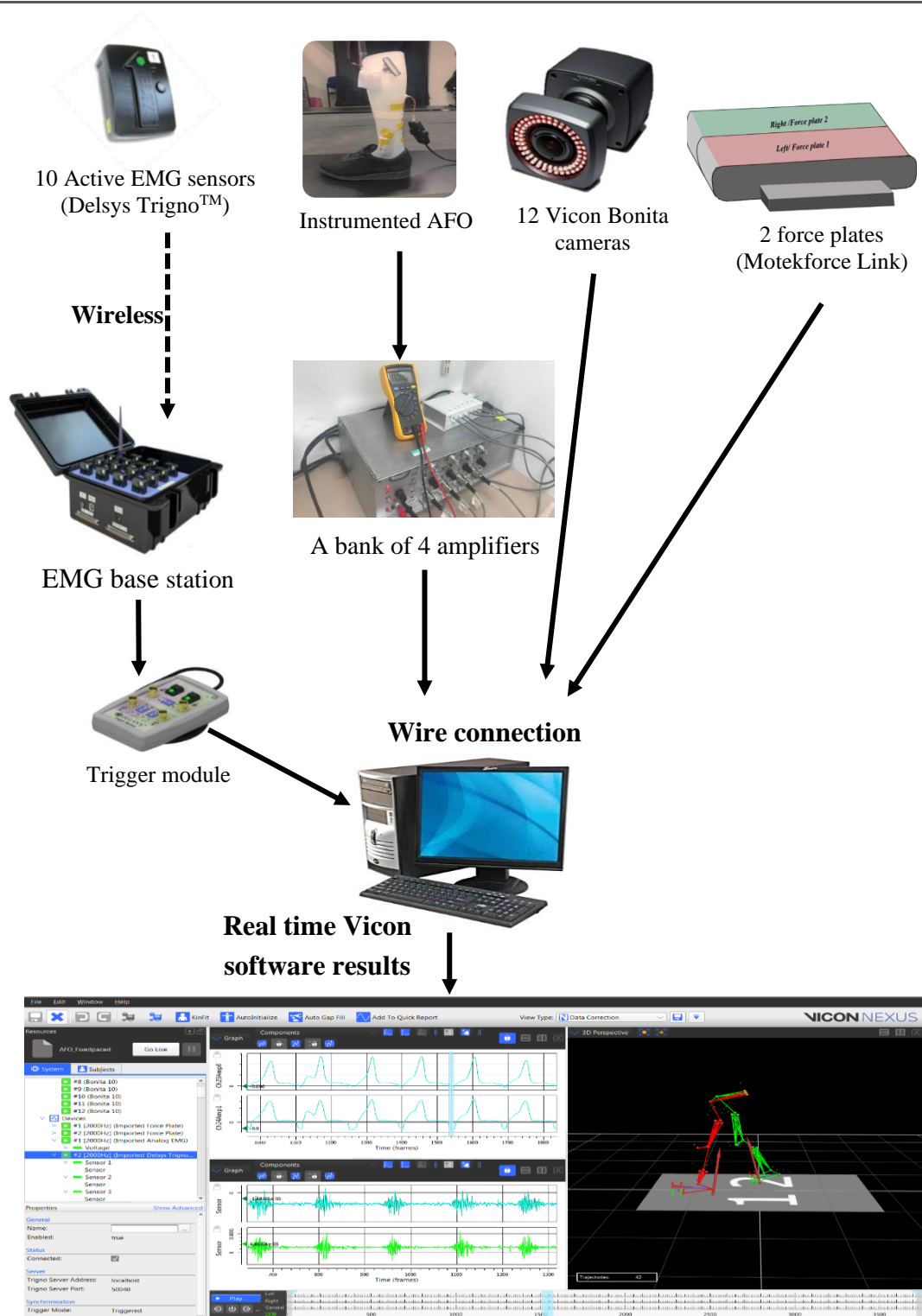


Figure 3.21: The experimental set up for gait analysis.

- The origin of the lab was defined, and the force plates were set to zero (as mentioned in section 3.3.2 under the heading “The instrumented treadmill”).
- The batteries of the ten EMG signals were checked to ensure that they were fully charged. Then, the EMG system was synchronised with the gait laboratory software, and the trigger module was checked if it was able to allow simultaneous data collection with force plates and 3-D markers trajectories (as mentioned in 3.3.3 under the heading “EMG signal placements”).
- Retro-reflective markers and EMG sensors were prepared with double-sided adhesive tape, and the elastic bandages to bind on top of the marker clusters were made available. Appropriate sizes of standard shoes (Potenza, Renace limited, UK) (Figure 3.22), shaving razors, EMG gel, alcoholic wipes, cleaning wipes, scissors, a pen, a shoe horn, shoe sterilising spray, heel wedges and towels were all made ready in preparation for testing.

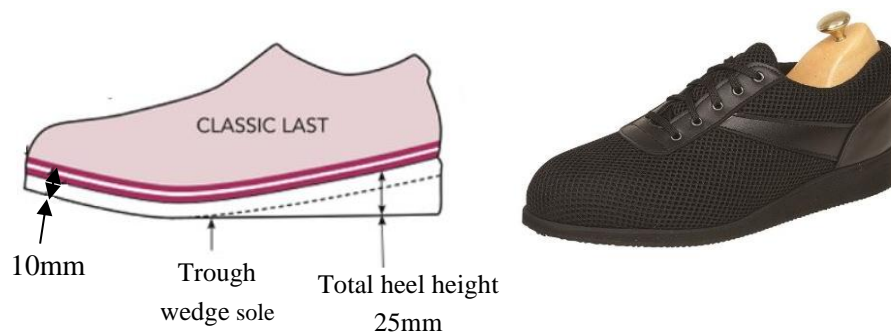


Figure 3.22: Standard Shoes (Potenza Renace).

-
- A 15-metre long multicore shielded cable was used to connect the instrumented AFO to a bank of four amplifiers. This cable was lifted up to the ceiling, passing through the harness system’s hook then dropped down to be connected with the instrumented AFO. The cable length was adjusted in order not to restrict the participant’s walking on the treadmill and to avoid creating stress over the wire circuit.
 - The bridge voltage output from each strain gauge (channel) was connected to the amplifier. The amplifier was linked to Vicon laboratory software to synchronise

the strain gauge data with force plates and 3-D markers trajectories. Prior to data collection, the bridge voltage, gain and output for each channel were set at 3V, 200 and 0, respectively (as mentioned in section 3.3.1 under the heading “‘AFO calibration’’”).

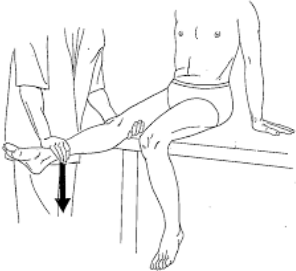
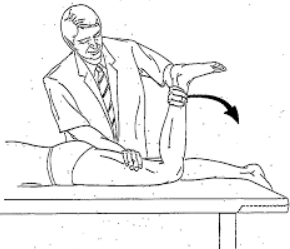
3.4.2 Manual muscle test (MMT)

The test procedures and equipment used were briefly explained to each participant. All participants were asked to change into close-fitting shorts, like cycling shorts, (Figure 3.23) so that accurate motion of the participant’s leg could be recorded.

The participant’s skin was prepared in order to attach ten wireless active EMG sensors (Delsys Trigno™, Boston, USA) as mentioned in details in section 3.3.3 under the heading “‘EMG signal placements’”. Comparing muscle activity among muscles, conditions and participants cannot be accomplished without normalizing it to a reference value (Criswell, 2010, De Luca et al., 2010). This is because EMG data can vary based on several factors related to electrode placement, amplification, skin impedance, difference between muscles and participants, etc... These factors can cause significant fluctuations in the recorded EMG data by increasing variation within and between tested muscles and participants (Kasprisin and Grabiner, 1998, Sinclair et al., 2015).

The most convenient reference for the normalization process is recording the muscle activity during a maximum manual muscle test (MMT) (Lin et al., 2008, Perry and Burnfield, 2010). MMT is a rehabilitation method used to evaluate the muscle strength. In this study, the MMT was used as a reference to normalize the EMG data by recording the contraction of two muscle groups (Knee flexors and extensors). To test each muscle group manual resistance was applied against muscle group action (Flexion for knee extensors and extension for knee flexors). Muscle contraction was considered to reach maximum when the resistance provided prevents the muscle group from completing the range of motion of its action, so that muscle contraction almost reaches an isometric state. This test was repeated three times on each muscle group and on each lower limb; starting with one side followed by the other side to minimise muscle fatigue. The EMG signal of each muscle was recorded over a period of 3-5 seconds starting from no contraction reaching to maximum and ending in no contraction. The MMT positions for quadriceps and hamstring muscles are illustrated in table (Table 3.2).

Table 3.2: Manual muscle test for quadriceps and hamstring muscles (Halaki and Ginn, 2012, Konrad, 2005).

| Muscle group investigated | Manual muscle test |
|---------------------------------------------------------------------------------------------------------------------------------------------------------|--------------------------------------------------------------------------------------------------------------------------------------------------------------------------------------------------------------------------------------------------------------------------------------------------------------------------------------------------------------------------------------------------------------------------------------------------------------------------------------------------------------------------------------------------------------------------------------------------------------------------------------------------------------------------------------------------------------------------------------------------------------------------------------------------------------------------------------------|
| <p data-bbox="277 389 533 425"><i>Quadriceps muscle</i></p>  | <p data-bbox="657 358 919 394"><u>Participant position:</u></p> <p data-bbox="657 407 1383 488">The participant sits on a chair with 60° knee flexion and 90° hip flexion.</p> <p data-bbox="657 510 903 546"><u>Examiner position:</u></p> <p data-bbox="657 560 1383 694">The examiner stands at the side of the tested limb placing one hand over the anterior surface of the distal leg just above the ankle and placing the other hand under the distal thigh.</p> <p data-bbox="657 712 724 748"><u>Test:</u></p> <p data-bbox="657 761 1383 945">The participant extends his/her knee through the available range of motion while the examiner is applying manual resistance over the anterior surface of the distal leg just above the ankle and stabilising the thigh by the other hand.</p> |
| <p data-bbox="277 1030 526 1066"><i>Hamstring muscle</i></p>  | <p data-bbox="657 1003 919 1039"><u>Participant position:</u></p> <p data-bbox="657 1052 1383 1133">The participant lays in prone position with 90° knee flexion and 0° hip extension.</p> <p data-bbox="657 1151 903 1187"><u>Examiner position:</u></p> <p data-bbox="657 1200 1383 1335">The examiner stands at the side of the tested limb placing one hand over the posterior surface of the distal leg just above the ankle and placing the other hand above the distal thigh.</p> <p data-bbox="657 1352 724 1388"><u>Test:</u></p> <p data-bbox="657 1402 1383 1585">The participant bends his/her knee through available range of motion while the examiner is applying manual resistance over the posterior surface of the distal leg just above the ankle and stabilising the thigh by the other hand.</p> |

3.4.3 Gait laboratory testing procedure

Participants were given appropriate sizes of standard shoes (Potenza, Renace limited, UK) (Figure 3.22). To minimize the influence of footwear, all participants wore the same type of standard shoes (Potenza Renace, Figure 3.22) to perform the test. The shoes were sterilised before and after the test session with an antibacterial/antifungal sterilising spray to prevent foot infection due to using shared shoes. The anatomical reflective markers were directly placed on the skin of both lower limbs using hypoallergenic double-sided adhesive tape. The pelvis cluster and the other four fixed clusters (technical markers) were placed on the lateral aspect of each lower limb segment at the mid-segment level (as aforementioned in section 3.3.2 under the heading ‘‘Reflective marker positions’’ (Figure 3.23).

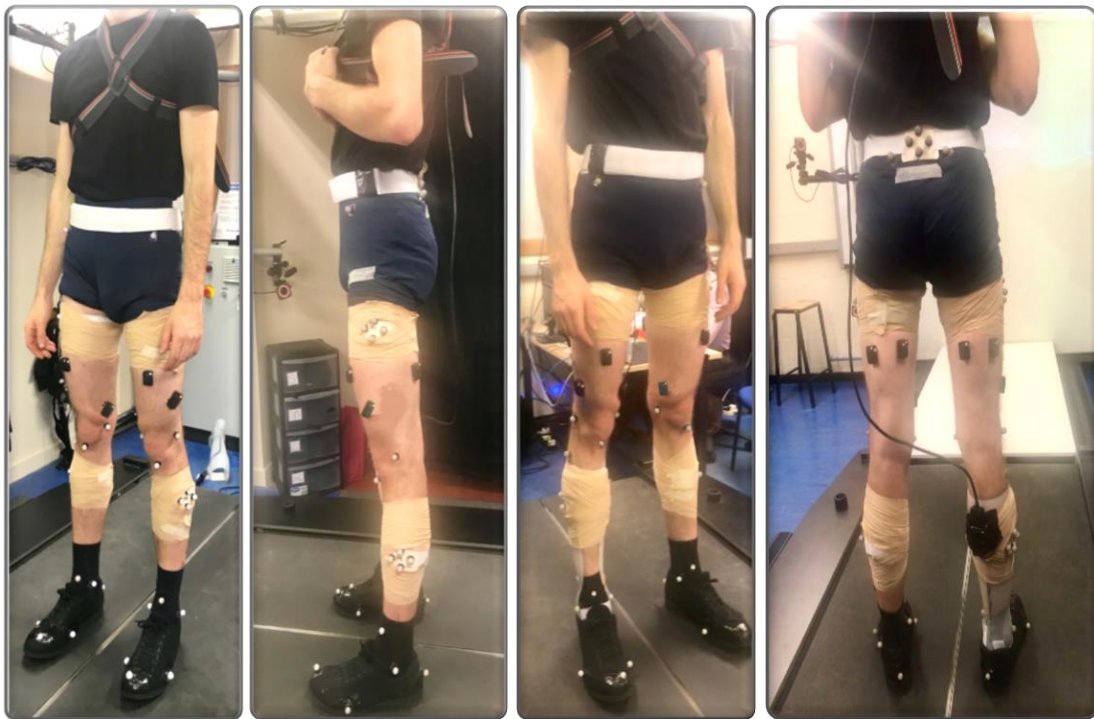


Figure 3.23: Anatomical and technical markers.

Prior to data collection, all participants had the opportunity to become familiar with the instrumented AFO; they were asked to walk overground for ten minutes to ensure proper fit of the shoes and the AFO, and acceptable comfort level.

Before the walking test commenced, a supportive harness was fitted around the participant's chest and shoulders. This harness is hung from the ceiling and tightened comfortably around the participant's chest and shoulders with the aim of eliminating the risk of tripping or falling off the treadmill (Figure 3.24). Afterwards, the participants were allowed to familiarise themselves with the treadmill and to measure their Comfortable Walking Speed (CWS) by asking them to walk at a self-selected speed for two minutes. The average of their maximum and minimum CWSs was then calculated to find their CWS. Walking with AFO may affect the participant's CWS; therefore, at the beginning of each test condition, the CWS was found and applied on the treadmill for that tested condition. Thus, the speed could be compared among test conditions. For each test condition, the participants walked for 2 minutes on the treadmill (to find their CWS and to allow familiarization), and 30 seconds of walking was then captured. The treadmill speed was controlled using the position and acceleration of the participant (as measured by Vicon motion capture system) by Motek D-Flow software (Motekforce Link, the Netherlands). The D-flow is a visual programming tool that uses virtual reality applications to improve clinical research in rehabilitation. In this study, the D-flow system was only used to control the participant's speed and to project a virtual scene on both wall and floor screens ahead of the participants by two mounted projectors as shown in Figure 3.9.

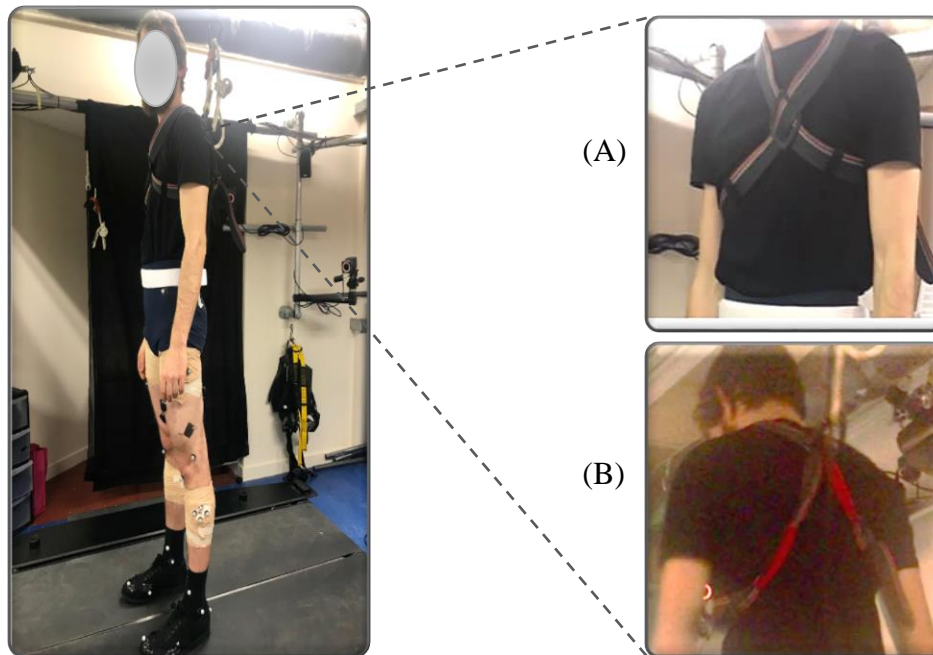


Figure 3.24: The supportive harness used during treadmill walking. The focused pictures show anterior (A) and posterior (B) views of the supportive harness.

Furthermore, static 3D image was taken prior to each walking condition. The participants were asked to stand steady on the two force plates (left foot on force plate 1 and the right foot on force plate 2) with their feet parallel to each other and pointing forward toward the walking direction. After ensuring that all of the markers were able to be seen by the cameras, all participants were asked to walk on the treadmill where their gait was recorded at their CWS. All participants were given time to have a rest after every tested condition, if required. Three conditions were performed in random order:

❖ *Condition 1: Standard Shoes Only (SSO)*

The participants were asked to walk while wearing standard shoes only (Potenza Renace, Figure 3.22) to perform the test. This provided a baseline dataset for the footwear conditions.

❖ *Condition 2: AFO*

The participants were asked to walk while wearing the standard shoes with the instrumented AFO (before tuning).

❖ *Condition 3: Tuned-AFO*

The participants were asked to walk while wearing the standard shoes with the same instrumented AFO in condition 2 but with temporary tuning wedge(s). The tuning wedge(s) was/were inserted under the heel of the AFO (inside the standard shoes) to achieve an optimal SVA, see section 2.5.4 under the heading “The AFO alignment”. Additionally, the same number of tuning wedges was also placed under the other foot in order to equalise the leg length. These wedges were custom made by an experienced technician, and were made from a synthetic cork (Birkocork, Algeos, UK), a high-density material. The heel wedge was either placed under the heel only or was extended from the heel to terminate at the metatarsophalangeal joints; this was done based on the participant’s comfort. If more than one wedge was used, the wedges were adhered together using a super glue material (Kövuifix, Polychloroprene, Germany), as illustrated in Figure 3.25.



Figure 3.25: Tuning heel wedges.

The AFO for each participant was tuned by an experienced orthotist to achieve the optimal SVA (Figure 3.26). Initially, a visual assessment was performed. This was followed by 3D motion analysis. The target was reaching 10°-12° of SVA at mid stance period of the gait cycle (dynamic SVA) or at static condition (quiet standing). Measuring the SVA during static condition showed reliable results to the dynamic SVA values measured at mid stance (Eddison et al., 2017). Measuring the SVA during testing either during static or dynamic conditions was not applicable; as this requires an immediate analysis of the participant’s data and accurately estimating the SVA using multiple software not available in the laboratory PC. Measuring the SVA during testing was also not applicable due to the limited testing time.

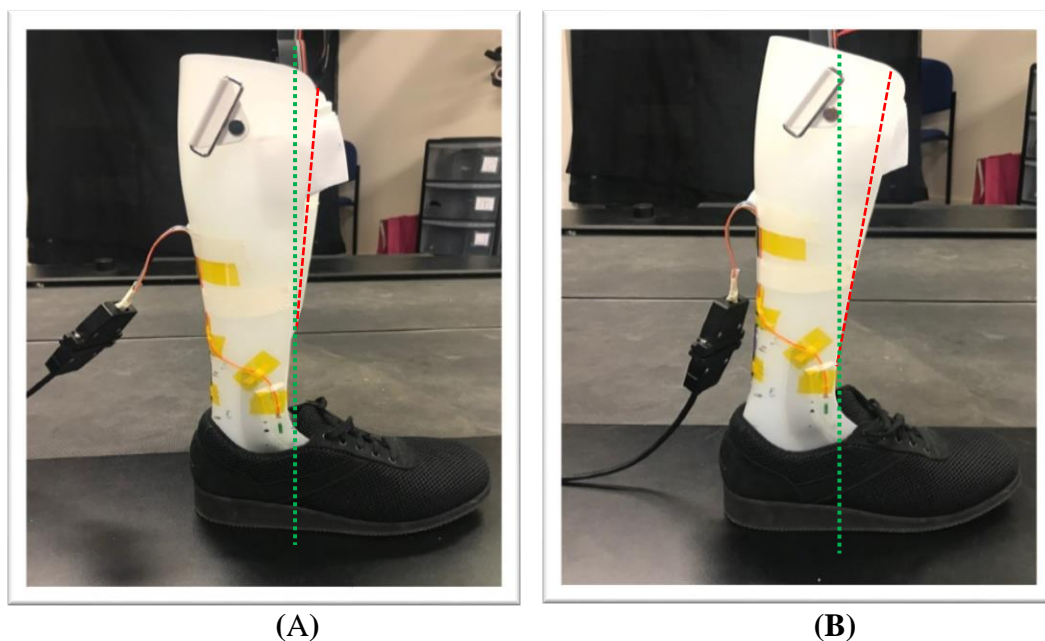


Figure 3.26: Example of an AFO before tuning (A) and after tuning (B). The red line represents the long axis of the shank of the AFO. The green line represents the vertical line. The red line tilts more forward with tuning (B) than before tuning (A).

One of the main purposes of performing tuning is to align the GRF as close as possible, to hip and knee joints centres during mid stance to late stance (Eddison and Chockalingam, 2015, Owen, 2005a). During testing, the tuning process was performed firstly by eye, and then it was confirmed by detecting the GRF alignment at mid stance to late stance period using the motion capture system. The tuning process was performed following Owen’s procedure (Owen, 2005a). To adjust the AFO tuning, adequate temporary heel wedges were inserted under the heel of the AFO, inside an appropriate size of standard shoes. The participants were asked to walk on the treadmill, at a self-selected speed, for two minutes to allow familiarisation with the Tuned-AFO, only ten seconds were recorded to ensure that the GRF is passing, as closely as possible, anterior to the knee joint and posterior to the hip joint during mid stance to late stance. The location of hip and knee joint centres were estimated and were showed as virtual points in the recorded data using Vicon software as shown in Figure 3.27 (this will be discussed further in section 3.5.1 under the heading “Lower limb modelling”). This process was repeated until reaching the optimal possible alignment of the GRF, (aligning the GRF as closer as possible to the hip and knee joints). Once the AFO was optimally tuned, the participant

was asked to walk on the treadmill for another two minutes to become familiar with Tuned-AFO, and to find their CWS. Afterwards, 30 seconds of walking were recorded for each participant for the purpose of the data analysis.

The SVA was measured again at the end of the testing after processing and analysing the data. In the sagittal plane, the SVA is measured as the angle between the shank and the vertical (Owen, 2005a) (Figure 3.28). In this study, the anterior surface of tibia was used to identify the long axis of the shank (see section 2.4.4 under the heading ‘‘Shank alignment’’) (Kerkum et al., 2015b, Kessels et al., 2013). Using the anterior surface of tibia allows the markers to be directly attached to the participant’s skin. If the lateral markers placement method is used, the markers will be attached to the AFO (at the lateral malleolus) rather than the participant’s skin which is expected to result in larger artefacts due to relative motion between the shank and the AFO. In a recent study, this method was more accurate and more repeatable than using lateral markers placement method (Nguyen et al., 2020). For this purpose, extra reflective markers were attached at the tibial tuberosity and the anterior distal edge of tibia to the participant’s skin using hypoallergenic double-sided adhesive tape as shown in figures (Figure 3.28). Based on these markers’ locations, the SVA was calculated using a code written in Matlab software (MathWorks 2017, Massachusetts, USA) by the author (Matlab codes SVA angle Appendix (I)). This equation was used to calculate the SVA:

$$SVA = \tan^{-1} \left[\frac{TT_{AP} - TD_{AP}}{TT_v - TD_v} \right] \quad \text{Equation 2}$$

Where TT_{AP} and TD_{AP} denote the anterior-posterior location of tibial tuberosity and distal tibial markers, respectively. TT_v and TD_v denote the vertical location of tibial tuberosity and distal tibial markers, respectively.

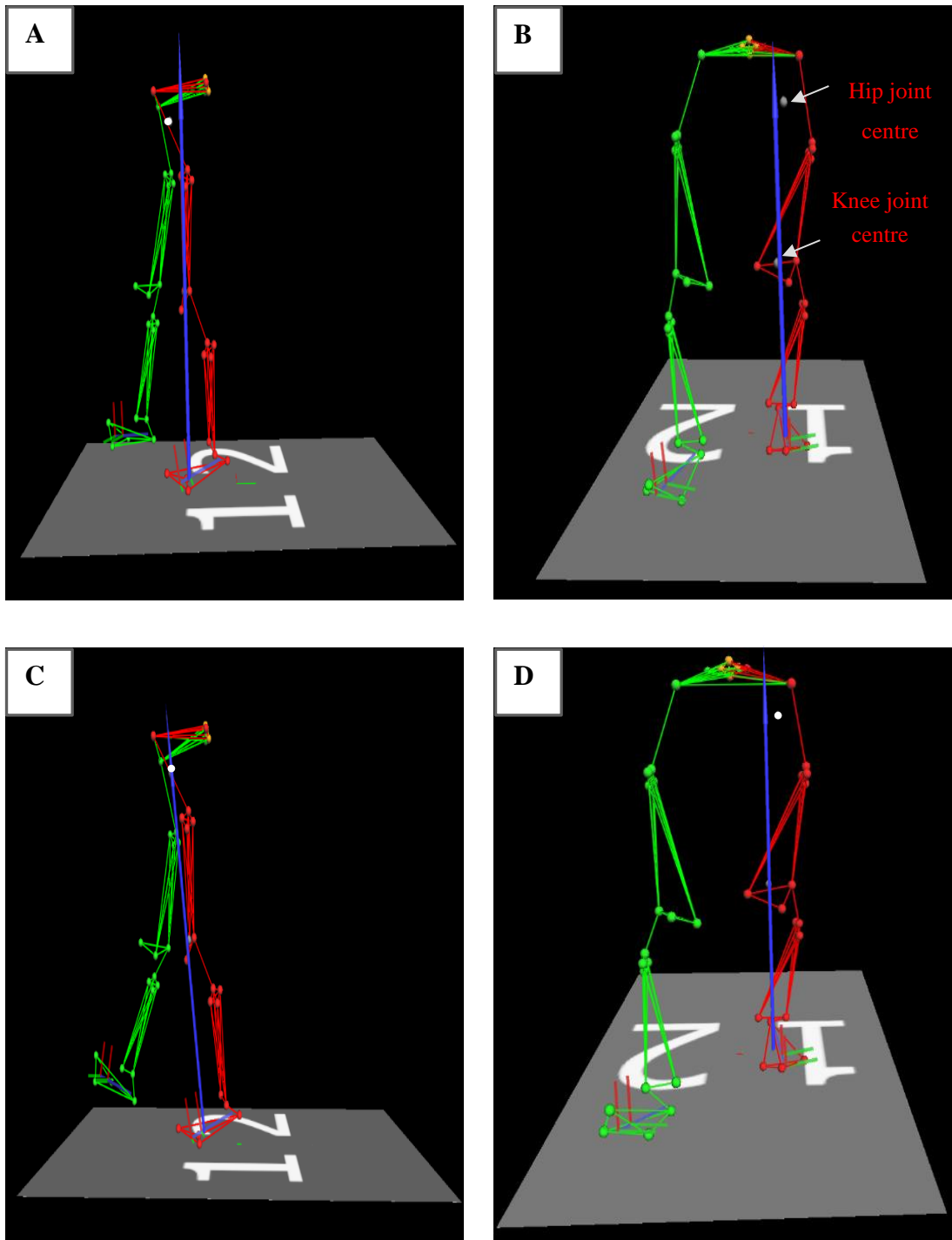


Figure 3.27: The GRF (blue arrow) location relative to hip and knee joints in left Tuned-AFO (red) during midstance (Lateral view (A), Anterior view (B)) and terminal stance (Lateral view (C), Anterior view (D)).

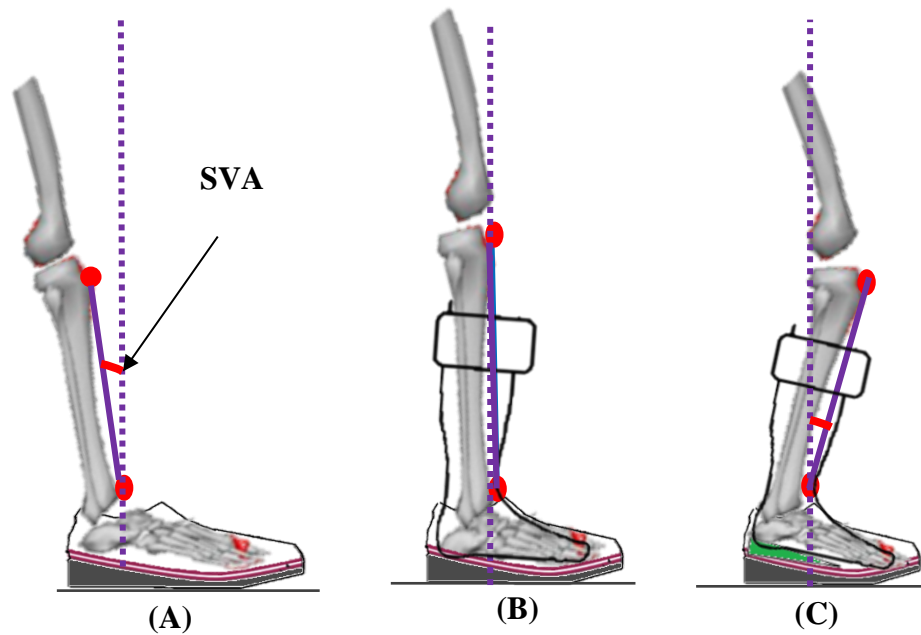


Figure 3.28: Demonstration of SVA with SSO (A), AFO (in this diagram, it was assumed that the AFO was set at 90°) (B), and Tuned-AFO (C).

3.5 Motion data processing

After kinematic and kinetic data were collected, they were processed using Vicon Nexus software (Oxford Metrics Ltd., UK). Raw EMG and SG data were stored as analogue data in Vicon Nexus software, and were exported as C3D files to be analysed using Matlab software (MathWorks 2017, Massachusetts, USA), this will be discussed further in section 3.6 under the headings (“EMG data analysis” and “SG data analysis”).

Following that, each trajectory marker was digitised and labelled as shown in Figure 3.29. Cubic spline interpolation was used, if needed, to fill gaps of a maximum of ten missing frames in the trajectory.

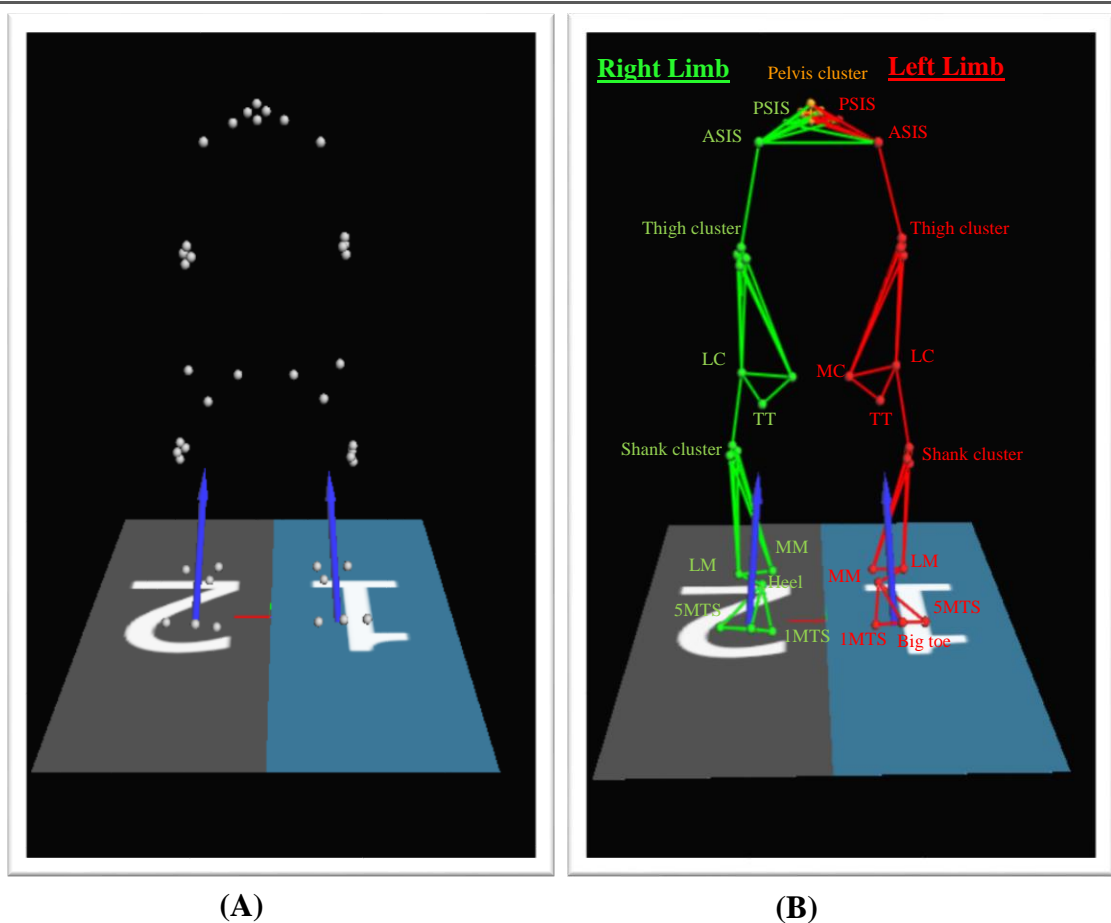


Figure 3.29: Static participant's markers before (A) and after (B) labelling.

All raw data were truncated to contain only the relevant portion needed for analysis. For instance, if the participant had not completely placed his/her left foot only on the left force plate (left treadmill belt) and his/her right foot only on the right force plate (right treadmill belt) during stance phase for each foot, this part of data was trimmed out to not affect the kinetic results (Figure 3.30).

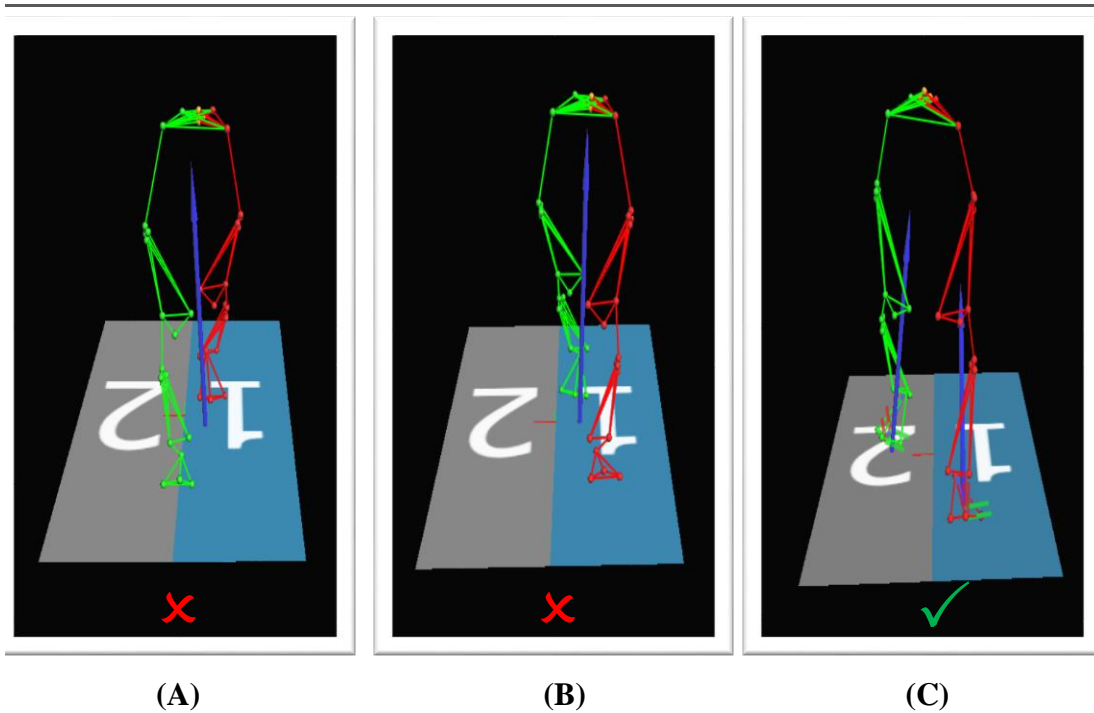


Figure 3.30: Examples of some walking scenarios. Only (C) was considered successful trial, while (A) and (B) were considered unsuccessful ones.

3.5.1 Lower limb modelling

A six-degree of freedom model for the lower limbs developed at the biomedical engineering department at University of Strathclyde (Papi et al., 2014) was used in this study. This model was built using Bodybuilder software (Vicon, Oxford Metrics Ltd., UK) based on CAST method (Cappozzo et al., 1995). The six-degree model of freedom is used to define both translational and rotational movements of a rigid segment in 3D space (Figure 3.31). Rigid clusters were used to track each segment independently and to link them to the joints. Thus, the segments' translation in three perpendicular axes (vertical, medial-lateral and anterior- posterior) and their rotation about each axis of the segment (sagittal, frontal and transverse) were defined. Consequently, the pose (position and orientation) of each segment in 3D space was detected. Pelvis, thigh, shank, and foot segments were then modelled by determining the proximal and distal joint/radius and the tracking (technical) markers as illustrated in table (Table 3.3). The foot was considered as one rigid segment and thus, this model did not differentiate between the ankle and

subtalar joints. Subsequently, the subtalar joint in this study was neglected and assumed as ankle joint.

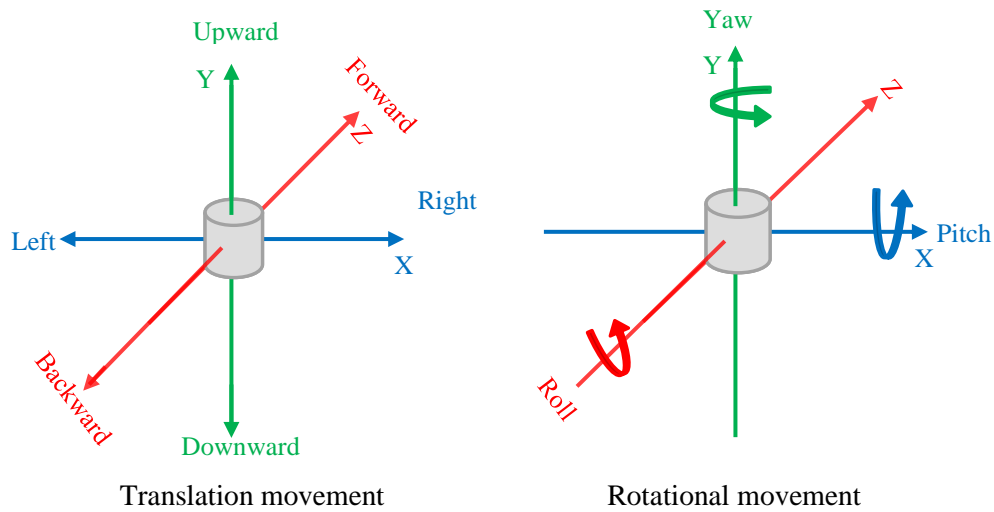


Figure 3.31: Six- degrees of freedom movements.

Joint centre locations were identified using the positions of the anatomical markers surrounding the joint, as the following;

✓ **Hip joint:** The right hip joint centre was predicted based on Harrington's (2007) method using the following linear regression equations:

$$\mathbf{X} = -0.24 \text{ PD} - 9.9$$

$$\mathbf{Y} = -0.30 \text{ PW} - 10.9$$

$$\mathbf{Z} = 0.33 \text{ PW} + 7.3$$

Equation 3

Where **X**: the position of hip joint centre in the anterior-posterior axis, **Y**: the position of hip joint centre in the vertical axis, **Z**: the position of hip joint centre in the medio-lateral axis, **PD**: pelvic depth (the distance between the midpoints of the line segments connecting the two ASISs and the two PSISs), and **PW**: pelvic width (the inter ASISs distance), Figure 3.32.

Similarly, the left hip joint centre was predicted using the same equations above but with negating the position of the hip joint in medial-lateral axis (Z) (Harrington et al., 2007).

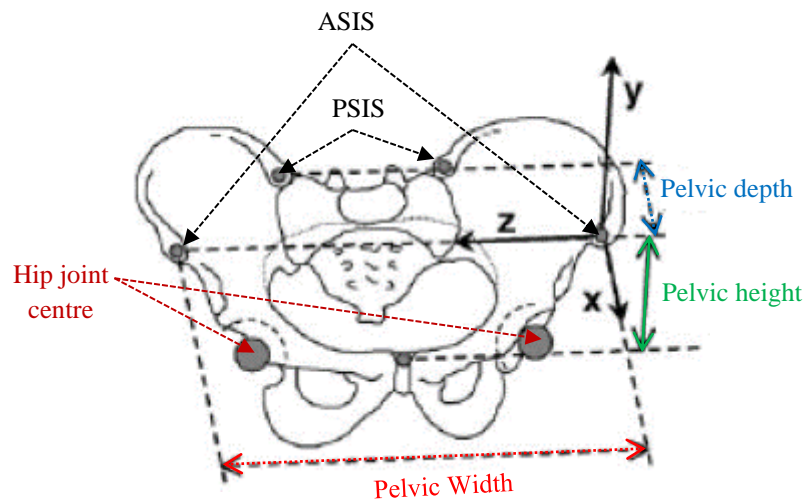


Figure 3.32: Pelvic depth, height and width. Adpated from (Della Croce et al., 2005).

- ✓ **Knee joint:** The knee joint centre was estimated at halfway of the line between medial and lateral condyles of femur in the anterior-posterior axis, the medio-lateral axis and the vertical axis.
- ✓ **Ankle joint:** The ankle joint was estimated at halfway of the line between medial and lateral malleoli in the anterior-posterior axis, the medio-lateral axis and the vertical axis.

The anatomical coordinate systems (frames) were defined for each segment (Table 3.3). For pelvis, femur and tibia/fibula segments, the anatomical frames were defined in agreement with ISB recommendations (Wu et al., 2002) (Table 3.3 and Figure 3.33). For the foot segment, the vertical axis was the X-axis (not the Y-axis as in ISB convention), and the Y-axis was defined as anterior-posterior axis. Changing the arrangement of ISB convention for foot segment to the aforementioned arrangement was done to keep the rotation definitions of ankle joint consistent with clinical terminology (Baker, 2003).

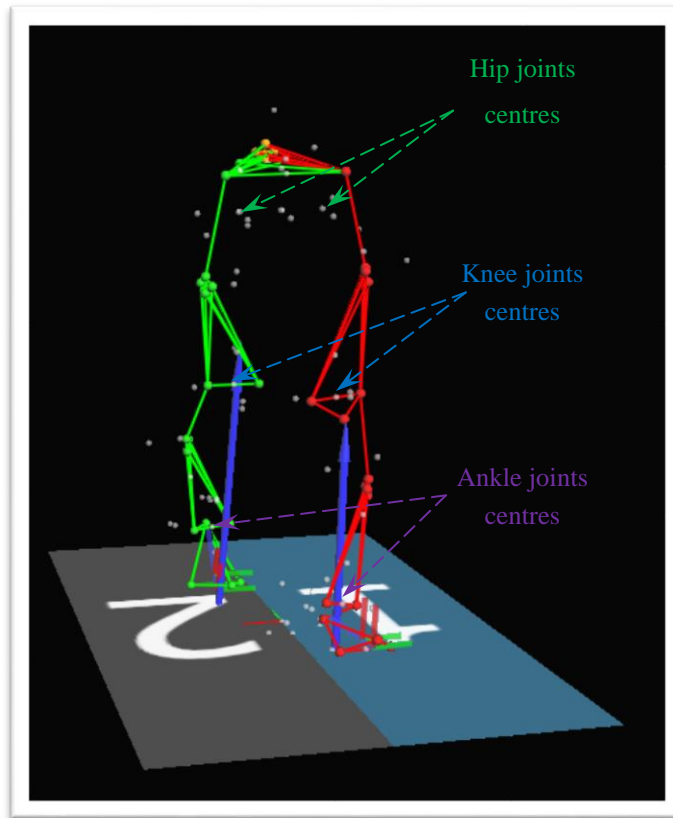


Figure 3.33: The modelled markers that represent the hip, knee, and ankle joints centres.

Table 3.3: The model segments and their anatomical reference frames definitions. Adapted from (Papi et al., 2014).

| <i>Segments</i> | | <i>Anatomical frames</i> |
|--------------------------------|-------------------------------------------------------------|--------------------------|
| ❖ Pelvis | | |
| <i>Proximal radius</i> | Left and right ASIS | |
| <i>Distal radius</i> | Left and right PSIS | |
| <i>Tracking marker</i> | Pelvis cluster | |
| <i>Anatomical frame origin</i> | Midpoint between LASIS and RASIS | |
| ❖ Femur | | |
| <i>Proximal radius</i> | Hip joint centre | |
| <i>Distal radius</i> | MC and LC | |
| <i>Tracking marker</i> | Thigh cluster | |
| <i>Anatomical frame origin</i> | Knee joint centre | |
| ❖ Tibia/Fibula | | |
| <i>Proximal radius</i> | MC and LC | |
| <i>Distal radius</i> | MM and LM | |
| <i>Tracking marker</i> | Shank cluster | |
| <i>Anatomical frame origin</i> | Ankle joint centre | |
| ❖ Foot | | |
| <i>Proximal radius</i> | MM and LM | |
| <i>Distal radius</i> | 1 MTS and 5 MTS | |
| <i>Tracking marker</i> | Heel, Toe cap and mid foot (midpoint between 1MTS and 5MTS) | |
| <i>Anatomical frame origin</i> | Heel | |

3.5.2 Kinematics calculation

The angle between two adjacent segments was calculated using joint coordinate system (JCS) (Grood and Suntay, 1983). This method defines the rotation of the joints in relation to the clinical and anatomical definitions. The JCS method defines each joint by a non-orthogonal “working” axis system, which consists of three axes (fixed medio-lateral axis of the proximal segment (e_1), fixed long axis of the distal segment (e_3), and a not fixed (floating) perpendicular axis to the other two axes (e_2), (Figure 3.34)). The rotation about each axis describes the relevant motion occurring at the joint; the rotation about the proximal medio-lateral axis, distal long axis and floating axis represent flexion/extension, internal/external rotation, and abduction/adduction, respectively (Figure 3.34). The lower limb joints angles were calculated using the following equations:

$$\sigma = \cos^{-1}(e_{2ij} \cdot t_i) \times B$$

Equation 4

where $B = 1$ if $(e_{2ij} \cdot l_i) > 0$ else $B = -1$

σ : Flexion/extension angle, e_{2ij} : floating axis, t_i : the third axis of the proximal segment (the flexion/extension reference axis), l_i is the proximal longitudinal axis. B^* determines the sign of the angle.

$$\gamma = \cos^{-1}(e_{2ij} \cdot t_j) \times D$$

Equation 5

where $D = 1$ if $(e_{2ij} \cdot f_j) > 0$ else $D = -1$

γ : Internal/external rotation angle, t_j : third axis of the distal segment, f_j : flexion axis of the distal segment. D^* determines the sign of the angle.

$$\beta = \cos^{-1}(r \cdot l_j) \times C$$

Equation 6

where $r = \left(\frac{f_i \times e_{2ij}}{|f_i \times e_{2ij}|} \right)$

and $C = 1$ if $(f_i \cdot l_j) > 0$ else $C = -1$

β : Abduction/adduction angle, r : axis mutually orthogonal to the proximal flexion axis (f_i) and the floating axis and orientated downwards, l_j : distal longitudinal axis. C^* determines the sign of the angle.

*Counter-clockwise rotations about each axis were considered positive.

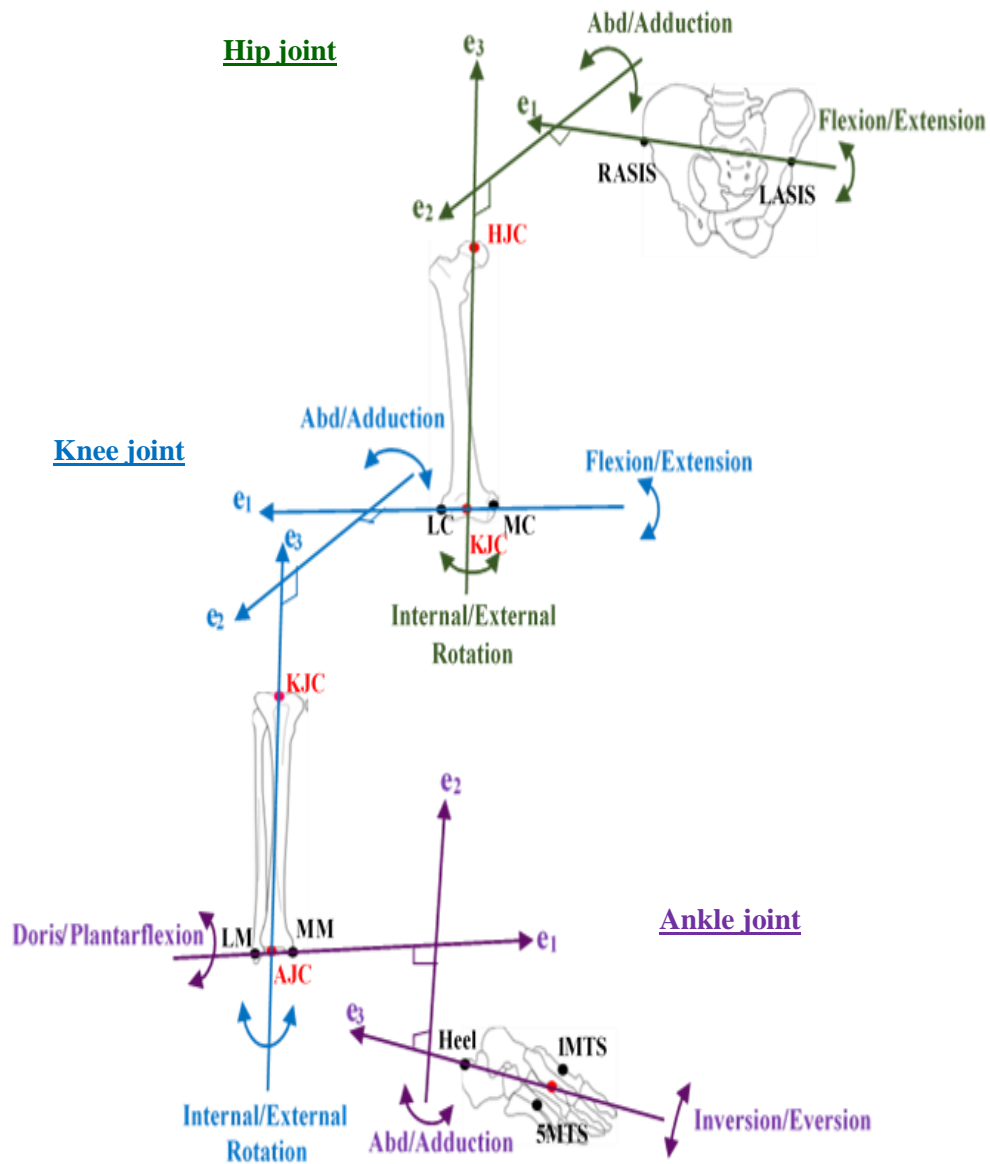


Figure 3.34: The hip, knee, and Ankle coordinate systems. Adapted from (Papi et al., 2014)

3.5.3 Kinetics calculation

Joint Kinetics were calculated using an inverse dynamics method. This method calculates net forces and moments acting in a rigid linked segment model in 3D space, using external forces (GRFs) and moments on the anatomical joints (based on the kinematics and inertial properties of the segments) (Vaughan et al., 1992). The GRFs were measured using two force plates (Motekforce Link, Amsterdam, Netherlands) while performing the walking trials. The segment kinematics, particularly accelerations, were calculated by differentiating the displacement of the segments in order to measure the joint moment. Segment inertial properties were estimated based on the anthropometric data which were obtained from Winter (2009).

Forces and moments were calculated at the hip, knee, and ankle in the anatomical frame of the distal segment (femur, tibia/fibula, and foot, respectively) (Table 3.3). The basic equations to calculate the force (F) and moment (M) in inverse dynamics are:

$$\sum F = ma = F_{\text{dist}} + F_{\text{prox}} + mg \quad \text{Equation 7}$$

m : mass of the limb segment, a : the acceleration of the limb segment, F_{dist} : the force of the distal limb segment acting on the limb segment of interest, F_{prox} : the force of the proximal limb segment acting on the limb segment of interest, and g is the acceleration due to gravity.

$$\sum M = I\alpha = M_{\text{dist}} + M_{\text{prox}} + F_{\text{dist}} * r_{\text{dist}} + F_{\text{prox}} * r_{\text{prox}} \quad \text{Equation 8}$$

I : the moment of inertia of the limb segment, α : the angular acceleration of the limb segment, M_{dist} : the moment of the distal limb segment acting on the limb segment of interest, M_{prox} : the moment of the proximal limb segment acting on the limb segment of interest, r_{dist} : the lever arm between the line of action of F_{dist} and the limb segment centre of mass, and r_{prox} is the moment arm between the line of action of F_{prox} and the limb segment centre of mass.

Hip, knee and ankle moments model outputs were normalized to the participants' body mass and height in order to reduce variability among participants by about 50% (Winter,

2009). Variability among participants, may result from factors like gender, body mass and height (Moisio et al., 2003).

3.6 Data analysis

Prior to data analysis, a low pass filter was applied to eliminate high frequency noise with a cut-off frequency of 6 Hz for kinematic and kinetic model outputs data using a Butterworth fourth order filter. All data (kinematic and kinetic model outputs, GRFs, marker trajectories, EMG and strain gauge analogue data) were exported as C3D files, which were then loaded into Matlab software (MathWorks 2017, Massachusetts, USA) to carry out further subsequent analyses and to be graphically illustrated. A Matlab Biomechanical toolkit (BTK), which was developed by Barre (2014), was used to read, write, modify and visualize the exported C3D files from Vicon Nexus software to Matlab software.

The primary outcome measures in this study were:

- ✓ ***Kinematic data in the sagittal plane***: ankle motion, Knee motion, hip motion and SVA.
- ✓ ***Kinetic data***: vertical GRF, ankle sagittal plane moment, knee sagittal plane moment and hip sagittal plane moment.
- ✓ ***Temporal-spatial parameters***: speed, stride length, stance and swing time.
- ✓ ***EMG data***: EMG amplitude and activation period.
- ✓ ***Strain gauge data***: orthotic and anatomical ankle moments in sagittal and frontal planes.

3.6.1 Kinetic and kinematic analysis

The gait events were determined in all conditions based on the vertical GRFs using a Matlab code that was written by the author (Matlab codes: gait events Appendix I). The gait cycle was defined from initial contact of the foot on the force platform to the subsequent ipsilateral (same foot) initial contact. Stance phase was defined from initial contact of the foot to the subsequent ipsilateral toe off, as illustrated in Figure 3.35. All kinematic and kinetic data were then interpolated with spline fills to 100 -time intervals across the gait cycle using Matlab software.

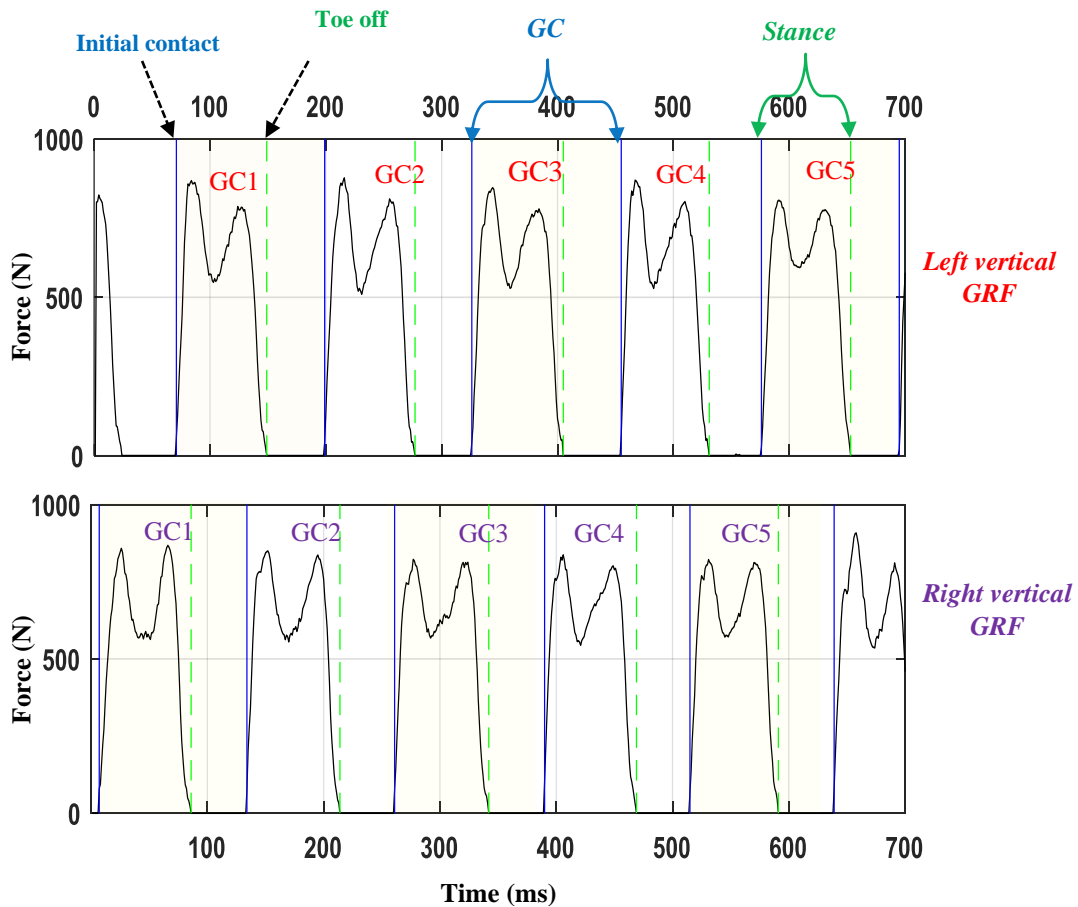


Figure 3.35: Determination of gait events using vertical GRF. This graph shows detection of five gait cycles (GCs) for both right and left limbs/GRF. The blue solid line represents the initial contact, and the green dashed line represents the toe off.

All kinetic and kinematic parameters were based on the mean and the standard deviation of the maximum/minimum peak values across fifteen gait cycles for each condition and for each participant (Figure 3.36). Regarding the SVA, as aforementioned in section 3.4.3, the SVA was also investigated at midstance of gait cycle, as this is the period of our interest in this study.

In addition, temporal-spatial parameters (speed, stance duration, single limb support interval (which is the period of stance phase where only one foot is in contact with the force plate), and double limb support interval (which is the period of stance phase when both feet are in contact with the force plates)) were also calculated to determine the differences between the tested conditions.

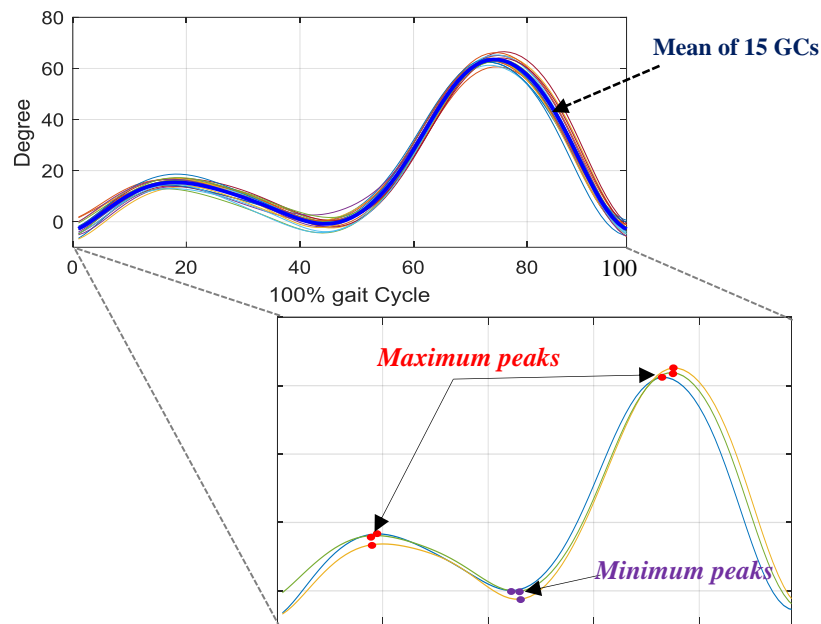


Figure 3.36: The maximum/minimum peak values calculation of the knee angle joint (as an example), which shows the mean for 15 GCs of the knee angle. The extended picture illustrates the peaks for only three GCs.

3.6.2 EMG data analysis

Raw EMG signal data, which were exported as C3D files into Matlab, represent the electrical action potential signals that were generated during muscle contraction (Figure 3.37, A).

(i). *EMG data processing*

The EMG data were processed following the guidelines provided by SENIAM (Stegeman and Hermens, 2007) using a Matlab code (Matlab codes: EMG Appendix I). The following steps were carried out to process the raw EMG data (Figure 3.37); (1) Second order Butterworth band pass filter (20-500 Hz) was used to eliminate low and high frequency noise from the signal, and to remove any direct current (DC) offset. (2) Full-wave rectification was performed by calculating the absolute values of the EMG signals, so that the negative and positive values do not cancel each other in subsequent processing. (3) The rectified data were then smoothed using infinite impulse response (IIR) notch filter at 50Hz (Hakonen et al., 2015). (4) Root mean square (RMS) was calculated to

measure the power of the EMG signal. The RMS represents the square root of the average amplitude of the EMG signal within a specific number of continuous time intervals (window length), which may also lead to smooth the signals. The window length was set at 0.01 second, as this was found to best represent the variation of EMG data (Burden et al., 2014), and to the best match the on/off time displayed by the raw EMG data (Perry and Burnfield, 2010).

(ii). Normalization of EMG data to MMT

The processed RMS data were then normalized to maximum muscle contraction that were provided from the three MMT recorded data as mentioned in section 3.4.2 under the heading ‘‘Manual muscle test (MMT)’’. Following the same aforementioned processing procedure, the RMS of the three MMT trials data was calculated for each muscle (A and B, Figure 3.38). To determine the maximum MMT magnitude, the mean value for the highest one second contraction of the MMT activation period was selected as reference value for each trial (Perry and Burnfield, 2010). Then the walking EMG data were normalized based on the maximum reference value across the three trials for each muscle (C and D, Figure 3.38), using the following equation:

$$\text{Normalised EMG}_{(x)} (\% \text{ MMT}) = \frac{\text{EMG}_{(x)} \text{ value during walking}}{\text{MMT}_{(\text{max})} \text{ value for EMG}_{(x)}} * 100 \quad \text{Equation 10}$$

Where **X**: The examined muscle, **EMG_(x) value during walking**: the RMS value of the examined muscle, **MMT_(max) value for EMG_(x)**: the maximum RMS of the maximum RMS values during MMT trials for the examined muscle.

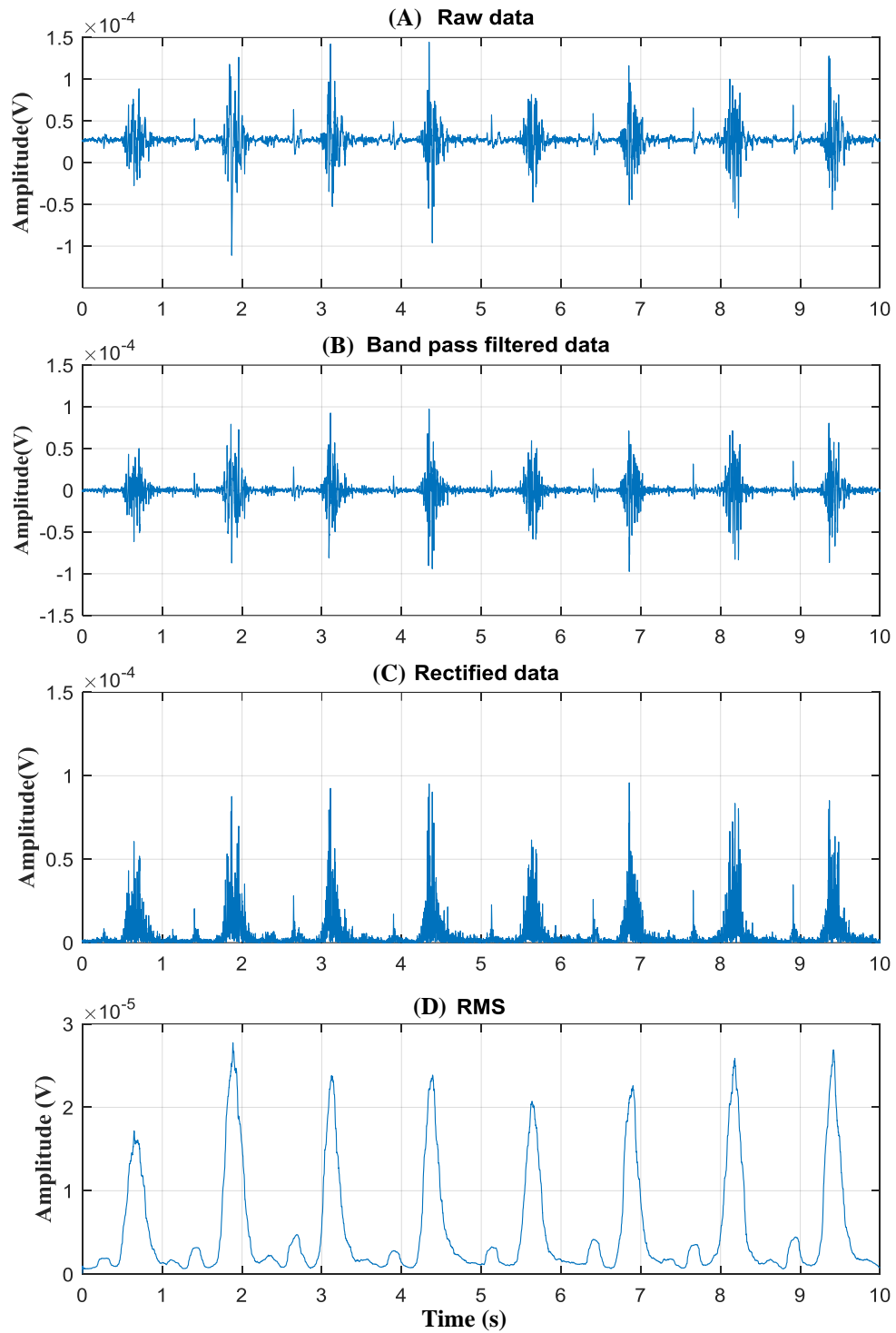


Figure 3.37: An example of EMG data processing steps (Left Vastus medialis muscle), X-axis displays time in second (s), and Y-axis displays the muscle amplitude in volts (V). Raw EMG data (A). Band pass filtered data (B). Rectified and smoothed data (C). Processed EMG data using RMS method (D).

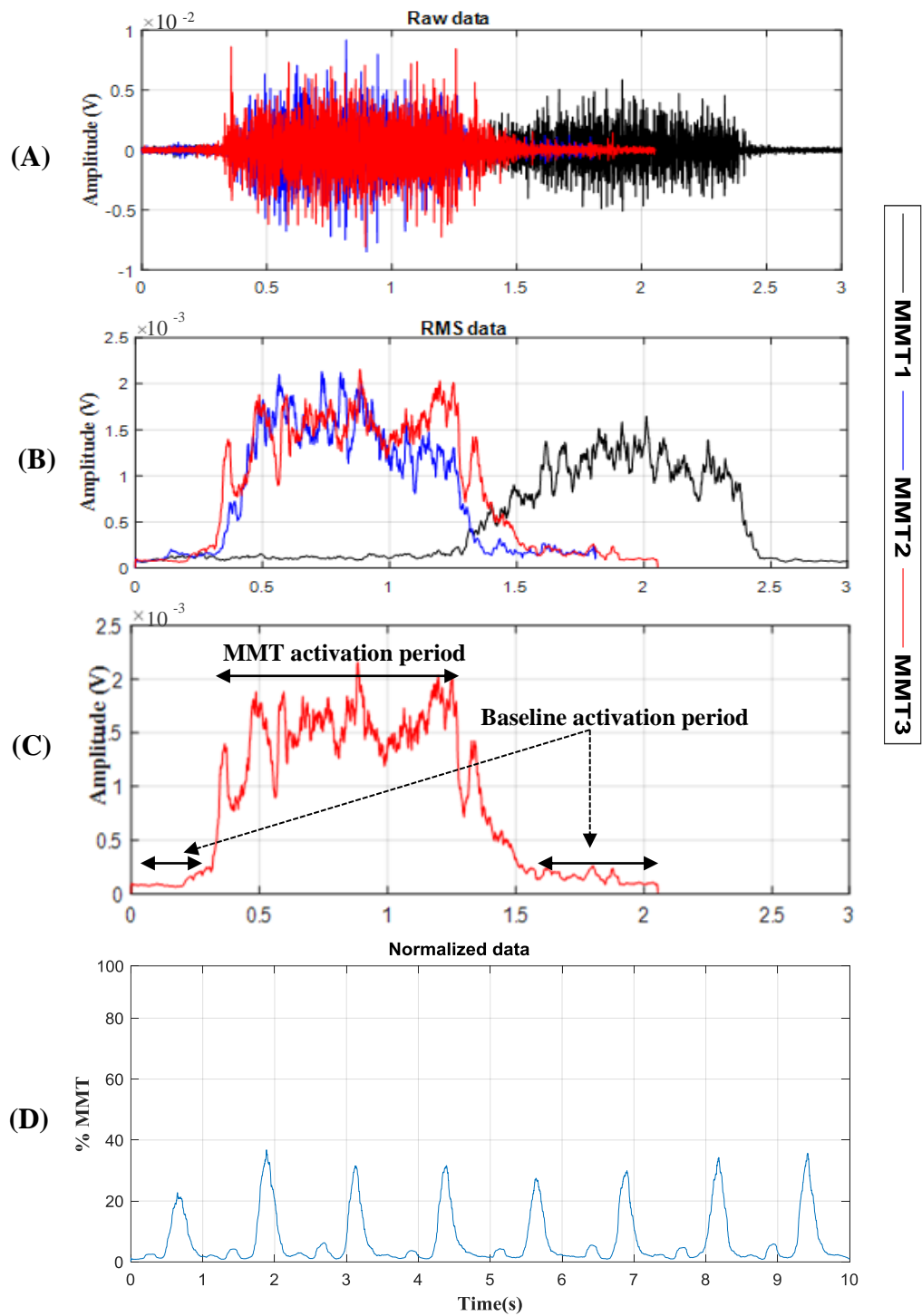


Figure 3.38: An example of EMG normalization processes (Left Vastus medialis muscle): The three raw MMT trials (A). Processed MMT trials (RMS) (B). MMT trial showing the baseline and the activation MMT periods (C). Normalized walking trial to the maximum MMT (D).

(iii). *Identification of muscle activation period*

The raw and processed EMG data were investigated to identify muscle activation period by finding the starting (on) and ending (off) points of muscle activation (Criswell, 2010). Although this has been estimated based on visual inspection of EMG graph, the muscle was only considered active when the EMG amplitude and the activation period reached at least 5% of MMT and 5% GC time (Bogey et al., 1992, Chimera et al., 2009, Perry and Burnfield, 2010, Takada et al., 1995) (Figure 3.39). This is because the threshold of (5%) of muscle contraction is considered clinically ineffective muscle contraction (grade 2; poor contraction) (Beasley, 1961).

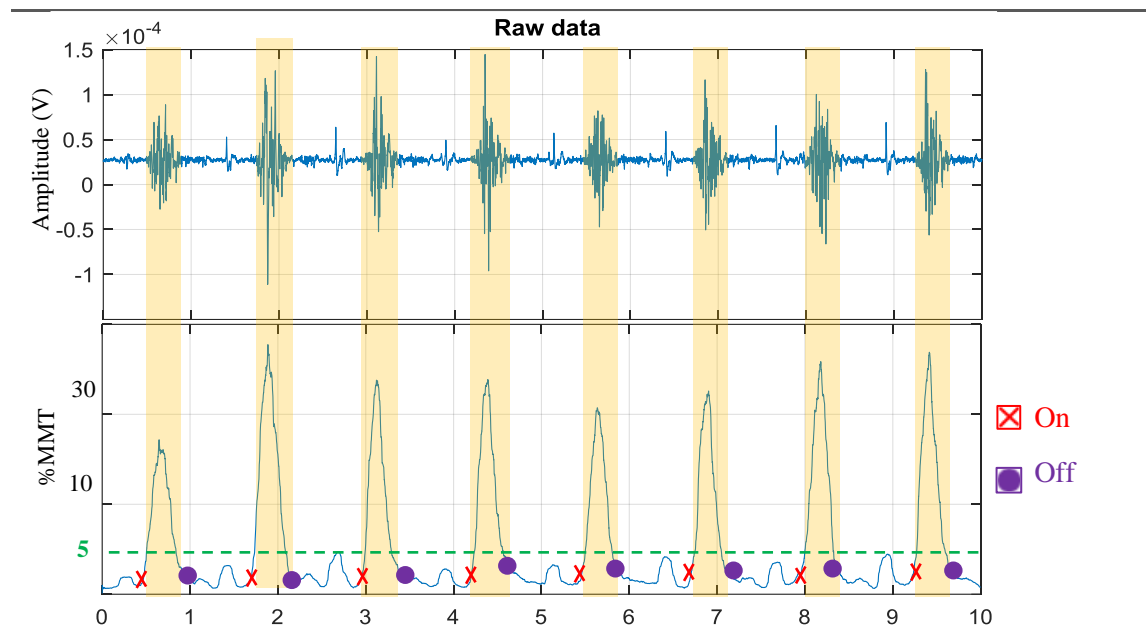


Figure 3.39: An example of determining the activation period (Left Vastus medialis muscle). Shaded regions indicate the muscle activation period. The red X and purple circle represent the starting (on) and ending (off) points of muscle activation, respectively. The horizontal green dashed line represents the threshold of (5%) of muscle contraction.

(iv). *Normalization of EMG data to gait cycle*

Based on synchronized vertical GRF data, the normalized EMG data were divided into gait cycles using the identified initial contact and toe off. Afterwards, all EMG data were presented over a complete gait cycle. The mean and the standard deviation of the

maximum peak values during the activation periods across the fifteen gait cycles for each condition and for each participant were then calculated (Figure 3.40).

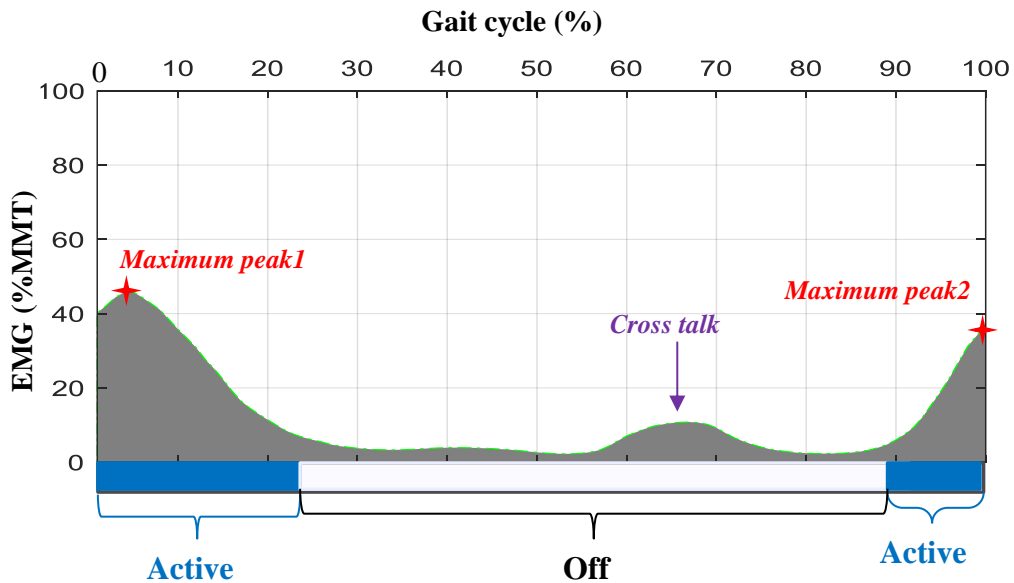


Figure 3.40: An example of processed EMG data. This graph shows the RMS for left vastus medialis muscle that is normalised to maximum MMT during 100% of the gait cycle. An example of cross talk interference from rectus femoris is also shown in the graph.

3.6.3 SG data analysis

(i). Normalization of SG data to gait cycle

Raw SG data, which were exported as C3D files into Matlab, represent the dynamic electrical resistance change (which represents the dynamic strain change) in the AFO during walking on treadmill (Figure 3.41). The raw data were offset to zero, then interpolated with spline fills to 100 time intervals across the gait cycle based on the synchronized gait events; that is derived from vertical GRF data as mentioned in section 3.6.1 under the heading “Kinetic and kinematic analysis”).

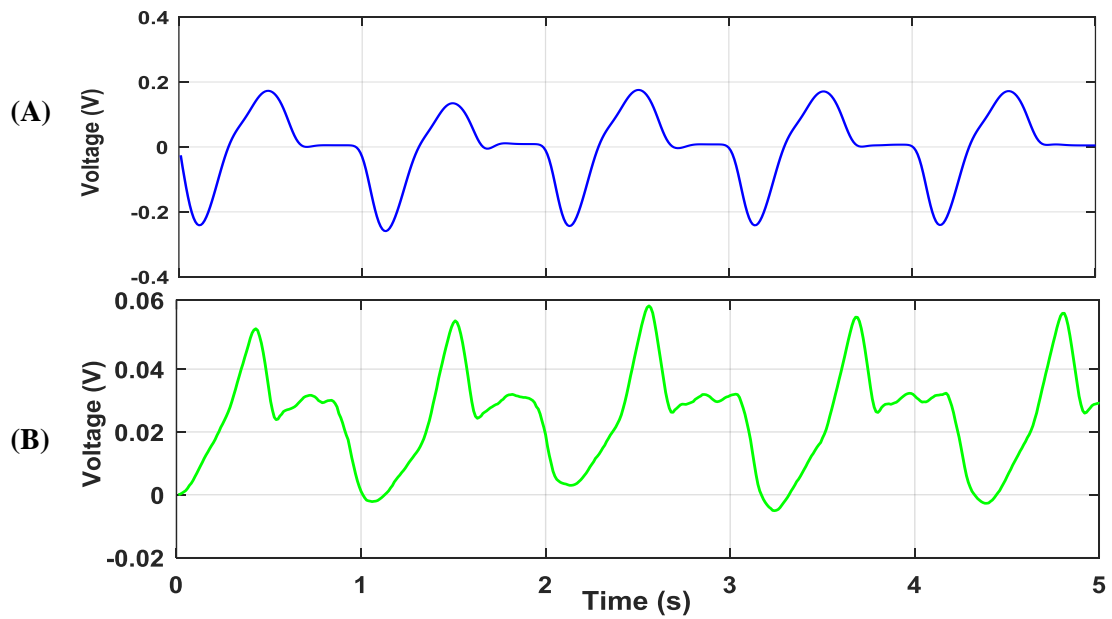


Figure 3.41: SGs raw data examples for SG2 (A) and SG4 (B).

(ii). Calculating the orthotic moment

The SG data outputs were converted from voltage (V) to moment (Nm/kg). For this purpose, the output voltages of the AFO calibration were plotted against the load applied for dorsiflexion (DF), plantarflexion (PF), inversion and eversion to test the linear behaviour of the SGs (Figure 3.42) (see “Strain gauges attachments” in section 3.3.1). This was conducted for each AFO separately.

As the SGs output voltages showed a linear behaviour with the load applied for DF, PF, inversion and eversion, the moments generated by the Instron were then calculated using this equation:

$$M = F * d * \sin \theta \quad \text{Equation 11}$$

Where M is the moment, F is the load, d is the distance between the load application point and the axis of the ankle joint, θ is the angle between (F) and (d) (θ was kept at 90 degrees during the test as force was always applied perpendicularly to (d)).

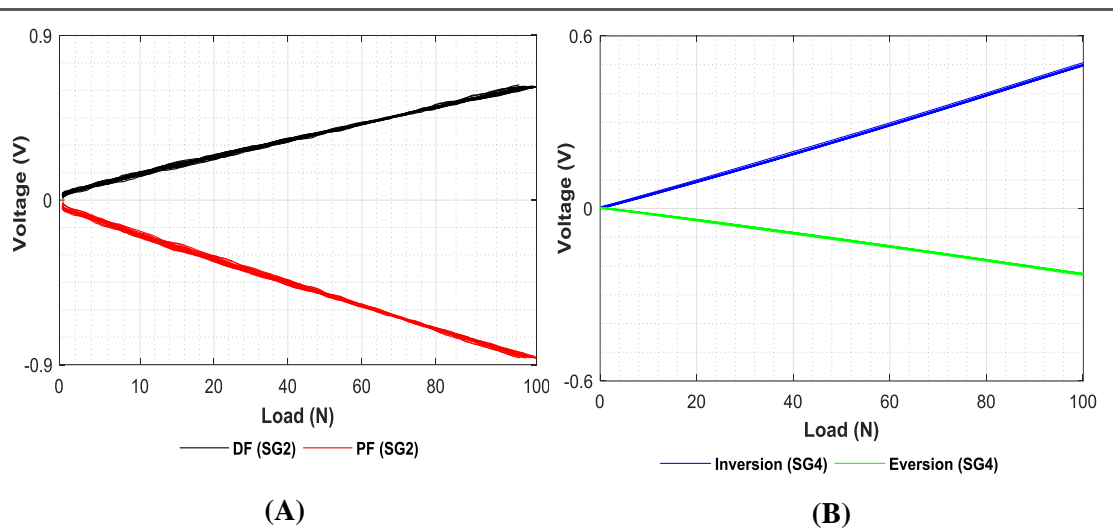


Figure 3.42: SGs AFO calibration outputs against load. Outputs of 19 cycles for SG2 in dorsiflexion (DF) and plantarflexion (PF) (A), SG4 in inversion and eversion AFO calibration (B).

The resulting moments for each AFO were normalized to the participant's body mass. Afterwards, the normalized AFO calibration moments were plotted against the SG outputs for DF/PF and inversion/eversion to generate the linear regression equations (Figure 3.43). The conversion factors (Nm/V) were then derived from the linear regression equations to be used to calculate the orthotic moments (the moments exerted by the AFO or Tuned-AFO around the ankle joint) during walking. Based on the locations and orientations of the SGs installation to the AFO; the outputs of SG2 and SG3 were used to calculate the DF and PF moments (Figure 3.43). Similarly, the outputs of SG1 and SG4 were used to calculate the inversion and eversion moments (Figure 3.43). For each SG, the mean of the 19 calibration cycles of the SG calibration outputs and loads were used to calculate the conversion factors. Thus, the SGs outputs data during walking were converted to orthotic moments using the derived conversion factors (Figure 3.44).

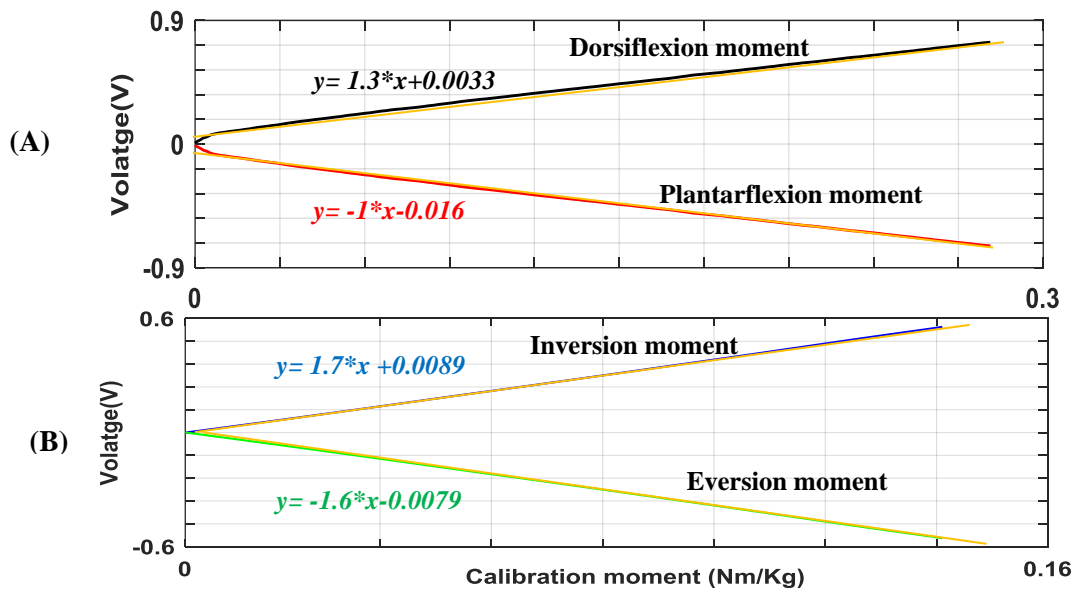


Figure 3.43: Linear regression of SG2 outputs versus dorsiflexion/plantarflexion moments (A), SG4 outputs versus inversion/eversion moments (B).

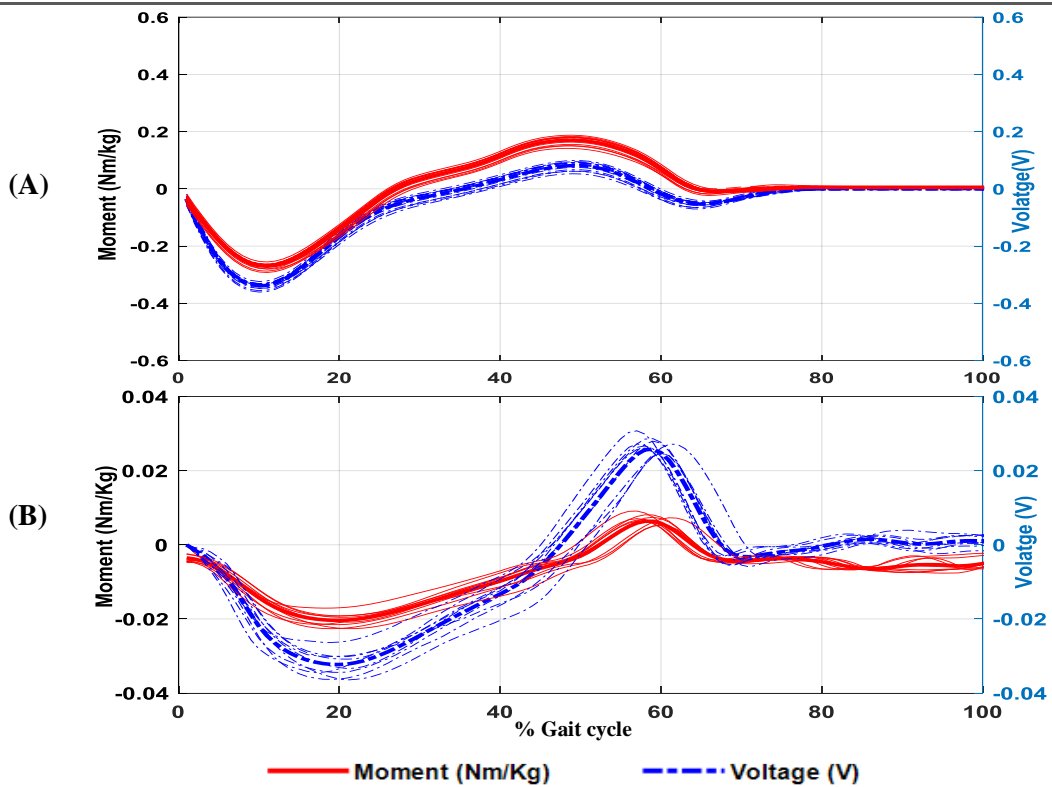


Figure 3.44: Orthotic moments in sagittal plane based on SG2 voltage output (A), and in frontal plane based on SG4 voltage outputs (B).

(iii). *Calculating the anatomical ankle moment*

Following Papi's (2015) method, the anatomical ankle moment (the moment produced by the muscles and other tissues around the ankle joint) was calculated using the following equation:

$$M_{Total} = M_{Orthotic} + M_{Anatomical} \quad \text{Equation 12}$$

Where M_{Total} is the total ankle moment about the ankle joint measured by force plate and the Vicon motion system, $M_{Orthotic}$ is the AFO moment, and the $M_{Anatomical}$ is the anatomical ankle moment.

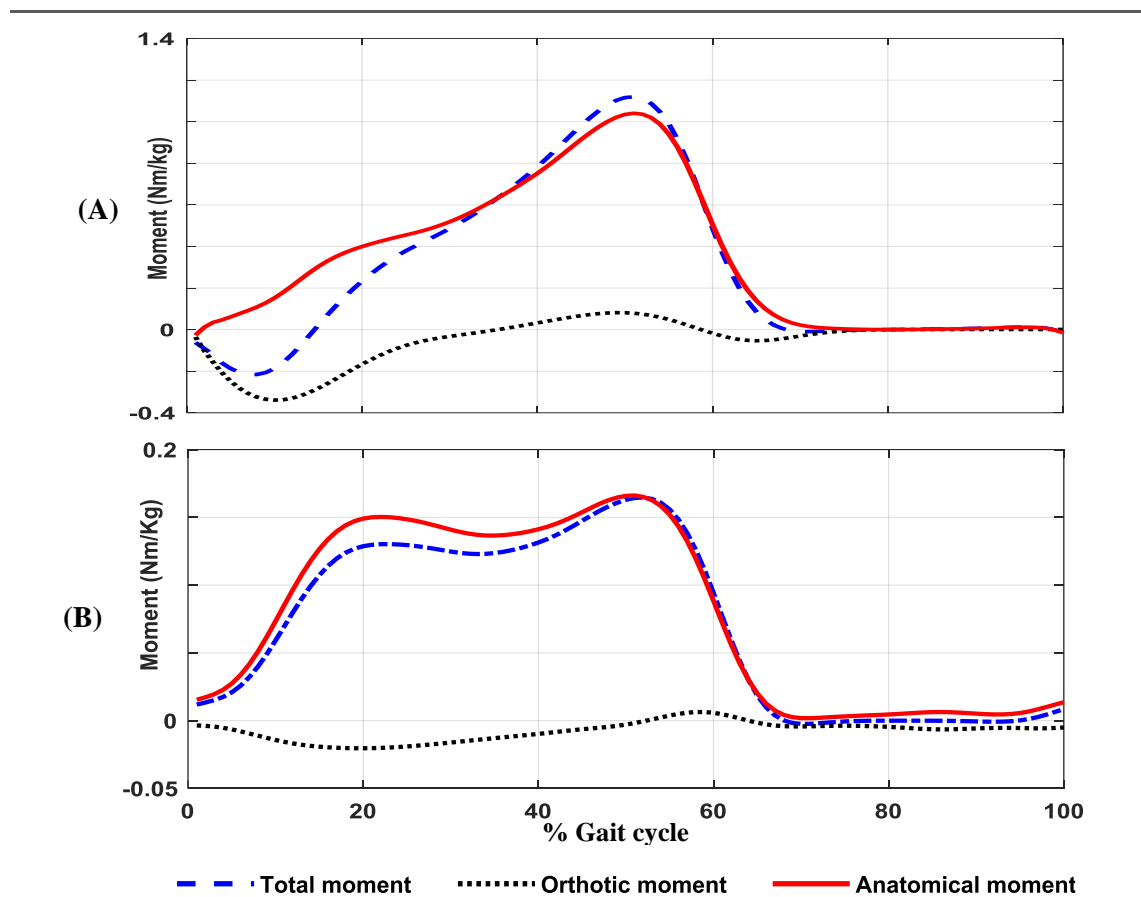


Figure 3.45: Ankle moments in sagittal plane (A) and in frontal plane (B).

Chapter 4 Case Studies: Results and Discussion.

The current study investigates the immediate effects of wearing a Tuned-AFO as compared to rigid AFO (before tuning) and Standard Shoes Only (SSO) on the gait of control and Stroke Participants (SP). Additionally, this study measures the orthotic and the anatomical moments at the ankle joint in the sagittal plane and at the assumed subtalar joint in the frontal plane and investigates the effects of tuning a rigid AFO on the orthotic moment and the anatomical moment.

The initial aim was to investigate the immediate effects of Tuned-AFO on a larger sample size of stroke participants (*SP*). However, the relatively small sample size recruited led to a decision to conduct case studies' analysis. Six case studies (*SP1*, *SP2*, *SP3*, *SP4*, *SP5*, and *SP6*) were performed for six stroke participants with equinovarus deformity using an AFO. Stroke participants recruited were only from Chest Heart & Stroke Scotland. Six control participants were also recruited in this study to provide a baseline group for comparison.

As a result of the vast amount of data obtained in this study, the results provided in this chapter only represent gait parameters that are directly relevant to the main objectives of this study (other results are presented in appendix (J)). Therefore, only the results of one side (the side fitted with an AFO) are presented in this chapter (for SSO condition, the same side fitted with an AFO was chosen). All gait parameters were compared across the three conditions: SSO, AFO and Tuned-AFO for both control and stroke participants. The symbols asterisk (★), circle (●) and cross (✕) were used in the graphs to identify the end of stance time in Tuned-AFO, AFO and SSO conditions, respectively. In the current study, the reported kinetic parameters (knee moments, hip moments, and ankle moments) represent the external moments. The term knee hyperextension was used when the knee angle is less than 5° of flexion during mid and terminal stance (Hullin et al., 1996). Furthermore, in the current study, the term improvement was used to define the change in any parameter towards normal, and the term deterioration was used to define the change in any parameter away from normal.

Regarding the strain gauge data, paired t-tests, at 0.05 level of significance, was performed at the minima and the maxima of the orthotic moments that were derived from

SG2 and SG3 outputs, and from SG1 and SG4 outputs (illustrated in section 3.6.3) in all control and stroke participants. No significant differences were found between the orthotic moments that were derived from SG2 and SG3 outputs nor in the orthotic moments that were derived from SG1 and SG4 outputs in all control and stroke participants ($p > 0.05$). Therefore, only the data derived from SG2 output to measure the orthotic moment at the ankle joint in the sagittal plane and only the data derived from SG4 output to measure the orthotic moment at the assumed subtalar joint in the frontal plane will be presented in this chapter (SG1 and SG3 results are presented in appendix (J)).

4.1 Control participants

Six participants (3 females and 3 males, age: 27 ± 3 years, height: 1.71 ± 0.11 m, body mass: 78 ± 13 kg) participated in this study. The AFO side was selected randomly for the control participants (4 Right and 2 left). The Comfortable Walking Speed (CWS) for the control participants was 1.2 m/s in SSO condition. This CWS is within the required walking speed to safely cross the road using pedestrian crossing in the United Kingdom (1.2 m/s) (Asher et al., 2012).

4.1.1 Comparing AFO condition with SSO condition:

The walking speed of control participants slightly decreased from (1.20 ± 0.12 m/s) in SSO condition to (1.14 ± 0.14 m/s) in AFO condition. This is reflected in the slightly increased stance percentage of the gait cycle and the decreased stride length (from $65.81 \pm 2.65\%$ in SSO to $66.12 \pm 2.95\%$ in AFO condition, and from 1.16 ± 0.20 m to 1.09 ± 0.25 m, respectively). SVA inclination during mid stance slightly decreased (by 0.7 degrees) from (10.21 ± 1.5 degrees) in SSO to (9.51 ± 2.4 degrees) in AFO condition (Table 4.1, Figure 4.1, A). Ankle motion on the other hand, greatly changed and showed decreased first (early stance) plantar flexion, second (late stance) dorsiflexion, and third (swing phase) plantar flexion peaks in AFO condition as compared to SSO condition (from -11.81 ± 1.15 degrees, 9.86 ± 2.09 degrees, -18.27 ± 0.87 degrees in SSO condition to -3.73 ± 0.94 degrees, 4.62 ± 0.51 degrees, -1.04 ± 0.76 degrees in AFO condition, respectively) (Table 4.1, Figure 4.1, B). On the contrary, knee motion showed increased early stance flexion peak, decreased late stance extension, and decreased early swing flexion peaks in AFO

condition as compared to SSO condition (13.47 ± 4.52 degrees, 5.59 ± 2.85 degrees, 64.45 ± 2.54 degrees in SSO condition, 16.43 ± 1.60 degrees, 4.84 ± 2.32 degrees, 59.44 ± 2.48 degrees in AFO condition, respectively) (Table 4.1, Figure 4.1, C). Hip flexion that occurs during swing phase slightly increased in AFO condition (34.95 ± 1.82 degrees) as compared to SSO condition (32.45 ± 1.51 degrees), and late stance hip extension also slightly increased in AFO condition (-9.01 ± 2.74 degrees) as compared to SSO condition (-8.63 ± 1.74 degrees) (Table 4.1, Figure 4.1, D).

Changes in the kinetics in control participants were also observed in AFO condition as compared to SSO condition (Table 4.1, Figure 4.2). The values of the first and second peaks of the GRFv were lower in AFO condition (786 ± 26.0 N and 766 ± 12.8 N) as compared to SSO condition (821 ± 26.4 N and 827 ± 11.5 N) and the trough was higher (608 ± 24.2 N and 683 ± 21.2 N). At the ankle, peak plantar flexion moment which occurs early in stance did not show any noticeable change in AFO condition as compared to SSO condition, and the dorsiflexion moment peak which occurs late in stance showed a decrease (1.34 ± 0.01 Nm/kg in AFO condition as compared to 1.12 ± 0.01 Nm/kg in SSO condition). The change at the knee in AFO condition as compared to SSO condition was very mild; early stance, and swing flexion moment peaks were very slightly increased and late stance extension peak decreased very slightly as well. The same holds true at the hip.

Fitting an AFO also showed variable changes in the EMG activity of muscles as compared to SSO condition (Table 4.2, Figure 4.3). Vastus Lateralis (VL) and Vastus Medialis VM generally showed similar activity patterns and thus, will be presented together. VL and VM were active from initial contact to the end of mid stance in SSO condition. An AFO only reduced stance period of activity of VL to halfway in mid stance. Swing peak of VL and stance and swing peaks of VM decreased in AFO condition (13.41 ± 3.14 %MMT, 35.41 ± 3.21 %MMT, 23.42 ± 3.14 %MMT in AFO condition respectively, 15.11 ± 1.90 %MMT, 36.73 ± 2.29 %MMT, 29.31 ± 1.90 %MMT in SSO condition, respectively). Stance peak of VL on the other hand very slightly increased (25.21 ± 3.21 %MMT, 24.10 ± 2.29 %MMT). Rectus Femoris (RF) was active from the beginning of pre swing to the end of initial swing in all three conditions in control participants. RF showed decreased terminal stance-pre swing peak (29.42 ± 0.88 %MMT) in AFO condition as

compared to SSO condition (34.42 ± 0.67 %MMT). The activity of the Biceps Femoris (BF) was recorded during loading response, early mid stance, and during mid and terminal swing, but it was also slightly prolonged in stance and swing in AFO condition. Semitendinosus (ST) muscle activity was the same as BF. Fitting and AFO only slightly shortened stance period of activity. BF and ST showed decreased stance peak and swing peaks in AFO condition (BF: 17.84 %MMT, 26.81 ± 2.05 %MMT, respectively, ST: 19.08 ± 1.82 %MMT, 27.89 ± 1.90 %MMT, respectively) as compared to SSO condition (BF: 19.37 ± 1.69 %MMT, 31.39 ± 1.74 %MMT, respectively, ST: 20.86 ± 1.79 %MMT, 34.31 ± 1.88 %MMT, respectively).

4.1.2 Comparing Tuned-AFO condition with AFO condition:

The walking speed of control participants slightly increased in Tuned-AFO condition (1.16 ± 0.13 m/s) as compared to AFO condition (1.14 ± 0.14 m/s). Stride length very slightly increased and stance percentage of the gait cycle very slightly decreased. SVA inclination during mid stance slightly increased (by 1.48 degrees) from (9.51 ± 2.4 degrees) in AFO condition to (10.99 ± 2.4 degrees) in Tuned-AFO condition (Table 4.1, Figure 4.1, A). Slight change in ankle motion resulted in Tuned-AFO condition as compared to AFO condition (Table 4.1, Figure 4.1, B); as first plantar flexion peak slightly decreased (-2.32 ± 0.82 degrees, -3.73 ± 0.94 degrees, respectively), second plantar flexion peak reversed to very slight dorsiflexion (0.59 ± 1.16 degrees, -1.04 ± 0.76 degrees, respectively), and the dorsiflexion peak slightly increased (5.65 ± 0.54 degrees, 4.62 ± 0.51 , respectively). Knee motion showed, in Tuned-AFO condition as compared to AFO condition (Table 4.1, Figure 4.1, C), increased early stance flexion (18.45 ± 2.15 degrees, 16.43 ± 1.60 degrees, respectively), decreased knee extension (6.32 ± 1.59 degrees, 4.84 ± 2.32 degrees, respectively), and decreased knee flexion in swing phase (58.06 ± 1.88 degrees, 59.44 ± 2.48 degrees, respectively). Hip flexion peak in control participants slightly decreased in Tuned-AFO condition (33.04 ± 1.01 degrees) as compared to AFO condition (34.95 ± 1.82 degrees), and hip extension peak slightly increased in Tuned-AFO condition (-10.11 ± 1.87 degrees) as compared to AFO condition (33.04 ± 1.01 degrees).

GRFv in control participants after AFO tuning did not show any change in the first peak nor in the trough (Table 4.1, Figure 4.2, D). Second peak also showed very slight increase only. Moments at the ankle showed an increase in peak plantar flexion moment in Tuned-

AFO condition (-0.33 ± 0.12 Nm/kg) as compared to AFO condition (-0.22 ± 0.11 Nm/kg). Dorsiflexion moment peak on the other hand showed no change (Table 4.1, Figure 4.2, A). Moments at the knee showed unnoticeable changes at the knee joint in Tuned-AFO condition as compared to AFO condition (Table 4.1, Figure 4.2, B). Again, the changes in the moments at the hip in Tuned-AFO condition were very slight and unnoticeable (Table 4.1, Figure 4.2, C).

The Tuned-AFO condition resulted in greater change in the EMG of knee muscles (Table 4.2, Figure 4.3). VL and VM were active from initial contact to end of mid stance and then during terminal swing, and thus, only VL period of activity in stance is slightly longer in Tuned-AFO condition than in AFO condition. VL stance and swing peaks and VM stance peak were slightly larger in Tuned-AFO condition (26.60 ± 2.62 %MMT, 14.10 ± 1.37 %MMT, 38.33 ± 2.62 %MMT, respectively) as compared to AFO condition (25.21 ± 3.21 %MMT, 13.41 ± 3.14 %MMT, 35.41 ± 3.21 %MMT, respectively). VM swing peak was slightly smaller in Tuned-AFO condition (21.61 ± 1.37 %MMT). Tuning the AFO did not result in any change in the activation periods of RF muscle. RF activity showed slight increase in terminal stance-pre swing peak in Tuned-AFO condition (32.14 ± 0.92 %MMT) as compared to AFO condition (29.42 ± 0.88 %MMT). Tuned-AFO condition did not change the period of activity of ST as compared to AFO condition (Table 4.2, Figure 4.3). BF activity on the other hand was slightly longer in stance in Tuned-AFO condition as compared to AFO condition (Table 4.2, Figure 4.3). BF and ST showed decreased stance peak and swing peaks in Tuned-AFO condition (BF: 11.67 ± 1.82 %MMT, 22.78 ± 1.92 %MMT, respectively, ST: 15.40 ± 1.75 %MMT, 22.37 ± 1.85 %MMT, respectively) as compared to AFO condition (BF: 17.84 ± 1.68 %MMT, 26.81 ± 2.05 %MMT, respectively, ST: 19.08 ± 1.82 %MMT, 27.89 ± 1.90 %MMT, respectively).

The orthotic moment in control participants showed a plantarflexion moment peak during loading response and a slight orthotic dorsiflexion moment during terminal stance (Table 4.3, Figure 4.4). In contrast, the anatomical moment only showed a dorsiflexion moment during the whole stance. Walking with a Tuned-AFO in control participants showed increased plantar flexion moment peak (-0.47 ± 0.07 Nm/kg) as compared to AFO condition (-0.33 ± 0.05 Nm/kg), and no change in the orthotic dorsiflexion moment (Table 4.3, Figure 4.4).

Control participants in SSO showed only inversion moment during stance. Control participants showed reduced early stance total inversion moment in AFO condition and reversed the first peak of total inversion moment to eversion moment in Tuned-AFO condition (Table 4.3, Figure 4.4). Orthotic moment showed eversion moment in early stance in AFO condition (-0.03 ± 0.01 Nm/kg) that is greater in Tuned-AFO condition (-0.08 ± 0.01 Nm/kg), and inversion moment late in stance with no difference between AFO and Tuned-AFO conditions.

The effect of AFO and Tuned-AFO on the speed of control participants was minimal, as control participants' gait speed decreased by (0.04m/s) and (0.02m/s), respectively. This does not have any effect on their classification according to the classification by Perry et al. (1995). Additionally, as the speed changes were much lower than the Minimal Clinically Important Differences (MCID: 0.16m/s), these changes are thus considered clinically insignificant (Tilson et al., 2010).

In contrast, AFO and Tuned-AFO have greater effects on the kinematics of control participants. SVA in Tuned-AFO condition was within the target range (10-12 degrees) compared to 10.21 degrees in SSO condition; indicating sufficient tuning. The values also indicate that normal persons do not necessarily need tuning, as their SVA in SSO were considered sufficient. The hip was 1.48 degrees more extended than normal (control participants in SSO condition are considered the normal baseline in this study) in Tuned-AFO condition and 1.1 degrees less extended than normal in AFO condition, the knee was 4.98 degrees more flexed during early stance in Tuned-AFO condition and 2.96 degrees more flexed in AFO condition. Further discussion on the effect of Tuned-AFO condition and AFO condition on the gait parameters of control and stroke participants will be addressed in the next chapter (Chapter 5 Discussion).

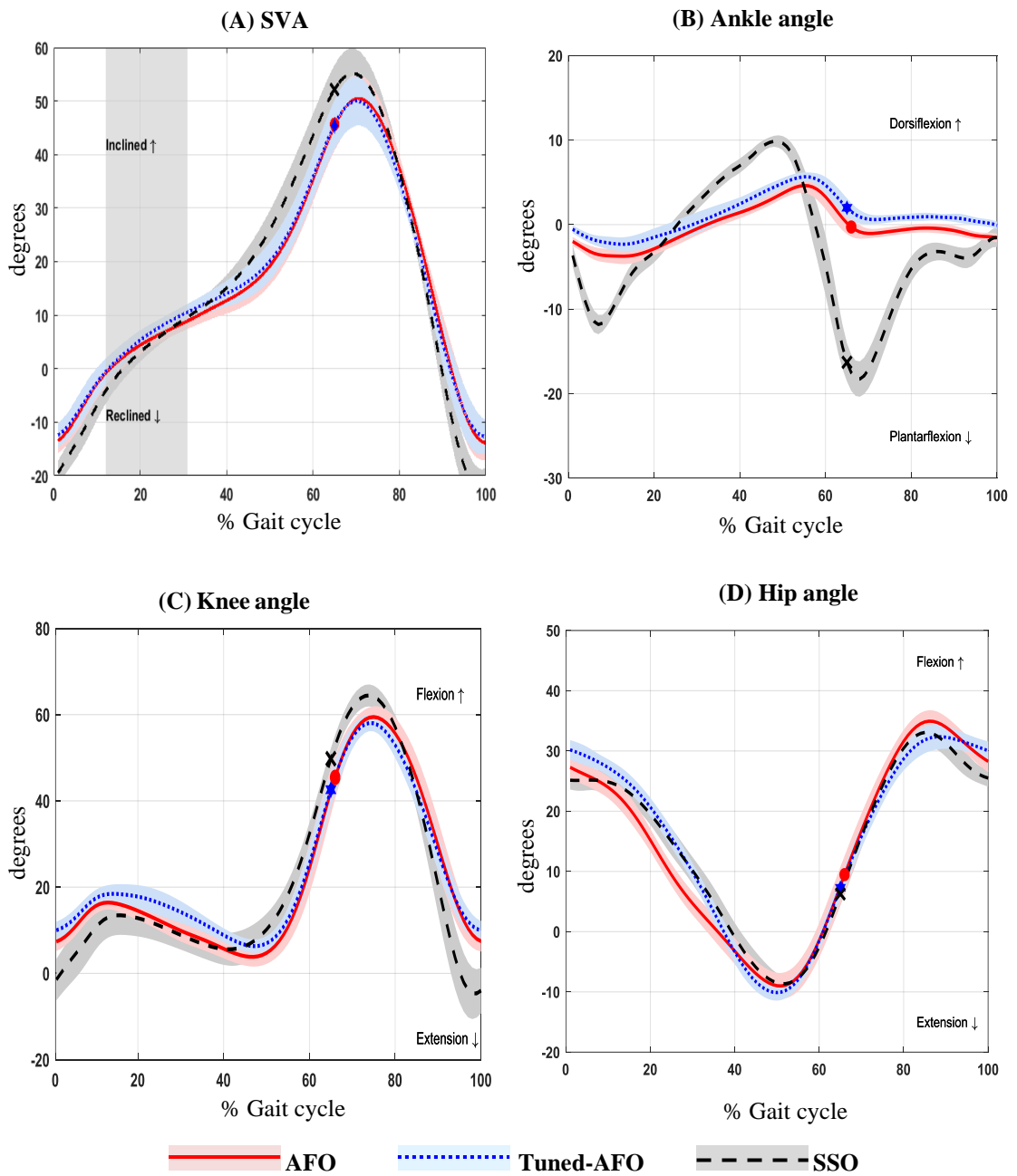


Figure 4.1: Sagittal kinematic graphs for control participants while walking on treadmill wearing Tuned-AFO, AFO, and SSO.

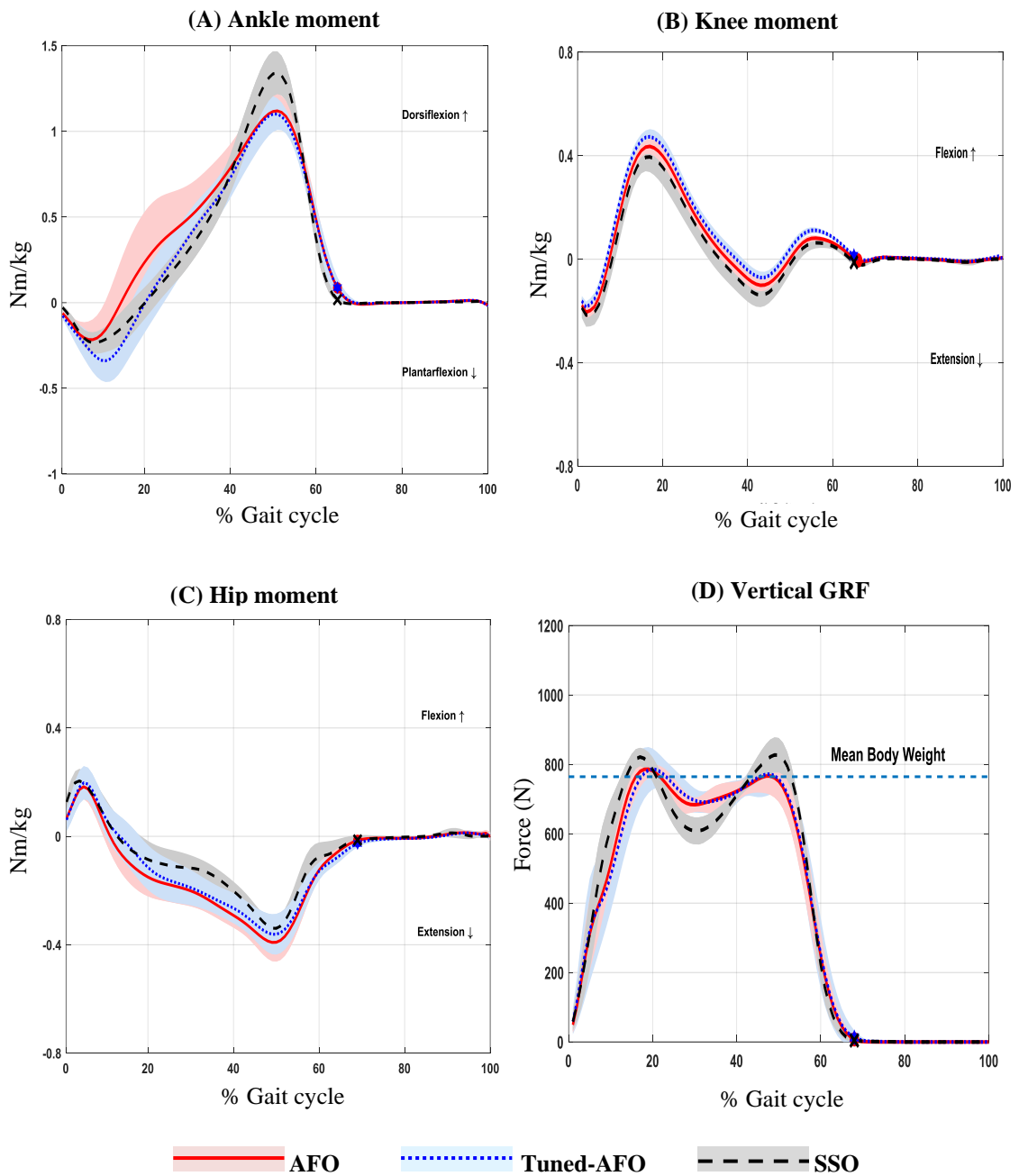


Figure 4.2: Sagittal kinetic graphs and the vertical GRF graph for control participant while walking on treadmill wearing Tuned-AFO, AFO, and SSO.

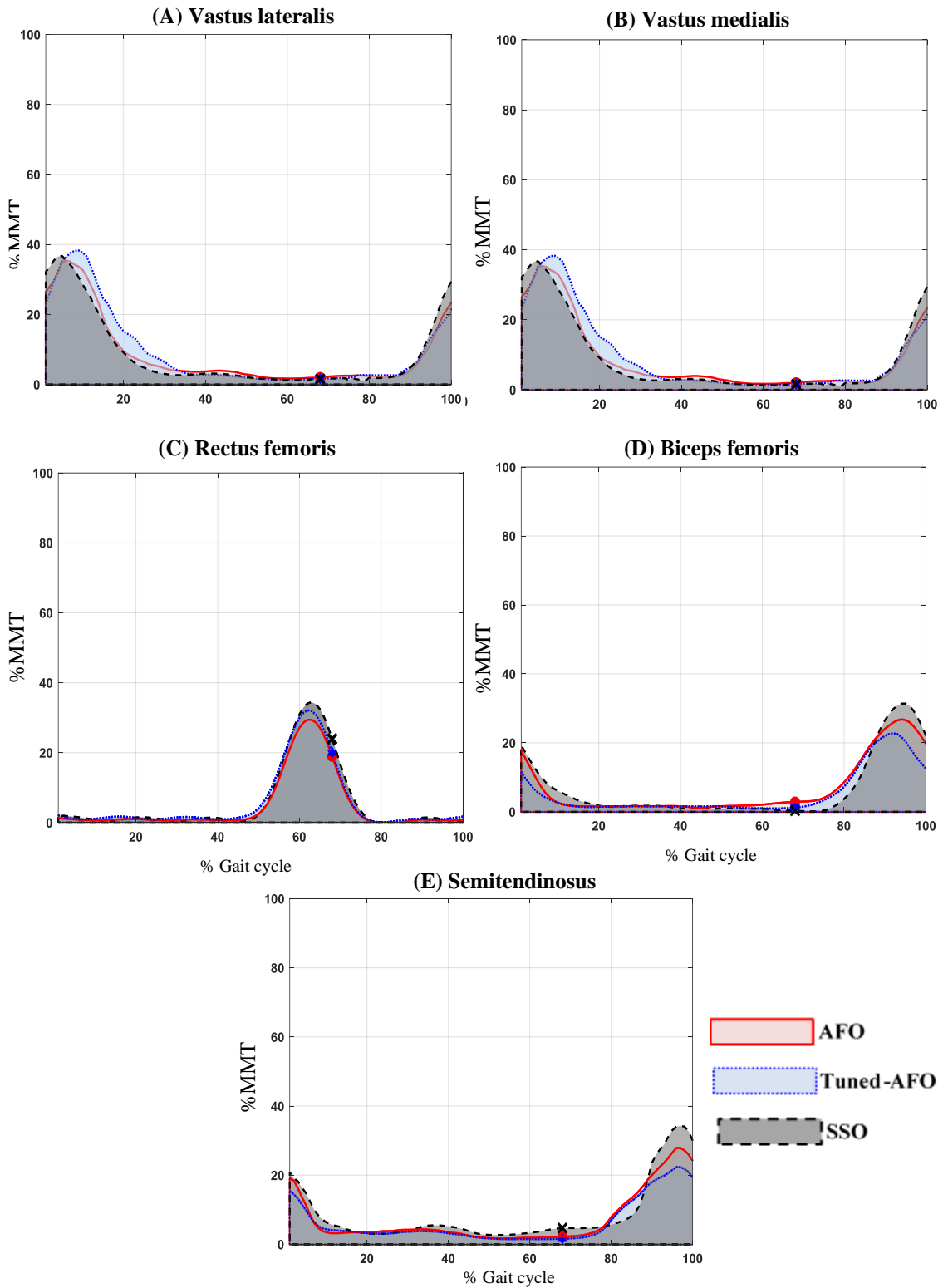


Figure 4.3: Quadriceps and hamstring EMG RMS amplitude and timing during walking on treadmill for control participant. The RMS is presented as a percentage of maximum manual muscle test value (% MMT).

Table 4.1: Temporal-spatial, kinematic and kinetic data for control participant.

| Parameter description | | <u>Mean±(SD)</u> | | |
|------------------------------|-----------------------------|------------------|---------------|---------------|
| | | AFO | Tuned | SSO |
| SVA (degrees) | Mid stance | 9.51±(2.4) | 10.99±(2.4) | 10.21±(1.5) |
| Temporal-spatial | Speed (ms ⁻¹) | 1.14±(0.14) | 1.16±(0.13) | 1.20±(0.12) |
| | Stance time (%) | 66.12±(2.95) | 66.22±(2.44) | 65.81±(2.65) |
| | Stride length (m) | 1.09±(0.25) | 1.12±(0.22) | 1.16±(0.20) |
| Ankle angle (degrees) | PF peak (early stance) | -3.73±(0.94) | -2.32±(0.82) | -11.81±(1.15) |
| | Dorsiflexion peak | 4.62±(0.51) | 5.65±(0.54) | 9.86±(2.09) |
| | PF peak (swing phase) | -1.04±(0.76) | 0.59±(1.16) | -18.27±(0.87) |
| Knee angle (degrees) | Flexion peak (stance) | 16.43±(1.60) | 18.45±(2.15) | 13.47±(4.52) |
| | Extension (terminal stance) | 4.84±(2.32) | 6.32±(1.59) | 5.59±(2.85) |
| | Flexion peak (swing) | 59.44±(2.48) | 58.06±(1.88) | 64.45±(2.54) |
| Hip angle (degrees) | Extension peak | -9.01±(2.74) | -10.11±(1.87) | -8.63±(1.74) |
| | Flexion peak (swing phase) | 34.95±(1.82) | 33.04±(1.01) | 32.45±(1.51) |
| Ankle moment (Nm/kg) | PF peak (early stance) | -0.22±(0.11) | -0.33±(0.12) | -0.23±(0.06) |
| | Dorsiflexion peak | 1.12±(0.01) | 1.11±(0.01) | 1.34±(0.01) |
| Knee moment (Nm/kg) | Flexion peak1 | 0.41±(0.03) | 0.43±(0.03) | 0.39±(0.05) |
| | Extension peak | -0.10±(0.01) | -0.09±(0.01) | -0.12±(0.01) |
| | Flexion peak2 | 0.09±(0.03) | 0.11±(0.03) | 0.08±(0.05) |
| Hip moment (Nm/kg) | Flexion peak | 0.19±(0.04) | 0.20±(0.06) | 0.20±(0.04) |
| | Extension peak | -0.39±(0.02) | -0.37±(0.01) | -0.35±(0.01) |
| GRFv (N) | 1 st peak | 786±(26.0) | 786±(28.8) | 821±(26.4) |
| | Trough | 683±(21.2) | 684±(21.4) | 608±(24.2) |
| | 2 nd peak | 766±(12.8) | 771±(10.9) | 827±(11.5) |

Table 4.2: Quadriceps and hamstring EMG RMS amplitude for control participant.

| Parameter description | | <u>Mean±(SD)</u> | | |
|-----------------------|-------------|------------------|--------------|--------------|
| | | AFO | Tuned | SSO |
| VL RMS (%MMT) | Stance peak | 25.21±(3.21) | 26.60±(2.62) | 24.10±(2.29) |
| | Swing peak | 13.41±(3.14) | 14.10±(1.37) | 15.11±(1.90) |
| VM RMS (%MMT) | Stance peak | 35.41±(3.21) | 38.33±(2.62) | 36.73±(2.29) |
| | Swing peak | 23.42±(3.14) | 21.61±(1.37) | 29.31±(1.90) |
| RF RMS (%MMT) | T-PS peak | 29.42±(0.88) | 32.14±(0.92) | 34.42±(0.67) |
| BF RMS (%MMT) | Stance peak | 17.84±(1.68) | 11.67±(1.82) | 19.37±(1.69) |
| | Swing peak | 26.81±(2.05) | 22.78±(1.92) | 31.39±(1.74) |
| ST RMS (%MMT) | Stance peak | 19.08±(1.82) | 15.40±(1.75) | 20.86±(1.79) |
| | Swing peak | 27.89±(1.90) | 22.37±(1.85) | 34.31±(1.88) |

T-PS peak: the maximum activity during terminal stance and pre swing phase

Table 4.3: The anatomical and the orthotic ankle moment for control participant derived from SG2 and SG4 data outputs.

| Moment (Nm/kg) | | <u>Anatomical</u> (mean±(SD)) | | <u>Orthotic</u> (mean±(SD)) | |
|----------------|----------------------|-------------------------------|-------------|-----------------------------|--------------|
| | | AFO | Tuned | AFO | Tuned |
| SG2 | Early stance peak | 0.11±(0.10) | 0.14±(0.06) | -0.33±(0.05) | -0.47±(0.07) |
| | Terminal stance peak | 1.01±(0.02) | 1.00±(0.01) | 0.11±(0.01) | 0.11±(0.01) |
| SG4 | Mid stance peak | 0.04±(0.01) | 0.03±(0.01) | -0.03±(0.01) | -0.08±(0.01) |
| | Terminal stance peak | 0.11±(0.02) | 0.02±(0.01) | 0.03±(0.01) | 0.11±(0.01) |

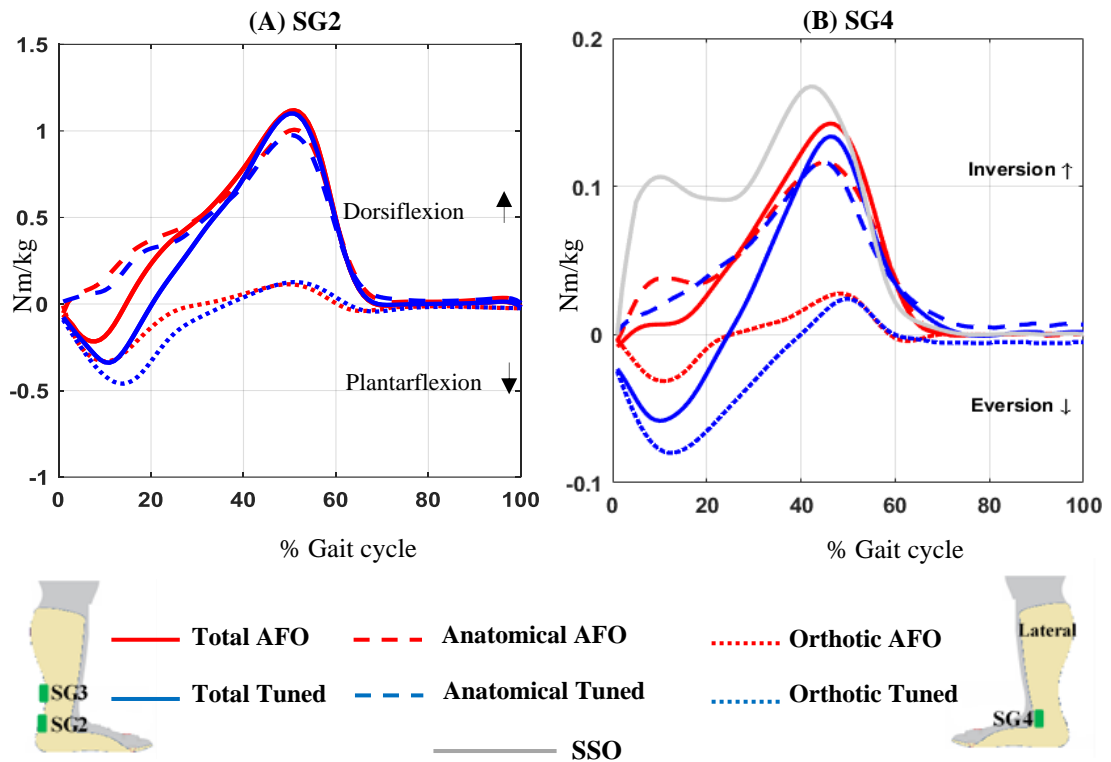


Figure 4.4: Total ankle moment, orthotic moment, and anatomical moment in sagittal plane (A) and frontal plane (B) for control participants derived from SG2 and SG4 data outputs, respectively.

4.2 Case study one (SPI)

SPI was a 56-year-old female with a mass of 72kg and height of 1.56m. *SPI* had hemorrhagic stroke in 2015 affecting her left hemisphere, resulting in right side hemiparesis. *SPI* started a daily physical therapy regimen in 2015 for two years. *SPI* own orthosis was rigid plastic AFO, similar to the AFO used in this study. The CWS for *SPI* was 0.2 m/s in SSO condition. Based on walking speed classification in stroke patients (Perry et al., 1995), *SPI* is classified as a “household walking” (speed <0.4 m/s).

4.2.1 Comparing AFO condition with SSO condition:

The walking speed of *SPI* increased from (0.20 ± 0.02) m/s in SSO condition to (0.61 ± 0.02) m/s in AFO condition. This is reflected in the decreased stance percentage of the gait cycle and increased stride length (from $79.01 \pm 0.45\%$ in SSO to $69.02 \pm 0.20\%$ in

AFO condition, and from $0.19\pm 0.05\text{m}$ to $0.62\pm 0.06\text{m}$, respectively). SVA inclination during mid stance increased (by 5.94 degrees) from (3.14 ± 0.55) in SSO to (9.13 ± 0.55) in AFO condition (Table 4.4, Figure 4.5, A). Ankle motion on the other hand, showed decreased first (early stance) plantar flexion, second (late stance) dorsiflexion, and third (swing phase) plantar flexion peaks in AFO condition as compared to SSO condition (from -2.17 ± 0.62 degrees, 3.70 ± 0.52 degrees, -1.84 ± 0.42 degrees in SSO condition to -1.04 ± 0.56 degrees, 0.98 ± 0.54 degrees, -0.55 ± 0.21 degrees in AFO condition, respectively) (Table 4.4, Figure 4.5, B). On the contrary, knee motion showed increased early stance and swing flexion peaks and decreased late stance extension peak in AFO condition as compared to SSO condition (2.91 ± 1.26 degrees, -2.44 ± 0.37 degrees, 18.32 ± 1.79 degrees in SSO condition, 15.22 ± 1.51 degrees, 2.93 ± 0.26 degrees, 53.16 ± 2.60 degrees in AFO condition, respectively) (Table 4.4, Figure 4.5, C). Hip motion in *SPI* reversed from flexion in SSO condition to extension in AFO condition by the end of single limb support (from 18.61 ± 1.12 degrees to -6.04 ± 0.99 degrees). Maximum hip flexion in swing phase increased in AFO condition (37.31 ± 1.25 degrees) as compared to SSO condition (40.22 ± 1.24 degrees) (Table 4.4, Figure 4.5, D).

Changes in the kinetics in *SPI* were also observed in AFO condition as compared to SSO condition (Table 4.4, Figure 4.6). The values of the first and second peaks and the trough of the GRFv were all higher in AFO condition ($768\pm 8.52\text{N}$, $811\pm 8.05\text{N}$ and $697\pm 12.14\text{N}$, respectively) as compared to SSO condition ($488\pm 7.52\text{N}$, $740\pm 9.22\text{N}$ and $381\pm 10.62\text{N}$, respectively). Additionally, the first and second peaks are higher than *SPI* body weight in AFO condition ($107\%\text{BW}$ and $113\%\text{BY}$, respectively). First peak in SSO condition was much less than *SPI* body weight ($68\%\text{BW}$). The trough is slightly less than body weight in AFO condition ($97\%\text{BW}$). At the ankle, peak plantar flexion moment which occurs early in stance was absent in SSO condition and appeared in AFO condition (-0.27 ± 0.02 Nm/kg). Additionally, the dorsiflexion moment peak decreased in AFO condition (0.95 ± 0.03 Nm/kg) as compared to SSO condition (0.71 ± 0.04 Nm/kg). The change was also observed at the knee; especially that in SSO condition knee extension moment was dominant and wearing an AFO ends this dominance. Knee moments reversed in early stance from extension moments in SSO condition (-0.09 ± 0.01 Nm/kg) to flexion moments in AFO condition (0.14 ± 0.01 Nm/kg), peak extension moments in late stance decreased in AFO condition (-0.45 ± 0.01 Nm/kg) as compared to SSO

condition (-0.64 ± 0.01 Nm/kg), and the second flexion moments peak that occur by the end of stance increased from (0.01 ± 0.01 Nm/kg) in SSO condition to (0.05 ± 0.01 Nm/kg) in AFO condition. At the hip in SSO condition, only small extension moment occurs during mid and terminal stance, AFO condition increases this extension moment. Flexion moment peak at the hip that occurs early in stance showed slight increase in AFO condition (0.38 ± 0.03 Nm/kg) as compared to SSO condition (0.37 ± 0.05 Nm/kg), however, the extension moment peak showed great increase in AFO condition (-0.64 ± 0.04 Nm/kg) as compared to SSO condition (-0.14 ± 0.05 Nm/kg).

Fitting an AFO also showed changes in the EMG activity of muscles as compared to SSO condition (Table 4.5, Figure 4.7). VL and VM generally showed similar activity patterns and thus, will be presented together. VL and VM showed longer periods of activity and continued to be active during mid and terminal stance in SSO condition and AFO condition in *SPI*. VL and VM showed increased stance (33.48 ± 4.50 %MMT, 38.17 ± 0.41 %MMT, respectively) and swing (28.02 ± 3.30 %MMT, 27.90 ± 0.33 %MMT, respectively) peaks in AFO condition as compared to SSO condition (VL: 13.23 ± 3.16 %MMT, 6.44 ± 1.50 %MMT, VM: 20.72 ± 0.31 %MMT, 14.50 ± 0.33 %MMT, respectively). RF activity was different from normal in SSO condition. RF in AFO condition showed extremely longer activation period than in normal starting at IC and continuing until 80%GC (except the period from 40%GC to 55%GC). RF showed increased stance peak (11.15 ± 0.09 %MMT), terminal stance-pre swing peak (18.26 ± 0.08 %MMT), and swing peak (12.40 ± 0.12 %MMT) in AFO condition as compared to SSO condition (8.85 ± 0.19 %MMT, 11.63 ± 0.12 %MMT, 6.25 ± 0.09 %MMT, respectively). The activity of the BF and ST muscles was recorded during loading response, early mid stance, and during mid and terminal swing, but it was also prolonged to the end of mid stance and initial swing in SSO condition. Wearing an AFO resulted in slightly longer periods of activity in stance and swing. As is the case in VL and VM, BF and ST also generally showed similar activity pattern and will thus, be presented together. Wearing an AFO resulted in slightly longer periods of activity in stance and swing. BF and ST showed decreased stance peak (15.92 ± 0.23 %MMT, 16.51 ± 0.32 %MMT, respectively) and swing peak (29.64 ± 0.41 %MMT, 16.05 ± 0.29 %MMT, respectively) in AFO condition as compared to SSO condition (BF: 26.17 ± 0.23 %MMT, 45.91 ± 0.40 %MMT, respectively, ST: 27.66 ± 0.35 %MMT, 49.24 ± 0.56 %MMT, respectively).

4.2.2 Comparing Tuned-AFO condition with AFO condition:

The walking speed of *SPI* remained almost the same in Tuned-AFO condition (0.60 ± 0.02 m/s) as compared to AFO condition (0.61 ± 0.02 m/s). Stride length and stance percentage of the gait cycle also remained almost the same (0.63 ± 0.06 m and $69.04\pm 0.18\%$ in Tuned-AFO condition as compared to 0.62 ± 0.06 m and $69.02\pm 0.20\%$ in AFO condition). SVA inclination during mid stance was further increased in Tuned-AFO (by 2.23 degrees) from (9.13 ± 0.55 degrees) in AFO condition to (11.39 ± 0.56 degrees) in Tuned-AFO condition (Table 4.1, Figure 4.5, A). Slight change in ankle motion resulted in Tuned-AFO condition as compared to AFO condition; as first plantar flexion peak decreased (-0.90 ± 0.45 degrees and -1.04 ± 0.56 degrees, respectively), second plantar flexion peak increased (-0.57 ± 0.22 degrees and -0.55 ± 0.21 degrees, respectively), and the dorsiflexion peak increased (1.05 ± 0.52 and 0.98 ± 0.54 degrees, respectively) (Table 4.1, Figure 4.5, B). Knee motion showed, in Tuned-AFO condition as compared to AFO condition, only increased early stance flexion (19.59 ± 1.11 degrees and 15.22 ± 1.51 degrees, respectively), decreased knee extension (5.90 ± 0.71 degrees and, 2.93 ± 0.26 degrees, respectively), and decreased knee flexion in swing phase (50.73 ± 1.53 degrees and 53.16 ± 2.60 degrees) (Table 4.1, Figure 4.5, C). Hip motion flexion and extension peaks in *SPI* slightly changed in Tuned-AFO condition (40.37 degrees, ± 1.14 degrees and -5.56 degrees ± 0.97 degrees, respectively) as compared to AFO condition (40.22 ± 1.24 degrees and -6.04 ± 0.99 degrees, respectively) (Table 4.1, Figure 4.5, D).

GRFv in *SPI* after AFO tuning also changed (Table 4.1, Figure 4.6, D). The first peak and the second peak were higher, and the trough was lower in Tuned-AFO condition (109%BW, 113%BW, and 94%BW, respectively) as compared to AFO condition (107%BW, 113%BW, and 97%BW, respectively). Changes in the moments in *SPI* were most apparent on the knee joint, where the first flexion peak increased, second flexion peak increased, and the extension peak decreased in Tuned-AFO condition (0.20 ± 0.01 Nm/kg 0.06 ± 0.01 Nm/kg and -0.32 ± 0.01 Nm/kg respectively) as compared to AFO condition (0.14 ± 0.01 Nm/kg 0.05 ± 0.01 Nm/kg and -0.45 ± 0.01 Nm/kg respectively) (Table 4.1, Figure 4.6, B). At the ankle, Slight decrease in peak plantar flexion moment and in peak dorsiflexion moment were recorded in Tuned-AFO condition (-0.24 ± 0.03 Nm/kg and 0.70 ± 0.02 Nm/kg respectively) as compared to AFO condition (-0.27 ± 0.02 Nm/kg and 0.71 ± 0.04 Nm/kg respectively) (Table 4.1, Figure 4.6, A). Again, very slight

change was recorded at the hip in Tuned-AFO condition (Flexion peak: 0.38 ± 0.04 Nm/kg, Extension peak: -0.62 ± 0.04 Nm/kg) as compared to AFO condition (Flexion peak: 0.38 ± 0.03 Nm/kg, Extension peak: -0.64 ± 0.04 Nm/kg) (Table 4.1, Figure 4.6, C).

The Tuned-AFO condition resulted in greater change in the EMG of knee muscles (Table 4.5, Figure 4.7). VL and VM showed an increase in their activity in Tuned-AFO condition (40.04 ± 5.12 %MMT, 33.48 ± 4.50 %MMT for VL, and 48.72 ± 0.28 %MMT, 33.81 ± 0.31 %MMT for VM, respectively) as compared to AFO condition (31.60 ± 3.50 and 28.02 ± 3.30 %MMT for VL, and 38.17 ± 0.41 %MMT, 27.90 ± 33 %MMT for VM, respectively). RF in AFO-Tuned condition showed extremely longer activation period than in normal starting at IC and continuing until 80%GC (except the period from 40%GC to 55%GC). RF activity showed reduction in the stance peak, terminal stance-pre swing peak, and swing peak in Tuned-AFO condition (10.44 ± 0.14 %MMT, 17.44 ± 0.09 %MMT, and 9.26 ± 0.13 %MMT, respectively) as compared to AFO condition (11.15 ± 0.09 %MMT, 18.26 ± 0.08 %MMT, and 12.40 ± 0.12 %MMT, respectively). Tuned-AFO condition did not change the period of activity of BF and ST as compared to AFO condition, but showed decreased stance peak and swing peak in Tuned-AFO condition (BF: 12.86 ± 0.25 %MMT, 24.85 ± 0.41 %MMT, ST: 14.26 ± 0.37 %MMT, 17.51 ± 0.27 %MMT, respectively).

The orthotic moment showed a plantarflexion moment peak during loading response but with almost no orthotic dorsiflexion moment during terminal stance (Table 4.9, Figure 4.8, A). In contrast, the anatomical moment only showed a dorsiflexion moment during most of stance. Walking with a Tuned-AFO or an AFO in *SPI*, showed no noticeable differences in the orthotic plantarflexion moment during loading response (0.25 ± 0.03 Nm/kg and 0.26 ± 0.03 Nm/kg, respectively), nor in the anatomical dorsiflexion moment in late stance (0.76 ± 0.02 Nm/kg and 0.73 ± 0.04 Nm/kg, respectively).

SPI showed a noticeable reduction in the total inversion moment while walking with an AFO or Tuned-AFO as compared to walking with SSO as illustrated in Figure 4.8 (A). The orthotic moment peaks showed an eversion moment peak during the whole of stance. Walking with a Tuned-AFO or an AFO, showed no noticeable differences in the orthotic eversion moment nor in the anatomical inversion moment.

The effect of AFO and Tuned-AFO on the speed of *SPI* was obvious, as *SPI* gait speed increased by (0.41m/s) and (0.40m/s), respectively. This moves *SPI* from “household walking” to “limited community walking” according to the classification by Perry et al. (1995). Additionally, as the speed increments were higher than the MCID (0.16 m/s), these increments are considered clinically significant (Tilson et al., 2010).

Additionally, AFO and Tuned-AFO changed the kinematics so that they are closer to normal than in SSO (except for the ankle motion). SVA in Tuned-AFO condition was within the target range (10-12 degrees) compared to 3.19 degrees in SSO condition; indicating sufficient tuning. The hip was 3.07 degrees less extended than normal (control participants in SSO condition are considered the normal baseline in this study) in Tuned-AFO condition and 2.59 degrees less than normal in AFO condition compared to 27.24 degrees more flexed than normal in SSO condition, the knee was 6.12 degrees more flexed during early stance in Tuned-AFO condition and 1.75 degrees more flexed in AFO condition compared to 10.56 degrees less flexed than normal in SSO condition.

The effects of altering SVA by fitting a rigid AFO and a Tuned-AFO are obvious on the kinematics, kinetics, and EMG of knee muscles. As the change in SVA was greater in AFO condition as compared to Tuned-AFO condition, changes in gait parameters are expected to be greater in AFO condition as compared to SSO condition than in Tuned-AFO condition as compared to AFO condition. This does not underestimate the importance of tuning; as tuning improved the gait of *SPI* and made it closer to normal than in AFO condition. Further discussion on the effect of Tuned-AFO condition and AFO condition on the gait parameters of control and stroke participants will be addressed in the next chapter (Chapter 5 Discussion).

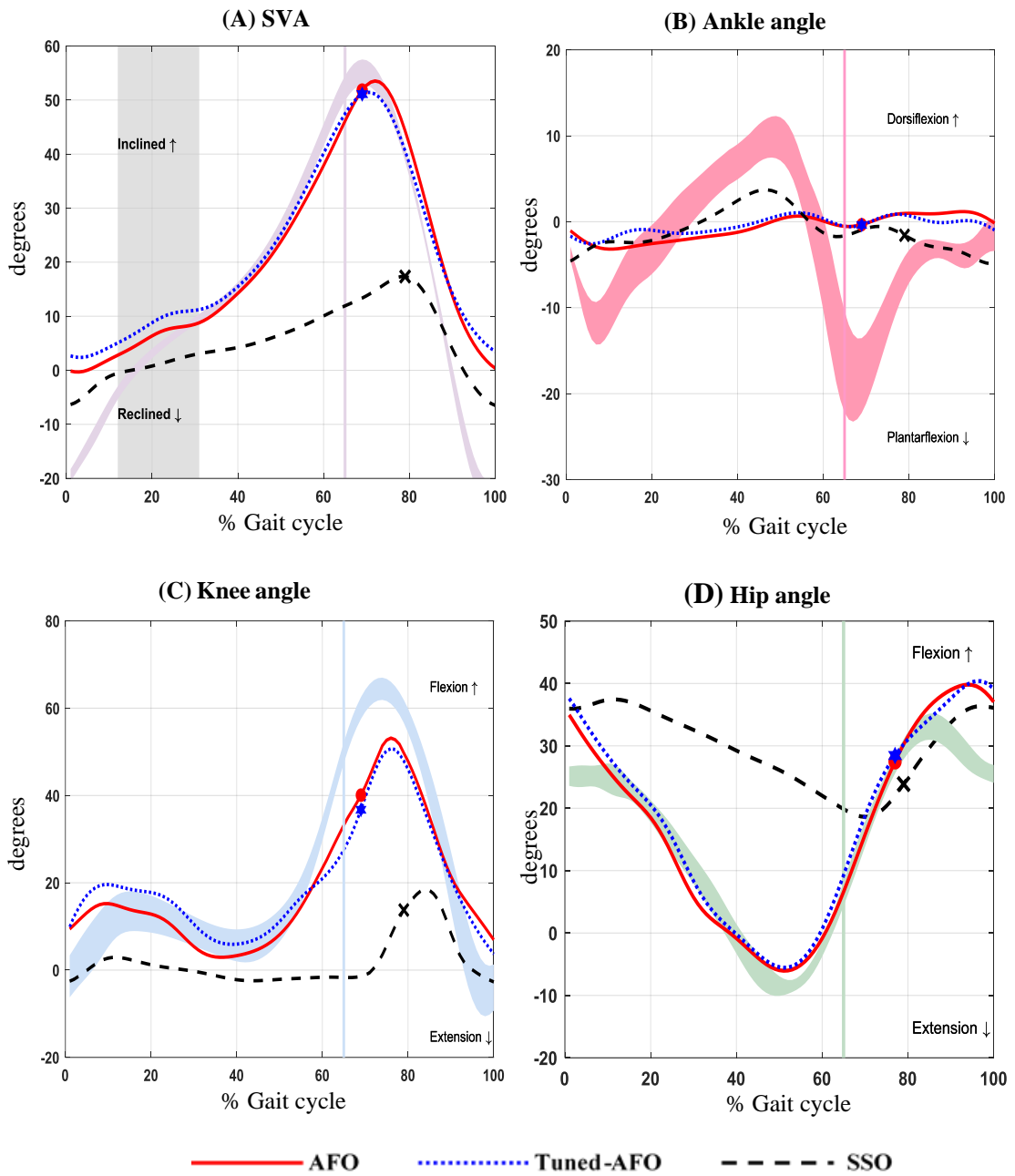


Figure 4.5: Sagittal kinematic graphs for case study 1 (*SPI*) while walking on treadmill wearing Tuned-AFO, AFO, and SSO with reference to control participants while wearing SSO (shaded lines).

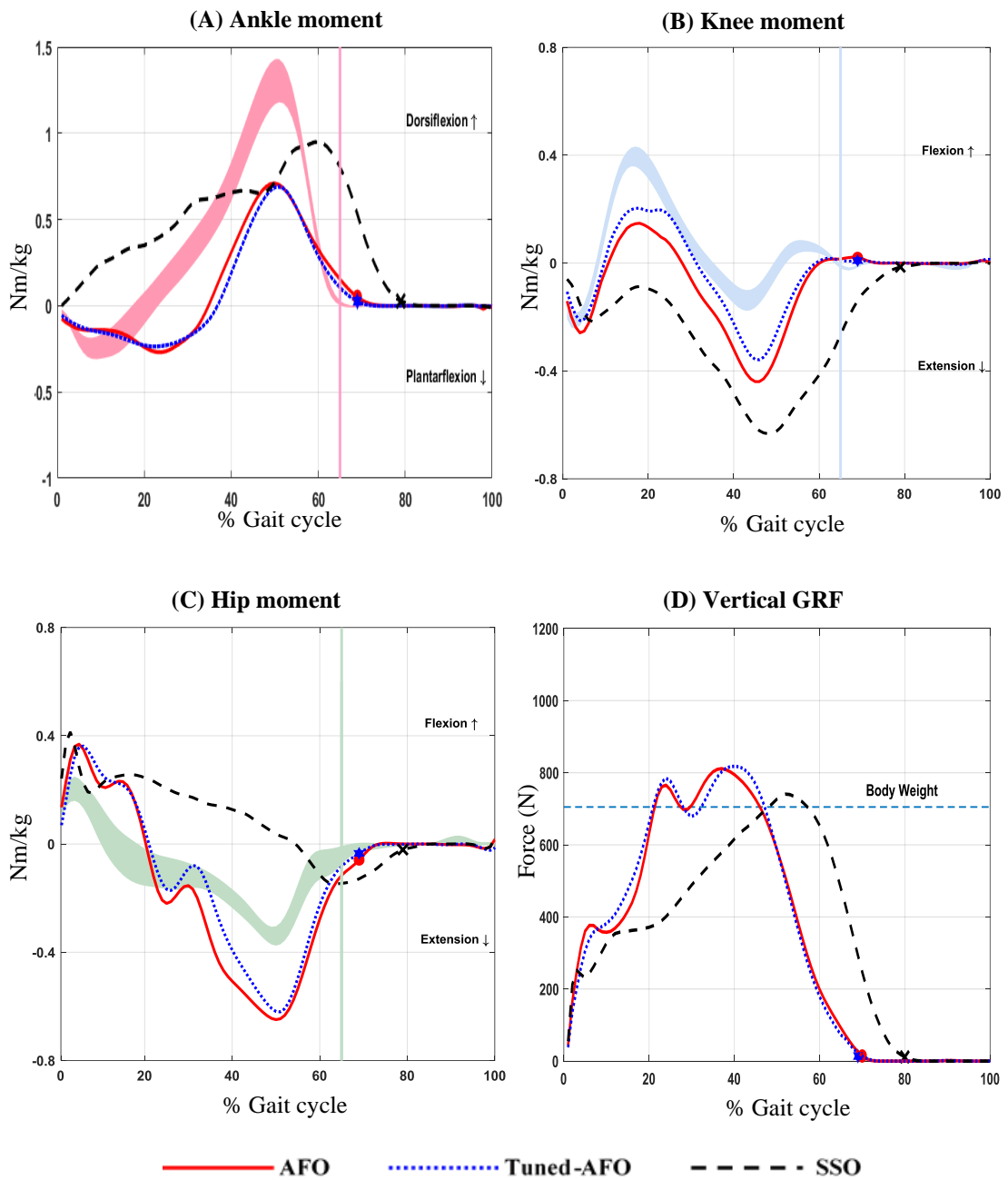


Figure 4.6: Sagittal kinetic graphs and the vertical GRF graph for case study 1 (*SPI*) while walking on treadmill wearing Tuned-AFO, AFO, and SSO with reference to control participants while wearing SSO (shaded lines).

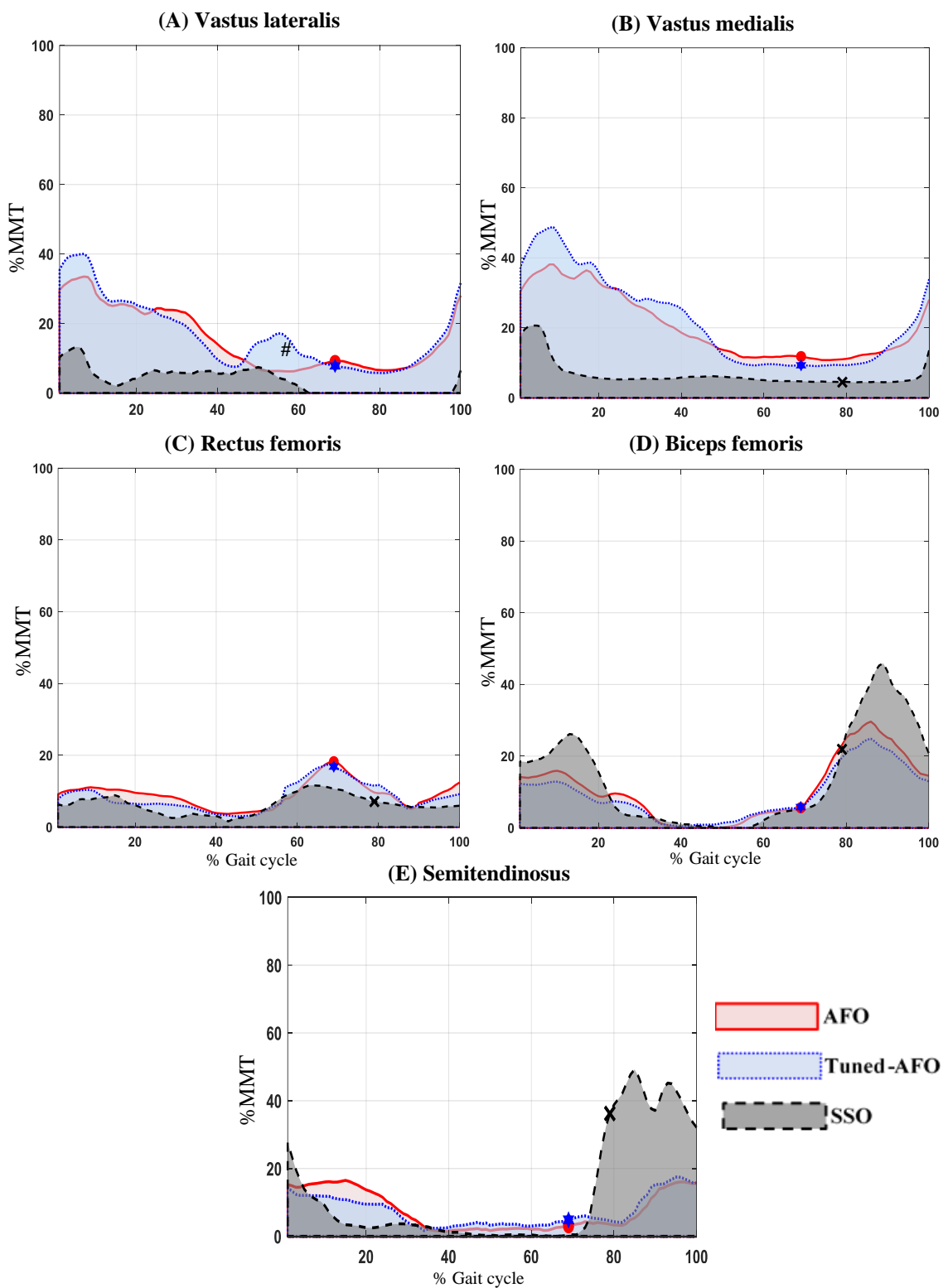


Figure 4.7: Quadriceps and hamstring EMG RMS amplitude and timing during walking on treadmill for case study 1 (*SPI*). The RMS is presented as a percentage of maximum manual muscle test value (% MMT) # Represents an example of Rectus Femoris cross talk.

Table 4.4: Temporal-spatial, kinematic and kinetic data for *SPI*.

| Parameter description | | <u>Mean±(SD)</u> | | |
|------------------------------|-----------------------------|------------------|--------------|--------------|
| | | AFO | Tuned | SSO |
| SVA (degrees) | Mid stance | 9.13±(0.55) | 11.36±(0.56) | 3.19±(0.55) |
| Temporal-spatial | Speed (ms ⁻¹) | 0.61±(0.02) | 0.60±(0.02) | 0.20±(0.02) |
| | Stance time (%) | 69.02±(0.20) | 69.04±(0.18) | 79.01±(0.45) |
| | Stride length (m) | 0.62±(0.06) | 0.63±(0.06) | 0.19±(0.05) |
| Ankle angle (degrees) | PF peak (early stance) | -1.04±(0.56) | -0.90±(0.45) | -2.17±(0.62) |
| | Dorsiflexion peak | 0.98±(0.54) | 1.05±(0.52) | 3.70±(0.52) |
| | PF peak (swing phase) | -0.55±(0.21) | -0.57±(0.22) | -1.84±(0.42) |
| Knee angle (degrees) | Flexion peak (stance) | 15.22±(1.51) | 19.59±(1.11) | 2.91±(1.26) |
| | Extension (terminal stance) | 2.93±(0.26) | 5.90±(0.71) | -2.44±(0.37) |
| | Flexion peak (swing) | 53.16±(2.60) | 50.73±(1.53) | 18.32±(1.79) |
| Hip angle (degrees) | Extension peak | -6.04±(0.99) | -5.56±(0.97) | 18.61±(1.12) |
| | Flexion peak (swing phase) | 40.22±(1.24) | 40.37±(1.14) | 37.31±(1.25) |
| Ankle moment (Nm/kg) | PF peak (early stance) | -0.27±(0.02) | -0.24±(0.03) | - |
| | Dorsiflexion peak | 0.71±(0.04) | 0.70±(0.02) | 0.95±(0.03) |
| Knee moment (Nm/kg) | Flexion peak1 | 0.14±(0.01) | 0.20±(0.01) | -0.09±(0.01) |
| | Extension peak | -0.45±(0.01) | -0.32±(0.01) | -0.64±(0.01) |
| | Flexion peak2 | 0.05±(0.01) | 0.06±(0.01) | 0.01±(0.01) |
| Hip moment (Nm/kg) | Flexion peak | 0.38±(0.03) | 0.38±(0.04) | 0.37±(0.05) |
| | Extension peak | -0.64±(0.04) | -0.62±(0.04) | -0.14±(0.05) |
| GRFv (N) | 1 st peak | 768±(8.52) | 784±(8.48) | 488±(7.52) |
| | Trough | 697±(12.14) | 678±(9.42) | 381±(10.62) |
| | 2 nd peak | 811±(8.05) | 817±(8.04) | 740±(9.22) |

Table 4.5: Quadriceps and hamstring EMG RMS amplitude for case study 1 (*SPI*).

| Parameter description | | <u>Mean±(SD)</u> | | |
|-----------------------|--------------------------|------------------|--------------|--------------|
| | | AFO | Tuned | SSO |
| VL RMS (%MMT) | Stance peak | 33.48±(4.50) | 40.04±(5.12) | 13.23±(3.16) |
| | Swing peak | 28.02±(3.30) | 31.60±(3.50) | 6.44±(1.50) |
| VM RMS (%MMT) | Stance peak | 38.17±(0.41) | 48.72±(0.28) | 20.72±(0.31) |
| | Swing peak | 27.90±(.33) | 33.81±(0.31) | 14.50±(0.33) |
| RF RMS (%MMT) | Stance peak [#] | 11.15±(0.09) | 10.44±(0.14) | 8.85±(0.19) |
| | T-PS peak | 18.26±(0.08) | 17.44±(0.09) | 11.63±(0.12) |
| | Swing peak | 12.40±(0.12) | 9.26±(0.13) | 6.25±(0.09) |
| BF RMS (%MMT) | Stance peak | 15.92±(0.23) | 12.86±(0.25) | 26.17±(0.23) |
| | Swing peak | 29.64±(0.41) | 24.85±(0.41) | 45.91±(0.40) |
| ST RMS (%MMT) | Stance peak | 16.51±(0.32) | 14.26±(0.37) | 27.66±(0.35) |
| | Swing peak | 16.05±(0.29) | 17.51±(0.27) | 49.24±(0.56) |

T-PS peak: the maximum activity during terminal stance and pre swing phase

Table 4.6: The anatomical and the orthotic ankle moment for case study 1 (*SPI*) derived from SG2 and SG4 data outputs.

| Moment (Nm/kg) | | <u>Anatomical</u> (mean±(SD)) | | <u>Orthotic</u> (mean±(SD)) | |
|----------------|----------------------|-------------------------------|-------------|-----------------------------|--------------|
| | | AFO | Tuned | AFO | Tuned |
| SG2 | Early stance peak | -0.01±(0.03) | 0.01±(0.03) | -0.26±(0.03) | -0.25±(0.03) |
| | Terminal stance peak | 0.73±(0.04) | 0.76±(0.02) | 0.02±(0.03) | -0.06±(0.02) |
| SG4 | Mid stance peak | 0.07±(0.01) | 0.07±(0.01) | -0.05±(0.01) | -0.06±(0.01) |
| | Terminal stance peak | 0.19±(0.01) | 0.18±(0.01) | 0.01±(0.01) | 0.01±(0.01) |

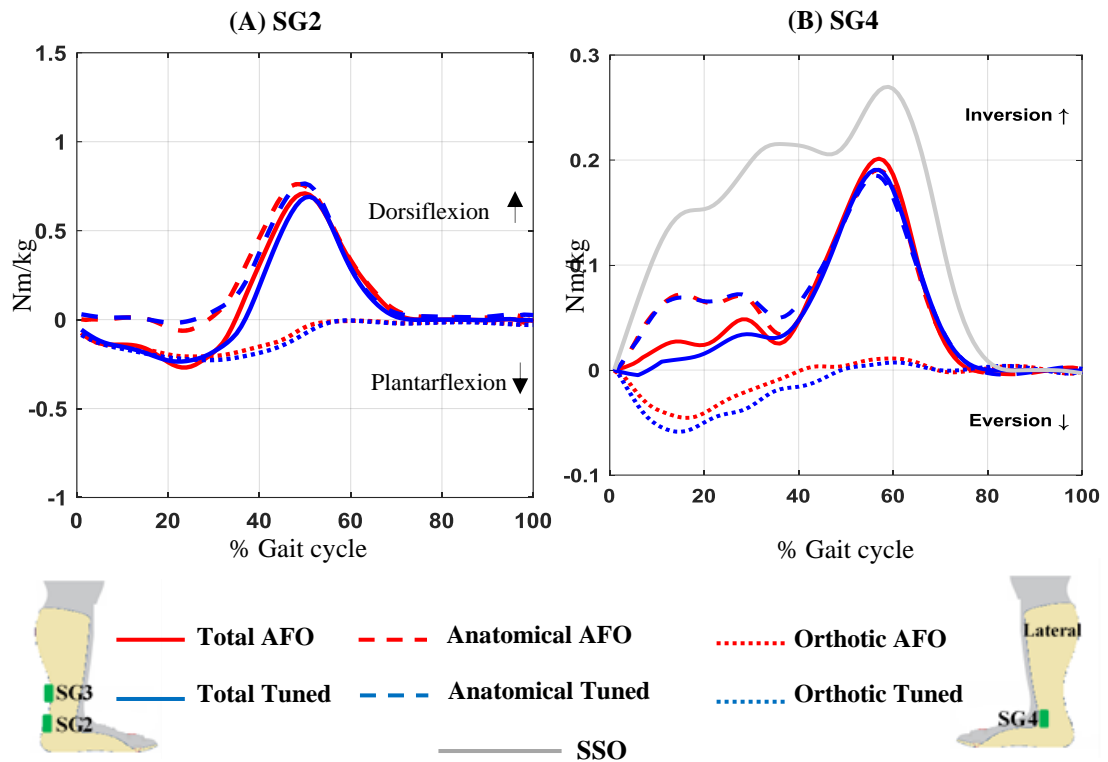


Figure 4.8: Total ankle moment, orthotic moment, and anatomical moment in sagittal plane (A) and frontal plane (B) for case study 1 (*SP1*) derived from SG2 and SG4 data outputs, respectively.

4.3 Case study two (*SP2*)

SP2 was a 55-year-old male with a mass of 77kg and height of 1.65m. *SP2* had hemorrhagic stroke in 2015 affecting his left hemisphere resulting in right side hemiparesis. *SP2* started a daily physical therapy regimen in 2015 for three years (lower limbs) and still receiving a daily physical therapy for his upper limb only. Initially, *SP2* was prescribed a rigid plastic AFO but he prefers flexible articulated AFO (Orliman Boxia Drop Foot AFO that consists of two separate components; a cuff situated above the ankle and a non-slip hook section which fits between the laces/Velcro straps of the shoes) which allows some movement at the ankle. The CWS for *SP2* was 0.40 m/s in SSO condition. Based on walking speed classification in stroke patients (Perry et al., 1995), *SP2* is classified as a “limited community walking” (speed 0.4–0.8 m/s).

4.3.1 Comparing AFO condition with SSO condition:

The walking speed of **SP2** increased from $(0.40 \pm 0.02 \text{ m/s})$ in SSO condition to $(0.60 \pm 0.02 \text{ m/s})$ in AFO condition. This is reflected in the slightly decreased stance percentage of the gait cycle and in the increased stride length (from $69.06 \pm 0.12\%$ in SSO to $69 \pm 0.15\%$ in AFO condition, and from $0.36 \pm 0.09\text{m}$ to $0.58 \pm 0.06\text{m}$, respectively). SVA inclination during mid stance merely increased (only by 0.38 degrees) from $(8.33 \pm 0.26 \text{ degrees})$ in SSO to $(8.71 \pm 0.26 \text{ degrees})$ in AFO condition (Table 4.7, Figure 4.9, A). Ankle motion on the other hand, showed decreased first (early stance) plantar flexion, increased second (late stance) dorsiflexion, and decreased third (swing phase) plantar flexion peaks in AFO condition as compared to SSO condition (from $-1.51 \pm 0.51 \text{ degrees}$, $-0.03 \pm 0.01 \text{ degrees}$, $-3.24 \pm 0.18 \text{ degrees}$ in SSO condition to $-0.46 \pm 0.12 \text{ degrees}$, $0.40 \pm 0.05 \text{ degrees}$, $-0.31 \pm 0.09 \text{ degrees}$ in AFO condition, respectively) (Table 4.7, Figure 4.9, B). On the contrary, knee motion showed increased early stance and swing flexion peaks and decreased late stance extension in AFO condition as compared to SSO condition ($7.01 \pm 1.22 \text{ degrees}$, $27.88 \pm 1.72 \text{ degrees}$, $-0.27 \pm 0.36 \text{ degrees}$ in SSO condition, $18.49 \pm 1.53 \text{ degrees}$, $51.41 \pm 1.58 \text{ degrees}$, $2.63 \pm 0.27 \text{ degrees}$ in AFO condition, respectively) (Table 4.7, Figure 4.9, C). Hip extension in **SP2** by the end of single limb support increased (but the hip remained flexed) from $(15.89 \pm 0.82 \text{ degrees})$ in SSO condition to $(13.59 \pm 0.84 \text{ degrees})$. Maximum hip flexion in swing phase decreased in AFO condition ($28.27 \pm 2.03 \text{ degrees}$) as compared to SSO condition ($34.34 \pm 2.10 \text{ degrees}$) (Table 4.7, Figure 4.9, D).

Changes in the kinetics in **SP2** were also observed in AFO condition as compared to SSO condition (Table 4.7, Figure 4.10). The value of the first peak of GRFv was lower in AFO condition ($805 \pm 12.24\text{N}$) as compared to SSO condition ($818 \pm 14.15\text{N}$). The values of the trough and the second peak of the GRFv were higher in AFO condition ($755 \pm 2.24\text{N}$ and $803 \pm 9.85\text{N}$, respectively) as compared to SSO condition ($709\text{N} \pm 6.14\text{N}$ and $721 \pm 7.88\text{n}$, respectively). Additionally, the first is higher than **SP2** body weight in AFO condition (105%BW). First peak in SSO condition was higher than **SP2** body weight (106%BW). The second peak of GRFv in **SP2** is slightly more than body weight in AFO condition (104%BW). The trough was (92%BW) in SSO condition and became (98%BW) in AFO condition. At the ankle, peak plantar flexion moment which occurs early in stance was absent in SSO condition and appeared in AFO condition ($-0.14 \pm 0.05 \text{ Nm/kg}$), the same

as in *SPI*. Additionally, the dorsiflexion moment peak decreased in AFO condition (0.41 ± 0.01 Nm/kg) as compared to SSO condition (0.80 ± 0.01 Nm/kg). The change was also observed at the knee; especially that in SSO condition knee extension moment was dominant and wearing an AFO ends this dominance. Knee moments reversed in early stance from extension moments in SSO condition (0.52 ± 0.06 Nm/kg) to flexion moments in AFO condition (0.26 ± 0.01 Nm/kg), the slight flexion moment in late stance in SSO condition (0.06 ± 0.06 Nm/kg) reversed to extension moment in AFO condition (-0.46 ± 0.01 Nm/kg), and the second flexion moment peak that occurs by the end of stance decreased from (0.08 ± 0.01 Nm/kg) in SSO condition to (0.06 ± 0.01 Nm/kg) in AFO condition. At the hip in SSO condition, only small extension moment occurs during mid and terminal stance, AFO condition increases this extension moment. Flexion moment peak at the hip that occurs early in stance showed a decrease in AFO condition (0.15 ± 0.02 Nm/kg) as compared to SSO condition (0.35 ± 0.02 Nm/kg), however, the extension moment peak showed great increase in AFO condition (-0.31 ± 0.03 Nm/kg) as compared to SSO condition (-0.08 ± 0.01 Nm/kg).

As in *SPI*, fitting an AFO also showed changes in the EMG activity of muscles of *SP2* as compared to SSO condition (Table 4.8, Figure 4.11). VL and VM generally showed similar activity patterns and thus, will be presented together. VL and VM showed longer periods of activity and continued to be active during mid and terminal stance in SSO condition, and even longer period of activity in AFO condition in *SP2*. VL and VM showed increased stance (37.46 ± 3.20 %MMT, 41.80 ± 0.29 %MMT, respectively) and swing (17.57 ± 3.40 %MMT, 19.82 ± 0.50 %MMT, respectively) peaks in AFO condition as compared to SSO condition (VL: 27.83 ± 4.13 %MMT, 12.01 ± 2.40 %MMT, VM: 26.02 ± 0.31 %MMT, 14.74 ± 0.51 %MMT, respectively). In SSO condition, RF started activity during the second half of mid stance and continued until the end of stance, and then resumed activity in mid and terminal swing. Wearing an AFO resulted in RF activity that starts in the second half of terminal stance and continued through most of swing. It also showed increased terminal stance-pre swing peak (9.52 ± 0.09 %MMT) in AFO condition as compared to SSO condition (7.85 ± 0.10 %MMT) and increased swing phase peak in AFO condition (6.54 ± 0.05 %MMT) as compared to SSO condition (3.97 ± 0.06 %MMT). BF and ST also showed similar activity pattern and will thus, be presented together. BF and ST were active from initial contact to the end of mid stance and during

almost of swing phase in SSO condition. Wearing an AFO did not change the period of activity of these muscles. BF and ST showed decreased stance peak (34.01 ± 0.38 %MMT, 23.28 ± 0.27 %MMT, respectively) and swing peak (43.26 ± 0.52 %MMT, 27.51 ± 0.33 %MMT, respectively) in AFO condition as compared to SSO condition (BF: 48.78 ± 0.38 %MMT, 51.68 ± 0.51 %MMT, respectively, ST: 29.01 ± 0.25 %MMT, 31.40 ± 0.38 %MMT, respectively).

4.3.2 Comparing Tuned-AFO condition with AFO condition:

The walking speed of *SP2* remained almost the same in Tuned-AFO condition (0.58 ± 0.02 m/s) as compared to AFO condition (0.60 ± 0.02 m/s). Stride length and stance percentage of the gait cycle also remained almost the same (0.54 ± 0.05 m and 69.01 ± 0.20 % in Tuned-AFO condition as compared to 0.58 ± 0.06 m and 69.00 ± 0.15 % in AFO condition). SVA inclination during mid stance was further increased in Tuned-AFO (by 3 degrees) from (8.71 ± 0.26 degrees) in AFO condition to (11.71 ± 0.26 degrees) in Tuned-AFO condition (Table 4.7, Figure 4.9, A). Slight change in ankle motion resulted in Tuned-AFO condition as compared to AFO condition; as first plantar flexion peak decreased (-0.14 ± 0.08 degrees, -0.46 ± 0.12 degrees, respectively), second slight plantar flexion peak reversed to slight dorsiflexion (0.12 ± 0.05 degrees and, -0.31 ± 0.09 degrees, respectively), and the dorsiflexion peak slightly increased (0.49 ± 0.10 degrees and 0.40 ± 0.05 degrees, respectively) (Table 4.7, Figure 4.9, B). Knee motion showed, in Tuned-AFO condition as compared to AFO condition, increased early stance flexion (20.69 ± 1.42 degrees and 18.49 ± 1.53 degrees, respectively), decreased knee extension (6.25 degrees ± 0.57 degrees and 2.63 ± 0.27 degrees, respectively), and increased knee flexion in swing phase (53.78 ± 1.69 degrees and 51.41 ± 1.58 degrees) (Table 4.7, Figure 4.9, C). Hip flexion peak decreased and extension peak increased (but remained flexed) in *SP2* in Tuned-AFO condition (24.2 ± 2.02 degrees and 9.35 ± 0.75 degrees, respectively) as compared to AFO condition (28.27 ± 2.03 degrees and 13.59 ± 0.84 degrees, respectively) (Table 4.7, Figure 4.9, D).

GRFv in *SP2* after AFO tuning also changed (Table 4.7, Figure 4.10, D). The first peak, trough, and the second peak were higher (110%BW, 105%BW, and 110%BW, respectively) as compared to AFO condition (105%BW, 98%BW, and 104%BW, respectively). Changes in the moments in *SP2* were, as in *SP1*, most apparent on the knee

joint, where the first flexion peak increased, second flexion peak increased, and the extension peak decreased in Tuned-AFO condition ($0.34\pm 0.01\text{Nm/kg}$, $0.12\pm 0.01\text{Nm/kg}$, and $-0.31\pm 0.01\text{Nm/kg}$, respectively) as compared to AFO condition ($0.26\pm 0.01\text{Nm/kg}$, $0.06\pm 0.01\text{Nm/kg}$, and $-0.46\pm 0.01\text{Nm/kg}$, respectively) (Table 4.7, Figure 4.10, B). At the ankle, slight decrease in peak plantar flexion moment and in peak dorsiflexion moment were recorded in Tuned-AFO condition ($-0.12\pm 0.04\text{ Nm/kg}$, and $0.43\pm 0.01\text{ Nm/kg}$, respectively) as compared to AFO condition ($0.14\pm 0.05\text{ Nm/kg}$, and $0.41\pm 0.01\text{ Nm/kg}$, respectively) (Table 4.7, Figure 4.10, A). Again, very slight change was recorded at the hip in Tuned-AFO condition (Flexion peak: $0.20\pm 0.02\text{ Nm/kg}$, Extension peak: $-0.29\pm 0.02\text{ Nm/kg}$) as compared to AFO condition (Flexion peak: $0.15\pm 0.02\text{ Nm/kg}$, Extension peak: $-0.31\pm 0.03\text{ Nm/kg}$) (Table 4.7, Figure 4.10, C).

The Tuned-AFO condition resulted in greater change in the EMG of knee muscles (Table 4.8, Figure 4.11). VL and VM showed an increase in their activity in Tuned-AFO condition (VL: $50.6\pm 7.15\% \text{MMT}$, $27.31\pm 3.80\% \text{MMT}$, VM: $46.58\pm 0.32\% \text{MMT}$, $29.87\pm 0.50\% \text{MMT}$, respectively) as compared to AFO condition (37.46 ± 3.20 and 17.57 ± 3.40 for VL, and $41.80\pm 0.29\% \text{MMT}$, $19.82\pm 0.50\% \text{MMT}$ for VM, respectively). Wearing a Tuned-AFO resulted in RF activity that starts in the second half of terminal stance and continued through most of swing as is the case in AFO condition, but RF activity showed no early stance peak, increased terminal stance-pre swing peak, and decreased swing peak in Tuned-AFO condition ($11.61\pm 0.11\% \text{MMT}$ and $5.83\pm 0.09\% \text{MMT}$, respectively) as compared to AFO condition ($9.52\pm 0.09\% \text{MMT}$ and $6.54\pm 0.05\% \text{MMT}$, respectively). Period of activity of Biceps Femoris and Semitendinosus did not show a change in Tuned-AFO condition as compared to AFO condition but showed slightly decreased stance and swing peaks in Tuned-AFO condition (BF: 31.01 ± 0.36 , 35.26 ± 0.49 , ST: 22.15 ± 0.24 , $24.23\pm 0.31\% \text{MMT}$, respectively).

The orthotic moment showed plantarflexion moment during loading response and reduced plantar flexion orthotic moment during terminal stance (Table 4.9, Figure 4.12, A). In contrast, the anatomical moment only showed a dorsiflexion moment during most of stance. Walking with a Tuned-AFO or an AFO in *SP2*, showed no noticeable differences in the orthotic plantarflexion moment during loading response (-0.14 ± 0.04 and -0.15 ± 0.05 , respectively), nor in the anatomical dorsiflexion moment in late stance (0.52 ± 0.01 and 0.50 ± 0.01 , respectively).

SP2 showed a noticeable reduction in the total inversion moment while walking with an AFO or Tuned-AFO as compared to walking with SSO as illustrated in Figure 4.12 (B). The orthotic moment peaks showed an eversion moment peak during the whole of stance. Walking with a Tuned-AFO or an AFO, showed no noticeable differences in the orthotic eversion moment nor in the anatomical inversion moment.

The effect of AFO and Tuned-AFO on the speed of **SP2** was obvious, as **SP2** gait speed increased by (0.2m/s) and (0.18m/s), respectively. Although the classification of **SP2** remained a “limited community walking” according to the classification by Perry et al. (1995) the speed increments were higher than the MCID (0.16 m/s); and thus these increments are considered clinically significant (Tilson et al., 2010).

Additionally, AFO and Tuned-AFO changed the kinematics so that they are closer to normal than in SSO (except for the ankle motion). SVA in Tuned-AFO condition was within the target range (10-12 degrees) compared to 8.33 degrees in SSO condition; indicating sufficient tuning. The hip was 17.71 degrees less extended than normal (control participants in SSO condition are considered the normal baseline in this study) in Tuned-AFO condition and 22.22 degrees less than normal in AFO condition compared to 24.52 degrees more flexed than normal in SSO condition, the knee was 7.22 degrees more flexed during early stance in Tuned-AFO condition and 5.20 degrees more flexed in AFO condition compared to 6.46 degrees less flexed than normal in SSO condition.

The effects of tuning the AFO are more obvious in **SP2** as compared to **SP1**. This could be justified by the greater alteration of SVA that occurred in Tuned-AFO condition as compared to AFO condition. The inability of the AFO to change the SVA greatly may be due to very rigid equinus that could not be changed by the AFO. Additionally, it is important to note that SVA of **SP2** in SSO condition was very close to the target SVA (as compared to other SPs), which means that **SP2**'s gait in SSO condition can be considered close to normal (again as compared to other SPs). Further discussion on the effect of Tuned-AFO condition and AFO condition on the gait parameters of control and stroke participants will be addressed in the next chapter (Chapter 5 Discussion).

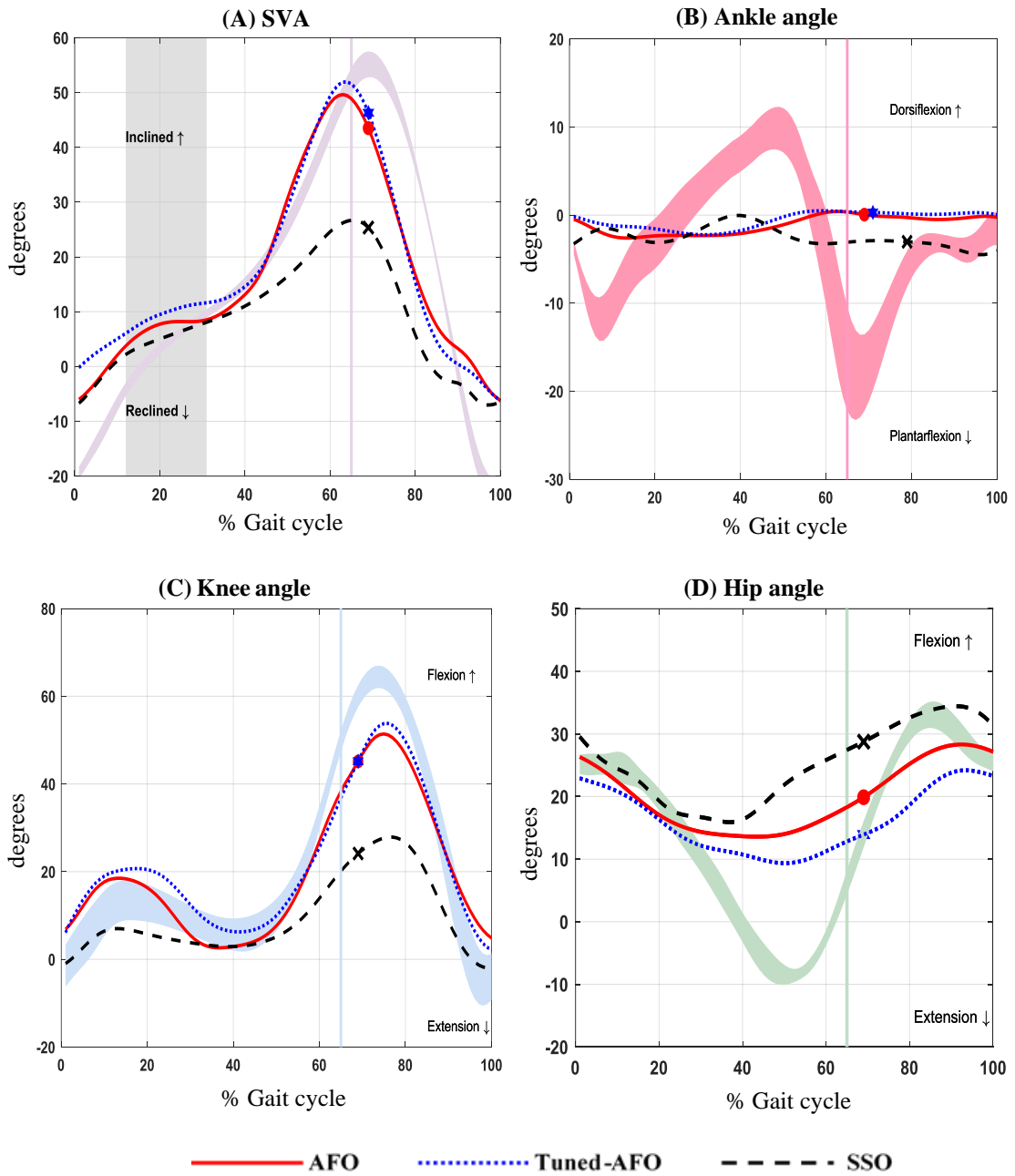


Figure 4.9: Sagittal kinematic graphs for case study 2 (*SP2*) while walking on treadmill wearing Tuned-AFO, AFO, and SSO with reference to control participants while wearing SSO (shaded lines).

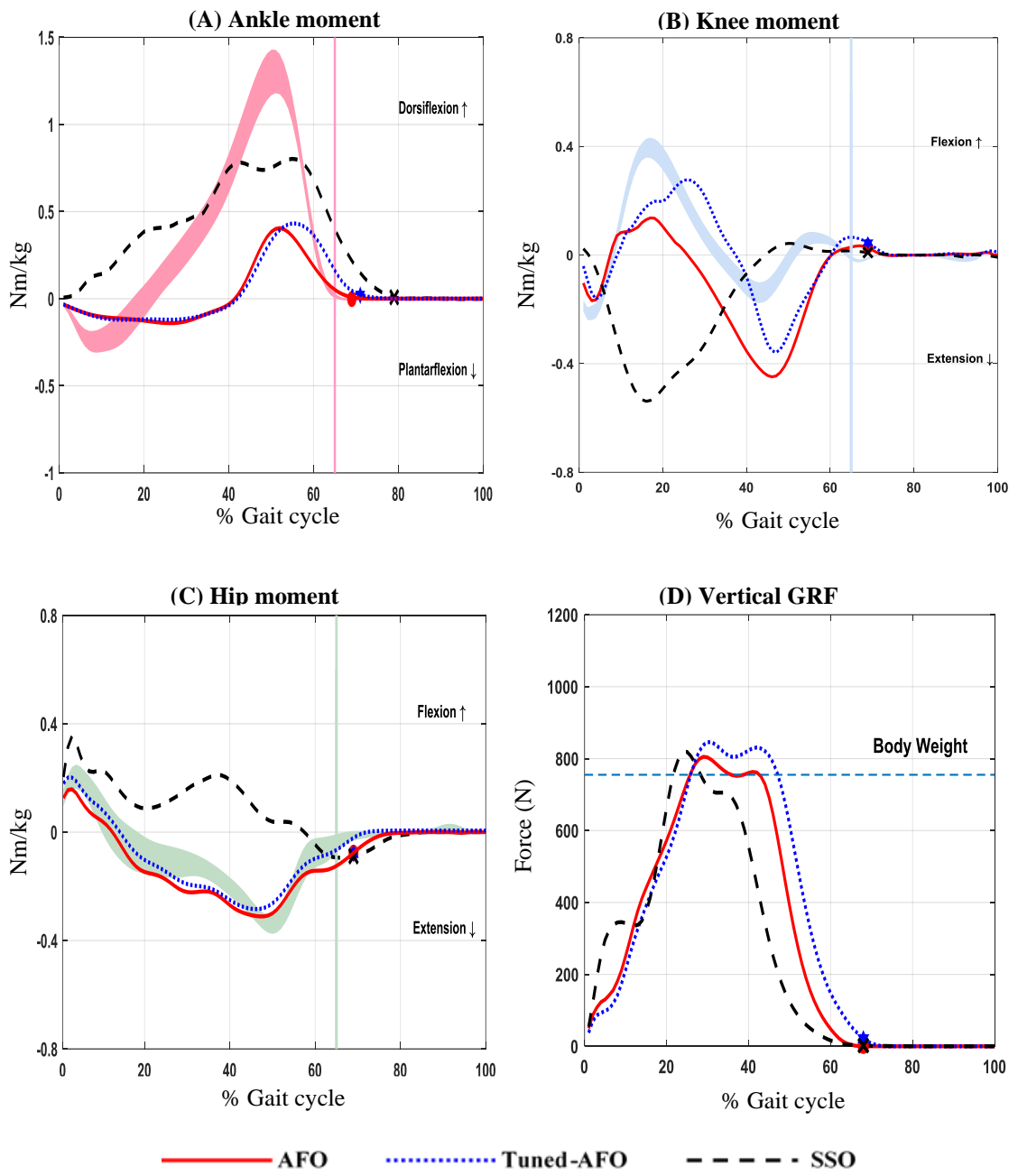


Figure 4.10: Sagittal kinetic graphs and the vertical GRF graph for case study 2 (*SP2*) while walking on treadmill wearing Tuned-AFO, AFO, and SSO with reference to control participants while wearing SSO (shaded lines).

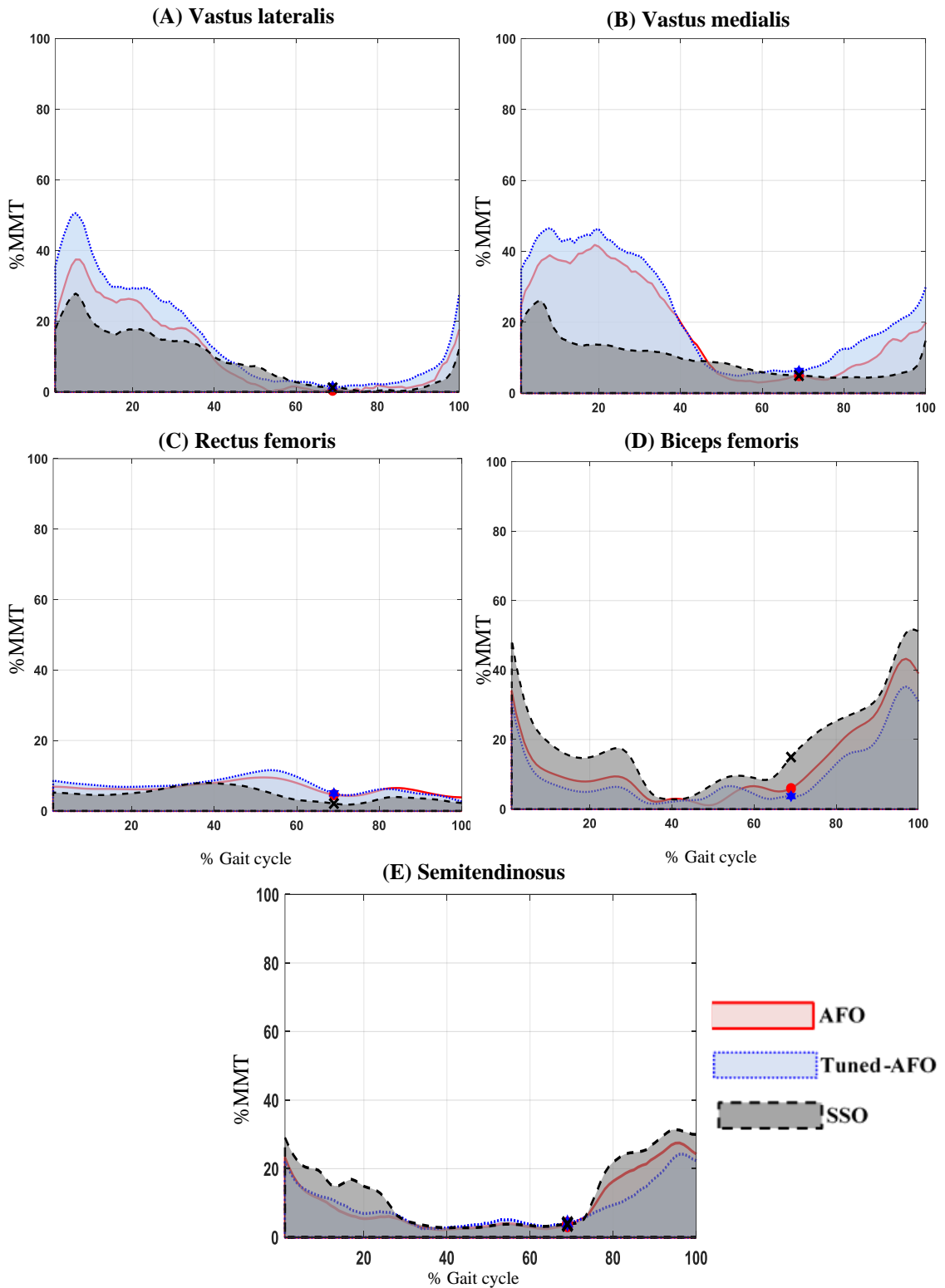


Figure 4.11: Quadriceps and hamstring EMG RMS amplitude and timing during walking on treadmill for case study 2 (*SP2*). The RMS is presented as a percentage of maximum manual muscle test value (% MMT).

Table 4.7: Temporal-spatial, kinematic and kinetic data for *SP2*.

| Parameter description | | <u>Mean±(SD)</u> | | |
|------------------------------|-----------------------------|------------------|--------------|--------------|
| | | AFO | Tuned | SSO |
| SVA (degrees) | Mid stance | 8.71±(0.26) | 11.71±(0.26) | 8.33±(0.26) |
| Temporal-spatial | Speed (ms ⁻¹) | 0.60±(0.02) | 0.58±(0.02) | 0.40±(0.02) |
| | Stance time (%) | 69.00±(0.15) | 69.01±(0.20) | 69.06±(0.12) |
| | Stride length (m) | 0.58±(0.06) | 0.54±(0.05) | 0.36±(0.09) |
| Ankle angle (degrees) | PF peak (early stance) | -0.46±(0.12) | -0.14±(0.08) | -1.51±(0.51) |
| | Dorsiflexion peak | 0.40±(0.05) | 0.49±(0.10) | -0.03±(0.01) |
| | PF peak (swing phase) | -0.31±(0.09) | 0.12±(0.05) | -3.24±(0.18) |
| Knee angle (degrees) | Flexion peak (stance) | 18.49±(1.53) | 20.69±(1.42) | 7.01±(1.22) |
| | Extension (terminal stance) | 2.63±(0.27) | 6.25±(0.57) | -0.27±(0.36) |
| | Flexion peak (swing) | 51.41±(1.58) | 53.78±(1.69) | 27.88±(1.72) |
| Hip angle (degrees) | Extension peak | 13.59±(0.84) | 9.35±(0.75) | 15.89±(0.82) |
| | Flexion peak (swing phase) | 28.27±(2.03) | 24.2±(2.02) | 34.34±(2.10) |
| Ankle moment (Nm/kg) | PF peak (early stance) | -0.14±(0.05) | -0.12±(0.04) | - |
| | Dorsiflexion peak | 0.41±(0.01) | 0.43±(0.01) | 0.80±(0.01) |
| Knee moment (Nm/kg) | Flexion peak1 | 0.26±(0.01) | 0.34±(0.01) | -0.52±(0.06) |
| | Extension peak | -0.46±(0.01) | -0.31±(0.01) | 0.06±(0.06) |
| | Flexion peak2 | 0.06±(0.01) | 0.12±(0.01) | 0.08±(0.01) |
| Hip moment (Nm/kg) | Flexion peak | 0.15±(0.02) | 0.20±(0.02) | 0.35±(0.02) |
| | Extension peak | -0.31±(0.03) | -0.29±(0.02) | -0.08±(0.01) |
| GRFv (N) | 1 st peak | 805±(12.24) | 845±(11.28) | 818±(14.15) |
| | Trough | 755±(2.24) | 805±(2.28) | 709±(6.14) |
| | 2 nd peak | 803±(9.85) | 845±(8.55) | 721±(7.88) |

Table 4.8: Quadriceps and hamstring EMG RMS amplitude for case study 2 (*SP2*).

| Parameter description | | <u>Mean±(SD)</u> | | |
|-----------------------|--------------------------|------------------|--------------|--------------|
| | | AFO | Tuned | SSO |
| VL RMS (%MMT) | Stance peak | 37.46±(3.20) | 50.60±(7.15) | 27.83±(4.13) |
| | Swing peak | 17.57±(3.40) | 27.31±(3.80) | 12.01±(2.40) |
| VM RMS (%MMT) | Stance peak | 41.80±(0.29) | 46.58±(0.32) | 26.02±(0.31) |
| | Swing peak | 19.82±(0.50) | 29.87±(0.50) | 14.74±(0.51) |
| RF RMS (%MMT) | Stance peak [#] | - | - | - |
| | T-PS peak | 9.52±(0.09) | 11.61±(0.11) | 7.85±(0.10) |
| | Swing peak | 6.54±(0.05) | 5.83±(0.09) | 3.97±(0.06) |
| BF RMS (%MMT) | Stance peak | 34.01±(0.38) | 31.01±(0.36) | 48.78±(0.38) |
| | Swing peak | 43.26±(0.52) | 35.26±(0.49) | 51.68±(0.51) |
| ST RMS (%MMT) | Stance peak | 23.28±(0.27) | 22.15±(0.24) | 29.01±(0.25) |
| | Swing peak | 27.51±(0.33) | 24.23±(0.31) | 31.40±(0.38) |

T-PS peak: the maximum activity during terminal stance and pre swing phase

Table 4.9: The anatomical and the orthotic ankle moment for case study 2 (*SP2*) derived from SG2 and SG4 data outputs.

| Moment (Nm/kg) | | <u>Anatomical</u> (mean±(SD)) | | <u>Orthotic</u> (mean±(SD)) | |
|----------------|----------------------|-------------------------------|-------------|-----------------------------|--------------|
| | | AFO | Tuned | AFO | Tuned |
| SG2 | Early stance peak | 0.01±(0.05) | 0.02±(0.04) | -0.15±(0.05) | -0.14±(0.04) |
| | Terminal stance peak | 0.50±(0.01) | 0.52±(0.01) | -0.09±(0.05) | -0.09±(0.01) |
| SG4 | Mid stance peak | 0.10±(0.01) | 0.10±(0.01) | -0.03±(0.01) | -0.04±(0.01) |
| | Terminal stance peak | 0.15±(0.01) | 0.15±(0.01) | -0.05±(0.01) | -0.05±(0.01) |

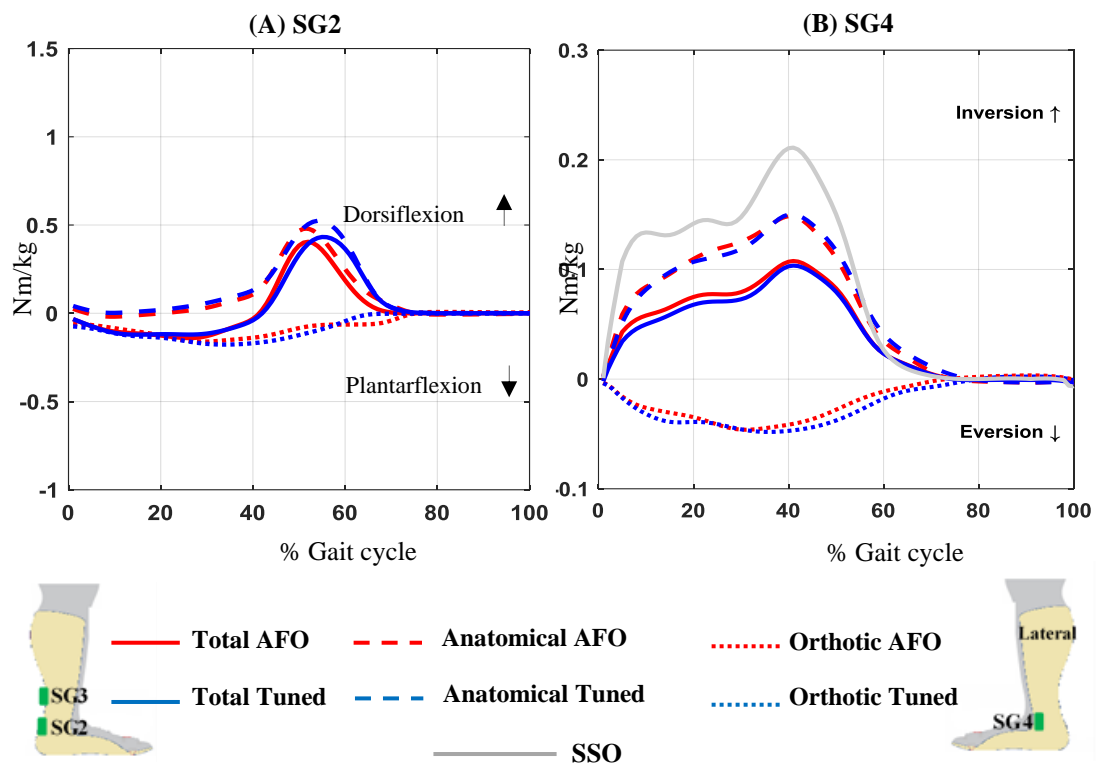


Figure 4.12: Total ankle moment, orthotic moment, and anatomical moment in sagittal plane (A) and frontal plane (B) for case study 2 (*SP2*) derived from SG2 and SG4 data outputs, respectively.

4.4 Case study three (*SP3*)

SP3 was a 37-year-old male with a mass of 95kg and height of 1.93m. *SP3* had ischemic stroke in 2018 affecting his left hemisphere resulting in right side hemiparesis. *SP3* started a daily physical therapy regimen in 2015 for two years. *SP3* own orthosis was rigid AFO (with tuning), the same as the AFO used in this study (but without reinforcements at the ankle region). The CWS for *SP3* was 0.60 m/s in SSO condition. Based on walking speed classification in stroke patients (Perry et al., 1995), *SP3* is classified as a “limited community walking” (speed 0.4–0.8 m/s).

4.4.1 Comparing AFO condition with SSO condition:

The walking speed of *SP3* increased from (0.60±0.02 m/s) in SSO condition to (0.90±0.02 m/s) in AFO condition. This is reflected only in the increased stride length

($0.59\pm 0.09\text{m}$ in SSO condition and $0.88\pm 0.07\text{m}$ in AFO condition). Stance time percentage did not show any change. SVA inclination during mid stance merely increased (only by 0.57 degrees) from (7.51 ± 0.42 degrees) in SSO to (8.08 ± 0.42 degrees) in AFO condition (Table 4.10, Figure 4.13, A). Ankle motion on the other hand, showed increased first (early stance) plantar flexion, decreased second (late stance) dorsiflexion, and decreased third (swing phase) plantar flexion peaks in AFO condition as compared to SSO condition (from 1.14 ± 0.09 degrees, 7.65 ± 0.32 degrees, -2.89 ± 0.13 degrees in SSO condition to, -0.22 ± 0.04 degrees, 2.77 ± 0.08 degrees, -0.76 ± 0.07 in AFO condition, respectively) (Table 4.10, Figure 4.13, B). Knee motion showed slightly increased early stance and swing flexion and decreased late stance extension in AFO condition as compared to SSO condition (12.13 ± 1.25 degrees, 45.12 ± 1.10 degrees, 0.67 ± 0.22 degrees in SSO condition, 14.38 ± 1.53 degrees, 47.04 ± 1.04 degrees, 3.51 ± 0.23 degrees in AFO condition, respectively) (Table 4.10, Figure 4.13, C). Hip extension in **SP3** by the end of single limb support increased from (17.84 ± 0.94) in SSO condition to (12.65 ± 0.59 degrees) but remained flexed (Table 4.10, Figure 4.13, D). Maximum hip flexion in swing phase slightly decreased in AFO condition (37.14 ± 1.34 degrees) as compared to SSO condition (38.58 ± 1.41 degrees).

Changes in the kinetics in **SP3** were also observed in AFO condition as compared to SSO condition (Table 4.10, Figure 4.14). The values of the first and second peaks of GRFv were higher in AFO condition ($1088\pm 8.12\text{N}$ and $963\pm 9.22\text{N}$, respectively) as compared to SSO condition ($931\pm 5.05\text{N}$ and $879\pm 7.35\text{N}$, respectively). The value of the trough was lower in AFO condition ($625\pm 9.13\text{N}$) as compared to SSO condition ($830\pm 6.23\text{N}$). Additionally, the first and second peaks are higher than **SP3** body weight in AFO condition ($115\% \text{BW}$ and $101\% \text{BW}$, respectively) as compared to ($98\% \text{BW}$ and $93\% \text{BW}$, respectively) in SSO condition. The trough was ($87\% \text{BW}$) in SSO condition and became ($66\% \text{BW}$) in AFO condition. At the ankle, peak plantar flexion moment which occurs early in stance was absent in SSO condition and appeared in AFO condition (-0.17 ± 0.07 Nm/kg), the same as in **SP1** and **SP2**. Additionally, the dorsiflexion moment peak slightly decreased in AFO condition (1.04 ± 0.04 Nm/kg) as compared to SSO condition (0.89 ± 0.03 Nm/kg). The change was merely observed at the knee; the values of first flexion moment peak, the extension moment peak, and the second flexion moment peak slightly changed in AFO condition (0.24 ± 0.01 Nm/kg, -0.29 ± 0.01 Nm/kg, 0.001 ± 0.01

Nm/kg, respectively) as compared to SSO condition (0.19 ± 0.04 , -0.25 ± 0.06 Nm/kg, 0.01 ± 0.01 Nm/kg, respectively). Flexion moment peak at the hip that occurs early in stance showed a slight decrease in AFO condition (0.43 ± 0.02 Nm/kg) as compared to SSO condition (0.58 ± 0.05 Nm/kg), however, the extension moment peak showed slight increase in AFO condition (-0.51 ± 0.02 Nm/kg) as compared to SSO condition (-0.43 ± 0.01 Nm/kg).

As in *SP1* and *SP2*, fitting an AFO also showed changes in the EMG activity of knee muscles as compared to SSO condition (Table 4.11, Figure 4.15). VL and VM generally showed similar activity patterns and thus, will be presented together. VL and VM showed longer periods of activity than normal and continued to be active during the whole of mid stance VL and to mid terminal stance VM in SSO and AFO conditions. VL and VM showed increased stance (33.91 ± 5.30 %MMT, 30.85 ± 0.41 %MMT, respectively) and swing (22.14 ± 3.60 %MMT, 20.91 ± 0.36 %MMT, respectively) peaks in AFO condition as compared to SSO condition (VL: 29.99 ± 5.02 %MMT, 21.84 ± 3.50 %MMT, VM: 26.91 ± 0.25 %MMT, 18.47 ± 0.33 %MMT, respectively). In SSO condition, RF in *SP3* started activity at initial contact and continued to halfway in mid stance and then from late terminal stance to end of initial swing. AFO did not change the activation periods of RF (Table 4.11, Figure 4.15). RF showed slightly increased early stance peak (7.88 ± 0.07 %MMT) in AFO condition as compared to SSO condition (7.18 ± 0.09) and slightly increased terminal stance-pre swing peak in AFO condition (9.15 ± 0.07 %MMT) as compared to SSO condition (7.16 ± 0.09 %MMT). BF and ST also showed similar activity pattern and will thus, be presented together. BF and ST were active from initial contact to the halfway in mid stance and during almost all of swing phase in SSO condition. Wearing an AFO did not change the period of activity of these muscles. BF and ST showed decreased stance peak (15.67 ± 0.31 %MMT, 26.24 ± 0.43 %MMT, respectively) and swing peak (22.71 ± 0.33 %MMT, 33.32 ± 0.36 %MMT, respectively) in AFO condition as compared to SSO condition (BF: 20.13 ± 0.32 %MMT, 26.09 ± 0.34 %MMT, respectively, ST: 27.88 ± 0.40 %MMT, 37.32 ± 0.38 %MMT, respectively).

4.4.2 Comparing Tuned-AFO condition with AFO condition:

The walking speed of *SP3* did not change between Tuned-AFO condition and AFO condition (0.90 ± 0.02 m/s). Stride length and stance percentage of the gait cycle also did

not change (69.04 ± 0.12 and 0.89 ± 0.06 in Tuned-AFO condition). SVA inclination during mid stance increased in Tuned-AFO (by 3.53 degrees) from (8.08 ± 0.42 degrees) in AFO condition to (11.61 ± 0.42 degrees) in Tuned-AFO condition (Table 4.10, Figure 4.13, A). Slight change in ankle motion resulted in Tuned-AFO condition as compared to AFO condition; as first plantar flexion peak decreased (-1.14 ± 0.00 and -0.22 ± 0.04 degrees, respectively), second slight plantar flexion peak reversed to slight dorsiflexion (0.36 ± 0.07 degrees and -0.76 ± 0.07 degrees, respectively), and the dorsiflexion peak slightly increased (4.36 ± 0.25 and 2.77 ± 0.08 degrees, respectively) (Table 4.10, Figure 4.13, B). Knee motion showed, in Tuned-AFO condition as compared to AFO condition, increased early stance flexion (21.35 ± 1.50 degrees and 14.38 ± 1.53 degrees, respectively), decreased knee extension (5.37 ± 0.31 degrees and 3.51 ± 0.23 degrees, respectively), and increased knee flexion in swing phase (52.59 ± 1.24 degrees and 47.04 ± 1.04 degrees) (Table 4.10, Figure 4.13, C). Hip flexion and extension peaks increased (but remained flexed throughout gait cycle) in **SP3** in Tuned-AFO condition (40.72 ± 1.32 degrees and 8.63 ± 0.59 degrees, respectively) as compared to AFO condition (37.14 ± 1.34 and 12.65 ± 0.59 degrees, respectively) (Table 4.10, Figure 4.13, D).

GRFv in **SP3** after AFO tuning also changed (Table 4.10, Figure 4.14). The first peak, trough, and the second peak were higher (125%BW, 83%BW, and 102%BW, respectively) as compared to AFO condition (115%BW, 66%BW, and 101%BW, respectively). Changes in the moments in **SP3** varied from slight to great. Ankle plantar flexion moment peak increased (-0.31 ± 0.06 Nm/kg) and dorsiflexion moment peak slightly decreased (0.87 ± 0.03) in Tuned-AFO condition as compared to AFO condition (-0.17 ± 0.07 Nm/kg and 0.89 ± 0.03 Nm/kg, respectively). Knee first flexion moment peak increased (0.36 ± 0.01 Nm/kg) in Tuned-AFO condition, while the second flexion peak remained unchanged (0.001 ± 0.01 Nm/kg) when compared with AFO condition (0.24 ± 0.01 Nm/kg and 0.001 ± 0.01 Nm/kg, respectively). Extension moment peak, on the other hand, decreased in Tuned-AFO condition (-0.17 ± 0.01 Nm/kg). Very slight change was recorded in the hip extension moment peak in Tuned-AFO condition (-0.52 ± 0.02 Nm/kg) as compared to AFO condition (-0.51 ± 0.02). Flexion moment peak showed greater decrease (0.30 ± 0.01 Nm/kg in Tuned-AFO condition and 0.43 ± 0.02 Nm/kg in AFO condition).

Tuning an AFO showed very little changes in the EMG activity of knee muscles as compared to AFO condition (Table 4.11, Figure 4.15). VL and VM showed similar activity patterns and thus, will be presented together. VL and VM showed longer periods of activity than normal and continued to be active during the whole of mid stance VL and to mid terminal stance VM in SSO and AFO conditions. VL and VM showed increased stance (41.97 ± 6.12 %MMT and 36.22 ± 0.28 %MMT, respectively) and swing (30.07 ± 4.60 %MMT and 26.85 ± 0.34 %MMT, respectively) peaks in Tuned-AFO condition as compared to AFO condition (VL: 33.91 ± 5.30 %MMT, 22.14 ± 3.60 %MMT, VM: 30.85 ± 0.41 %MMT, 20.91 ± 0.36 %MMT, respectively). Tuning the AFO did not change the activation periods of RF in *SP3*. RF showed slightly increased early stance peak (8.82 ± 0.07 %MMT) in Tuned-AFO condition as compared to AFO condition (7.88 ± 0.07 %MMT) and slightly decreased terminal stance-pre swing peak in Tuned-AFO condition (8.82 ± 0.07 %MMT) as compared to AFO condition (9.15 ± 0.07 %MMT). BF and ST also showed similar activity pattern and will thus, be presented together. BF and ST were active from initial contact to the halfway in mid stance and during almost all of swing phase in AFO condition. Tuning the AFO did not change the period of activity of these muscles. BF and ST showed decreased stance peak (13.79 ± 0.32 %MMT and 23.47 ± 0.39 %MMT, respectively) and swing peak (27.61 ± 0.36 %MMT and 17.36 ± 0.33 , respectively) in Tuned-AFO condition as compared to AFO condition (BF: 15.67 ± 0.31 %MMT, 22.71 ± 0.33 %MMT, respectively, ST: 26.24 ± 0.43 %MMT, 33.32 ± 0.36 %MMT, respectively).

In *SP3*, and as in *SP2*, the orthotic moment showed plantarflexion moment during loading response and reduced plantar flexion orthotic moment during terminal stance (Table 4.12, Figure 4.16, A). In contrast, the anatomical moment only showed a dorsiflexion moment during most of stance. Walking with a Tuned-AFO *SP3* resulted in higher plantar flexion orthotic moment (-0.31 ± 0.06) as compared to AFO condition (-0.20 ± 0.04). Terminal stance moment peak showed no noticeable differences in the orthotic plantarflexion moment between Tuned-AFO and AFO conditions.

SP3 showed a noticeable reduction in the total inversion moment while walking with an AFO or Tuned-AFO as compared to walking with SSO as illustrated in Figure 4.16 (B). The orthotic moment peaks showed an eversion moment peak during the whole of stance.

Walking with a Tuned-AFO or an AFO, showed no noticeable differences in the orthotic eversion moment nor in the anatomical inversion moment.

The effect of AFO and Tuned-AFO on the speed of **SP3** was obvious, as **SP3** gait speed increased by (0.3m/s) in both conditions. This means that **SP3** converted to “full community walking” according to the classification by Perry et al. (1995). Additionally, as the speed increments were higher than the MCID (0.16 m/s), these increments are considered clinically significant (Tilson et al., 2010).

Additionally, AFO and Tuned-AFO changed the kinematics so that they are closer to normal than in SSO (except for the ankle motion). SVA in Tuned-AFO condition was within the target range (10-12 degrees) compared to 7.51 degrees in SSO condition; indicating sufficient tuning. The hip was 17.26 degrees less extended than normal (control participants in SSO condition are considered the normal baseline in this study) in Tuned-AFO condition and 21.19 degrees less than normal in AFO condition compared to 26.47 degrees more flexed than normal in SSO condition, the knee was 7.88 degrees more flexed during early stance in Tuned-AFO condition and 0.91 degrees more flexed in AFO condition compared to 1.34 degrees less flexed than normal in SSO condition.

The effect of Tuning a rigid AFO on gait parameters was greater than the effect of AFO. This may be due to the fact that most of the SVA alteration was due to tuning not to fitting the AFO. Consequently, gait improvements in **SP3** are well noticed in Tuned-AFO condition. Further discussion on the effect of Tuned-AFO condition and AFO condition on the gait parameters of control and stroke participants will be addressed in the next chapter (Chapter 5 Discussion).

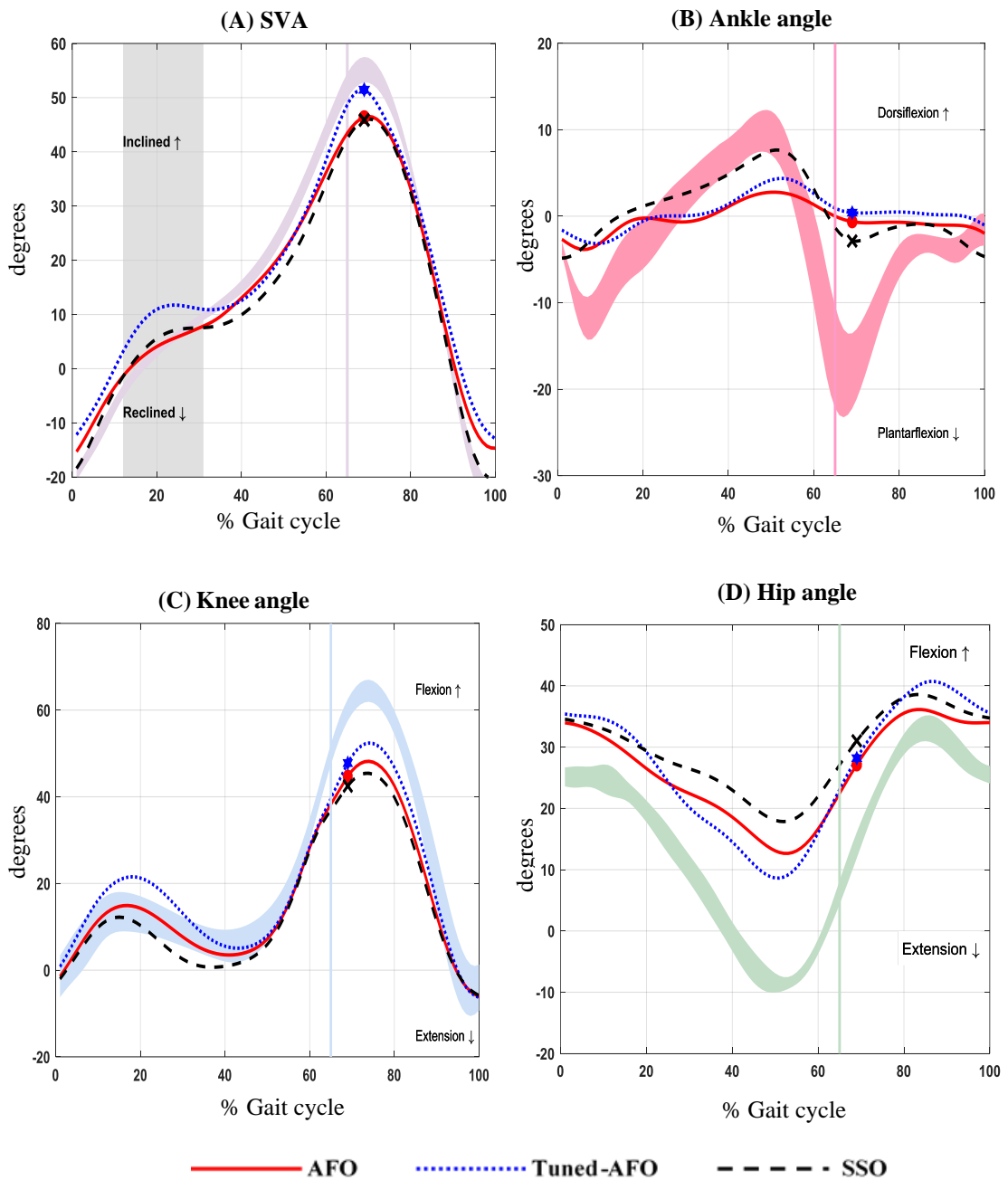


Figure 4.13: Sagittal kinematic graphs for case study 3 (*SP3*) while walking on treadmill wearing Tuned-AFO, AFO, and SSO with reference to control participants while wearing SSO (shaded lines).

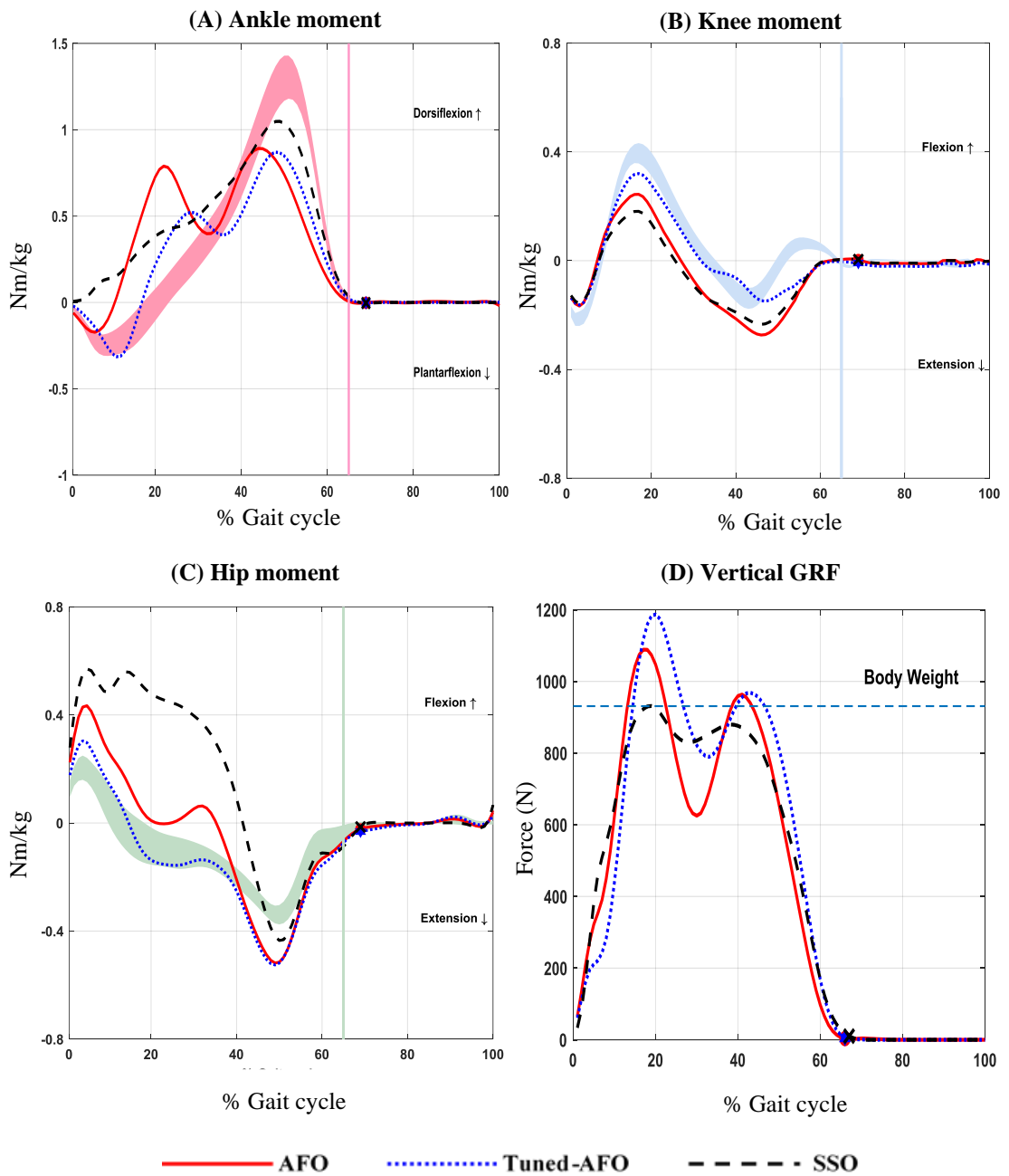


Figure 4.14: Sagittal kinetic graphs and the vertical GRF graph for case study 3 (*SP3*) while walking on treadmill wearing Tuned-AFO, AFO, and SSO with reference to control participants while wearing SSO (shaded lines).

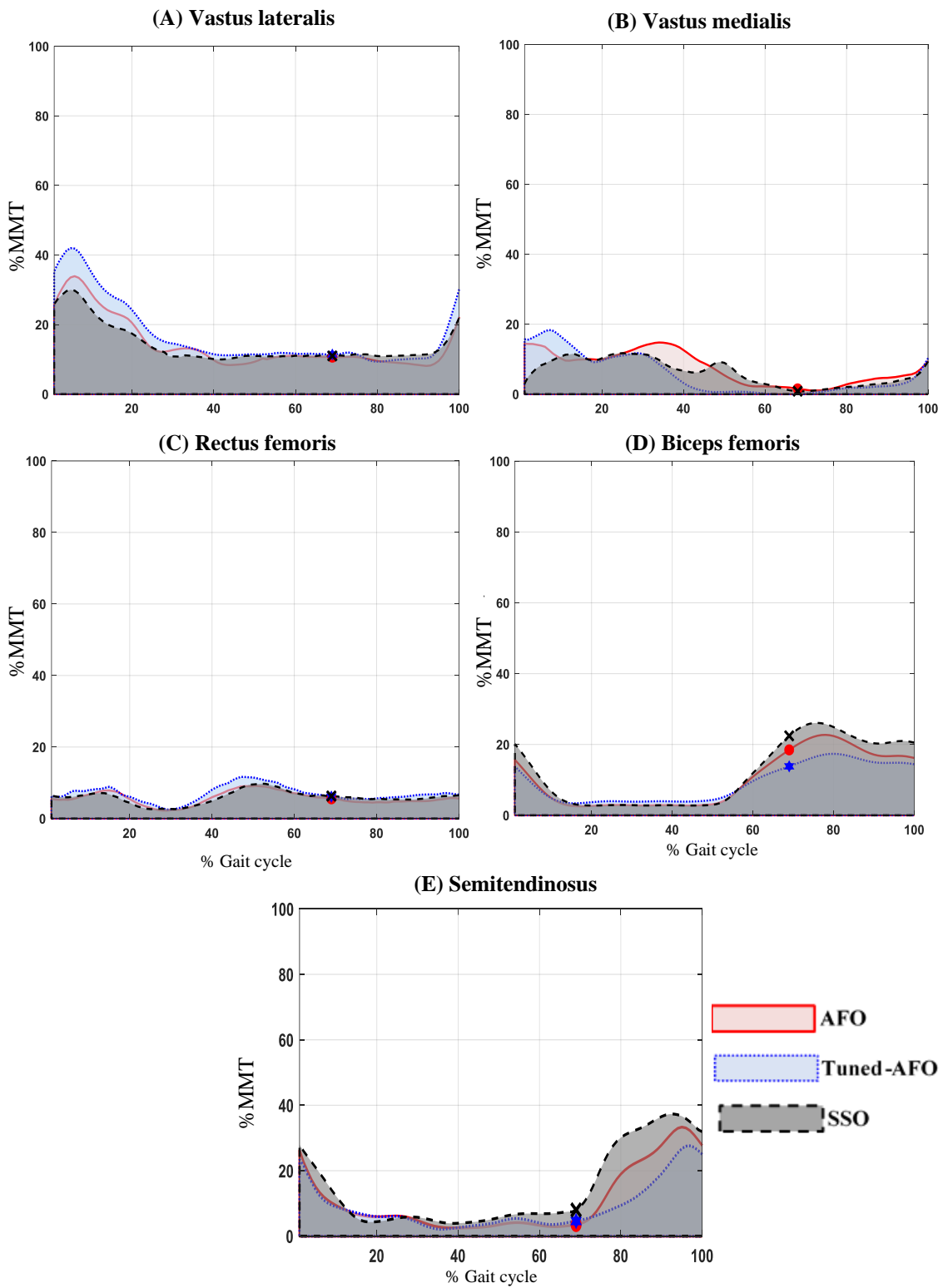


Figure 4.15: Quadriceps and hamstring EMG RMS amplitude and timing during walking on treadmill for case study 3 (*SP3*). The RMS is presented as a percentage of maximum manual muscle test value (% MMT).

Table 4.10: Temporal-spatial, kinematic and kinetic data for *SP3*.

| Parameter description | | <u>Mean±(SD)</u> | | |
|------------------------------|-----------------------------|------------------|--------------|--------------|
| | | AFO | Tuned | SSO |
| SVA (degrees) | Mid stance | 8.08±(0.42) | 11.61±(0.42) | 7.51±(0.42) |
| Temporal-spatial | Speed (ms ⁻¹) | 0.90±(0.02) | 0.90±(0.02) | 0.60±(0.02) |
| | Stance time (%) | 69.04±(0.11) | 69.04±(0.12) | 69.03±(0.12) |
| | Stride length (m) | 0.88±(0.07) | 0.89±(0.06) | 0.59±(0.09) |
| Ankle angle (degrees) | PF peak (early stance) | -0.22±(0.04) | -0.56±(0.06) | -1.14±(0.09) |
| | Dorsiflexion peak | 2.77±(0.08) | 4.36±(0.25) | 7.65±(0.32) |
| | PF peak (swing phase) | -0.76±(0.07) | 0.36±(0.07) | -2.89±(0.13) |
| Knee angle (degrees) | Flexion peak (stance) | 14.38±(1.53) | 21.35±(1.50) | 12.13±(1.25) |
| | Extension (terminal stance) | 3.51±(0.23) | 5.37±(0.31) | 0.67±(0.22) |
| | Flexion peak (swing) | 47.04±(1.04) | 52.59±(1.24) | 45.12±(1.10) |
| Hip angle (degrees) | Extension peak | 12.65±(0.59) | 8.63±(0.59) | 17.84±(0.94) |
| | Flexion peak (swing phase) | 37.14±(1.34) | 40.72±(1.32) | 38.58±(1.41) |
| Ankle moment (Nm/kg) | PF peak (early stance) | -0.17±(0.07) | -0.31±(0.06) | - |
| | Dorsiflexion peak | 0.89±(0.03) | 0.87±(0.03) | 1.04±(0.04) |
| Knee moment (Nm/kg) | Flexion peak1 | 0.24±(0.01) | 0.36±(0.01) | 0.19±(0.04) |
| | Extension peak | -0.29±(0.01) | -0.17±(0.01) | -0.25±(0.06) |
| | Flexion peak2 | 0.001±(0.01) | 0.001±(0.01) | 0.01±(0.01) |
| Hip moment (Nm/kg) | Flexion peak | 0.43±(0.02) | 0.30±(0.01) | 0.58±(0.05) |
| | Extension peak | -0.51±(0.02) | -0.52±(0.02) | -0.43±(0.01) |
| GRFv (N) | 1 st peak | 1088±(8.12) | 1186±(8.10) | 931±(5.05) |
| | Trough | 625±(9.13) | 789±(7.57) | 830±(6.23) |
| | 2 nd peak | 963±(9.22) | 968±(7.18) | 879±(7.35) |

Table 4.11: Quadriceps and hamstring EMG RMS amplitude for case study 3 (*SP3*).

| Parameter description | | <u>Mean±(SD)</u> | | |
|-----------------------|--------------------------|------------------|--------------|--------------|
| | | AFO | Tuned | SSO |
| VL RMS (%MMT) | Stance peak | 33.91±(5.30) | 41.97±(6.12) | 29.99±(5.02) |
| | Swing peak | 22.14±(3.60) | 30.07±(4.60) | 21.84±(3.50) |
| VM RMS (%MMT) | Stance peak | 30.85±(0.41) | 36.22±(0.28) | 26.91±(0.25) |
| | Swing peak | 20.91±(0.36) | 26.85±(0.34) | 18.47±(0.33) |
| RF RMS (%MMT) | Stance peak [#] | 7.88±(0.07) | 8.82±(0.07) | 7.18±(0.09) |
| | T-PS peak | 9.15±(0.07) | 8.82±(0.07) | 7.16±(0.09) |
| | Swing peak | - | - | - |
| BF RMS (%MMT) | Stance peak | 15.67±(0.31) | 13.79±(0.32) | 20.13±(0.32) |
| | Swing peak | 22.71±(0.33) | 17.36±(0.33) | 26.09±(0.34) |
| ST RMS (%MMT) | Stance peak | 26.24±(0.43) | 23.47±(0.39) | 27.88±(0.40) |
| | Swing peak | 33.32±(0.36) | 27.61±(0.36) | 37.32±(0.38) |

T-PS peak: the maximum activity during terminal stance and pre swing phase

Table 4.12: The anatomical and the orthotic ankle moment for case study 3 (*SP3*) derived from SG2 and SG4 data outputs.

| Moment (Nm/kg) | | <u>Anatomical</u> (mean±(SD)) | | <u>Orthotic</u> (mean±(SD)) | |
|----------------|----------------------|-------------------------------|-------------|-----------------------------|--------------|
| | | AFO | Tuned | AFO | Tuned |
| SG2 | Early stance peak | 0.03±(0.05) | 0.00±(0.06) | -0.20±(0.04) | -0.31±(0.06) |
| | Terminal stance peak | 0.90±(0.03) | 0.89±(0.03) | -0.01±(0.03) | -0.02±(0.03) |
| SG4 | Mid stance peak | 0.11±(0.01) | 0.10±(0.01) | -0.05±(0.01) | -0.07±(0.01) |
| | Terminal stance peak | 0.11±(0.01) | 0.12±(0.01) | 0.01±(0.03) | 0.01±(0.01) |

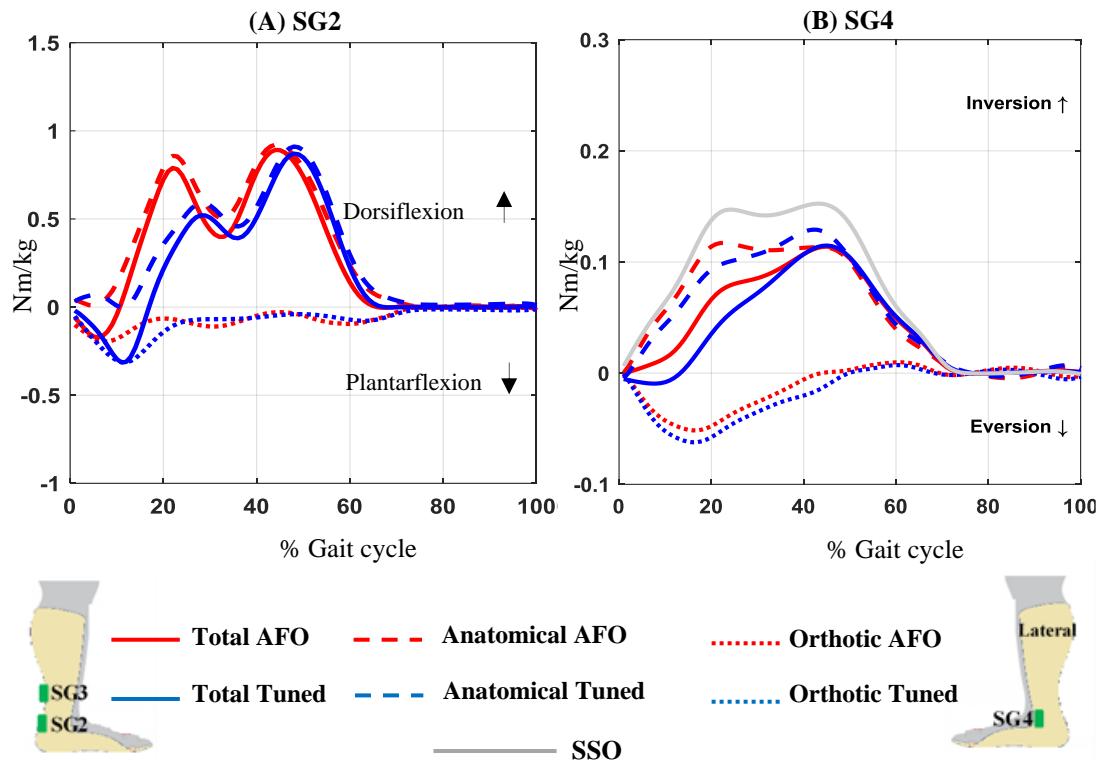


Figure 4.16: Total ankle moment, orthotic moment, and anatomical moment in sagittal plane (A) and frontal plane (B) for case study 3 (*SP3*) derived from SG2 and SG4 data outputs, respectively.

4.5 Case study four (*SP4*)

SP4 was a 58-year-old female with a mass of 68Kg and height of 1.52m. *SP4* had ischemic stroke in 2014 affecting her right hemisphere resulting in left side hemiparesis. *SP4* had type II diabetes and hypertension. *SP4* started a daily physical therapy regimen in 2014 till now. *SP4* own orthosis was PLS AFO, different from the AFO used in this study. Initially, *SP4* was prescribed with a rigid plastic AFO. She prefers PLS AFO due to the better cosmesis and easy donning compared to rigid AFO. The CWS for *SP4* was 0.20 m/s in SSO condition. Based on walking speed classification in stroke patients (Perry et al., 1995), *SP4* is classified as a “household walking” (speed < 0.4 m/s).

4.5.1 Comparing AFO condition with SSO condition:

The walking speed of *SP4* increased from $(0.20\pm 0.02$ m/s) in SSO condition to $(0.34\pm 0.02$ m/s) in AFO condition. This is reflected only in the increased stride length (0.18 ± 0.08 m in SSO condition and 0.32 ± 0.06 m in AFO condition). Stance time percentage only showed slight change (Table 4.13). SVA inclination during mid stance increased (by 1.86 degrees) from $(6.78\pm 0.19$ degrees) in SSO to $(8.64\pm 0.19$ degrees) in AFO condition (Table 4.13, Figure 4.17, A). Ankle motion on the other hand, showed decreased first (early stance) plantar flexion, increased second (late stance) dorsiflexion, and decreased third (swing phase) plantar flexion peaks in AFO condition as compared to SSO condition (from -3.76 ± 0.09 degrees, 0.74 ± 0.14 degrees, -2.33 ± 0.16 degrees in SSO condition to, -0.01 ± 0.04 degrees, 2.00 ± 0.12 degrees, -1.39 ± 0.09 degrees in AFO condition, respectively) (Table 4.13, Figure 4.17, B). Knee motion showed increased early stance and swing flexion and decreased late stance extension in AFO condition as compared to SSO condition (6.46 ± 0.22 , 16.02 ± 1.08 degrees, 0.78 ± 0.28 degrees in SSO condition, 17.21 ± 0.92 degrees, 25.33 ± 1.14 degrees, 8.57 ± 0.26 degrees in AFO condition, respectively) (Table 4.13, Figure 4.17, C). Hip extension in *SP4* by the end of single limb support increased from $(42.2\pm 1.01$ degrees) in SSO condition to $(27.56\pm 0.87$ degrees) but the hip remained flexed (Table 4.13, Figure 4.17, D). Maximum hip flexion in swing phase decreased in AFO condition (48.30 ± 1.21 degrees) as compared to SSO condition (34.23 ± 1.22 degrees).

Changes in the kinetics in *SP4* were also observed in AFO condition as compared to SSO condition (Table 4.13, Figure 4.18). *SP4* did not show any distinguishable first peak or trough. Walking with an AFO resulted only in a second peak that is less (660 ± 10.18 N) than in SSO condition (669 ± 13.18 N). Additionally, the second peak is higher than *SP4* body weight in SSO condition (97%BW) as compared to SSO condition (98%BW). At the ankle, *SP4* did not show any plantar flexion moment in stance in the three conditions. Dorsiflexion moment peak decreased slightly in AFO condition (0.90 ± 0.05 Nm/kg) as compared to SSO (1.06 ± 0.05 Nm/kg). As the case in *SP3*, the change was merely observed at the knee; the values of first flexion moment peak, the extension moment peak, and the second flexion moment peak slightly changed in AFO condition (0.10 ± 0.040 , -0.11 ± 0.01 Nm/kg, -0.02 ± 0.01 Nm/kg, respectively) as compared to SSO condition (0.05 ± 0.04 Nm/kg, -0.42 ± 0.05 Nm/kg, -0.021 ± 0.01 Nm/kg respectively). Flexion moment

peak at the hip that occurs early in stance showed a slight increase in AFO condition (0.18 ± 0.01 Nm/kg) as compared to SSO condition (0.16 ± 0.01 Nm/kg), and the extension moment peak showed an increase in AFO condition (-0.21 ± 0.01 Nm/kg) as compared to SSO condition (-0.07 ± 0.01 Nm/kg).

As in *SP1*, *SP2*, and *SP3*, fitting an AFO also showed changes in the EMG activity of knee muscles as compared to SSO condition (Table 4.14, Figure 4.19). VL and VM showed similar activity patterns and thus, will be presented together. VL and VM showed longer periods of activity than normal in SSO condition and continued to be active the whole of stance. AFO condition reduced the period of activity of only VL to end of mid stance. VL and VM showed increased stance (40.85 ± 6.10 %MMT, 14.70 ± 0.22 %MMT, respectively) and swing (19.82 ± 4.40 %MMT, 9.67 ± 0.17 %MMT, respectively) peaks in AFO condition as compared to SSO condition (VL: 33.21 ± 5.43 %MMT, 17.29 ± 4.10 %MMT, VM: 11.71 ± 0.21 %MMT, 9.32 ± 0.17 %MMT, respectively). In SSO condition, RF in *SP4* started activity at initial contact and continued to 80%GC. RF's activity in AFO condition only showed a period of inactivity in the first half of terminal stance and then continued to be active to end of mid swing. RF showed increased early stance peak (27.10 ± 0.21) in AFO condition as compared to SSO condition (9.93 ± 0.14 %MMT) and increased terminal stance-pre swing peak in AFO condition (14.05 ± 0.09 %MMT) as compared to SSO condition (10.41 ± 0.12 %MMT). BF and ST also showed similar activity pattern and will thus, be presented together. BF and ST were active during loading response and throughout swing phase. Wearing an AFO did not change the period of these muscles activity. BF showed increased stance peak (30.62 ± 0.25 %MMT) and decreased swing peak (43.39 ± 0.18 %MMT) in AFO condition as compared to SSO condition (12.27 ± 0.26 , 59.03 ± 0.16 %MMT, respectively). ST showed decreased stance peak (9.22 ± 0.18 %MMT) and swing peak (12.85 ± 0.09 %MMT) in AFO condition as compared to SSO condition (12.39 ± 0.16 %MMT, 30.52 ± 0.09 %MMT, respectively).

4.5.2 Comparing Tuned-AFO condition with AFO condition:

The walking speed of *SP4* increased in Tuned-AFO condition (0.38 ± 0.02 m/s) as compared to AFO condition (0.34 ± 0.02 m/s). Stride length increased and stance percentage of the gait cycle decreased in Tuned-AFO condition (0.34 ± 0.08 m and $65.22\pm 0.09\%$ in Tuned-AFO condition). SVA inclination during mid stance increased in Tuned-

AFO (by 1.8 degrees) from (8.64 ± 0.19 degrees) in AFO condition to (10.44 ± 0.19 degrees) in Tuned-AFO condition (Table 4.13, Figure 4.17, A). Slight change in ankle motion resulted in Tuned-AFO condition as compared to AFO condition; as first slight plantar flexion peak reversed to dorsiflexion (1.81 ± 0.06 degrees, -0.01 ± 0.04 degrees, respectively), second slight plantar flexion peak decreased (-0.25 ± 0.04 , -1.39 ± 0.09 degrees, respectively), and the dorsiflexion peak slightly increased (3.69 ± 0.32 degrees, 2.00 ± 0.12 degrees, respectively) (Table 4.13, Figure 4.17, B). Knee motion showed, in Tuned-AFO condition as compared to AFO condition, slightly increased early stance flexion (18.61 ± 0.18 degrees, 17.21 ± 0.92 degrees, respectively), slightly decreased knee extension (10.75 ± 0.21 degrees, 8.57 ± 0.26 degrees, respectively), and increased knee flexion in swing phase (30.32 ± 1.15 degrees, 25.33 ± 1.14 degrees, respectively) (Table 4.13, Figure 4.17, C). Hip flexion and extension peaks increased (but remained flexed throughout gait cycle) in **SP4** in Tuned-AFO condition (35.90 ± 1.09 degrees, 22.99 ± 0.87 degrees, respectively) as compared to AFO condition (34.23 ± 1.22 degrees, 27.56 ± 0.87 degrees, respectively) (Table 4.13, Figure 4.17, D).

GRFv in **SP4** after AFO tuning slightly changed (Table 4.13, Figure 4.18, D). The first peak and trough remained absent. The second peak increased (101%BW) as compared to AFO condition (97%BW) and SSO condition (98%BW). Changes in the moments in **SP4** were slight (Table 4.13, Figure 4.18). Ankle plantar flexion moment peak remained absent and the dorsiflexion moment peak slightly decreased in Tuned-AFO condition (0.84 ± 0.04 Nm/kg) as compared to AFO condition (0.90 ± 0.05 Nm/kg). Knee first and second flexion moment peaks slightly increased (0.20 ± 0.05 Nm/kg, 0.04 ± 0.01 Nm/kg, respectively) in Tuned-AFO condition when compared with AFO condition (0.10 ± 0.04 Nm/kg, -0.02 ± 0.01 Nm/kg, respectively). Extension moment peak, on the other hand, decreased in Tuned-AFO condition (-0.05 ± 0.01 Nm/kg). Very slight change was recorded in the hip extension moment and flexion peaks in Tuned-AFO condition as they remained almost unchanged.

Tuning an AFO showed very little changes in the EMG activity of knee muscles as compared to AFO condition (Table 4.14, Figure 4.19). VL and VM showed similar activity patterns and thus, will be presented together. VL showed no change in the periods of activity in Tuned-AFO condition as compared to AFO condition. VM showed shorter activity in stance, as its activity ends around midway in terminal stance. VL and VM

showed increased stance (46.62 ± 5.08 %MMT, 18.44 ± 0.22 %MMT, respectively) and swing (26.38 ± 3.90 %MMT, 10.31 ± 0.19 %MMT, respectively) peaks in Tuned-AFO condition as compared to AFO condition (VL: 40.85 ± 6.10 %MMT, 19.82 ± 4.40 %MMT, VM: 14.70 ± 0.22 %MMT, 9.67 ± 0.17 %MMT, respectively). Tuning the AFO did not change the activation periods of RF in *SP4*. RF showed no change in early stance peak in Tuned-AFO condition as compared to AFO condition, and increased terminal stance-pre swing peak in Tuned-AFO condition (24.79 ± 0.11 %MMT) as compared to AFO condition (14.05 ± 0.09 %MMT). BF and ST also showed similar activity pattern and will thus, be presented together. BF and ST did not change their period of activity in Tuned-AFO condition as compared to AFO condition. BF showed slightly decreased stance peak (29.79 ± 0.28 %MMT) and BF and ST showed slightly decreased swing peaks (41.98 ± 0.14 %MMT, 12.28 ± 0.07 %MMT) respectively) in Tuned-AFO condition as compared to AFO condition (BF: 30.62 ± 0.25 %MMT, ST: 9.22 ± 0.18 %MMT, 12.85 ± 0.09 %MMT, respectively). ST showed slightly increased stance peak in Tuned-AFO condition (10.16 ± 0.16 %MMT) as compared to AFO condition (9.22 ± 0.18 %MMT).

As in *SP4*, the orthotic moment showed plantarflexion moment during loading response, and reduced (or almost absent) plantar flexion orthotic moment during terminal stance, (Table 4.14, Figure 4.19, A). In contrast, the anatomical moment only showed a dorsiflexion moment during most of stance. Walking with a Tuned-AFO *SP4* did not change orthotic moment as compared to AFO condition.

SP4 showed a noticeable reduction in the total inversion moment while walking with an AFO or Tuned-AFO as compared to walking with SSO as illustrated in Figure 4.19 (B). The orthotic moment peaks showed an eversion moment peak during the whole of stance. Like in *SPI*, *2*, and *3*, walking with a Tuned-AFO or an AFO, showed no noticeable differences in the orthotic eversion moment nor in the anatomical inversion moment.

The effect of AFO and Tuned-AFO on the speed of *SP4* was obvious, as *SP4* gait speed increased by (0.14m/s) and (0.18m/s) in AFO and Tuned-AFO conditions. This means that although *SP4* remained in “household walking” according to the classification by Perry et al. (1995), the speed increments in AFO and Tuned-AFO conditions were higher than the MCID (0.16 m/s). These increments are considered clinically significant (Tilson et al., 2010).

Additionally, AFO and Tuned-AFO improved the kinematics so that they are closer to normal than in SSO (except for the ankle motion). SVA in Tuned-AFO condition was within the target range (10-12 degrees) compared to 6.78 degrees in SSO condition; indicating sufficient tuning. The hip was 31.62 degrees less extended than normal (control participants in SSO condition are considered the normal baseline in this study) in Tuned-AFO condition and 35.92 degrees less than normal in AFO condition compared to 50.56 degrees more flexed than normal in SSO condition, the knee was 5.14 degrees more flexed during early stance in Tuned-AFO condition and 3.74 degrees more flexed in AFO condition compared to 7.01 degrees less flexed than normal in SSO condition.

Changes in SVA in *SP4* were very close, which does not necessarily mean that changes between SSO and AFO condition, and AFO and Tuned-AFO condition are close. The more inclined SVA means that the knee and hip are free to flex and extend in stance, respectively (this will be discussed further in the following chapter). AFO condition resulted in a more inclined SVA than SSO condition, which results in knee flexion and hip extension. Tuned-AFO condition further increases SVA inclination, which results in the fine adjustments in kinematics closer to normal. Further discussion on the effect of Tuned-AFO condition and AFO condition on the gait parameters of control and stroke participants will be addressed in the next chapter (Chapter 5 Discussion).

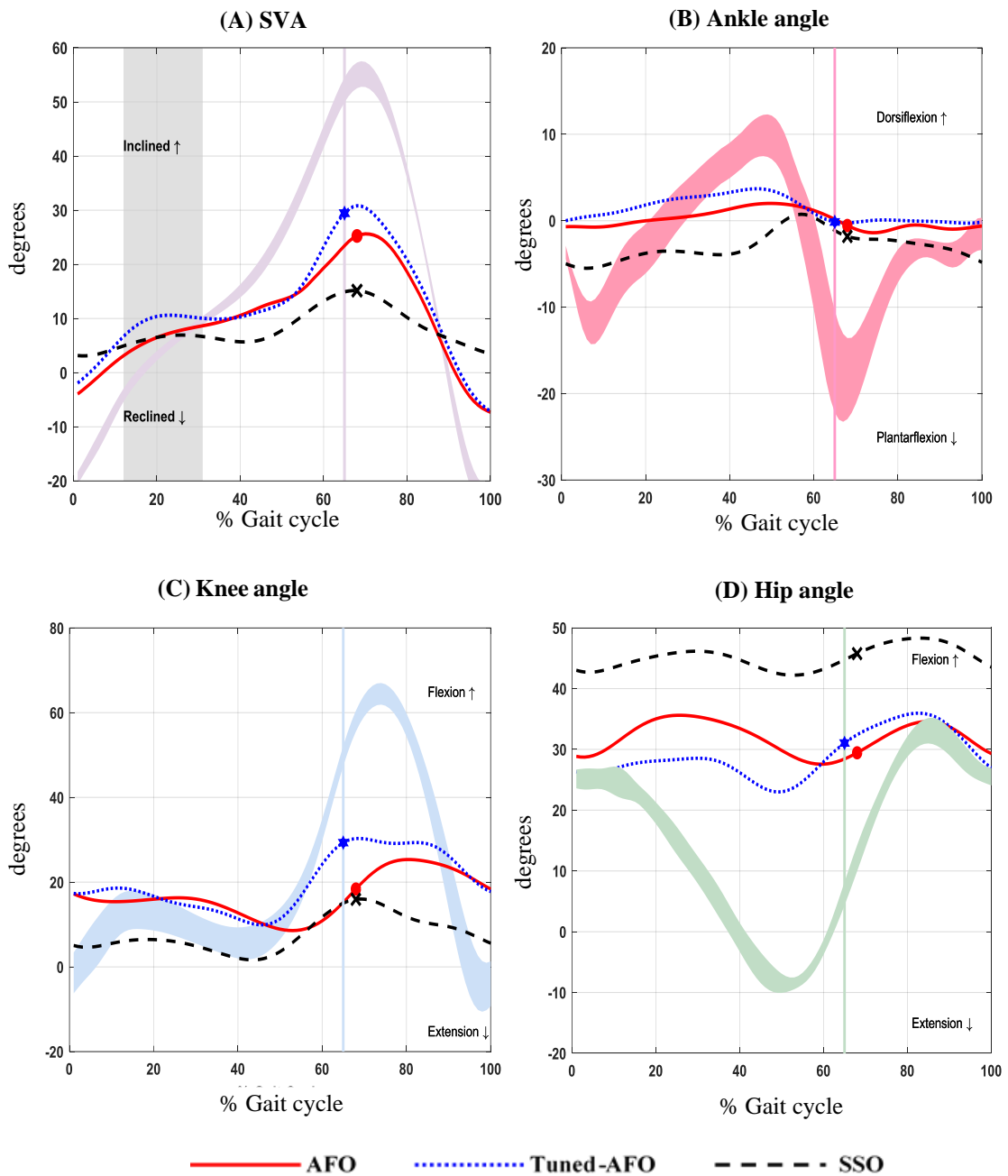


Figure 4.17: Sagittal kinematic graphs for case study 4 (*SP4*) while walking on treadmill wearing Tuned-AFO, AFO, and SSO with reference to control participants while wearing SSO (shaded lines).

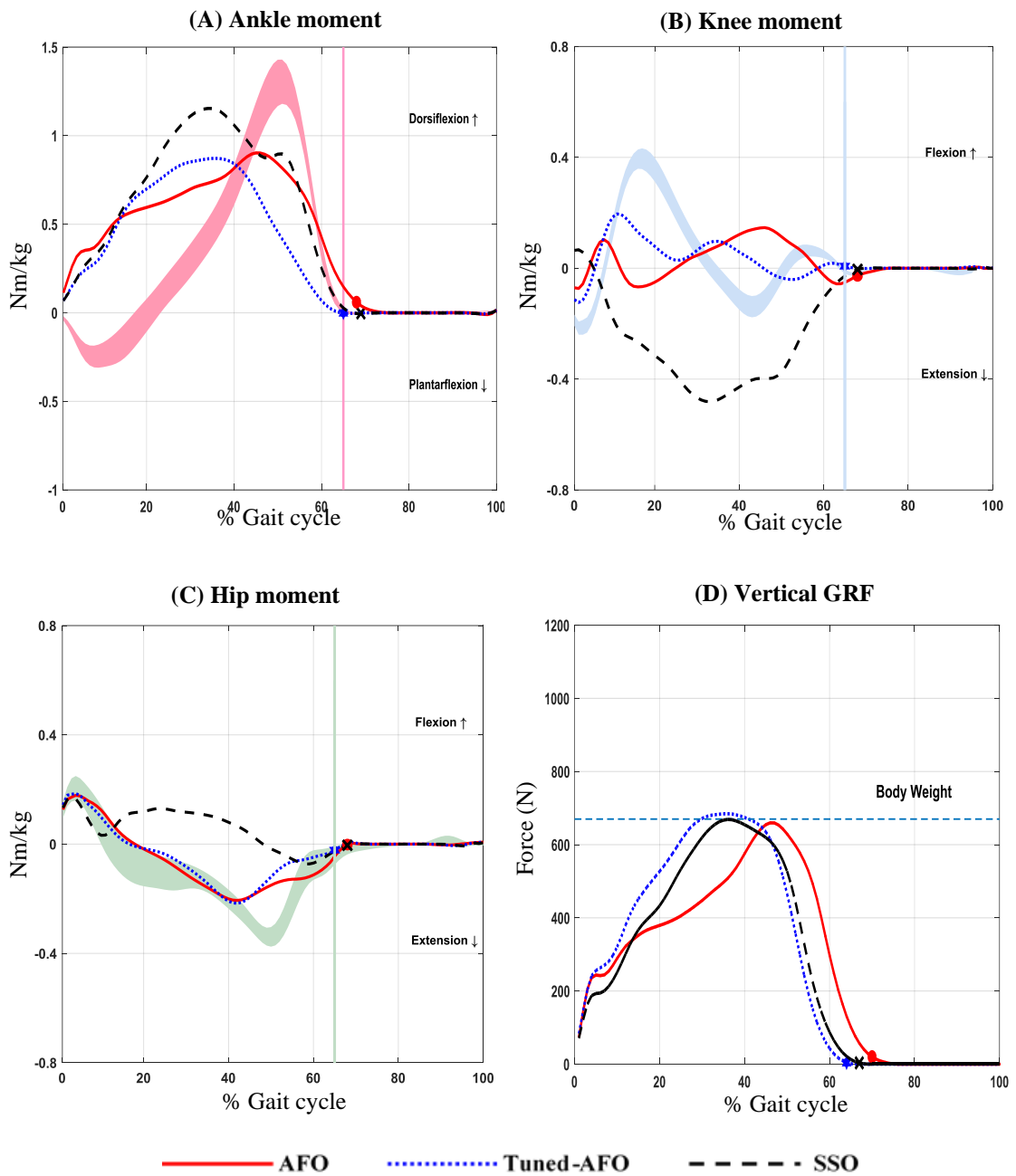


Figure 4.18: Sagittal kinetic graphs and the vertical GRF graph for case study 4 (*SP4*) while walking on treadmill wearing Tuned-AFO, AFO, and SSO with reference to control participants while wearing SSO (shaded lines).

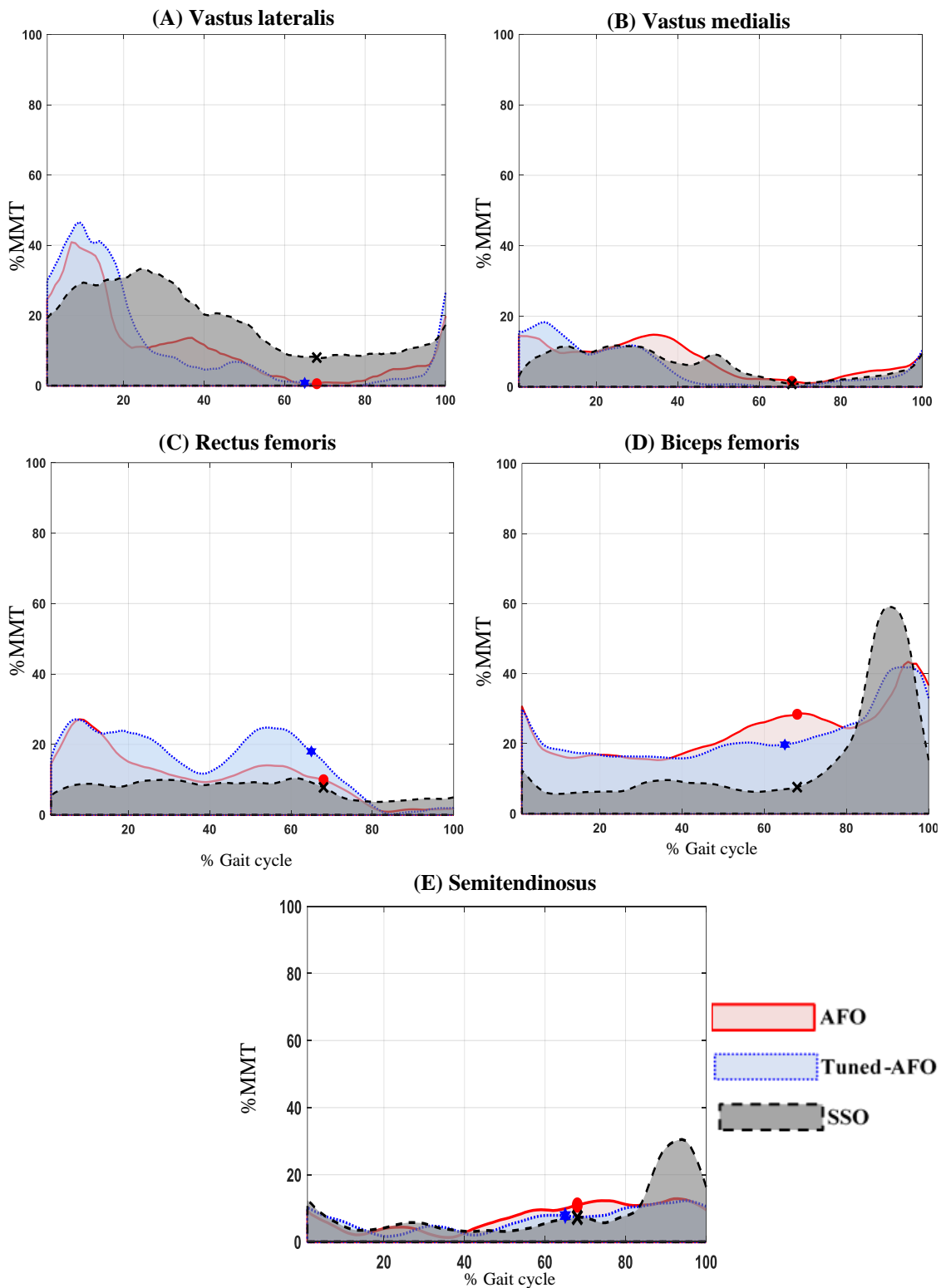


Figure 4.19: Quadriceps and hamstring EMG RMS amplitude and timing during walking on treadmill for case study 4 (*SP4*). The RMS is presented as a percentage of maximum manual muscle test value (% MMT).

Table 4.13: Temporal-spatial, kinematic and kinetic data for *SP4*.

| Parameter description | | <u>Mean±(SD)</u> | | |
|------------------------------|-----------------------------|------------------|--------------|---------------|
| | | AFO | Tuned | SSO |
| SVA (degrees) | Mid stance | 8.64±(0.19) | 10.44±(0.19) | 6.78±(0.19) |
| Temporal-spatial | Speed (ms ⁻¹) | 0.34±(0.02) | 0.38±(0.02) | 0.20±(0.02) |
| | Stance time (%) | 68.14±(0.15) | 65.22±(0.09) | 68.00±(0.55) |
| | Stride length (m) | 0.32±(0.06) | 0.34±(0.08) | 0.18±(0.08) |
| Ankle angle (degrees) | PF peak (early stance) | -0.01±(0.04) | 1.81±(0.06) | -3.76±(0.09) |
| | Dorsiflexion peak | 2.00±(0.12) | 3.69±(0.32) | 0.74±(0.14) |
| | PF peak (swing phase) | -1.39±(0.09) | -0.25±(0.04) | -2.33±(0.16) |
| Knee angle (degrees) | Flexion peak (stance) | 17.21±(0.92) | 18.61±(0.18) | 6.46±(0.22) |
| | Extension (terminal stance) | 8.57±(0.26) | 10.75±(0.21) | 0.78±(0.28) |
| | Flexion peak (swing) | 25.33±(1.14) | 30.32±(1.15) | 16.02±(1.08) |
| Hip angle (degrees) | Extension peak | 27.56±(0.87) | 22.99±(0.87) | 42.20±(1.01) |
| | Flexion peak (swing phase) | 34.23±(1.22) | 35.90±(1.09) | 48.30±(1.21) |
| Ankle moment (Nm/kg) | PF peak (early stance) | - | - | - |
| | Dorsiflexion peak | 0.90±(0.05) | 0.84±(0.04) | 1.06±(0.05) |
| Knee moment (Nm/kg) | Flexion peak1 | 0.10±(0.04) | 0.20±(0.05) | 0.05±(0.04) |
| | Extension peak | -0.11±(0.01) | -0.05±(0.01) | -0.42±(0.05) |
| | Flexion peak2 | -0.02±(0.01) | 0.04±(0.01) | -0.021±(0.01) |
| Hip moment (Nm/kg) | Flexion peak | 0.18±(0.01) | 0.17±(0.01) | 0.16±(0.01) |
| | Extension peak | -0.21±(0.01) | -0.22±(0.01) | -0.07±(0.01) |
| GRFv (N) | 1 st peak | - | - | - |
| | Trough | - | - | - |
| | 2 nd peak | 660±(10.18) | 685±(10.14) | 669±(13.18) |

Table 4.14: Quadriceps and hamstring EMG RMS amplitude for case study 4 (*SP4*).

| Parameter description | | <u>Mean±(SD)</u> | | |
|-----------------------|--------------------------|------------------|--------------|--------------|
| | | AFO | Tuned | SSO |
| VL RMS (%MMT) | Stance peak | 40.85±(6.10) | 46.62±(5.08) | 33.21±(5.43) |
| | Swing peak | 19.82±(4.40) | 26.38±(3.90) | 17.29±(4.10) |
| VM RMS (%MMT) | Stance peak | 14.70±(0.22) | 18.44±(0.22) | 11.71±(0.21) |
| | Swing peak | 9.67±(0.17) | 10.31±(0.19) | 9.32±(0.17) |
| RF RMS (%MMT) | Stance peak [#] | 27.10±(0.21) | 27.11±(0.15) | 9.93±(0.14) |
| | T-PS peak | 14.05±(0.09) | 24.79±(0.11) | 10.41±(0.12) |
| | Swing peak | - | - | - |
| BF RMS (%MMT) | Stance peak | 30.62±(0.25) | 29.79±(0.28) | 12.27±(0.26) |
| | Swing peak | 43.39±(0.18) | 41.98±(0.14) | 59.03±(0.16) |
| ST RMS (%MMT) | Stance peak | 9.22±(0.18) | 10.16±(0.16) | 12.39±(0.16) |
| | Swing peak | 12.85±(0.09) | 12.28±(0.07) | 30.52±(0.09) |

T-PS peak: the maximum activity during terminal stance and pre swing phase

Table 4.15: The anatomical and the orthotic ankle moment for case study 4 (*SP4*) derived from SG2 and SG4 data outputs.

| Moment (Nm/kg) | | <u>Anatomical</u> (mean±(SD)) | | <u>Orthotic</u> (mean±(SD)) | |
|----------------|----------------------|-------------------------------|--------------|-----------------------------|--------------|
| | | AFO | Tuned | AFO | Tuned |
| SG2 | Early stance peak | 0.62±(0.04)- | 0.61±(0.06)- | -0.09±(0.04) | -0.11±(0.06) |
| | Terminal stance peak | 0.88±(0.03) | 0.84±(0.04) | 0.02±(0.01) | 0.00±(0.04) |
| SG4 | Mid stance peak | 0.09±(0.01)- | 0.08±(0.01)- | -0.03±(0.01) | -0.03±(0.01) |
| | Terminal stance peak | 0.16±(0.01) | 0.15±(0.01) | -0.03±(0.01) | -0.03±(0.01) |

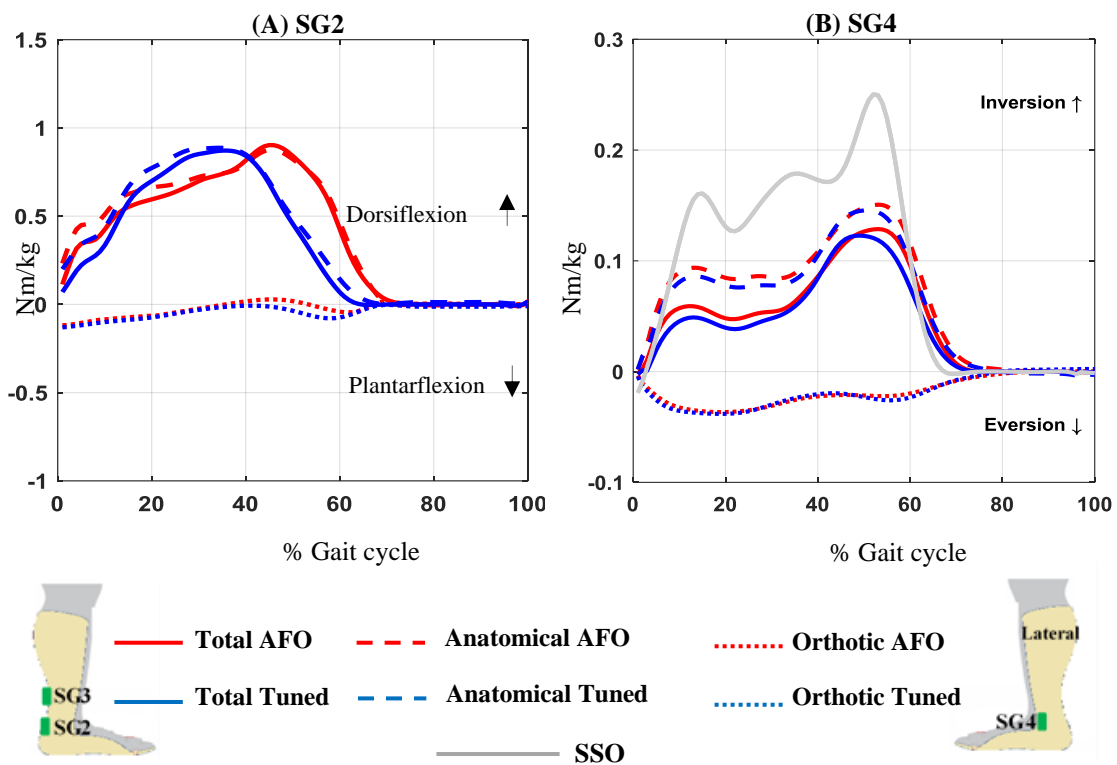


Figure 4.20: Total ankle moment, orthotic moment, and anatomical moment in sagittal plane (A) and frontal plane (B) for case study 4 (*SP4*) derived from SG2 and SG4 data outputs, respectively.

4.6 Case study four (*SP5*)

SP5 was a 53-year-old male with a mass of 92kg and height of 1.8m. *SP5* had ischemic stroke in 2012 affecting his right hemisphere resulting in left side hemiparesis. *SP5* started a daily physical therapy regimen in 2013 for 6 months only. *SP5* own orthosis was rigid AFO, similar to the AFO used in this study but without carbon fibre reinforcement at the ankle region of the AFO. He reported infrequent use of his rigid AFO for community ambulation, preferring the use of a walker for enhanced stability. The CWS for *SP5* was 0.54 m/s in SSO condition. Based on walking speed classification in stroke patients (Perry et al., 1995), *SP5* is classified as a “limited community walking” (speed 0.4 – 0.8 m/s).

4.5.1 Comparing AFO condition with SSO condition:

The walking speed of *SP5* increased from $(0.54\pm 0.02$ m/s) in SSO condition to $(0.67\pm 0.02$ m/s) in AFO condition. This is reflected only in the increased stride length (0.55 ± 0.02 m in SSO condition and 0.64 ± 0.05 m in AFO condition). Stance time percentage only showed slight change (Table 4.16). SVA inclination during mid stance increased (by 1.1 degrees) from $(2.55\pm 0.25$ degrees) in SSO to $(3.65\pm 0.25$ degrees) in AFO condition (Table 4.16, Figure 4.21, A). Ankle motion on the other hand, showed slightly decreased first (early stance) and second (swing phase) plantar flexion, and slightly decreased dorsiflexion peak in AFO condition as compared to SSO condition (from -2.17 ± 0.14 degrees, -1.84 ± 0.08 degrees, 3.70 ± 0.24 degrees in SSO condition respectively to, -1.04 ± 0.05 degrees, -0.55 ± 0.07 degrees, 0.98 ± 0.04 degrees, in AFO condition, respectively) (Table 4.16, Figure 4.21, B). Knee motion showed slightly increased early stance flexion and late stance extension in AFO condition as compared to SSO condition (15.98 ± 0.86 degrees, 1.45 ± 0.22 degrees, respectively and 12.32 ± 0.82 degrees, 2.06 ± 0.22 degrees, respectively), and decreased swing flexion peak in AFO condition (22.04 ± 1.11 degrees) as compared to SSO condition (23.25 ± 1.12 degrees) (Table 4.16, Figure 4.21, C). Hip extension in *SP5* by the end of single limb support increased from $(25.08\pm 0.69$ degrees) in SSO condition to $(21.09\pm 0.72$ degrees) but the hip remained flexed (Table 4.16, Figure 4.21, D). Maximum hip flexion in swing phase decreased in AFO condition (30.20 ± 1.33 degrees) as compared to SSO condition (36.88 ± 1.41 degrees).

Changes in the kinetics in *SP5* were also observed in AFO condition as compared to SSO condition (Table 4.16, Figure 4.22). *SP5* showed slightly decreased first GRFv peak in AFO condition (895 ± 8.20 N) as compared to SSO condition (928 ± 9.21 N), and slightly increased trough and second peak (855 ± 9.24 , 914 ± 10.32 , in AFO condition, and 788 ± 8.46 , 848 ± 10.29 in SSO condition, respectively). Additionally, the first peak is lower than *SP5* body weight in AFO condition (97%BW). First peak in SSO condition was higher than *SP5* body weight (101%BW). The second peak of GRFv in *SP5* is lower than body weight in AFO condition (99%BW) as compared to (92%) in SSO condition. The trough was (86%BW) in SSO condition and became (93%BW) in AFO condition. At the ankle, *SP5* did not show any plantar flexion moment in stance in SSO condition but showed slight plantar flexion moment peak in AFO condition (-0.16 ± 0.03 Nm/kg).

Dorsiflexion moment peak decreased slightly in AFO condition (0.62 ± 0.06 Nm/kg) as compared to SSO (0.78 ± 0.06 Nm/kg). At the knee, the values of first flexion moment peak increased in AFO condition (0.23 ± 0.02 Nm/kg) as compared to SSO condition (0.10 ± 0.01 Nm/kg). The extension moment peak and the second flexion moment peak slightly decreased in AFO condition (-0.16 ± 0.02 Nm/kg, 0.10 ± 0.01 Nm/kg, respectively) as compared to SSO condition (-0.31 ± 0.01 Nm/kg, 0.15 ± 0.01 Nm/kg, respectively). Flexion moment peak at the hip that occurs early in stance showed a slight increase in AFO condition (0.25 ± 0.01 Nm/kg) as compared to SSO condition (0.14 ± 0.01 Nm/kg), and the extension moment peak showed an increase in AFO condition (-0.20 ± 0.01 Nm/kg) as compared to SSO condition (-0.07 ± 0.01 Nm/kg).

As in in the previous stroke participants, fitting an AFO also showed changes in the EMG activity of knee muscles as compared to SSO condition (Table 4.17, Figure 4.23). VL and VM showed similar activity patterns and thus, will be presented together. AFO condition and Tuned-AFO condition did not have an effect on periods of activity of VL and VM as compared to SSO condition. Different from the previous stroke participants, VL showed very slight increase in stance peak (39.99 ± 5.12 %MMT) and VM showed a reduction in stance peak (27.74 ± 0.40 %MMT). Both muscles showed a slightly reduced swing peak (33.43 ± 4.65 %MMT, 25.15 ± 0.33 %MMT, respectively) in AFO condition as compared to SSO condition (VL: 39.22 ± 5.55 %MMT, 38.01 ± 5.17 %MMT, VM: 28.44 ± 0.38 %MMT, 27.42 ± 0.34 %MMT, respectively). In SSO condition, RF in *SP5* started activity at initial until halfway in mid stance, and then from the end of terminal stance to the end of swing phase with very short period in activity midway in swing. AFO condition and Tuned-AFO condition did not change the period of RF's activity. RF showed almost no change in the early stance peak nor in the terminal stance-pre swing peak but showed slightly reduced swing phase peak in AFO condition (13.43 ± 0.11 %MMT) as compared to SSO condition (15.51 ± 0.13 %MMT). BF and ST also showed similar activity pattern and will thus, be presented together. BF and ST were active during loading response and throughout swing phase. Wearing an AFO only lengthened the second period of activity of only BF. BF and ST showed decreased stance (20.53 ± 0.24 %MMT, 25.42 ± 0.11 %MMT, respectively) and swing (40.65 ± 0.25 %MMT, 33.14 ± 0.21 %MMT, respectively) peaks in AFO condition as compared to SSO condition (BF: 38.19 ± 0.28

%MMT, 46.74 ± 0.26 %MMT, ST: 28.36 ± 0.10 %MMT, 41.37 ± 0.21 %MMT, respectively).

4.6.2 Comparing Tuned-AFO condition with AFO condition:

The walking speed of *SP5* slightly increased in Tuned-AFO condition (0.69 ± 0.02 m/s) as compared to AFO condition (0.67 ± 0.02 m/s). Stride length slightly increased and stance percentage of the gait cycle slightly decreased in Tuned-AFO condition (0.65 ± 0.05 and 69.08 ± 0.08 in Tuned-AFO condition). SVA inclination during mid stance increased in Tuned-AFO (by 4.48 degrees) from (3.65 ± 0.25 degrees) in AFO condition to (8.13 ± 0.25 degrees) in Tuned-AFO condition (Table 4.16, Figure 4.21, A). Slight change in ankle motion resulted in Tuned-AFO condition as compared to AFO condition; as first slight plantar flexion peak decreased (-0.90 ± 0.06 degrees, -1.04 ± 0.05 degrees, respectively), second slight plantar flexion peak slightly increased (-0.57 ± 0.07 degrees, -0.55 ± 0.07 degrees, respectively), and the dorsiflexion peak slightly increased (1.05 ± 0.06 degrees, 0.98 ± 0.04 degrees, respectively) (Table 4.16, Figure 4.21, B). Knee motion showed, in Tuned-AFO condition as compared to AFO condition, greatly increased early stance flexion (22.96 ± 0.65 degrees, 15.98 ± 0.86 degrees, respectively), decreased knee extension (8.33 ± 0.24 degrees, 1.45 ± 0.22 degrees, respectively), and slightly increased knee flexion in swing phase (25.67 ± 1.09 degrees, 22.04 ± 1.11 degrees, respectively) (Table 4.16, Figure 4.21, C). Hip flexion peak decreased and extension peak increased (but remained flexed throughout gait cycle) in *SP5* in Tuned-AFO condition (25.95 ± 1.21 degrees, 30.20 ± 1.33 degrees, respectively) as compared to AFO condition (16.46 ± 0.76 degrees, 21.09 ± 0.72 degrees, respectively) (Table 4.16, Figure 4.21, D).

GRFv in *SP5* after AFO tuning slightly changed (Table 4.16, Figure 4.22, D). The first peak increased and the trough decreased in Tuned-AFO condition ($112\%BW$, $86\%BW$, respectively) as compared to AFO condition ($97\%BW$, $93\%BW$, respectively). The second peak remained unchanged. Changes in the moments in *SP5* were generally slight (Table 4.16, Figure 4.22). Ankle plantar flexion moment peak increased and the dorsiflexion moment peak slightly decreased in Tuned-AFO condition (-0.25 ± 0.05 Nm/kg and 0.59 ± 0.05 Nm/kg, respectively) as compared to AFO condition (-0.16 ± 0.03 Nm/kg and 0.62 ± 0.06 Nm/kg, respectively). Knee first and second flexion moment peaks slightly increased (0.38 ± 0.03 Nm/kg, 0.14 ± 0.01 Nm/kg, respectively) in Tuned-AFO

condition when compared with AFO condition (0.23 ± 0.02 Nm/kg, 0.10 ± 0.01 Nm/kg, respectively). Extension moment peak, on the other hand, slightly decreased in Tuned-AFO condition (-0.09 ± 0.03 Nm/kg). Hip flexion moment peak slightly increased in Tuned-AFO condition (0.29 ± 0.01 Nm/kg) as compared to AFO condition (0.25 ± 0.01 Nm/kg), while extension moment remained almost unchanged.

Tuning an AFO showed changes in the EMG activity of knee muscles as compared to AFO condition in *SP5* (Table 4.17, Figure 4.23). VL and VM showed similar activity patterns and thus, will be presented together. VL and VM showed no change in the periods of activity in Tuned-AFO condition as compared to AFO condition. VL showed increased stance (46.49 ± 6.16 %MMT) and swing (35.91 ± 5.82 %MMT) peaks in Tuned-AFO condition as compared to AFO condition (39.99 ± 5.12 %MMT, 33.43 ± 4.65 %MMT, respectively). VM showed increased stance peak and decreased swing peak in Tuned-AFO condition (29.61 ± 0.38 %MMT, 24.72 ± 0.34 %MMT, respectively) as compared to AFO condition (27.74 ± 0.40 %MMT, 25.15 ± 0.33 %MMT, respectively). Tuning the AFO did not change the activation periods of RF in *SP5*. RF showed increased early stance peak, terminal stance-pre swing peak, and swing peak in Tuned-AFO condition (21.02 ± 0.09 %MMT, 13.46 ± 0.15 %MMT, 14.31 ± 0.10 , respectively) as compared to AFO condition (16.24 ± 0.10 %MMT, 12.94 ± 0.13 %MMT, 13.43 ± 0.11 %MMT, respectively). BF and ST also showed similar activity pattern and will thus, be presented together. BF and ST did not change their period of activity in Tuned-AFO condition as compared to AFO condition except for slightly shorter BF activity in swing. BF showed slightly increased stance peak (25.52 ± 0.21 %MMT) in Tuned-AFO condition as compared to AFO condition (20.53 ± 0.24 %MMT). BF and ST showed slightly decreased swing peaks (35.82 ± 0.29 %MMT, 26.69 ± 0.19 %MMT, respectively) in Tuned-AFO condition as compared to AFO condition (40.65 ± 0.25 %MMT, 33.14 ± 0.21 %MMT, respectively). ST showed decreased stance peak in Tuned-AFO condition (17.50 ± 0.10 %MMT) as compared to AFO condition (25.42 ± 0.11 %MMT).

The orthotic moment showed plantarflexion moment during loading response, and reduced (or almost absent) plantar flexion orthotic moment during terminal stance (Table 4.21, Figure 4.24, A). In contrast, the anatomical moment only showed a dorsiflexion moment during most of stance. Walking with a Tuned-AFO *SP5* showed slight change in orthotic moment as compared to AFO condition.

SP5 showed a noticeable reduction in the total inversion moment while walking with an AFO or Tuned-AFO as compared to walking with SSO as illustrated in Figure 4.24 (B). The orthotic moment peaks showed an eversion moment peak during the whole of stance. Like in all previous stroke participants, walking with a Tuned-AFO or an AFO, showed no noticeable differences in the orthotic eversion moment nor in the anatomical inversion moment.

The effect of AFO and Tuned-AFO on the speed of *SP5* was obvious but not clinically significant, as *SP5* gait speed increased by (0.13m/s) and (0.15m/s) in AFO and Tuned-AFO conditions. This means that *SP5* remained in the “limited community walking” according to the classification by Perry et al. (1995). Nevertheless, as the speed increment in Tuned-AFO condition was lower than the MCID (0.16 m/s), this increment is considered clinically insignificant (Tilson et al., 2010).

Additionally, AFO and Tuned-AFO changed the kinematics so that they are closer to normal than in SSO (except for the ankle motion). SVA in Tuned-AFO condition was not within the target range (10-12 degrees) compared to 2.55 degrees in SSO condition; indicating insufficient tuning. This is because *SP5* did not feel comfortable walking with the tuning actually needed. The hip was 25.09 degrees less extended than normal (control participants in SSO condition are considered the normal baseline in this study) in Tuned-AFO condition and 29.72 degrees less than normal in AFO condition compared to 33.71 degrees more flexed than normal in SSO condition, the knee was 9.49 degrees more flexed during early stance in Tuned-AFO condition and 2.51 degrees more flexed in AFO condition compared to 1.15 degrees less flexed than normal in SSO condition.

As much greater change in SVA occurred in Tuned-AFO condition than in AFO condition, changes in gait parameters were greater in Tuned-AFO condition. As tuning was less than the target range (as *SP5* did not feel comfortable walking with the target tuning), improvements in gait parameters were not sufficient. Further discussion on the effect of Tuned-AFO condition and AFO condition on the gait parameters of control and stroke participants will be addressed in the next chapter (Chapter 5 Discussion).

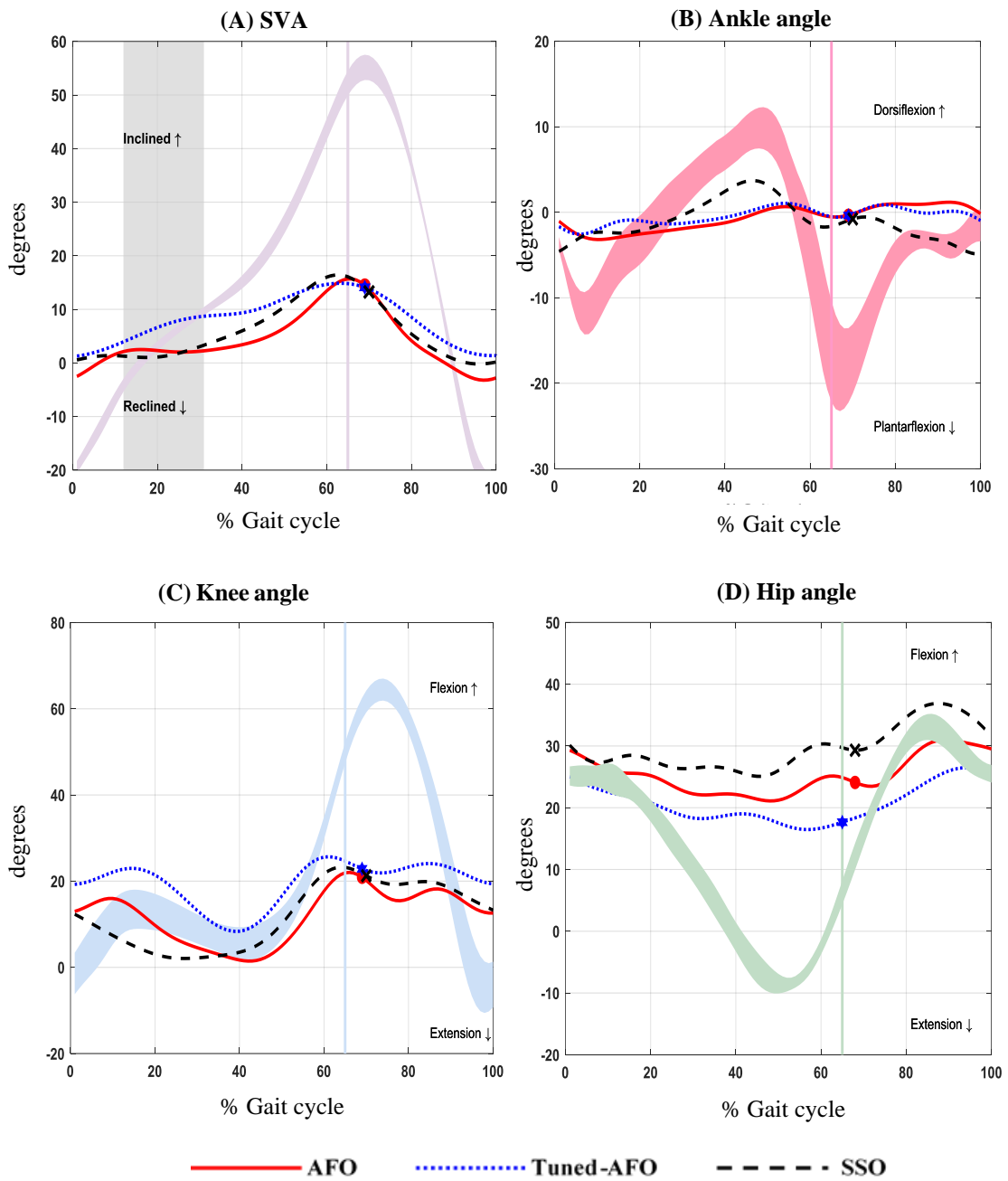


Figure 4.21: Sagittal kinematic graphs for case study 5 (*SP5*) while walking on treadmill wearing Tuned-AFO, AFO, and SSO with reference to control participants while wearing SSO (shaded lines).

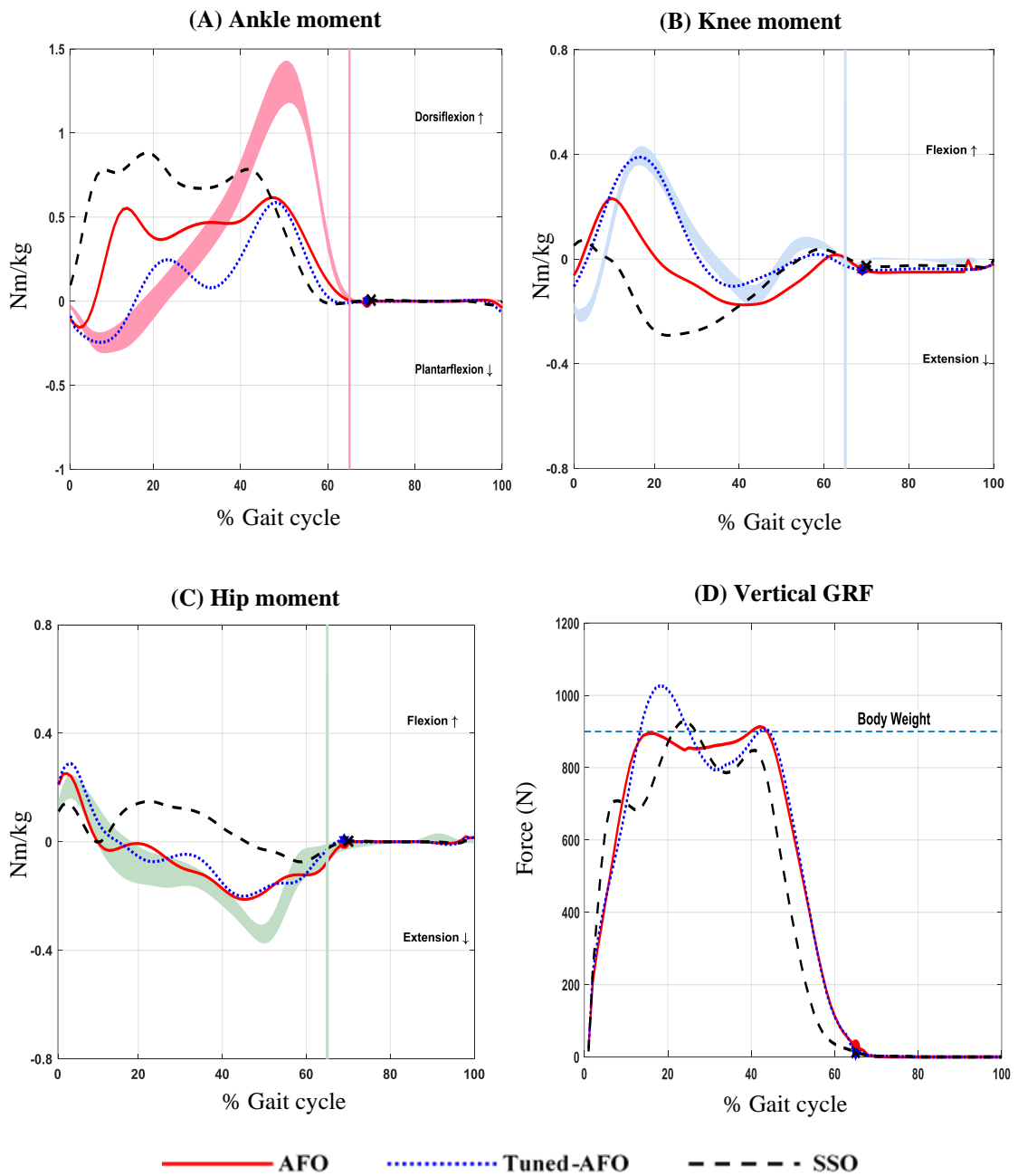


Figure 4.22: Sagittal kinetic graphs and the vertical GRF graph for case study 5 (*SP5*) while walking on treadmill wearing Tuned-AFO, AFO, and SSO with reference to control participants while wearing SSO (shaded lines).

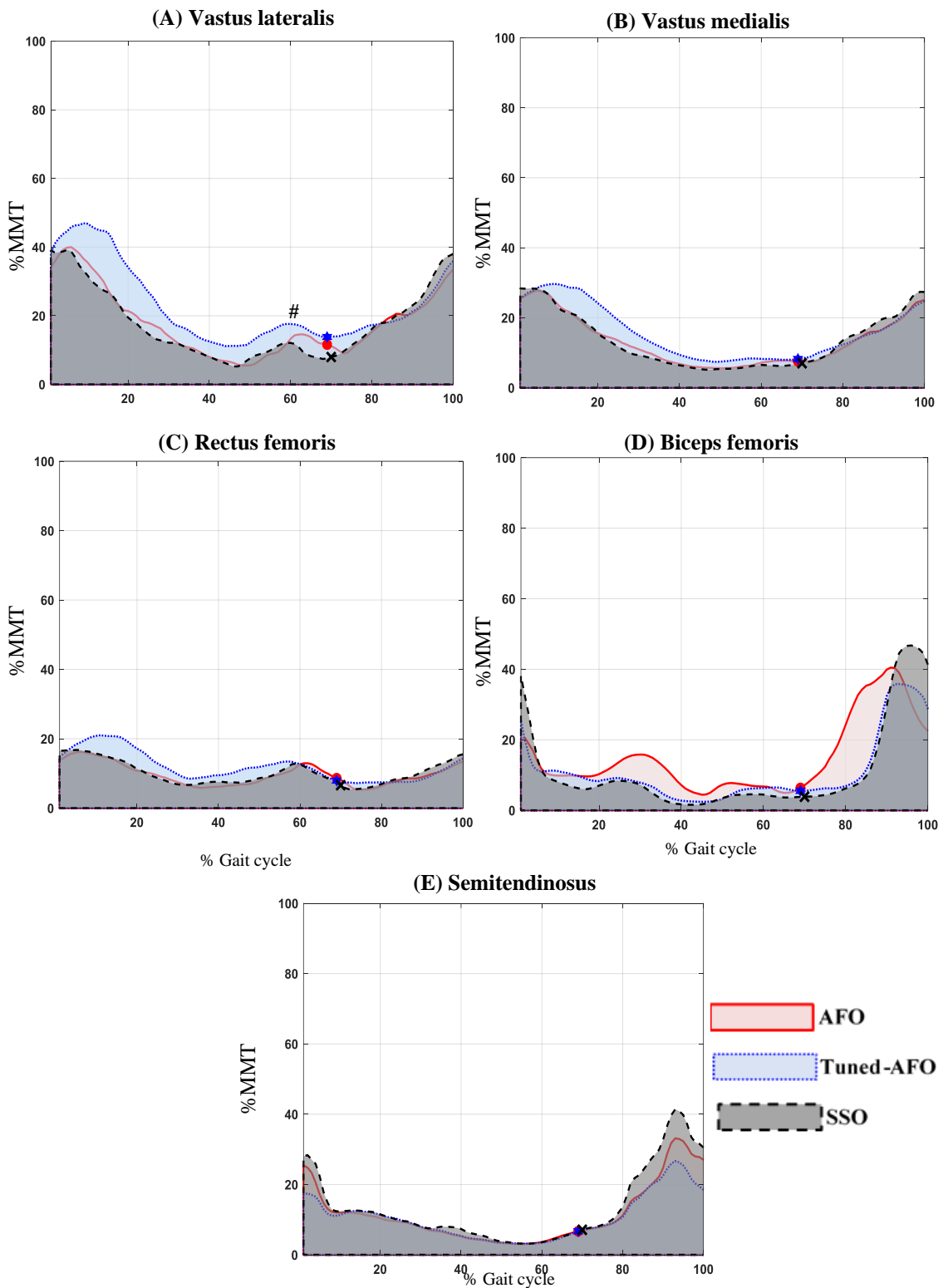


Figure 4.23: Quadriceps and hamstring EMG RMS amplitude and timing during walking on treadmill for case study 5 (*SP5*). The RMS is presented as a percentage of maximum manual muscle test value (% MMT). # Represents an example of Rectus Femoris cross talk.

Table 4.16: Temporal-spatial, kinematic and kinetic data for *SP5*.

| Parameter description | | <u>Mean±(SD)</u> | | |
|------------------------------|-----------------------------|------------------|--------------|--------------|
| | | AFO | Tuned | SSO |
| SVA (degrees) | Mid stance | 3.65±(0.25) | 8.13±(0.25) | 2.55±(0.25) |
| Temporal-spatial | Speed (ms ⁻¹) | 0.67±(0.02) | 0.69±(0.02) | 0.54±(0.02) |
| | Stance time (%) | 69.24±(0.10) | 69.08±(0.08) | 70.02±(0.10) |
| | Stride length (m) | 0.64±(0.05) | 0.65±(0.05) | 0.55±(0.02) |
| Ankle angle (degrees) | PF peak (early stance) | -1.04±(0.05) | -0.90±(0.06) | -2.17±(0.14) |
| | Dorsiflexion peak | 0.98±(0.04) | 1.05±(0.06) | 3.70±(0.24) |
| | PF peak (swing phase) | -0.55±(0.07) | -0.57±(0.07) | -1.84±(0.08) |
| Knee angle (degrees) | Flexion peak (stance) | 15.98±(0.86) | 22.96±(0.65) | 12.32±(0.82) |
| | Extension (terminal stance) | 1.45±(0.22) | 8.33±(0.24) | 2.06±(0.22) |
| | Flexion peak (swing) | 22.04±(1.11) | 25.67±(1.09) | 23.25±(1.12) |
| Hip angle (degrees) | Extension peak | 21.09±(0.72) | 16.46±(0.76) | 25.08±(0.69) |
| | Flexion peak (swing phase) | 30.20±(1.33) | 25.95±(1.21) | 36.88±(1.41) |
| Ankle moment (Nm/kg) | PF peak (early stance) | -0.16±(0.03) | -0.25±(0.05) | - |
| | Dorsiflexion peak | 0.62±(0.06) | 0.59±(0.05) | 0.78±(0.06) |
| Knee moment (Nm/kg) | Flexion peak1 | 0.23±(0.02) | 0.38±(0.03) | 0.10±(0.01) |
| | Extension peak | -0.16±(0.02) | -0.09±(0.03) | -0.31±(0.01) |
| | Flexion peak2 | 0.10±(0.01) | 0.14±(0.01) | 0.15±(0.01) |
| Hip moment (Nm/kg) | Flexion peak | 0.25±(0.01) | 0.29±(0.01) | 0.14±(0.01) |
| | Extension peak | -0.20±(0.01) | -0.19±(0.01) | -0.07±(0.01) |
| GRFv (N) | 1 st peak | 895±(8.20) | 1030±(9.19) | 928±(9.21) |
| | Trough | 855±(9.24) | 794±(9.36) | 788±(8.46) |
| | 2 nd peak | 914±(10.32) | 915±(10.30) | 848±(10.29) |

Table 4.17: Quadriceps and hamstring EMG RMS amplitude for case study 5 (*SP5*).

| Parameter description | | <u>Mean±(SD)</u> | | |
|-----------------------|--------------------------|------------------|--------------|--------------|
| | | AFO | Tuned | SSO |
| VL RMS (%MMT) | Stance peak | 39.99±(5.12) | 46.49±(6.16) | 39.22±(5.55) |
| | Swing peak | 33.43±(4.65) | 35.91±(5.82) | 38.01±(5.17) |
| VM RMS (%MMT) | Stance peak | 27.74±(0.40) | 29.61±(0.38) | 28.44±(0.38) |
| | Swing peak | 25.15±(0.33) | 24.72±(0.34) | 27.42±(0.34) |
| RF RMS (%MMT) | Stance peak [#] | 16.24±(0.10) | 21.02±(0.09) | 16.77±(0.10) |
| | T-PS peak | 12.94±(0.13) | 13.46±(0.15) | 12.84±(0.13) |
| | Swing peak | 13.43±(0.11) | 14.31±(0.10) | 15.51±(0.13) |
| BF RMS (%MMT) | Stance peak | 20.53±(0.24) | 25.52±(0.21) | 38.19±(0.28) |
| | Swing peak | 40.65±(0.25) | 35.82±(0.29) | 46.74±(0.26) |
| ST RMS (%MMT) | Stance peak | 25.42±(0.11) | 17.50±(0.10) | 28.36±(0.10) |
| | Swing peak | 33.14±(0.21) | 26.69±(0.19) | 41.37±(0.21) |

T-PS peak: the maximum activity during terminal stance and pre swing phase

Table 4.18: The anatomical and the orthotic ankle moment for case study 5 (*SP5*) derived from SG2 and SG4 data outputs.

| Moment (Nm/kg) | | <u>Anatomical</u> (mean±(SD)) | | <u>Orthotic</u> (mean±(SD)) | |
|----------------|----------------------|-------------------------------|--------------|-----------------------------|--------------|
| | | AFO | Tuned | AFO | Tuned |
| SG2 | Early stance peak | 0.04±(0.03) | -0.01±(0.03) | -0.20±(0.03) | -0.24±(0.02) |
| | Terminal stance peak | 0.63±(0.06) | 0.60±(0.05) | 0.01±(0.03) | -0.01±(0.05) |
| SG4 | Mid stance peak | 0.08±(0.01) | 0.07±(0.01) | -0.02±(0.01) | -0.02±(0.01) |
| | Terminal stance peak | 0.10±(0.01) | 0.09±(0.01) | -0.01±(0.01) | -0.02±(0.01) |

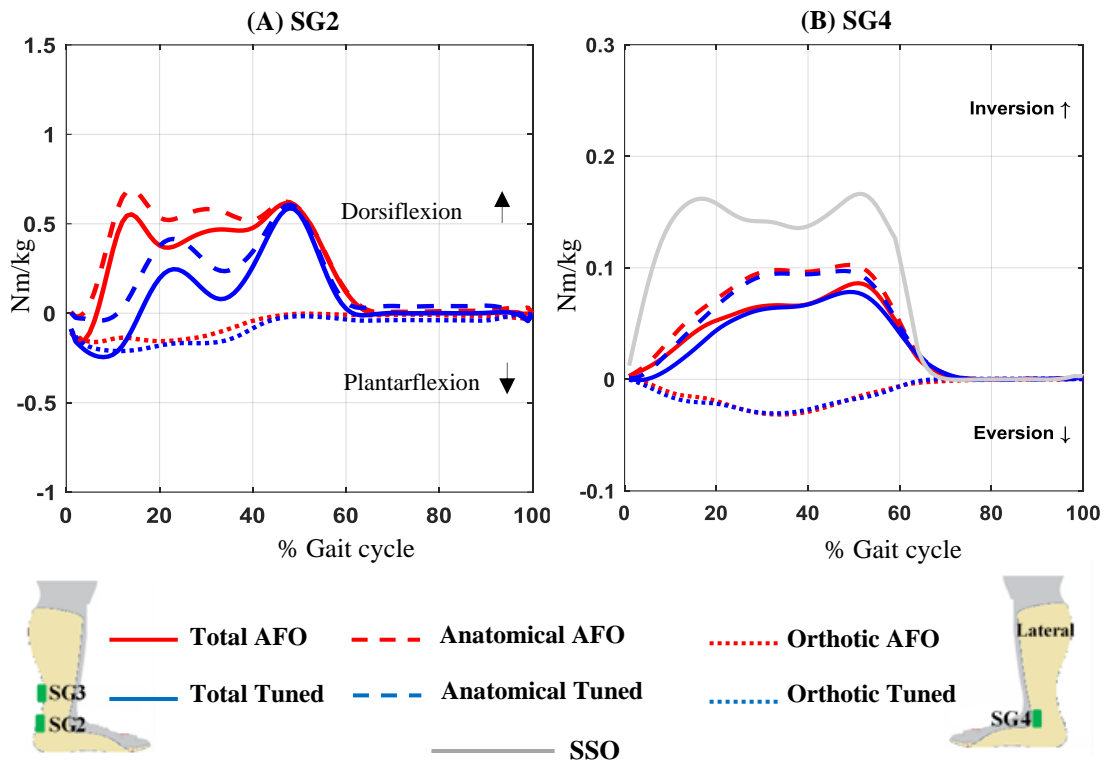


Figure 4.24: Total ankle moment, orthotic moment, and anatomical moment in sagittal plane (A) and frontal plane (B) for case study 5 (*SP5*) derived from SG2 and SG4 data outputs, respectively.

4.7 Case study four (*SP6*)

SP6 was a 50-year-old male with a mass of 91kg and height of 1.78m. *SP6* had hemorrhagic stroke in 2013 affecting his right hemisphere resulting in left side hemiparesis. *SP6* started a daily physical therapy regimen in 2014 for two years. *SP6* own orthosis was articulated AFO (metal and leather AFO with plantarflexion stop) different from the AFO used in this study. *SP6* felt unsecure to walk on a treadmill with SSO (i.e. without an AFO or a Tuned-AFO), thus his gait was only recorded during walking with an AFO and a Tuned-AFO. The CWS for *SP6* was 0.45 m/s in AFO condition. Based on walking speed classification in stroke patients (Perry et al., 1995), *SP6* is classified as a “limited community walking” (speed 0.4 – 0.8 m/s).

4.7.1 Comparing Tuned-AFO condition with AFO condition:

The walking speed of *SP6* slightly increased in Tuned-AFO condition (0.47 ± 0.02 m/s) as compared to AFO condition (0.45 ± 0.02 m/s). Stride length and stance percentage of the gait cycle merely changed in Tuned-AFO condition (Table 4.19). SVA inclination during mid stance increased in Tuned-AFO (by 4.18 degrees) from (-3.80 ± 0.12 degrees) in AFO condition to (0.38 ± 0.09 degrees) in Tuned-AFO condition (Table 4.19, Figure 4.25, A). Slight change in ankle motion resulted in Tuned-AFO condition as compared to AFO condition; as first slight plantar flexion peak decreased (-1.22 ± 0.10 degrees, -0.18 ± 0.03 degrees, respectively), second slight plantar flexion peak reversed to slight dorsiflexion (0.79 ± 0.08 degrees, -0.25 ± 0.04 degrees, respectively), and the dorsiflexion peak slightly increased (2.56 ± 0.14 degrees, 1.59 ± 0.12 degrees, respectively) (Table 4.19, Figure 4.25, B). Knee motion showed, in Tuned-AFO condition as compared to AFO condition, greatly increased early stance flexion (6.66 ± 0.55 degrees, 0.55 ± 0.42 degrees, respectively), decreased knee extension (-2.25 ± 0.92 degrees, -10.99 ± 0.97 degrees, respectively), and slightly increased knee flexion in swing phase (22.09 ± 0.55 , 20.49 ± 0.42 degrees, respectively) (Table 4.19, Figure 4.25, A). Hip flexion peak and extension peaks slightly increased (but the hip remained flexed throughout gait cycle) in *SP6* in Tuned-AFO condition (36.94 ± 1.01 degrees, 4.65 ± 0.81 degrees, respectively) as compared to AFO condition (34.35 ± 0.81 degrees, 6.33 ± 0.82 degrees, respectively) (Table 4.19, Figure 4.25, A).

GRFv in *SP6* after AFO tuning slightly changed (Table 4.19, Figure 4.26, D). The first peak, second peak, and trough slightly increased (978 ± 9.50 N, 974 ± 9.53 N, 943 ± 9.24 N, respectively) as compared to AFO condition (955 ± 8.54 N, 942 ± 9.50 N, 895 ± 8.57 N, respectively). Additionally, the first and second peaks and the trough are higher than *SP2* body weight in Tuned-AFO condition (107%BW, 107%BBW, and 104%BW, respectively) as compared to AFO condition (105%BW, 104%BW, and 98%BW, respectively). Changes in the moments in *SP6* were generally slight (Table 4.19, Figure 4.26). Ankle plantar flexion moment peak and the dorsiflexion moment peak slightly decreased Tuned-AFO condition (-0.11 ± 0.04 Nm/kg, 0.42 ± 0.05 Nm/kg, respectively) as compared to AFO condition (-0.13 ± 0.04 Nm/kg, 0.51 ± 0.06 Nm/kg, respectively). Knee first flexion moment peak slightly increased (0.32 ± 0.02 Nm/kg) in Tuned-AFO condition when compared with AFO condition (0.25 ± 0.02 Nm/kg). Extension moment peak, on the

other hand, reversed to slight flexion moment in Tuned-AFO condition (0.19 ± 0.02 Nm/kg) as compared to AFO condition (-0.30 ± 0.01 Nm/kg). Hip flexion moment peak slightly increased in Tuned-AFO condition (0.38 ± 0.01 Nm/kg) as compared to AFO condition (0.31 ± 0.01 Nm/kg), while extension moment remained almost unchanged.

Tuning an AFO showed changes in the EMG activity of knee muscles as compared to AFO condition in *SP6* (Table 4.20, Figure 4.27). VL and VM showed similar activity patterns and thus, will be presented together. VL and VM showed no change in the periods of activity in Tuned-AFO condition as compared to AFO condition. They were both active during early stance and late in swing. VL showed increased stance (26.36 ± 3.39 %MMT) and swing (18.40 ± 2.62 %MMT) peaks in Tuned-AFO condition as compared to AFO condition (18.63 ± 4.08 %MMT, 9.86 ± 2.55 %MMT, respectively). VM showed increased stance peak and decreased swing peak in Tuned-AFO condition (29.3 ± 0.37 %MMT, 15.6 ± 0.24 %MMT, respectively) as compared to AFO condition (24.17 ± 0.37 %MMT, 16.71 ± 0.25 %MMT, respectively). Tuning the AFO did not change the activation periods of RF in *SP6*. RF was active starting from the end of mid stance to almost 80%GC. RF showed only terminal stance-pre swing peak which slightly increased in Tuned-AFO condition (18.52 ± 0.12 %MMT) as compared to AFO condition (16.52 ± 0.17 %MMT). BF and ST also showed similar activity pattern and will thus, be presented together. BF and ST were active during loading response and terminal swing. Their period of activity did not change in Tuned-AFO condition as compared to AFO condition. BF and ST showed slightly increased stance peaks (29.68 ± 0.32 %MMT, 34.86 ± 0.17 %MMT, respectively) and decreased swing peaks (41.90 ± 0.38 %MMT, 32.22 ± 0.15 %MMT, respectively) in Tuned-AFO condition as compared to AFO condition (BF: 28.47 ± 0.31 %MMT, 47.36 ± 0.46 %MMT, respectively, ST: 32.64 ± 0.18 %MMT, 46.04 ± 0.15 %MMT, respectively).

The orthotic moment showed plantarflexion moment during loading response, and reduced (or almost absent) plantar flexion orthotic moment during terminal stance (Table 4.21, Figure 4.28, A). In contrast, the anatomical moment only showed a dorsiflexion moment during most of stance. Walking with a Tuned-AFO *SP6* showed no change in orthotic moment as compared to AFO condition.

SP6 showed a noticeable reduction in the total inversion moment while walking with an AFO or Tuned-AFO Figure 4.28 (B). The orthotic moment peaks showed an eversion moment during the whole of stance. Like in all previous stroke participants, walking with a Tuned-AFO or an AFO, showed no noticeable differences in the orthotic eversion moment nor in the anatomical inversion moment.

The effect of Tuned-AFO on the speed of *SP6* was slight and not clinically significant, as *SP* gait speed only increased by (0.02m/s) Tuned-AFO condition as compared to AFO condition. This means that *SP6* remained in the “limited community walking” according to the classification by Perry et al. (1995). Nevertheless, as the speed increment in Tuned-AFO condition was lower than the MCID (0.16 m/s), this increment is considered clinically insignificant (Tilson et al., 2010).

Additionally, Tuned-AFO improved the kinematics so that they are slightly closer to normal than in AFO (except for the ankle motion). SVA in Tuned-AFO condition was far from being within the target range (only 0.38 degrees); indicating insufficient tuning. This is because *SP6* did not feel comfortable walking with the tuning actually needed. This could highlight the need for gradual tuning process in certain stroke patients to reach the actually needed tuning. The hip was 13.28 degrees less extended than normal (control participants in SSO condition are considered the normal baseline in this study) in Tuned-AFO condition and 14.96 degrees less than normal in AFO condition, the knee was 6.81 degrees less flexed during early stance in Tuned-AFO condition and 12.92 degrees less flexed in AFO condition.

All changes in gait parameters in *SP6* are caused by the tuning process. As tuning was insufficient and far from the target range, changes in gait parameters were slight. The tibia is not inclined and thus the knee ability to flex and the hip ability to extend are very limited. Further discussion on the effect of Tuned-AFO condition and AFO condition on the gait parameters of control and stroke participants will be addressed in the next chapter (Chapter 5 Discussion).

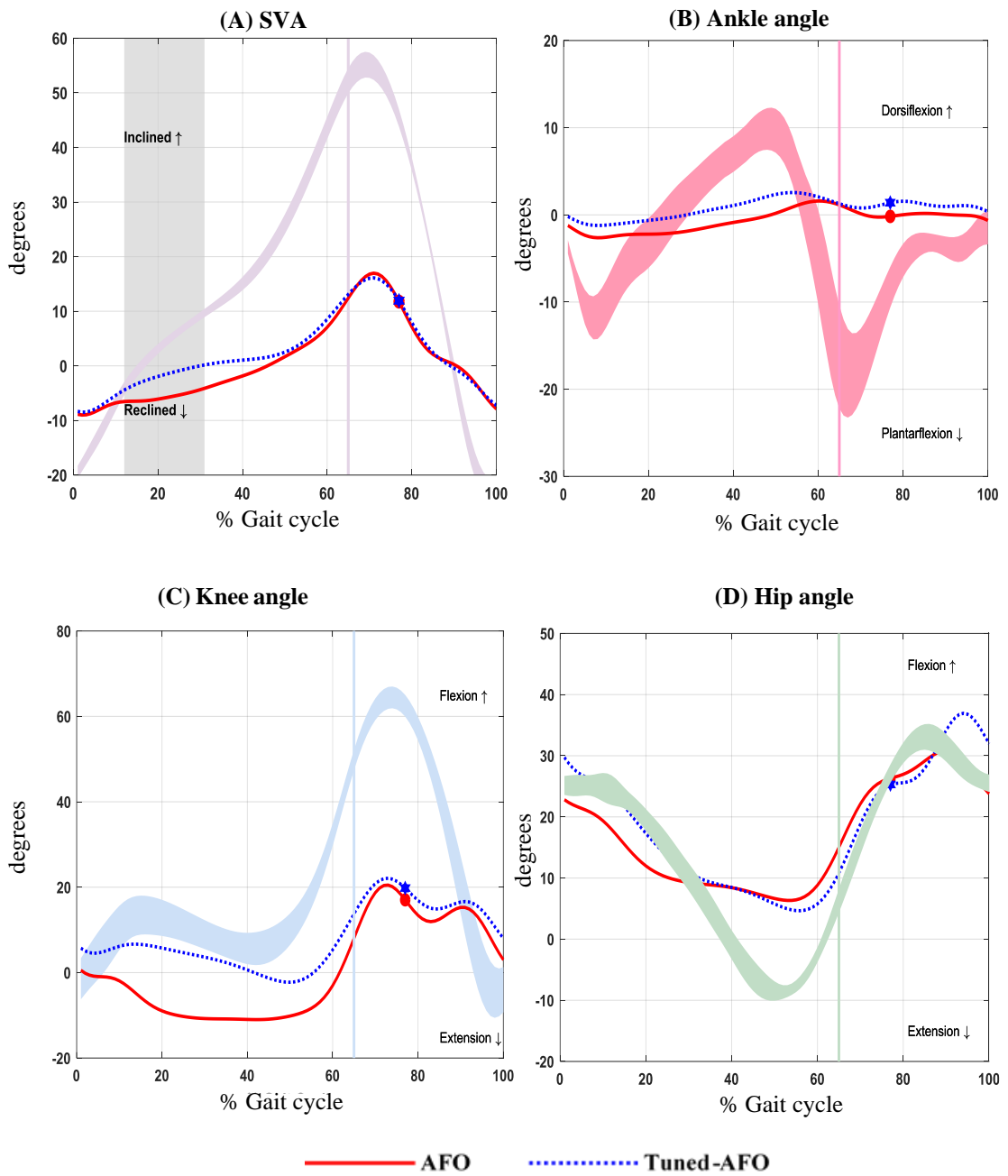


Figure 4.25: Sagittal kinematic graphs for case study 6 (*SP6*) while walking on treadmill wearing Tuned-AFO and AFO with reference to control participants while wearing SSO (shaded lines).

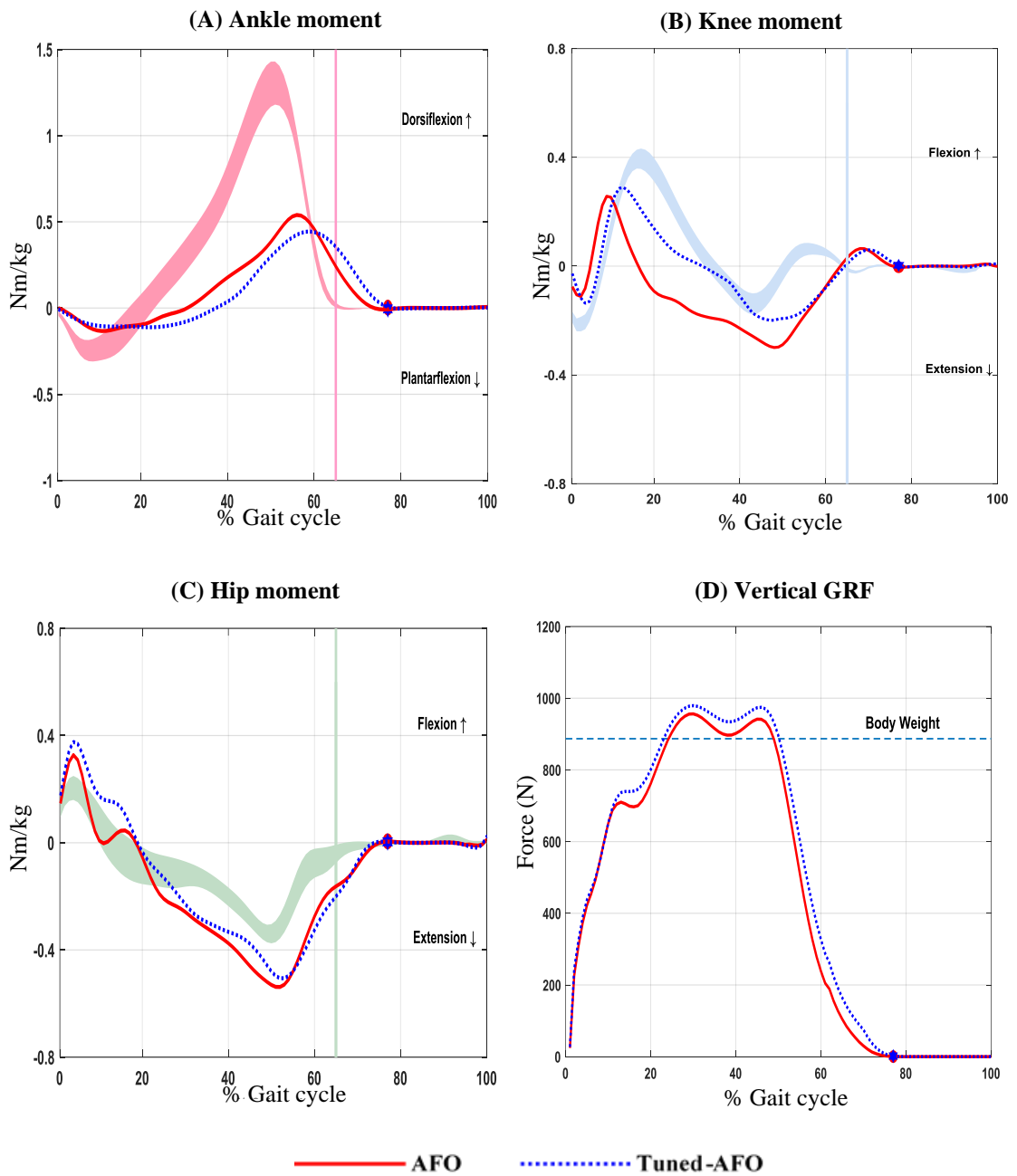


Figure 4.26: Sagittal kinetic graphs and the vertical GRF graph for case study 6 (*SP6*) while walking on treadmill wearing Tuned-AFO and AFO with reference to control participants while wearing SSO (shaded lines).

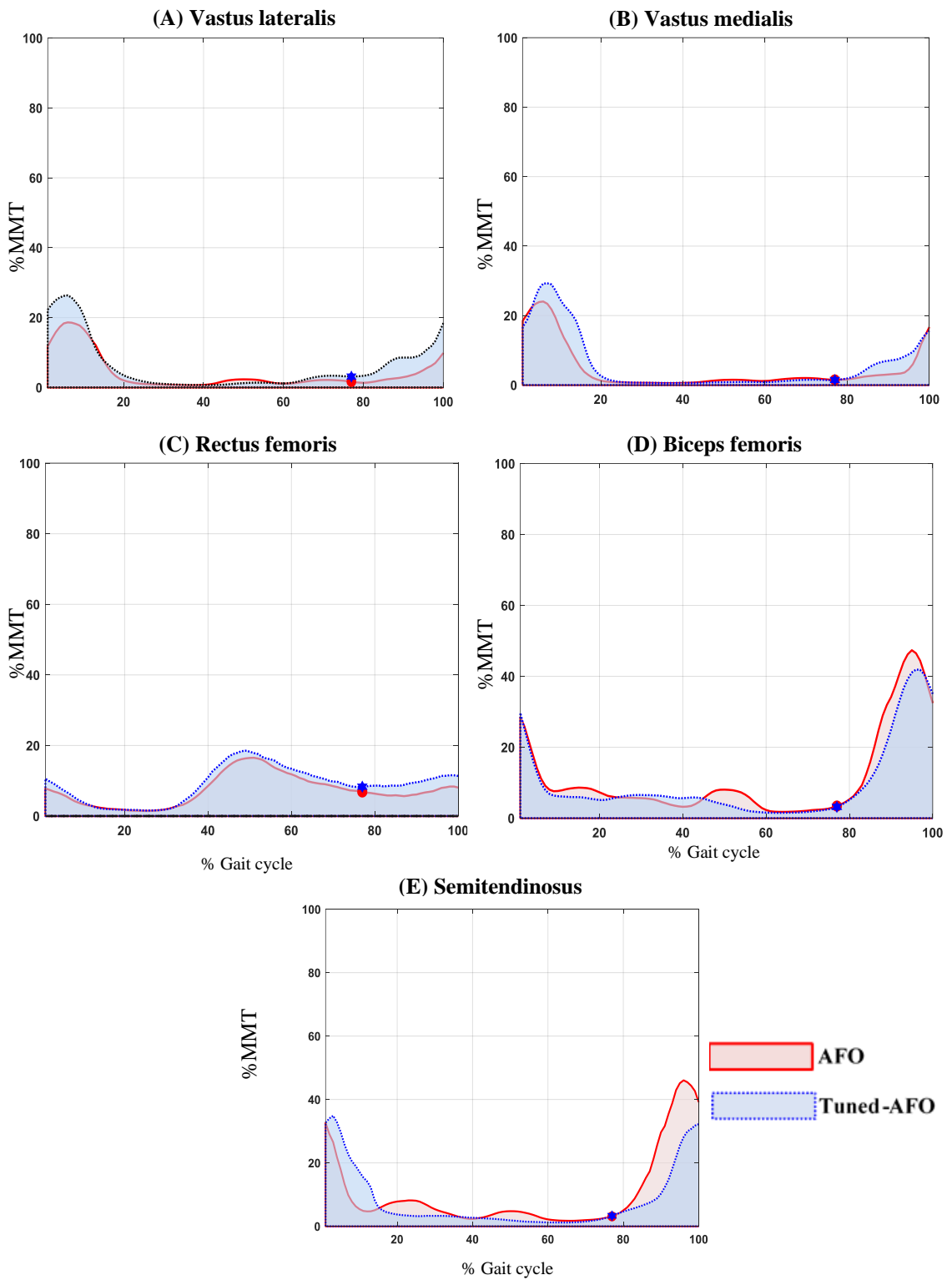


Figure 4.27: Quadriceps and hamstring EMG RMS amplitude and timing during walking on treadmill for case study 6 (*SP6*). The RMS is presented as a percentage of maximum manual muscle test value (% MMT).

Table 4.19: Temporal-spatial, kinematic and kinetic data for *SP6*.

| Parameter description | | <u>Mean±(SD)</u> | | |
|------------------------------|-----------------------------|------------------|--------------|-----|
| | | AFO | Tuned | SSO |
| SVA (degrees) | Mid stance | -3.80±(0.12) | 0.38±(0.09) | - |
| Temporal-spatial | Speed (ms ⁻¹) | 0.45±(0.02) | 0.47±(0.02) | - |
| | Stance time (%) | 77.01±(0.35) | 77.02±(0.32) | - |
| | Stride length (m) | 0.42±(0.04) | 0.43±(0.05) | - |
| Ankle angle (degrees) | PF peak (early stance) | -1.22±(0.10) | -0.18±(0.03) | - |
| | Dorsiflexion peak | 1.59±(0.12) | 2.56±(0.14) | - |
| | PF peak (swing phase) | -0.25±(0.04) | 0.79±(0.08) | - |
| Knee angle (degrees) | Flexion peak (stance) | 0.55±(0.42) | 6.66±(0.55) | - |
| | Extension (terminal stance) | -10.99±(0.97) | -2.25±(0.92) | - |
| | Flexion peak (swing) | 20.49±(0.42) | 22.09±(0.55) | - |
| Hip angle (degrees) | Extension peak | 6.33±(0.82) | 4.65±(0.81) | - |
| | Flexion peak (swing phase) | 34.35±(0.81) | 36.94±(1.01) | - |
| Ankle moment (Nm/kg) | PF peak (early stance) | -0.13±(0.04) | -0.11±(0.04) | - |
| | Dorsiflexion peak | 0.51±(0.06) | 0.42±(0.05) | - |
| Knee moment (Nm/kg) | Flexion peak1 | 0.25±(0.02) | 0.32±(0.02) | - |
| | Extension peak | -0.30±(0.01) | 0.19±(0.02) | - |
| | Flexion peak2 | 0.12±(0.01) | 0.12±(0.01) | - |
| Hip moment (Nm/kg) | Flexion peak | 0.31±(0.01) | 0.38±(0.01) | - |
| | Extension peak | -0.53±(0.01) | -0.51±(0.01) | - |
| GRFv (N) | 1 st peak | 955±(8.54) | 978±(9.50) | - |
| | Trough | 895±(8.57) | 943±(9.24) | - |
| | 2 nd peak | 942±(9.50) | 974±(9.53) | - |

Table 4.20: Quadriceps and hamstring EMG RMS amplitude for case study 6 (*SP6*).

| Parameter description | | <u>Mean±(SD)</u> | | |
|-----------------------|--------------------------|------------------|--------------|-----|
| | | AFO | Tuned | SSO |
| VL RMS (%MMT) | Stance peak | 18.63±(4.08) | 26.36±(3.39) | - |
| | Swing peak | 9.86±(2.55) | 18.40±(2.62) | - |
| VM RMS (%MMT) | Stance peak | 24.17±(0.37) | 29.3±(0.37) | - |
| | Swing peak | 16.71±(0.25) | 15.6±(0.24) | - |
| RF RMS (%MMT) | Stance peak [#] | - | - | - |
| | T-PS peak | 16.52±(0.17) | 18.52±(0.12) | - |
| | Swing peak | - | - | - |
| BF RMS (%MMT) | Stance peak | 28.47±(0.31) | 29.68±(0.32) | - |
| | Swing peak | 47.36±(0.46) | 41.90±(0.38) | - |
| ST RMS (%MMT) | Stance peak | 32.64±(0.18) | 34.86±(0.17) | - |
| | Swing peak | 46.04±(0.15) | 32.22±(0.15) | - |

T-PS peak: the maximum activity during terminal stance and pre swing phase

Table 4.21: The anatomical and the orthotic ankle moment for case study 6 (*SP6*) derived from SG2 and SG4 data outputs.

| Moment (Nm/kg) | | <u>Anatomical</u> (mean±(SD)) | | <u>Orthotic</u> (mean±(SD)) | |
|----------------|----------------------|-------------------------------|-------------|-----------------------------|--------------|
| | | AFO | Tuned | AFO | Tuned |
| SG2 | Early stance peak | 0.01±(0.02) | 0.03±(0.04) | -0.14±(0.04) | -0.14±(0.04) |
| | Terminal stance peak | 0.52±(0.04) | 0.42±(0.05) | 0.01±(0.06) | 0.00±(0.05) |
| SG4 | Mid stance peak | 0.09±(0.01) | 0.08±(0.01) | -0.02±(0.01) | -0.02±(0.01) |
| | Terminal stance peak | 0.14±(0.01) | 0.13±(0.01) | -0.03±(0.01) | -0.03±(0.01) |

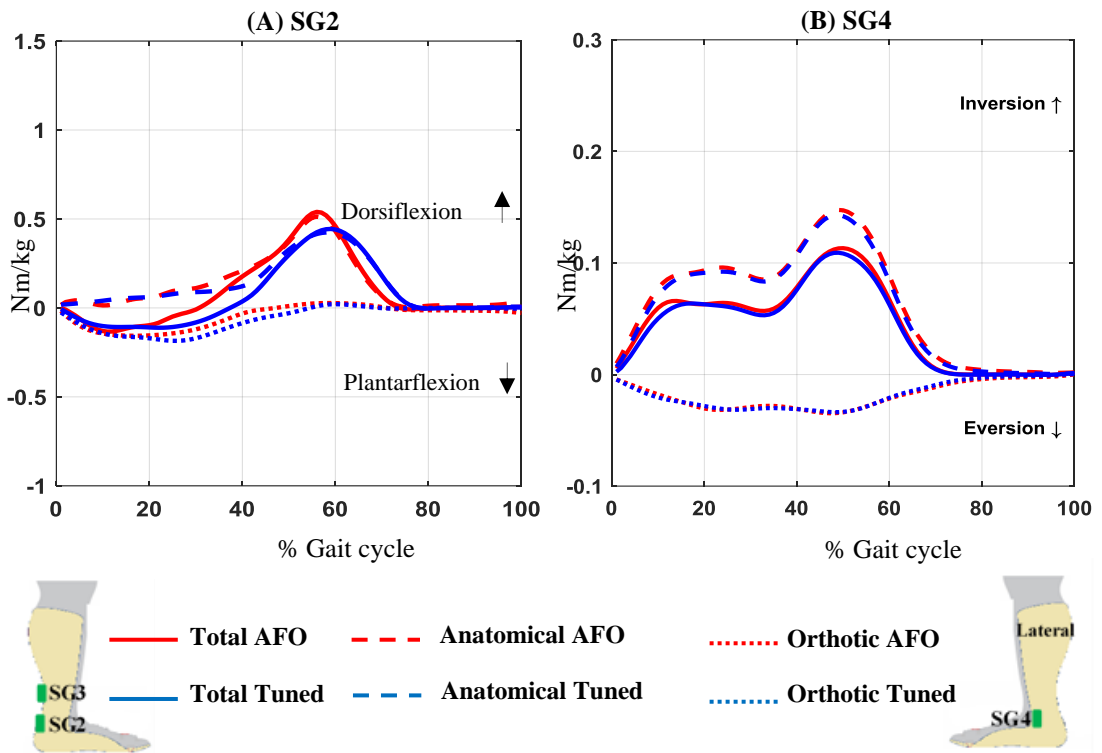


Figure 4.28: Total ankle moment, orthotic moment, and anatomical moment in sagittal plane (A) and frontal plane (B) for case study 6 (*SP6*) derived from SG2 and SG4 data outputs, respectively.

Chapter 5 Discussion

The current study evaluates the immediate effects of wearing a Tuned-AFO as compared to rigid AFO (before tuning) and Standard Shoes Only (SSO) on the gait parameters of control participants and stroke participants during walking on a treadmill. The study also measures the orthotic and the anatomical moments at the ankle joint in the sagittal plane and at the assumed subtalar joint in the frontal plane and compares the effects of tuning rigid AFO on the orthotic moments.

Hypothesis 1 is accepted as the results obtained in this study support the hypothesis. The gait parameters improved were walking speed, SVA inclination in mid stance, knee flexion in loading response and initial swing, hip extension in mid and terminal stance, external dorsiflexion moment, external inversion moment, external knee extension moment, external hip extension moment in terminal stance, quadriceps muscle activity, and hamstring muscle activity.

Hypothesis 2 is partially accepted as the obtained in this study partially support the hypothesis. The gait parameters further improved were: SVA inclination in mid stance, knee flexion in loading response, knee extension in terminal stance, external knee flexion moment in mid stance, and external knee extension moment during terminal stance.

It is important to note that, although uncontrolled variables were made to a minimum, several variables were very difficult to control in the protocol of this study. These should be considered before discussing the results and before conclusions are drawn from this study.

Among the most important variables is the spasticity level of the stroke participants which controls how far equinus deformity can be reduced during casting. The inclusion criteria of this study limit the spasticity level to mild-moderate evaluated through the Modified Ashworth Scale. Yet, mild-moderate spasticity may contain a large difference. Based on clinical practice, spasticity level controls how controllable the equinus deformity is. High spasticity makes it difficult to reduce equinus during casting for the AFO especially that the ankle was set in a position to accommodate the available gastrocnemius length, resulting in less correction of SVA in AFO condition. In these cases, it is fair to expect

that, tuning is the main factor correcting SVA. Low spasticity, on the other hand, will result in greater correction of SVA in AFO condition than in Tuned-AFO condition.

Another variable that cannot be controlled in this study is the geometry of the AFO. Geometry of the AFO depends on the shape and dimensions of the affected limb of the stroke participants and thus cannot be controlled. Geometry is among the factors that can determine the AFO stiffness (Convery et al., 2004, Kobayashi et al., 2011, Major et al., 2004).

Another variable that may have an effect on the results of this study is the timing and the length of period of the rehabilitation programme underwent by the stroke participants. These may have different effects on the general condition of the stroke participants' gait and consequently, on the results of the current study. Similarly, different types of orthoses are used by stroke participants in their everyday life. Different types of orthoses have been shown to have different effects on the gait of stroke patients (Daryabor et al., 2018, Daryabor et al., 2020, Ferreira et al., 2013, Leung and Moseley, 2003, Padilla et al., 2014, Shahabi et al., 2020, Totah et al., 2019, Tyson et al., 2013), which may have led to different or unexplainable results in the current study. Additionally, adherence of the stroke participants to using their orthoses is another factor that is absolutely out of control (Yüzer et al., 2018). Not using the prescribed orthoses has been shown to have a negative effect on the general wellbeing of patients (Davidson et al., 2009, McMonagle, 2019, NHS Quality Improvement Scotland, 2009, Yamane, 2019). Several efforts have been previously made to monitor the use of patients to their orthoses, as patients may not use their orthoses yet state to use them upon being asked for a variety of reasons (McMonagle, 2019, Yüzer et al., 2018).

Length of the tuning wedge, heel wedge or wedge extended from the heel to the metatarsophalangeal joints, may also be another variable that may have an effect. Length of the tuning wedge was decided upon participants' preference, as some participants did not feel comfortable with heel wedge. The density of the material used in tuning wedges in this study was the same for all participants regardless of their body weight. It is expected that high weight participants may require denser materials to gain the complete effects of tuning (Kerkum et al., 2015a). In the current study, weight range of participants

was large (72-95 kg). Consequently, using the same density materials for all participants may not be ideal.

Some stroke participants, especially those who needed 3cm or more tuning wedges, did not feel comfortable using the required tuning wedges to reach the target SVA. This may indicate that some stroke patients need gradual tuning process to reach the optimal alignment. The limited time of the current study and its protocol did not provide the privilege of gradual tuning. These variables –among others- may have effects on the results and conclusions of this study and should be considered when making clinical implications out of it.

This chapter is composed of three sections. The first section discusses the effects of Tuned-AFO on stroke and control participants gait when compared to AFO (before tuning) and SSO condition. The second section discusses the effects of Tuned-AFO on the orthotic and the anatomical moments at the ankle joint in the sagittal plane and at the assumed subtalar joint in the frontal plane compared to AFO (before tuning) during walking for stroke and control participants. In the last section, the limitations of the current study will be discussed.

The gait pattern obtained from control participants while walking with SSO showed similar results to the previous reported results of overground gait (Perry and Burnfield, 2010, Richards, 2018) or treadmill gait (Riley et al., 2007, Watt et al., 2010) in healthy participants. Treadmill gait has been reported to be similar to overground gait (Parvataneni et al., 2009, Riley et al., 2007, Watt et al., 2010), however, other studies have reported that minor differences may exist in the temporal-spatial parameters between walking overground and walking on a treadmill in healthy individuals (Hollman et al., 2016, Nymark et al., 2005, Papegaaij and Steenbrink, 2017) and stroke patients (Kautz et al., 2011); walking on a treadmill showed a higher cadence and shorter strides as compared to overground gait at comparable speeds. The results obtained from stroke patients walking on a treadmill have been shown to be reliable and repeatable results (Kesar et al., 2011). Consequently, using an instrumented treadmill is considered as a valid method to detect gait deviations that are present in post stroke gait during overground gait (Kesar et al., 2011).

In general, stroke participants in this study can be seen to have a different gait pattern as compared to control participants. Stroke participants walked with inadequate hip extension during stance, excessive knee extension during stance, reduced ankle dorsiflexion during stance and swing, and reduced knee flexion peak in swing on the affected side limb while wearing SSO, as compared to control participants wearing SSO. Additionally, the walking speed of the stroke participants in this study was slower while wearing SSO as compared to control participants while wearing SSO. Stroke participants showed decreased stance time on the affected limb relative to the unaffected limb, thus demonstrating a temporally asymmetric gait pattern.

5.1 The immediate effects of rigid Tuned-AFO, rigid AFO (before tuning), and SSO on control and stroke participants gait.

The primary aim of this study was to investigate the immediate effects of optimising the SVA alignment during mid stance with the use of a rigid AFO on several gait parameters including ankle, knee, hip kinematic and kinetic parameters, temporal-spatial parameters, and vertical GRF. Understanding the influence of rigid AFO (before and after tuning) on quadriceps and hamstring muscles activity during walking was also investigated.

It is important to know that *SP3* in particular may be described as being fairly active as he showed almost a similar gait pattern to that obtained from control participants. Moreover, in this section, the results of SSO for *SP6* will not be discussed as his gait was only recorded during walking with an AFO and a Tuned-AFO, as *SP6* felt unsecure to walk on a treadmill with SSO.

5.1.1 Shank to vertical angle (SVA)

The results from this study demonstrate obvious alterations of SVA magnitude when walking with a Tuned-AFO as compared to walking with an AFO or SSO during mid stance (Figure 5.1).

In control participants, the SVA mean value during mid stance was (10.21 ± 1.5 degrees) while walking with SSO. This result shows that the alignment of the shank in control participants during mid stance was within the optimum inclination (10-12 degrees) as indicated in the literature (Meadows et al., 2008, Owen, 2010). The results from the

current study demonstrate the abnormality in SVA in stroke participants. In the current study, the SVA value among stroke participants ranged from 2.55 degrees to 8.33 degrees while walking with SSO. Wearing an AFO improved the inclination of the tibia for all stroke participants; however, the SVA value was still not adequate when compared with control participants (Figure 5.1). In control and all stroke participants, wearing a Tuned-AFO resulted in greater inclination of the tibia during mid stance as compared to the untuned AFO or SSO conditions. This agrees with a previous case study (Jagadamma et al., 2010), which reported that SVA of a stroke patient was improved to be inclined 12 degrees in mid stance after AFO tuning. This was explained in other studies (Kerkum et al., 2015b, Kessels et al., 2013) by the fact that tuning an AFO elevates the heel of the foot, yet keeping it in contact with the ground, which results in tibial forward inclination and thus greater SVA. It could be noticed that Tuned-AFO improved the SVA to be more inclined and closer to normal compared to AFO or SSO. However, the SVA was still inadequate in *SP5* and *SP6* as the tuning process did not accomplish the target SVA values (10-12 degrees); this was because *SP5* and *SP6* did not feel secure with the required wedges to achieve target SVA. Based on this, it is expected that some patients may need more time to adapt to the effects of tuning than others.

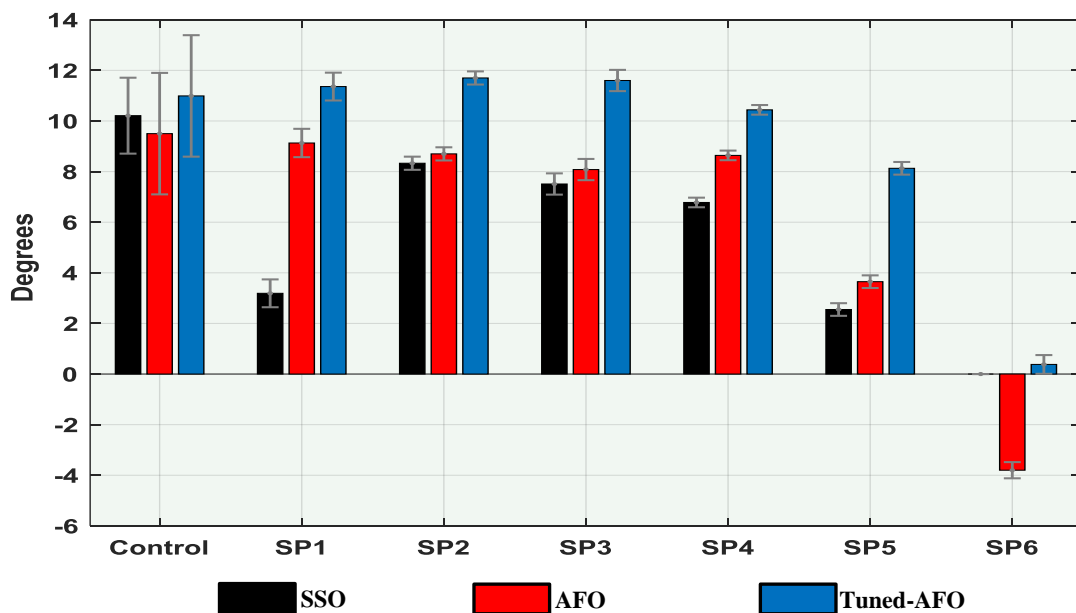


Figure 5.1: The SVA values for stroke participants and the mean SVA value for control participants during mid stance.

5.1.2 Temporal-spatial parameters

Stride length was longer and walking speed was faster with wearing a Tuned-AFO or an AFO compared to SSO among all stroke participants. This agrees with the previous studies (Daryabor et al., 2018, Ferreira et al., 2013, Leung and Moseley, 2003, Padilla et al., 2014, Shahabi et al., 2020, Tyson et al., 2013, Tyson and Kent, 2013). In the current study, the walking speed of stroke participants while wearing SSO ranged (0.20 m/s to 0.60 m/s) and showed clinically significant improvement while wearing a Tuned-AFO (ranging from 0.15 m/s to 0.40 m/s) or an AFO (in SPs except in **SP5**, ranging from 0.13 m/s to 0.40 m/s). However, the walking speed remained slower than in control participants (1.2 m/s) with SSO. The walking speed in all stroke participants while walking with a Tuned-AFO or an AFO was less than 0.8 m/s (except in **SP3**) which may clinically be considered insufficient to accomplish the basic community walking activities based on Perry classification (Perry et al., 1995). The walking speed in **SP3** while walking with Tuned-AFO or AFO was the highest (0.9m/s), but is still below the required walking speed to safely cross the road using pedestrian crossing in the United Kingdom (1.2 m/s) (Asher et al., 2012).

Improvements in temporal-spatial parameters in the current study may be related to the changes in the SVA and proximal joint kinematics (This will be further discussed below under the heading “kinematic parameters”). Improving the alignment of the tibia to be closer to the normal inclination during mid to terminal stance results in a more normal tibial progression during early and terminal stance (Roelker et al., 2019).

In the current study, no obvious differences in the temporal-spatial parameters (speed, stride length, and stance duration) in all participants were found while walking with AFO or Tuned-AFO. Literature only report comparison in temporal-spatial parameters between rigid tuned AFO and a baseline (shoes or barefoot) or with other types/designs of AFO (Choi et al., 2016, Wening et al., 2009), and thus making explanations based on previous studies difficult. Only one single case study compared the effects of tuning on temporal-spatial parameters among others (Jagadamma et al., 2010). The immediate effect of tuning the rigid AFO was a reduction in walking speed after tuning (Jagadamma et al., 2010). Prolonged use of the rigid AFO (after 3 months) resulted in an increase in walking speed and stride length. The study by Jagadamma et al. (2010) does not show levels of

significance, which makes comparison difficult. The fact that no obvious improvements were noticed in the current study in temporal-spatial parameters may be due to the small sample size. It also can be expected that temporal-spatial parameters may improve upon prolonged use of the Tuned-AFO.

5.1.3 Kinematic parameters

The kinematic results of the current study can be explained in the scope of healthy and stroke patients' gait as described in section 2.3 under the heading "Normal and post stroke gait". It was previously shown that changes in walking speed result in changes in the kinematics (Choi et al., 2017, Kirtley et al., 1985, Sousa and Tavares, 2012, Tyrell et al., 2011). It is important to address that no changes in walking speed were reported in the current study between AFO and Tuned-AFO conditions, although kinematic changes were noted and some of them were obvious. Consequently, and as variables in this study were made to a minimum, it is fair to refer the changes in the kinematics to tuning the AFO.

❖ *Ankle joint kinematics (sagittal plane)*

➤ Control participants

Wearing an AFO or a Tuned-AFO in control participants resulted in altered (from SSO/normal) ankle motion pattern. This is expected as AFO and Tuned-AFO's main effect is to limit ankle motion in dorsiflexion/plantarflexion. The less the movement that occurs at the ankle, the more effective the AFO and Tuned-AFO are. The greater limitation to ankle plantarflexion occurs during pre swing, which is consistent with previous studies (Choi et al., 2016, Cruz and Dhaher, 2009). Perry and Burnfield (2010) state that this plantarflexion occurs due to previously (during mid and terminal stance) stretched plantarflexors which shorten once body weight is being shifted to the contralateral limb. Given that rigid AFO/Tuned-AFO are designed primarily to prevent all motions at the foot and ankle (Condie and Bowers, 2008), it was not surprising that ankle range of motion was very limited. In AFO and in Tuned-AFO conditions, controlling tibial alignment results in reducing knee hyperextension. This is mainly because normally all the dorsiflexion that occurs during mid stance results from tibia moving on the foot (Perry and Burnfield, 2010). Limited dorsiflexion hinders progression

during mid stance (ankle rocker). During swing phase, dorsiflexion normally occurs due to dorsiflexors' contraction. The need for this is crucial as it facilitates in lifting the foot off the ground. Two points can be noticed here, the ankle is not plantarflexed (as it is the case in normal gait) during initial and mid swing, reducing the need for dorsiflexors contraction, which was not recorded in this study as dorsiflexors EMG is beyond the scope of the current study. The other point is that the effect of an AFO or a Tuned-AFO is more obvious during swing, as the dorsiflexion mechanism during swing is much weaker than the proposed dorsiflexion and plantarflexion mechanisms during the rest of the gait cycle.

The current study demonstrated that ankle dorsiflexion angle throughout the gait cycle tended to be higher with Tuned-AFO compared to AFO. This finding is consistent with previous studies (Fatone et al., 2009, Kerkum et al., 2015b). This can be explained by the effect of attaching the reflective markers to the standard shoes rather than the anatomical foot. The reflective markers on the standard shoes remained on their specific locations between testing conditions. Thus, inserting a heel wedge(s) inside the standard shoes in Tuned-AFO condition leads to elevating the heel of the foot inside the standard shoes, moving the reflective markers of the leg forward (increase in SVA). This results in a change in the relative positions of the reflective markers resulting in the apparent increase in dorsiflexion.

➤ Stroke participants

In agreement with the literature (Gard and Fatone, 2003, Meadows et al., 2008), walking with SSO showed one of the characteristic patterns of stroke gait, which is a plantarflexed ankle. The ankle is plantarflexed at initial contact and in loading response in all participants. During mid and terminal stance, some participants (*SP1*, *SP3*, and *SP5*) showed slight dorsiflexion (mean = 5.05 degrees, much less than in control participants mean = 9.86 degrees), while others (*SP2* and *SP4*) only reduced their ankle plantarflexed position slightly. During swing phase, the ankle remained plantarflexed in all participants. These results of limited ankle dorsiflexion are due to plantarflexors' hypertonus/spasticity.

Wearing an AFO or a Tuned-AFO in stroke participants resulted in ankle motion pattern that is close to control participants while wearing an AFO or Tuned-AFO. This suggests

that the same mechanisms affecting ankle motion in control participants while wearing an AFO or Tuned-AFO are also effective in stroke participants and are acting in the same way. Two points to raise are that ankle total range of motion in stroke participants during walking with an AFO or a Tuned-AFO was less than ankle total range of motion in control participants walking with an AFO or a Tuned-AFO. The total range of motion was very limited in all stroke participants while walking with an AFO or a Tuned-AFO (the mean total range of motion that occurred at the ankle joint in control and stroke participants was 8.35 and 1.98 degrees, respectively). This range of motion occurring at the ankle does not necessary reflect the deflection of the orthosis. It may have occurred as a result of the relative motion between the orthosis and leg due to soft tissue compression within the orthosis, or relative motion between the orthosis and the shoes. The other point is that some stroke participants (*SP1*, *SP3*, and *SP5*) still showed plantarflexed posture of the ankle especially during loading response and early mid stance. This plantarflexion is slight (less than 2 degrees) and it is irrelevant of the plantarflexion they showed while wearing SSO. An example on this is *SP4*, who showed the greatest plantarflexion while wearing SSO, but showed no plantarflexion while wearing an AFO or a Tuned-AFO. The decreased plantarflexion during swing indicates that foot ground clearance has been improved with AFO and Tuned-AFO.

❖ *Knee joint kinematics (sagittal plane)*

➤ Control participants

Control participants wearing an AFO or a Tuned-AFO showed greater knee flexion during loading response than when wearing SSO. The reason behind this is as the foot descends towards the ground while wearing AFO or a Tuned-AFO, the tibia follows the foot at the same rate (creating knee flexion moment). This occurs because the AFO and Tuned-AFO prevent motion between these two segments and thus they can be considered as one segment. As the foot descends towards the ground it pulls the tibia with it. In SSO condition (without wearing an AFO or a Tuned-AFO), this foot descent is controlled by the ankle dorsiflexors, allowing the foot to descend at a controlled rate. The presence of an AFO or Tuned-AFO cancels the effect of dorsiflexors control because plantarflexion is prevented, and the tibia accurately follows the foot. This quickens tibial advancement and inclination, and thus increases knee flexion. This effect continues until terminal

stance. In terminal stance, as the AFO and Tuned-AFO continue their work to prevent ankle motion, dorsiflexion in terminal stance will be reduced, decreasing tibial advancement. Proximally, the femur is free to move forward. Femoral advancement occurs due to knee extension moment created by GRF being anterior to the knee and due to momentum effect from other lower limb swinging forward. Consequently, femur is free to move forward while tibia is not. The net effect will be an increase in knee extension in terminal stance compared to walking with SSO.

➤ Stroke participants

In this study, the main characteristic of knee motion in stroke participants while walking with SSO is the extremely reduced or absent knee flexion during loading response (except *SP3*). This is due to the absent heel rocker affecting tibial advancement and knee flexion. The foot is usually plantarflexed at initial contact in stroke participants and foot descent towards the ground is extremely reduced or absent. Consequently, dorsiflexors control on foot descent is no longer necessary, cancelling their pulling effect on the tibia, and thus, retaining the extended position of the knee present in terminal swing (Meadows et al., 2008, Perry and Burnfield, 2010). This continues throughout stance and even causes stance phase to be longer than in control participants, as the knee is very hard to bend. In swing phase, the typical knee motion in stroke participants is characterised by reduced knee flexion. Two reasons may cause this. Firstly; knee flexion is very difficult during stance in stroke participants (for the aforementioned reason). Knee flexion in initial swing is the result of knee flexion starting in terminal stance and continuing in pre swing due to gastrocnemius rebound and knee flexion moments, respectively. As knee flexion in these two phases is reduced, knee flexion in initial swing is reduced as well. Secondly, hip flexion in stroke participants is decreased in pre swing and initial swing (This will be further discussed below under the heading “Hip joint kinematics”). Knee flexion that occurs during initial swing is believed to be enhanced by hip flexion; inertial characteristics of tibia resisting forward motion following hip flexion, resulting in knee flexion (Perry and Burnfield, 2010).

The increase in knee flexion during loading response with the use of AFO when compared with SSO is consistent with the findings of several previous studies (Fatone et al., 2009, Mulroy et al., 2010). However, some studies found no change in knee flexion during

loading response with the use of AFO (Gatti et al., 2012, Zollo et al., 2015). These contradictory results could be related to the different designs and/or stiffness of AFOs and participants impairments. The increased knee flexion during loading response while wearing an AFO may have resulted from the reduction of the excessive plantar flexion position of the ankle made by the AFO; which reduces the plantarflexed position of the foot at initial contact; re-establishing initial contact with the heel which improves the knee flexion moment rather than starting the initial contact with forefoot; which leads to losing the heel rocker and to moving the tibia backward creating a knee extension moment. Nevertheless, *SP6* showed knee hyperextension while wearing an AFO, which may suggest that the participant walks with extreme plantarflexion that leads to transferring the weight of the limb through the front part of the foot rather than smoothly transferring it from the heel throughout the length of the foot, thus the tibia is driven backward as the heel drops to the ground. This may also suggest that this participant walks with extreme hip flexion during stance in SSO; which may explain the inability of this participant to walk securely on a treadmill with SSO.

Wearing a Tuned-AFO resulted in greater knee flexion during loading response in all stroke participants compared to wearing AFO, which is consistent with a previous case study (Jagadamma et al., 2010). The inserted tuning wedges in Tuned-AFO led to an increase in heel height. It was shown that increased heel height of the shoes (Simonsen et al., 2012) and adding heel wedges underneath an AFO (Kerkum et al., 2015b) alter knee kinematics and cause an increase in knee flexion in early stance. In addition to the reasons explained above, a Tuned-AFO realigns the tibia from an initial reclined position to allow it to be slightly more inclined compared to AFO, the increased tibial inclination allows the knee to flex even more by the end of loading response. Those effects continue throughout stance and will place the knee further anteriorly (compared to AFO) during mid to terminal stance, resulting in reduction in knee extension and in improving knee flexion during pre swing and initial swing. The results of the current study showed an obvious decrease of knee extension during terminal stance and an increase in the knee flexion peak during swing in all stroke participants. In a previous case study (Choi et al., 2016), when comparing the effects of altering the alignment of SVA from 15° to 12° in a rigid AFO, it was found that reducing the SVA decreased the knee extension in terminal stance and increased the knee flexion peak during swing. In contrast, another case study

(Jagadamma et al., 2010) found no difference in knee flexion peak during swing, and a reduction in the knee extension during terminal stance when comparing walking with a rigid AFO (SVA 0°) to a rigid AFO after tuning (SVA 12°). These contradictions between findings may be due to the different participants' characteristics and/or the variation of the rigid AFO characteristics such as the AA-AFO, materials and trimlines.

❖ *Hip joint Kinematics*

➤ Control participants

In control participants, wearing an AFO and a Tuned-AFO had minimal effect on hip motion as compared to SSO. This may be explained by the fact that an AFO or a Tuned-AFO are likely to have minimal effect on the proximal joints, as they do not extend beyond the proximal leg region, especially in a participant showing normal gait pattern. The main striking difference is that the hip is slightly more flexed during initial contact and loading response in AFO and Tuned-AFO compared to SSO. This may have resulted from the more flexed knee joint position in terminal swing in these two conditions. Contacting the ground with a flexed knee dictates that hip flexion is greater as foot is in contact with ground, and knee flexion is associated with hip flexion.

➤ Stroke participants

In this study, the main characteristic of hip motion in stroke participants while wearing SSO is that the hip is flexed throughout stance. The persistent plantarflexion and the maintained knee hyperextension will limit the advancement of the body. The location of the GRF (in front of the knee and hip) and the knee hyperextension position make hip extension difficult due to the presence of an external hip flexion moment. Stroke participants try to lean their upper body anteriorly to improve the forward reach of the opposite limb. This creates progression by forward fall of their body weight, substituting the lost progression effect from losing heel and ankle rocker.

Wearing an AFO or a Tuned-AFO resulted in less hip flexion in all participants. In fact, *SPI* showed an almost normal hip joint motion in AFO and Tuned-AFO. Although the other stroke participants showed less-normal hip motion with varying degrees of improvement, the hip flexion peak was improved (reduced) in all stroke participants. Wearing an AFO or a Tuned-AFO realigns the tibia to be more inclined, an issue that in

turn facilitates stroke participants' progression. Altering the alignment of tibia to be more inclined induces realigning the femur to be inclined forward; which leads to GRF moving posteriorly relative to the hip during mid to terminal stance and the hip joint to be shifted anteriorly. This can reduce the undesirable hip flexion moment and facilitate hip extension, and thus participants could walk with less flexed hips in stance. Wearing a Tuned-AFO results in a more decrease in hip flexion, as tibia is more inclined in a Tuned-AFO as compared to an AFO. As discussed earlier, controlling the tibial alignment to be more inclined would facilitate the GRF to be as close as possible to the joint centre so that it passes anterior to the knee and posterior to the hip. Thus, more hip extension is facilitated. There is limited information in the literature with regard to the biomechanical effects of a rigid AFO/Tuned-AFO on hip motion in stroke patients. In a previous study (Carse et al., 2015), the consequences of tuning rigid AFOs on hip motion for 8 early stroke patients varied among the participants making comparison/conclusion among them difficult. In agreement with our findings, walking with a rigid AFO with AA-AFO set at 90° and a rocker bar (as an alternative way of tuning) statistically significant increased hip extension compared to AFO without rocker bar or barefoot conditions (Farmani et al., 2016a). In contrast, another study (Zollo et al., 2015) found no statistically significant differences in the hip motion when walking with non-tuned AFOs compared to shoes condition. The design and/or tuning and/or the stiffness of the AFO may influence the effectiveness of the AFO at hip joint. In the study by Zollo et al. (2015) an AFO with heel opening was used (the authors considered it as off-the-shelf rigid AFO but this is questionable based on the image of the AFO presented in their study). In the current study a custom made rigid AFO with carbon fibre reinforcement at the ankle region of the AFO was used, suggesting that the AFO used in the current study is stiffer than the AFO used in the study by Zollo et al. (2015). Although there is a low evidence of the impact of AFO stiffness on hip kinematics, these contradictory results could be related to the different designs and/or tuning and/or stiffness of AFOs. This is especially so as higher stiffness materials are considered to be more effective in controlling and supporting the foot and ankle than lower stiffness materials (NHS Quality Improvement Scotland, 2009, Totah et al., 2019).

5.1.4 Kinetic parameters

The kinetics results of the current study can be explained in the scope of healthy and stroke patients' gait as described in section 2.3 under the heading "Normal and post stroke gait".

❖ *External ankle moments*

➤ Control participants

In control participants, the plantarflexion moment peak during loading response was greater with Tuned-AFO compared to AFO. The tuning wedge(s) was/were inserted under the heel of the AFO (inside the standard shoes) to optimise the SVA alignment. Using different type/design of tuning wedges may have an effect on moment acting on the tibia (Waters and Bontrager, 1979). In both Tuned-AFO and AFO (before tuning) conditions, the participants were fitted with the same type of shoes. However, there was alteration at the heels in the Tuned-AFO as high-density tuning wedge(s) made from synthetic cork was used to tune the AFO. Higher density materials have been found to produce a greater moment than lower density materials (Kerkum et al., 2015a, Waters and Bontrager, 1979). Thus, using the high-density materials may have led to an increase in plantarflexion moment. These changes highlight the importance of considering the heel design/materials when tuning orthoses.

➤ Stroke participants

In this study, the ankle moments in stroke participants while wearing SSO showed only dorsiflexion moment during the whole of stance except in pre swing, when dorsiflexion moment decreases. Stroke participants walking with SSO start their gait cycle contacting the ground with their forefoot making the point of application of the GRF anterior to the ankle and generating a dorsiflexion moment and a knee extension moment. The flexed hip and extended (or hyperextended) knee posture place GRF far anterior to the ankle leading to the absence of plantarflexion moment and an increasing dorsiflexion moment throughout stance.

The rigid AFO role in reducing the plantarflexion position of the ankle has a great direct effect on modifying GRF alignment in relation to the foot. Consequently, this will alter

the moments acting on the ankle after using the AFO (Bowker et al., 1993, Meadows et al., 2008). The rigid AFO uses a “three-force system” to block motion at the ankle as discussed in section 2.5.3 under the heading “Biomechanical effects of rigid AFO”. In this study, controlling the ankle plantarflexion deformity allows the stroke participants to start the gait cycle with heel contact which allows the GRF to start its application posteriorly to the ankle generating a plantarflexion moment and knee flexion moment. Tuning an AFO further facilitates starting the gait cycle with heel contact as tuning enhances alignment of the foot in relation to the ground.

In agreement with a previous case study (Choi et al., 2016), wearing an AFO or a Tuned-AFO resulted in a first peak of plantarflexion moment during early stance in all participants except *SP4*. The plantarflexion moment during early stance in an AFO or a Tuned-AFO may have resulted from changes in knee and hip postures; i.e. increased hip and knee flexion, resulting in a near-normal body alignment. Consequently, GRF is posterior to the ankle during early stance causing a plantarflexion moment. As the body progresses forward (by hip and knee extension), GRF moves anterior to the ankle resulting in a dorsiflexion moment. Reviewing the kinematics of the hip, knee, and ankle, and SVA of *SP4*, shows that SVA improvement (increment in inclination) is the least amongst the stroke participants. Additionally, hip motion in this participant shows very little improvement (hip flexion remained high). Both postures will cause the GRF to be anterior to the foot throughout stance, causing the absence of plantarflexion moment in this participant.

❖ *External knee moment*

➤ Control participants

To understand knee moments pattern while wearing an AFO or a Tuned-AFO, it is first important to note that during normal gait GRF travels anteriorly throughout stance. This creates a dorsiflexion moment at the ankle and a flexion moment at the hip. The knee presents a special case, as the knee moves forward and backward in relation to the GRF as it moves into flexion and extension. In early loading response, the GRF is anterior to the knee creating an extension moment. The knee then flexes (due to the effect of heel rocker on tibia) and moves anteriorly to GRF, creating a flexion moment. This moment increases as the knee is in flexion and then decreases as the knee extends in mid and

terminal stance. Knee flexion in pre swing moves the GRF posterior to the knee creating a flexion moment. In control participants, wearing the AFO or Tuned-AFO increases knee flexion in early stance and afterwards, causing knee flexion moment to increase in early stance. As Tuned-AFO results in greater knee flexion in early stance (this positions the knee further anterior to the GRF as explained earlier), knee flexion moment is greater in a Tuned-AFO than in an AFO.

➤ Stroke participants

In all stroke participants (except *SP3*), knee extension moment predominates in stance while walking with SSO. As explained earlier, the persistent plantarflexion of the ankle leads to knee hyperextension and large hip flexion that are noticed in stroke participants. Thus, the GRF alignment is inappropriately altered to pass further anteriorly to the knee centre and anteriorly to the hip joint centre, which will lead to an increase in the moment arms and thus an increase in the magnitude of the external moments at these two joints. As AFO and Tuned-AFO realign the tibia to be more inclined, the knee joint will be placed anteriorly during mid to terminal stance. This will realign the GRF to pass closer to the knee joint; resulting in the knee flexion moment noticed. Again, as Tuned-AFO resulted in greater increase in knee flexion and a greater decrease in hip flexion, it is now obvious why knee flexion moment while wearing a Tuned-AFO is greater than while wearing an AFO. Thus, the knee flexion moment peak at mid stance increased after tuning, while the external knee extension moment peak at terminal stance decreased after tuning. These findings are Consistent with previous studies (Choi et al., 2016, Jagadamma et al., 2010, Kerkum et al., 2015b, Kessels et al., 2013, Mulroy et al., 2010).

❖ **External hip moment**

➤ Control participants

Although all control participants accomplished the SVA target (10-12 degrees), no considerable difference was found in the hip moment among all walking conditions.

➤ Stroke participants

In stroke participants, the absent (or almost absent) hip extension moment while walking with SSO is caused by inappropriate anterior placement of the GRF as explained earlier.

The persistent plantarflexion and the resulting knee hypertension will lead to losing the heel and ankle rocker. If there is no heel rise (as the heel is already raised due to the plantarflexion deformity), the advancement of the body is limited to the extent that knee hyperextension and trunk lean improve the forward reach of the opposite limb. The location of the GRF is always in front of the hip creating a flexion moment. Wearing an AFO or a Tuned-AFO allows the tibia to be more inclined over the stance foot and allows the GRF moves in a near normal path relative to the hip, creating an extension moment during late stance.

In the current study, there were no obvious effects of Tuned-AFO in improving hip moment compared to AFO. This finding suggests that tuning an AFO may result in improvement in the hip kinematics but may have no effects on hip kinetics. However, it should be noted that the SVA in *SP5* and *SP6* was not adequate (less than 10 degrees) suggesting that some patients may need time to adapt to the tuning. A previous study (Carse et al., 2015) stated that tuning an AFO can be more valuable for patients with limited mobility and low level of motivation.

❖ *Vertical ground reaction force (GRF_v)*

➤ Control participants

In control participants, wearing an AFO or Tuned-AFO resulted in a shallower trough and slightly lower first and second peaks of GRF_v compared to wearing SSO. The lower first peak may reflect a slower walking speed or fear from fall as participants may have not be accustomed efficiently to the orthosis. The shallower trough may reflect reduced movement of the ankle, which is expected as the ankle is controlled by the orthosis. The lower second peak may be the result of inability of the participants to take the foot off the ground (Richards, 2018, Winter, 2009). This may be due to the slightly reduced knee flexion angle in pre swing.

➤ Stroke participants

In stroke participants, walking with SSO resulted in distorted GRF_v pattern as compared to normal. According to the study by Wong et al. (2004), the GRF_v in stroke patients is either bimodal M pattern, inverted U pattern, or A pattern. In the current study, *SP3* and

SP5 exhibited a bimodal M pattern that is similar in shape to the normal GRFv, but it has smaller first and second peaks, with magnitude less than the patient's body weight agreeing previous studies (Chen et al., 2007, Wong et al., 2004). The GRFv pattern of *SP2* can also be considered as a bimodal M pattern but with lower second peak compared to the first peak. *SP1* and *SP4* exhibited the A pattern; no clear first peak, second peak, nor a trough is noticed. This reflects the inability of the participants to load their limbs, transfer weight over the stance foot, and the inability or reduced ability to take the foot off the ground (Chen et al., 2007, Wong et al., 2004). These signs may be the result of the plantarflexion deformity exhibited by these participants. This deformity produces abnormal loading of the foot during loading response affecting the first GRF peak. The deformity then diminishes the limb ability to advance over the stance foot affecting the trough. The deformity also hinders the ability of the participant to lift the foot off the ground, resulting in delayed and inefficient toe off. Altering the alignment of the tibia and changing the knee and hip moment during mid to terminal stance will lead to a change in the magnitude/production of the second peak of the GRF. Reducing the SVA, increasing knee extension moment, and decreasing hip extension result in smaller or absent second peak of the GRF (Condie and Meadows, 1993, Lehmann, 1986, Meadows, 1984).

Stroke participants (except *SP4*) showed a closer to normal GRF pattern after wearing an AFO or a Tuned-AFO although the first and second peaks were generally lower than normal, and the trough was shallower. Appearance of the first GRF peak may imply that stroke participants were able to load their limbs more efficiently wearing an AFO or Tuned-AFO than with SSO (Richards, 2018, Winter, 2009). Generally, Tuned-AFO resulted in higher first peak of GRF suggesting better loading of the foot. This may be the result of the more neutral angle ankle due to the AFO and the wedges underneath of the orthosis when approaching the ground. The most striking finding was the appearance of a trough in stroke participants after wearing an AFO or a Tuned-AFO. This may imply better transfer of body weight forward, in other words, more efficient progression. This is expected as wearing an AFO or a Tuned-AFO resulted in more normal knee and hip joint posture and motion as the tibia was more inclined. All stroke participants (except *SP4*) in Tuned-AFO showed higher second GRF peak as compared to AFO. This reflects more efficient toe off and alteration in the alignment of the GRF in relation to the knee and hip resulting in reducing the excessive knee extension moment and in generating hip

extension moment in mid and late stance as the excessive plantarflexion was controlled by the AFO and Tuned-AFO.

SP4 presents a different case scenario as no clear first peak, second peak, nor trough were found while walking with AFO or Tuned-AFO. This participant showed very little improvement in knee moment and hip moment. This may have resulted in the participant's inability to move her body forward. Although the walking speed in *SP4* was improved with AFO/Tuned-AFO compared to SSO, *SP4* is still the slowest among all stroke participants (0.34 ± 0.2 m/s). This slow walking speed may also lead to the absence of the first peak of the GRFv pattern (Chen et al., 2007, Richards, 2018, Winter, 2009, Wong et al., 2004).

5.1.5 EMG outputs

Inspecting the EMG results of the current study reveals that vastus medialis and vastus lateralis exhibit approximately similar activation patterns in all conditions. This also holds true for the long head of biceps femoris and semitendinosus. Therefore, these pairs of muscle will be discussed together. Rectus femoris, on the other hand, will be discussed separately as it does not share the same activation pattern.

❖ *Vastus Lateralis (VL) and Vastus Medialis (VM) muscles activity*

➤ Control participants

In control participants, the EMG amplitude and timing of VL and VM activities (Figure 5.2) while walking with SSO were consistent with the expected normal patterns reported in Perry and Burnfield (2010). The need for VL and VM activation during loading response and early stance results from knee instability (flexion) during this time of stance. Heel rocker action on the knee results in knee flexion (and an anterior alignment of the knee in relation to GRF). In control participants, the slight increased VL and VM activity during loading response and early mid stance while wearing an AFO or a Tuned-AFO compared to SSO suggests increased need to stabilise the knee joint. This may be explained by the increased knee flexion motion reported in these conditions. In early mid stance, the activity of VL and VM while wearing an AFO was lower than with Tuned-AFO. As the foot contacts the ground, tibial advancement (dorsiflexion) is restricted by the AFO and thus the tibia is now held in position while the femur is free to move forward

(due to normally occurring knee extension). This eliminates the need for knee stabilisation by VL and VM. As the same mechanisms are active while wearing a tuned AFO, the larger knee flexion angle recorded in the Tuned-AFO necessitates the need for stronger and longer vastus lateralis and medialis activity.

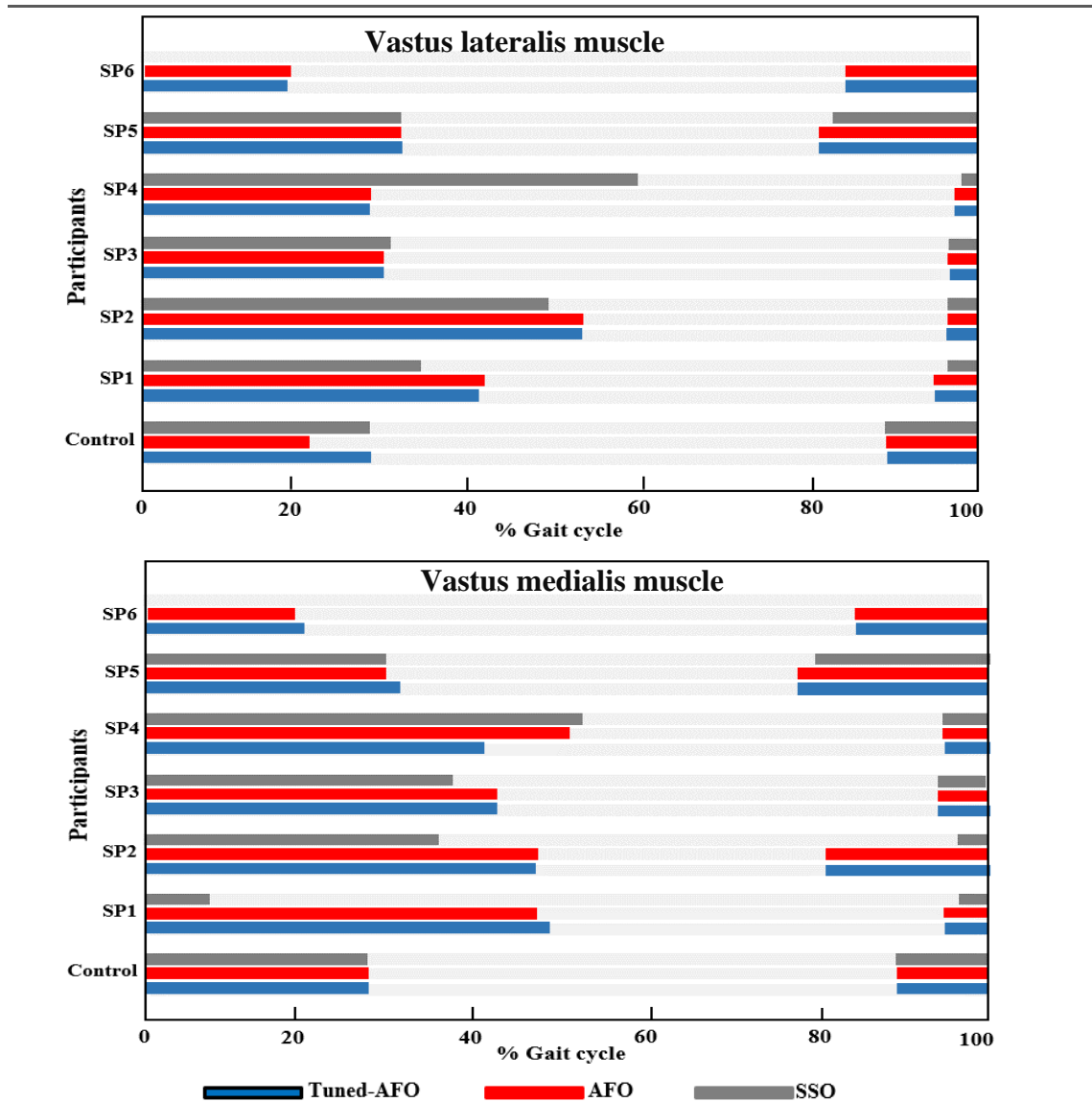


Figure 5.2: Vastus lateralis and Vastus medialis muscles activation time duration for all participants.

➤ Stroke participants

In stroke participants while wearing SSO (except *SP6*), the knee is in full extension or even in hyperextension due to the lost heel rocker action on the knee. The need for

stabilisation by VL and VM is not needed anymore; however, most of stroke participants showed prolonged activity of VL and VM during stance (Figure 5.2). This has been explained by the substitutive movements that stroke patients generally use to provide additional stability in the presence of insufficient function of plantarflexors. Plantarflexors generally are the major source of support during stance in normal gait. The insufficient function of plantarflexors in stroke patients is usually substituted by simultaneous contraction of knee extensors and flexors (Den Otter et al., 2007).

In the current study, wearing an AFO or a Tuned-AFO restores heel rocker action on the knee and thus the knee flexes, creating the need for VL and VM action. As knee flexion in an AFO or a Tuned-AFO continues further in stance; the excessive activity of VL and VM is required and continues for longer time to provide knee stability (Perry and Burnfield, 2010). To the best of the author's knowledge, the effects of tuning a rigid AFO (compared to non-tuned AFO) on knee extensor muscles for healthy and stroke patients during walking have not been evaluated. Few studies have investigated the effect of AFO on knee extensor muscles (Den Otter et al., 2007, Hesse et al., 1999). The findings of these studies were varying and inconclusive. The varying results may be due to the different participants' characteristics that are often not fully described in the literature, evaluating different muscles, and using different AFO types/designs. In agreement with our finding, a previous study showed that wearing a Valens caliper AFO (metal and leather AFO) showed an increase of the VL activity during early stance and mid stance due to quicker loading of the affected limb (Hesse et al., 1999). The Valens caliper AFO also lengthened the single support period (Hesse et al., 1999). Loading the affected limb in human and animal studies resulted in strong activation effects of antigravity muscles (Barbeau and Rossignol, 1994, Duysens and Pearson, 1980). A study by Mulroy et al. (2010) found no significant difference in vastus intermedius activity when walking with rigid AFO compared to wearing shoes only. Comparing the results in the current study to the results in the study by Mulroy et al. (2010) is difficult as different muscles were investigated.

In the current study, the excessive activity of VL and VM with the use of AFO/Tuned-AFO may be related to the fact that participants were anxious when walking with AFO on the treadmill and that they may require more time to familiarise themselves with the

treadmill and AFO. Further studies are required to investigate the prolonged effects of using AFO/Tuned-AFO on VL and VM activity.

The EMG sensors in the current study were placed over tested muscles according to SENIAM guidelines (SENIAM Organisation, 1999) in order to get the optimal EMG signal amplitude with the minimum cross talk interference from undesired/adjacent muscles (De Luca et al., 2010). However, VL activation pattern in *SP1* (Tuned-AFO condition) and *SP5* (all conditions) showed a clear small activation period of the VL during the end of terminal stance. This was considered as a cross talk of rectus femoris muscle, especially because VL activity in the end of terminal stance resembles the rectus femoris activity. A previous study (Howard et al., 2015) also showed that even when placing the EMG sensors ideally, they may still pick up cross talk from the adjacent muscles however, it is not considered as significant when the standard EMG protocol is followed.

❖ *Rectus Femoris (RF) muscle activity*

➤ Control participants

In control participants, the EMG amplitude and timing of RF activity while walking with SSO were consistent with the expected normal pattern reported in Perry and Burnfield (2010). RF activity is brief and occurs mainly during pre swing and initial swing (Figure 5.3). RF is believed to be active to control any increased knee flexion and hip extension that may occur during pre swing, which may lead to premature swing. Wearing an AFO or a Tuned-AFO restricts knee flexion in mid and terminal stance. This occurs because ankle dorsiflexion is prevented by the effect of the AFO or Tuned-AFO on tibial advancement. Combined with femur freedom to advance, the relative motion on the knee is extension, which is greater in an orthosis. Consequently, the need for RF to control excessive knee flexion is no longer the case.

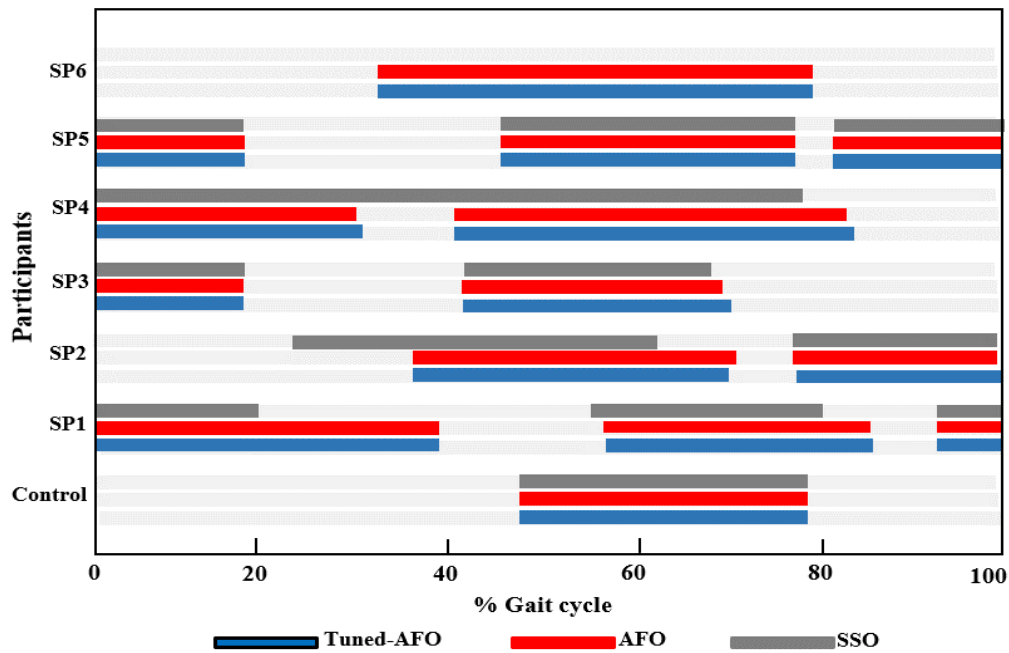


Figure 5.3: Rectus femoris muscle activation time duration for all participants.

➤ Stroke participants

In stroke participants, activation timing of RF differs greatly from control participants and also differs greatly among stroke participants while walking with SSO (Figure 5.3). This may suggest cross talk from nearby muscles, especially because RF activity in early stance resembles those of VL and VM (De Luca et al., 2010, Howard et al., 2015). It may also suggest abnormal RF activation pattern in an attempt to stabilise an instable knee in early stance, and to extend the knee in terminal swing. All stroke participants while walking with AFO or Tuned-AFO retained the period of muscle activation between 55% and 70% of the gait cycle, but with some added periods (Figure 5.3). Depending on knee motion pattern in AFO and Tuned-AFO conditions, RF contraction activity is expected to be greater than in SSO condition. This is particularly because AFO and Tuned-AFO resulted in greater knee flexion angles during pre swing and early swing than in the SSO condition. As aforementioned, to the best of the author's knowledge, the effects of tuning a rigid AFO (compared to non-tuned AFO) on knee extensor muscles have not been evaluated. However, a previous study by Zollo et al. (2015) compared the effects of walking with an AFO with heel opening (the authors considered them as off-the-shelf rigid AFO) on the co-contraction activity of the rectus femoris-biceps femoris with

walking with patient's own shoes. They found that AFO led to an increase, but not statistically significant, of co-contraction of the rectus femoris-biceps femoris. Although a similar effect has been reported in the study by Zollo et al. (2015) compared to our study, the results of their study were not statistically significant. This difference in the results may be due to using different AFO type/design. In addition, the participants in the study by Zollo et al. (2015) wore their own shoes; the type of shoes worn was not a constant condition in their study. Different shoes have been shown to affect the magnitude of lower limb muscle activity during walking (Murley et al., 2009, Stefanyshyn et al., 2000) which might be another factor leading to the difference between the two studies.

❖ *Biceps femoris(Long head) and Semitendinosus muscles activity*

➤ Control participants

In normal gait, Biceps Femoris (BF) and Semitendinosus (ST) are active primarily during terminal swing to control knee extension and prevent the knee from going in undesirable hyperextension (Perry and Burnfield, 2010). In the current study, this pattern was found in control participants while walking with SSO. As the knee was greatly flexed in AFO and Tuned-AFO conditions, the need for these muscles to check for knee extension is less and thus their contraction activity is expected to be less in these conditions. The activity of these muscles in the current study was found to be less in AFO and Tuned-AFO conditions as compared to SSO condition.

➤ Stroke participants

The pattern of BF and ST was found to be very similar in stroke participants, the activity of the BF and ST was recorded during loading response, early mid stance, and during mid and terminal swing, but it was also prolonged to the end of mid stance and initial swing. Major point to note is that the activity of BF and ST was less in AFO and Tuned-AFO conditions as compared to SSO condition. This might be due to the greater knee flexion recorded in these conditions. Stroke participants showed also increased activity in the BF and ST during mid stance in the SSO condition. This may be explained as an attempt to control the increased hip flexion that stroke participants use to move the GRF anteriorly to facilitate progression. As this hip flexion is reduced greatly in AFO and Tuned-AFO conditions, the need for these muscles' activation in this time is no longer needed, which

may explain the reduced activity of these muscles in AFO and Tuned-AFO conditions. It was also found that biceps femoris showed less activity in Tuned-AFO as compared to AFO in all stroke participants, and that semitendinosus activity was less in all stroke participants.

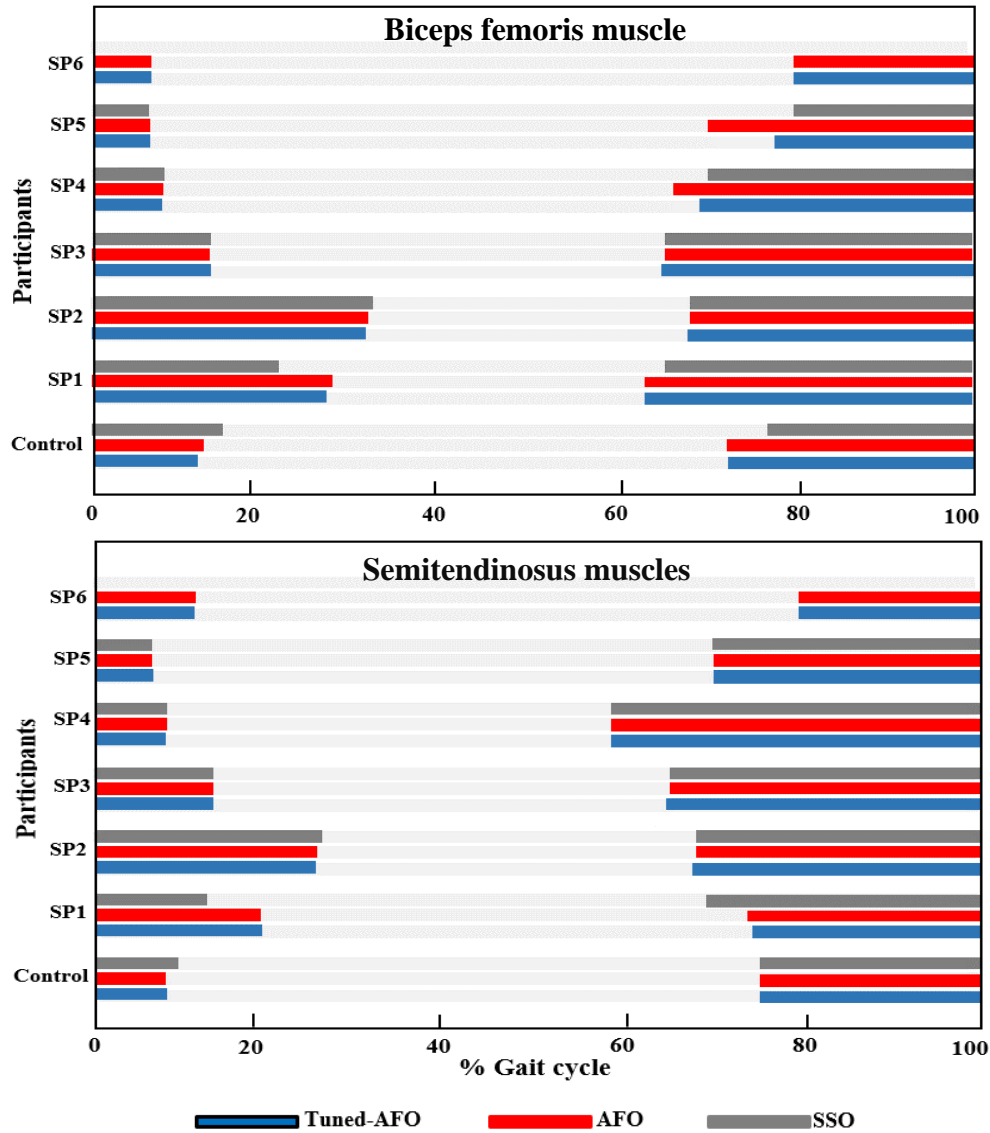


Figure 5.4: Biceps femoris and Semitendinosus muscles activation time duration for all participants.

5.2 The immediate effects of Tuned-AFO and rigid AFO (before tuning) on the orthotic and the anatomical moments

The secondary aim of this study was to measure the orthotic and the anatomical moments at the ankle joint in the sagittal plane and at the assumed subtalar joint in frontal plane and to investigate the immediate effects of optimising the SVA alignment during mid stance with the use of a rigid AFO on the orthotic and anatomical moments.

In the current study, the orthotic moment that is exerted by a rigid Homopolymer Polypropylene (HPP) AFO around the ankle joint during walking was measured following the same methods introduced by Papi et al (2015). In this study, four strain gauges (SGs) were attached to the AFO (SG1 and SG4 on the medial and lateral aspects of the AFO at the medial and lateral malleoli, respectively; SG2 on the posterior aspect of the AFO at the level of a line extended between the medial and lateral malleoli; SG3 on the posterior aspect of the AFO 30mm above and in line with SG2) as illustrated in section 3.3.1 under the heading ‘‘Strain gauges attachments’’. The SGs in current study were attached to the AFO in agreement with SG manufacture’s recommendations (Techni Measure Lab (TML), Tokyo, Japan) without the need for using UV light in the preparation of the HPP AFO surface. In the study by Papi et al (2015), the UV light was used in order to facilitate attachment of the SGs on the HPP. Using a cyanoacrylate adhesive (200 Catalyst-C and M-Bond 200, Micro-Measurements, UK) which is used specifically for attaching SGs to any plastic materials, eliminated the need for using the UV light. The SGs reading in this study showed a good consistency and repeatability (Appendix H), and this may support/indicate that this attachment technique may be considered as an adequate technique without the need for using the UV light.

Furthermore, similar to the methods used Papi et al (2015) study, a static calibration test was conducted on the strain gauged AFO to investigate the linearity and the repeatability of the SGs responses. However, instead of performing the static calibration manually using a calibration bench (Figure 2.43), an Instron tensile testing machine (Electroplus™ E10000 Instron, USA) was used in this study in order to assure accurate and repeatable results of the static calibration (Figure 3.6). The accuracy of static calibration depends on the accuracy of the calibration procedure (Choi et al., 2012, Karimi and Jamshidi, 2012). Performing the static calibration manually may increase the risk of

errors and mistakes. It is also a time-consuming procedure. Reliable and accurate measurement of orthotic moments is, however, subject to several challenges such as cross talk from non-axial load. Each SG in the current study was connected to three compensating resistors to create a full Wheatstone bridge circuit in order to detect any changes in the electrical resistance of the SG and to minimize the cross talk errors from non-axial load (Choi et al., 2012). The AFO was attached in a position that only allows for dorsiflexion/plantarflexion moments (measured by SG2 and SG3) to occur eliminating any frontal plane moments (measured by SG1 and SG4). In spite of this the SG1 and SG4 recorded a small electrical resistance. Likewise, when the AFO was attached in a position that only allows for inversion/eversion moments to occur eliminating any sagittal plane moment, SG2 and SG3 pick up a small electrical resistance. These small electrical resistances were considered as cross talk of non-axial load, especially because the viscoelastic nature of the HPP (the material of which the AFO was made in current study) involves molecular movement and rearrangement when a load is applied (Crawford and Martin, 2019). Thus, it is impossible to eliminate the cross talk effects. In an attempt to suppress these cross talks, the load was confirmed to be perpendicularly applied to the measurement direction and the calibration frame and the stainless-steel loading bar were firmly attached to the Instron to prevent any undesired movement during the test. Additionally, each SG was arranged in a quarter Wheatstone bridge configuration in order to eliminate any source of errors such errors arising from the non-axial load and temperature dependent errors (Choi et al., 2012).

The aim of using two SGs to measure the ankle moment for both sagittal and frontal planes (i.e. SG2 and SG3 in sagittal plane and SG1 and SG4 in frontal plane) was to provide a backup of the data in case of any failure that might occur in the SGs during the data collection. As expected, inspecting the SGs results of the current study reveals that no statistically significant differences were found between the orthotic moments that were derived from SG2 and SG3 outputs nor between the orthotic moments that were derived from SG1 and SG4. However, some results showed slight differences, that were not statistically significant, between the orthotic moments from SG2 and SG3 and between the orthotic moments from SG1 and SG4. These slight differences between findings may be due to the different geometry/curvature of the AFO where the SGs were attached which may have led to the observed differences of the SGs' outputs especially in the presence

of the viscoelastic nature of the HPP material (the material of which the AFO was made in this study) that is characterised by a non-instantaneous time-dependant response to the applied stresses.

5.2.1 Anatomical and Orthotic moments at the ankle in the sagittal plane

The anatomical and the orthotic moments at the ankle in the sagittal plane were measured using the strain gauged AFOs (as illustrated in section 3.6.3 under the heading ‘‘SG data analysis’’) during walking on a treadmill in control and stroke participants.

In all control and stroke participants, the orthotic moment was higher in the plantarflexion than in the dorsiflexion direction reflecting the need to counteract the dorsiflexion moment that predominates in stance. The main contribution of the AFO was to provide a plantarflexion moment at early stance counteracting the anatomical dorsiflexion moment measured at early stance. The orthotic moment during late stance provide dorsiflexion moment and was minimal in normal participants suggesting that the AFO provides no counteracting moments against the dorsiflexion moments present late in stance. In stroke participants, no orthotic dorsiflexion moment was measured during late stance supporting the finding in control participants. These findings are consistent with previous studies (Kobayashi et al., 2017, Miyazaki et al., 1993, Yamamoto et al., 1993b); however, these studies used an experimental AFO design that approximates the rigidity of a plastic AFO through the use of springs.

In the current study, the AFO is clearly capable of providing more than the contribution recorded in terminal stance. An explanation of why AFO do not provide a contribution in terminal stance is that the plantarflexors are doing all the effort needed to control dorsiflexion. Further studies are required to investigate the contribution that same AFO type/design has in different pathologies (flaccid vs spastic). It can be expected that AFOs may change their contribution depending on the needs placed upon them; i.e. the contribution of the AFOs in flaccid paralysis cases may be much greater than in spastic paralysis cases. Consequently, the orthotic moment provides information about the patient needs, rather than the information about what the AFO is capable of.

In control participants, Tuned-AFO showed higher peak orthotic plantarflexion moment as compared to AFO in early stance. This is also noticed in stroke participants *SP3* and

SP5. Anatomical dorsiflexion moment also increased in these participants. Other stroke participants show no differences in orthotic plantarflexion moment between AFO and Tuned-AFO.

In control participants and during mid stance, orthotic moment was greater in the Tuned-AFO condition compared to AFO, although the total ankle moment was less than in AFO. This also holds true for **SP3** and **SP5**. In these participants, anatomical dorsiflexion moment was less in Tuned-AFO as compared to AFO. The increased orthotic moment in the Tuned-AFO condition, is accompanied by a decrease in the anatomical moment when the total ankle moment decreases. Additionally, the orthotic moment increases in Tuned-AFO, and the anatomical moment increases when the total ankle moment increases. This suggests that the contribution of Tuned-AFO is greater than the AFO in resisting the total ankle moment, reflecting a smaller demand on the muscles of the participant. However, in the other stroke participants, there was no change noticed in all of the moments between AFO and Tuned-AFO. This may be due to the different characteristics of the stroke participants.

In control participants, AFO and Tuned-AFO can generate approximately (0.33 ± 0.05 Nm/kg, 0.47 ± 0.07 Nm/kg, respectively) of orthotic plantarflexion moment during early stance. In stroke participants, based on the mean, AFO and Tuned-AFO can generate approximately (0.17 ± 0.06 Nm/kg, 0.20 ± 0.08 Nm/kg, respectively) of orthotic plantarflexion moment during early stance. These results indicate that the orthotic plantarflexion moment generated in Tuned-AFO is higher than AFO (before tuning). However, these results are misleading because only **SP3** and **SP5** showed this while the other stroke participants showed no differences. Therefore, no clear conclusion can be drawn regarding the effectiveness of tuning on the orthotic moment.

Inspecting the relationship between total ankle moment and ankle angle, and orthotic moment and ankle angle reveals that whenever the ankle motion increases, the moments increase, either total ankle moment or orthotic moment (Figure 7.35, Figure 7.36). However, the orthotic moment increases in a greater manner in the plantarflexion motion, and the total ankle moment increases in a greater manner in dorsiflexion motion.

Increased orthotic moment in the plantarflexion direction may be explained by an increase in the resistance by the orthosis when the motion increases. Increased total moment in the

dorsiflexion direction may be explained by tibial alignment control that allows the knee to flex in early stance and to extend later on in stance, which in turn facilitates hip extension during stance. These factors allow smooth progression of GRF anteriorly resulting in greater total dorsiflexion moment.

Although in the current study both ankle motion and moments changed with AFO or Tuned-AFO, it is important to note that the change in ankle motion does not purely reflect orthosis deflection. Several possible factors may have led to the measured motion including; relative motion between the orthosis and the leg due to soft tissue compression within the orthosis, relative motion between the orthosis and shoes, the change in the positions of the reflective markers after tuning, and the short neck of the standard shoes which may not provide enough volume to accommodate all of the heel wedges which may have elevated the ankle region of the AFO above the upper edge of the shoes possibly making the fit of the tuned AFO inside the shoes in this region looser than other regions.

5.2.2 Anatomical and Orthotic moments at assumed subtalar joint in the frontal plane

In normal gait, the GRF is medial to the ankle throughout stance phase, causing a total inversion moment (Perry and Burnfield, 2010). However, and as the foot normally contacts the ground in an inversion position and then everts during stance, the GRF keeps moving in a medial direction from a position that is closer to the centre of the heel at initial contact (Chiu et al., 2013), as illustrated in Figure 2.5. This causes the total inversion moment to increase and reach a first peak during loading response, and then a second peak by the end of terminal stance. To the best of the author's knowledge, the effects of AFO on frontal subtalar joint have not been evaluated.

In the current study, first peak total inversion moment showed a decrease in AFO condition as compared to SSO condition for all participants. This may be due to the orthosis minimising frontal plane motion, and thus the GRF is no longer travelling in a medial direction causing the total inversion moment to be reduced.

In the Tuned-AFO condition, the first peak total inversion moment is reversed to eversion moment in control participants. This may be due to tuning effect on the foot. The tuning wedges can be considered as acting as a heel. Wearing a shoe with a heel was shown to

be causing an eversion moment during loading response (Barkema et al., 2012). Consequently, and as the wedges can be considered a heel, an eversion moment is expected.

In control participants, no differences were found between the Tuned-AFO and AFO conditions in the magnitude of anatomical moment. The anatomical moment shows a first peak inversion moment in control participants which is due to the action of invertor muscles to control heel eversion that occurs normally during gait after initial contact. The orthotic moment, however, is higher in the Tuned-AFO as compared to AFO. Orthotic moment, which counteracts anatomical moment but follows total moment, is expected to be higher in Tuned-AFO as the total moment is higher in Tuned-AFO.

In all stroke participants (except *SP3* and *SP5*), the first peak total inversion moment was higher than in control participants in the SSO. This may be due to the inverted position of the heel at initial contact. In normal gait, the eversion motion that occurs after limb loading is due to the alignment of the calcaneus lateral to the talus (Perry and Burnfield, 2010). In stroke patients, this alignment is faulty, and the calcaneus is medial in relation to the talus due to the spasticity of the invertor muscles. Consequently, varus deformity increases the lever arm medially of the GRF, causing greater inverting moment. Varus deformity in *SP3* and *SP5* was mild as compared to other stroke participants (who showed moderate deformity), and total inversion moment was less in *SP3* and *SP5* as compared to other stroke participants, supporting that the above justification is valid.

Anatomical moment in all stroke participants shows inversion moment which may be due to the spasticity of invertor muscles. Orthotic moment as expected is in the opposite direction, that is; eversion, to control the inversion anatomical moment.

5.3 The limitations of the study

There were several limitations of the current study including:

- ◆ The relatively small sample size which limits generalisation of the results. Recruitment of stroke and control participants was limited by time and budget restrictions. To give more statistical power to the results, future research on the effects of tuning a rigid AFO on post stroke gait should include a larger sample size (at least 20 stroke participants, based on sample size calculation with 95% confidence interval, power 0.8 and 0.05

significance level), which is powered to evaluate the clinical significance of the statistical differences found. Increasing the sample size will lead to further analysis of the post stroke gait.

- ◆ The sample included in the current study will most likely not represent the wider stroke patients due to the heterogeneous nature of stroke.
- ◆ During SSO condition the data collected do not accurately reflect actual foot motion. This is because the reflective markers were attached to the shoes rather than the foot which is expected to result in larger artefacts due to relative motion between the foot and the shoes, and/or relative motion between the AFO and the shoes. In an attempt to reduce these artefacts, well-fitting shoes and tight lacing were confirmed for each subject.
- ◆ This study has only evaluated the immediate effects of using a rigid AFO/Tuned-AFO as the participants wore the AFO/Tuned-AFO for no more than 10 minutes before the test to become familiar with them.
- ◆ No surrogate limb was fitted within the AFO during the static calibration test. Consequently, the AFO could potentially rotate and bend in all planes, although no marked rotation/bending changes were noticed by the investigators. Additionally, performing the static calibration with a surrogate limb would provide more precise results as this would provide approximate forces to the forces applied via the limb during walking with AFO. However, in this study a wooden foot block was inserted in the foot section of the AFO and the AFO was firmly attached to the calibration frame in order to minimise any undesired rotation or motion during the static calibration test.
- ◆ All stroke participants who took part in current study already use various type/designs of their own AFO prescribed by their health own orthotic centres. This variation among participants' own orthosis may have had an effect on their gait pattern which in turn may have had an effect on the outcomes of this study.

Chapter 6 Conclusions and suggested future studies

6.1 Clinical implications

As has been shown in the results chapter and discussed in the discussion chapter of this thesis, the primary drawback of post stroke gait is the results of excessive plantar flexion during initial contact and loading response phases of gait. This results in a group of asymmetries and inefficiencies in post stroke gait. These include increased stance time percentage of the gait cycle, decreased stride length, decreased speed of walking, lost heel, ankle, and sometimes forefoot rocker, hyperextended knee gait, and excessively flexed hip gait. Some of these cause (and others are the result of) reduced progression. Secondary drawbacks of post stroke gait include reduced shock absorption function of the lower limbs (due to the lost normal ankle motion, knee motion, and hip motion).

Using Rigid AFO and Tuned-AFO improved the gait of stroke participants, mainly at the knee and the hip. Putting the study limitations into consideration, the following can be implied:

- 1- SVA can be used as a measure of overall improvement in post stroke gait (particularly at the knee), as has been shown in previous studies.
- 2- Rigid AFO/Tuned-AFO have the potential to improve swing phase quality by reducing equinus of the ankle and by providing better push off during pre swing (indicated by higher second peak of GRFv).
- 3- Rigid AFO/Tuned-AFO have the potential to improve initial contact of the foot by the heel, with the resulting improvement in heel rocker.
- 4- Rigid AFO/Tuned-AFO have the potential to reduce knee hyperextension during early stance with subsequent reduction of shock taken by the joints of lower limb.
- 5- Rigid AFO/Tuned-AFO have the potential to reduce hip excessive flexion during stance with subsequent reduction of biceps femoris and semitendinosus amplitude of activity. This may result in lower energy cost of walking; it may also prevent fatigue in these muscles.
- 6- Rigid AFO/Tuned-AFO have the potential to improve progression in post stroke gait. This can be concluded from the increased walking speed, decreased stance percentage of gait cycle, and increased stride length in stroke participants.

- 7- Rigid AFO/Tuned-AFO may have the potential to reduce energy cost of walking as closer to normal kinematics at the knee and the hip, and closer to normal rockers at the ankle and foot have been achieved by AFO/Tuned-AFO. However, further studies are required to directly measure improvements in energy cost of walking.
- 8- Rigid AFO/Tuned-AFO may have the potential to reduce shock taken by the joints of the lower limb, with subsequent reduction of lower limb joints deterioration. However, further studies are required to directly measure improvements in shock absorption function of the lower limbs.

6.2 Conclusions

Hypothesis 1 is accepted as the results obtained in this study support the hypothesis. On the other hand, hypothesis 2 is partially accepted as the obtained in this study partially support the hypothesis. An individual analysis for each patient would be more meaningful in order to understand individual responses to the AFO. Although there are variations between stroke participants, there are also some important common features.

The following points can be concluded from the findings of the current study:

- ✓ The gait pattern of post stroke patients is different from normal gait.
- ✓ The results have shown noticeable influences on the resulting gait patterns immediately after wearing a rigid AFO or a rigid Tuned-AFO.
- ✓ The rigid AFO demonstrated improvements in the gait parameters in terms of temporal-spatial, sagittal kinematics and kinetics (hip, knee and ankle), GRF, and knee muscle activity.
- ✓ Tuning of a rigid AFO also demonstrated improvements in the gait parameters in terms of temporal-spatial, kinematics, GRF, kinetics, and knee muscle activity as compared to SSO and with improvement in SVA, knee kinematics and kinetics compared to the rigid AFO before tuning.
- ✓ The results support the potential to use strain gauges to quantify/evaluate the orthotic moment that is exerted by a rigid homopolymer polypropylene AFO around the ankle joint during walking, as the SGs reading showed a good consistency and repeatability. The similar results found in SG1 and SG4, and in SG2 and SG3 reveal that one SG for

each plane would be enough to measure the orthotic moment. However, considering that the viscoelastic nature of the homopolymer polypropylene and the geometry of the AFO may have an effect on the readings of the SGs, further study should be performed by attaching more than two SGs in the sagittal plane and in the frontal plane to compare the results of SGs and to confirm that changing the location of SG within the same plane does not affect the resulting orthotic moment so that the time and efforts spent in precisely positioning the strain gauges can be saved.

✓ The current study quantified the orthotic moments generated from a rigid AFO/Tuned-AFO to control ankle joint motion in the sagittal plane. No clear evidence was found that tuning an AFO can change the orthotic moment. However, increased orthotic plantarflexion moment was associated with increased total plantarflexion moment and no changes were found in the anatomical moment, which suggests that any increase in the magnitude of the total ankle moment is modulated by the orthosis adding no burden on the patients' ankle muscles.

✓ Rigid AFO/Tuned-AFO showed improvement in the total frontal plane moment at the assumed subtalar joint. The orthotic moments at the assumed subtalar joint generated from a rigid AFO/Tuned-AFO were quantified and no clear evidence was found that tuning an AFO can change the orthotic moment. Tuning a rigid AFO did not alter the anatomical moment at the assumed subtalar joint.

✓ The results also provide an important finding about the interaction between the leg and the orthosis, as the orthosis has minimum or no contribution to ankle moment at late stance in this study. Thus, the orthotic moment provides information about the patient needs, rather than the information about what the AFO is capable of. This should ultimately improve AFO prescription procedure to provide an AFO that best fits the functional needs of the patients.

6.3 Suggested future studies

- In the current study only the effects of tuning on sagittal plane motion and moments of the major joints (and the assumed subtalar joint frontal moment) were investigated. 3-D kinematic and kinetic analysis of knee and hip in the frontal and transverse planes should be considered.

- This study has only evaluated the immediate effects of tuning a rigid AFO. Longitudinal studies would be beneficial to determine the long-term influence of tuning a rigid AFO on post stroke gait. The long-term impact of tuning a rigid AFO on muscle activity/spasticity and muscle length, particularly the muscles within the orthosis (ankle plantarflexor and dorsiflexor), is advised in order to provide better understanding of their role in influencing the magnitudes and directions of the external moments generated.
- Although the ankle was encompassed by a rigid AFO, a small range of motion was recorded at the ankle in the sagittal plane. The source of this motion is a point of debate and further investigation into how effectively the rigid AFO can block motion is required. Further studies to identify the source of the recorded total ankle range of motion are needed. The source may be due to deflection of the orthosis, compression of soft tissues or slippage in the shoes.
- Investigating the influence of gradually changing the tuning wedges' characteristics; such as the heel height (greater and less than the target heel height), length, and stiffness before using them as a part of tuning is also required.
- Further research is needed to evaluate the effects of tuning a rigid AFO on improving balance in several mobility tasks such as walking overground on various surfaces (such as polished floor as in the clinic room or carpet, slopes and cambers), sit-to-stand and climbing up and down stairs.
- Investigating the impact of improving the SVA in relation to the Centre of Mass (COM) may provide a thorough understanding for improving stroke patients balance and walking performance, and thus, ultimately improve their quality of life.
- Further research is required to compare the effects of using different type/design/alignment of AFOs on the orthotic and anatomical moments. Investigating the contribution of the AFO with different stiffness will provide more information that should be considered in orthotic prescription.
- Further study is required to investigate the contribution of the AFO in different pathologies.

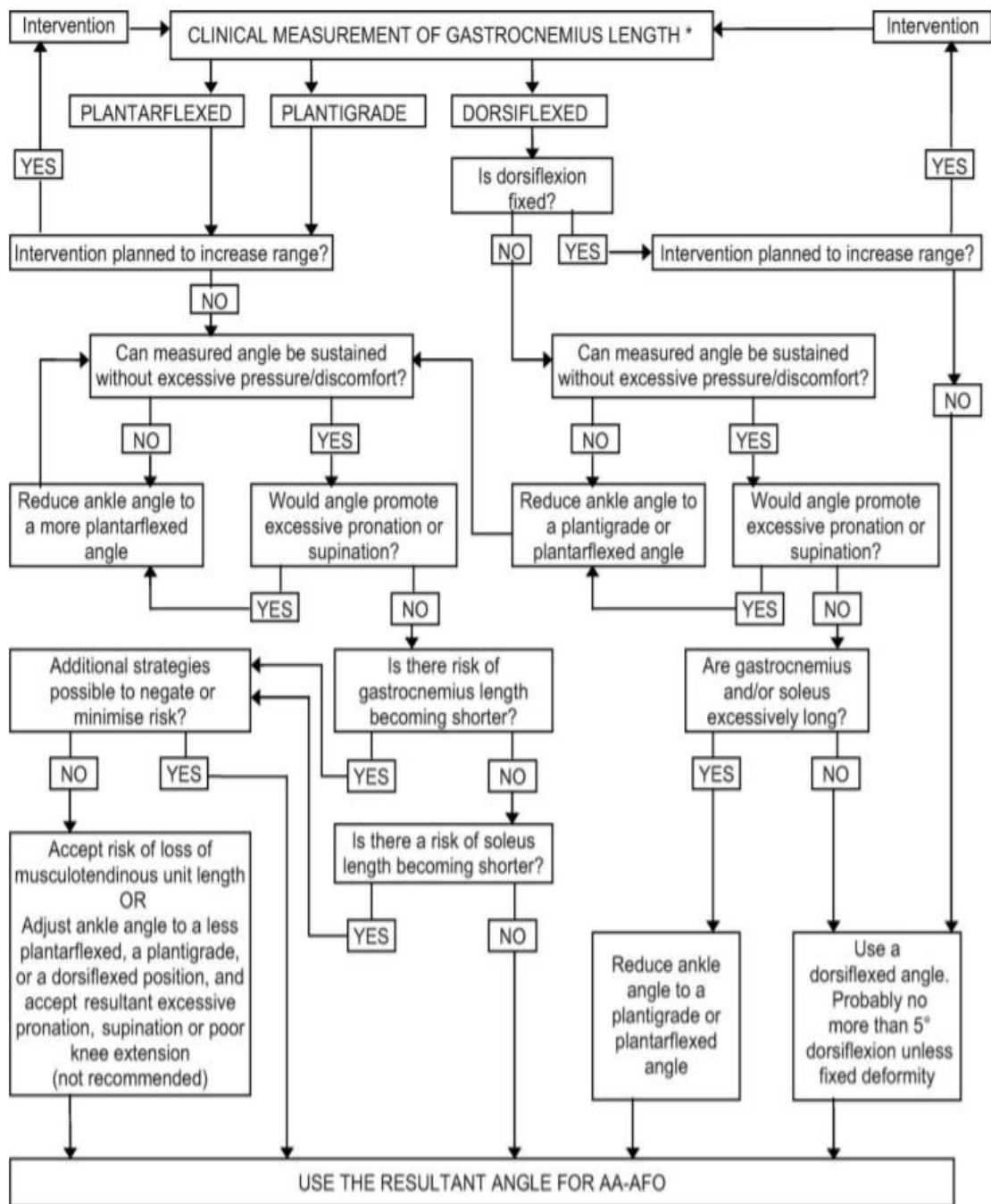
Chapter 7 Appendices

Appendix (A)

- Clinical recommendations for AFO prescription from ISPO consensus conference (Condie et al., 2004).

| <u><i>AFO Type</i></u> | <u><i>Clinical Indication</i></u> |
|-------------------------------------|----------------------------------------------------------------------------------------------------------------------------------------------------------------------------------------------------------------------------------------------------------------------------------------------------------------------------------------------------------------------------------------------------------------------------------------------------------------|
| <i>Rigid AFO</i> | <ul style="list-style-type: none"> ✓ Poor balance, instability in stance ✓ Inability to transfer weight onto affected leg in stance ✓ Moderate to severe foot abnormality; equinus, valgus or varus, or a combination ✓ Moderate to severe hypertonicity ✓ As above, but with mild recurvatum or instability of the knee ✓ To improve walking speed and cadence |
| <i>Articulated AFO</i> | <ol style="list-style-type: none"> 1. Dorsiflexor weakness only 2. Where passive or active range of dorsiflexion is present 3. Where dorsiflexion is needed for sit-to-stand or stair climbing 4. To control knee flexion instability only, articulated AFO with dorsiflexion stop 5. To control recurvatum only, articulated AFO with plantarflexion stop 6. To improve walking speed and cadence |
| <i>Posterior Leaf Spring</i> | <ul style="list-style-type: none"> ✓ Isolated dorsiflexors weakness ✓ No significant problem with tone ✓ No significant medio-lateral instability ✓ No need for orthotic influence on the knee or hip |

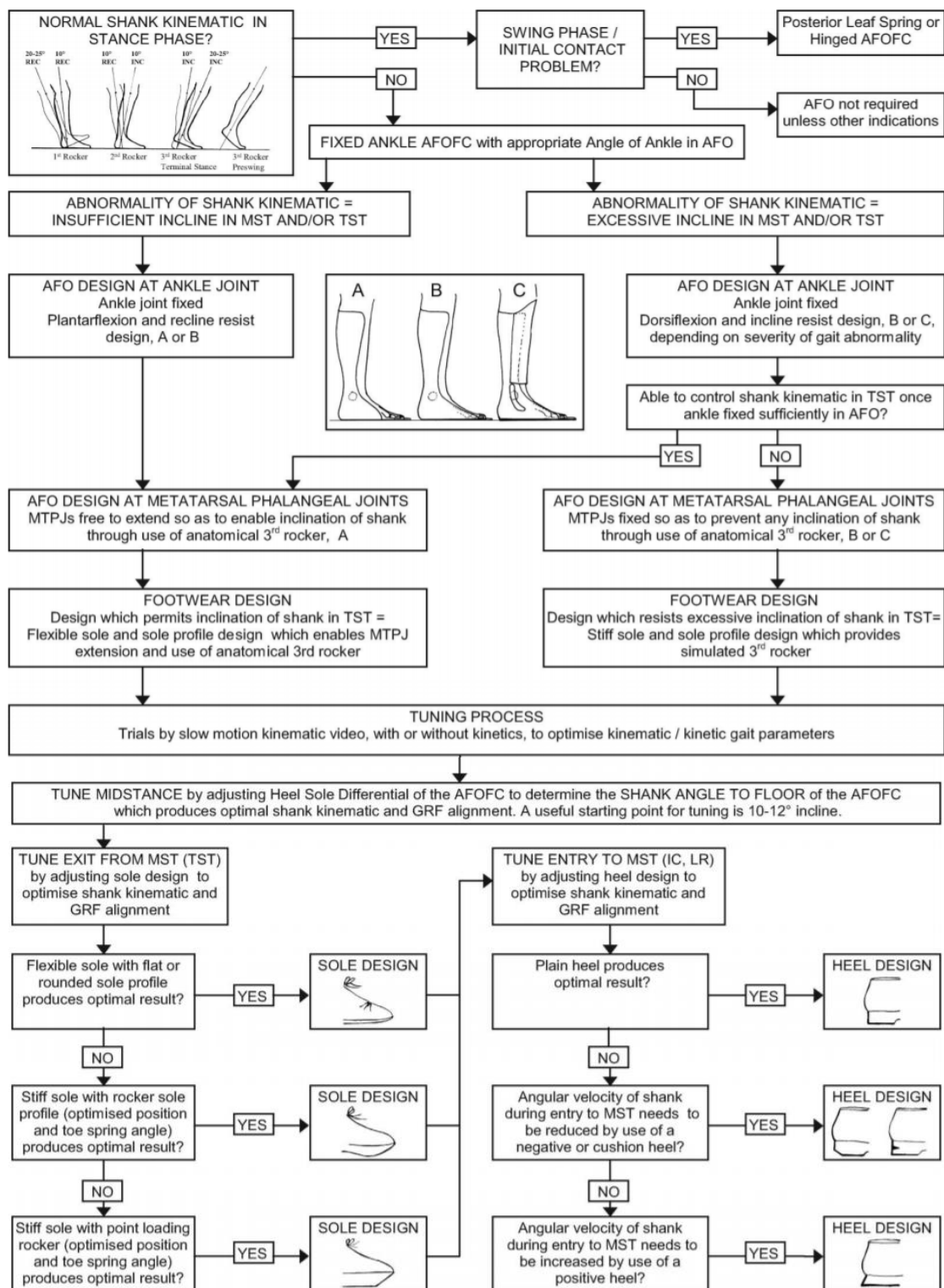
➤ Proposed algorithm for deciding AA-AFO casting sagittal angle (Owen, 2010).



*Note about measurement

Position to measure gastrocnemius length: the knee: extended, the foot: dorsiflexed and supinated, neutral or pronated depending on which is associated with the least range. The supinated foot position will therefore be used for feet that escape into a pronated position and the neutral or pronated position will be used for feet that escape into supination.

- A clinical algorithm for the design and tuning of ankle-foot orthosis footwear combinations (AFO-FCs) based on shank kinematics (Owen, 2010).



Appendix (B): Randomization plan from (www.randomization.com)

1. _____
 - AFO
 - SSO
 - Tuned-AFO
2. _____
 - SSO
 - Tuned-AFO
 - AFO
3. _____
 - Tuned-AFO
 - SSO
 - AFO
4. _____
 - Tuned-AFO
 - AFO
 - SSO
5. _____
 - Tuned-AFO
 - SSO
 - AFO
6. _____
 - SSO
 - AFO
 - Tuned-AFO
7. _____
 - Tuned-AFO
 - AFO
 - SSO
8. _____
 - AFO
 - SSO
 - Tuned-AFO
9. _____
 - AFO
 - SSO
 - Tuned-AFO
10. _____
 - Tuned-AFO
 - AFO
 - SSO
11. _____
 - SSO
 - Tuned-AFO
 - AFO
12. _____
 - AFO
 - Tuned-AFO
 - SSO

Appendix (C): West of Scotland Research Ethics Service letter.

WoSRES
West of Scotland Research Ethics Service



Mr Stephanos Solomonidis
Visiting Senior Lecturer
The University of Strathclyde
40 George Street,
Graham Hills Building, Biomedical Engineering
department Glasgow
8 floor
G1 1QE

West of Scotland REC 3
Research Ethics
Clinical Research and Development
West Glasgow Ambulatory Care Hospital
Dalnair Street
Glasgow
G3 8SJ
(Formerly Yorkhill Childrens Hospital)

Date 12 November 2018
Direct line 0141 232 1807
E-mail WoSREC3@ggc.scot.nhs.uk

Dear Mr Solomonidis

Study title: An investigation into mechanical and biomechanical effects of using solid Ankle Foot Orthoses in stroke patients during walking
REC reference: 18/WS/0178
Protocol number: N/A
IRAS project ID: 240196

Thank you for your letter of 10 October 2018, responding to the Committee's request for further information on the above research and submitting revised documentation.

The further information was considered in correspondence by a Sub-Committee of the REC. A list of the Sub-Committee members is attached.

We plan to publish your research summary wording for the above study on the HRA website, together with your contact details. Publication will be no earlier than three months from the date of this opinion letter. Should you wish to provide a substitute contact point, require further information, or wish to make a request to postpone publication, please contact hra.studyregistration@nhs.net outlining the reasons for your request.

Confirmation of ethical opinion

On behalf of the Committee, I am pleased to confirm a favourable ethical opinion for the above research on the basis described in the application form, protocol and supporting documentation as revised, subject to the conditions specified below.

As a feedback only, with regards to the statistical aspects, please note that it is the test that is parametric (e.g. a t-test or ANOVA) or nonparametric (e.g. Wilcoxon test) and not the data. The data is assessed for normality and then the choice of a parametric or nonparametric test is taken.

Conditions of the favourable opinion

The REC favourable opinion is subject to the following conditions being met prior to the start of the study.

Management permission must be obtained from each host organisation prior to the start of the study at the site concerned.

Management permission should be sought from all NHS organisations involved in the study in accordance with NHS research governance arrangements. Each NHS organisation must confirm through the signing of agreements and/or other documents that it has given permission for the research to proceed (except where explicitly specified otherwise).

Guidance on applying for HRA and HCRW Approval (England and Wales)/ NHS permission for research is available in the Integrated Research Application System, at www.hra.nhs.uk or at <http://www.rdforum.nhs.uk>.

Where a NHS organisation's role in the study is limited to identifying and referring potential participants to research sites ("participant identification centre"), guidance should be sought from the R&D office on the information it requires to give permission for this activity.

For non-NHS sites, site management permission should be obtained in accordance with the procedures of the relevant host organisation.

Sponsors are not required to notify the Committee of management permissions from host organisations

Registration of Clinical Trials

All clinical trials (defined as the first four categories on the IRAS filter page) must be registered on a publically accessible database within 6 weeks of recruitment of the first participant (for medical device studies, within the timeline determined by the current registration and publication trees).

There is no requirement to separately notify the REC but you should do so at the earliest opportunity e.g. when submitting an amendment. We will audit the registration details as part of the annual progress reporting process.

To ensure transparency in research, we strongly recommend that all research is registered but for non-clinical trials this is not currently mandatory.

If a sponsor wishes to request a deferral for study registration within the required timeframe, they should contact hra.studyregistration@nhs.net. The expectation is that all clinical trials will be registered, however, in exceptional circumstances non registration may be permissible with prior agreement from the HRA. Guidance on where to register is provided on the HRA website.

It is the responsibility of the sponsor to ensure that all the conditions are complied with before the start of the study or its initiation at a particular site (as applicable).

Ethical review of research sites

NHS sites

The favourable opinion applies to all NHS sites taking part in the study, subject to management permission being obtained from the NHS/HSC R&D office prior to the start of the study (see "Conditions of the favourable opinion" below).

Non-NHS sites (if applicable)

The Committee has not yet completed any site-specific assessment (SSA) for the non-NHS research site(s) taking part in this study. The favourable opinion does not therefore apply to any non-NHS site at present. We will write to you again as soon as an SSA application(s) has been reviewed. In the meantime no study procedures should be initiated at non-NHS sites.

Approved documents

The final list of documents reviewed and approved by the Committee is as follows:

| <i>Document</i> | <i>Version</i> | <i>Date</i> |
|--------------------------------------------------------------------------------------------------------------------------------|----------------|-------------------|
| Copies of advertisement materials for research participants [Advert] | 2.0 | 10 October 2018 |
| Copies of advertisement materials for research participants [Study Poster] | 3.0 | 05 November 2018 |
| Evidence of Sponsor insurance or indemnity (non NHS Sponsors only) [Univ of Strathclyde Employers Liability] | | 16 July 2018 |
| Instructions for use of medical device [NHS best practice of using leg splint] | | 01 August 2009 |
| IRAS Application Form [IRAS_Form_01112018] | | 01 November 2018 |
| Non-validated questionnaire [Questionnaire] | Version 2 | 30 October 2018 |
| Other [Certificate of eGCP] | | 03 September 2018 |
| Other [Certificate of eConsent] | | 03 September 2018 |
| Other [Figures] | 2.0 | 06 September 2018 |
| Participant consent form [Consent Form] | 2.0 | 10 October 2018 |
| Participant information sheet (PIS) [PIS] | 2.0 | 10 October 2018 |
| Research protocol or project proposal [Research Protocol] | 2.0 | 10 October 2018 |
| Response to Request for Further Information [Reply to NHS_Cover Letter] | 1.0 | 10 October 2018 |
| Summary CV for Chief Investigator (CI) [Chief Investigator CV] | 1.0 | 10 August 2018 |
| Summary CV for student [Amneh Alshwabka CV] | 1.0 | 10 August 2018 |
| Summary CV for supervisor (student research) [Stephanos Solomondis CV] | 1.0 | 10 August 2018 |
| Summary CV for supervisor (student research) [Roy Bowers CV] | 1.0 | 14 August 2018 |
| Summary of any applicable exclusions to sponsor insurance (non-NHS sponsors only) [Univ of Strathclyde Professional Indemnity] | | 16 July 2018 |
| Summary, synopsis or diagram (flowchart) of protocol in non technical language [Flowchart] | 1.0 | 03 September 2018 |

Statement of compliance

The Committee is constituted in accordance with the Governance Arrangements for Research Ethics Committees and complies fully with the Standard Operating Procedures for Research Ethics Committees in the UK.

After ethical review

Reporting requirements

The attached document "After ethical review – guidance for researchers" gives detailed guidance on reporting requirements for studies with a favourable opinion, including:

- Notifying substantial amendments
- Adding new sites and investigators
- Notification of serious breaches of the protocol
- Progress and safety reports
- Notifying the end of the study

The HRA website also provides guidance on these topics, which is updated in the light of changes in reporting requirements or procedures.

User Feedback

The Health Research Authority is continually striving to provide a high quality service to all applicants and sponsors. You are invited to give your view of the service you have received and the application procedure. If you wish to make your views known please use the feedback form available on the HRA website: <http://www.hra.nhs.uk/about-the-hra/governance/quality-assurance/>

HRA Training

We are pleased to welcome researchers and R&D staff at our training days – see details at <http://www.hra.nhs.uk/hra-training/>

| | |
|-------------------|-------------------------------------------------------|
| 18/WS/0178 | Please quote this number on all correspondence |
|-------------------|-------------------------------------------------------|

With the Committee's best wishes for the success of this project.

Yours sincerely

Abibat Adewumi

On behalf of

**Mrs Rosie Rutherford
Chair**

Enclosures: List of names and professions of members who were present at the meeting and those who submitted written comments

"After ethical review – guidance for researchers"

West of Scotland REC 3

Attendance at Sub-Committee of the REC meeting in November 2018

Committee Members:

| Name | Profession | Present | Notes |
|----------------------|--------------------------------------------------|---------|------------------|
| Dr Sarah J E Barry | Consultant Biostatistician & Chancellor's Fellow | Yes | |
| Mrs Lorna Hammond | Senior Clinical Pharmacist | Yes | |
| Mrs Rosie Rutherford | Volunteer - Lay Plus Member and Chair | Yes | Chair of Meeting |

Also in attendance:

| Name | Position (or reason for attending) |
|-----------------------------|------------------------------------|
| Mrs Abibat Adewumi-Ogunjobi | REC Manager |

Appendix (D): The Study poster

A study of the effectiveness of a leg splint during walking.

*Have you had a **Stroke**?*

*Do you wear a **lower leg splint**?*

*Would you take part in a **research study**?*

We are looking for people aged over 18 years and have had a stroke to help in a study investigating the performance of load sensors attached to a lower leg splint during walking.

If you take part, you will be invited to come to the National Centre for Prosthetics and Orthotics at the University of Strathclyde for three visits , approximately 2 hours each and we will record your walking whilst wearing a lower leg splint. The purpose of this study is to improve the design of the splint and prevent failures.

Travelling expenses incurred will be reimbursed.

For further information of how to participate in this study, please contact:

Mrs. Amneh Alshawabka
Postgraduate Research Student
Mobile: 07491978925
Mail: amneh.alshawabka.2016@strath.ac.uk



Study Poster, IRAS: 240196, Version 3.0 , 5/11/2018

Appendix (E): The Study Advert

Title of the investigation:

A study of the effectiveness of a leg splint in stroke patients during walking

The Biomedical Engineering Department of the University of Strathclyde would like to recruit stroke patients in order to study the performance of load sensors attached to a lower leg splint during walking.

This sensor allows the measurement of forces and bending or twisting actions on the splint generated during walking. This study aims to gain a thorough understanding of ankle joint load during walking in stroke patients and the effects of wearing a leg splint on this load. The results of this study may influence clinical decision making in choosing splint design and material that best matches the patient needs.

If you were to participate in the study, you will be invited to attend three sessions for no longer than 2 hours each at the National Centre for Prosthetics and Orthotics (NCPO) at the University of Strathclyde.

The first session will be a screening session to determine whether you can be included in the study, if so a plaster of Paris cast of your lower leg will be taken. The second session (one week later) will be to check the splint fitting, comfort and function. The third session (two weeks later) will be to record your walking on a treadmill.

Travelling expenses incurred will be reimbursed.

In order to meet our study criteria, we are seeking participants who:

- ✓ Have no or mild to moderate spasticity
- ✓ Are using a leg splint
- ✓ Are able to give informed consent.
- ✓ Are not pregnant
- ✓ Are over 18 years of age
- ✓ Are able to walk without walking aids up to 3minutes
- ✓ Have no hip or knee muscle shortening.

If you are interested in participating or would like further information, please get in touch with the research team below, and we will arrange a meeting, to discuss the study.

Mrs. Amneh Alshwabka
Postgraduate Research Student
Email: amneh.alshwabka.2016@strath.ac.uk
Tel: 07491978925
Biomedical Engineering Department
Graham Hills Building
40 George Street, Glasgow
Post Code G1 1QE

Or
Mr. Stephan Solomonidis
Senior Lecturer
Email: s.e.solomonidis@strath.ac.uk
Tel. 0141 548 3778
Department of Biomedical Engineering
University of Strathclyde
Graham Hills Building
40 George Street
Glasgow G1 1QE

Appendix (F): Participant information sheet and consent form

- Participant Information Sheet

A study of the effectiveness of a leg splint during walking.

We would like to invite you to take part in a research study. The study is being organised by the University of Strathclyde. Before you decide, it is important for you to understand why the research is being done and what you would need to do.

Please take time to read the following information carefully. Talk to others about the study if you wish. You are free to choose whether to not to take part. If you decide not to take part this will not affect the care you get.

If you have any questions about this study, you can talk to one of the researchers organising it: Amneh Alshawabka **07491978925**.

This information sheet is divided into two parts:

- Part 1 tells you the purpose of this study and what will happen to you if you take part.
- Part 2 gives you more detailed information about the conduct of the study.

Version: 2.0, 10/10/2018

IRAS ID: 240196

Part 1 – Purpose of the study

What is the purpose of the study?

During standing or walking, bodyweight is transmitted through the lower limb joints. This transmitted weight is called load and can be measured. This study aims to gain a thorough understanding of ankle joint load during walking and the effects of wearing leg splint on this load. Therefore, a sensor has been designed to record the loads in the splint during walking. The results of this study may influence clinical decision making in choosing splint design and material that best matches the patient's needs.

Why have I been invited to take part?

You have been invited to take part because you have had a stroke, and you meet all of the following inclusion criteria. You:

- ✓ Are over 18 years of age
- ✓ Are able to walk 10-15 steps on the treadmill, which correspond to 10 meters, without walking aids.
- ✓ Have no spasticity or with mild to moderate spasticity
- ✓ Have no hip or knee muscle shortening.
- ✓ Are not pregnant.
- ✓ Are using lower leg splint (Ankle-foot orthosis).

If you have any existing condition or have had any previous surgical procedure that will limit the required range of motion needed for normal walking (e.g. arthritis, joint fusion), or if you suffer from motion sickness, have epilepsy, or balance conditions other than stroke you will be excluded from the study. If you are living outside the Greater Glasgow and Clyde, and Lanarkshire health board areas, you will also be excluded from the study.

Do I have to take part in the study?

No, it is up to you to decide whether or not to take part, since participating in this study is completely voluntary and you may withdraw at any time. Also, even after agreeing to participate in our study, you are still free to withdraw at any time and without giving a reason. However, your anonymised data (i.e. data which do not identify you personally) cannot be withdrawn once they have been included in the study.

What will I have to do in the study?

If you decide that you would like to take part in the study, please contact the researcher (contact details are at the end of this sheet), who will arrange an appointment to check your suitability for the study and to answer any questions you may have.

You will be invited to attend **three sessions** for no longer than 2 hours each at the National Centre for Prosthetics and Orthotics (NCPO) at the University of Strathclyde. **The first session** will be a screening session to determine whether you can be included in the study; if so, a plaster of paris cast of your lower leg will be taken. **The second session** (one week later) will be to check the splint fitting, comfort and function. **The third session** (two weeks later) will be to record your walking.

In the first visit, you will be asked to sign a consent form if you are happy to take part. If you match all the selection criteria, a research team member will take a plaster of Paris cast of your lower leg. The cast will be removed after it dries, approximately 10 minutes. Then, you will be free to leave. This cast will be used to make a splint which will be fitted after one week.

In the second visit, once the splint has been made, you will be invited to visit the NCPO for checking the fitting, comfort and function of the splint. A heel wedge will be inserted under the splint to achieve a better posture for your lower legs. Additionally, another heel wedge will be placed under the other foot in order to equalise the leg length. Then, you will be free to leave. A load sensor will be attached to the splint before your third visit, Figure (1).

In the third visit, one week after your second visit, you will be invited to visit the laboratory at the NCPO. This laboratory is fitted with a treadmill and other equipment to record your walking patterns, Figure (3). You will need to wear close-fitting shorts (like cycling shorts, Figure 4) so that accurate motion of your legs can be recorded (appropriate, a clean laundered shorts will be provided to you by the department, if necessary, but you may feel more comfortable wearing your own clothes). You will have the opportunity to become familiar with the splint which you will wear with a long sock underneath. Additionally, you will wear standard shoes which will be provided in all sizes. The shoes will be sterilised before and after the test session using a sterilising spray.

It is important to note that the splint will only be used within the building in which the movement laboratory is housed.

Reflective markers will be attached at various anatomical landmarks on your legs and pelvis. These markers will be attached to your skin or to the close-fitting shorts using non-allergenic adhesive tape as shown in Figure (2). Other markers will be attached to plastic pads. These plastic pads will be attached to various parts of your leg using elastic strap. Additionally, to measure the electrical activity of your knee muscles, electrical sensors -called electrodes- will be placed on your skin (Figure 2). The location of the electrodes will be determined only by vision. However, you should note that some of these anatomical landmarks are in an intimate location (pelvis landmarks), therefore, at least two of the research members (a male and a female) will be present during each test session, and will be located by a researcher of the gender of your choice. For secure attachment of these electrical sensors, any hair on their locations will be removed using a standard disposable safety razor, and the shaved skin will be cleansed with mild gel abrasive and an alcohol wipe.

Before the walking test commences, a supportive harness will be fitted around your chest and shoulders. The harness is a set of bands hung from the ceiling and tightened comfortably around your chest and shoulders with the aim of eliminating the risk of falling. Afterwards, you will be asked to walk on the treadmill where your walking will be recorded. You will be asked to walk at different speeds, all within a range that is comfortable to you. Three tests will be performed in random order:

Test 1: Standard shoes only – you will be asked to walk while wearing standard shoes with no splint.

Test 2: Standard shoes with splint – you will be asked to walk while wearing standard shoes with the splint.

Test 3: Standard shoes with splint and heel wedge – you will be asked to walk while wearing standard shoes with the same splint as in test 2, with a heel wedge.

What are the possible benefits of taking part?

There are no direct benefits to you from participation. However, the study will help researchers and orthotists to learn more about the mechanical and the biomechanical properties of leg splints. This information might be taken into account in the future and may inform clinical decision making in choosing which splint design and materials would most match individual patient needs.

What are the possible disadvantages and risks of taking part?

1. Removing the plaster of Paris cast from your leg may cause mild skin abrasion, however, the casting and cast removal will be done by an experienced clinician.
2. There is a slight chance that you may experience discomfort from the splint. However, the splint will be made by an experienced orthotist and the test will be stopped if any discomfort is being experienced, so that the splint can be adjusted.
3. The testing requires some markers and electrodes to be attached to the skin with non-allergenic adhesive tape. Very occasionally this can cause a mild irritation to the skin. This should only be a temporary irritation since the markers and the electrodes will only be in place for a short time and will be very carefully removed. If you develop a reaction to the tape, the markers will be removed immediately. Removing the reflective markers and the electrodes attached with tape may cause mild discomfort, but these will be removed very carefully, or if you prefer, you can remove them yourself.
4. To reduce the risk of tripping or falling, you will be fitted with a supportive harness attached to the ceiling and tightened comfortably around your chest and shoulders. Moreover, if this happens the researchers will stop the treadmill immediately.
5. You will not be active throughout the entire session. Rest breaks are built in between tests while equipment is prepared. Moreover, you will be able to rest as required and refreshments will be provided. You will not be asked to perform any activity which causes distress to you.

What happens when the research study stops?

You will continue to receive your standard clinical care. Being involved in the study will not lead to a change in treatment or to a change of splint. The lower leg splint that has been made for this study will not be delivered to you and it will only be used during the walking trials within the university. Therefore, you will not be given the splint for outside use.

THIS COMPLETES PART 1 OF THE INFORMATION SHEET.

Part 2 – Further information about the study

What will happen if I do not want to carry on with the study?

You can withdraw from the study at any time by speaking to a member of the research team or by writing to us. You do not have to give a reason for not wanting to carry on with the study and the care you receive will not be affected because of your decision.

The data for the study will be written up by a PhD student as part of her degree. If you decide you want to stop being in the study before the data has been analysed it can be removed from the study. If you decide after this point it will not be possible to take your data out of the study.

If the study is stopped for any reason, you will be told why. Your care will not be affected.

What if there is a problem?

If you have a concern about any aspect of this study, you should ask to speak to any or all of the researchers who will do their best to answer your questions. Please contact the chief investigator, Mr Stephan Solomonidis, on 01415483778 or by email to s.e.solomonidis@strath.ac.uk.

If you remain unhappy and wish to complain formally, please contact:

Research & Knowledge Exchange Services
University of Strathclyde
50 George street, Graham Hills Building,
Glasgow
G1 1QE
Telephone 0141 548 4364
Email to ethics@strath.ac.uk.

The University of Strathclyde has insurance policies that provide cover for any professional negligence of its staff and/or students.

Will my study data be kept confidential?

The consent form will be kept confidential, in a secured locked cabinet of the chief investigators office in the department of Biomedical Engineering and will be only used as instructed in University Data Management Plan. Consent forms will be retained indefinitely and will not be destroyed.

All personal details will remain confidential. All generated data will be allocated a unique identifiable code (a number to be stored) to make it anonymous. The identified code will be password protected and will be accessible only by the research team of this study. All anonymous data will be stored on secure university website, Strathcloud, with access only by the named researchers. Its access and destruction will be in accordance with the University Data Management Plan. The anonymization code will be destroyed at the completion of the study (13 months).

None of your personal details (name, contact details and other identifiable personal information) will be used in any publication related to the study. Consent will be obtained to use images in publications and for teaching if needed. Facial and other identifying features will be obscured from the images, so that you will not be identified. The University of Strathclyde is registered with the Information Commissioner's Office who implements the General Data Protection Regulation (GDPR). All personal data on participants will be processed in accordance with the provisions of the GDPR.

What will happen to the results of the study?

The findings will be written up in the form of a report, which will be included in a thesis that forms part of a post-graduate student's PhD. Furthermore, it is also likely that this post-graduate student will write papers based on our findings, and these papers will be published in a professional, peer-reviewed journal. If you consent to be photographed, images may be taken during the test and will be used for publication/teaching purposes, however, your identity will be kept confidential.

Who is organising and funding the study?

The research is being organised and funded by the Biomedical engineering department at the University of Strathclyde.

Who has reviewed the study?

All research in the NHS is looked at by an independent group of people, called a Research Ethics Committee, to protect your interests. This study has been reviewed and approved by the West of Scotland Research Ethics Committee.

What happens next?

If you are interested to take part in the study, please contact any of the research team members using the information that is provided at the end of this participant information sheet.

If you have a concern about any aspect of the study to discuss, you can kindly e-mail or call one of the researchers to get more information about the study and/or to arrange for possible study visits.

It is entirely your choice to decide whether or not to take part in the study. If you are happy to take part and you are considered suitable for participation in the study, the researchers will schedule suitable appointment dates and times. The consent form can be handed to any of the investigators/researchers on the first visit.

In the case that you do not wish to be involved in the study, then the investigators of this study would like to take the opportunity to thank you for taking an interest in this research study.

If required, the researchers will arrange and pay for a taxi to pick you up and to take you back home at the end of your visit. Alternatively, if you would like to make your own transport arrangements, you will receive reimbursement of travel costs.

Once the study is over, a summary of the results can be provided to you, if requested, by contacting any of the investigators on the contact details given below.

Researcher contact details:

Thank you for reading this information – please ask any questions if you are unsure about what is written here. If you have any questions about this study, you can talk to one of the researchers organising it:

❖ Mrs Amneh Alshawabka
Postgraduate Research Student
Biomedical Engineering Department
Graham Hills Building
40 George Street, Glasgow
Post Code G1 1QE
Telephone: 07491978925
E-mail: amneh.alshawabka.2016@strath.ac.uk

❖ Mr Roy Bowers
Principal Teaching Fellow
Biomedical Engineering Department
Graham Hills Building
40 George Street, Glasgow
Post Code G1 1QE
Telephone: 0141 548 4699
E-mail: r.j.bowers@strath.ac.uk

❖ Mr Stephanos Solomonidis
Senior Lecturer
Biomedical Engineering Department
Graham Hills Building
40 George Street, Glasgow
Post Code G1 1QE
Telephone: 01415483778
E-mail: s.e.solomonidis@strath.ac.uk

❖ Mrs Karyn Ross
Senior Teaching Fellow
Biomedical Engineering Department
Graham Hills Building
40 George Street, Glasgow
Post Code G1 1QE
Telephone: 0141 548 3525/5952
E-mail: k.ross@strath.ac.uk



Figure (1): The instrumented leg splint

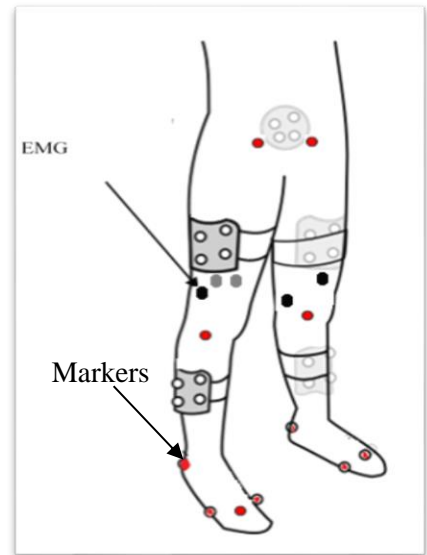


Figure (2): Markers and electrodes position



Figure (3): The Motek lab

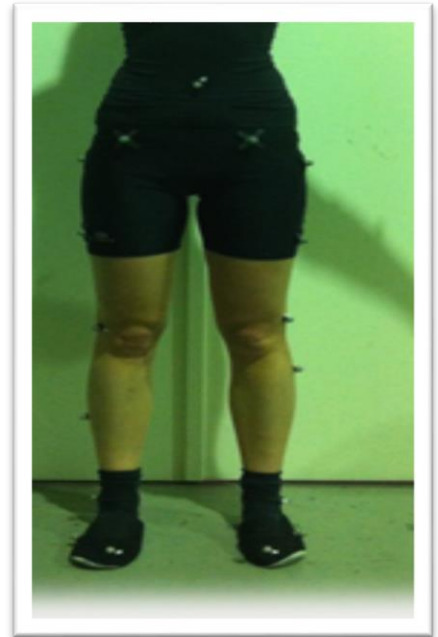


Figure (4): participant wearing appropriate clothing

➤ Consent form



Participant Identification Number for this trial: ____

CONSENT FORM

Title of Study: A study of the effectiveness of a leg splint during walking.

Name of Researcher: Amneh Alshwabka

Please initial box

1. I confirm that I have read and understood the information sheet (dated 10/10/2018, version 2.0) for the above study and the researcher has answered any queries to my satisfaction.
2. I understand that my participation is voluntary and that I am free to withdraw at any time without giving any reason, without my medical care or legal rights being affected.
3. I understand that I can withdraw from the study any personal data (i.e. data which identify me personally) at any time.
4. I understand that anonymised data (i.e. data which do not identify me personally) cannot be withdrawn once they have been included in the study.
5. I understand that any information recorded in the investigation will remain confidential and no information that identifies me will be made publicly available.
6. I consent to having my photograph taken as part of the study. Images which do not identify me personally may be used in scientific publications, teaching and conference presentations where their use would aid better understanding of the results.

| | |
|--------------------------|--------------------------|
| Yes | No |
| <input type="checkbox"/> | <input type="checkbox"/> |
7. I give my consent for my data stored at the University of Strathclyde (the study sponsor) for long term storage as part of an anonymised database with access only granted to the research team members in accordance with the University Data Management Plan.
8. I consent to being a participant in the study.
9. I confirm that I have received a copy of this consent form.

Name of Participant _____ Date _____ Signature _____

Name of person taking consent _____ Date _____ Signature _____

Researcher _____ Date _____ Signature _____

Appendix (G): Demographic data collection

A study of the effectiveness of a leg splint during walking.

Subject Number: _____.

Date: _____.

Subject group: Stroke patient

❖ Demographic collection

Gender: Male / Female

Age: _____.

Height (M): _____.

Weight (Kg): _____.

Tested AFO side: Right / Left.

Shoe size: _____.

Tuning Note: _____

_____.

Appendix (H): Strain Gauge Reliability Test

A reliability tensile test was conducted on homopolymer polypropylene plastic (North Sea Plastics Ltd., Glasgow, UK) samples of 5mm thickness (the same thickness and material used in AFOs fabrication). The aim of this test was to investigate the accuracy, repeatability, and the performance of the strain gauges (SGs) attached to homopolymer polypropylene plastic.

❖ *Materials and Methods*

Six dumbbell-shaped samples were cut from 5 mm thick homopolymer polypropylene plastic sheets (North Sea Plastics Ltd., Glasgow, UK) following the dimensions indicated in the British Standard ('BS 527-2', 1996) (Figure 7.1). This shape was assumed to reduce local stress concentration while allowing for an even distribution of stresses in the region where measurements are taken ('BS 527-2', 1996).

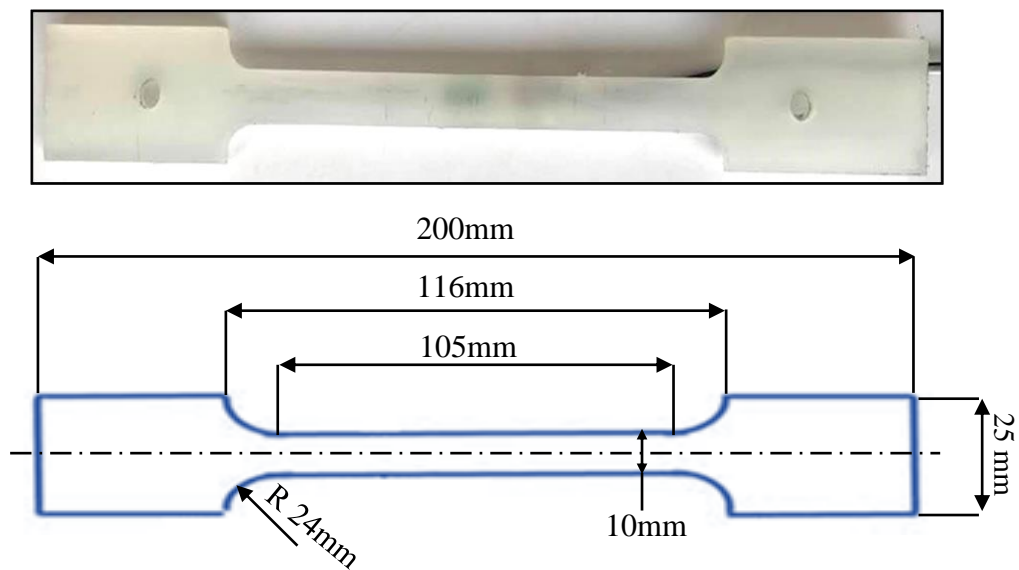


Figure 7.1: Test sample dimensions as obtained from the 5mm thick homopolymer polypropylene plastic sheet.

Two, two-element 90° degrees rosette strain gauges (2 mm long, 120 Ω; Techni Measure Lab (TML), Tokyo, Japan) were used and connected to create a full Wheatstone bridge circuit (Figure 7.2). This allowed small changes in electric resistance in the SG wires to

be detected and the strain to be determined. The two-element 90° rosette SGs were conducted to determine the Poisson's ratio of the homopolymer polypropylene material. Poisson's ratio is a measure of the Poisson effect which describes both the longitudinal and the transverse strains of the material. Therefore, a half Wheatstone bridge configuration on each sample side was created to measure the Poisson's ratio (transverse strain/longitudinal strain) (Figure 7.2).

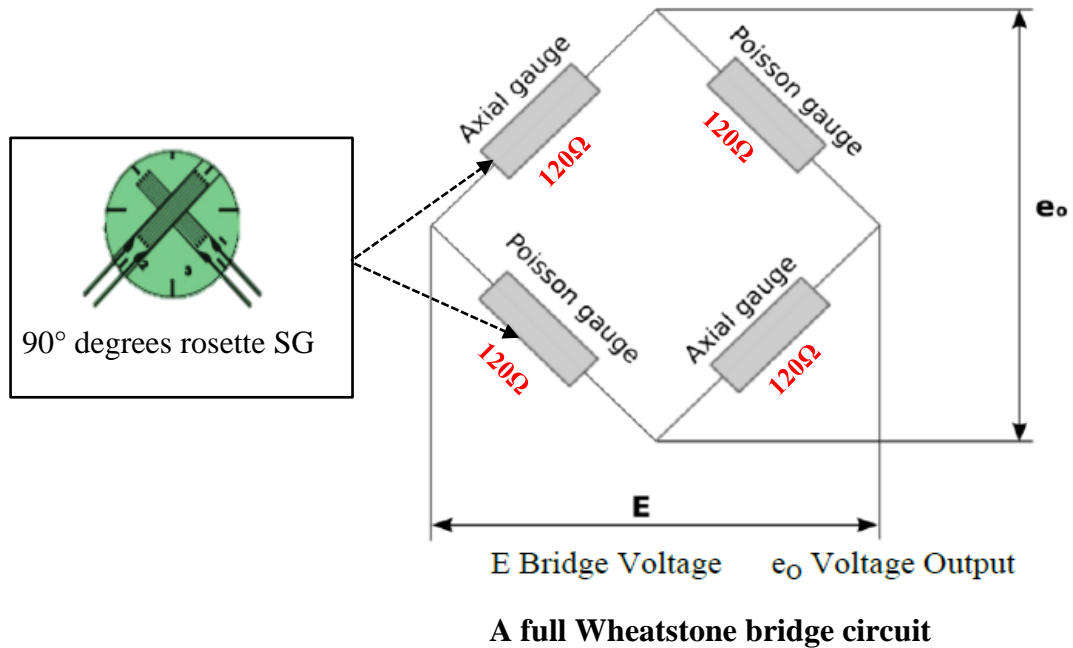
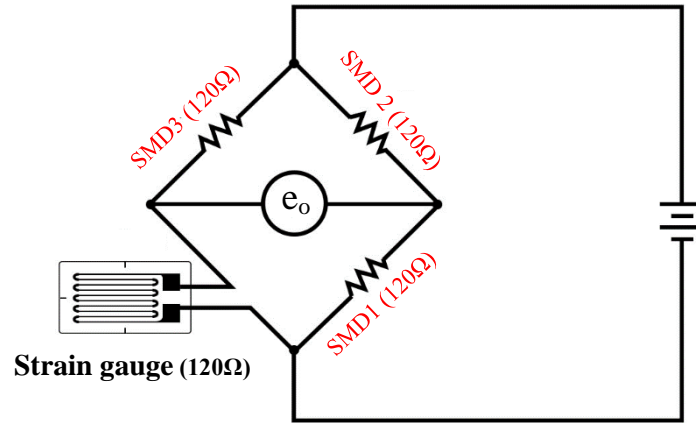


Figure 7.2: Two-element 90° degrees rosette SG used for strain measurement (Techni Measure Lab (TML), Tokyo, Japan) and the full Wheatstone bridge circuit.

However, using two two-element rosette SGs showed a non-linear stress/strain relationship on plastic AFOs (Papi, 2012). The curvature of the AFO, where the SGs were attached, caused the Wheatstone bridge to be unbalanced, which led to the observed non-linear behaviour of the SGs' outputs. This could be overcome by using a different set up of SGs' positions on the AFO where the shape is identical for each SG. This, however, is not promising due to the geometry of AFO. Hence, using one SG could eliminate the AFO's geometry problem, and thus no need to find two identical positions on the AFO. Consequently, a single SG (arranged in a quarter Wheatstone bridge configuration, 5 mm length, 120 Ω ; Techni Measure Lab (TML), Tokyo, Japan) was also used in this study to assess the single SG repeatability and performance as this type will be attached to the

AFO (Figure 7.3). The single SG was connected to three compensating resistors (Surface Mount Device (SMD) resistor, $120\ \Omega$, Panasonic, New Jersey, USA) to compensate/complete the Wheatstone bridge circuit, which is used to measure changes in electrical resistance that are caused by strain (Figure 7.3).



A full Wheatstone bridge circuit

Figure 7.3: Single SG used for strain measurement (Techni Measure Lab (TML), Tokyo, Japan) and the full Wheatstone bridge circuit.

The two, two-element 90° degrees rosette SGs were attached to four homopolymer polypropylene samples (two, two-element SGs for each sample, one on each side of the sample) and the single SGs were attached to two homopolymer polypropylene samples (one single SG for each sample) (Figure 7.4). The SGs were attached to the homopolymer polypropylene samples, using the standard surface preparation technique (Window and Holister, 1992). This technique was performed as follows: **(1)** degreasing and cleaning a larger area than the area required for SG attachment from all dust, paint, oil and grease with a solvent (Chlorothene, Micro-Measurements). **(2)** abrading the surface to make it slightly rough using fine sandpaper (400 grit size) to allow good bonding surface of the SGs. **(3)** scrubbing the area with a conditioner (M-Prep Conditioner A, Micro-Measurements) to remove any contamination caused by the abrading procedure. **(4)** neutralising the area by scrubbing the surface using absorbent cotton with a neutralizer (M-Prep Neutralizer 5A, Micro-Measurements) to bring the surface alkalinity to the optimum condition of PH value of around seven in order to facilitate bonding the SGs; as

some adhesives will not bond to an acidic surface. (5) transferring the SGs to the samples using a specific SG installation tape (MJG-2 MYLAR tape, Micro-Measurements, UK). (6) aligning the transferred SGs in the principal stress direction (i.e. the SG foil was aligned in line with the main axes of the tensile sample, to be parallel to the long direction of the sample). (7) adhering the SG to the prepared surface using cyanoacrylate adhesive (200 Catalyst-C and M-Bond 200, Micro-Measurements, UK). Constant thumb pressure was immediately applied to the SG for at least two minutes. Once the adhesive was cured, the SG installation tape was then carefully removed. (8) soldering the SG lead wires to the soldering path (connecting the two, two-element 90° degrees rosette SGs together to create the full Wheatstone bridge or connecting the single SG to the three compensating resistors to create the quarter Wheatstone bridge). (9) applying a coating agent (M-Coat-A Polyurethane, Micro-Measurements) over the SGs and the lead wires, and this was allowed to dry for at least two hours. The aim of using the coating agent was to prevent the SGs from absorbing moisture in outdoor or long-term measurement and to protect them from any excessive movements of the wire that may damage them.

Each strain-gauged sample was then clamped into the upper and lower jaws of the Instron tensile testing machine (Electroplus™ E10000 Instron, USA) (Figure 7.5). Then, the extensometer (Instron reference 2620-60, USA) was attached on the side of the sample using rubber O-rings allowing a simultaneous measurement of strain by the extensometer and the SGs (Figure 7.5). Before data collection, the O-rings were checked to ensure they were not loose, and the extensometer was checked to ensure it is firmly attached to the strain-gauged sample to prevent slippage during the data collection. Following this, the full Wheatstone bridge of the strain-gauged sample was connected to a bank of amplifier. For each strain-gauged sample, the amplifier gain, and the bridge voltage were set at 200 and 3 Volts, respectively. Then, the output for each strain-gauged sample was zeroed before starting the tensile test.

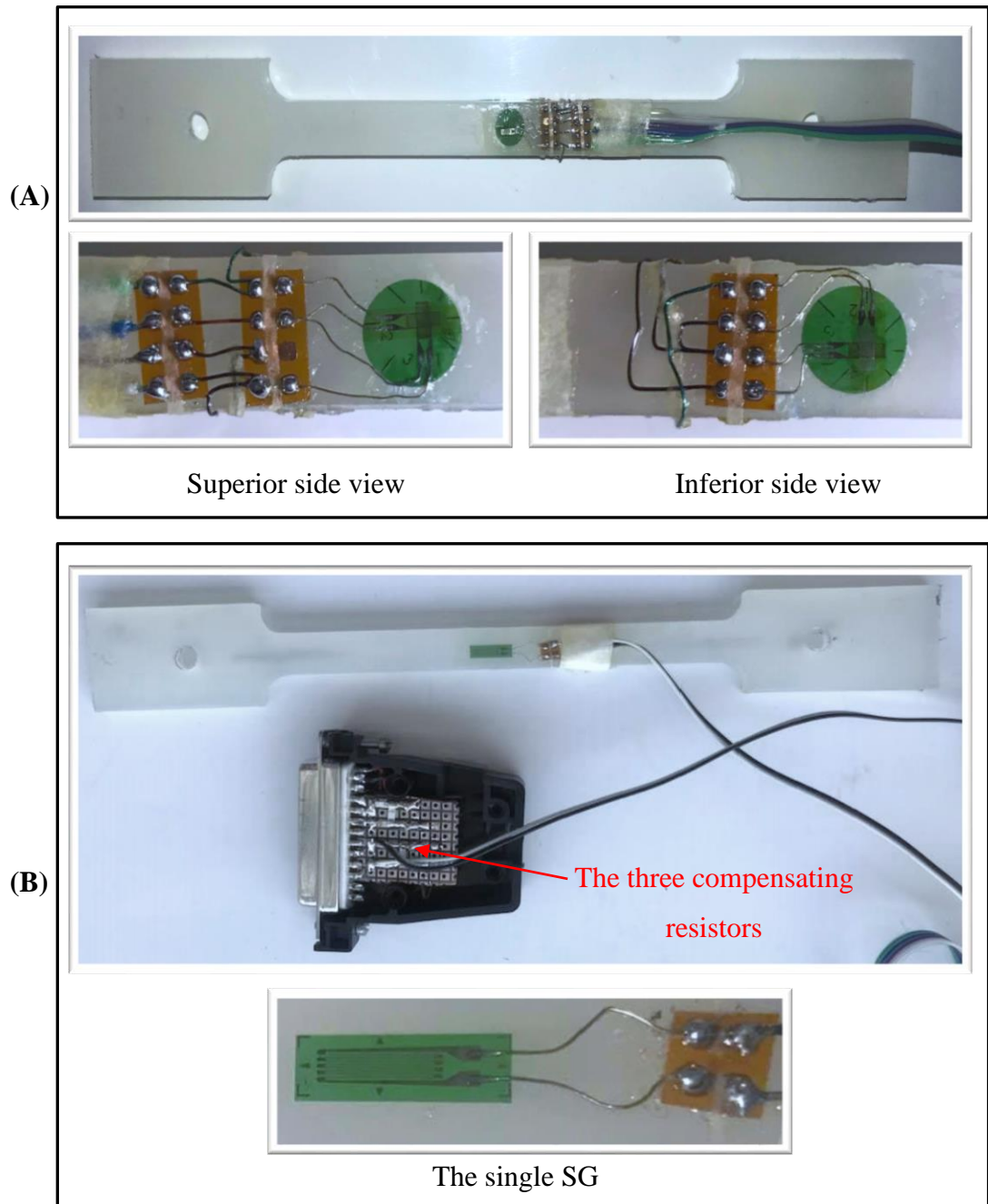


Figure 7.4: Strain-gauged samples with the two two-element 90° degrees rosette SGs on the upper (superior side view) and lower (inferior side view) surfaces of the sample (A) and with single SG (B).

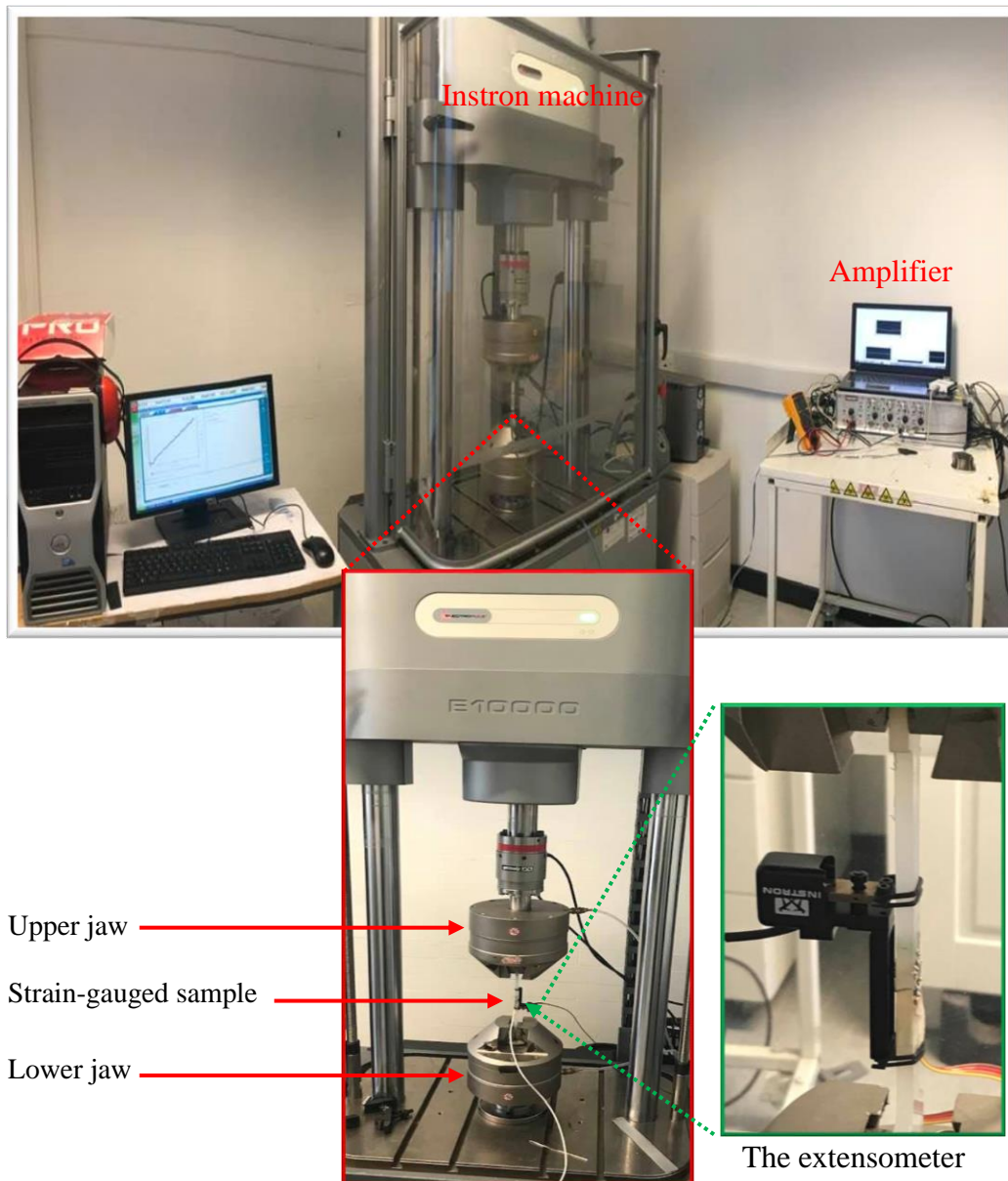


Figure 7.5: The Instron tensile testing machine (Electroplus™ E10000 Instron, USA). The focused pictures show attachment of the strain-gauged sample to the Instron and the Instron extensometer (Instron reference 2620-60, USA) to the strain-gauged sample.

A tensile test protocol was created and applied to each strain-gauged sample using the Instron WaveMatrix software at a sample rate of 50Hz. The protocol consisted of 100 loading cycles up to 100 N. For each cycle, five seconds were allowed for the load to reach the maximum value and five seconds to return to 0 N (Figure 7.6). The load was chosen to be approximating the load expected to be exerted on an AFO (Papi et al., 2015)

(derived from the 2 MPa based on experimental and finite element analysis studies conducted on a plastic AFO (Chu and Feng, 1998, Chu, 2000)). Output data from the SGs were transferred to a laptop via data acquisition system (Analog-to-digital convertor, National Instruments (USB-8009), USA). Data from the Instron extensometer were collected using Instron WaveMatrix software. While data from the SGs were collected using a custom –built LabVIEW programme (LabVIEW software 18, National Instruments, USA) installed on the laptop. The data from both WaveMatrix and the LabVIEW were exported to Excel (Microsoft Office Professional Edition 2016, Microsoft Corporation, USA) for further analysis. The synchronization of both sets of data was not feasible at the time of data collection. Therefore, synchronization was performed manually by using the first load cycle as the starting point. Matlab software (MathWorks 2017, Massachusetts, USA) was used to analysis 100 cycles (loading and unloading). The strain was measured using both the attached strain gauges on the homopolymer polypropylene plastic samples and an Instron extensometer (Instron reference 2620-60, USA).

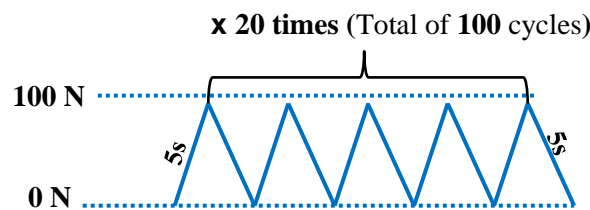


Figure 7.6: The tensile test protocol applied to strain-gauged samples with an Instron tensile testing machine (Electroplus™ E10000 Instron, USA).

Data collected were filtered, prior to analysis, to reduce the noise introduced by the recording system used. For this purpose, a custom-made moving average filter implemented via Matlab signal processing software (MathWorks 2017, Massachusetts, USA), was applied to the data stored.

The strain was calculated for the full Wheatstone bridge (two two-element 90° degrees rosette SGs) using this equation (Papi, 2012):

$$\varepsilon = \frac{2 \cdot e_o}{(1 + \nu) E \cdot K_S \cdot G} \quad \text{Equation 1}$$

Where: ε = Strain (mm/mm); e_o = Bridge output (V); ν = Poisson's Ratio; E = Bridge voltage (V); K_S = Gauge Factor; G = Amplifier Gain.

While the voltage output from the quarter Wheatstone bridge (single SG) was applied to calculate the strain using this equation (Papi, 2012):

$$\varepsilon = \frac{4 e_o}{E K_S G} \quad \text{Equation 2}$$

Where: ε = Strain (mm/mm); e_o = Bridge output (V); ν = Poisson's Ratio; E = Bridge voltage (V); K_S = Gauge Factor; G = Amplifier Gain.

As aforementioned, the amplifier gain (G) and bridge voltage (E) were set at 200 and 3 volts respectively. The gauge factor (K_S) was 2.15 (provided by the strain gauges supplier), and a Poisson's Ratio for homopolymer polypropylene of 0.36 was used (Crawford and Martin, 2019). Additionally, the strains from the Instron extensometer were also calculated by dividing the extensometer reading by its gauge length (50 mm).

The strain measurements obtained through SGs (full and quarter Wheatstone bridge) were assessed by means of a comparison with simultaneously recorded extensometer readings under the given load conditions. The difference between the systems (both types of SGs and the extensometer) was expressed as percentage of difference (Equation 3) of the strain outputs (highest and lowest values) computed with both methods for loading and unloading steps of the test protocol. The percentage of difference was calculated relatively to the strain outputs obtained by the strain gauges by using the equation:

$$\% \text{ Difference} = \frac{\text{SG outputs} - \text{Extensometer outputs}}{\text{SG outputs}} * 100 \quad \text{Equation 3}$$

❖ *Results*

Figure 7.7 shows the stress-strain graph of selected strain-gauged samples with full Wheatstone bridge (two two-element 90° degrees rosette SGs) and quarter Wheatstone

bridge (single SG) under tensile loads. The speed of testing (relative rate of motion of the grips) for the tests conducted was found to be $(0.030 \pm 0.001 \text{ mm/min})$ and $(0.031 \pm 0.001 \text{ mm/min})$ for full and quarter Wheatstone bridge strain-gauged samples, respectively. The strain-gauged samples after a preconditioning phase (the first 3 cycles), reached a steady state as the number of cycles increased, with reduced differences among the cycles. For the applied test speed between 0 and 2 MPa, the stress-strain relationship for the strain-gauged samples showed a linear relationship and thus Hooke's law can be applied to determine the Young's Modulus (the mechanical property that measures the stiffness of a material or the relationship between stress and strain) (Table 7.1). Although during the test cycles the strain-gauged samples were stressed within the linear region, hysteresis occurred as another manifestation of viscoelasticity. The stress-strain curve highlights a small difference between loading and unloading paths (hysteresis). Hysteresis can be noticed, for example, when comparing the strain in cycle 1 before applying the load 0.00 to the magnitude of strain in cycle 100 at the end of the test (after removing the load) 0.000006, Figure 7.7, While the strain in cycle 4 before applying the load was 0.000003.

Table 7.1: Young's Modulus mean (100 cycles).

| Strain-gauged sample | Wheatstone bridge arrangement | <u>Young's Modulus Mean(MPa)±(SD)</u> |
|-------------------------------|--------------------------------------|----------------------------------------------|
| Strain-gauged sample 1 | Full bridge | 2022.±(1.4) |
| Strain-gauged sample 2 | Full bridge | 2021±(1.2) |
| Strain-gauged sample 3 | Full bridge | 2014±(0.9) |
| Strain-gauged sample 4 | Full bridge | 2024±(1.5) |
| Strain-gauged sample 5 | Quarter bridge | 2020±(0.7) |
| Strain-gauged sample 6 | Quarter bridge | 2018±(0.9) |

Unpaired two sample t-tests, at 0.05 level of significance on the mean values of Young's Modulus, were conducted between the full Wheatstone bridge strain-gauged samples (2020.3 ± 4.35) and the quarter Wheatstone bridge strain-gauged samples (2019.0 ± 1.41) . The p-value obtained was $(p=0.29)$, which is greater than the chosen level of significance.

Thus, the strain-gauged samples stiffness did not change with changing the type of SG or the changing the Wheatstone bridge arrangements.

Strains calculated from the full and quarter Wheatstone bridge outputs using equation 1 and 2, respectively, were compared to strain values obtained from the extensometer. Similar trends of strain against time can be generally noticed (Figure 7.8, Figure 7.9).

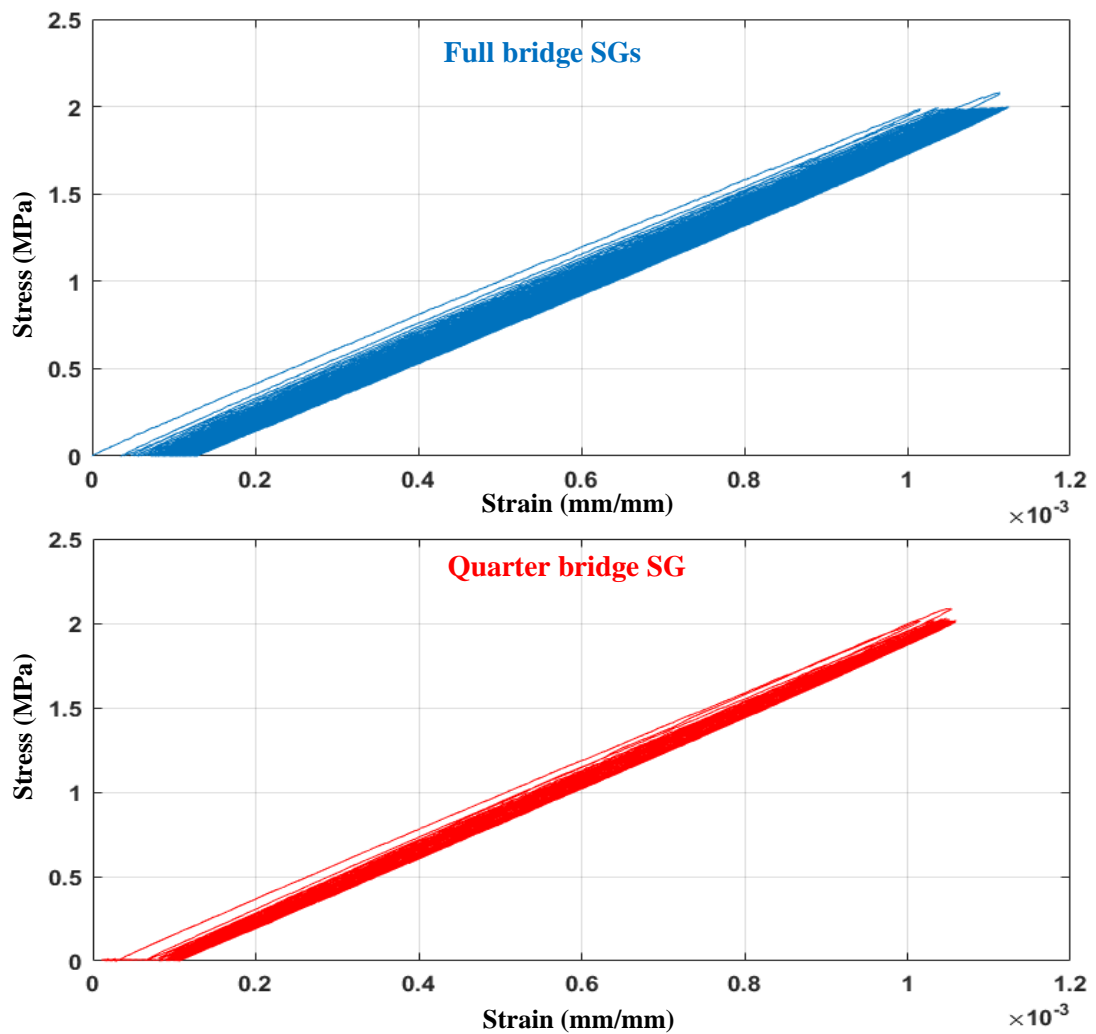


Figure 7.7: Stress-strain graph of selected strain-gauged samples with full Wheatstone bridge (two two-element 90° degrees rosette SGs) and quarter Wheatstone bridge (single SG) under tensile loads.

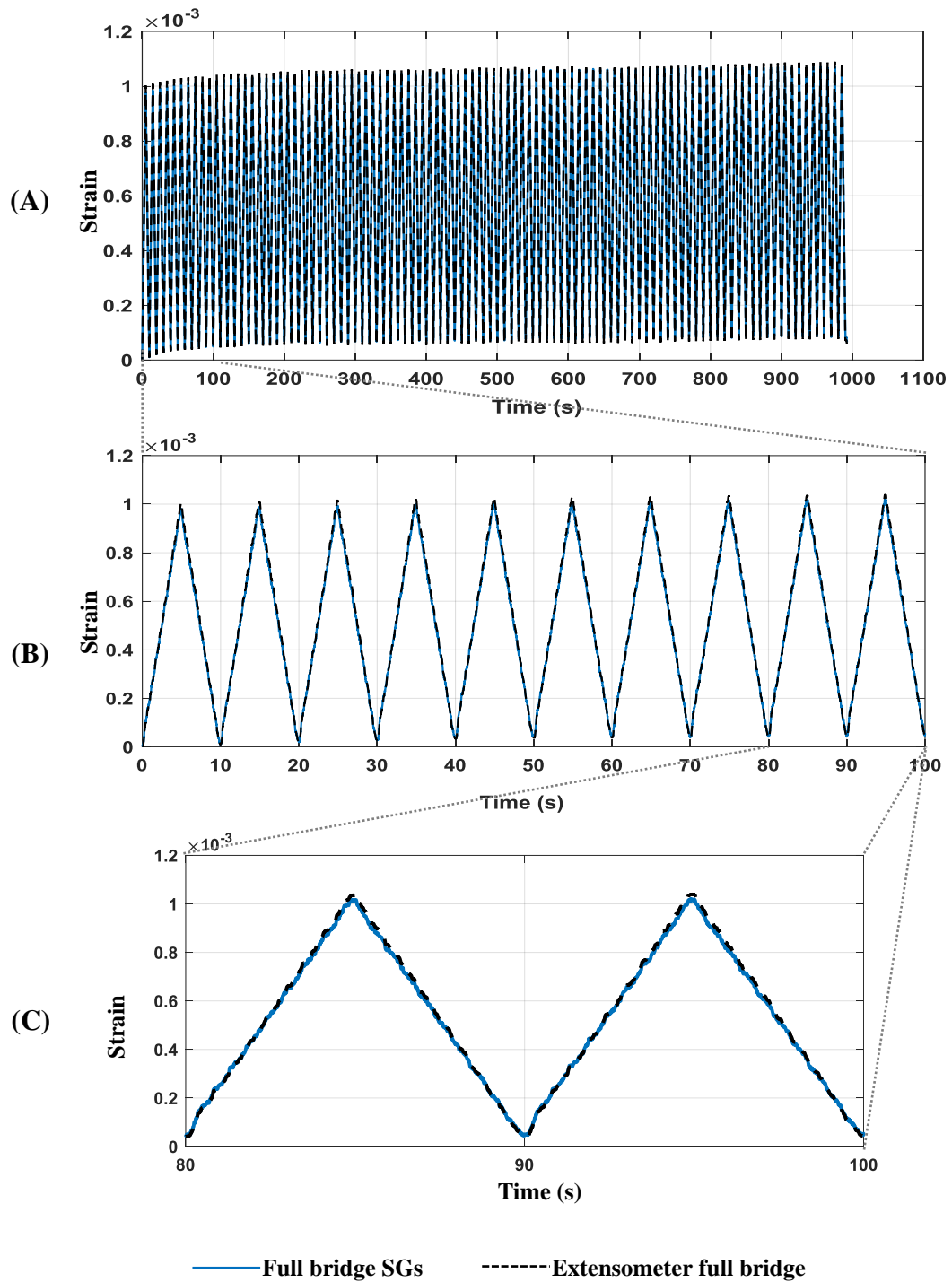


Figure 7.8: Strain against time measured by the extensometer and full Wheatstone bridge SGs (two two-element SGs) during 100 cycles (A). The focused pictures show the first 10 cycles (B) and two cycles (cycle 8 and 9) (C).

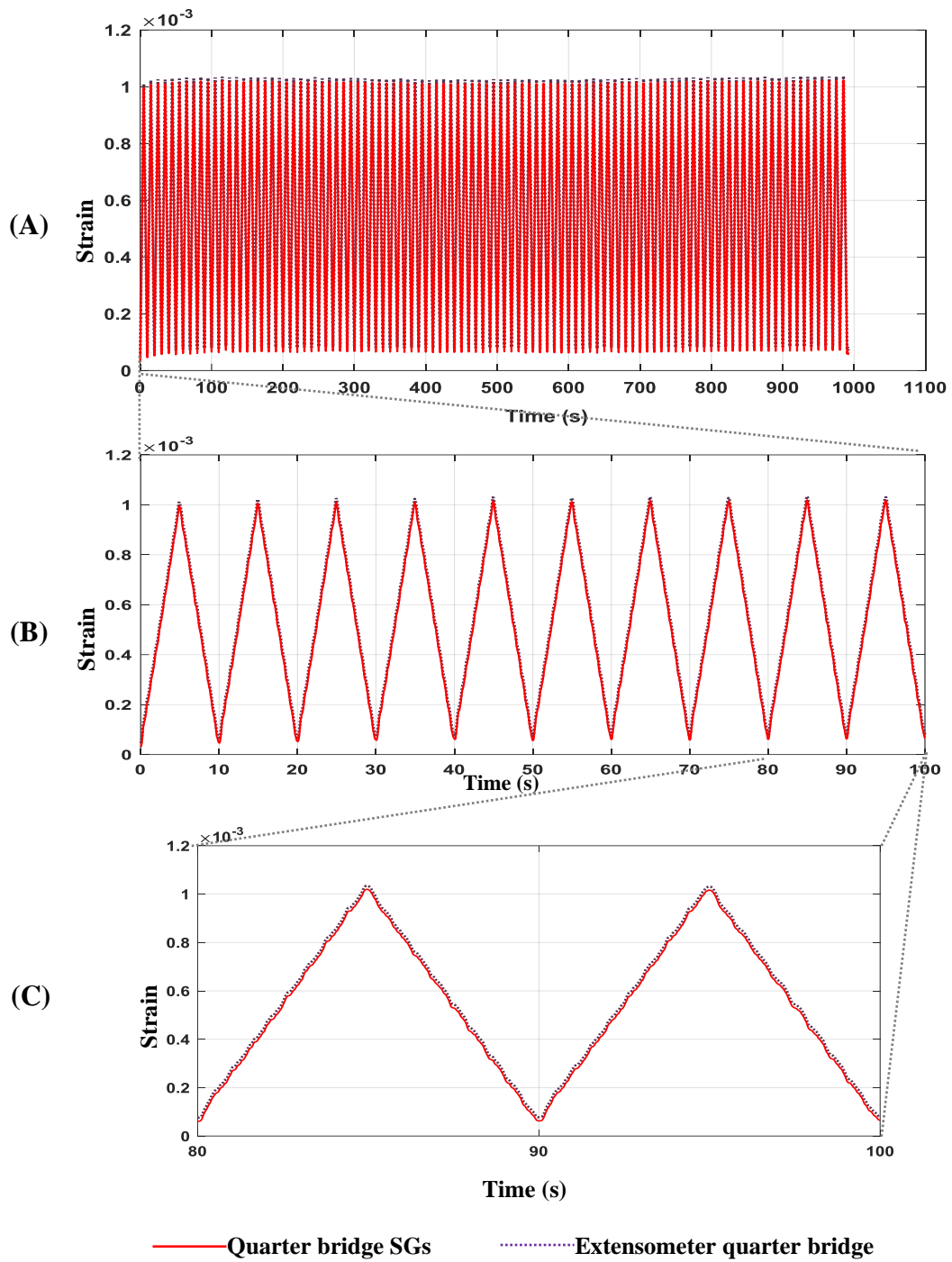


Figure 7.9: Strain against time measured by the extensometer and quarter Wheatstone bridge SG (single SG) during 100 cycles (A). The focused pictures show the first 10 cycles (B) and two cycles (cycle 8 and 9) (C).

The percentage of difference in the measurements from each strain-gauged sample from both SGs outputs and the extensometer was calculated separately for loading and unloading path (value at 2 MPa and value at 0 MPa, respectively) for the 100 cycles. Then the means of the percentage of difference for loading and unloading path were calculated as illustrated in Table 7.2. Negative values indicate a strain measurement from SGs outputs lower than the extensometer outputs.

Table 7.2: Means percentage of difference between strain gauges and extensometer values of strain for the 100 cycles.

| Strain-gauged sample | Strain Direction | <i>Mean percentage of differences (%)</i> | <u>p value</u> |
|----------------------|------------------|-------------------------------------------------------|------------------------------------------------|
| | | ((SGs outputs- Extensometer outputs)/SGs outputs*100) | SGs outputs mean vs. Extensometer outputs mean |
| S-G S1 | Loading | -2.38±0.22% | 0.161 |
| | Unloading | 0.25± 0.06% | 0.485 |
| S-G S2 | Loading | -1.86± 0.25% | 0.171 |
| | Unloading | 0.39± 0.03% | 0.405 |
| S-G S3 | Loading | 6.45± 0.52% | 0.093 |
| | Unloading | 1.01± 0.13% | 0.232 |
| S-G S4 | Loading | -2.15± 0.18% | 0.1491 |
| | Unloading | 0.44± 0.07% | 0.152 |
| S-G S5 | Loading | -0.68± 0.13% | 0.525 |
| | Unloading | -1.40± 0.07% | 0.374 |
| S-G S6 | Loading | -4.72± 0.16% | 0.093 |
| | Unloading | 0.27± 0.08% | 0.372 |

S-G S: Strain-gauged sample

The first four S-G-S were arranged in full Wheatstone bridge, S-G S5 and S-G S6 were arranged in quarter Wheatstone bridge.

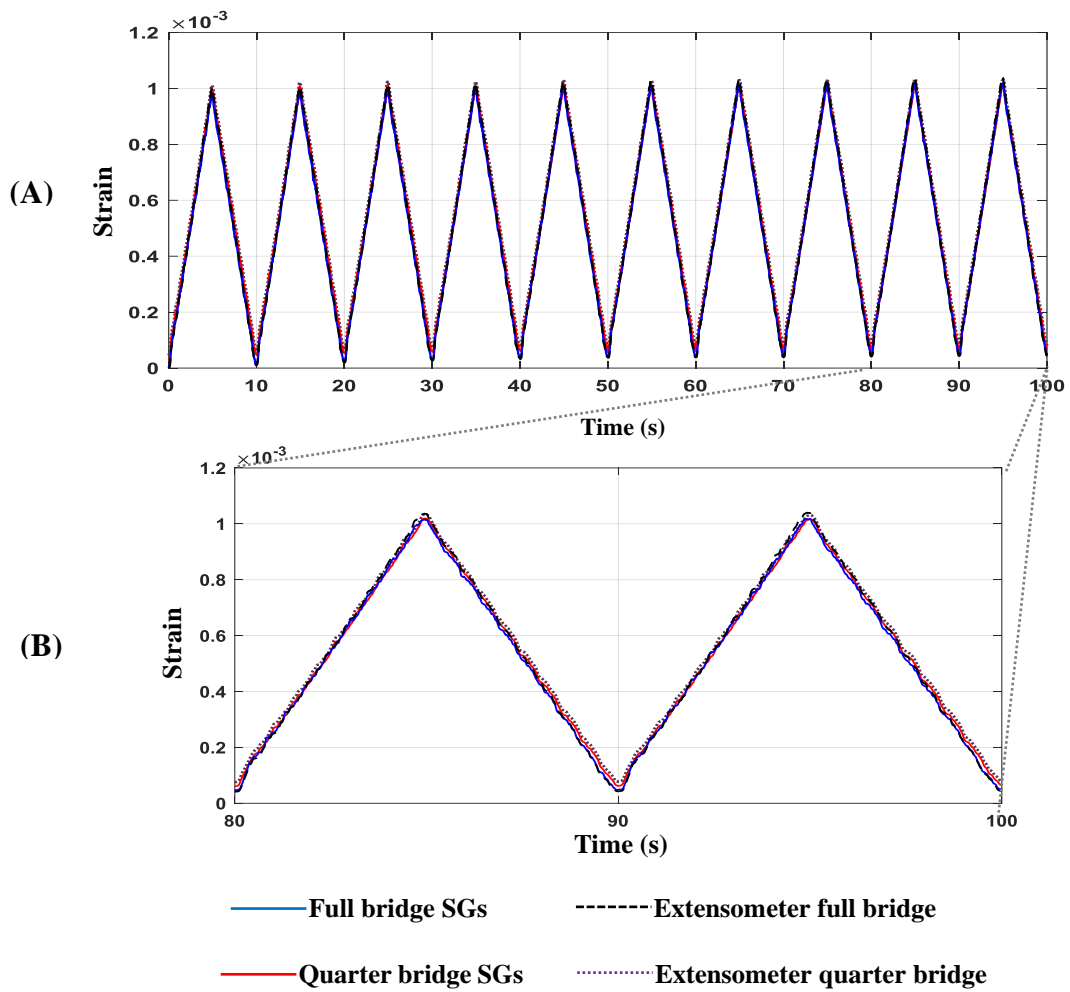


Figure 7.10: The first 10 cycles of strain against time measured by the extensometer, quarter Wheatstone bridge SG (strain-gauged sample 5) and full Wheatstone bridge (strain-gauged sample 1) (A). The focused picture shows two cycles (cycle 8 and 9) (B).

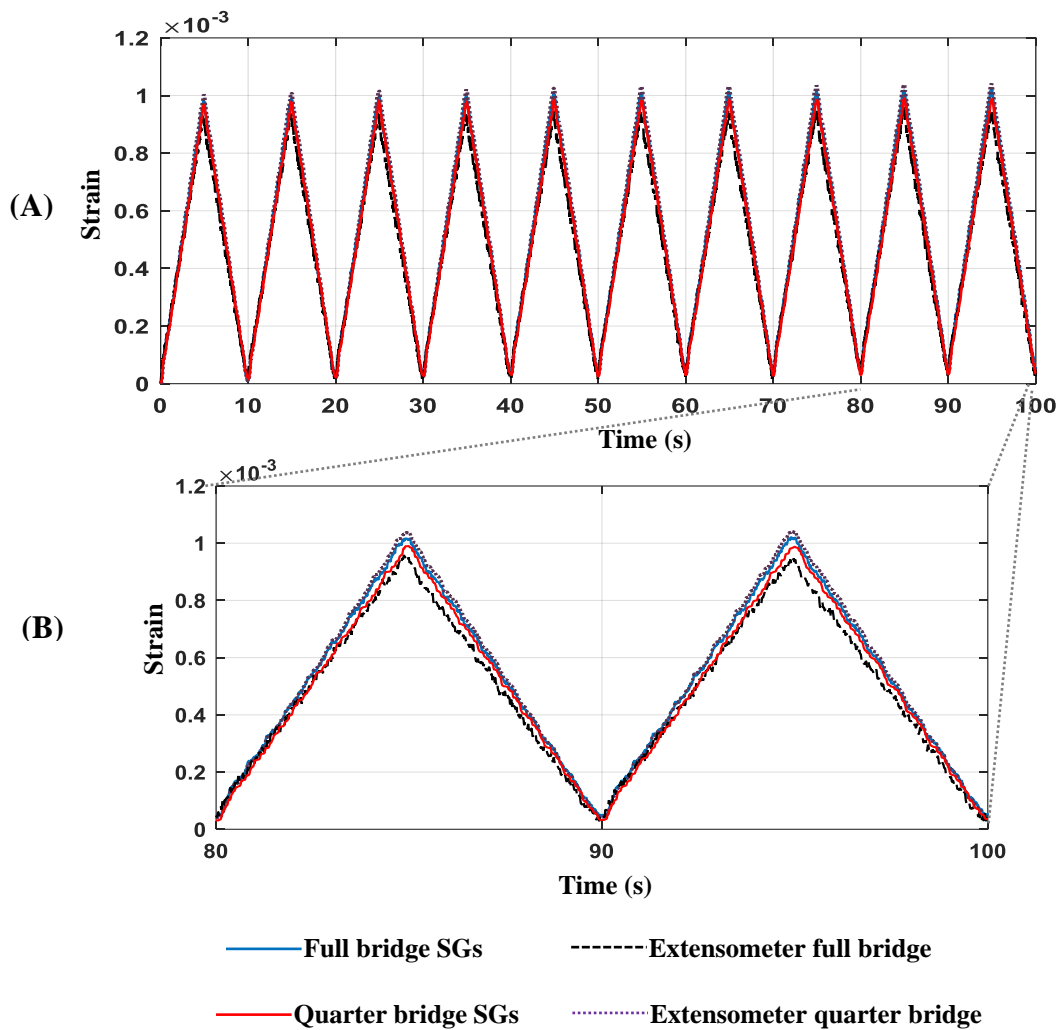


Figure 7.11: The first 10 cycles of strain against time measured by the extensometer, quarter Wheatstone bridge SG (strain-gauged sample 6) and full Wheatstone bridge (strain-gauged sample 3) (A). The focused picture shows two cycles (cycle 8 and 9) (B).

Unpaired two sample t-tests, at 0.05 level of significance on the mean percentage of difference, were conducted between the two measurement systems (SGs and the extensometer). No significant differences were found between the two measurement systems for the six strain-gauged samples (Table 7.2). The maximum difference of $6.45 \pm 0.52\%$ was obtained between the two measurement systems during loading for strain-gauged sample 3, Table 7.2.

In all strain-gauged samples, the SGs' output values during loading were found to be slightly lower than extensometer output values except in strain-gauged sample 3, which showed slightly higher values (Table 7.2). While during unloading, the SGs output values were found to be slightly higher than extensometer output values except in strain-gauged sample 5, which showed slightly lower values (Table 7.2). It was also observed that data measured by both systems were found to be repeatable all over the 100 cycles with slight differences (Figure 7.8, Figure 7.9).

Furthermore, a repeated measure ANOVA test was also used to compare the full Wheatstone bridge arrangement outputs, quarter Wheatstone bridge arrangement outputs, and the extensometer outputs. The significance level was adjusted using a Bonferroni correction and p-values were defined as significant when $p < 0.05$. The Wheatstone bridge arrangements and the extensometer outputs showed no significant differences (Figure 7.10, Figure 7.11).

❖ *Discussion and Conclusion*

Homopolymer polypropylene behaviour under tensile load condition was investigated through the tests conducted. Its viscoelastic nature was revealed showing a linear stress-strain relation at low stresses (0-2 MPa). Although within the encompassed stress range during the tests, homopolymer polypropylene was within its linear region, hysteresis was observed, and a full recovery of the deformation did not occur when the load was removed. This can be explained by the nature of viscoelastic materials that tend to flow under tensile loads rearranging their polymeric chains. Intermolecular bonds that keep polymers stable in position, break during this process dissipating energy and hence hysteresis occurs. The reestablishment of broken bonds for viscoelastic materials is time-demanding and consequentially recovery is slow. To return to its original length each sample would have necessitated a longer time than the one allowed during the performed tests and this explains the residual strain observed at zero load condition. As the number of cycles increased, curves in the stress-strain graphs were closer to each other, hysteresis loops overlapped, and the residual strain was constant. A preconditioned state that corresponds to a certain strain value for a given stress was reached. Preconditioning should be taken into account when testing a homopolymer polypropylene AFO to avoid misleading results.

The Young's Modulus was calculated experimentally from the stress and strain values obtained from the tests of each strain-gauged sample. The values of Young's Modulus were similar to the values obtained in the study by Papi et al. (2015) study.

Comparison between strains calculated by the two types of SGs to those measured by the extensometer provided an insight into SGs accuracy when attached to a viscoelastic material. A viscoelastic material is characterised by a non-instantaneous time-dependant response to applied stresses. The comparison showed that the SGs were measuring reasonable results, and the outcomes obtained were comparable with a previous study (Papi et al., 2015). Good consistency was found among the tests carried out with regards to discrepancy between measures. In strain-gauged sample 3, the SGs indicated a higher strain than the extensometer at a given stress. This was thought to be an extensometer fault rather than to strain gauges producing wrong strains as the outputs from them showed greater repeatability across tests (Figure 7.11).

The slight differences of the strains between the two types of SGs and the extensometer might be because the extensometer could not be placed directly alongside the SGs in the strain-gauged samples and, consequently, the measurements were taken from different positions on the samples, the SGs from the central parts of the sample and the extensometer slightly to the peripheral. The different positioning of the two systems could explain the discrepancy in strain values. While slight differences of the strains between the two two-element SGs and the single SG might be because the two two-element SGs report the average strain over 2mm of length, while the single SG report the average strain over 5mm of length. The extensometer readings were representative of an area of 50 mm in length, which also could contribute in the obtained strain differences. Given that the material is viscoelastic and thus the strain response is time dependant, averaging the strains over a larger area (the extensometer) could have resulted in a reduced value of strain in comparison to the value obtained from a more concentrate region (the strain gauge), as this contrarily would have raised the value of strain.

In spite of the discrepancies found, the overall results obtained from the SGs were considered acceptable to proceed toward the strain gauging of an AFO with single SG type arranged in a quarter Wheatstone bridge.

Appendix (I): Matlab codes

- Detect gait event code

```
%%Import acquisition
acq = btkReadAcquisition(Control_1);

%%%%%%%%%%%%%%%%%%%%%%%%%%%%%%%%%%%%%%%%%%%%%%%%%%%%%%%%%%%%%%%%%%%%%%%%%%
% import markers
markers = btkGetMarkers(acq);
% Import the model output/forces:
forces = btkGetForces(acq);

%% Detect the gait event:
analog = btkGetAnalog(acq);
ratio = btkGetAnalogSampleNumberPerFrame(acq);
analogDownsampled = [];
labels = fieldnames(analog);
for i = 1:btkGetAnalogNumber(acq);
    analogDownsampled.(labels{i}) =
analog.(labels{i})(1:ratio:end);
    % ...
end

Fz1=analogDownsampled.Force_Fz1;
Fz2=analogDownsampled.Force_Fz2;

% Left side
d=0;
for c=1:length(Fz1)-15;
    if
(Fz1(c)==0) && (Fz1(c+1)<0) && (Fz1(c+2)<0) && (Fz1(c+3)<0) &
& (Fz1(c+15)<0)
        LeftHS(d+1,1)=(c+1);
        d=d+1;
    elseif (Fz1(c)==0) && (Fz1(c+1)==0);
    end
    if (Fz1(c)<0) && (Fz1(c+1)<0);
    end
end;

d=0;
for c=1:length(Fz1)-15;
    if (Fz1(c)<0) && (Fz1(c-1)<0) && (Fz1(c-2)<0) && (Fz1(c-
3)<0) && (Fz1(c-15)<0) && (Fz1(c+1)==0)
```

```

        LeftTO(d+1,1)=(c+1);
        d=d+1;
    end

end

% Right side
d=0;
for c=1:length(Fz1)-15;
    if
        (Fz1(c)==0) && (Fz1(c+1)<0) && (Fz1(c+2)<0) && (Fz1(c+3)<0) &
        & (Fz1(c+15)<0)
            RightHS(d+1,1)=(c+1);
            d=d+1;
        elseif (Fz1(c)==0) && (Fz1(c+1)==0);
        end
        if (Fz1(c)<0) && (Fz1(c+1)<0);
        end
    end;

d=0;
for c=1:length(Fz1)-15;
    if (Fz1(c)<0) && (Fz1(c-1)<0) && (Fz1(c-2)<0) && (Fz1(c-
3)<0) && (Fz1(c-15)<0) && (Fz1(c+1)==0)
        RightTO(d+1,1)=(c+1);
        d=d+1;
    end
end

% GRF graph to check the gait events:
figure
h1 = subplot(2,1,1);
h2 = subplot(2,1,2);
plot(h1,Fz1,'k');
axes(h1);
y1=get(h1,'YLim');
y2=get(h2,'YLim');
line([LeftHS LeftHS],y1,'Color','b');
line([LeftTO LeftTO],y1,'Color','g');
title(h1,'Fz1 Left');xlabel('Frames');ylabel('N');grid
on;
plot(h2,Fz2,'k');
axes(h2);
line([RightHS RightHS],get(h2,'YLim'),'Color','b');
line([RightTO RightTO],get(h2,'YLim'),'Color','g');
title(h2,'Fz2
Right');xlabel('Frames');ylabel('N');grid on;

```

➤ SVA calculation code

```
%% TO CALCULATE THE left SVA :
L_Proximal =markers.LTT';
L_Distal=markers.LDT';

for i=1:size(L_KneeJoint,2)
    Tibial_inc(i) = atand((L_Proximal(2,i) - L_Distal
(2,i))/(L_Proximal(3,i) - L_Distal (3,i)));
end

    Tibial_inc= Tibial_inc';

% Time of gait cycle normalized to 100%
    for f =1:length(LeftHS)-1
        L_SVA = Tibial_inc_L(LeftHS(f):(LeftHS(f+1)-1));
        T_L_SVA_GaitCycle=1:numel(L_SVA)/101:numel(L_SVA);
        L_SVA_GC(:,f) = interp1(1:numel(
L_SVA),L_SVA,T_L_SVA_GaitCycle);
    end;
```

➤ EMG code

```
%Row Data
EMG_path='Sensor_1_Sensor';
EMG=analoggs.(EMG_path);
det_EMG= detrend(EMG);

%Band Pass filiter
% FcL = 20, FcH = 500, FSA = 2000 (Staudemann et al
2007)
FcL=20; % Cut-off frequency, low
FcH = 500; % Cut-off frequency, high
N=6; % butter Filter Order
NqF = FSA*0.5;% Nyquist frequency nqf is 5Hz
[B, A] = butter(N, ([FcL,FcH]/NqF));
x1_EMG = filtfilt(B,A,det_EMG);

% Rectification & Smoothing(x2)

[b2, a2] = iirnotch(0.111,(0.111/80));
x2_EMG=abs(filter(b2, a2,x1_EMG));%ABS(X) is the
absolute value of the elements of X3
```

```

% Root mean Squar (RMS) (x3)
windowlength=0.01;
overlap=0;
zeropad=0;

x3_EMG = rms(x2_EMG, windowlength, overlap, zeropad);
delta = windowlength - overlap;
indices = 1:delta:length(x2_EMG);

if length(x2_EMG) - indices(end) + 1 < windowlength;
    if zeropad
        x2_EMG(end+1:indices(end)+windowlength-1) = 0;
    else
        indices = indices(1:find(indices+windowlength-
1 <= length(x2_EMG), 1, 'last'));
    end
end

x3_EMG = zeros(1, length(indices));
x2_EMG = x2_EMG.^2;

index = 0;
for i = indices
    index = index+1;
    % Average and take the square root of each window
    x3_EMG (index) =
sqrt(mean(x2_EMG(i:i+windowlength-1)));
end

% Down sample Ration of the EMGs
Dx3_EMG1_Shoe_FixedPaced=x3_EMG1_Shoe_FixedPaced(1:ratio:end)';

% Normalization of EMG data to MMT%
% After calculate the RMS    x3_MVC1_EMG, x3_MVC2_EMG,
x3_MVC3_EMG
% Max points of MVCs
    M_x3_MVC1_EMG=max(x3_MVC1_EMG);
    M_x3_MVC2_EMG=max(x3_MVC2_EMG);
    M_x3_MVC3_EMG=max(x3_MVC3_EMG);

    M_x3_MVC_EMG=[M_x3_MVC1_EMG M_x3_MVC2_EMG
M_x3_MVC3_EMG];
    Max_x3_MVC_EMG=max(M_x3_MVC_EMG);
    NMVC_Dx3_EMG=(Dx3_EMG/Max_x3_MVC_EMG)*100;

```

```

        x2_EMG(end+1:indices(end)+windowlength-1) = 0;
    else
        indices = indices(1:find(indices+windowlength-
1 <= length(x2_EMG), 1, 'last'));
    end
end

x3_EMG = zeros(1, length(indices));
x2_EMG = x2_EMG.^2;

index = 0;
for i = indices
    index = index+1;
    % Average and take the square root of each window
    x3_EMG(index) =
sqrt(mean(x2_EMG(i:i+windowlength-1)));
end

% Down sample Ration of the EMGs
Dx3_EMG1_Shoe_FixedPaced=x3_EMG1_Shoe_FixedPaced(1:ratio:end)';

```

Appendix (J): Supplementary Results

The results of the unaffected side for stroke participants (SPs) while walking on treadmill wearing Tuned-AFO, AFO and SSO are presented in this chapter. The unaffected side for control participants refers to the side not fitted with the orthosis (non-orthotic side). All gait parameters were compared across the three conditions: SSO, AFO and Tuned-AFO for both control and stroke participants. The symbols asterisk (\star), circle (\bullet) and cross (\times) were used in the graphs to identify the end of stance time in Tuned-AFO, AFO and SSO conditions, respectively. In this study, the reported kinetic parameters (Knee moments, hip moments and ankle moments) represent the external moments.

❖ Control participants for the side not fitted with the orthosis

➤ Shank to vertical angle (SVA)

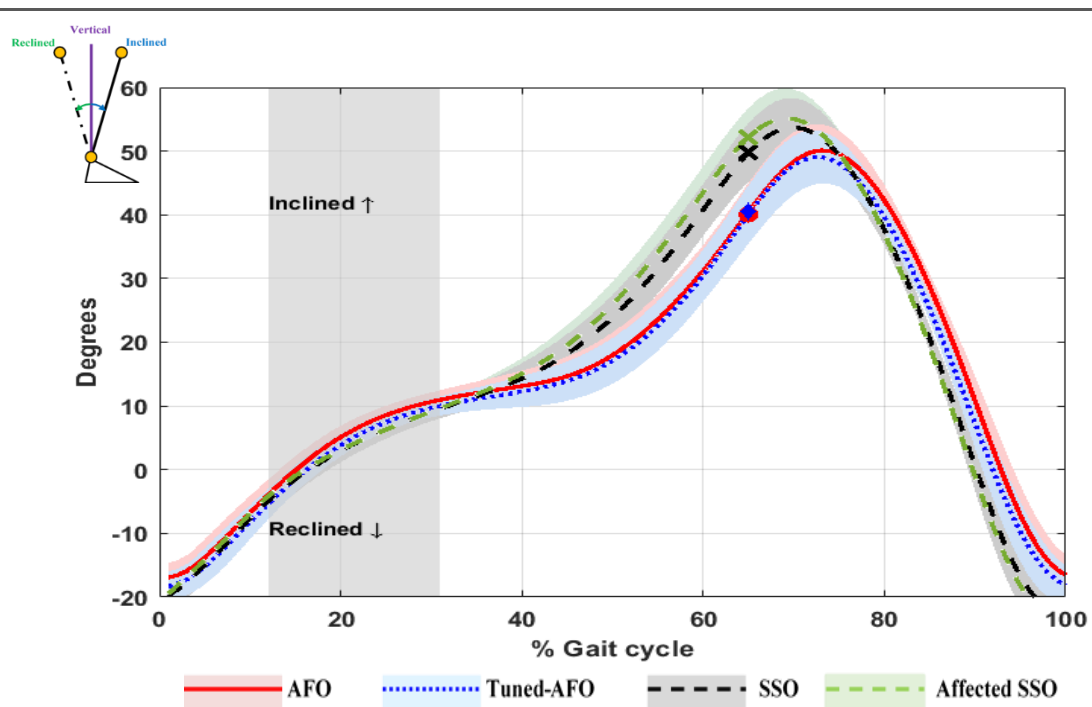


Figure 7.12: The SVAs mean of the non-orthotic side for control participants while walking on treadmill. The shaded area represents the mid stance phase.

➤ Ankle joint kinematics (sagittal plane)

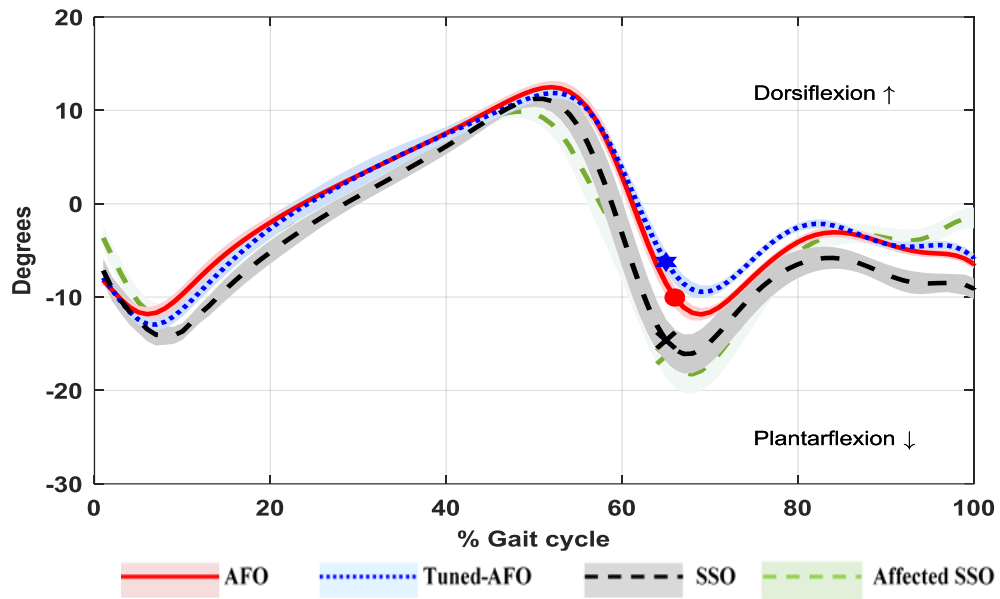


Figure 7.13: Sagittal ankle motion of non-orthotic side for control participants while walking on treadmill.

➤ Knee joint kinematics (sagittal plane)

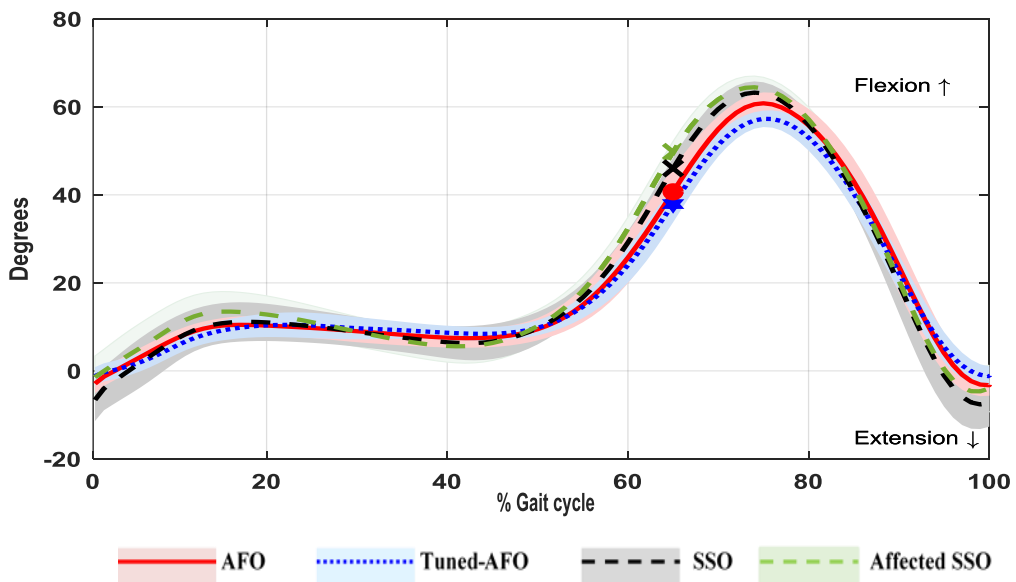


Figure 7.14: Sagittal knee motion of non-orthotic side for control participants while walking on treadmill.

➤ Hip joint kinematics (sagittal plane)

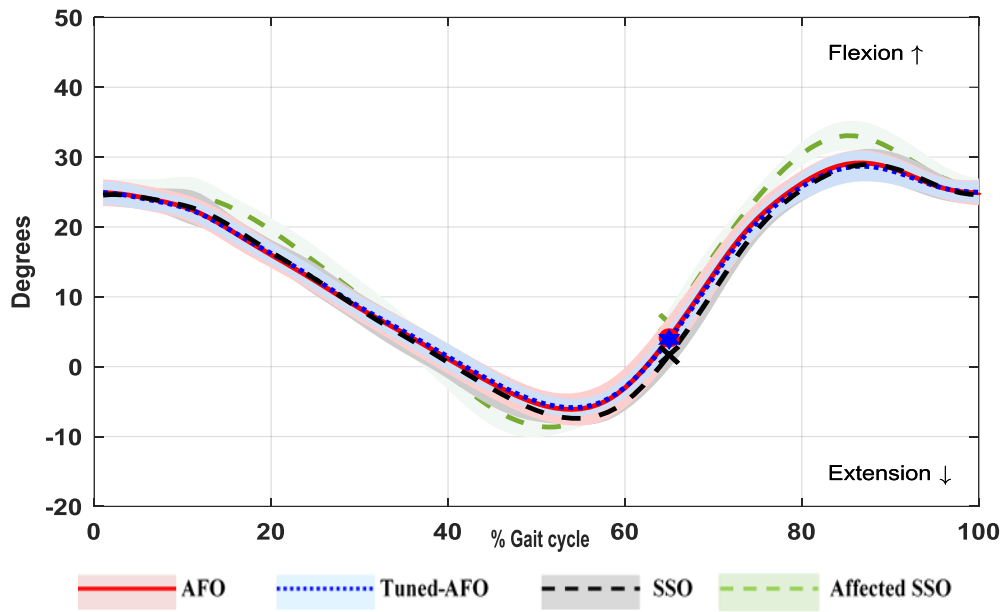


Figure 7.15: Sagittal hip motion of non-orthotic side for control participants while walking on treadmill.

➤ Ankle joint kinetics (sagittal plane)

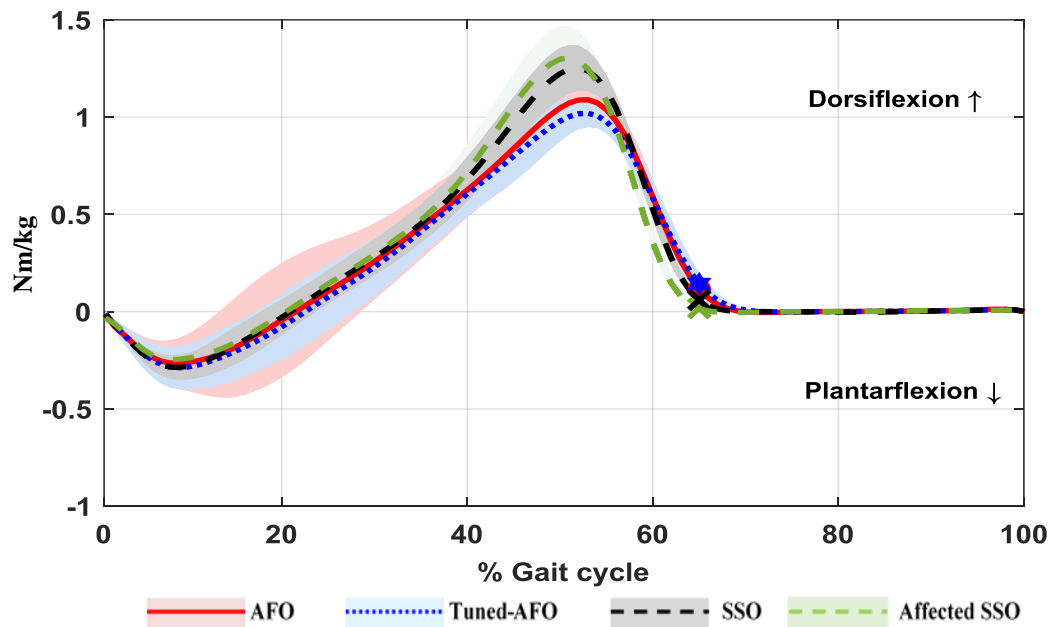


Figure 7.16: Sagittal ankle moment of non-orthotic side for control participants while walking on treadmill.

➤ Knee joint kinetics (sagittal plane)

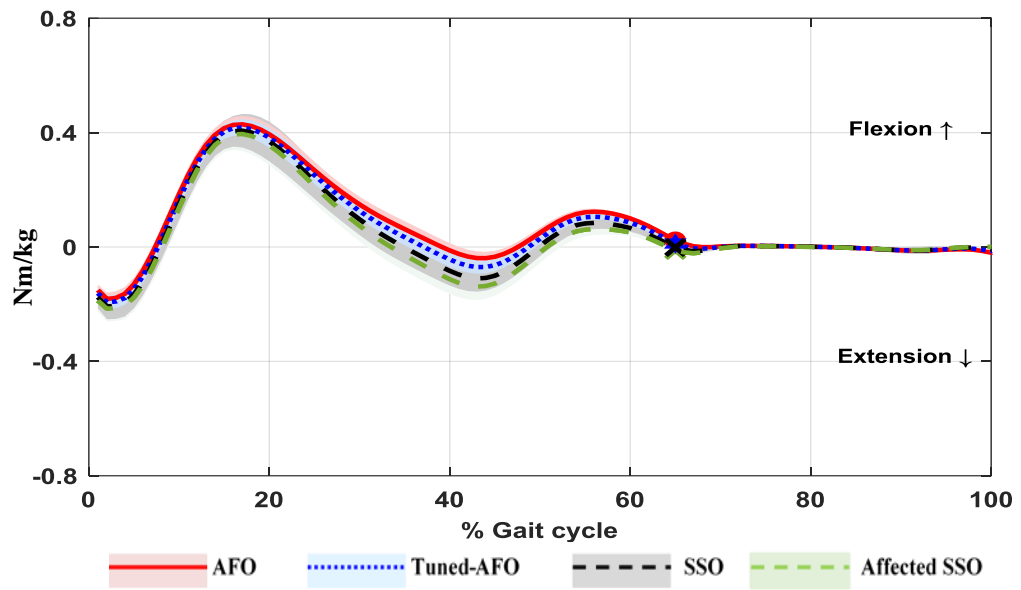


Figure 7.17: Sagittal knee moment of non-orthotic side for control participants while walking on treadmill.

➤ Hip joint kinetics (sagittal plane)

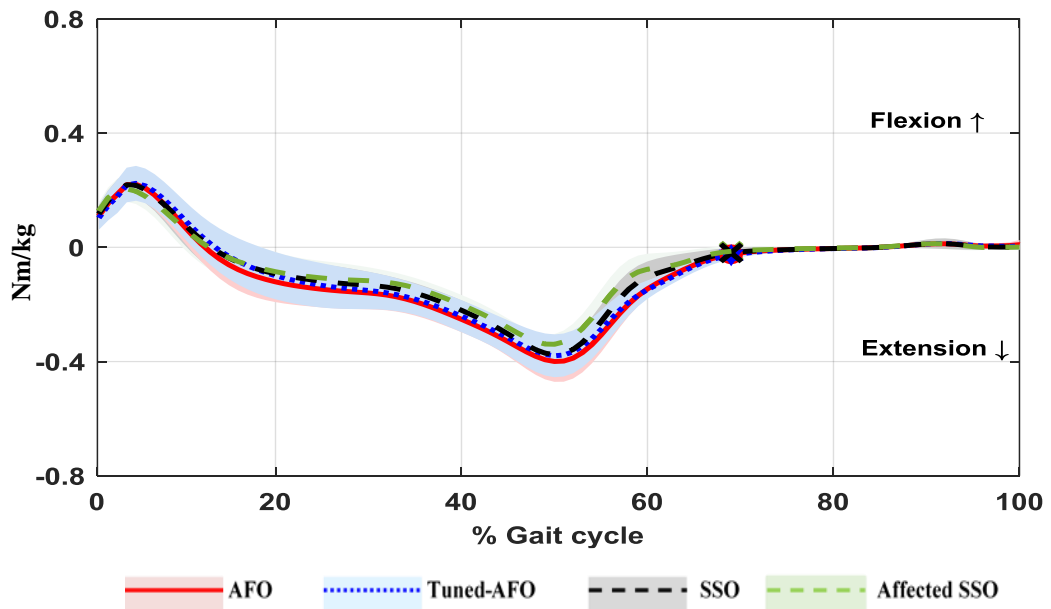


Figure 7.18: Sagittal hip moment for control participants while walking on treadmill.

➤ Vertical ground reaction force (GRFv)

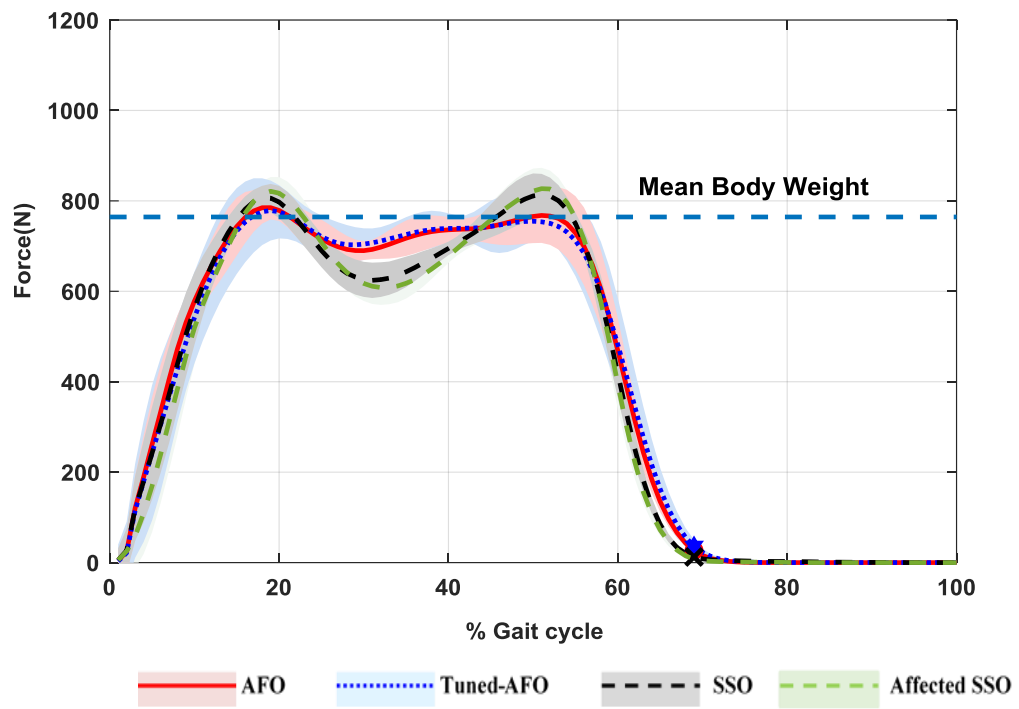


Figure 7.19: Vertical GRF for control participants while walking on treadmill.

❖ **Stroke participants for unaffected side**

➤ Temporal-spatial parameters for unaffected side

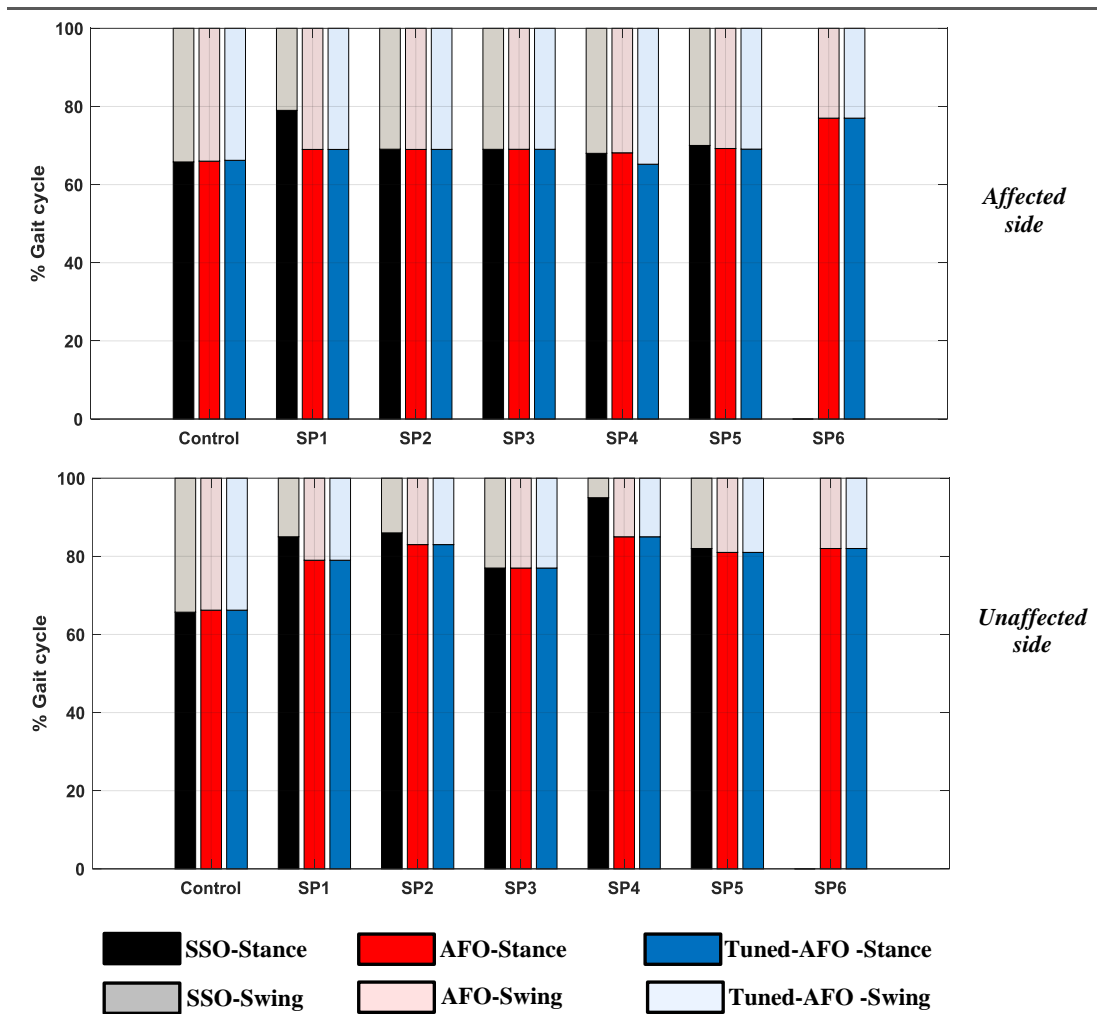


Figure 7.20: Stance (dark coloured bars) and swing (light coloured bars) as a percentage of %100 gait cycle for the affected and unaffected sides. In control participants, affected and unaffected sides refer to fitted and unfitted sides with the orthosis, respectively.

➤ Shank to vertical angle (SVA) for unaffected side

Table 7.3: The SVA values in mid stance of the non-orthotic side and unaffected side for control and stroke participants, respectively.

| Participants | <u>Mean±(SD)</u> | | |
|----------------|------------------|--------------|--------------|
| | AFO | Tuned-AFO | SSO |
| Control | 10.32±(0.98) | 9.93±(1.01) | 9.99±(0.99) |
| SP1 | 5.80±(0.32) | 6.52±(0.31) | 13.10±(0.35) |
| SP2 | 7.90±(0.22) | 9.72±(0.21) | 8.53±(0.20) |
| SP3 | 7.99±(0.32) | 6.96±(0.32) | 9.63±(0.33) |
| SP4 | 16.86±(0.17) | 11.65±(0.17) | 11.54±(0.18) |
| SP5 | 7.81±(0.21) | 7.80±(0.21) | 7.82±(0.24) |
| SP6 | 15.07±(0.22) | 4.56±(0.07) | - |

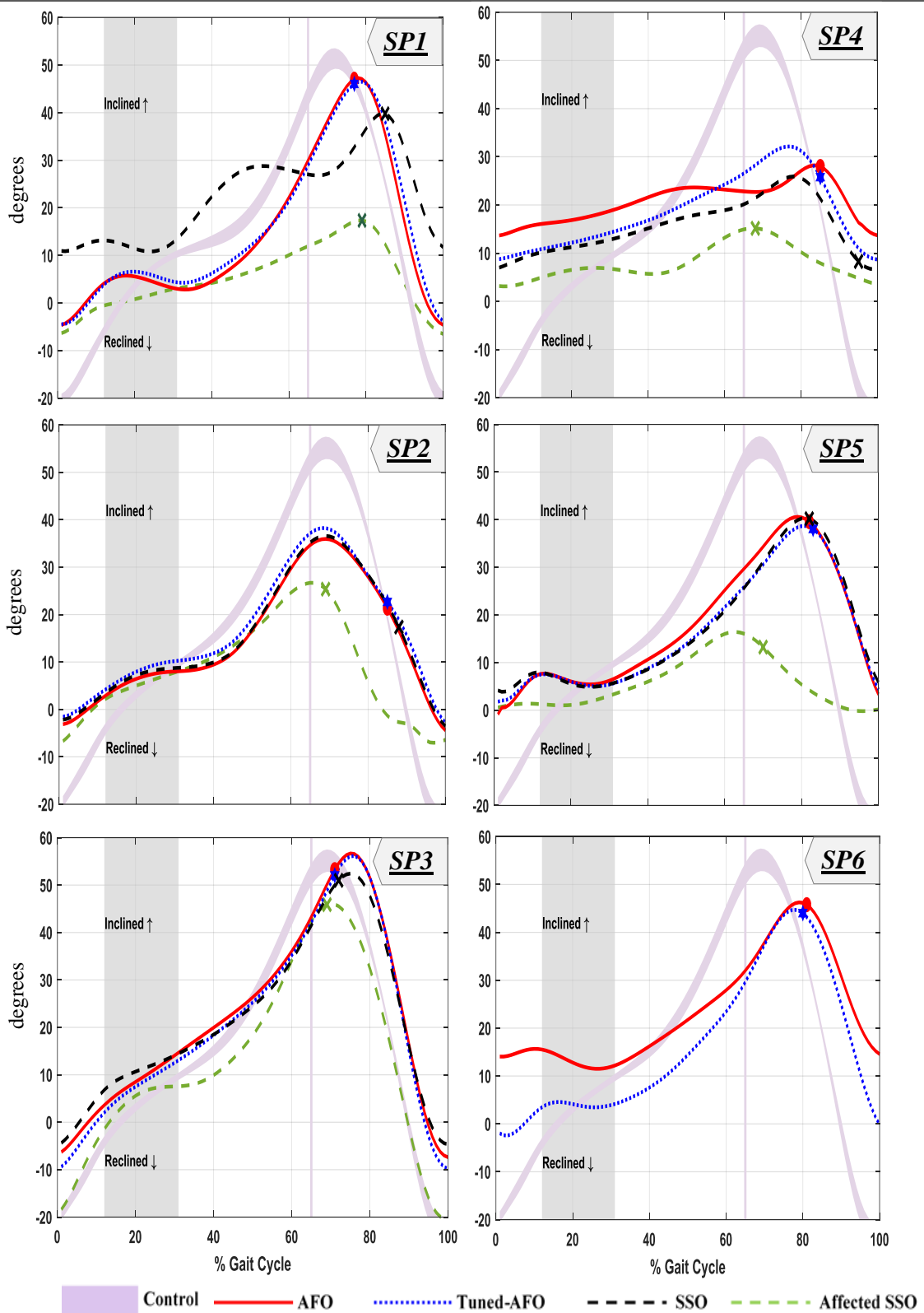


Figure 7.21: The SVA of the unaffected side for stroke participants (SPs) while walking on treadmill wearing Tuned-AFO, AFO and SSO with reference to control participants while wearing SSO.

➤ Knee joint kinematics (sagittal plane)

Table 7.4: Sagittal knee angle of the non-orthotic side and unaffected side for control and stroke participants, respectively.

| Participants | Knee angle (degrees) | <i>Mean±(SD)</i> | | |
|----------------|----------------------|------------------|--------------|--------------|
| | | AFO | Tuned | SSO |
| Control | KF peak (stance) | 11.82±(2.20) | 10.48±(2.10) | 11.95±(3.12) |
| | KE (stance) | 7.64±(2.32) | 8.13±(1.52) | 6.88±(2.44) |
| | KF peak (swing) | 60.81±(2.12) | 57.28±(1.45) | 62.97±(2.54) |
| SP1 | KF peak (stance) | 16.14±(1.52) | 17.70±(1.14) | 26.68±(1.24) |
| | KE(stance) | 0.04±(0.22) | 2.45±(0.65) | 35.87±(0.42) |
| | KF peak (swing) | 61.14±(2.21) | 62.60±(1.55) | 59.57±(1.55) |
| SP2 | KF peak (stance) | 13.50±(1.65) | 13.25±(1.62) | 14.11±(1.20) |
| | KE (stance) | -0.95±(0.25) | -0.96±(0.50) | -0.95±(0.34) |
| | KF peak (swing) | 43.62±(1.50) | 43.58±(1.62) | 43.93±(1.42) |
| SP3 | KF peak (stance) | 16.50±(1.50) | 17.93±(1.20) | 26.98±(1.20) |
| | KE (stance) | 16.33±(0.29) | 14.76±(0.25) | 19.52±(0.26) |
| | KF peak (swing) | 68.35±(1.21) | 67.25±(1.71) | 70.22±(1.09) |
| SP4 | KF peak (stance) | 17.61±(0.85) | 21.38±(0.14) | 24.06±(0.26) |
| | KE (stance) | 2.12±(0.15) | 5.11±(0.24) | 26.67±(0.32) |
| | KF peak (swing) | 57.87±(1.10) | 57.80±(1.10) | 39.48±(1.12) |
| SP5 | KF peak (stance) | 24.85±(0.80) | 21.38±(0.61) | 17.61±(0.85) |
| | KE (stance) | 15.43±(0.42) | 4.68±(0.14) | 2.26±(0.26) |
| | KF peak (swing) | 62.67±(1.15) | 57.81±(1.12) | 57.92±(1.10) |
| SP6 | KF peak (stance) | 30.08±(0.52) | 31.38±(0.50) | - |
| | KE (stance) | 9.62±(0.95) | 12.22±(0.85) | - |
| | KF peak (swing) | 64.91±(0.60) | 67.64±(0.59) | - |

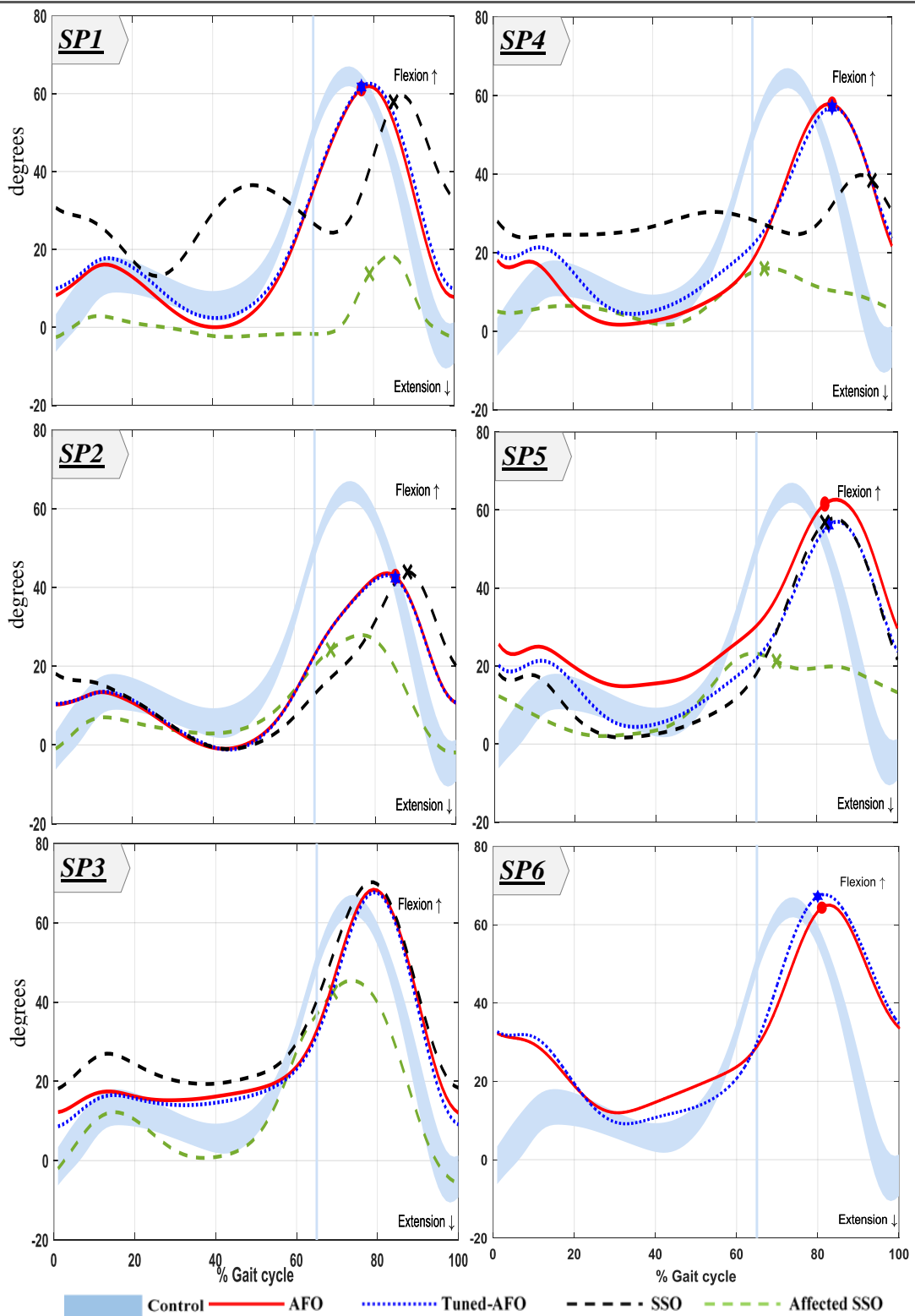


Figure 7.22: Sagittal knee motion of the unaffected side for stroke participants (SPs) while walking on treadmill wearing Tuned-AFO, AFO and SSO with reference to control participants while wearing SSO.

➤ Hip joint kinematics (sagittal plane)

Table 7.5: Hip extension and flexion angle peaks of the non-orthotic side and unaffected side for control and stroke participants, respectively.

| Participants | Hip angle (degrees) | <i>Mean±(SD)</i> | | |
|----------------|------------------------|------------------|--------------|--------------|
| | | AFO | Tuned | SSO |
| Control | HE peak | -5.81±(2.10) | -5.90±(1.62) | -7.39±(1.44) |
| | HF peak | 29.25±(1.92) | 29.24±(1.26) | 29.25±(1.66) |
| SP1 | HE peak | 1.87±(0.90) | -1.70±(0.90) | 14.44±(0.99) |
| | HF peak | 42.06±(0.98) | 40.10±(1.10) | 40.50±(1.12) |
| SP2 | HE peak | -1.01±(0.75) | -3.59±(0.72) | 2.56±(0.70) |
| | HF peak | 26.23±(1.05) | 29.56±(0.80) | 32.87±(2.10) |
| SP3 | HE peak | 19.33±(0.60) | 16.55±(0.55) | 31.5±(0.50) |
| | HF peak | 44.84±(0.64) | 39.54±(0.57) | 43.43±(0.58) |
| SP4 | HE peak | 27.56±(0.87) | 10.91±(0.85) | 42.20±(1.01) |
| | HF peak | 49.83±(0.75) | 35.96±(0.80) | 45.39±(0.85) |
| SP5 | HE peak | 0.31±(0.55) | 0.04±(0.72) | 4.96±(0.62) |
| | HF peak | 36.15±(0.44) | 36.26±(0.35) | 33.09±(0.48) |
| SP6 | HE peak | 7.94±(0.75) | 1.76±(0.82) | - |
| | HF peak | 41.76±(0.86) | 40.43±(0.95) | - |

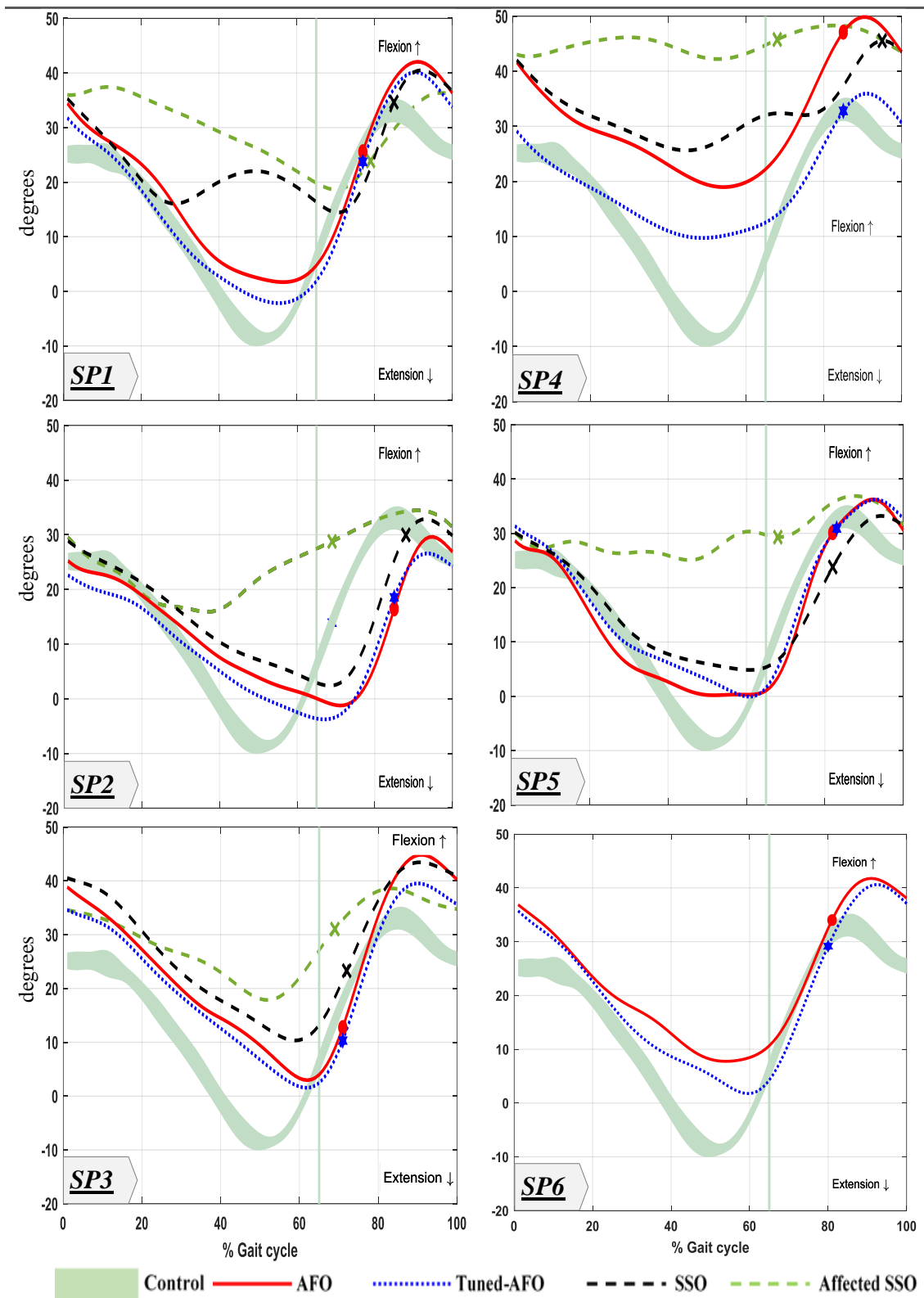


Figure 7.23: Sagittal hip motion of the unaffected side for stroke participants (SPs) while walking on treadmill wearing Tuned-AFO, AFO and SSO with reference to control participants while wearing SSO.

➤ Ankle joint kinematics (sagittal plane)

Table 7.6: Sagittal ankle motion peaks of the non-orthotic side and unaffected side for control and stroke participants, respectively.

| Participants | Ankle angle (degrees) | <i>Mean±(SD)</i> | | |
|----------------|--------------------------|------------------|---------------|---------------|
| | | AFO | Tuned | SSO |
| Control | PF peak1 | -11.68±(0.95) | -12.95±(0.95) | -14.12±(1.05) |
| | DF peak | 12.48±(0.84) | 11.86±(1.05) | 11.13±(2.05) |
| | PF peak 2 | -11.04±(0.80) | -9.44±(1.00) | -16.27±(0.87) |
| SP1 | PF peak1 | -0.42±(0.50) | -5.37±(0.42) | -0.02±(0.50) |
| | DF peak | 12.76±(0.60) | 7.08±(0.54) | 16.59±(0.75) |
| | PF peak 2 | -21.25±(0.77) | -26.47±(0.78) | -7.45±(0.85) |
| SP2 | PF peak1 | -6.30±(0.14) | -9.78±(0.54) | -11.38±(0.22) |
| | DF peak | 4.86±(0.15) | 3.79±(0.14) | -1.43±(0.20) |
| | PF peak 2 | -4.24±(0.18) | -6.19±(0.15) | -8.67±(0.15) |
| SP3 | PF peak1 | -9.15±(0.12) | -18.67±(0.16) | -4.59±(0.12) |
| | DF peak | 9.17±(0.10) | 2.36±(0.20) | 13.22±(0.32) |
| | PF peak 2 | -0.74±(0.07) | -8.22±(0.09) | -2.32±(0.10) |
| SP4 | PF peak1 | 2.99±(0.09) | -6.89±(0.04) | -1.61±(0.08) |
| | DF peak | 4.07±(0.10) | 2.45±(0.12) | 7.48±(0.18) |
| | PF peak 2 | -9.33±(0.15) | -16.09±(0.24) | -4.91±(0.08) |
| SP5 | PF peak1 | -3.44±(0.05) | -9.65±(0.06) | -6.34±(0.10) |
| | DF peak | 15.44±(0.14) | 14.83±(0.11) | 10.95±(0.20) |
| | PF peak 2 | 0.07±(0.09) | -6.73±(0.09) | -5.72±(0.07) |
| SP6 | PF peak1 | 0.09±(0.11) | -5.13±(0.11) | - |
| | DF peak | 14.09±(0.10) | 12.15±(0.12) | - |
| | PF peak 2 | -6.46±(0.08) | -6.99±(0.09) | - |

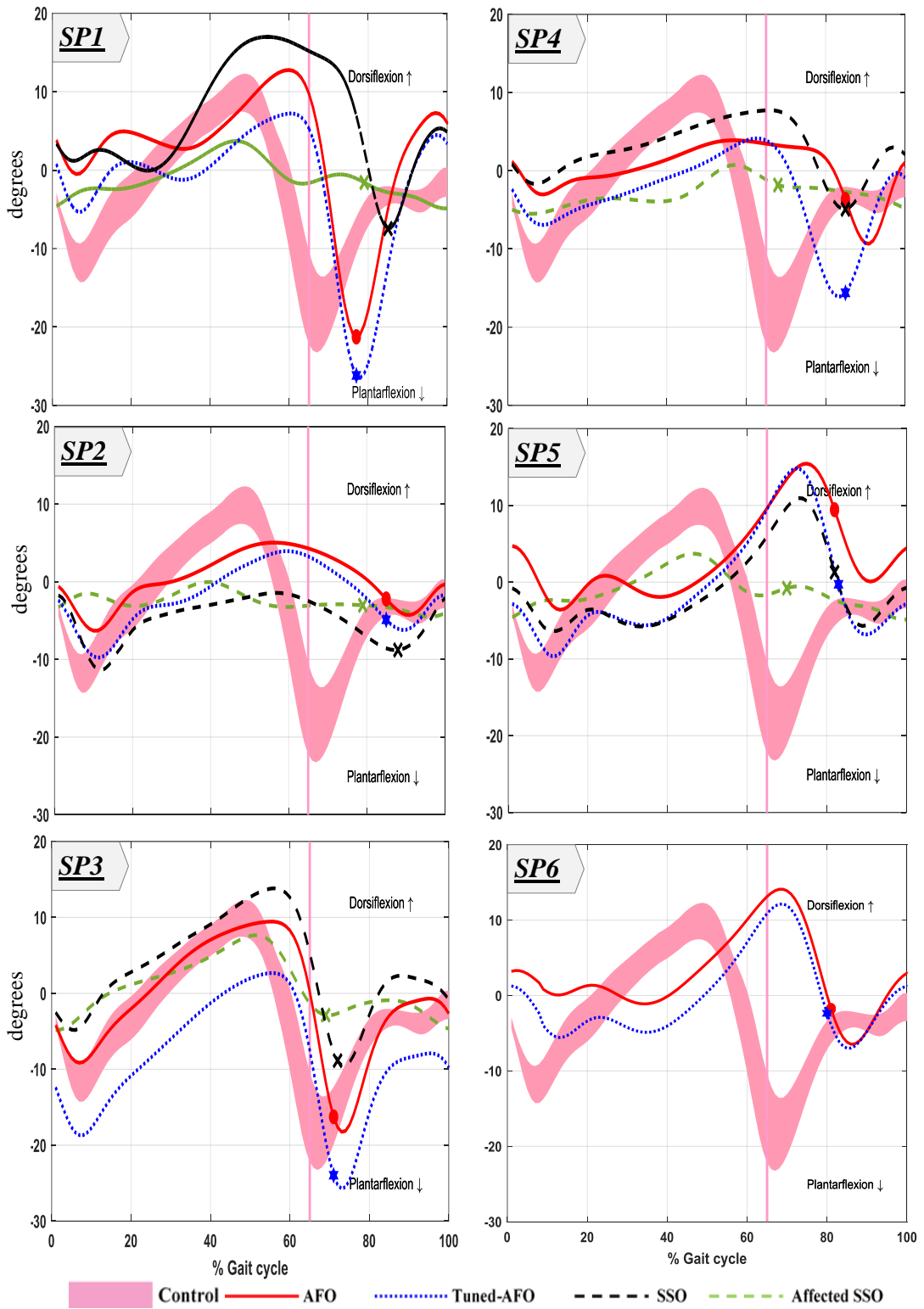


Figure 7.24: Sagittal ankle motion of the unaffected side for stroke participants (SPs) while walking on treadmill wearing Tuned-AFO, AFO and SSO with reference to control participants while wearing SSO.

➤ Knee joint kinetics (sagittal plane)

Table 7.7: Sagittal knee moment of the non-orthotic side and unaffected side for control and stroke participants, respectively.

| Participants | Knee moment (Nm/kg) | <i>Mean±(SD)</i> | | |
|----------------|------------------------|------------------|--------------|--------------|
| | | AFO | Tuned | SSO |
| Control | KF peak1 | 0.42±(0.03) | 0.43±(0.03) | 0.40±(0.06) |
| | KE peak | -0.20±(0.01) | -0.18±(0.01) | -0.22±(0.01) |
| | KF peak2 | 0.19±(0.03) | 0.22±(0.03) | 0.18±(0.05) |
| SP1 | KF peak1 | 0.24±(0.04) | 0.31±(0.02) | 0.35±(0.01) |
| | KE peak | -0.14±(0.01) | -0.12±(0.01) | 0.03±(0.01) |
| | KF peak2 | -0.02±(0.01) | 0.00±(0.02) | 0.06±(0.01) |
| SP2 | KF peak1 | 0.45±(0.01) | 0.44±(0.01) | 0.44±(0.06) |
| | KE peak | -0.06±(0.01) | -0.10±(0.01) | -0.01±(0.01) |
| | KF peak2 | 0.05±(0.01) | 0.06±(0.02) | 0.16±(0.01) |
| SP3 | KF peak1 | 0.43±(0.01) | 0.44±(0.01) | 0.39±(0.04) |
| | KE peak | -0.07±(0.01) | -0.09±(0.01) | -0.13±(0.06) |
| | KF peak2 | 0.20±(0.01) | 0.18±(0.01) | 0.06±(0.01) |
| SP4 | KF peak1 | 0.38±(0.04) | 0.37±(0.04) | 0.38±(0.04) |
| | KE peak | 0.08±(0.01) | 0.14±(0.01) | 0.19±(0.05) |
| | KF peak2 | 0.19±(0.01) | 0.25±(0.01) | 0.29±(0.01) |
| SP5 | KF peak1 | 0.38±(0.02) | 0.32±(0.02) | 0.35±(0.02) |
| | KE peak | 0.00±(0.02) | -0.01±(0.02) | -0.01±(0.01) |
| | KF peak2 | 0.20±(0.01) | 0.20±(0.01) | 0.24±(0.01) |
| SP6 | KF peak1 | 0.39±(0.02) | 0.42±(0.02) | - |
| | KE peak | 0.08±(0.01) | 0.04±(0.02) | - |
| | KF peak2 | 0.25±(0.01) | 0.17±(0.01) | - |

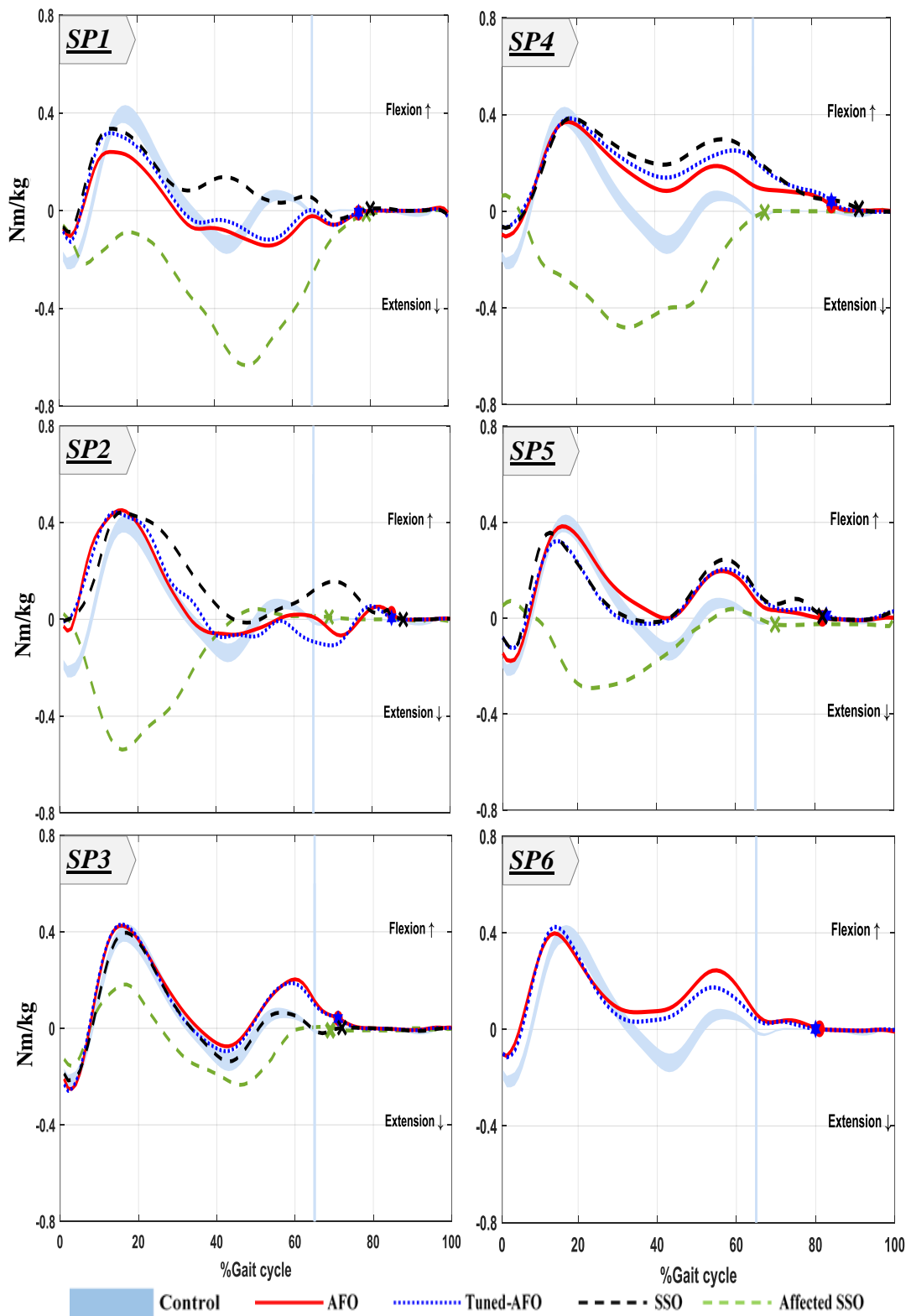


Figure 7.25: Sagittal knee moment for stroke participants (SPs) while walking on treadmill wearing Tuned-AFO, AFO and SSO with reference to control participants while wearing SSO.

➤ Hip joint kinetics (sagittal plane)

Table 7.8: Sagittal hip moment of the non-orthotic side and unaffected side for control and stroke participants, respectively.

| Participants | Hip moment (Nm/kg) | <i>Mean±(SD)</i> | | |
|----------------|-----------------------|------------------|--------------|--------------|
| | | AFO | Tuned | SSO |
| Control | HF peak | 0.22±(0.04) | 0.21±(0.06) | 0.22±(0.04) |
| | HE peak | -0.39±(0.02) | -0.38±(0.01) | -0.38±(0.01) |
| SP1 | HF peak | 0.30±(0.03) | 0.34±(0.04) | 0.13±(0.05) |
| | HE peak | -0.19±(0.04) | -0.15±(0.04) | -0.05±(0.05) |
| SP2 | HF peak | 0.09±(0.02) | 0.07±(0.02) | 0.05±(0.02) |
| | HE peak | -0.24±(0.03) | -0.26±(0.02) | -0.37±(0.01) |
| SP3 | HF peak | 0.30±(0.02) | 0.29±(0.01) | 0.28±(0.05) |
| | HE peak | -0.26±(0.02) | -0.27±(0.02) | -0.11±(0.01) |
| SP4 | HF peak | 0.23±(0.01) | 0.24±(0.01) | 0.28±(0.01) |
| | HE peak | -0.36±(0.01) | -0.34±(0.01) | -0.42±(0.01) |
| SP5 | HF peak | 0.26±(0.01) | 0.31±(0.01) | 0.22±(0.01) |
| | HE peak | -0.31±(0.01) | -0.37±(0.01) | -0.43±(0.01) |
| SP6 | HF peak | 0.27±(0.01) | 0.31±(0.01) | - |
| | HE peak | -0.47±(0.01) | -0.46±(0.01) | - |

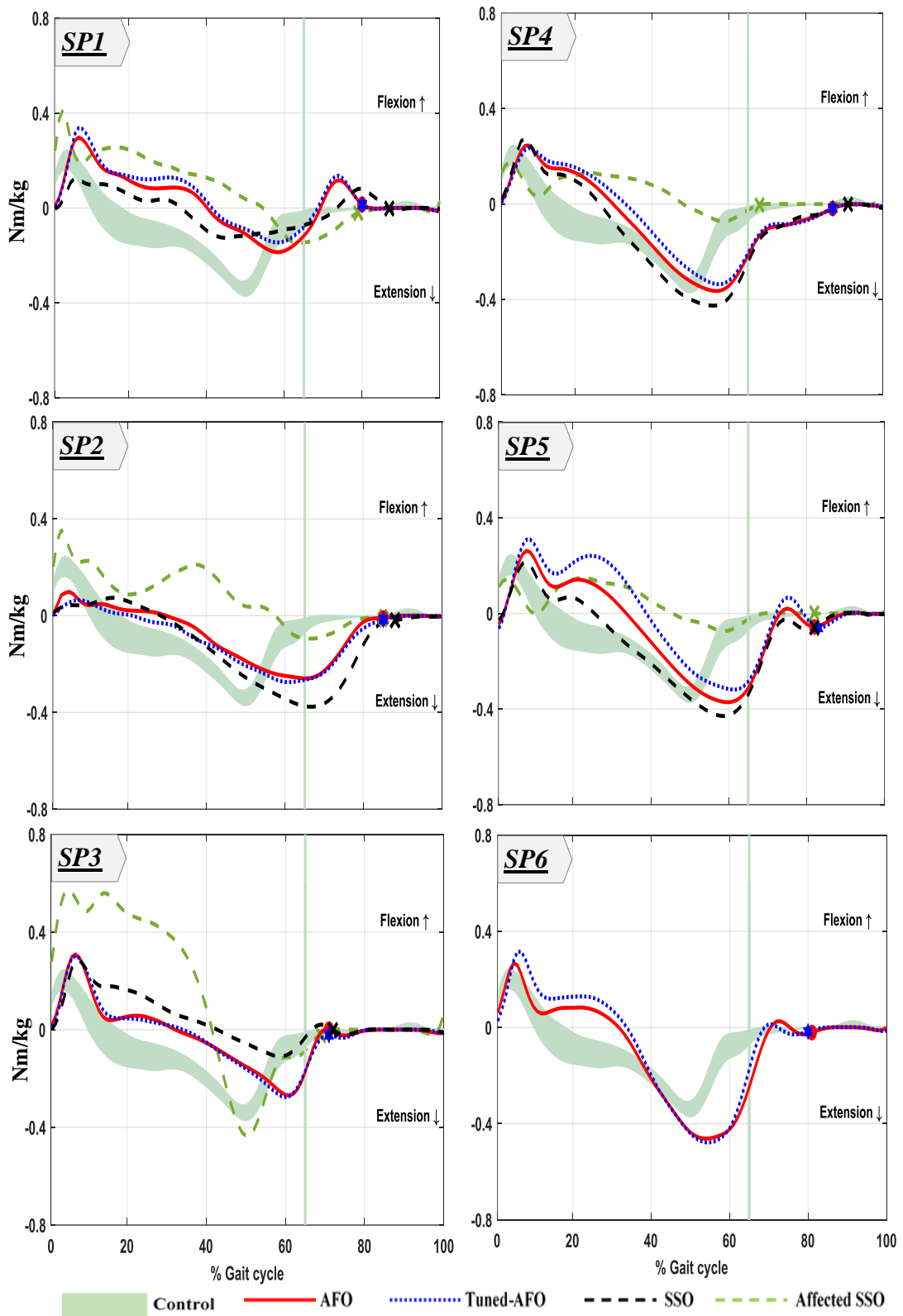


Figure 7.26: Sagittal hip moment for stroke participants (SPs) while walking on treadmill wearing Tuned-AFO, AFO and SSO with reference to control participants while wearing SSO.

➤ Ankle joint kinetics (sagittal plane)

Table 7.9: Sagittal ankle moment of the non-orthotic side and unaffected side for control and stroke participants, respectively.

| Participants | Ankle moment (Nm/kg) | <i>Mean±(SD)</i> | | |
|----------------|-------------------------|------------------|--------------|--------------|
| | | AFO | Tuned | SSO |
| Control | PF peak | -0.24±(0.11) | -0.26±(0.10) | -0.26±(0.05) |
| | DF peak | 1.08±(0.04) | 1.02±(0.04) | 1.25±(0.09) |
| SP1 | PF peak | -0.07±(0.02) | -0.12±(0.03) | -0.01±(0.03) |
| | DF peak | 1.33±(0.04) | 1.25±(0.02) | 1.39±(0.03) |
| SP2 | PF peak | -0.12±(0.06) | -0.13±(0.04) | -0.06±(0.02) |
| | DF peak | 1.24±(0.02) | 1.11±(0.03) | 1.37±(0.03) |
| SP3 | PF peak | -0.07±(0.05) | -0.18±(0.06) | -0.06±(0.05) |
| | DF peak | 1.39±(0.03) | 1.41±(0.03) | 1.37±(0.04) |
| SP4 | PF peak | -0.06±(0.05) | -0.05±(0.06) | -0.08±(0.05) |
| | DF peak | 0.92±(0.05) | 0.92±(0.04) | 1.00±(0.05) |
| SP5 | PF peak | -0.04±(0.03) | -0.04±(0.05) | -0.04±(0.05) |
| | DF peak | 1.21±(0.08) | 1.08±(0.06) | 1.36±(0.08) |
| SP6 | PF peak | -0.01±(0.04) | -0.02±(0.04) | - |
| | DF peak | 1.12±(0.05) | 1.13±(0.07) | - |

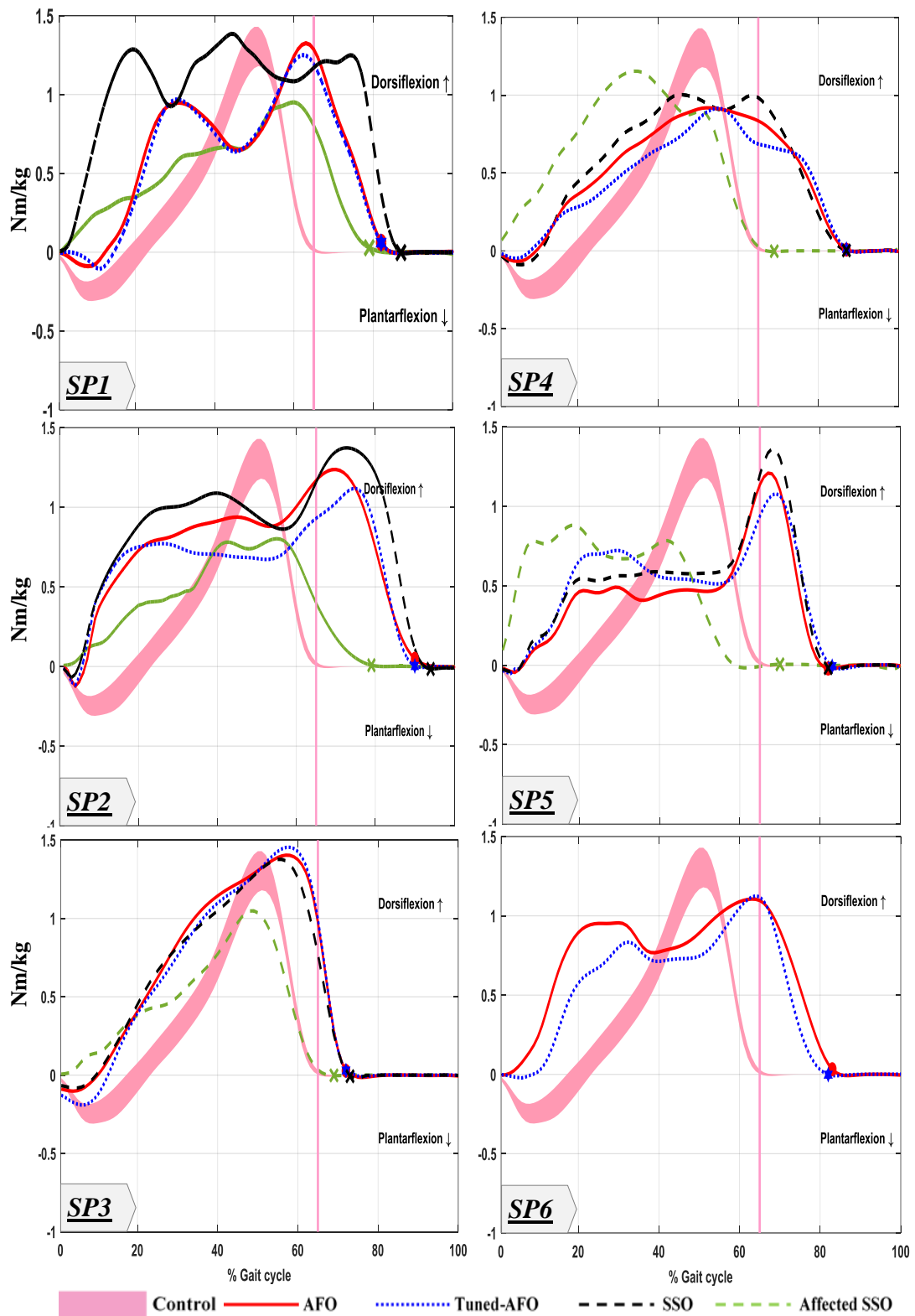


Figure 7.27: Sagittal ankle moment for stroke participants (SPs) while walking on treadmill wearing Tuned-AFO, AFO and SSO with reference to control participants while wearing SSO.

➤ Vertical ground reaction force (GRFv)

Table 7.10: Vertical GRF of the non-orthotic side and unaffected side for control and stroke participants, respectively.

| Participants | GRFv (N) | <i>Mean±(SD)</i> | | |
|----------------|----------------------|------------------|--------------|-------------|
| | | AFO | Tuned | SSO |
| Control | 1 st peak | 785±(25.0) | 784±(26.2) | 833±(27.2) |
| | Trough | 693±(20.2) | 705±(22.7) | 628±(25.0) |
| | 2 nd peak | 766±(12.5) | 755±(11.5) | 815±(11.2) |
| SP1 | 1 st peak | 695±(8.55) | 709±(9.40) | 735±(7.50) |
| | Trough | 702±(10.55) | 700±(11.05) | 708±(10.50) |
| | 2 nd peak | 772±(8.20) | 783±(8.80) | 663±(10.24) |
| SP2 | 1 st peak | 791±(10.50) | 771±(10.85) | 763±(11.05) |
| | Trough | 779±(4.08) | 780±(4.25) | 781±(6.10) |
| | 2 nd peak | 788±(11.10) | 794±(10.05) | 762±(9.85) |
| SP3 | 1 st peak | 960±(10.05) | 981±(10.15) | 964±(8.12) |
| | Trough | 930±(9.15) | 932±(7.80) | 929±(6.29) |
| | 2 nd peak | 992±(10.02) | 1053±(10.00) | 1008±(8.55) |
| SP4 | 1 st peak | 651±(10.00) | 636±(10.00) | 638±(9.50) |
| | Trough | 624±(4.19) | 637±(4.25) | 635±(6.10) |
| | 2 nd peak | 630±(10.00) | 630±(9.80) | 577±(10.00) |
| SP5 | 1 st peak | 808±(5.05) | 823±(5.12) | 784±(6.10) |
| | Trough | 924±(8.85) | 940±(7.58) | 855±(5.15) |
| | 2 nd peak | 839±(7.50) | 845±(7.50) | 816±(8.57) |
| SP6 | 1 st peak | 838±(7.52) | 837±(7.58) | - |
| | Trough | 775±(8.00) | 742±(8.75) | - |
| | 2 nd peak | 856±(9.00) | 817±(9.02) | - |

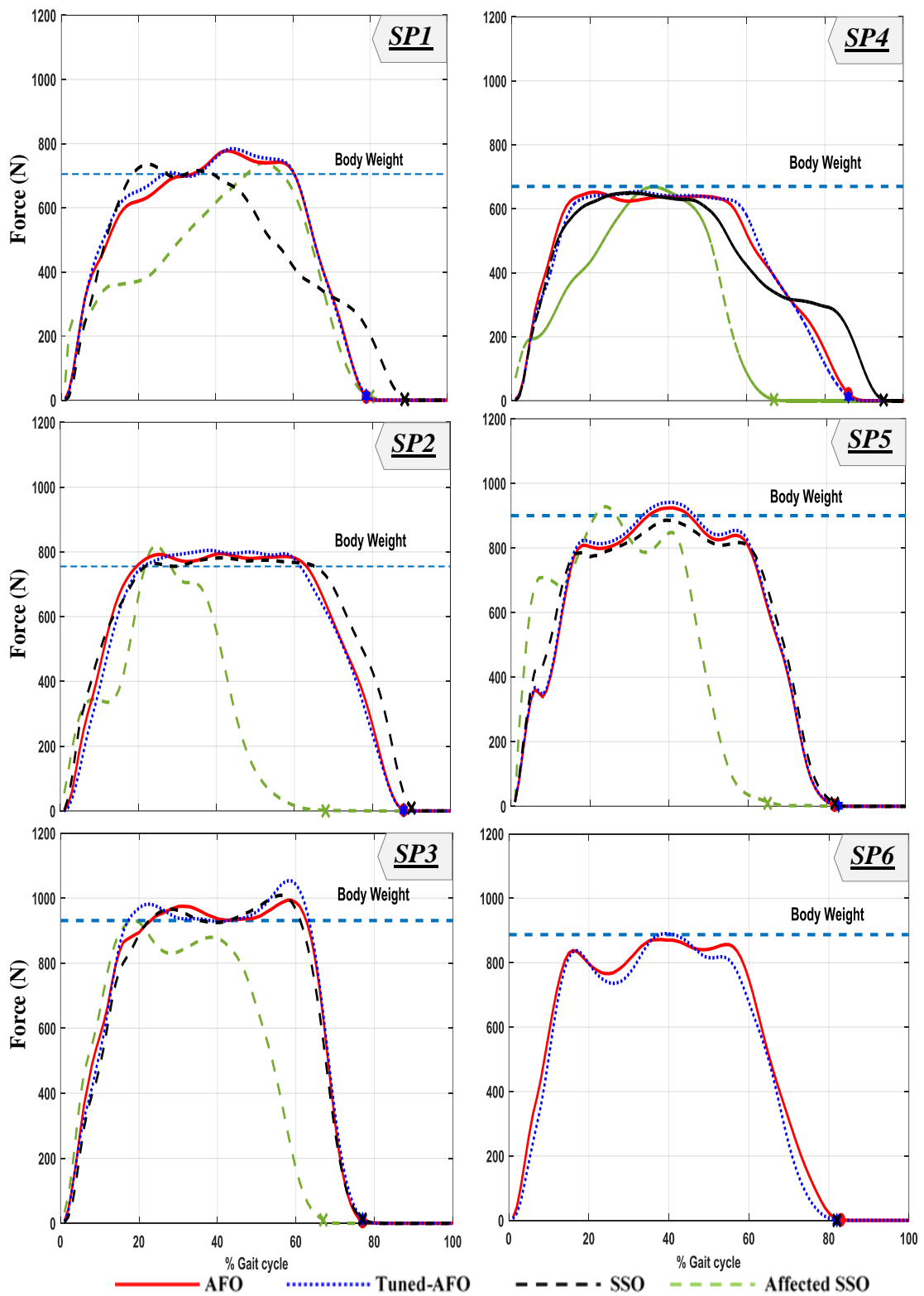


Figure 7.28: Vertical GRF for stroke participants (SPs) while walking on treadmill wearing Tuned-AFO, AFO and SSO with reference to their body weights'.

❖ EMG outputs peaks and their time of occurrence

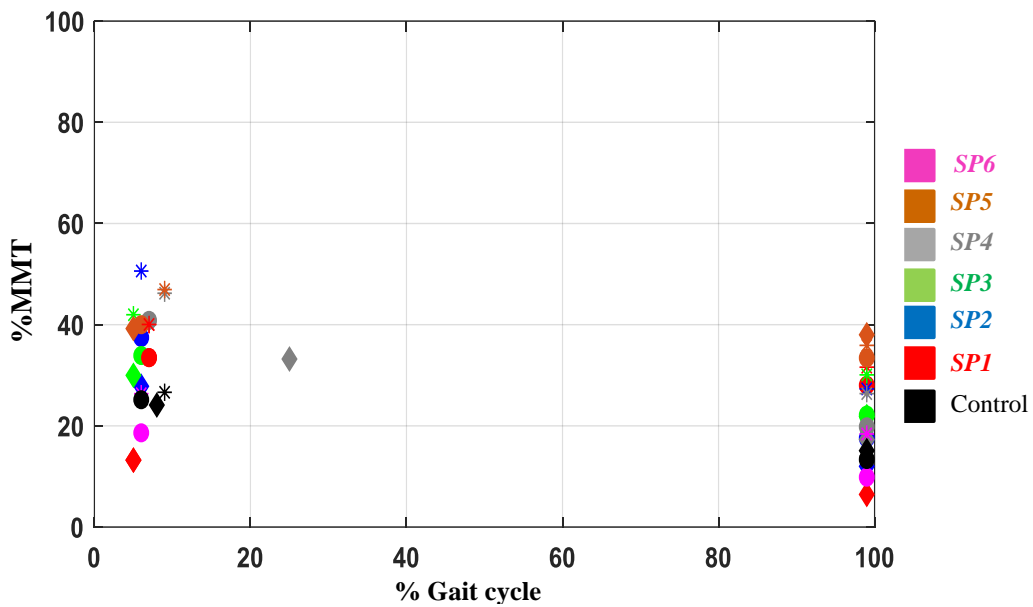


Figure 7.29: Vastus lateralis muscle peaks and their time of occurrence for all participants. The VL peaks for each participant were assigned with different colour to represent the walking conditions as follows; AFO (●), Tuned-AFO (*) and SSO (◆).

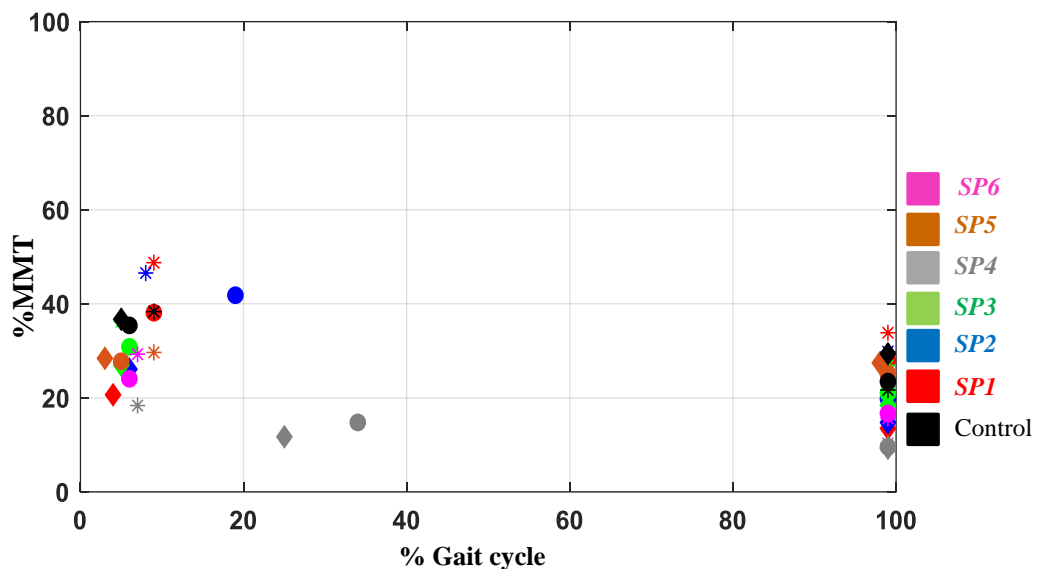


Figure 7.30: Vastus medialis muscle peaks and their time of occurrence for all participants. The VM peaks for each participant were assigned with different colour to represent the walking conditions as follows; AFO (●), Tuned-AFO (*) and SSO (◆).

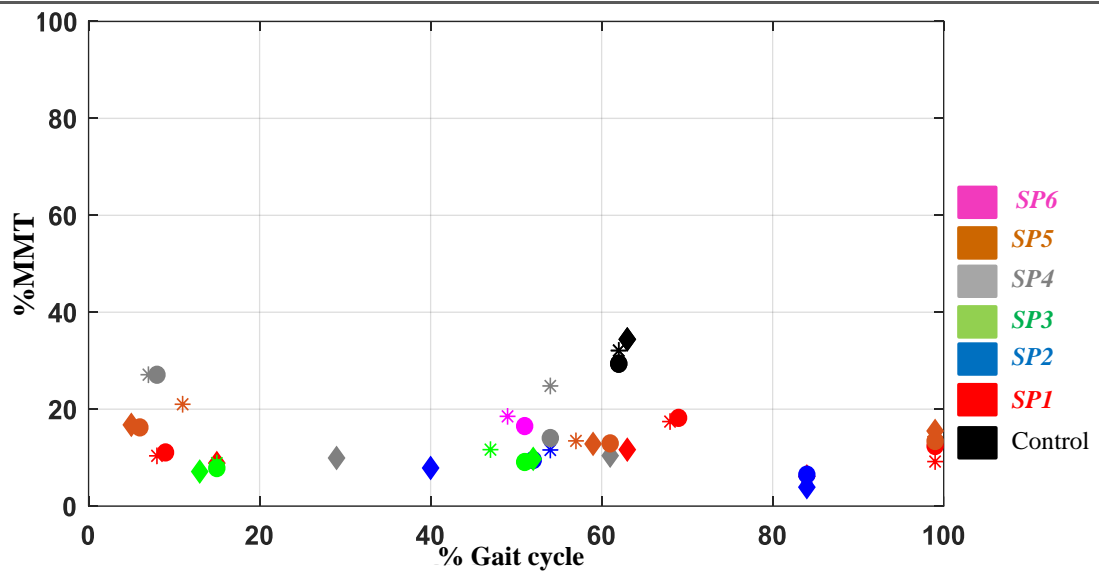


Figure 7.31: Rectus femoris muscle peaks and their time of occurrence for all participants. The RF peaks for each participant were assigned with different colour to represent the walking conditions as follows; AFO (●), Tuned-AFO (*) and SSO (◆).

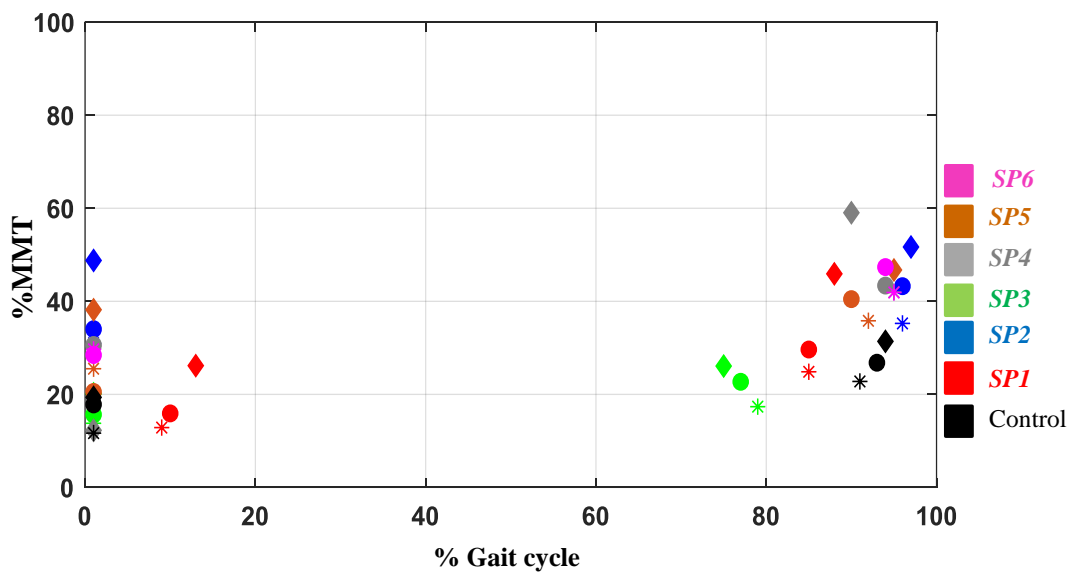


Figure 7.32: Biceps femoris muscle peaks and their time of occurrence for all participants. The BF peaks for each participant were assigned with different colour to represent the walking conditions as follows; AFO (●), Tuned-AFO (*) and SSO (◆).

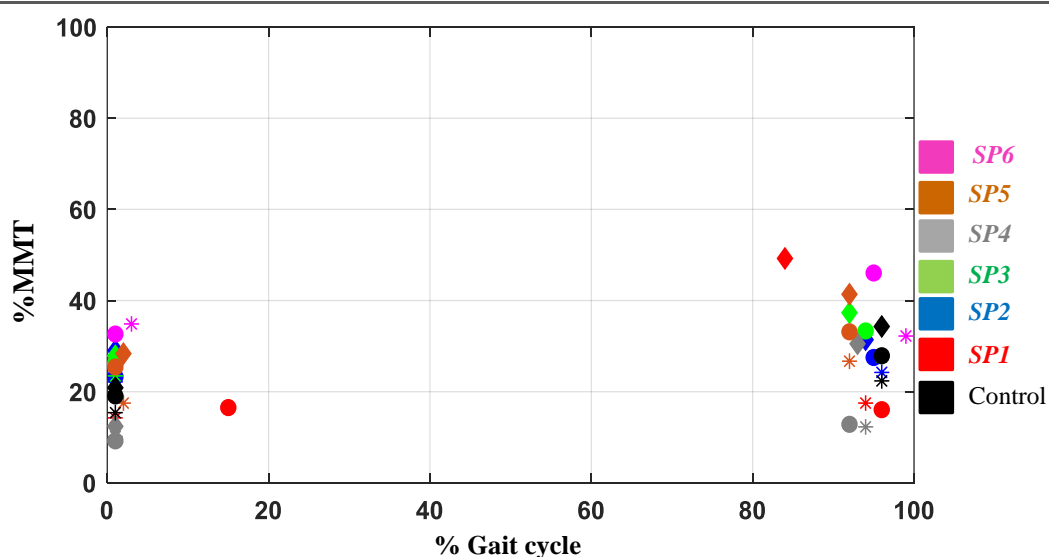


Figure 7.33: Semitendinosus muscle peaks and their time of occurrence for all participants. The ST peaks for each participant were assigned with different colour to represent the walking conditions as follows; AFO (●), Tuned-AFO (*) and SSO (◆).

❖ The relationship between ankle moments and the ankle angle in sagittal plane

The relationship between the total ankle moment and the ankle angle, and the orthotic moment and the ankle angle under AFO and Tuned-AFO conditions for control and stroke participants during a complete gait cycle are shown in Figure 7.34, Figure 7.35 and Figure 7.36. In these figures, the negative sign represents the plantarflexion angle and plantarflexion moments, and the positive sign represents the dorsiflexion angle and dorsiflexion moment.

❖ *Control participants*

In control participants, the orthotic plantarflexion moment during loading response increases with increased ankle plantarflexion angle and then decreases as the plantarflexion angle decreases towards the end of loading response (Figure 7.34). The peak orthotic plantarflexion moment in Tuned-AFO (-0.46 ± 0.02 Nm/kg at -2.28 ± 0.04 degrees) is greater than in AFO (-0.32 ± 0.02 Nm/kg at -3.73 ± 0.03 degrees). During the rest of stance, the orthotic dorsiflexion moment increases as the dorsiflexion angle of the ankle increases and decreases as the ankle dorsiflexion angle decreases (Figure 7.34). Peak orthotic dorsiflexion moment in Tuned-AFO (0.11 ± 0.02 Nm/kg at 5.59 ± 0.04

degrees) is slightly and slightly higher than in AFO (0.09 ± 0.02 Nm/kg at 4.56 ± 0.04 degrees) ($p > 0.05$). The Figure 7.34 (B) shows that orthotic plantarflexion moment increases greatly with plantarflexion, on the other hand, the increment of the orthotic dorsiflexion are much less.

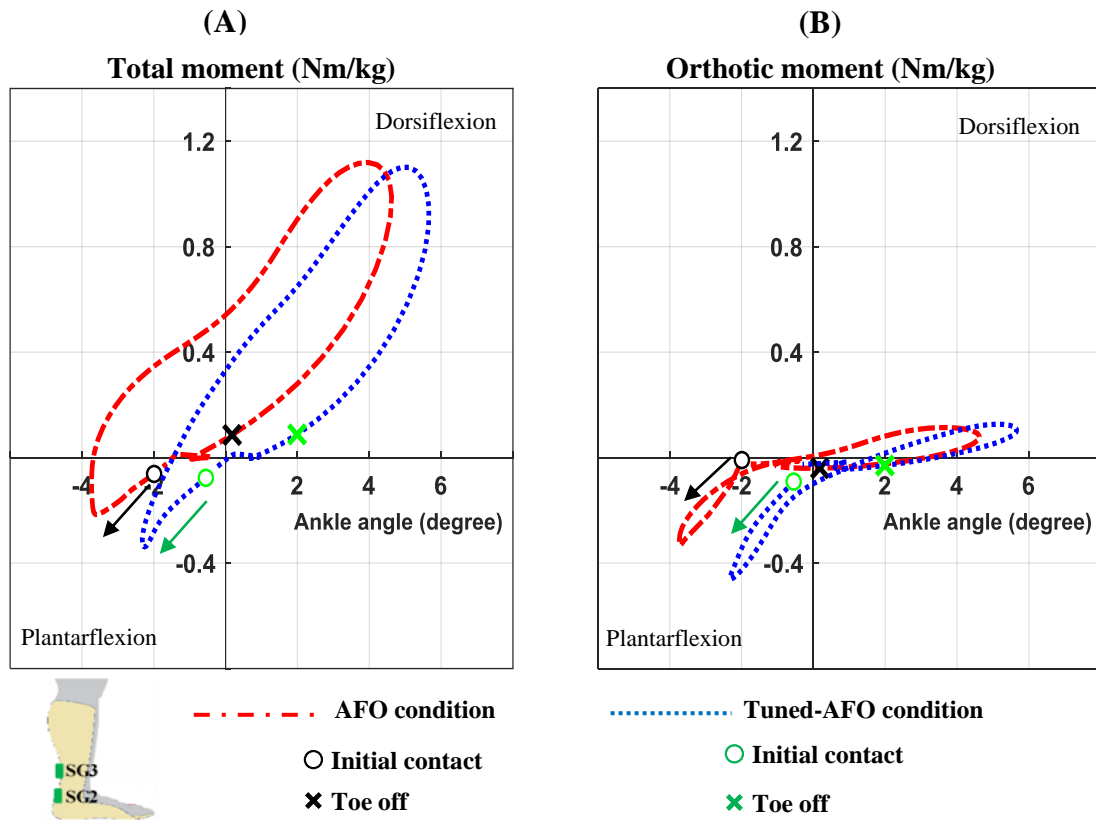


Figure 7.34: The relationship between the total ankle moment and the ankle angle (A), the relationship between the orthotic ankle moment (derived from SG2) and the ankle angle (B) under AFO and Tuned-AFO conditions during a complete gait cycle for control participants.

❖ *Stroke participants*

In stroke participants, the same relationship between orthotic moment and ankle angle is noticed as is the case in control participants, but with main general difference, that is; the ankle angle shows very limited changes and thus orthotic moment changes will be limited as well (Figure 7.35 and Figure 7.36). Additionally, orthotic plantarflexion moment is greater than orthotic dorsiflexion moment. In fact, none of the stroke participants shows

orthotic dorsiflexion moment at any point in the gait cycle (the maximum value of the orthotic dorsiflexion moment among all stroke participants was in **SP4** (0.02 ± 0.01 Nm/kg). Orthotic plantarflexion moment was higher in Tuned-AFO than in AFO in all stroke participants.

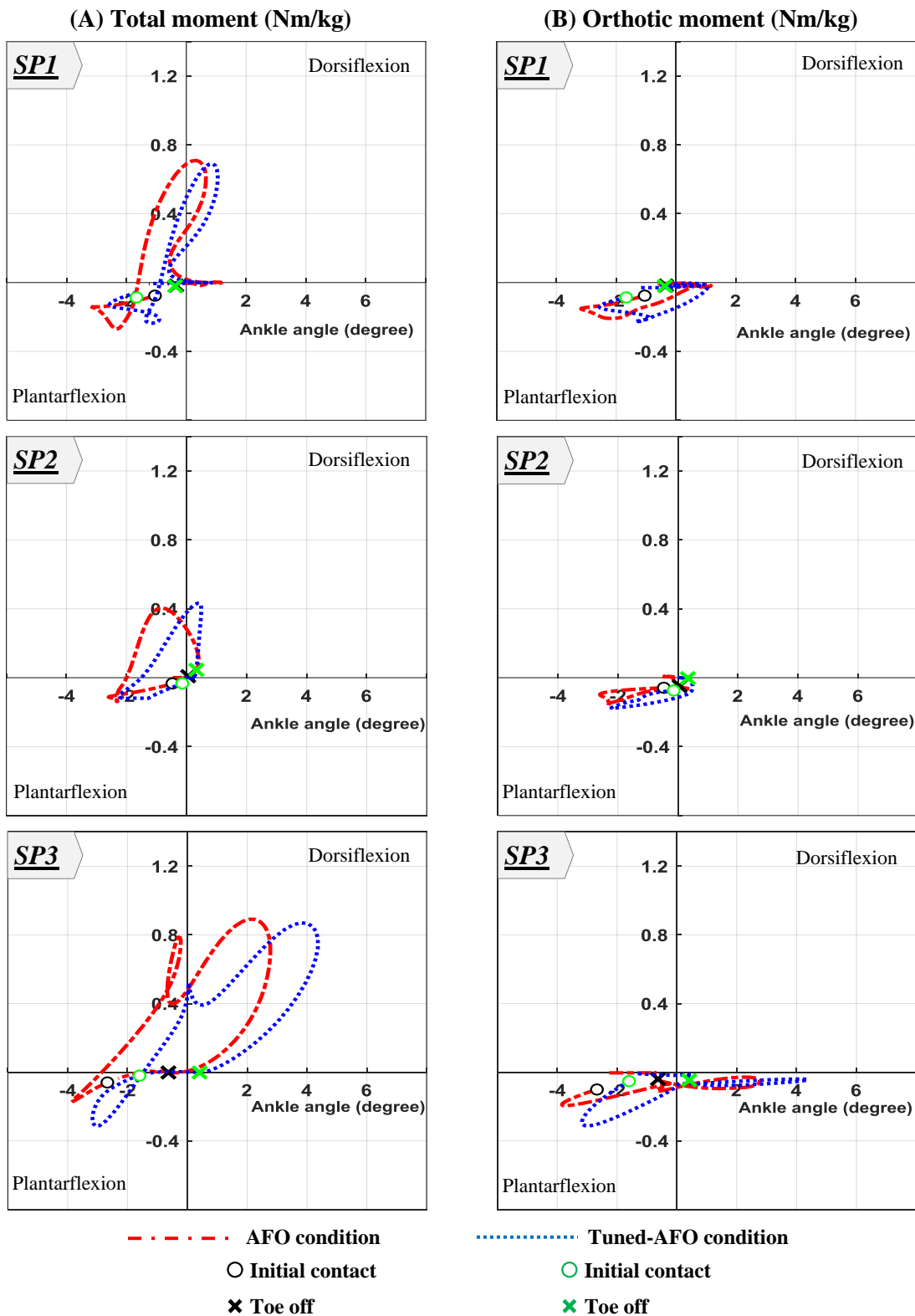


Figure 7.35: The relationship between the total ankle moment and the ankle angle (A), the relationship between the orthotic ankle moment (derived from SG2) and the ankle angle (B) under an AFO and a Tuned-AFO conditions during a complete gait cycle for *SP1*, *SP2*, and *SP3*.

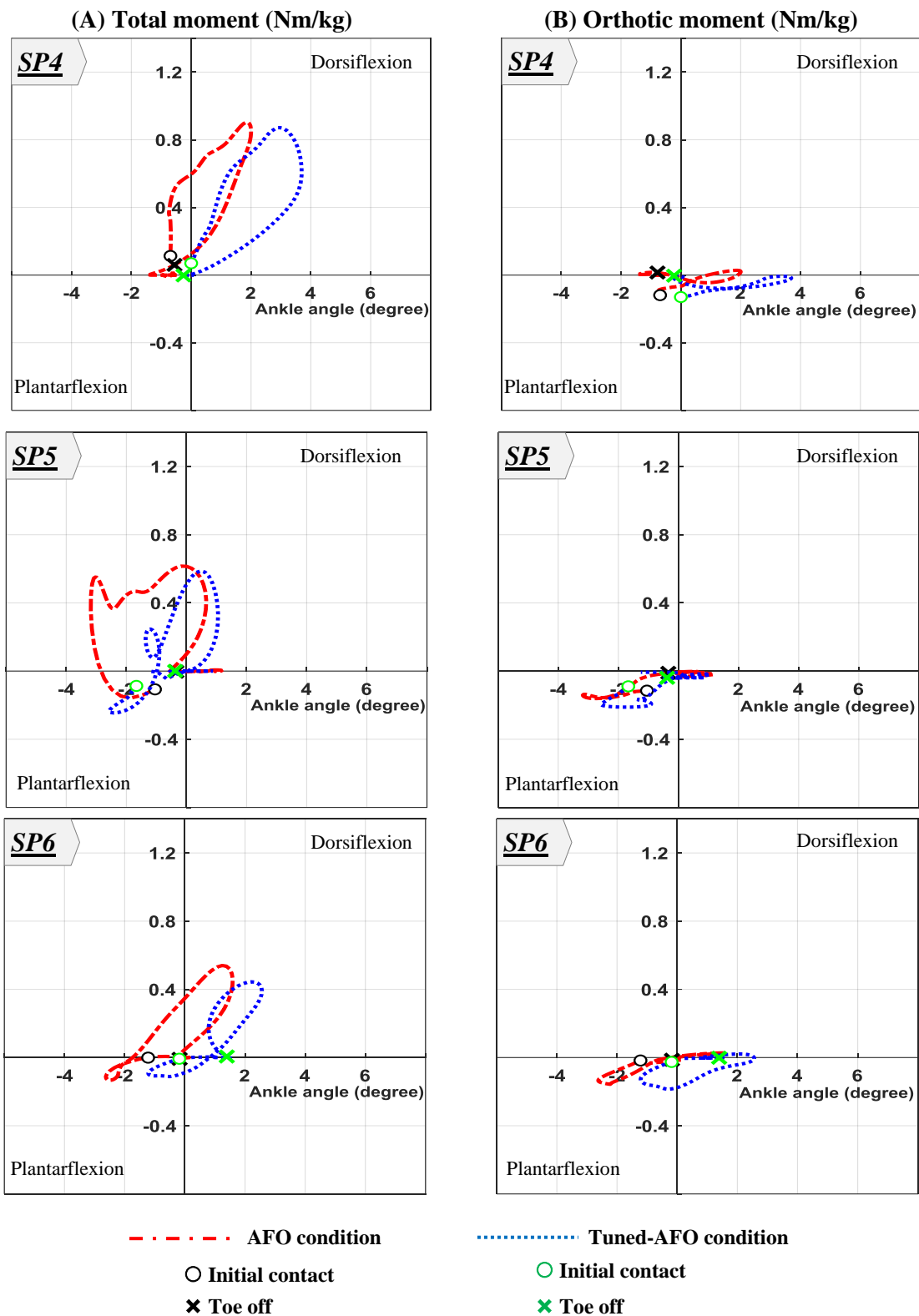


Figure 7.36: The relationship between the total ankle moment and the ankle angle (A), the relationship between the orthotic ankle moment (derived from SG2) and the ankle angle (B) under an AFO and a Tuned-AFO conditions during a complete gait cycle for *SP4*, *SP5*, and *SP6*.

References

- 'BS 527-2' 1996. Plastics-Determination of tensile properties-Part 2:Test conditions for moulding and extrusion plastic. *British Standard Institution, London*.
- Abe H, Michimata A, Sugawara K, Sugaya N,Izumi S-I 2009. Improving gait stability in stroke hemiplegic patients with a plastic ankle-foot orthosis. *The Tohoku journal of experimental medicine*, 218, 193-199.
- Ada L, Dean C M, Morris M E, Simpson J M,Katrak P 2010a. Randomized trial of treadmill walking with body weight support to establish walking in subacute stroke: the MOBILISE trial. *Stroke*, 41, 1237-1242.
- Ada L, Dean C M, Vargas J,Ennis S 2010b. Mechanically assisted walking with body weight support results in more independent walking than assisted overground walking in non-ambulatory patients early after stroke: a systematic review. *Journal of physiotherapy*, 56, 153-161.
- Adeoye O,Broderick J P 2010. Advances in the management of intracerebral hemorrhage. *Nature Reviews Neurology*, 6, 593.
- Ali M, Lyden P,Brady M 2015. Aphasia and dysarthria in acute stroke: recovery and functional outcome. *International journal of stroke*, 10, 400-406.
- Allen D G, Lamb G D,Westerblad H 2008. Skeletal muscle fatigue: cellular mechanisms. *Physiological reviews*.
- Amrutha N,Arul V 2017. A Review on Noises in EMG Signal and its Removal. *Int. J. Sci. Res. Publ*, 7, 23-27.
- Andersen M S, Benoit D L, Damsgaard M, Ramsey D K,Rasmussen J 2010. Do kinematic models reduce the effects of soft tissue artefacts in skin marker-based motion analysis? An in vivo study of knee kinematics. *Journal of biomechanics*, 43, 268-273.
- Andriacchi T, Ogle J,Galante J 1977. Walking speed as a basis for normal and abnormal gait measurements. *Journal of biomechanics*, 10, 261-268.
- Arnold A S, Blemker S S,Delp S L 2001. Evaluation of a deformable musculoskeletal model for estimating muscle–tendon lengths during crouch gait. *Annals of biomedical engineering*, 29, 263-274.
- Asher L, Aresu M, Falaschetti E,Mindell J 2012. Most older pedestrians are unable to cross the road in time: a cross-sectional study. *Age and ageing*, 41, 690-694.
- Awad L N, Binder-Macleod S A, Pohlig R T,Reisman D S 2015. Paretic propulsion and trailing limb angle are key determinants of long-distance walking function after stroke. *Neurorehabilitation and neural repair*, 29, 499-508.

- Baker R 2003. ISB recommendation on definition of joint coordinate systems for the reporting of human joint motion-part I: ankle, hip and spine. *Journal of Biomechanics*, 2, 300-302.
- Banerjee G, Stone S P, Werring D J 2018. Posterior circulation ischaemic stroke. *Bmj*, 361, k1185.
- Barbeau H, Rossignol S 1994. Enhancement of locomotor recovery following spinal cord injury. *Current opinion in neurology*, 7, 517-524.
- Barkema D D, Derrick T R, Martin P E 2012. Heel height affects lower extremity frontal plane joint moments during walking. *Gait & posture*, 35, 483-488.
- Barre A, Armand S 2014. Biomechanical ToolKit: Open-source framework to visualize and process biomechanical data. *Computer methods and programs in biomedicine*, 114, 80-87.
- Barrett C, Taylor P 2010. The effects of the Odstock drop foot stimulator on perceived quality of life for people with stroke and multiple sclerosis. *Neuromodulation: Technology at the Neural Interface*, 13, 58-64.
- Baumgart F 2000. Stiffness-an unknown world of mechanical science? *Injury-International Journal for the Care of the Injured*, 31, 14-23.
- Beasley W 1961. Quantitative muscle testing: principles and applications to research and clinical services. *Archives of Physical Medicine and Rehabilitation*, 42, 398.
- Becher J G 2002. Pediatric rehabilitation in children with cerebral palsy: general management, classification of motor disorders. *JPO: Journal of Prosthetics and Orthotics*, 14, 143-149.
- Begg R, Galea M P, James L, Sparrow W T, Levinger P, Khan F, Said C M 2019. Real-time foot clearance biofeedback to assist gait rehabilitation following stroke: a randomized controlled trial protocol. *Trials*, 20, 317.
- Belagaje S, Kissela B 2010. Epidemiology of stroke recovery. *Brain Repair After Stroke*, 2, 163.
- Belda-Lois J-M, Mena-del Horno S, Bermejo-Bosch I, Moreno J C, Pons J L, Farina D, Iosa M, Molinari M, Tamburella F, Ramos A 2011. Rehabilitation of gait after stroke: a review towards a top-down approach. *Journal of neuroengineering and rehabilitation*, 8, 66.
- Bennett B C, Russell S D, Abel M F 2012. The effects of ankle foot orthoses on energy recovery and work during gait in children with cerebral palsy. *Clinical Biomechanics*, 27, 287-291.
- Berenpas F, Schiemanck S, Beelen A, Nollet F, Weerdesteyn V, Geurts A 2018. Kinematic and kinetic benefits of implantable peroneal nerve stimulation in people with

post-stroke drop foot using an ankle-foot orthosis. *Restorative neurology and neuroscience*, 36, 547-558.

Berg K, Wood-Dauphine S, Williams J, Gayton D 1989. Measuring balance in the elderly: preliminary development of an instrument. *Physiotherapy Canada*, 41, 304-311.

Bernhardt J, Chan J, Nicola I, Collier J M 2007. Little therapy, little physical activity: rehabilitation within the first 14 days of organized stroke unit care. *Journal of rehabilitation medicine*, 39, 43-48.

Bethoux F, Rogers H L, Nolan K J, Abrams G M, Annaswamy T M, Brandstater M, Browne B, Burnfield J M, Feng W, Freed M J 2014. The effects of peroneal nerve functional electrical stimulation versus ankle-foot orthosis in patients with chronic stroke: a randomized controlled trial. *Neurorehabilitation and neural repair*, 28, 688-697.

Bielby S A, Warrick T J, Benson D, Brooks R E, Skewes E, Alvarez E, Dunning C, DesJardins J D 2010. Trimline severity significantly affects rotational stiffness of ankle-foot orthosis. *JPO: Journal of Prosthetics and Orthotics*, 22, 204-210.

Birkenmeier R L, Prager E M, Lang C E 2010. Translating animal doses of task-specific training to people with chronic stroke in 1-hour therapy sessions: a proof-of-concept study. *Neurorehabilitation and neural repair*, 24, 620-635.

Boake C, Noser E A, Ro T, Baraniuk S, Gaber M, Johnson R, Salmeron E T, Tran T M, Lai J M, Taub E 2007. Constraint-induced movement therapy during early stroke rehabilitation. *Neurorehabilitation and neural repair*, 21, 14-24.

Bogey R A, Barnes L A, Perry J 1992. Computer algorithms to characterize individual subject EMG profiles during gait. *Archives of physical medicine and rehabilitation*, 73, 835-841.

Bohannon R 1987. Gait performance of hemiparetic stroke patients: selected variables. *Archives of physical medicine and rehabilitation*, 68, 777-781.

Bohannon R W, Andrews A W 2011. Normal walking speed: a descriptive meta-analysis. *Physiotherapy*, 97, 182-189.

Bohannon R W, Larkin P A, Smith M B, Horton M G 1987. Relationship between static muscle strength deficits and spasticity in stroke patients with hemiparesis. *Physical therapy*, 67, 1068-1071.

Bohannon R W, Smith M B 1987. Interrater reliability of a modified Ashworth scale of muscle spasticity. *Physical Therapy*, 67, 206-7.

Bonnì S, Ponzio V, Caltagirone C, Koch G 2014. Cerebellar theta burst stimulation in stroke patients with ataxia. *Functional neurology*, 29, 41.

Bowers R, Ross K 2010. Development of a best practice statement on the use of ankle-foot orthoses following stroke in Scotland. *Prosthetics and orthotics international*, 34, 245-253.

- Bowker P, Condie D, Bader D, Pratt D, Wallace W 1993. *Biomechanical basis of orthotic management*, Butterworth-Heinemann Oxford.
- Boyd R N, Graham H K 1999. Objective measurement of clinical findings in the use of botulinum toxin type A for the management of children with cerebral palsy. *European Journal of Neurology*, 6, s23-s35.
- Braund M, Kroontje D, Brooks J, Self B, Aaron G, Bearden K 2005. Analysis of stiffness reduction in varying curvature ankle foot orthoses. *Biomedical Sciences Instrumentation*, 41, 19-24.
- Bray B D, Smith C J, Cloud G C, Enderby P, James M, Paley L, Tyrrell P J, Wolfe C D, Rudd A G 2017. The association between delays in screening for and assessing dysphagia after acute stroke, and the risk of stroke-associated pneumonia. *J Neurol Neurosurg Psychiatry*, 88, 25-30.
- Bregman D, Rozumalski A, Koops D, De Groot V, Schwartz M, Harlaar J 2009. A new method for evaluating ankle foot orthosis characteristics: BRUCE. *Gait & posture*, 30, 144-149.
- Bregman D, Van der Krogt M, De Groot V, Harlaar J, Wisse M, Collins S 2011. The effect of ankle foot orthosis stiffness on the energy cost of walking: a simulation study. *Clinical Biomechanics*, 26, 955-961.
- Bregman D J, De Groot V, Van Diggele P, Meulman H, Houdijk H, Harlaar J 2010. Polypropylene ankle foot orthoses to overcome drop-foot gait in central neurological patients: a mechanical and functional evaluation. *Prosthetics and orthotics international*, 34, 293-304.
- Bruel-Jungerman E, Davis S, Laroche S 2007. Brain plasticity mechanisms and memory: a party of four. *The Neuroscientist*, 13, 492-505.
- Brunner R, Meier G, Ruepp T 1998. Comparison of a stiff and a spring-type ankle-foot orthosis to improve gait in spastic hemiplegic children. *Journal of Pediatric Orthopaedics*, 18, 719-726.
- Bulley C, Shiels J, Wilkie K, Salisbury L 2011. User experiences, preferences and choices relating to functional electrical stimulation and ankle foot orthoses for foot-drop after stroke. *Physiotherapy*, 97, 226-233.
- Burden A M, Lewis S E, Willcox E 2014. The effect of manipulating root mean square window length and overlap on reliability, inter-individual variability, statistical significance and clinical relevance of electromyograms. *Manual therapy*, 19, 595-601.
- Burrige J, Taylor P, Hagan S, Wood D E, Swain I D 1997. The effects of common peroneal stimulation on the effort and speed of walking: a randomized controlled trial with chronic hemiplegic patients. *Clinical rehabilitation*, 11, 201-210.
- Butler P B, Nene A V 1991. The biomechanics of fixed ankle foot orthoses and their potential in the management of cerebral palsied children. *Physiotherapy*, 77, 81-88.

- Cahill L S, Lannin N A, Mak-Yuen Y Y, Turville M L, Carey L M 2018. Changing practice in the assessment and treatment of somatosensory loss in stroke survivors: protocol for a knowledge translation study. *BMC health services research*, 18, 34.
- Cakar E, Durmus O, Tekin L, Dincer U, Kiralp M 2010. The ankle-foot orthosis improves balance and reduces fall risk of chronic spastic hemiparetic patients. *Eur J Phys Rehabil Med*, 46, 363-368.
- Campanini I, Merlo A 2009. Reliability, smallest real difference and concurrent validity of indices computed from GRF components in gait of stroke patients. *Gait & posture*, 30, 127-131.
- Cappa P, Patanè F, Di Rosa G 2005. A continuous loading apparatus for measuring three-dimensional stiffness of ankle-foot orthoses.
- Cappozzo A, Catani F, Della Croce U, Leardini A 1995. Position and orientation in space of bones during movement: anatomical frame definition and determination. *Clinical biomechanics*, 10, 171-178.
- Cappozzo A, Catani F, Leardini A, Benedetti M, Della Croce U 1996. Position and orientation in space of bones during movement: experimental artefacts. *Clinical biomechanics*, 11, 90-100.
- Carr J H 2011. *Neurological rehabilitation: optimizing motor performance*, Elsevier India.
- Carse B, Bowers R, Meadows B C, Rowe P 2015. The immediate effects of fitting and tuning solid ankle-foot orthoses in early stroke rehabilitation. *Prosthetics and orthotics international*, 39, 454-462.
- Carse B, Bowers R J, Meadows B C, Rowe P J 2011. Visualisation to enhance biomechanical tuning of ankle-foot orthoses (AFOs) in stroke: study protocol for a randomised controlled trial. *Trials*, 12, 254.
- Celnik P, Webster B, Glasser D M, Cohen L G 2008. Effects of action observation on physical training after stroke. *Stroke*, 39, 1814-1820.
- Charalambous C P 2014. Interrater reliability of a modified Ashworth scale of muscle spasticity. *Classic papers in orthopaedics*. Springer.
- Chen C-C, Hong W-H, Wang C-M, Chen C-K, Wu K P-H, Kang C-F, Tang S F 2010. Kinematic features of rear-foot motion using anterior and posterior ankle-foot orthoses in stroke patients with hemiplegic gait. *Archives of physical medicine and rehabilitation*, 91, 1862-1868.
- Chen C-L, Chen H-C, Wong M-K, Tang F-T, Chen R-S 2001. Temporal stride and force analysis of cane-assisted gait in people with hemiplegic stroke. *Archives of physical medicine and rehabilitation*, 82, 43-48.

- Chen C, Hong P, Chen C, Chou S W, Wu C, Cheng P, Tang F, Chen H 2007. Ground reaction force patterns in stroke patients with various degrees of motor recovery determined by plantar dynamic analysis. *Chang Gung medical journal*, 30, 62.
- Chen G, Patten C, Kothari D H, Zajac F E 2005. Gait differences between individuals with post-stroke hemiparesis and non-disabled controls at matched speeds. *Gait & posture*, 22, 51-56.
- Chimera N J, Benoit D L, Manal K 2009. Influence of electrode type on neuromuscular activation patterns during walking in healthy subjects. *Journal of electromyography and kinesiology*, 19, e494-e499.
- Chisholm A E 2012. *Dropped Foot Impairment Post Stroke: Gait Deviations and the Immediate Effects of Ankle-Foot Orthotics and Functional Electrical Stimulation*, University of Toronto (Canada).
- Chisholm A E, Perry S D, McIlroy W E 2011. Inter-limb centre of pressure symmetry during gait among stroke survivors. *Gait & posture*, 33, 238-243.
- Chiu M-C, Wu H-C, Chang L-Y 2013. Gait speed and gender effects on center of pressure progression during normal walking. *Gait & posture*, 37, 43-48.
- Choi H, Bjornson K, Fatone S, Steele K M 2016. Using musculoskeletal modeling to evaluate the effect of ankle foot orthosis tuning on musculotendon dynamics: a case study. *Disability and Rehabilitation: Assistive Technology*, 11, 613-618.
- Choi H, Peters K M, MacConnell M B, Ly K K, Eckert E S, Steele K M 2017. Impact of ankle foot orthosis stiffness on Achilles tendon and gastrocnemius function during unimpaired gait. *Journal of biomechanics*, 64, 145-152.
- Choi S-y, Kim T-K, Kim D Y, Kim B-S, Hwang J-H, Park C-W. Development of joint torque sensor applied to compensate crosstalk error. 2012 IEEE International Conference on Automation Science and Engineering (CASE), 2012. IEEE, 1086-1088.
- Chu T-M, Feng R 1998. Determination of stress distribution in various ankle-foot orthoses: experimental stress analysis. *JPO: Journal of Prosthetics and Orthotics*, 10, 11-16.
- Chu T 2000. Determination of peak stress on polypropylene ankle-foot orthoses due to weight change using strain gage technology. *Experimental Techniques*, 24, 28-30.
- Chu T T 2001. Biomechanics of ankle-foot orthoses: past, present, and future. *Topics in stroke rehabilitation*, 7, 19-28.
- Churchill A J, Halligan P W, Wade D T 2003. Relative contribution of footwear to the efficacy of ankle-foot orthoses. *Clinical rehabilitation*, 17, 553-557.
- Classen J, Liepert J, Wise S P, Hallett M, Cohen L G 1998. Rapid plasticity of human cortical movement representation induced by practice. *Journal of neurophysiology*, 79, 1117-1123.

- Collins S H, Wiggin M B, Sawicki G S 2015. Reducing the energy cost of human walking using an unpowered exoskeleton. *Nature*, 522, 212-215.
- Combs-Miller S A, Kalpathi Parameswaran A, Colburn D, Ertel T, Harmeyer A, Tucker L, Schmid A A 2014. Body weight-supported treadmill training vs. overground walking training for persons with chronic stroke: a pilot randomized controlled trial. *Clinical rehabilitation*, 28, 873-884.
- Condie D, Meadows C 1993. Ankle-Foot Orthoses. In: Bowker P, Condie D, Bader D, Pratt D, editors., editors. *Biomechanical Basis of Orthotic Management*. Oxford[England], Boston: Butterworth and Heinemann.
- Condie D N 2008. International organization for standardization (ISO) terminology. *AAOS Atlas of Orthoses and Assistive Devices*. 4th ed. Philadelphia, PA: Mosby Elsevier, 3-7.
- Condie E, Campbell H, Martina D. Report of a consensus conference on the orthotic management of stroke patients. Report of a Consensus Conference on the Orthotic Management of Stroke., 2004. International Society for Prosthetics and Orthotics (ISPO).
- Condie M, Bowers R 2008. Lower limb orthoses for persons who have had a stroke. In: 'Atlas of orthoses and assistive devices', ed Hsu J, Michael J, Fisk JR, 4th edition. *American Academy of Orthopedic Surgeons*, pp 433-440.
- Convery P, Greig R, Ross R, Sockalingam S 2004. A three centre study of the variability of ankle foot orthoses due to fabrication and grade of polypropylene. *Prosthetics and orthotics international*, 28, 175-182.
- Cramer S C, Riley J D 2008. Neuroplasticity and brain repair after stroke. *Current opinion in neurology*, 21, 76-82.
- Cramer S C, Sur M, Dobkin B H, O'Brien C, Sanger T D, Trojanowski J Q, Rumsey J M, Hicks R, Cameron J, Chen D 2011. Harnessing neuroplasticity for clinical applications. *Brain*, 134, 1591-1609.
- Crawford R J, Martin P 2019. *Plastics engineering*, Butterworth-Heinemann, Oxford.
- Criswell E 2010. *Cram's introduction to surface electromyography*, Jones & Bartlett Publishers.
- Cruz T H, Dhaher Y Y 2009. Impact of ankle-foot-orthosis on frontal plane behaviors post-stroke. *Gait & posture*, 30, 312-316.
- Daryabor A, Arazpour M, Aminian G 2018. Effect of different designs of ankle-foot orthoses on gait in patients with stroke: A systematic review. *Gait & posture*, 62, 268-279.
- Daryabor A, Yamamoto S, Orendurff M, Kobayashi T 2020. Effect of types of ankle-foot orthoses on energy expenditure metrics during walking in individuals with stroke: a systematic review. *Disability and Rehabilitation*, 1-11.

- Davidson A C, Auyeung V, Luff R, Holland M, Hodgkiss A, Weinman J 2009. Prolonged benefit in post-polio syndrome from comprehensive rehabilitation: a pilot study. *Disability and rehabilitation*, 31, 309-317.
- Davis III R B, Ounpuu S, Tyburski D, Gage J R 1991. A gait analysis data collection and reduction technique. *Human movement science*, 10, 575-587.
- Dayan E, Cohen L G 2011. Neuroplasticity subserving motor skill learning. *Neuron*, 72, 443-454.
- De Luca C J, Gilmore L D, Kuznetsov M, Roy S H 2010. Filtering the surface EMG signal: Movement artifact and baseline noise contamination. *Journal of biomechanics*, 43, 1573-1579.
- de Wit D C, Buurke J, Nijlant J M, IJzerman M J, Hermens H J 2004. The effect of an ankle-foot orthosis on walking ability in chronic stroke patients: a randomized controlled trial. *Clinical rehabilitation*, 18, 550-557.
- Dean C M, Richards C L, Malouin F 2000. Task-related circuit training improves performance of locomotor tasks in chronic stroke: a randomized, controlled pilot trial. *Archives of physical medicine and rehabilitation*, 81, 409-417.
- Della Croce U, Leardini A, Chiari L, Cappozzo A 2005. Human movement analysis using stereophotogrammetry: Part 4: assessment of anatomical landmark misplacement and its effects on joint kinematics. *Gait & posture*, 21, 226-237.
- Delp S L, Anderson F C, Arnold A S, Loan P, Habib A, John C T, Guendelman E, Thelen D G 2007. OpenSim: open-source software to create and analyze dynamic simulations of movement. *IEEE transactions on biomedical engineering*, 54, 1940-1950.
- DELSYS Trigno 2019. Trigno™ Wireless Biofeedback System. *Download EMGworks® at www.delsys.com/emgworks*, User's Guide, PM-W05.
- Den Otter A, Geurts A, Mulder T, Duysens J 2007. Abnormalities in the temporal patterning of lower extremity muscle activity in hemiparetic gait. *Gait & posture*, 25, 342-352.
- Desloovere K, Molenaers G, Van Gestel L, Huenaerts C, Van Campenhout A, Callewaert B, Van de Walle P, Seyler J 2006. How can push-off be preserved during use of an ankle foot orthosis in children with hemiplegia? A prospective controlled study. *Gait & posture*, 24, 142-151.
- DeToro W W 2001. Plantarflexion resistance of selected ankle-foot orthoses: A pilot study of commonly prescribed prefabricated and custom-molded alternatives. *JPO: Journal of Prosthetics and Orthotics*, 13, 39-44.
- Dickstein R 2008. Rehabilitation of gait speed after stroke: a critical review of intervention approaches. *Neurorehabilitation and neural repair*, 22, 649-660.

- Dimyan M A, Cohen L G 2011. Neuroplasticity in the context of motor rehabilitation after stroke. *Nature Reviews Neurology*, 7, 76.
- Dorsch S, Ada L, Canning C G, Al-Zharani M, Dean C 2012. The strength of the ankle dorsiflexors has a significant contribution to walking speed in people who can walk independently after stroke: an observational study. *Archives of physical medicine and rehabilitation*, 93, 1072-1076.
- Duncan P W, Sullivan K J, Behrman A L, Azen S P, Wu S S, Nadeau S E, Dobkin B H, Rose D K, Tilson J K, Cen S 2011. Body-weight–supported treadmill rehabilitation after stroke. *New England Journal of Medicine*, 364, 2026-2036.
- Duysens J, Pearson K 1980. Inhibition of flexor burst generation by loading ankle extensor muscles in walking cats. *Brain research*, 187, 321-332.
- Eddison N, Chockalingam N 2015. Response: Tuning of rigid ankle-foot orthoses is essential. *Prosthetics and orthotics international*, 39, 260-260.
- Eddison N, Chockalingam N, Osborne S 2015. Ankle foot orthosis–footwear combination tuning: an investigation into common clinical practice in the United Kingdom. *Prosthetics and orthotics international*, 39, 126-133.
- Eddison N, Healy A, Needham R, Chockalingam N 2017. Shank-to-vertical angle in ankle-foot orthoses: A comparison of static and dynamic assessment in a series of cases. *JPO: Journal of Prosthetics and Orthotics*, 29, 161-167.
- Embrey D G, Holtz, S. L., Alon, G., Brandsma, B. A., & McCoy, S. W. 2010. Functional electrical stimulation to dorsiflexors and plantar flexors during gait to improve walking in adults with chronic hemiplegia. *Archives of Physical Medicine and Rehabilitation*, 91(5), 687-696.
- Emos M C, Agarwal S 2018. Neuroanatomy, Upper Motor Neuron Lesion. *StatPearls [Internet]*. StatPearls Publishing.
- Esposito E R, Blanck R V, Harper N G, Hsu J R, Wilken J M 2014. How does ankle-foot orthosis stiffness affect gait in patients with lower limb salvage? *Clinical Orthopaedics and Related Research*®, 472, 3026-3035.
- Esquenazi A 2008. Assessment and orthotic management of gait dysfunction in individuals with traumatic brain injury. In: *'Atlas of orthoses and assistive devices'*, ed Hsu J, Michael J, Fisk JR, 4th edition, American Academy of Orthopedic Surgeons, Philadelphia, 441.
- Esquenazi A, Ofluoglu D, Hirai B, Kim S 2009. The effect of an ankle-foot orthosis on temporal spatial parameters and asymmetry of gait in hemiparetic patients. *PM&R*, 1, 1014-1018.
- Evers S M, Struijs J N, Ament A J, van Genugten M L, Jager J C, van den Bos G A 2004. International comparison of stroke cost studies. *Stroke*, 35, 1209-1215.

- Farmani F, Mohseni-Bandpei M-A, Bahramizadeh M, Aminian G, Abdoli A, Sadeghi-Goghari M 2016a. The influence of rocker bar ankle foot orthosis on gait in patients with chronic hemiplegia. *Journal of Stroke and Cerebrovascular Diseases*, 25, 2078-2082.
- Farmani F, Mohseni Bandpei M A, Bahramizadeh M, Aminian G, Nikoo M R, Sadeghi-goghari M 2016b. The effect of different shoes on functional mobility and energy expenditure in post-stroke hemiplegic patients using ankle-foot orthosis. *Prosthetics and orthotics international*, 40, 591-597.
- Fasoli S E, Krebs H I, Stein J, Frontera W R, Hughes R, Hogan N 2004. Robotic therapy for chronic motor impairments after stroke: Follow-up results. *Archives of physical medicine and rehabilitation*, 85, 1106-1111.
- Fatone S, Gard S A, Malas B S 2009. Effect of ankle-foot orthosis alignment and foot-plate length on the gait of adults with poststroke hemiplegia. *Archives of physical medicine and rehabilitation*, 90, 810-818.
- Feeney D M, Baron J-C 1986. Diaschisis. *Stroke*, 17, 817-830.
- Ferreira L A B, Neto H P, Christovão T C L, Duarte N A, Lazzari R D, Galli M, Oliveira C S 2013. Effect of ankle-foot orthosis on gait velocity and cadence of stroke patients: a systematic review. *Journal of physical therapy science*, 25, 1503-1508.
- Finger S, Koehler P J, Jagella C 2004. The Monakow concept of diaschisis: origins and perspectives. *Archives of Neurology*, 61, 283-288.
- Francisco G E, McGuire J R 2012. Poststroke spasticity management. *Stroke*, 43, 3132-3136.
- French B, Thomas L, Leathley M, Sutton C, McAdam J, Forster A, Langhorne P, Price C, Walker A, Watkins C 2010. Does repetitive task training improve functional activity after stroke? A Cochrane systematic review and meta-analysis. *Journal of rehabilitation medicine*, 42, 9-15.
- French B, Thomas L H, Coupe J, McMahon N E, Connell L, Harrison J, Sutton C J, Tishkovskaya S, Watkins C L 2016. Repetitive task training for improving functional ability after stroke. *Cochrane database of systematic reviews*.
- Gao F, Carlton W, Kapp S 2011. Effects of joint alignment and type on mechanical properties of thermoplastic articulated ankle-foot orthosis. *Prosthetics and orthotics international*, 35, 181-189.
- Gard S, Fatone S. Biomechanics of lower limb function and gait. Report of a consensus conference on the orthotic management of stroke patients. Copenhagen (Denmark): International Society for Prosthetics and Orthotics, 2003. 55-63.
- Gatti M A, Freixes O, Fernández S A, Rivas M E, Crespo M, Waldman S V, Olmos L E 2012. Effects of ankle foot orthosis in stiff knee gait in adults with hemiplegia. *Journal of biomechanics*, 45, 2658-2661.

- Geboers J F, Drost M R, Spaans F, Kuipers H, Seelen H A 2002. Immediate and long-term effects of ankle-foot orthosis on muscle activity during walking: a randomized study of patients with unilateral foot drop. *Archives of physical medicine and rehabilitation*, 83, 240-245.
- Getliffe K, Thomas L 2019. Promoting Continence. *Stroke Nursing*, 2, 229-258.
- Gibbons E M, Thomson A N, de Noronha M, Joseph S 2016. Are virtual reality technologies effective in improving lower limb outcomes for patients following stroke—a systematic review with meta-analysis. *Topics in stroke rehabilitation*, 23, 440-457.
- Giraldo E A 2018. Overview of Stroke. <https://www.msmanuals.com/home/brain,-spinal-cord,-and-nerve-disorders/stroke-cva/overview-of-stroke>.
- Glanz M, Klawansky S, Stason W, Berkey C, Chalmers T C 1996. Functional electrostimulation in poststroke rehabilitation: a meta-analysis of the randomized controlled trials. *Archives of physical medicine and rehabilitation*, 77, 549-553.
- Gök H, Küçükdeveci A, Altinkaynak H, Yavuzer G, Ergin S 2003. Effects of ankle-foot orthoses on hemiparetic gait. *Clinical rehabilitation*, 17, 137-139.
- Golay W, Lunsford T, Lunsford B R, Greenfield J 1989. The effect of malleolar prominence on polypropylene AFO rigidity and buckling. *JPO: Journal of Prosthetics and Orthotics*, 1, 231-241.
- Goldie P A, Matyas T A, Evans O M 1996. Deficit and change in gait velocity during rehabilitation after stroke. *Archives of physical medicine and rehabilitation*, 77, 1074-1082.
- Goldstein E M 2001. Spasticity management: an overview. *Journal of child neurology*, 16, 16-23.
- Good D, Supan T, Aisen M 1989. Basic principles of orthotics in neurologic disorders. *Orthotics in neurologic rehabilitation*, ML Aisen, ed., Demos Publications, New York.
- Gregson J M, Leathley M, Moore A P, Sharma A K, Smith T L, Watkins C L 1999. Reliability of the Tone Assessment Scale and the modified Ashworth scale as clinical tools for assessing poststroke spasticity. *Archives of physical medicine and rehabilitation*, 80, 1013-1016.
- Grood E S, Suntay W J 1983. A joint coordinate system for the clinical description of three-dimensional motions: application to the knee. *Journal of biomechanical engineering*, 105, 136-144.
- Guichet J-M, Javed A, Russell J, Saleh M 2003. Effect of the foot on the mechanical alignment of the lower limbs. *Clinical Orthopaedics and Related Research*®, 415, 193-201.

- Hakonen M, Piitulainen H, Visala A 2015. Current state of digital signal processing in myoelectric interfaces and related applications. *Biomedical Signal Processing and Control*, 18, 334-359.
- Halaki M, Ginn K 2012. Normalization of EMG signals: to normalize or not to normalize and what to normalize to? *Computational intelligence in electromyography analysis-a perspective on current applications and future challenges*. IntechOpen.
- Halim I, Omar A R, Saman A M, Othman I 2012. Assessment of muscle fatigue associated with prolonged standing in the workplace. *Safety and health at work*, 3, 31-42.
- Hallett M 2001. Plasticity of the human motor cortex and recovery from stroke. *Brain research reviews*, 36, 169-174.
- Handelzalts S, Melzer I, Soroker N 2019. Analysis of brain lesion impact on balance and gait following stroke. *Frontiers in human neuroscience*, 13, 149.
- Hans J 2011. *Clinical neuroanatomy: brain circuitry and its disorders*, Springer Science & Business Media.
- Harper N G, Esposito E R, Wilken J M, Neptune R R 2014. The influence of ankle-foot orthosis stiffness on walking performance in individuals with lower-limb impairments. *Clinical Biomechanics*, 29, 877-884.
- Harrington M, Zavatsky A, Lawson S, Yuan Z, Theologis T 2007. Prediction of the hip joint centre in adults, children, and patients with cerebral palsy based on magnetic resonance imaging. *Journal of biomechanics*, 40, 595-602.
- Harvey R L, Macko R F, Stein J, Winstein C J, Zorowitz R D 2008. *Stroke recovery and rehabilitation*, Demos Medical Publishing.
- Hausdorff J M, Alexander N B 2005. *Gait disorders: evaluation and management*, Taylor & Francis US.
- Hausdorff J M, Ring H 2008. Effects of a new radio frequency-controlled neuroprosthesis on gait symmetry and rhythmicity in patients with chronic hemiparesis. *American journal of physical medicine & rehabilitation*, 87, 4-13.
- Hayward K S, Brauer S G 2015. Dose of arm activity training during acute and subacute rehabilitation post stroke: a systematic review of the literature. *Clinical rehabilitation*, 29, 1234-1243.
- Heimer L 2012. *The human brain and spinal cord: functional neuroanatomy and dissection guide*, Springer Science & Business Media.
- Helldén J, Bergström L, Karlsson S 2018. Experiences of living with persisting post-stroke dysphagia and of dysphagia management—a qualitative study. *International Journal of Qualitative Studies on Health and Well-being*, 13.

- Hermens H J, Freriks B, Disselhorst-Klug C, Rau G 2000. Development of recommendations for SEMG sensors and sensor placement procedures. *Journal of electromyography and Kinesiology*, 10, 361-374.
- Hesse S, Luecke D, Jahnke M, Mauritz K 1996. Gait function in spastic hemiparetic patients walking barefoot, with firm shoes, and with ankle-foot orthosis. *International journal of rehabilitation research. Internationale Zeitschrift für Rehabilitationsforschung. Revue internationale de recherches de readaptation*, 19, 133-141.
- Hesse S, Werner C, Matthias K, Stephen K, Bertheanu M 1999. Non-velocity-related effects of a rigid double-stopped ankle-foot orthosis on gait and lower limb muscle activity of hemiparetic subjects with an equinovarus deformity. *Stroke*, 30, 1855-1861.
- Hobbs B, Artemiadis P 2020. A review of robot-assisted lower-limb stroke therapy: unexplored paths and future directions in gait rehabilitation. *Frontiers in neurorobotics*, 14.
- Hodics T, Cohen L G, Cramer S C 2006. Functional imaging of intervention effects in stroke motor rehabilitation. *Archives of physical medicine and rehabilitation*, 87, 36-42.
- Hoffmann K 2012. An introduction to stress analysis and transducer design using strain gauges. The definitive work on strain gauge measurement.
- Hollman J H, Watkins M K, Imhoff A C, Braun C E, Akervik K A, Ness D K 2016. A comparison of variability in spatiotemporal gait parameters between treadmill and overground walking conditions. *Gait & posture*, 43, 204-209.
- Hong Z, Sui M, Zhuang Z, Liu H, Zheng X, Cai C, Jin D 2018. Effectiveness of neuromuscular electrical stimulation on lower limbs of patients with hemiplegia after chronic stroke: a systematic review. *Archives of physical medicine and rehabilitation*, 99, 1011-1022. e1.
- Howard R M, Conway R, Harrison A J. An exploration of eliminating cross-talk in surface electromyography using independent component analysis. 2015 26th Irish Signals and Systems Conference (ISSC). 2015. IEEE, 1-6.
- Hullin M, Robb J, Loudon I 1992. Ankle-foot orthosis function in low-level myelomeningocele. *Journal of pediatric orthopedics*, 12, 518-521.
- Hullin M, Robb J, Loudon I 1996. Gait patterns in children with hemiplegic spastic cerebral palsy. *Journal of pediatric orthopedics. Part B*, 5, 247-251.
- Hylin M J, Kerr A L, Holden R 2017. Understanding the Mechanisms of Recovery and/or Compensation following Injury. *Neural plasticity*.
- Inman V T, Ralston H J, Todd F 1981. *Human walking*, Williams & Wilkins.
- ISO 1989. ISO 8549-1. Prosthetics and orthotics -Vocabulary. Part 1: General terms for external limb prostheses and external orthoses.

- Jagadamma K C, Owen E, Coutts F J, Herman J, Yirrell J, Mercer T H, Van Der Linden M L 2010. The effects of tuning an ankle-foot orthosis footwear combination on kinematics and kinetics of the knee joint of an adult with hemiplegia. *Prosthetics and orthotics international*, 34, 270-276.
- Jamal M Z 2012. Signal acquisition using surface EMG and circuit design considerations for robotic prosthesis. *Computational Intelligence in Electromyography Analysis-A Perspective on Current Applications and Future Challenges*. IntechOpen.
- Jenkins G, Kemnitz C, Tortora G J 2006. *Anatomy and physiology: from science to life*, John Wiley & Sons Incorporated.
- Jorgensen H S, Nakayama H, Raaschou H O, Olsen T S 1995. Recovery of walking function in stroke patients: the Copenhagen Stroke Study. *Archives of physical medicine and rehabilitation*, 76, 27-32.
- Karimi M T, Jamshidi N 2012. The magnitude of errors associated in measuring the loads applied on an assistive device while walking. *Journal of Medical Signals and Sensors*, 2, 225.
- Kasprisin J, Grabiner M 1998. EMG variability during maximum voluntary isometric and anisometric contractions is reduced using spatial averaging. *Journal of Electromyography and Kinesiology*, 8, 45-50.
- Kautz S A, Bowden M G, Clark D J, Neptune R R 2011. Comparison of motor control deficits during treadmill and overground walking poststroke. *Neurorehabilitation and neural repair*, 25, 756-765.
- Kerkum Y L, Buizer A I, van den Noort J C, Becher J G, Harlaar J, Brehm M-A 2015a. The effects of varying ankle foot orthosis stiffness on gait in children with spastic cerebral palsy who walk with excessive knee flexion. *PloS one*, 10, e0142878.
- Kerkum Y L, Houdijk H, Brehm M-A, Buizer A I, Kessels M L, Sterk A, van den Noort J C, Harlaar J 2015b. The Shank-to-Vertical-Angle as a parameter to evaluate tuning of Ankle-Foot Orthoses. *Gait & posture*, 42, 269-274.
- Kerr A, Rowe P 2019. *An Introduction to Human Movement and Biomechanics*. Elsevier.
- Kerr A, Rowe P, Clarke A, Chandler E, Smith J, Ugbolue C, Pomeroy V 2019. Biomechanical correlates for recovering walking speed following a stroke. The potential of tibia to vertical angle as a therapy target. *Gait and Posture*.
- Kerrigan D C, Frates E P, Rogan S, Riley P O 2000. Hip hiking and circumduction: quantitative definitions. *American journal of physical medicine & rehabilitation*, 79, 247-252.
- Kesar T M, Binder-Macleod S A, Hicks G E, Reisman D S 2011. Minimal detectable change for gait variables collected during treadmill walking in individuals post-stroke. *Gait & posture*, 33, 314-317.

- Kesar T M, Perumal R, Jancosko A, Reisman D S, Rudolph K S, Higginson J S, Binder-Macleod S A 2010. Novel patterns of functional electrical stimulation have an immediate effect on dorsiflexor muscle function during gait for people poststroke. *Physical therapy*, 90, 55-66.
- Kesikburun S, Yavuz F, Güzelküçük Ü, Yaşar E, Balaban B 2017. Effect of ankle foot orthosis on gait parameters and functional ambulation in patients with stroke. *Turkish Journal of Physical Medicine and Rehabilitation*, 63, 143.
- Kessels M, Sterk A, Kerkum Y, Harlaar J, Steenbrink F, Roeles S 2013. The Shank Angle to Vertical as a control parameter for tuning of Ankle Foot Orthoses.
- Kim C M, Eng J J 2003. Symmetry in vertical ground reaction force is accompanied by symmetry in temporal but not distance variables of gait in persons with stroke. *Gait & posture*, 18, 23-28.
- Kim C S, Gong W, Kim S G 2011. The effects of lower extremity muscle strengthening exercise and treadmill walking exercise on the gait and balance of stroke patients. *Journal of Physical Therapy Science*, 23, 405-408.
- Kinsella S, Moran K 2008. Gait pattern categorization of stroke participants with equinus deformity of the foot. *Gait & posture*, 27, 144-151.
- Kirtley C, Whittle M W, Jefferson R 1985. Influence of walking speed on gait parameters. *Journal of biomedical engineering*, 7, 282-288.
- Kluding P M, Dunning K, O'Dell M W, Wu S S, Ginosian J, Feld J, McBride K 2013. Foot drop stimulation versus ankle foot orthosis after stroke: 30-week outcomes. *Stroke*, 44, 1660-1669.
- Kobayashi T, Leung A K, Hutchins S W 2011. Techniques to measure rigidity of ankle-foot orthosis: a review. *Journal of rehabilitation research and development*.
- Kobayashi T, Orendurff M S, Hunt G, Gao F, LeCursi N, Lincoln L S, Foreman K B 2019. The effects of alignment of an articulated ankle-foot orthosis on lower limb joint kinematics and kinetics during gait in individuals post-stroke. *Journal of biomechanics*, 83, 57-64.
- Kobayashi T, Orendurff M S, Singer M L, Gao F, Daly W K, Foreman K B 2016. Reduction of genu recurvatum through adjustment of plantarflexion resistance of an articulated ankle-foot orthosis in individuals post-stroke. *Clinical Biomechanics*, 35, 81-85.
- Kobayashi T, Orendurff M S, Singer M L, Gao F, Foreman K B 2017. Contribution of ankle-foot orthosis moment in regulating ankle and knee motions during gait in individuals post-stroke. *Clinical Biomechanics*, 45, 9-13.
- Kobayashi T, Singer M L, Orendurff M S, Gao F, Daly W K, Foreman K B 2015. The effect of changing plantarflexion resistive moment of an articulated ankle-foot orthosis

on ankle and knee joint angles and moments while walking in patients post stroke. *Clinical Biomechanics*, 30, 775-780.

Kolb B, Teskey C, Gibb R 2010. Factors influencing cerebral plasticity in the normal and injured brain. *Frontiers in human neuroscience*, 4, 204.

Konrad P 2005. The abc of emg. *A practical introduction to kinesiological electromyography*, 1, 30-35.

Kottink A I, Tenniglo M J, de Vries W H, Hermens H J, Buurke J H 2012. Effects of an implantable two-channel peroneal nerve stimulator versus conventional walking device on spatiotemporal parameters and kinematics of hemiparetic gait. *Journal of rehabilitation medicine*, 44, 51-57.

Krakauer J W, Marshall R S 2015. The proportional recovery rule for stroke revisited. *Annals of neurology*, 78, 845-847.

Kwakkel G, Kollen B, Lindeman E 2004. Understanding the pattern of functional recovery after stroke: facts and theories. *Restorative neurology and neuroscience*, 22, 281-299.

Kwakkel G, Kollen B, Wagenaar R 2002. Long term effects of intensity of upper and lower limb training after stroke: a randomised trial. *Journal of Neurology, Neurosurgery & Psychiatry*, 72, 473-479.

Lairamore C, Garrison M K, Bandy W, Zabel R 2011. Comparison of tibialis anterior muscle electromyography, ankle angle, and velocity when individuals post stroke walk with different orthoses. *Prosthetics and orthotics international*, 35, 402-410.

Lance J W 1980. The control of muscle tone, reflexes, and movement: Robert Wartenbeg Lecture. *Neurology*, 30, 1303-1303.

Langhorne P, Bernhardt J, Kwakkel G 2011. Stroke rehabilitation. *The Lancet*, 377, 1693-1702.

Leardini A, Chiari L, Della Croce U, Cappozzo A 2005. Human movement analysis using stereophotogrammetry: Part 3. Soft tissue artifact assessment and compensation. *Gait & posture*, 21, 212-225.

Lee H Y, Lee J H, Kim K 2015. Changes in angular kinematics of the paretic lower limb at different orthotic angles of plantar flexion limitation of an ankle-foot-orthosis for stroke patients. *Journal of physical therapy science*, 27, 825-828.

Lee S-J, Lee D-G, Moon H-J, Lee T-K 2017. Lesion pattern, mechanisms, and long-term prognosis in patients with monoparetic stroke: a comparison with nonmonoparetic stroke. *BioMed research international*, 2017.

Lee S I, Adans-Dester C P, Grimaldi M, Dowling A V, Horak P C, Black-Schaffer R M, Bonato P, Gwin J T 2018. Enabling stroke rehabilitation in home and community settings:

a wearable sensor-based approach for upper-limb motor training. *IEEE journal of translational engineering in health and medicine*, 6, 1-11.

Lehmann J 1979. BIOMECHANICS OF ANKLE-FOOT ORTHOSES: PRESCRIPTION AND DESIGN.

Lehmann J 1986. Lower limb orthotics. *Orthotics Etcetera. 3rd ed. Baltimore, Md: Williams & Wilkins*, 278-351.

Lehmann J F, Esselman P, Ko M, Smith J, Dralle A 1983. Plastic ankle-foot orthoses: evaluation of function. *Archives of physical medicine and rehabilitation*, 64, 402-407.

Lennon S, Bassile C 2018. Guiding principles in neurological rehabilitation. *Neurological Physiotherapy Pocketbook E-Book*, 1.

Leung J, Moseley A 2003. Impact of ankle-foot orthoses on gait and leg muscle activity in adults with hemiplegia: systematic literature review. *Physiotherapy*, 89, 39-55.

Lin H-T, Hsu A-T, Chang J-H, Chien C-S, Chang G-L 2008. Comparison of EMG activity between maximal manual muscle testing and cybex maximal isometric testing of the quadriceps femoris. *Journal of the Formosan Medical Association*, 107, 175-180.

Lin R 2007. Ankle-Foot Orthoses In: Lusardi M, Nielsen C, editors. *Orthotics and Prosthetics in Rehabilitation. Saunders: Elsevier*.

Lindquist A R, Prado C L, Barros R M, Mattioli R, Da Costa P H L, Salvini T F 2007. Gait training combining partial body-weight support, a treadmill, and functional electrical stimulation: effects on poststroke gait. *Physical therapy*, 87, 1144-1154.

Loetscher T, Potter K J, Wong D, das Nair R 2019. Cognitive rehabilitation for attention deficits following stroke. *Cochrane Database of Systematic Reviews*.

Logan L R 2011. Rehabilitation techniques to maximize spasticity management. *Topics in stroke rehabilitation*, 18, 203-211.

Lugade V, Kaufman K 2014. Center of pressure trajectory during gait: a comparison of four foot positions. *Gait & posture*, 40, 719-722.

Macleod P 2002. *A review of flexible circuit technology and its applications*, PRIME Faraday Partnership.

Major R, Hewart P, MacDonald A 2004. A new structural concept in moulded fixed ankle foot orthoses and comparison of the bending stiffness of four constructions. *Prosthetics and orthotics international*, 28, 44-48.

Malas B S 2011. What variables influence the ability of an AFO to improve function and when are they indicated? *Clinical Orthopaedics and Related Research*®, 469, 1308-1314.

Marasović T, Cecić M, Zanchi V 2009. Analysis and interpretation of ground reaction forces in normal gait. *WSEAS transactions on systems*, 8, 1105-14.

- Marigold D S, Eng J J 2006. The relationship of asymmetric weight-bearing with postural sway and visual reliance in stroke. *Gait & posture*, 23, 249-255.
- May B J, Lockard M A 2011. *Chapter 12: Biomechanical principles in prosthetics and orthotics, in Prosthetics & orthotics in clinical practice: a case study approach. p 11-27, FA Davis.*
- McDonald S, Tavener G 1999. Pronation and supination of the foot: confused terminology. *The Foot*, 9, 6-11.
- McHugh B 1999. Analysis of body-device interface forces in the sagittal plane for patients wearing ankle-foot orthoses. *Prosthetics and orthotics international*, 23, 75-81.
- McMonagle C. 2019. *Understanding adherence to ankle-foot orthoses: an application of the theory of planned behaviour.* University of Strathclyde.
- Meadows B, Bowers R, Owen E 2008. *Biomechanics of the hip, knee and ankle. In: Hsu J, Michael J, Fisk J, editors. AAOS atlas of orthoses and assistive devices, Philadelphia: American Academy of Orthopedic Surgeons. p. 299-309.*
- Meadows C B. 1984. *The influence of polypropylene ankle-foot orthoses on the gait of cerebral palsied children.* University of Strathclyde.
- Mehrholz J, Thomas S, Elsner B 2017. Treadmill training and body weight support for walking after stroke. *Cochrane Database of Systematic Reviews.*
- Michael K M, Allen J K, Macko R F 2005. Reduced ambulatory activity after stroke: the role of balance, gait, and cardiovascular fitness. *Archives of physical medicine and rehabilitation*, 86, 1552-1556.
- Mills P M, Morrison S, Lloyd D G, Barrett R S 2007. Repeatability of 3D gait kinematics obtained from an electromagnetic tracking system during treadmill locomotion. *Journal of biomechanics*, 40, 1504-1511.
- Miyazaki S, Yamamoto S, Ebina M, Iwasaki M 1993. A system for the continuous measurement of ankle joint moment in hemiplegic patients wearing ankle-foot orthoses. *Frontiers of medical and biological engineering: the international journal of the Japan Society of Medical Electronics and Biological Engineering*, 5, 215-232.
- Miyazaki S, Yamamoto S, Kubota T 1997. Effect of ankle-foot orthosis on active ankle moment in patients with hemiparesis. *Medical and Biological Engineering and Computing*, 35, 381-385.
- Moisio K C, Sumner D R, Shott S, Hurwitz D E 2003. Normalization of joint moments during gait: a comparison of two techniques. *Journal of biomechanics*, 36, 599-603.
- Momosaki R, Abo M, Watanabe S, Kakuda W, Yamada N, Kinoshita S 2015. Effects of ankle-foot orthoses on functional recovery after stroke: a propensity score analysis based on Japan rehabilitation database. *PLoS One*, 10, e0122688.

Moseley A M, Stark A, Cameron I D, Pollock A 2005. Treadmill training and body weight support for walking after stroke. *Cochrane database of systematic reviews*.

Motion Lab Systems 2016. Support: Documentation Manual. URL https://www.motion-labs.com/support_docs_manuals.html.

Mueller M 2014. Homeopathic Treatment of Brain Hemorrhage – Several Cases. *The American Homeopath*, vol 19. <https://hpathy.com/clinical-cases/homeopathic-treatment-brain-hemorrhage-several-cases/>.

Mulroy S J, Eberly V J, Gronely J K, Weiss W, Newsam C J 2010. Effect of AFO design on walking after stroke: impact of ankle plantar flexion contracture. *Prosthetics and orthotics international*, 34, 277-292.

Murley G S, Landorf K B, Menz H B, Bird A R 2009. Effect of foot posture, foot orthoses and footwear on lower limb muscle activity during walking and running: a systematic review. *Gait & posture*, 29, 172-187.

Nagaya M 1997. Shoehorn-type ankle-foot orthoses: prediction of flexibility. *Archives of physical medicine and rehabilitation*, 78, 82-84.

Nardone A, Godi M, Grasso M, Guglielmetti S, Schieppati M 2009. Stabilometry is a predictor of gait performance in chronic hemiparetic stroke patients. *Gait & Posture*, 30, 5-10.

National Stroke Foundation 2010. Clinical guidelines for stroke management 2010. National Stroke Foundation.

Ng S S, Hui-Chan C W 2012. Contribution of ankle dorsiflexor strength to walking endurance in people with spastic hemiplegia after stroke. *Archives of physical medicine and rehabilitation*, 93, 1046-1051.

Nguyen B T, Baicoianu N A, Howell D B, Peters K M, Steele K M 2020. Accuracy and repeatability of smartphone sensors for measuring shank-to-vertical angle. *Prosthetics and Orthotics International*, 0309364620911314.

NHS Quality Improvement Scotland 2009. Best Practice Statement, Use of Ankle Foot Orthoses Following Stroke. *Edinburgh: NHS Quality Improvement Scotland: http://www.healthcareimprovementscotland.org/previous_resources/best_practice_statement/use_of_ankle-foot_orthoses_fol.aspx*.

NHS Scotland 2019. Scottish Stroke Statistics *NHS National Services Scotland 2018*.

NICE Stroke rehabilitation 2013. Stroke rehabilitation in adults: Clinical guideline. *National Institute for Health and Care Excellence, Available at: <https://www.nice.org.uk/guidance/cg162/resources/stroke-rehabilitation-in-adults-pdf-35109688408261>*.

Nickel V L 1995. Gait parameters following stroke: a practical assessment. *Journal of Rehabilitation Research and Development*, 32, 25-31.

- Nikamp C, Buurke J, Schaake L, Van der Palen J, Rietman J, Hermens H 2019. Effect of long-term use of ankle-foot orthoses on tibialis anterior muscle electromyography in patients with sub-acute stroke: A randomized controlled trial. *Journal of rehabilitation medicine*, 51, 11-17.
- Novacheck T F, Beattie C, Rozumalski A, Gent G, Kroll G 2007. Quantifying the spring-like properties of ankle-foot orthoses (AFOs). *JPO: Journal of Prosthetics and Orthotics*, 19, 98-103.
- Nudo R J 2007. Postinfarct cortical plasticity and behavioral recovery. *Stroke*, 38, 840-845.
- Nudo R J 2011. Neural bases of recovery after brain injury. *Journal of communication disorders*, 44, 515-520.
- Nudo R J, Milliken G W, Jenkins W M, Merzenich M M 1996. Use-dependent alterations of movement representations in primary motor cortex of adult squirrel monkeys. *Journal of Neuroscience*, 16, 785-807.
- Nudo R J, Plautz E J, Frost S B 2001. Role of adaptive plasticity in recovery of function after damage to motor cortex. *Muscle & Nerve: Official Journal of the American Association of Electrodiagnostic Medicine*, 24, 1000-1019.
- Nymark J R, Balmer S J, Melis E H, Lemaire E D, Millar S 2005. Electromyographic and kinematic nondisabled gait differences at extremely slow overground and treadmill walking speeds. *Journal of Rehabilitation Research & Development*, 42.
- Olney S J, Richards C 1996. Hemiparetic gait following stroke. Part I: Characteristics. *Gait & posture*, 4, 136-148.
- Otterman N, Veerbeek J, Schiemanck S, van der Wees P, Nollet F, Kwakkel G 2017. Selecting relevant and feasible measurement instruments for the revised Dutch clinical practice guideline for physical therapy in patients after stroke. *Disability and rehabilitation*, 39, 1449-1457.
- Ounpuu S, Bell K, Davis III R, DeLuca P 1996. An evaluation of the posterior leaf spring orthosis using joint kinematics and kinetics. *Journal of Pediatric Orthopaedics*, 16, 378-384.
- Owen E 2002. Shank angle to floor measures of tuned 'ankle-foot orthosis footwear combinations' used with children with cerebral palsy, spina bifida and other conditions. *Gait Posture*, 16, S132-S133.
- Owen E 2004a. The point of 'point-loading rockers' in ankle-foot orthosis footwear combinations used with children with cerebral palsy, spina bifida and other conditions. *Gait Posture*, 20, S86.
- Owen E 2004b. Tuning of ankle-foot orthosis combinations for children with cerebral palsy, spina bifida and other conditions. *Proceedings of ESMAC Seminars. Warsaw, European Society for Movement Analysis of Children and Adults.*

- Owen E 2005a. A clinical algorithm for the design and tuning of ankle-foot orthosis footwear combinations (AFOFCs) based on shank kinematics. *Gait Posture*, 22, S36-37.
- Owen E 2005b. Proposed clinical algorithm for deciding the sagittal angle of the ankle in an ankle-foot orthosis footwear combination. *Gait Posture*, 22, 38-9.
- Owen E 2010. The importance of being earnest about shank and thigh kinematics especially when using ankle-foot orthoses. *Prosthetics and orthotics international*, 34, 254-269.
- Owen E 2016. Normal gait kinematics and kinetics. *Physical therapy for children with cerebral palsy: an evidence-based approach*. SLACK Incorporated.
- Owen E, Bowers R, Meadows C. Tuning of AFO-footwear combinations for neurological disorders. Proceedings of the 11th World Congress of the International Society for Prosthetics and Orthotics, 2004. 1-6.
- Owen E, Fatone S, Hansen A 2018. Effect of walking in footwear with varying heel sole differentials on shank and foot segment kinematics. *Prosthetics and orthotics international*, 42, 394-401.
- Padilla M G, Rueda F M, Diego I A 2014. Effect of ankle-foot orthosis on postural control after stroke: A systematic review. *Neurología (English Edition)*, 29, 423-432.
- Page S J, Levine P, Leonard A 2007. Mental practice in chronic stroke: results of a randomized, placebo-controlled trial. *Stroke*, 38, 1293-1297.
- Papegaaij S, Steenbrink F 2017. Clinical gait analysis: Treadmill-based vs overground. *Motek Inc.: Amsterdam, The Netherlands*.
- Papi E 2008. Investigate the use of strain gauge technology for the determination of the mechanical characteristics of polypropylene ankle-foot orthoses. *MSc thesis, The University of Strathclyde*.
- Papi E. 2012. *An investigation of the methodologies for biomechanical assessment of stroke rehabilitation*. PhD Thesis, University of Strathclyde, Glasgow.
- Papi E, Maclean J, Bowers R J, Solomonidis S E 2015. Determination of loads carried by polypropylene ankle-foot orthoses: A preliminary study. *Proceedings of the Institution of Mechanical Engineers, Part H: Journal of Engineering in Medicine*, 229, 40-51.
- Papi E, Ugbolue U C, Solomonidis S, Rowe P J 2014. Comparative study of a newly cluster based method for gait analysis and plug-in gait protocol. *Gait & Posture*, 39, S9-S10.
- Park B-S, Kim M-Y, Lee L-K, Yang S-M, Lee W-D, Noh J-W, Shin Y-S, Kim J-H, Lee J-U, Kwak T-Y 2015. Effects of conventional overground gait training and a gait trainer with partial body weight support on spatiotemporal gait parameters of patients after stroke. *Journal of physical therapy science*, 27, 1603-1607.

- Park J H, Chun M H, Ahn J S, Yu J Y, Kang S H 2009. Comparison of gait analysis between anterior and posterior ankle foot orthosis in hemiplegic patients. *American journal of physical medicine & rehabilitation*, 88, 630-634.
- Parmar P 2019. Stroke: classification and diagnosis. *pharmaceutical-journal*, 10, 00.
- Party I S W 2010. National clinical guideline for stroke, London: Royal College of Physicians, 2008.
- Parvataneni K, Ploeg L, Olney S J, Brouwer B 2009. Kinematic, kinetic and metabolic parameters of treadmill versus overground walking in healthy older adults. *Clinical biomechanics*, 24, 95-100.
- Patterson K K, Parafianowicz I, Danells C J, Closson V, Verrier M C, Staines W R, Black S E, McIlroy W E 2008. Gait asymmetry in community-ambulating stroke survivors. *Archives of physical medicine and rehabilitation*, 89, 304-310.
- Paul S L, Sturm J W, Dewey H M, Donnan G A, Macdonell R A, Thrift A G 2005. Long-term outcome in the North East Melbourne Stroke Incidence Study: predictors of quality of life at 5 years after stroke. *Stroke*, 36, 2082-2086.
- Payton C J, Burden A 2008. *Biomechanical evaluation of movement in sport and exercise: the British Association of Sport and Exercise Sciences guide*, Routledge.
- Pereira S, Mehta S, McIntyre A, Lobo L, Teasell R W 2012. Functional electrical stimulation for improving gait in persons with chronic stroke. *Topics in stroke rehabilitation*, 19, 491-498.
- Perry J, Burnfield J 2010. Gait analysis: normal and pathological function. 2nd. *Thorofare, NJ: Slack Incorporated*.
- Perry J, Davids J R 1992. Gait analysis: normal and pathological function. *Journal of Pediatric Orthopaedics*, 12, 815.
- Perry J, Garrett M, Gronley J K, Mulroy S J 1995. Classification of walking handicap in the stroke population. *Stroke*, 26, 982-989.
- Peters A, Galna B, Sangeux M, Morris M, Baker R 2010. Quantification of soft tissue artifact in lower limb human motion analysis: a systematic review. *Gait & posture*, 31, 1-8.
- Platts M M, Rafferty D, Paul L 2006. Metabolic cost of overground gait in younger stroke patients and healthy controls. *Medicine & Science in Sports & Exercise*, 38, 1041-1046.
- Plautz E J, Milliken G W, Nudo R J 2000. Effects of repetitive motor training on movement representations in adult squirrel monkeys: role of use versus learning. *Neurobiology of learning and memory*, 74, 27-55.

- Polliack A A, Swanson C, Landsberger S E, McNeal D R 2001. Development of a testing apparatus for structural stiffness evaluation of ankle-foot orthoses. *JPO: Journal of Prosthetics and Orthotics*, 13, 74-82.
- Pollock A, Baer G, Langhorne P, Pomeroy V 2007. Physiotherapy treatment approaches for the recovery of postural control and lower limb function following stroke: a systematic review. *Clinical rehabilitation*, 21, 395-410.
- Popovic M, Curt A, Keller T, Dietz V 2001. Functional electrical stimulation for grasping and walking: indications and limitations. *Spinal cord*, 39, 403-412.
- Prabhakaran S, Zarah E, Riley C, Speizer A, Chong J Y, Lazar R M, Marshall R S, Krakauer J W 2008. Inter-individual variability in the capacity for motor recovery after ischemic stroke. *Neurorehabilitation and neural repair*, 22, 64-71.
- Pratt E, Durham S, Ewins D 2007. Normal databases for orthotic tuning in children. *Gait Posture*, 26, S92.
- Ramstrand N, Ramstrand S. AAOP state-of-the-science evidence report: the effect of ankle-foot orthoses on balance—a systematic review. *JPO: Journal of Prosthetics and Orthotics*, 2010. LWW, P4-P23.
- Rao N, Chaudhuri G, Hasso D, D'Souza K, Wening J, Carlson C, Aruin A S 2008. Gait assessment during the initial fitting of an ankle foot orthosis in individuals with stroke. *Disability and rehabilitation: Assistive technology*, 3, 201-207.
- Rathore S S, Hinn A R, Cooper L S, Tyroler H A, Rosamond W D 2002. Characterization of incident stroke signs and symptoms: findings from the atherosclerosis risk in communities study. *Stroke*, 33, 2718-2721.
- Reynard F, Deriaz O, Bergeau J 2009. Foot varus in stroke patients: muscular activity of extensor digitorum longus during the swing phase of gait. *The Foot*, 19, 69-74.
- Richards J 2018. *The Comprehensive Textbook of Biomechanics-E-Book: with access to e-learning course [formerly Biomechanics in Clinic and Research]*, Elsevier Health Sciences.
- Richards L G, Stewart K C, Woodbury M L, Senesac C, Cauraugh J H 2008. Movement-dependent stroke recovery: a systematic review and meta-analysis of TMS and fMRI evidence. *Neuropsychologia*, 46, 3-11.
- Riley P O, Della Croce U, Kerrigan D C 2001. Effect of age on lower extremity joint moment contributions to gait speed. *Gait & posture*, 14, 264-270.
- Riley P O, Paolini G, Della Croce U, Paylo K W, Kerrigan D C 2007. A kinematic and kinetic comparison of overground and treadmill walking in healthy subjects. *Gait & posture*, 26, 17-24.

- Rodgers M, Forrester L, Mizelle C, Harris-Love M. Effects of gait velocity on COP symmetry measures in individuals with stroke. 28th annual meeting of the American Society of Biomechanics, 2004.
- Roelker S A, Bowden M G, Kautz S A, Neptune R R 2019. Paretic propulsion as a measure of walking performance and functional motor recovery post-stroke: a review. *Gait & posture*, 68, 6-14.
- Romkes J, Brunner R 2002. Comparison of a dynamic and a hinged ankle-foot orthosis by gait analysis in patients with hemiplegic cerebral palsy. *Gait & posture*, 15, 18-24.
- Roper B A 1982. Rehabilitation after a stroke. *Journal of bone and joint surgery* 64(B), 156-163.
- Ross R, Greig R, Convery P 1999. Comparison of bending stiffness of six different colours of copolymer polypropylene. *Prosthetics and orthotics international*, 23, 63-71.
- Rothi L J, Horner J 1983. Restitution and substitution: Two theories of recovery with application to neurobehavioral treatment. *Journal of Clinical and Experimental Neuropsychology*, 5, 73-81.
- Roy S H, De Luca G, Cheng M S, Johansson A, Gilmore L D, De Luca C J 2007. Electro-mechanical stability of surface EMG sensors. *Medical & biological engineering & computing*, 45, 447-457.
- Salbach N, Mayo N, Wood-Dauphinee S, Hanley J, Richards C, Cote R 2004. A task-orientated intervention enhances walking distance and speed in the first year post stroke: a randomized controlled trial. *Clinical rehabilitation*, 18, 509-519.
- Sangeux M, Marin F, Charleux F, Dürselen L, Tho M H B 2006. Quantification of the 3D relative movement of external marker sets vs. bones based on magnetic resonance imaging. *Clinical Biomechanics*, 21, 984-991.
- Sannyasi G. 2019. *Comparison of Gait with Ankle Foot Orthosis (AFO) and Functional Electrical Stimulation (FES) in patients following Stroke*. Christian Medical College, Vellore.
- Saposnik G, Levin M, Group S O R C W 2011. Virtual reality in stroke rehabilitation: a meta-analysis and implications for clinicians. *Stroke*, 42, 1380-1386.
- Sathian K, Buxbaum L J, Cohen L G, Krakauer J W, Lang C E, Corbetta M, Fitzpatrick S M 2011. Neurological principles and rehabilitation of action disorders: common clinical deficits. *Neurorehabilitation and neural repair*, 25, 21S-32S.
- Schmalz T, Blumentritt S, Drewitz H, Freslier M 2006. The influence of sole wedges on frontal plane knee kinetics, in isolation and in combination with representative rigid and semi-rigid ankle-foot-orthoses. *Clinical Biomechanics*, 21, 631-639.
- SENIAM Organisation 1999. Recommendations for sensor locations in hip or upper leg muscles. http://seniam.org/leg_location.htm.

- Shahabi S, Shabaninejad H, Kamali M, Jalali M, Ahmadi Teymurlouy A 2020. The effects of ankle-foot orthoses on walking speed in patients with stroke: a systematic review and meta-analysis of randomized controlled trials. *Clinical Rehabilitation*, 34, 145-159.
- Sheffler L R, Hennessey M T, Naples G G, Chae J 2006. Peroneal nerve stimulation versus an ankle foot orthosis for correction of footdrop in stroke: impact on functional ambulation. *Neurorehabilitation and neural repair*, 20, 355-360.
- Showers D, Strunck M 1984. Sheet plastics and their applications in orthotics and prosthetics. *Orthotics and Prosthetics*, 38, 41-48.
- Shumway-Cook A, Woollacott M H 2007. *Motor control: translating research into clinical practice*, Lippincott Williams & Wilkins.
- Silva P C, Silva M T, Martins J M 2010. Evaluation of the contact forces developed in the lower limb/orthosis interface for comfort design. *Multibody System Dynamics*, 24, 367-388.
- Silver-Thorn B, Herrmann A, Current T, McGuire J 2011. Effect of ankle orientation on heel loading and knee stability for post-stroke individuals wearing ankle-foot orthoses. *Prosthetics and orthotics international*, 35, 150-162.
- Simons C D, van Asseldonk E H, van der Kooij H, Geurts A C, Buurke J H 2009. Ankle-foot orthoses in stroke: effects on functional balance, weight-bearing asymmetry and the contribution of each lower limb to balance control. *Clinical biomechanics*, 24, 769-775.
- Simonsen E B, Svendsen M B, Nørreslet A, Baldvinsson H K, Heilskov-Hansen T, Larsen P K, Alkjær T, Henriksen M 2012. Walking on high heels changes muscle activity and the dynamics of human walking significantly. *Journal of applied biomechanics*, 28, 20-28.
- Sinclair J, Taylor P J, Hebron J, Brooks D, Hurst H T, Atkins S 2015. The reliability of electromyographic normalization methods for cycling analyses. *Journal of human kinetics*, 46, 19-27.
- Singer M L, Kobayashi T, Lincoln L S, Orendurff M S, Foreman K B 2014. The effect of ankle-foot orthosis plantarflexion stiffness on ankle and knee joint kinematics and kinetics during first and second rockers of gait in individuals with stroke. *Clinical Biomechanics*, 29, 1077-1080.
- Sousa A S, Tavares J M R 2012. Effect of gait speed on muscle activity patterns and magnitude during stance. *Motor Control*, 16, 480-492.
- Stagni R, Fantozzi S, Cappello A, Leardini A 2005. Quantification of soft tissue artefact in motion analysis by combining 3D fluoroscopy and stereophotogrammetry: a study on two subjects. *Clinical Biomechanics*, 20, 320-329.
- Stefanyshyn D J, Nigg B M, Fisher V, O'Flynn B, Liu W 2000. The influence of high heeled shoes on kinematics, kinetics, and muscle EMG of normal female gait. *Journal of Applied Biomechanics*, 16, 309-319.

- Stegeman D, Hermens H 2007. Standards for surface electromyography: The European project Surface EMG for non-invasive assessment of muscles (SENIAM). *Enschede: Roessingh Research and Development*, 108-12.
- Stein R B, Everaert D G, Thompson A K, Chong S L, Whittaker M, Robertson J, Kuether G 2010. Long-term therapeutic and orthotic effects of a foot drop stimulator on walking performance in progressive and nonprogressive neurological disorders. *Neurorehabilitation and neural repair*, 24, 152-167.
- Stevens A, Raftery J, Mant J, Simpson S 2018. *Health Care Needs Assessment, First Series, Volume 2*, CRC Press.
- Stewart C, Roberts A, Jonkers I 2004. Gastrocnemius: a three joint muscle. *Gait & posture*, 20.
- Stewart J D 2008. Foot drop: where, why and what to do? *Practical neurology*, 8, 158-169.
- Sumiya T, Suzuki Y, Kasahara T 1996. Stiffness control in posterior-type plastic ankle-foot orthoses: effect of ankle trimline Part 1: a device for measuring ankle moment. *Prosthetics and Orthotics International*, 20, 129-131.
- Summan R, Pierce S, Macleod C, Dobie G, Gears T, Lester W, Pritchett P, Smyth P 2015. Spatial calibration of large volume photogrammetry based metrology systems. *Measurement*, 68, 189-200.
- Sungkarat S, Fisher B E, Kovindha A 2011. Efficacy of an insole shoe wedge and augmented pressure sensor for gait training in individuals with stroke: a randomized controlled trial. *Clinical rehabilitation*, 25, 360-369.
- Swaffield L 1996. *Stroke: the complete guide to recovery and rehabilitation*, Thorsons.
- Takada K, Yashiro K, Morimoto T 1995. Application of polynomial regression modeling to automatic measurement of periods of EMG activity. *Journal of neuroscience methods*, 56, 43-47.
- Takahashi C D, Der-Yeghiaian L, Le V, Motiwala R R, Cramer S C 2008. Robot-based hand motor therapy after stroke. *Brain*, 131, 425-437.
- Teasell R W, Bhogal S K, Foley N C, Speechley M R 2003. Gait retraining post stroke. *Topics in stroke rehabilitation*, 10, 34-65.
- Teasell R W, McRae M P, Foley N, Bhardwaj A 2001. Physical and functional correlations of ankle-foot orthosis use in the rehabilitation of stroke patients. *Archives of physical medicine and rehabilitation*, 82, 1047-1049.
- Teixeira-Salmela L F, Olney S J, Nadeau S, Brouwer B 1999. Muscle strengthening and physical conditioning to reduce impairment and disability in chronic stroke survivors. *Archives of physical medicine and rehabilitation*, 80, 1211-1218.

- Telfer S, Pallari J, Munguia J, Dalgarno K, McGeough M, Woodburn J 2012. Embracing additive manufacture: implications for foot and ankle orthosis design. *BMC musculoskeletal disorders*, 13, 84.
- Tesio L, Rota V 2008. Gait analysis on split-belt force treadmills: validation of an instrument. *American journal of physical medicine & rehabilitation*, 87, 515-526.
- Tilley A R 2001. *The measure of man and woman: human factors in design*, John Wiley & Sons.
- Tilson J K, Sullivan K J, Cen S Y, Rose D K, Koradia C H, Azen S P, Duncan P W, Team L E A P S I 2010. Meaningful gait speed improvement during the first 60 days poststroke: minimal clinically important difference. *Physical therapy*, 90, 196-208.
- Total D, Menon M, Jones-Hershinow C, Barton K, Gates D H 2019. The impact of ankle-foot orthosis stiffness on gait: A systematic literature review. *Gait & Posture*, 69, 101-111.
- Tyrell C M, Roos M A, Rudolph K S, Reisman D S 2011. Influence of systematic increases in treadmill walking speed on gait kinematics after stroke. *Physical therapy*, 91, 392-403.
- Tyson S, Sadeghi-Demneh E, Nester C 2013. A systematic review and meta-analysis of the effect of an ankle-foot orthosis on gait biomechanics after stroke. *Clinical Rehabilitation*, 27, 879-891.
- Tyson S F, Kent R M 2013. Effects of an ankle-foot orthosis on balance and walking after stroke: a systematic review and pooled meta-analysis. *Archives of physical medicine and rehabilitation*, 94, 1377-1385.
- van de Port I G, Kwakkel G, Lindeman E 2008. Community ambulation in patients with chronic stroke: how is it related to gait speed? *Journal of Rehabilitation Medicine*, 40, 23-27.
- Van Peppen R P, Hendriks H, Van Meeteren N L, Helden P J, Kwakkel G 2007. The development of a clinical practice stroke guideline for physiotherapists in The Netherlands: a systematic review of available evidence. *Disability and rehabilitation*, 29, 767-783.
- van Swigchem R, Vloothuis J, den Boer J, Weerdesteyn V, Geurts A C 2010. Is transcutaneous peroneal stimulation beneficial to patients with chronic stroke using an ankle-foot orthosis? A within-subjects study of patients' satisfaction, walking speed and physical activity level. *Journal of rehabilitation medicine*, 42, 117-121.
- Vaughan C L, Davis B L, O'Connor J C 1992. *Dynamics of human gait*, Human Kinetics.
- Veerbeek J M, van Wegen E, van Peppen R, van der Wees P J, Hendriks E, Rietberg M, Kwakkel G 2014. What is the evidence for physical therapy poststroke? A systematic review and meta-analysis. *PloS one*, 9, e87987.

Verdie C, Daviet J, Borie M, Popielarz S, Munoz M, Salle J, Rebeyrotte I, Dudognon P. Epidemiology of pes varus and/or equinus one year after a first cerebral hemisphere stroke: apropos of a cohort of 86 patients. *Annales de readaptation et de medecine physique: revue scientifique de la Societe francaise de reeducation fonctionnelle de readaptation et de medecine physique*, 2004. 81-86.

VISHAY M-M 2008. Strain Gage Measurements on Plastics and Composites. Vishay Precision Group, Vishay Micro-Measurements. Application Note VMM-1. <https://pdfs.semanticscholar.org/fffca6b2b3b055158cc9c848e2d253ba9d19b1d9.pdf>.

Wall J, Ashburn A 1979. Assessment of gait disability in hemiplegics. *Hemiplegic gait. Scandinavian journal of rehabilitation medicine*, 11, 95-103.

Wang R-Y, Yen L-L, Lee C-C, Lin P-Y, Wang M-F, Yang Y-R 2005. Effects of an ankle-foot orthosis on balance performance in patients with hemiparesis of different durations. *Clinical rehabilitation*, 19, 37-44.

Wang Y, Rudd A G, Wolfe C D 2013. Age and ethnic disparities in incidence of stroke over time: the South London Stroke Register. *Stroke*, 44, 3298-3304.

Waters R L, Bontrager E L 1979. The influence of heel design on a rigid ankle-foot orthosis. *Orthot Prosthet*, 33, 3-10.

Watt J R, Franz J R, Jackson K, Dicharry J, Riley P O, Kerrigan D C 2010. A three-dimensional kinematic and kinetic comparison of overground and treadmill walking in healthy elderly subjects. *Clinical biomechanics*, 25, 444-449.

Webster J B, Darter B J 2019. Principles of Normal and Pathologic Gait. *Atlas of Orthoses and Assistive Devices*. Elsevier.

Wening J, Huskey M, Hasso D, Aruin C A, Rao N 2009. The effect of an ankle-foot orthosis on gait parameters of acute and chronic hemiplegic subjects. *The Academy Today*, 5, 1.

Whittle M W 2014. *Gait analysis: an introduction*, Butterworth-Heinemann.

Window A, Holister G 1992. Strain gauge technology. *Appl. Science Publishers, London*.

Winstein C J, Stein J, Arena R, Bates B, Cherney L R, Cramer S C, Deruyter F, Eng J J, Fisher B, Harvey R L 2016. Guidelines for adult stroke rehabilitation and recovery: a guideline for healthcare professionals from the American Heart Association/American Stroke Association. *Stroke*, 47, e98-e169.

Winter D A 2009. *Biomechanics and motor control of human movement*, John Wiley & Sons.

Winters C, van Wegen E E, Daffertshofer A, Kwakkel G 2015. Generalizability of the proportional recovery model for the upper extremity after an ischemic stroke. *Neurorehabilitation and neural repair*, 29, 614-622.

- Winters T, Gage J, Hicks R 1987. Gait patterns in spastic hemiplegia in children and young adults. *J Bone Joint Surg Am*, 69, 437-441.
- Wolf S L, Winstein C J, Miller J P, Taub E, Uswatte G, Morris D, Giuliani C, Light K E, Nichols-Larsen D, EXCITE Investigators f t 2006. Effect of constraint-induced movement therapy on upper extremity function 3 to 9 months after stroke: the EXCITE randomized clinical trial. *Jama*, 296, 2095-2104.
- Wong A M, Pei Y-C, Hong W-H, Chung C-Y, Lau Y-C, Chen C P 2004. Foot contact pattern analysis in hemiplegic stroke patients: an implication for neurologic status determination. *Archives of physical medicine and rehabilitation*, 85, 1625-1630.
- Woolley S M 2001. Characteristics of gait in hemiplegia. *Topics in stroke rehabilitation*, 7, 1-18.
- World Health Organisation 2002. The world Health Report 2002: reducing risks, Promoting health life. *World Health Report 2002*.
- Wu G, Siegler S, Allard P, Kirtley C, Leardini A, Rosenbaum D, Whittle M, D D'Lima D, Cristofolini L, Witte H 2002. ISB recommendation on definitions of joint coordinate system of various joints for the reporting of human joint motion—part I: ankle, hip, and spine. *Journal of biomechanics*, 35, 543-548.
- Yamamoto S, Ebina M, Iwasaki M, Kubo S, Kawai H, Hayashi T 1993a. Comparative study of mechanical characteristics of plastic AFOs. *JPO: Journal of Prosthetics and Orthotics*, 5, 59.
- Yamamoto S, Fuchi M, Yasui T 2011. Change of rocker function in the gait of stroke patients using an ankle foot orthosis with an oil damper: immediate changes and the short-term effects. *Prosthetics and orthotics international*, 35, 350-359.
- Yamamoto S, Hagiwara A, Mizobe T, Yokoyama O, Yasui T 2005. Development of an ankle-foot orthosis with an oil damper. *Prosthetics and orthotics international*, 29, 209-219.
- Yamamoto S, Miyazaki S, Kubota T 1993b. Quantification of the effect of the mechanical property of ankle-foot orthoses on hemiplegic gait. *Gait & Posture*, 1, 27-34.
- Yamamoto S, Tanaka S, Motojima N 2018. Comparison of ankle-foot orthoses with plantar flexion stop and plantar flexion resistance in the gait of stroke patients: a randomized controlled trial. *Prosthetics and orthotics international*, 42, 544-553.
- Yamane A 2019. *Chapter 1: Orthotic prescription in 'Atlas of Orthoses and Assistive Devices'*, Webster, Joseph Bradley Murphy, Douglas P, Elsevier.
- Yüzer G F N, Koyuncu E, Çam P, Özgirgin N 2018. The regularity of orthosis use and the reasons for disuse in stroke patients. *International Journal of Rehabilitation Research*, 41, 270-275.

Zakharov A V, Bulanov V A, Khivintseva E V, Kolsanov A V, Bushkova Y V, Ivanova G E 2020. Stroke affected lower limbs rehabilitation combining virtual reality with tactile feedback. *Frontiers in Robotics and AI*, 7.

Zarahn E, Alon L, Ryan S L, Lazar R M, Vry M-S, Weiller C, Marshall R S, Krakauer J W 2011. Prediction of motor recovery using initial impairment and fMRI 48 h poststroke. *Cerebral Cortex*, 21, 2712-2721.

Zollo L, Zaccheddu N, Ciancio A, Morrone M, Bravi M, Santacaterina F, Laineri Milazzo M, Guglielmelli E, Sterzi S 2015. Comparative analysis and quantitative evaluation of ankle-foot orthoses for foot drop in chronic hemiparetic patients. *Eur J Phys Rehabil Med*, 51, 185-9.

Zukowski L A, Feld J A, Giuliani C A, Plummer P 2019. Relationships between gait variability and ambulatory activity post stroke. *Topics in stroke rehabilitation*, 26, 255-260.